

TRIANGULAR $[\text{Mo}_3 (\mu_3\text{-E}) (\mu_2\text{-EE}')_3 (\text{Q}_3\text{LR}_2)_3]^+$ (E, E' = S or Se; L = CN
or P; Q = S or Se) CLUSTERS: SYNTHESIS, CRYSTALLOGRAPHY,
AND PHOTOCATALYTIC HYDROGEN EVOLUTION ACTIVITY
AND
EFFORTS TOWARD A SURFACE- TETHERED MOLYBDENUM
SULFIDE CLUSTER FOR SOLAR WATER SPLITTING.

AN ABSTRACT

SUBMITTED ON THE TWENTY-SECOND DAY OF FEBRUARY 2024

TO THE DEPARTMENT OF CHEMISTRY

IN PARTIAL FULFILLMENT OF THE REQUIREMENT

OF THE SCHOOL OF SCIENCE AND ENGINEERING

OF TULANE UNIVERSITY

FOR THE DEGREE

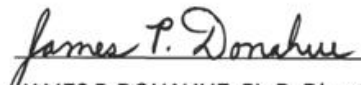
OF


DOCTOR OF PHILOSOPHY


BY

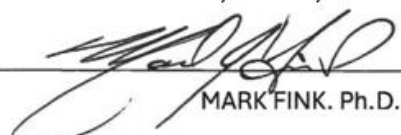


GAYATHRI RAGUNATHAN

APPROVED: 
JAMES P. DONAHUE, Ph.D. Director


RUSSELL H. SCHMEHL, Ph.D.


ALEXANDER, BURIN, Ph.D.


MARK FINK, Ph.D.

Abstract

Chapter 1 summarizes how global population and economic growth in the near future project to increase the global demand for energy. Hydrogen is expected to become an increasingly important energy carrier as part of the effort to move away from nonrenewable fossil fuels and more toward renewable sources with more benign environmental impact. This chapter reviews current technologies used for molecular dihydrogen (H_2) production from renewable and non-renewable sources. The massive production of H_2 worldwide is primarily from fossil fuels via steam reforming of methane (CH_4). “Green” hydrogen, however, is produced by electrolysis/photolysis technologies from water.

Chapter 2 of this dissertation considers the limitations for the synthesis of dithiocarbamate ligands directly from secondary amines and CS_2 . This ligand type is used as a supporting ligand for the catalysts described in Chapter 3. With secondary amines that are not sterically hindered, such as Et_2NH or tBu_2NH , the reaction $2R_2NH + CS_2 \rightarrow [R_2NH_2][R_2NCS_2]$ is facile, but with Cy_2NH , the reaction does not proceed cleanly. If the reaction is conducted in the presence of $NaOH/H_2O$ as proton acceptor, the reaction is complicated by the formation of S_8 , apparently via $[COS_2]^{2-}$ and by tetraalkylthiuram polysulfides. A cleaner, more effective route to $Cy_2NC(S)SSC(S)NCy_2$ was found by deprotonation of Cy_2NH with $tBuLi$ followed by oxidation coupling with I_2 . The conclusion from this work is that branching at the carbon atom that is alpha to the amine nitrogen decides the synthetic approach to tetraalkylthiuram disulfides that is viable.

The focus of Chapter 3 is upon the synthesis of a palette of triangular $[Mo_3(\mu_3-E)(\mu_2-EF)_3(Q_2LR_2)_3]^+$ ($E = S; F = S, \text{ or } Se; L = CN \text{ or } P; Q = S, \text{ or } Se$), clusters, which vary in the chalcogenide core composition (E,F) and in the identity of the ancillary chalcogen

donor ligand. The supporting ligand can be dithiocarbamate ($\text{R}_2\text{NCS}_2^{1-}$), diselenocarbamate ($\text{R}_2\text{NCS}_2^{1-}$), or dialkyldithiophosphate ($\text{R}_2\text{PS}_2^{1-}$). For consistency, R has been maintained as $i\text{Bu}$ or O^iPr . These clusters have been characterized structurally by X-ray crystallography and spectroscopically by UV-vis and NMR. With differing degrees of activity, these compounds function as homogeneous catalysts for H_2 formation from H_2O under photolysis with $[\text{Ru}(\text{bpy})_3]^{2+}$ as chromophore and 4-*N,N*-trimethylaniline (TMA) as reversible quencher in relay with triethylamine (TEA) as sacrificial electron donor. The source of H^+ is H_2O . Under identical conditions, $[\text{Mo}_3\text{S}_7(\text{S}_2\text{CN}^i\text{Bu}_2)_3]^+$ is the most effective H_2 evolution catalyst studied in this photosystem.

Chapter 4 summarizes efforts to synthesize a phosphonate-substituted dithiocarbamate ligand that might be chemically immobilized onto an electrode surface. If tethered to an electrode, a well-defined small molecule redox catalyst can enjoy the kinetic advantage of restricted proximity to the source of reducing equivalents. One of the well-developed choices for anchoring a metal complex to an oxide surface is the phosphonate group. As detailed in Chapter 3, trimolybdenum clusters of types $[\text{Mo}_3\text{S}_7(\text{S}_2\text{CNR}_2)_3]^+$ have been observed by us to be moderately active H_2 -evolving catalysts under photolysis in the presence of $[\text{Ru}(\text{bpy})_3]^{2+}$ as chromophore and triethylamine (TEA) as sacrificial electron donor. Several hundred turnovers in a period of several hours have been observed, and diminished activity over time appears to be due to chromophore deterioration rather than to degradation of catalyst. Thus, a surface-tethered version of the molybdenum sulfide cluster may allow a clearer view of its inherent activity without the complicating effect of dependency upon a chromophore of limited lifetime.

TRIANGULAR $[\text{Mo}_3 (\mu_3\text{-E}) (\mu_2\text{-EE}')_3 (\text{Q}_3\text{LR}_2)_3]^+$ (E, E' = S or Se; L = CN
or P; Q = S or Se) CLUSTERS: SYNTHESIS, CRYSTALLOGRAPHY,
AND PHOTOCATALYTIC HYDROGEN EVOLUTION ACTIVITY
AND
EFFORTS TOWARD A SURFACE- TETHERED MOLYBDENUM
SULFIDE CLUSTER FOR SOLAR WATER SPLITTING.

AN ABSTRACT

SUBMITTED ON THE TWENTY-SECOND DAY OF FEBRUARY 2024

TO THE DEPARTMENT OF CHEMISTRY

IN PARTIAL FULFILLMENT OF THE REQUIREMENT

OF THE SCHOOL OF SCIENCE AND ENGINEERING

OF TULANE UNIVERSITY

FOR THE DEGREE

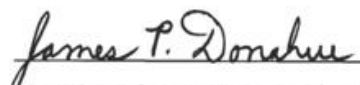
OF


DOCTOR OF PHILOSOPHY


BY

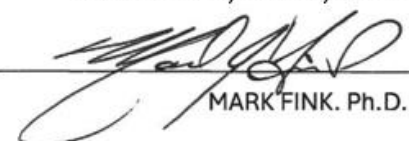


GAYATHRI RAGUNATHAN

APPROVED: 
JAMES P. DONAHUE, Ph.D. Director


RUSSELL H. SCHMEHL, Ph.D.


ALEXANDER, BURIN, Ph.D.


MARK FINK, Ph.D.

© Copyright by Gayathri Ragnathan, 2024
All Rights Reserved

Acknowledgements

First and foremost, I would like to thank and acknowledge my research advisor, Professor James P. Donahue. Throughout my journey of my graduate study, he has been kindly supporting and guiding and mentoring me in both my research projects and course works. Furthermore, he has supported and advised me to overcome difficulties during my study period at Tulane. He is an amazing instructor and fully dedicated professor for students. Moreover, he treats all his students with respect and gratitude.

I am also thankful to my dissertation committee members: Professor Russell H. Schmehl, Professor Mark Fink and Professor Alexander Burin. Thank you for your great suggestion and helpful discussions and valuable time in helping with my dissertation. Special thanks for our crystallographer, Dr. Joel Mague and Dr. Xiodong Zhang who helped me for my project.

I am thankful to all current and former postdoc, graduate students in the Donahue group including Dr. Satyendra kumar, Dr Saikat Mishra, Dr. Malathy Selvachandren, Dr. Bo Wang, Dr. Antony Obanda, Dr. Patricia Fontenot, Dr. Jared Taylor, Justin Barens, Atahar Rabby, Titir das gupta, Jimmy Martines. Special thanks is given to Dr. Malathy sevachandren's family who provided a lot of help from arriving in New Orleans to start my studies here.

Lastly, I am truly grateful for my father Ragunathan, mother Yogarani and brother Raguvarnan, without their support and blessings none of the things in my life is possible. I also want to express my thankfulness to my husband, Giridharan for his great support for my entire life in USA.

Table of Contents

Chapter 1

1.1 Introduction.....	1
1.2 Hydrogen Production Technologies.....	2
1.3 Homogeneous Systems for H ₂ Production.....	5
1.4 Conclusions.....	10
1.5 References.....	11

Chapter 2

2.1 Introduction.....	16
2.2 Summary and Concluding Remarks	26
2.3 Experimental.....	26
2.4 References.....	28

Chapter 3

3.1 Introduction.....	32
3.2 Experimental.....	36
3.3 Discussion.....	49
3.4 Discussion of Crystal Structures.....	61
3.5 Electrochemistry	73
3.6 Photolysis.....	93
3.7 Conclusion	116
3.8 References.....	118

Chapter 4

4.1 Introduction.....	126
4.2 Physical Methods and General Considerations	127
4.3 Result and Discussion.....	128
4.4 Future Work	136
4.5 References.....	137
Appendices.....	138

List of Tables

Chapter 1

Table 1.1. Hydrogen Production Methods.....	2
--	---

Chapter 2

Table 2.1. Crystal and Refinement Data for $\text{Cy}_2\text{NC}(\text{S})\text{SSC}(\text{S})\text{NCy}_2$ and $\text{Cy}_2\text{NC}(\text{S})\text{SSSSC}(\text{S})\text{NCy}_2$	20
---	----

Chapter 3

Table 3.1. Crystal and refinement data for bis(O,O'-di-isopropylphosphorothionyl)disulfide, and bis[[bis(2-methylpropyl)amino]selenoxomethyl] triselenide.....	65
---	----

Table 3.2. Crystal and refinement data for structurally characterized Mo_3 and Mo_2 compounds.....	66
---	----

Table 3.2., Cont'd. Crystal and refinement data for structurally characterized Mo_3 and Mo_2 compounds.....	67
--	----

Table 3.2., Cont'd. Crystal and refinement data for structurally characterized Mo_3 and Mo_2 compounds.....	67
--	----

Table 3.2., Cont'd. Crystal and refinement data for structurally characterized Mo_3 and Mo_2 compounds.....	69
--	----

Table 3.3. Selected interatomic distances (Å) and angles (deg.) for triangular M_3 cations. Averaged values ^a are presented for distances and angles that are chemically identical.....	73
--	----

Table 3.4. Comparison of first reduction potential for all clusters.....	92
---	----

Table 3.5. Comparison of reversible reduction between CV and DPV.....	92
--	----

List of Figures

Chapter 1

- Figure 1.1.** Homogeneous system for Mo-catalyst in water splitting. Reproduced with permission from American Chemical Society..... 7
- Figure 1.2.** Structure of Cobalt dithiolene complex. 7
- Figure 1.3** Cartoon that illustrates the relevant energies for H₂ production. dHA indicates dehydroascorbic acid. Potentials are shown versus that of NHE at pH = 4.5. Reproduced with permission from Science..... 8
- Figure 1.4** Catalyst design is organized around the first, second, and outer coordination spheres as well as the surrounding solvent, as exemplified by a [Ni(P^R₂N^{R'}₂)₂]²⁺ complex. Reproduced with permission from American Chemical Society. 9
- Figure 1.5.** (A) Structure of the cobaloxime linker in UU-100(Co) and (B) structural model of UU-100(Co) MOF viewed along [001]. Reproduced with permission from the American Chemical Society..... 10

Chapter 2

- Figure 2.1** Structures of tetracyclohexylthiuram tetrasulfide (a), tetracyclohexylthiuram disulfide (b), and the chiral C₂-symmetric cores of a typical tetraalkylthiuram disulfide (c). 17
- Figure 2.2.** Molecules 1 (a) and 2 (b) of Cy₂NC(S)SSC(S)NCy₂ in triclinic polymorph. Ellipsoids are drawn at the 30% level. Image (c) shows the monoclinic polymorph of Cy₂NC(S)SSC(S)NCy₂ with 50% ellipsoids. Tetrasulfide Cy₂NC(S)SSSSC(S)NCy₂ is presented in (d), also with 50% ellipsoids. For clarity, all H atoms are omitted, and disorder in the Cy groups in (b) and (c) is not shown. 21
- Figure 2.3.** (a) Arrangement of Cy₂NC(S)SSC(S)NCy₂ molecules (triclinic polymorph) into sheets in the *ab* plane. (b) Stacking of sheets of Cy₂NC(S)SSC(S)NCy₂ molecules (triclinic polymorph) along the *c* axis. 22
- Figure 2.4.** Symmetry-imposed disorder in the monoclinic form of Cy₂NC(S)SSC(S)NCy₂. A mirror plane coincides with C1, N1, C6 and N2 and generates a symmetry equivalent for all atoms that are off-plane. In addition to the symmetry-imposed disorder, the cyclohexyl groups have a static conformational disorder over two positions. 23
- Figure 2.5.** Packing arrangement for Cy₂NC(S)SSSSC(S)NCy₂ viewed along the *b* axis of the unit cell. All H atoms are omitted for clarity. The thermal ellipsoids are presented at the 50% level..... 25

Chapter 3

Figure 3.1. $(\text{NH}_4)_2(\text{Mo}_3\text{S}_{13})$ structures. Reproduced with permission from <i>Nature Chemistry</i> .	33
Figure 3.2. Synthesis for $\text{Ni}_3\text{Se}_4@\text{MoSe}_2$ nanostructures. Reproduced with permission from Applied Sciences.	34
Figure 3.3. ^1H NMR spectrum of complex $[\text{Mo}_3\text{S}_7(\text{S}_2\text{CN}^i\text{Bu}_2)_3]$ ($\text{S}_2\text{CN}^i\text{Bu}_2$).	53
Figure 3.4. ^1H NMR spectrum of complex $[\text{Mo}_3\text{S}_7(\text{S}_2\text{P}(\text{O}^i\text{Pr})_2)_3][\text{S}_2\text{P}(\text{O}^i\text{Pr})_2]$.	54
Figure 3.5. ^{31}P NMR spectrum of complex $[\text{Mo}_3\text{S}_7(\text{S}_2\text{P}(\text{O}^i\text{Pr})_2)_3][\text{S}_2\text{P}(\text{O}^i\text{Pr})_2]$.	54
Figure 3.6. ESI-MS spectrum of complex $[\text{Mo}_3\text{Se}_7(\text{S}_2\text{CN}^i\text{Bu}_2)_3]^+$ during the reaction at 170°C .	59
Figure 3.7. Thermal ellipsoid plots (50%) for bis(<i>O,O'</i> -diisopropylphosphorothionyl)disulfide (a), and bis[[bis(2-methylpropyl)amino]selenoxomethyl] triselenide (b). All H atoms are omitted for clarity.	63
Figure 3.8. Thermal ellipsoid plots (50%) of $[\mathbf{1a}]^+$, $[\mathbf{1e}]^+$, $[\mathbf{2a}][\text{SeCN}]$, $[\mathbf{2e}]^+$, $[\mathbf{3a}]^+$, and $[\mathbf{3c}]^+$. For clarity, all H atoms are omitted, and any disorder is edited to show only one of two parts.	70
Figure 3.9. Thermal ellipsoid plots (50%) of $[\mathbf{3f}]^+$, 4 , 5 , and 6 . For clarity, all H atoms are omitted, and any disorder is edited to show only one of two parts.	71
Figure 3.10. Illustration of the distinction between equatorial and axial positions in bridging dichalcogenide ligands.	72
Figure 3.11. The whole CV window for $[\text{Mo}_3\text{S}_7(\text{S}_2\text{CN}^i\text{Bu}_2)_3]\text{I}$ in DCM.	75
Figure 3.12. Reductive CV data for $[\text{Mo}_3\text{S}_7(\text{S}_2\text{CN}^i\text{Bu}_2)_3]\text{I}$ in DCM.	75
Figure 3.13. Reduction peak potentials for $[\text{Mo}_3\text{S}_7(\text{S}_2\text{CN}^i\text{Bu}_2)_3]\text{I}$ by DPV.	76
Figure 3.14. The whole CV window for $[\text{Mo}_3\text{S}_7(\text{S}_2\text{CN}^i\text{Bu}_2)_3]\text{Cl}$ in DCM.	77
Figure 3.15. Reductive CV data for $[\text{Mo}_3\text{S}_7(\text{S}_2\text{CN}^i\text{Bu}_2)_3]\text{Cl}$ in DCM.	77
Figure 3.16. Reduction peak potentials for $[\text{Mo}_3\text{S}_7(\text{S}_2\text{CN}^i\text{Bu}_2)_3]\text{Cl}$ by DPV.	78
Figure 3.17. The whole CV window for $[\text{Mo}_3\text{S}_4\text{Se}_3(\text{S}_2\text{CN}^i\text{Bu}_2)_3]\text{SeCN}$ in DCM.	79
Figure 3.18. Reductive CV data for $[\text{Mo}_3\text{S}_4\text{Se}_3(\text{S}_2\text{CN}^i\text{Bu}_2)_3]\text{SeCN}$ in DCM.	79
Figure 3.19. Reduction peak potentials for $[\text{Mo}_3\text{S}_4\text{Se}_3(\text{S}_2\text{CN}^i\text{Bu}_2)_3]\text{SeCN}$ by DPV.	80
Figure 3.20. The whole CV window for $[\text{Mo}_3\text{Se}_7(\text{S}_2\text{CN}^i\text{Bu}_2)_3]\text{I}$ in DCM.	81
Figure 3.21. Reductive CV data for $[\text{Mo}_3\text{Se}_7(\text{S}_2\text{CN}^i\text{Bu}_2)_3]\text{I}$ in DCM.	81
Figure 3.22. Reduction peak potentials for $[\text{Mo}_3\text{Se}_7(\text{S}_2\text{CN}^i\text{Bu}_2)_3]\text{I}$ by DPV.	82
Figure 3.23. The whole CV window for $[\text{Mo}_3\text{Se}_7(\text{Se}_2\text{CN}^i\text{Bu}_2)_3]\text{I}$ in DCM.	83
Figure 3.24. Reductive CV data for $[\text{Mo}_3\text{Se}_7(\text{Se}_2\text{CN}^i\text{Bu}_2)_3]\text{I}$ in DCM.	83
Figure 3.25. Reduction peak potentials for $[\text{Mo}_3\text{Se}_7(\text{Se}_2\text{CN}^i\text{Bu}_2)_3]\text{I}$ by DPV.	84

Figure 3.26. The whole CV window for $[\text{Mo}_3\text{S}_7(\text{S}_2\text{P}^i\text{Bu}_2)_3]\text{I}$ in DCM	84
Figure 3.27. Reductive CV data for $[\text{Mo}_3\text{S}_7(\text{S}_2\text{P}^i\text{Bu}_2)_3]\text{I}$ in DCM.	85
Figure 3.28. Reduction peak potentials for $[\text{Mo}_3\text{S}_7(\text{S}_2\text{P}^i\text{Bu}_2)_3]\text{I}$ by DPV.....	85
Figure 3.29. The whole CV window for $[\text{Mo}_3\text{S}_4\text{Se}_3(\text{S}_2\text{P}^i\text{Bu}_2)_3]\text{I}$ in DCM.....	86
Figure 3.30. Reductive CV data for $[\text{Mo}_3\text{S}_4\text{Se}_3(\text{S}_2\text{P}^i\text{Bu}_2)_3]\text{I}$ in DCM.....	86
Figure 3.31. Reduction peak potentials for $[\text{Mo}_3\text{S}_4\text{Se}_3(\text{S}_2\text{P}^i\text{Bu}_2)_3]\text{I}$ by DPV.	87
Figure 3.32. The whole CV window for $[\text{Mo}_3\text{Se}_7(\text{S}_2\text{P}^i\text{Bu}_2)_3]\text{I}$ in DCM.	88
Figure 3.33. Reductive CV data for $[\text{Mo}_3\text{Se}_7(\text{S}_2\text{P}^i\text{Bu}_2)_3]\text{I}$ in DCM.	89
Figure 3.34. Reduction peak potentials for $[\text{Mo}_3\text{Se}_7(\text{S}_2\text{P}^i\text{Bu}_2)_3]\text{I}$ by DPV.....	89
Figure 3.35. The whole CV window for $[\text{Mo}_3\text{Se}_7(\text{S}_2\text{P}(\text{O}^i\text{Pr})_2)_3](\text{S}_2\text{P}(\text{O}^i\text{Pr})_2)$ in DCM....	90
Figure 3.36. Reductive CV data for $[\text{Mo}_3\text{Se}_7(\text{S}_2\text{P}(\text{O}^i\text{Pr})_2)_3](\text{S}_2\text{P}(\text{O}^i\text{Pr})_2)$ in DCM.....	91
Figure 3.37. Reduction peak potentials for $[\text{Mo}_3\text{Se}_7(\text{S}_2\text{P}(\text{O}^i\text{Pr})_2)_3](\text{S}_2\text{P}(\text{O}^i\text{Pr})_2)$ by DPV.	91
Figure 3.38. TON for the $[\text{NBu}_4]_2[\text{Mo}_3\text{S}_{13}]$ catalyst at various concentrations	95
Figure 3.39. TON for the $[\text{Mo}_3\text{S}_7(\text{S}_2\text{CNEt}_2)_3]^+$ catalyst at various concentrations.....	95
Figure 3.40. MALDI-MS experiment during photolysis of $[\text{Mo}_3\text{S}_7(\text{S}_2\text{CNEt}_2)_3]^+$	96
Figure 3.41. Hydrogen production at various concentrations of $[\text{Mo}_3\text{S}_7(\text{S}_2\text{CN}^i\text{Bu}_2)_3]^+$..	97
Figure 3.42. Turnover number during 3-hour photolysis of $[\text{Mo}_3\text{S}_7(\text{S}_2\text{CN}^i\text{Bu}_2)_3]^+\text{I}^-$	97
Figure 3.43. Micromoles of hydrogen during 3-hour photolysis of $[\text{Mo}_3\text{S}_7(\text{S}_2\text{CN}^i\text{Bu}_2)_3]^+\text{I}^-$	98
Figure 3.44. Turnover number during 3-hour photolysis of $[\text{Mo}_3\text{S}_4\text{Se}_3(\text{S}_2\text{CN}^i\text{Bu}_2)_3]\text{SeCN}$	100
Figure 3.45. Micromoles of hydrogen during 3-hour photolysis of $[\text{Mo}_3\text{S}_4\text{Se}_3(\text{S}_2\text{CN}^i\text{Bu}_2)_3]\text{SeCN}$	100
Figure 3.46. photolysis measurement comparing $[\text{Mo}_3\text{S}_7(\text{S}_2\text{CN}^i\text{Bu}_2)_3]\text{I}$, versus $[\text{Mo}_3\text{S}_4\text{Se}_3(\text{S}_2\text{CN}^i\text{Bu}_2)_3]\text{SeCN}$	101
Figure 3.47. Turnover number during 3-hour photolysis of $[\text{Mo}_3\text{Se}_7(\text{S}_2\text{CN}^i\text{Bu}_2)_3] + \text{I}$..	102
Figure 3.48. Micromoles of hydrogen during 3-hour photolysis of $[\text{Mo}_3\text{Se}_7(\text{S}_2\text{CN}^i\text{Bu}_2)_3] + \text{I}$	102
Figure 3.49. Photolysis measurement comparing $[\text{Mo}_3\text{S}_7(\text{S}_2\text{CN}^i\text{Bu}_2)_3]\text{I}$, versus $[\text{Mo}_3\text{Se}_7(\text{S}_2\text{CN}^i\text{Bu}_2)_3]\text{I}$	103
Figure 3.50. Turnover number during 3-hour photolysis of $[\text{Mo}_3\text{Se}_7(\text{Se}_2\text{CN}^i\text{Bu}_2)_3] + \text{I}$	104
Figure 3.51. Micromoles of hydrogen during 3-hour photolysis of $[\text{Mo}_3\text{Se}_7(\text{Se}_2\text{CN}^i\text{Bu}_2)_3] + \text{I}$	104

Figure 3.52. photolysis measurement comparing $[\text{Mo}_3\text{Se}_7(\text{S}_2\text{CN}^i\text{Bu}_2)_3]\text{I}$ versus $[\text{MoSe}_7(\text{Se}_2\text{CN}^i\text{Bu}_2)_3]\text{I}$.	105
Figure 3.53. Turnover number during 3-hour photolysis of $[\text{Mo}_3\text{S}_7(\text{S}_2\text{P}^i\text{Bu}_2)_3] + \text{I}$	106
Figure 3.54. Micromoles of hydrogen during 3-hour photolysis of $[\text{Mo}_3\text{S}_7(\text{S}_2\text{P}^i\text{Bu}_2)_3] + \text{I}$	106
Figure 3.55. photolysis measurement comparing $[\text{Mo}_3\text{S}_7(\text{S}_2\text{CN}^i\text{Bu}_2)_3] \text{I}$, versus $[\text{Mo}_3\text{S}_7(\text{S}_2\text{P}^i\text{Bu}_2)_3] \text{I}$.	107
Figure 3.56. Turnover number during 3-hour photolysis of $[\text{Mo}_3\text{S}_4\text{Se}_3(\text{S}_2\text{P}^i\text{Bu}_2)_3]^+\text{I}^-$.	108
Figure 3.57. Micromoles of hydrogen during 3-hour photolysis of $[\text{Mo}_3\text{S}_4\text{Se}_3(\text{S}_2\text{P}^i\text{Bu}_2)_3]^+\text{I}^-$.	108
Figure 3.58. Photolysis measurement comparing $[\text{Mo}_3\text{S}_7(\text{S}_2\text{P}^i\text{Bu}_2)_3]\text{I}$, versus $[\text{Mo}_3\text{S}_4\text{Se}_3(\text{S}_2\text{P}^i\text{Bu}_2)_3]\text{I}$.	109
Figure 3.59. Turnover number during 3-hour photolysis of $[\text{Mo}_3\text{Se}_7(\text{S}_2\text{P}^i\text{Bu}_2)_3]\text{I}$.	110
Figure 3.60. Micromoles of hydrogen during 3-hour photolysis of $[\text{Mo}_3\text{Se}_7(\text{S}_2\text{P}^i\text{Bu}_2)_3]\text{I}$.	111
Figure 3.61. photolysis measurement comparing $[\text{Mo}_3\text{S}_7(\text{S}_2\text{P}^i\text{Bu}_2)_3]\text{I}$, versus $[\text{Mo}_3\text{S}_4\text{Se}_3(\text{S}_2\text{P}^i\text{Bu}_2)_3] \text{I}$ and $[\text{Mo}_3\text{Se}_7(\text{S}_2\text{P}^i\text{Bu}_2)_3]\text{I}$.	111
Figure 3.62. Turnover number during 3-hour photolysis of $[\text{Mo}_3\text{Se}_7(\text{S}_2\text{P}^i\text{PrO})_2)_3] (\text{S}_2\text{P}^i\text{PrO})_2$.	112
Figure 3.63. Micromoles of hydrogen during 3-hour photolysis of $[\text{Mo}_3\text{Se}_7(\text{S}_2\text{P}^i\text{PrO})_2)_3] (\text{S}_2\text{P}^i\text{PrO})_2$.	113
Figure 3.64. Turnover number during 3-hour photolysis of $[\text{Mo}_3\text{S}_7(\text{S}_2\text{CN}^i\text{Bu}_2)_3] \text{Cl}$.	114
Figure 3.65. Micromoles of hydrogen during 3-hour photolysis of $[\text{Mo}_3\text{S}_7(\text{S}_2\text{CN}^i\text{Bu}_2)_3] \text{Cl}$.	114
Figure 3.66. photolysis measurement comparing $[\text{Mo}_3\text{S}_7(\text{S}_2\text{CN}^i\text{Bu}_2)_3] \text{I}$, versus $[\text{Mo}_3\text{S}_7(\text{S}_2\text{CN}^i\text{Bu}_2)_3] \text{Cl}$.	115
Figure 3.67. Comparison of all clusters.	115
Chapter 4	
Figure 4.1. (Left) A Re catalysts for CO_2 reduction immobilized onto a Cu_2O photocathode by a bipyridyl ligand functionalized with phosphate groups. Reproduced with permission from American Chemical Society. (Right) A proposed $[\text{Mo}_3\text{S}_7]^{4+}$ cluster functionalized with a phosphate-substituted dithiocarbamate ligand.	126
Figure 4.2. ^1H NMR spectrum in CDCl_3 of diethyl <i>P</i> -[[4-(bromomethyl)phenyl]methyl]phosphonate.	129
Figure 4.4. ^1H NMR spectrum of diethyl [[4-[(phenylmethyl)amino]methyl]phenyl]methyl] phosphonate, (c).	131

Figure 4.3. ESI mass spectrum of diethyl [[4- [[phenylmethyl)amino]methyl]phenyl]methyl] phosphonate, (c)	131
Figure 4.6. ESI mass spectrum of bis([benzyl-4-methyl]diethylphosphonate) benzylamine.	132
Figure 4.5. ³¹ P NMR spectrum of diethyl [[4- [[phenylmethyl)amino]methyl]phenyl]methyl] phosphonate, (c)	132
Figure 4.8. ³¹ P NMR spectrum of bis([benzyl-4-methyl]diethylphosphonate) benzylamine.	133
Figure 4.7. ¹ H NMR spectrum of bis([benzyl-4-methyl]diethylphosphonate) benzylamine.	133
Figure 4.9. ¹ H NMR spectrum of product from reaction targeting tetrathiuram disulfide (d).....	135

List of Schemes

Chapter 2

Scheme 2.1. Approaches to the synthesis of tetraalkylthiuram disulfides. 16

Chapter 3

Scheme 3.1. Photocatalytic system employed in these studies. Conditions: $[\text{Ru}(\text{bpy})_3]^{2+} = 260 \mu\text{M}$; $[\text{TMA}] = 50 \text{ mM}$; $[\text{TEA}] = 0.4 \text{ M}$; solvent = 1:2:1 THF:MeCN:H₂O, 4 mL total; headspace = 4.7 mL. 35

Scheme 3.2. Synthetic routes to $[\text{Mo}_3\text{Q}_7\text{L}_3]^+$ type cluster cations from $\text{Mo}(\text{CO})_6$. 49

Scheme 3.3. Synthetic routes to $[\text{Mo}_3\text{Q}_7\text{L}_3]^+$ type cluster cations from $\text{Mo}(\text{CO})_6$. 50

Scheme 3.4. Known synthetic routes to $[\text{Mo}_3\text{S}_7\text{L}_3]^+$ type cluster cations from $[\text{Mo}_3\text{S}_{13}]^{2-}$ or $[\text{Mo}_3\text{S}_7\text{Br}_6]^{2-}$ 50

Scheme 3.5. Known synthetic routes to $[\text{Mo}_3\text{S}_7\text{L}_3]^+$ type cluster cations. 51

Scheme 3.6. Synthetic routes to $[\text{Mo}_3\text{S}_7\text{L}_3]^+$ type cluster cations from $\text{Mo}(\text{CO})_6$ 55

Scheme 3.7. Synthetic routes to $[\text{Mo}_3\text{S}_4\text{Se}_3\text{L}_3]^+$ type cluster cations. 56

Scheme 3.8. Known synthetic routes to $[\text{Mo}_3\text{Se}_7\text{L}_3]^+$ type cluster cations. 58

Scheme 3.9. Synthetic routes to $[\text{Mo}_3\text{Se}_7\text{L}_3]^+$ type cluster cations from $\text{Mo}(\text{CO})_6$ 60

Scheme 3.10. New synthetic routes to $[\text{Mo}_3\text{S}_4\text{Se}_3\text{L}_3]^+$ type cluster cations. 61

Scheme 3.11. New synthetic routes to $[\text{Mo}_3\text{Se}_4\text{S}_3\text{L}_3]^+$ type cluster cations. 61

Scheme 3.12. Proposed solution equilibrium for $t\text{Bu}_2\text{NC}(\text{Se})\text{SeSeSeC}(\text{Se})\text{N}^i\text{Bu}_2$, as deduced by ^{77}Se NMR. 64

Scheme 3.13. Four component photosystem using reductive quenching. 93

Chapter 4

Scheme 4.1. A proposed synthesis of an asymmetric phosphate-substituted dithiocarbamate ligand for surface immobilization. 127

Scheme 4.2. Synthesis of diethyl *P*-[[4-(bromomethyl)phenyl]methyl]phosphonate, which is targeted as precursor to phosphate-substituted-dithiocarbamate. 128

Scheme 4.3. Synthesis of diethyl [[4-[(phenylmethyl)amino]methyl]phenyl]methyl] phosphonate, (**c**). 130

Scheme 4.4. Synthesis of tetrathiuram disulfide (**d**). 134

Scheme 4.5. Synthesis targeting tetrathiuram disulfide (**e**). 135

Scheme 4.6. Alternative synthetic route to Mo_3 cluster. 136

Chapter 1

H₂ Production: A Brief Overview

1.1 Introduction

Hydrogen is the simplest, most abundant, and versatile energy carrier on earth. Hydrogen in molecular form can be found as part of another substance, such as fossil fuels, water, or alcohol. Hydrogen can be obtained from natural resources such as plants and animals, which is biomass. Because of this reason, it is considered as an energy carrier, which can help tackle various critical energy challenges.

The hydrogen produced with diverse, domestic resources such as nuclear, natural gas and biomass, coal and renewable energy resources such as solar, wind, sea wave etc. To extract hydrogen from diversity of domestic energy sources makes hydrogen in an excess quantity with promising energy carrier and important for energy security. It is desirable that hydrogen be produced using renewable energy resources and production technologies would allow for its sustainable production. The production of hydrogen can be achieved via main hydrogen production technologies will be set according to the raw material used such as fossil fuels or renewable energy resources.

Hydrogen is the most abundant element and has maximum energy content per unit of weight. However, it is not available in free form in nature. Hydrogen can be produced in various ways from initial raw materials. Nowadays, hydrogen is mainly produced by thermochemical processes using fossil fuels such as steam reforming of natural gas, coal

gasification, hydrocarbon pyrolysis and plasma reforming, process which leads to significant amounts of emissions of greenhouse gases^{1,2}.

Clean hydrogen is considered to be an energy vector, not as an energy source, of the future. However, the large-scale production of clean hydrogen and its sustainability depend upon an ecofriendly hydrogen production pathway and a source of renewable energy used during the process. Hence, renewable energy will play an important role during the decarbonization of the current energy system.

1.2 Hydrogen Production Technologies

Table 1.1. Hydrogen Production Methods.

Technology	Feedstock	Operating Conditions	Efficiency	Maturity
Steam reforming	Light hydrocarbons	800-1000 °C	70-85%	Commercial
Partial oxidation	Heavy hydrocarbons	> 1000 °C	60-75%	Commercial
Autothermal reforming	Light hydrocarbons	> 1000 °C	60-75%	Early commercial
Plasma reforming	Hydrocarbons	> 2000 °C	9-75%	Long term
Coal Gasification	Coal	700-1200 °C		Commercial
Biomass Gasification	Biomass	800-900 °C	35-50%	Commercial
Electrolysis	Electricity	50-900 °C	35-50%	Commercial
Photolysis	Sunlight	Ambient conditions	0.5%	Long term
Thermochemical water splitting	Heat	> 2500 °C		Long term

1.2.1 Hydrogen Production from Fossil Fuel

1.2.1.1 Steam Reforming

Steam reforming is currently the most developed technique for hydrogen production. This method is one of the least expensive processes for hydrogen production.³ Close to 50% of the world's hydrogen is currently generated by this method.⁴ The steam reforming reaction process uses a mixture of steam and methane at high temperature between (700-1100 °C) (1292-2012 F) in the presence of a nickel catalyst. This reaction is highly endothermic, and it produces molecular hydrogen and carbon monoxide.⁵ The carbon monoxide then passes through the water-gas shift reaction to produce carbon dioxide and additional hydrogen.



1.2.1.2 Partial Oxidation

Partial oxidation of hydrocarbons is one of the hydrogen production techniques to obtain hydrogen from heavy fuel oil.⁶ Partial oxidation is an exothermic process used to combust fuel-air or fuel-oxygen mixture to produce hydrogen and carbon monoxide and other partially oxidized species.⁷ The partial oxidation reaction depends on a sub stoichiometric fuel-air mixture or a fuel-oxygen that is constrained by a high reaction temperature >1000 C in a reformer or partial oxidation reactor. The catalytic partial oxidation reactions are usually carried out with a heterogeneous catalyst at lower temperature. Overall, thermal partial oxidation (TPOX), and catalytic partial oxidation reactions (CPOX) could be described as follows.



1.2.1.3 Plasma reforming

In the case of plasma reforming, energy and free radicals used for the reforming reaction are provided by a plasma converter typically produced with heat and electricity.⁸⁻

¹¹ Two types of plasma reforming, thermal and non-thermal, are used.¹¹ Hydrogen can be efficiently produced in a plasma converter from hydrocarbon fuels.⁸⁻¹¹ The plasma converter has a number of advantages, namely low cost, high conversion efficiencies, fast response time, compactness and low weight. Here, the high temperature conditions accelerate the thermodynamically favored reaction without a catalyst. The dependence on electricity and maintaining a high-pressure are the only disadvantages of this method.⁹

1.2.1.4 Coal gasification

Production of hydrogen from coal is defined as coal gasification. In the coal gasification process, coal is converted into gaseous mixtures, including hydrogen and carbon monoxide.¹²⁻¹⁴ In this thermochemical conversion process, steam and oxygen or air helps to convert to synthesis gas from coal at high temperature and pressure.¹⁵⁻¹⁷ The main disadvantage of this method is higher carbon dioxide emissions than other methods.

1.2.2 Hydrogen Production from Renewable Resources

1.2.2.1 Hydrogen from Biomass

Biomass is a primary renewable source which is available from plants, animal wastes, forest residues, crops, municipal solid waste products, microalgae, or animal byproducts.¹⁸⁻

¹⁹ Here, the hydrogen produced from biomass and waste products is via gasification, steam reforming or biological conversion processes such as fermentative hydrogen production. Compared with other hydrogen production methods, processes using biomass are more ecologically friendly. Moreover, a wide range of wastes sources can be utilized to produce

hydrogen through biochemical pathways. In 2050, biomass is projected to meet more than 25% of energy demand.²⁰

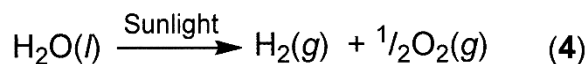
1.2.2.2 Hydrogen from Water

Although at present 95% of the global demand for hydrogen,²¹⁻²² is met with fossil fuels, renewable sources have attracted attention for the generation of “green” hydrogen.²⁰ Green hydrogen is produced without the use of fossil fuels by processes such as H₂O-splitting, which is the oxidative and reductive deconstruction of the water molecule into elemental hydrogen and oxygen. A source of energy for water splitting with a low carbon footprint can significantly reduce carbon dioxide emissions and limit global warming. Thus, such a process is referred to as “green” hydrogen generation. The conversion can be accomplished in many ways, such as electrolysis, thermolysis, photo-electrocatalysis, biophotolysis and photocatalytic water splitting. However, these methods are more expensive than hydrocarbon-based production methods.

1.3 Homogeneous Systems for H₂ Production

1.3.1 True H₂O-Splitting

True water splitting is the conversion of liquid water into gaseous hydrogen and oxygen.



The free energy change of this reaction is $\Delta G = 237.2$ kJ/mol or 2.46 eV/molecule. Here two electrons are involved, so $n = 2$ and the standard EMF = 1.23 eV/e. The photons in a solar energy system produce the energy to drive the reaction. This reaction can be driven thermally by heating water to 1500-2500 K.²³ However, the efficiency is below 2%.

1.3.2 Proton Reduction with Metal Catalysts

1.3.2.1 Photocatalytic Systems

An alternative method for electrolysis is multistep water splitting. In this system, an efficient photosensitizer is combined with one or more charge accumulation sites and one or more catalysts. Here in the system illustrated in **Figure 1.1**, light absorption drives a chromophore, $[\text{Ru}(\text{bipy})_3]^{2+}$, into an excited state, $[\text{Ru}^*(\text{bipy})_3]^{2+}$, which become quenched by a one-electron reduction from trimethylaniline (TMA). The reduced sensitizer is returned to its original state following electron transfer to the catalyst, and the oxidized TMA^+ is converted back to TMA by the sacrificial electron donor, triethylamine (TEA). The electrons received from $[\text{Ru}(\text{bipy})_3]^+$ are combined by the catalyst with protons from water to produce hydrogen gas. Lehn and co-workers have reported an early example of this method. They used $[\text{Ru}(\text{bpy})_3\text{Cl}_2]$, as sensitizer, triethanolamine as the sacrificial donor, and K_2PtCl_6 as catalyst.²⁴ Sasse and co-workers have produced a quantum efficiency of 93% for hydrogen evolution from 9-anthracenecarboxylate, EDTA and methyl viologen.²⁵

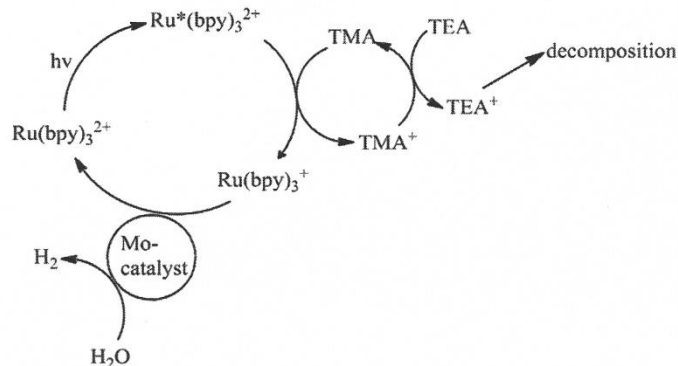


Figure 1.1. Homogeneous system for Mo-catalyst in water splitting. Reproduced with permission from American Chemical Society.

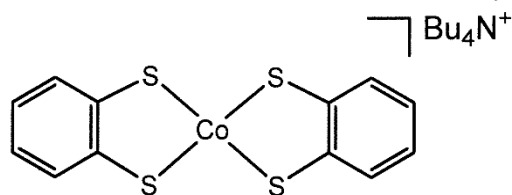


Figure 1.2. Structure of Cobalt dithiolene complex.

Another example of homogeneous catalytic H_2 evolution, reported in 2011 by McNamara *et al.*,²⁶ implements a cobalt bis(dithiolene) complex as catalyst as in both photocatalytic and electrocatalytic systems (**Figure 1.2**). This compound is a very active catalyst for hydrogen production from water in the presence of $[\text{Ru}(\text{bpy})_3]^{2+}$ as the photosensitizer and ascorbic acid as the sacrificial donor. This system was reported to produce over 2700 TON's hydrogen.

In general terms, a photolytically driven H₂-scheme features with a light absorbing molecule (chromophore) that transfers electrons to a catalyst that reduces protons.²⁷⁻²⁸ However, such homogeneous solution systems typically suffer short lifetimes because of decomposition of the chromophore over a period of time.²⁹ Semiconductor nanocrystals

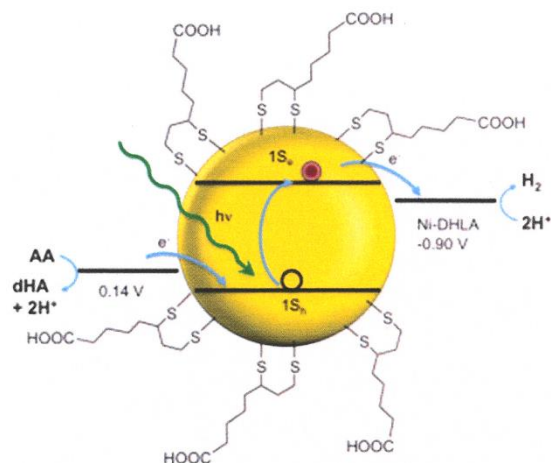


Figure 1.3 Cartoon that illustrates the relevant energies for H₂ production. dHA indicates dehydroascorbic acid. Potentials are shown versus that of NHE at pH = 4.5. Reproduced with permission from Science.

(NCs) are alternative chromophores for light-induced proton reduction.³⁰⁻³¹ Richard Eisenberg *et al.*³² reported that CdSe nanocrystals capped with dihydrolipoic acid (DHLA) as the light absorber, Ni²⁺-DHLA as catalyst for proton reduction, and ascorbic acid as an electron donor (**Figure 1.3**). This is one of the active system for solar hydrogen generation in water, producing over 600,000 TON's.

1.3.2.2 Electrocatalytic Systems

Cyclic diphosphine ligands with two amines serve as the basis for class of catalysts. These 1,5-diaza-3,7-diphosphacyclooctanes, referred to as P_2N_2 ligands, showed effects on the reactivity of many catalysts. The resulting $[Ni(P^{R_2}N^{R'_2})_2]^{2+}$ complexes have been shown to be remarkably effective in altering reaction pathways in catalysts and are excellent electrocatalyst for both production and oxidation of hydrogen.³³

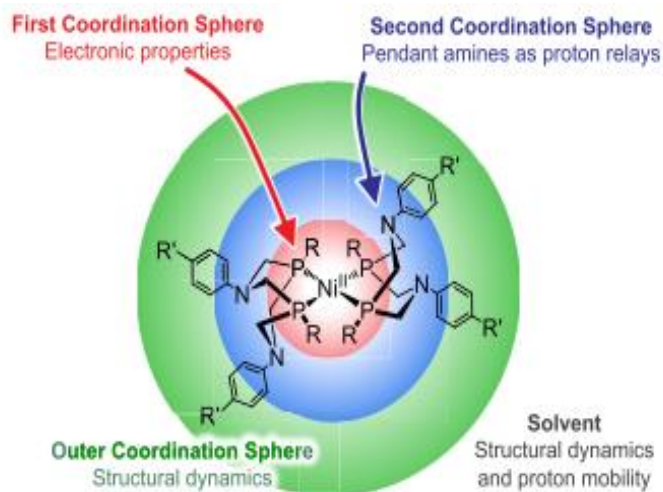


Figure 1.4 Catalyst design is organized around the first, second, and outer coordination spheres as well as the surrounding solvent, as exemplified by a $[Ni(P^{R_2}N^{R'_2})_2]^{2+}$ complex. Reproduced with permission from American Chemical Society.

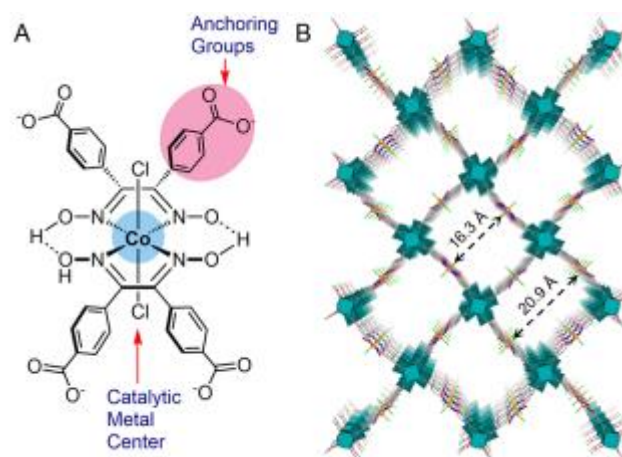


Figure 1.5. (A) Structure of the cobaloxime linker in UU-100(Co) and (B) structural model of UU-100(Co) MOF viewed along [001]. Reproduced with permission from the American Chemical Society.

Roy and co-workers³⁴ reported that structurally fragile molecular catalysts can be stabilized by incorporation into a metal-organic frameworks (MOF) so that they can be used as electrocatalysts for extended periods of time. Moreover, the structural integrity of the cobaloximes is greatly improved, as it produced at least 50-200 times higher TONs than those of any other related system that utilized similar cobaloxime.

1.4 Conclusions

Although significant effort and resources are being directed toward the development of hydrogen generation technologies, the most widely used technology is the reforming of hydrocarbons because production costs are correlated with fuel prices, which remain at acceptable levels. However, the main drawback of this method is the attending emission of a significant amount of greenhouse gases. To decrease carbon emissions, significant improvements in other hydrogen generation technologies from renewable sources such as water and biomass must be devised. Hydrogen can be generated from a wide range of renewable sources available almost everywhere. Development of hydrogen production

techniques that reduce the world's dependence on fossil fuels will also reduce environmental impact. Hydrogen can be produced from a wide variety of renewable feedstock, which may allow every region of the world able to produce its own energy. It is clear that, as future improvements in green hydrogen technologies are expected, hydrogen may prove to be the most widely available fuel.

1.5 References

- [1] M. Balat and M. Balat, "Political, economic and environmental impacts of biomass-based hydrogen," *International Journal of Hydrogen Energy*. **2009** vol. 34, no. 9, pp. 3589–3603.
- [2] A. Konieczny, K. Mondal, T. Wiltowski, and P. Dydo, "Catalyst development for thermocatalytic decomposition of methane to hydrogen," *International Journal of Hydrogen Energy*. **2008** vol. 33, no. 1, pp. 264–272.
- [3] J. M. Ogden, M. M. Steinbugler, and T. G. Kreutz, "Comparison of hydrogen, methanol and gasoline as fuels for fuel cell vehicles: implications for vehicle design and infrastructure development," *Journal of Power Sources*. **1999** vol. 79, no. 2, pp. 143–168.
- [4] N. Z. Muradov and T. N. Veziroglu, "From hydrocarbon to ~ hydrogen-carbon to hydrogen economy," *International Journal of Hydrogen Energy*. **2005** vol. 30, no. 3, pp. 225–237.

- [5] Press, Roman J.; Santhanam, K. S. V.; Miri, Massoud J.; Bailey, Alla V.; Takacs, Gerald A. (2008). Introduction to hydrogen Technology. *John Wiley & Sons*. p. 249. ISBN 978-0-471-77985-8.
- [6] Chen, H. L.; Lee, H. M.; Chen, S. H.; Chao, Y.; Chang, M. B. Review of Plasma Catalysis on Hydrocarbon Reforming for Hydrogen Production-Interaction, Integration, and Prospects. *Appl. Catal.*, B2008, 85 (1–2), 1–9.
- [7] Hariharan, D.; Yang, R.; Zhou, Y.; Gainey, B.; Mamalis, S.; Smith, R. E.; Lugo-Pimentel, M. A.; Castaldi, M. J.; Gill, R.; Davis, A.; Modroukas, D.; Lawler, B. Catalytic Partial Oxidation Reforming of Diesel, Gasoline, and Natural Gas for Use in Low Temperature Combustion Engines. *Fuel* **2019**, 246, 295–307.
- [8] L. Bromberg, D. R. Cohn, and A. Rabinovich, “Plasma reformer-fuel cell system for decentralized power applications,” *International Journal of Hydrogen Energy*. **1997** vol. 22, no. 1, pp. 83–94.
- [9] L. Bromberg, D. R. Cohn, A. Rabinovich, and N. Alexeev, “Plasma catalytic reforming of methane,” *International Journal of Hydrogen Energy*. **1999** vol. 24, no. 12, pp. 1131–1137.
- [10] T. Hammer, T. Kappes, and M. Baldauf, “Plasma catalytic hybrid processes: gas discharge initiation and plasma activation of catalytic processes,” *Catalysis Today*. **2004** vol. 89, no. 1-2, pp. 5–14.

- [11] T. Paulmier and L. Fulcheri, "Use of non-thermal plasma for hydrocarbon reforming," *Chemical Engineering Journal*. **2005** vol. 106, no. 1, pp. 59–71.
- [12] Stańczyk, K.; Kapusta, K.; Wiatowski, M.; Świądrowski, J.; Smoliński, A.; Rogut, J.; Kotyrba, A. Experimental Simulation of HardCoal Underground Gasification for Hydrogen Production. *Fuel* **2012**, 91 (1), 40–50.
- [13] Sutardi, T.; Wang, L.; Karimi, N.; Paul, M. C. Utilization of H₂O and CO₂ in Coal Particle Gasification with an Impact of Temperature and Particle Size. *Energy Fuels* **2020**, 34 (10), 12841–12852.
- [14] Emami Taba, L.; Irfan, M. F.; Wan Daud, W. A. M.; Chakrabarti, M. H. The Effect of Temperature on Various Parameters in Coal, Biomass and CO-Gasification: A Review. *Renewable Sustainable Energy Rev.* **2012**, 16 (8), 5584–5596.
- [15] Stiegel, G. J.; Ramezan, M. Hydrogen from Coal Gasification: An Economical Pathway to a Sustainable Energy Future. *Int. J. Coal Geol.* **2006**, 65 (3–4), 173–190.
- [16] Mularski, J.; Pawlak-Kruczek, H.; Modlinski, N. A Review of Recent Studies of the CFD Modelling of Coal Gasification in Entrained Flow Gasifiers, Covering Devolatilization, Gas-Phase Reactions, Surface Reactions, Models and Kinetics. *Fuel* **2020**, 271, 117620.
- [17] Dincer, I.; Acar, C. Review and Evaluation of Hydrogen Production Methods for Better Sustainability. *Int. J. Hydrogen Energy* **2015**, 40 (34), 11094–11111.

- [18] Ong, H. C.; Chen, W. H.; Farooq, A.; Gan, Y. Y.; Lee, K. T.; Ashokkumar, V. Catalytic Thermochemical Conversion of Biomass for Biofuel Production: A *Comprehensive Review*. *Renewable Sustainable Energy Rev.* **2019**, 113, 109266.
- [19] Gollakota, A. R. K.; Kishore, N.; Gu, S. A Review on Hydrothermal Liquefaction of Biomass. *Renewable Sustainable Energy Rev.* **2018**, 81, 1378–1392.
- [20] Hosseini, S. E.; Wahid, M. A. Hydrogen Production from Renewable and Sustainable Energy Resources: Promising Green Energy Carrier for Clean Development. *Renewable Sustainable Energy Rev.* **2016**, 57, 850–866.
- [21] Liu, Ke; Song, Chunshan; Subramani, Velu, eds. (2009). *Hydrogen and Syngas Production and Purification Technologies*. doi:10.1002/9780470561256. ISBN 9780470561256.
- [22] "Life cycle emissions of hydrogen". *4th generation energy*. Retrieved 2020-05-27.
- [23] Etievant, C. *Solar Energy Muter.* **1991**, 24, 413.
- [24] Lehn, J.-M.; Sauvage, J.-P. N O U L ~ . *J. Chim.* **1977**, 1, 449.
- [25] Johansen, O.; Mau, A. W. H.; Sass, W. H. F. *Chem. Phys. Lett.* **1983**, 94, 107, 113.
- [26] W. R. McNamara, Z. Han, P. J. Alperin, W. W. Brennessel, P. L. Holland and R. Eisenberg, *J. Am. Chem. Soc.*, **2011**, 133, 15368–15371.
- [27] Bard A. J., Fox M. A., Artificial photosynthesis: Solar splitting of water to hydrogen and oxygen. *Acc. Chem. Res.* **1995**, **28**, 141.

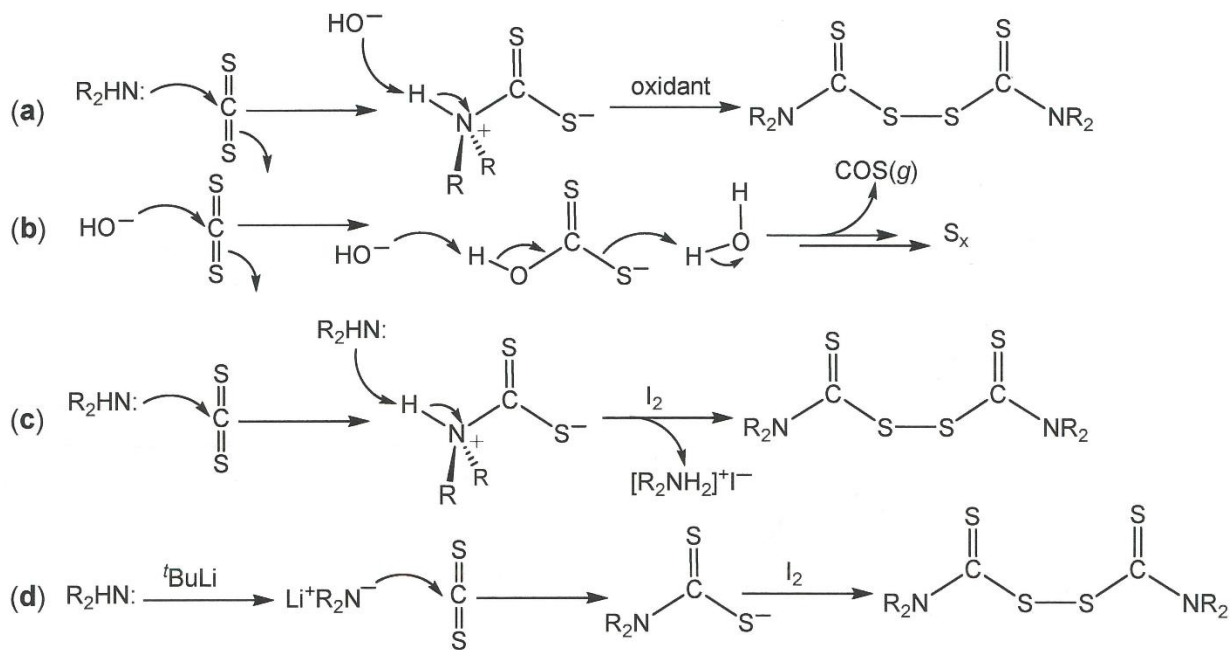
- [28] Esswein A. J., Nocera D. G., Hydrogen production by molecular photocatalysis. *Chem. Rev.* **2007**,**107**, 4022.
- [29] Eckenhoff W. T., Eisenberg R., Molecular systems for light driven hydrogen production. *Dalton Trans.* **2012**, **41**, 13004.
- [30] Amirav L., Alivisatos A. P., Photocatalytic hydrogen production with tunable nanorod heterostructures. *J. Phys. Chem. Lett.* **2010**, **1**, 1051.
- [31] Brown K. A., Dayal S., Ai X., Rumbles G., King P. W., Controlled assembly of hydrogenase-CdTe nanocrystal hybrids for solar hydrogen production. *J. Am. Chem. Soc.* **2010**,**132**, 9672.
- [32] Zhiji Han et al. Robust Photogeneration of H₂ in Water Using Semiconductor Nanocrystals and a Nickel Catalyst. *Science*. **2012**,**338**,1321-1324. DOI:[10.1126/science.1227775](https://doi.org/10.1126/science.1227775) .
- [33] Eric S. Wiedner, Aaron M. Appel, Simone Raugei, Wendy J. Shaw, and R. Morris Bullock *Chemical Reviews* **2022** *122* (14), 12427-12474 DOI: 10.1021/acs.chemrev.1c01001
- [34] Souvik Roy, Zhehao Huang, Asamanjoy Bhunia, Ashleigh Castner, Arvind K. Gupta, Xiaodong Zou, and Sascha Ott *Journal of the American Chemical Society* **2019** *141* (40), 15942-15950 DOI: 10.1021/jacs.9b07084.

Chapter 2

Probing the Limits of Tetraalkylthiuram Disulfide Synthesis by Direct Reaction of Secondary Amines with CS₂: The Structures of Cy₂NC(S)SSC(S)NCy₂ and Cy₂NC(S)SSSSC(S)NCy₂

2.1 Introduction

Tetraalkylthiuram disulfides comprise a class of organosulfur compounds of broad usefulness in both applied and synthetic chemistry. Tetraethylthiuram disulfide, for example, has long history of use as a treatment for alcohol use disorder^{1,2} but has more



Scheme 2.1. Approaches to the synthesis of tetraalkylthiuram disulfides.

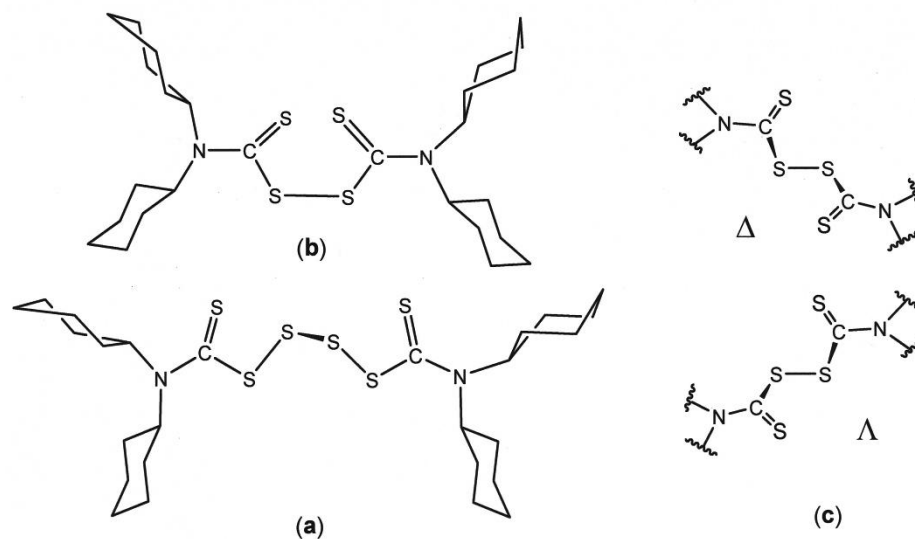


Figure 2.1 Structures of tetracyclohexylthiuram tetrasulfide (a), tetracyclohexylthiuram disulfide (b), and the chiral C₂-symmetric cores of a typical tetraalkylthiuram disulfide (c).

recently been repurposed for use as a potential anticancer therapeutic.³⁻⁵ and as a mitigant for the severe effects of advanced sepsis.⁶ (Klimiankou & Skokowa, 2021). Tetrathium disulfides have demonstrated utility for the synthesis of a wide range of dithiocarbamate coordination compounds, typically by oxidative addition to a suitable lower-valent precursor,⁷⁻¹⁰ and they serve as synthons toward such other useful compounds as thioureas,¹¹ dialkylthiocarbamoyl chlorides,¹² and organic dithiocarbamates.¹³ As such, optimal methods of synthesis of these compounds are of interest to for the further extension of their applications.

A commonly reported preparation of tetraalkylthiuram disulfides involve the reaction of the desired amine precursor, usually a secondary amine, with carbon disulfide in the presence of HO⁻ as a H⁺ scavenger (**Scheme 2.1**, path (a)) prior to oxidation coupling to the disulfide.¹⁴⁻¹⁵ We have observed this approach to be highly unsatisfactory because

hydroxide, both a smaller and more potent base than the amine, intercepts CS₂ to form dithiocarbonate, which then readily proceeds to extrude elemental sulfur (**Scheme 2.1**, path **(b)**). This sulfur further complicates the reaction mixture by enabling the facile formation of tetraalkylthiuram polysulfides, which differ little in visible or spectroscopic appearances from the intended disulfide. Consequently, an inseparable mixture is often the result.

In the course of a broadly ranging survey of the activity of [Mo₃S₇(S₂CNR₂)₃]^{+I} complexes as H₂-evolving catalysts,¹⁶ we contended with the problem illustrated in **Scheme 2.1 (b)** and, in the case of R = cyclohexyl (Cy), identified the tetrasulfide Cy₂NC(S)SSSSC(S)NCy₂ unequivocally by X-ray crystallography as one of the species occurring in the product mixture (**Figure 2.1 (a)**). Appreciable amounts of S₈, determined by its unit cell, were also present. A modified approach to R₂NC(S)SSC(S)NR₂ compounds involving the use of a second equivalent of the amine as H⁺ acceptor (**Scheme 2.1 (c)**) is effective with such alkyl substituents (R) as ^tBu.¹⁵ The R₂NH₂^{+I} salt generated after oxidative coupling with I₂ is readily separated from the R₂NC(S)SSC(S)NR₂ by an extraction that exploits their very different solubilities in nonpolar media. However, the method of **Scheme 2.1 (c)** is ineffective with Cy₂NH, possibly because clean reactivity with CS₂ is inhibited by its greater steric profile. Therefore, we resorted to deprotonation of Cy₂NH with ^tBuLi and subsequent introduction of the dicyclohexylamide anion to CS₂, followed by oxidative coupling (**Scheme 2.1 (d)**). In our hands, this procedure reliably produced Cy₂NC(S)SSC(S)NCy₂ in moderate yields of 74%. We note prior published syntheses of Cy₂NC(S)SSC(S)NCy₂ by the method of **Scheme 2.1 (a)**¹⁵ and by NaClO₂-mediated oxidative coupling of the corresponding dithiocarbamic acid.¹⁶ In the latter

report, a melting point of 88-89 °C is indicated for $\text{Cy}_2\text{NC}(\text{S})\text{SSC}(\text{S})\text{NCy}_2$, which is at variance with other literature data¹⁷ and our observation of a melting point of 169 °C.

In this account, we briefly relay the structures of both $\text{Cy}_2\text{NC}(\text{S})\text{SSC}(\text{S})\text{NCy}_2$ and $\text{Cy}_2\text{NC}(\text{S})\text{SSSSC}(\text{S})\text{NCy}_2$ the latter of which does not have a precedent for its type in the Cambridge Crystallographic Database. Crystal data and refinement statistics are presented in **Table 1**.

Two complete molecules occur in the asymmetric unit for the triclinic polymorph of $\text{Cy}_2\text{NC}(\text{S})\text{SSC}(\text{S})\text{NCy}_2$, both of which closely approximate C_2 symmetry around the central disulfide bond. The thione groups are disposed on the same side of the disulfide bond and define a 2-bladed propeller around the molecular C_2 . The molecule with S1-S4 bears a right-handed (clockwise) orientation to its thione groups, while the molecule with S5-S8 is left-handed. (*cf.* **Figure 2.2**, (a) and (b)) Consequently, the C13–S2–S3–C14 and C39–S6–S7–C40 torsion angles are similar in magnitude but opposite in sign at 88.52° and –87.72°, respectively. These values are within the range observed in the many other thiuram sulfides that have been crystallographically characterized.¹⁸ Slight disorder in the cyclohexyl groups of one molecule differentiates it from the other and likely contributes to the occurrence of $P-1$ as space group rather than a higher symmetry system.

The two molecules of $\text{Cy}_2\text{NC}(\text{S})\text{SSC}(\text{S})\text{NCy}_2$ that comprise the asymmetric unit of the triclinic polymorph are approximately planar in the ab plane, with the long axes of the two molecules meeting in a near orthogonal fashion. Replication of these two molecules in the ab plane (**Figure 3** (a)) produces a zig-zagged appearance to the arrangement. The sheets of molecules thus created stack along the c axis of the cell (**Figure 2.3** (b)) with the cyclohexyl groups protruding above and

Table 2.1. Crystal and Refinement Data for $\text{Cy}_2\text{NC}(\text{S})\text{SSC}(\text{S})\text{NCy}_2$ and $\text{Cy}_2\text{NC}(\text{S})\text{SSSSC}(\text{S})\text{NCy}_2$.

compound	$\text{Cy}_2\text{NC}(\text{S})\text{SSC}(\text{S})\text{NCy}_2$	$\text{Cy}_2\text{NC}(\text{S})\text{SSC}(\text{S})\text{NCy}_2$	$\text{Cy}_2\text{NC}(\text{S})\text{SSSSC}(\text{S})\text{NCy}_2$
structure code	JPD926	JPD1425	JPD864
formula	$\text{C}_{26}\text{H}_{44}\text{N}_2\text{S}_4$	$\text{C}_{26}\text{H}_{44}\text{N}_2\text{S}_4$	$\text{C}_{26}\text{H}_{44}\text{N}_2\text{S}_6$
FW	512.87	512.87	576.99
temperature, K	298	150	150
wavelength, Å	0.71073	1.54178	1.54178
2 θ range, deg.	3.334 – 51.450	9.06 – 144.56	6.528 – 144.506
crystal system	triclinic	monoclinic	monoclinic
space group	<i>P</i> -1	<i>P</i> 2 ₁ / <i>m</i>	<i>C</i> 2/ <i>c</i>
<i>a</i> , Å	12.8612(11)	10.3672(3)	28.1464(15)
<i>b</i> , Å	13.1642(11)	13.2293(3)	9.2015(5)
<i>c</i> , Å	18.3871(16)	10.6033(2)	12.0265(6)
α , deg.	109.965(1)	90	90
β , deg.	97.922(1)	109.518(1)	105.848(2)
γ , deg.	90.446(1)	90	90
volume, Å ³	2893.0(4)	1370.68(6)	2996.3(3)
<i>Z</i>	4	2	4
density, g/cm ³	1.178	1.243	1.279
μ , mm ⁻¹	0.345	3.296	4.343
F(000)	1112	556	1240
crystal size	0.083 x 0.357 x 0.397	0.093 x 0.103 x 0.290	0.026 x 0.143 x 0.183
color, habit	amber plate	pale yellow block	colorless plate
limiting indices, <i>h</i>	$-15 \leq h \leq 15$	$-11 \leq h \leq 12$	$-13 \leq h \leq 34$
limiting indices, <i>k</i>	$-16 \leq k \leq 15$	$-16 \leq k \leq 16$	$0 \leq k \leq 10$
limiting indices, <i>l</i>	$-22 \leq l \leq 22$	$-13 \leq l \leq 13$	$-14 \leq l \leq 14$
reflections collected	22600	27733	17752
independent data	10898	2745	2731
restraints	12	483	0
parameters refined	557	282	242
Goof ^a	0.965	1,097	1.043
R1, ^{b,c} wR2 ^{d,e}	0.0536, 0.0680	0.0347, 0.0946	0.0575, 0.1398
R1, ^{b,e} wR2 ^{d,e}	0.1276, 0.0716	0.0356, 0.0954	0.0767, 0.1489
largest diff. peak, e·Å ⁻³	0.339	0.217	0.395
largest diff. hole, e·Å ⁻³	-0.331	-0.189	-0.515

^aGoof = $\{\sum[w(F_o^2 - F_c^2)]/(n - p)\}^{1/2}$, where *n* = number of reflections and *p* is the total number of parameters refined; ^bR1 = $\sum||F_o| - |F_c||/\sum|F_o|$; ^cR indices for data cut off at $I > 2\sigma(I)$; ^dwR2 = $\{\sum[w(F_o^2 - F_c^2)^2]/\sum w(F_o^2)^2\}^{1/2}$; $w = 1/[\sigma^2(F_o^2) + (xP)^2 + yP]$, where $P = (F_o^2 + 2F_c^2)/3$; ^eR indices for all data.

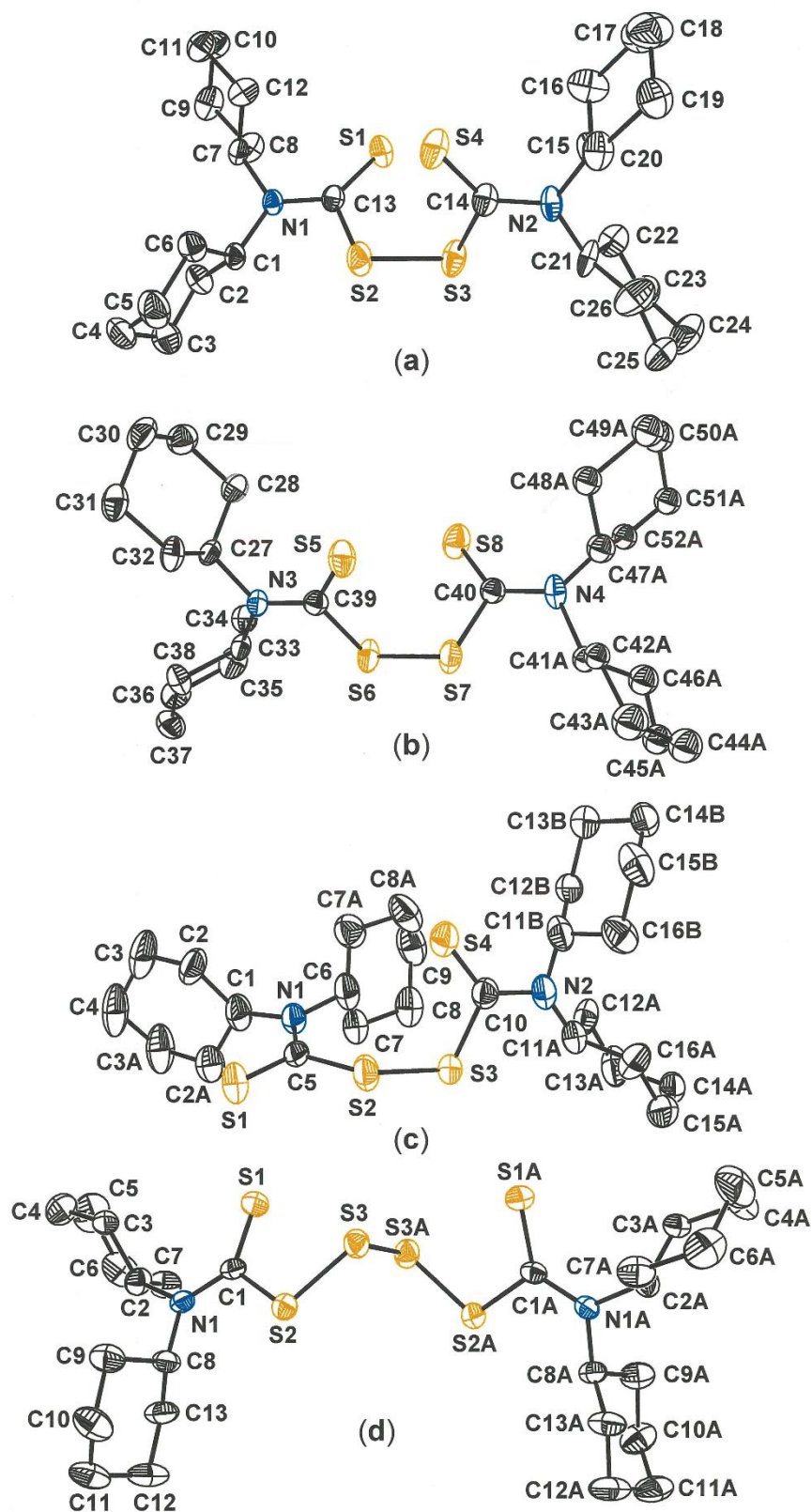


Figure 2.2. Molecules 1 (a) and 2 (b) of $\text{Cy}_2\text{NC}(\text{S})\text{SSC}(\text{S})\text{NCy}_2$ in triclinic polymorph. Ellipsoids are drawn at the 30% level. Image (c) shows the monoclinic polymorph of $\text{Cy}_2\text{NC}(\text{S})\text{SSC}(\text{S})\text{NCy}_2$ with 50% ellipsoids. Tetrasulfide $\text{Cy}_2\text{NC}(\text{S})\text{SSSSC}(\text{S})\text{NCy}_2$ is presented in (d), also with 50% ellipsoids. For clarity, all H atoms are omitted, and disorder in the Cy groups in (b) and (c) is not shown.

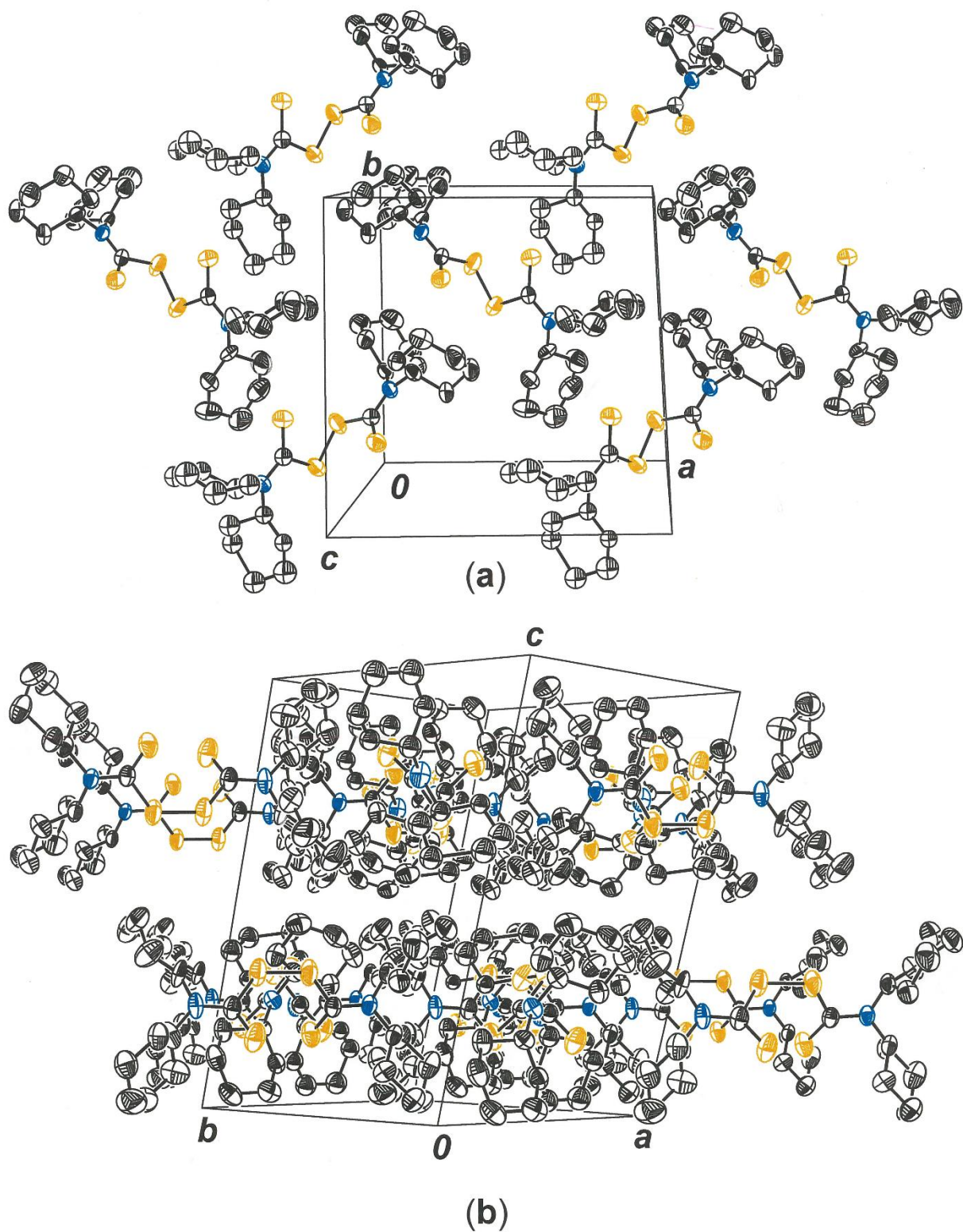


Figure 2.3. (a) Arrangement of $\text{Cy}_2\text{NC}(\text{S})\text{SSC}(\text{S})\text{NCy}_2$ molecules (triclinic polymorph) into sheets in the ab plane. (b) Stacking of sheets of $\text{Cy}_2\text{NC}(\text{S})\text{SSC}(\text{S})\text{NCy}_2$ molecules (triclinic polymorph) along the c axis.

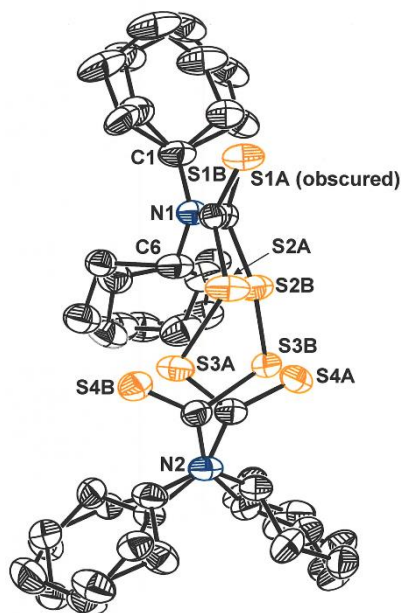


Figure 2.4. Symmetry-imposed disorder in the monoclinic form of $\text{Cy}_2\text{NC}(\text{S})\text{SSC}(\text{S})\text{NCy}_2$. A mirror plane coincides with C1, N1, C6 and N2 and generates a symmetry equivalent for all atoms that are off-plane. In addition to the symmetry-imposed disorder, the cyclohexyl groups have a static conformational disorder over two positions.

below such that intersheet contacts, and perhaps the packing pattern as whole, appear to be guided by hydrocarbon-hydrocarbon dispersion interactions.

The monoclinic polymorph of $\text{Cy}_2\text{NC}(\text{S})\text{SSC}(\text{S})\text{NCy}_2$ places the molecule on a mirror plane in $P2_1/m$, although it is not a symmetry element that is possessed by the molecule. This mirror plane is coincident with the plane defined by C1, N1, and C6 on one side and cleaves each of its two pendant cyclohexyl groups (**Figure 2.2 (c)**, **Figure 2.4**). However, these cyclohexyl groups are not quite symmetrically bisected such that the mirror plane also passes through C4 and C9, the carbon atoms in the 4-position of the ring. These rings thus have the appearance of being slightly pivoted off the mirror plane and are consequently disordered (**Figure 2.4**). Except for N2, which also coincides with the mirror plane, the remainder of the molecule's backbone (S1-C5-S2-S3-C10-S4) is off-plane to

varying degrees and necessarily subject to a symmetry-imposed disorder over two positions (**Figure 2.4**). One of the two cyclohexyl groups appended to N2 is unique, the other being generated by the reflection operation. However, this unique cyclohexyl group itself suffers from a static, highly overlapping conformational disorder over two positions, the second of which is shown in **Figure 2.4** but not in **Figure 2.2 (c)**. The disorder afflicting this unique Cy group was modeled as a 48.5:51.5 best fit distribution. Although it is not unusual for a molecule to crystallize on a symmetry element that it, as a free molecule does not possess, it is noteworthy that this monoclinic polymorph of $\text{Cy}_2\text{NC}(\text{S})\text{SSC}(\text{S})\text{NCy}_2$, is the only example, among the many structural characterizations that have been reported for the molecule type, to crystallize in such fashion. All prior instances reveal the molecule to either be on a general position or on a C_2 axis or inversion center that is coincident with the midpoint of the disulfide bond.¹⁹

In contrast to $\text{Cy}_2\text{NC}(\text{S})\text{SSC}(\text{S})\text{NCy}_2$, tetrasulfide $\text{Cy}_2\text{NC}(\text{S})\text{SSSSC}(\text{S})\text{NCy}_2$ coincides with a crystallographic C_2 axis in monoclinic $C2/c$ such that only half of one molecule is unique (**Figure 2.2 (d)**). The C1-S2-S3-S3A and S2-S3-S3A-S2A torsion angles within the molecule's core are -75.84° and -92.67° , respectively. A right-handed aspect is displayed by the thione groups around the C_2 axis, which bisects the central S3-S3A single bond. The packing arrangement for $\text{Cy}_2\text{NC}(\text{S})\text{SSSSC}(\text{S})\text{NCy}_2$ is such that molecules stack in well-ordered columns along the b axis of the cell, with the columns being replicated by simple unit translations in the a and c axis directions (**Figure 2.5**). The long axis of the molecule aligns approximately with the ab face diagonal. When the molecular packing is considered from a vantage that is orthogonal to the b axis, rather than down the b axis as

in **Figure 2.5**, it is clear that intermolecular contacts, and the pattern as a whole, are again decisively influenced by dispersion interactions between cyclohexyl groups.

Many tetraalkylthiuram disulfide molecules have been characterized structurally, but dithiocarbamoyl or diselenocarbamoyl groups with more than a two chalcogen connector

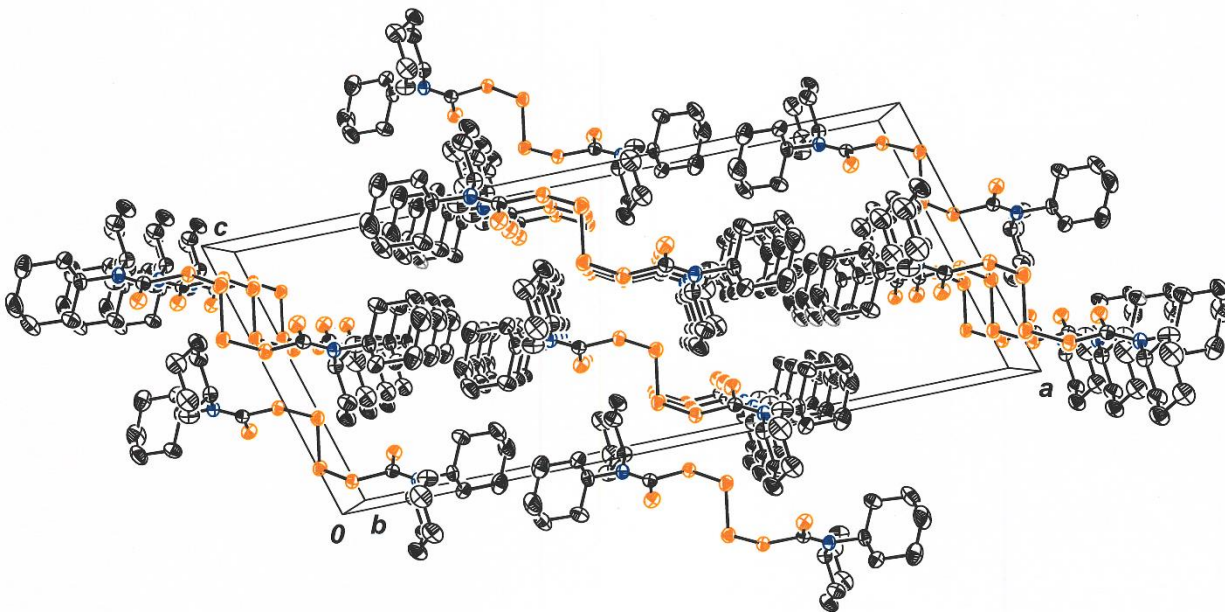


Figure 2.5. Packing arrangement for $\text{Cy}_2\text{NC}(\text{S})\text{SSSSC}(\text{S})\text{NCy}_2$ viewed along the b axis of the unit cell. All H atoms are omitted for clarity. The thermal ellipsoids are presented at the 50% level.

find scant occurrence in the structural database. The only such molecules with polysulfide linkages are $(\text{O}(\text{CH}_2\text{CH}_2)_2\text{N})\text{C}(\text{S})\text{SSSSC}(\text{S})(\text{N}(\text{CH}_2\text{CH}_2)_2\text{O})$, or bis(4-morpholine)dithiocarbamoyl monosulfide²⁰ and $(\text{C}_5\text{H}_{10})\text{NC}(\text{S})\text{S}_6\text{C}(\text{S})\text{N}(\text{C}_5\text{H}_{10})$, bis(piperidinyl)dithiocarbamoyl tetrasulfide.²¹ Among the selenium analogues, only bis(diethyldiselenocarbamoyl) triselenide, $\text{Et}_2\text{NC}(\text{Se})\text{SeSeSeC}(\text{Se})\text{NEt}_2$, has been subject to X-ray crystallographic characterization.^{22,23}

2.2 Summary and Concluding Remarks

The synthesis of tetracyclohexylthiuram disulfide via reaction of Cy_2NH with CS_2 in the presence of NaOH suffers from competing formation of S_8 and $\text{Cy}_2\text{NC}(\text{S})\text{SSSSC}(\text{S})\text{NCy}_2$, the identities of which were established by X-ray crystallography. Tetrasulfide $\text{Cy}_2\text{NC}(\text{S})\text{SSSSC}(\text{S})\text{NCy}_2$ is the first such molecule to be structurally characterized. The Cy_2N^- anion, generated from the amine with $t\text{BuLi}$, cleanly reacts with CS_2 and is oxidatively coupled to $\text{Cy}_2\text{NC}(\text{S})\text{SSC}(\text{S})\text{NCy}_2$. Triclinic and monoclinic polymorphs of $\text{Cy}_2\text{NC}(\text{S})\text{SSC}(\text{S})\text{NCy}_2$, grown by evaporation from Et_2O and acetone, respectively, are reported. The latter is disordered across a mirror plane in space group $P2_1/m$. A conclusion arising from this work is that secondary amines with branched alkyl groups are most effectively transformed to the tetraalkylthiuram disulfides by deprotonation with an alkylolithium agent prior to introduction of CS_2 and then oxidation. In continuing work, we are developing the synthesis of dithiocarbamate ligands with water-solubilizing functional groups such as diethyl phosphonate, $\text{OP}(\text{OEt})_2$.

2.3 Experimental

$\text{Cy}_2\text{NC}(\text{S})\text{SSC}(\text{S})\text{NCy}_2$. Under a N_2 atmosphere, a solution of *tert*-butyllithium in *n*-pentane (1.6 M, 25 mL, 2.56 g, 40 mmol) was added dropwise to 200 mL of THF solution of dicyclohexylamine (7.253 g, 40 mmol) held at -20° . Carbon disulfide (3.045 g, 40 mmol) was added via syringe, which induced a change in color from light yellow to red, and stirring was continued for 2 h. The solution was warmed to 50°C in an oil bath. Solid I_2 (5.076 g, 20 mmol) was then added as a single portion under an outward flow of N_2 , and stirring was continued overnight at 50°C . The solvent was removed under reduced pressure

to afford a pasty yellowish solid residue. This crude solid was extracted with EtOAc (3 x 100 mL), and the combined extracts were filtered to remove insoluble, finely-divided solids. The filtrate was taken to dryness under vacuum. Recrystallization of a portion of this solid by evaporation from a carefully filtered Et₂O solution produced Cy₂NC(S)SSC(S)NCy₂ in microcrystalline form, while evaporation of an acetone solution produced its monoclinic polymorph as pale-yellow blocks. Yield: 3.321 g, 6.475 mmol, 74%. MP: 169 °C. ¹H NMR (δ ppm in CDCl₃): 3.03 (m, 4 H, -NCH of cyclohexyl ring), 1.99 (br, -CH₂- of cyclohexyl group, 8 H), 1.86 (m, -CH₂- of cyclohexyl group, 8 H), 1.67 (m, -CH₂- of cyclohexyl group, 8 H), 1.38 (m, -CH₂- of cyclohexyl group, 8 H), 1.23-1.14 (m, -CH₂- of cyclohexyl group, 8 H). ¹³C NMR (δ ppm in CDCl₃): 206.94, 65.86, 30.95, 26.36, 15.29.

A modest number of colorless plate crystals of Cy₂NC(S)SSSSC(S)NCy₂, commingled with elemental sulfur, were obtained by evaporation of an EtOAc solution of the crude solid obtained following a literature procedure that invoked the use of Cy₂NH in reaction with CS₂/NaOH/EtOAc followed by oxidation with NaNO₂.¹⁵ Because Cy₂NC(S)SSSSC(S)NCy₂ was not easily distinguished from the other substances in the mixture by visual appearance, it could not be characterized more thoroughly. Slow evaporation of an Et₂O solution of this same crude product mixture yielded small amounts of the triclinic polymorph of Cy₂NC(S)SSC(S)NCy₂ as amber-hued plates. CCDC 2325220- 2325222 contain the supplementary crystallographic data for this structures.

2.4 References

- [1] Leggio, L.; Falk, D. E.; Ryan, M. L.; Fertig, J.; Litten, R. Z. Medication Development for Alcohol Use Disorder: A Focus on Clinical Studies. *Handbook of Experimental Pharmacology* **2020**, *258*, 443-462.
- [2] Brewer, C.; Streeb, E.; Skinner, M. Supervised Disulfiram's Superior Effectiveness in Alcoholism Treatment: Ethical, Methodological, and Psychological Aspects. *Alcohol and Alcoholism* **2017**, *52*(2), 213-219.
- [3] Lu, C.; Li, X.; Ren, Y.; Zhang, X. Disulfiram: A Novel Repurposed Drug for Cancer Therapy. *Cancer Chemotherapy and Pharmacology* **2021**, *87*, 159-172.
- [4] Lu, Y.; Pan, Q.; Gao, W.; Pu, Y.; Luo, K.; He, B.; Gu, Z. Leveraging Disulfiram to Treat Cancer: Mechanisms of Action, Delivery Strategies, and Treatment Regimens. *Biomaterials* **2022**, *281*, 121335.
- [5] Ekinci, E.; Rohondia, S.; Khan, R.; Dou, Q. P. Repurposing Disulfiram as an Anti-Cancer Agent: An Updated Review on Literature and Patents. *Recent Patents on Anti-Cancer Drug Discovery* **2019**, *14*(2), 113-132.
- [6] Klimiankou, M.; Skokowa, J. Old Drug Revisited: Disulfiram, NETs, and Sepsis. *Blood* **2021**, *138*(25), 2604-2605.
- [7] Naumann, D.; Roy, T.; Caeners, B.; Hütten, D.; Tebbe, K.-F.; Gilles, T. Syntheses and Properties of Pentafluoroethylcopper(I) and -copper(III) Compounds: CuC_2F_5 -D,

$[\text{Cu}(\text{C}_2\text{F}_5)_2]^-$, and $(\text{C}_2\text{F}_5)_2\text{CuSC}(\text{S})\text{N}(\text{C}_2\text{H}_5)_2$. *Zeit. Anorg. Allg. Chem.* **2000**, 626, 999-1003.

[8] Evans, W. J.; Montalvo, E.; Dixon, D. J.; Ziller, J. W.; Rheingold, A. L. Lanthanide Metallocene Complexes of the 1,3,4,6,7,8-Hexahydro-2*H*-pyrimido[1,2-*a*]pyrimidinato Ligand, (hpp)¹⁻. *Inorg. Chem.* **2008**, 47, 11376-11381.

[9] Karim, M. M.; Abser, M. N.; Hassan, M. R.; Ghosh, N.; Alt, H. G.; Richards, I.; Hogarth, G. Oxidative-Addition of Thiuram Disulfides to Osmium(0): Synthesis of *cis*- $[\text{Os}(\text{CO})_2(\text{S}_2\text{CNR}_2)_2]$ (R = Me, Et, Cy, CH₂CH₂OMe) and Molecular Structures of *cis*- $[\text{Os}(\text{CO})_2(\text{S}_2\text{CNMe}_2)_2]$ and $[(\text{MeOCH}_2\text{CH}_2)_2\text{NCS}]_2$. *Polyhedron* **2012**, 42, 84-88.

[10] Serpe, A.; Marchiò, L.; Artizzu, F.; Mercuri, M. L.; Deplano, P. Effective One-Step Gold Dissolution Using Environmentally Friendly Low-Cost Reagents. *Chem. Eur. J.* **2013**, 19, 10111-10114.

[11] Boi, L. V. Thiocarbamoylation of Amine-Containing Compounds 5.* The Mechanism of Reactions of Tetramethylthiuram Disulfide with Aliphatic Amines. *Russ. Chem. Bull.* **2000**, 49, 335-343.

[12] Adeppa, K., Rupainwar, D. C., Misra, K. Development of an Improved Method for Conversion of Thiuram Disulfides into *N,N*Dialkylcarbamoyl Halides and Derivatives. *Synth. Commun.* **2011**, 41, 285-290.

- [13] Peng, H.-Y., Dong, Z.-B. Transition-Metal-Free C(sp³)-S Coupling in Water: Synthesis of Benzyl Dithiocarbamates Using Thiuram Disulfides as an Organosulfur Source. *Eur. J. Org. Chem.* **2019**, 949-956.
- [14] Kapanda, C. N.; Muccioli, G. G.; Labar, G.; Poupaert, J. H.; Lambert, D, M. Bis(dialkylaminethiocarbonyl)disulfides as Potent and Selective Monoglyceride Lipase Inhibitors. *J. Med. Chem.* **2009**, *52*, 7310-7314.
- [15] Lal, N.; Jangir, S.; Bala, V.; Mandalapu, D.; Sarswat, A.; Kumar, L.; Jain, A.; Kumar, L.; Kushwaha, B.; Pandey, A. K.; Krishna, S.; Rawat, T.; Shukla, P. K.; Maikhuri, J. P.; Siddiqi, M. I.; Gupta, G.; Sharma, V. L. Role of Disulfide Linkage in Action of Bis(dialkylaminethiocarbonyl)disulfides as Potent Double-Edged Microbicidal Spermicide: Design, Synthesis and Biology. *Eur. J. Med. Chem.* **2016**, *115*, 275-290.
- [16] Ramadas, K.; Srinivasan, N. Sodium Chlorite – Yet Another Oxidant for Thiols to Disulphides. *Synth. Commun.* **1995**, *25*(2), 227-234.
- [17] Kaul, B. B.; Pandeya, K. B. Some Copper(III) Dithiocarbamates. *J. Inorg. Nucl. Chem.* **1981**, *43*, 1942-1944.
- [18] Fontenot, P. R.; Shan, B.; Wang, B.; Simpson, S.; Ragunathan, G.; Greene, A. F.; Obanda, A.; Hunt, L. A.; Hammer, N. I.; Webster, C. E.; Mague, J. T.; Schmehl, R. H.; Donahue, J. P. Photocatalytic H₂-Evolution by Homogeneous Molybdenum Clusters Supported by Dithiocarbamate Ligands. *Inorg. Chem.* **2019**, *58*, 16458-16474.

- [19] Fontenot, P.; Wang, B.; Chen, Y.; Donahue, J. P. Crystal Structure of Tetraisobutylthiuram Disulfide. *Acta Crystallogr., Sect. E* **2017**, *73*, 1764-1769.
- [20] Husebye, S. The Crystal Structure of Bis(4-morpholinthiocarbonyl) Trisulfide. *Acta Chem. Scand.* **1973**, *27*, 756-762.
- [21] Foss, O.; Maartmann-Moe, K. Crystal Structure and Rotameric Form of Bis(piperidinothiocarbonyl)hexasulfane. *Acta. Chem. Scand. A* **1986**, *40*, 664-668.
- [22] Bao, M.; Hong, M.; Su, W.; Cao, R. Bis(*N,N*-diethyl-1,1-diselenocarbamato-*Se*)selenium, [Se₂CNEt₂)₂Se]. *Acta Crystallogr., Sect. C* **2000**, *56*, e219-e220.
- [23] Klapötke, T. M.; Krumm, B.; Scherr, M. Studies on the Properties of Organoselenium(IV) Fluorides and Azides. *Inorg. Chem.* **2008**, *47*, 4712-4722.

Chapter 3

Tri molybdenum Triangular $[\text{Mo}_3(\mu_3\text{-E})(\mu_2\text{-EF})_3(\text{Q}_2\text{LR}_2)_3]^+$ (E = S; F = S, or Se; L = CN or P; Q = S, or Se) Clusters: Synthesis, Crystallographic, Electro- Physical and Photocatalytic H_2 Evolution Properties

3.1 Introduction

The present and future demand for energy is an important topic of discussion worldwide, not only because human population continues to grow but also because improved standards of living correlate to higher per capita energy consumption. The long-term energy supply to meet this demand remains uncertain.^{1,2} Further, fossil fuel combustion adds CO_2 to the atmosphere at a rate that is contributing to increases in average global temperatures.^{3,4} In turn, global warming threatens to increase sea levels by melting the polar ice caps, which would immerse low-lying coastal cities. Fossil fuel combustion also diminishes air quality by releasing nitrogen oxides (NO_x) that lead to smog and other breathing irritants. These environmental impacts of fossil fuel use, in conjunction with their nonrenewable nature, bring the issue of developing alternative energy sources to the forefront in world political discussion.⁵

Solar energy is a clean and renewable alternative to fossil fuels. The primary disadvantage of solar energy is its intermittent nature, which demands that energy that cannot be immediately consumed as electricity be stored. A practical form of energy storage is via

chemical bonds, and the simplest, energy-rich bond that can meet this use is the H–H bond in H₂.⁶⁻¹² Hydrogen gas is essential to other important industrial processes, such as hydrodesulfurization¹³ and ammonia production¹⁴ but is currently produced via steam reforming of CH₄ gas. Hence, photolytic and/or photo electrocatalytic water splitting to form H₂ is an attractive way to both to store solar energy and to meet industrial demand for H₂ without contributing to CO₂ emissions.

3.1.1 MoS₂ derivatives in H₂ production

Molybdenum disulfide, MoS₂, is one of the few H₂-evolving catalytic materials that is inexpensive enough to perhaps be scalable for commercial H₂ production. However, polymeric, or particulate MoS₂, while highly active at its surface and edge sites, is poorly active as a bulk material. Recent research studies on MoS₂ have aimed at making various types of MoS₂ to increase the surface area and reactive sites and depositing MoS₂ nanoparticles onto highly conducting supports to improve the kinetics of electron

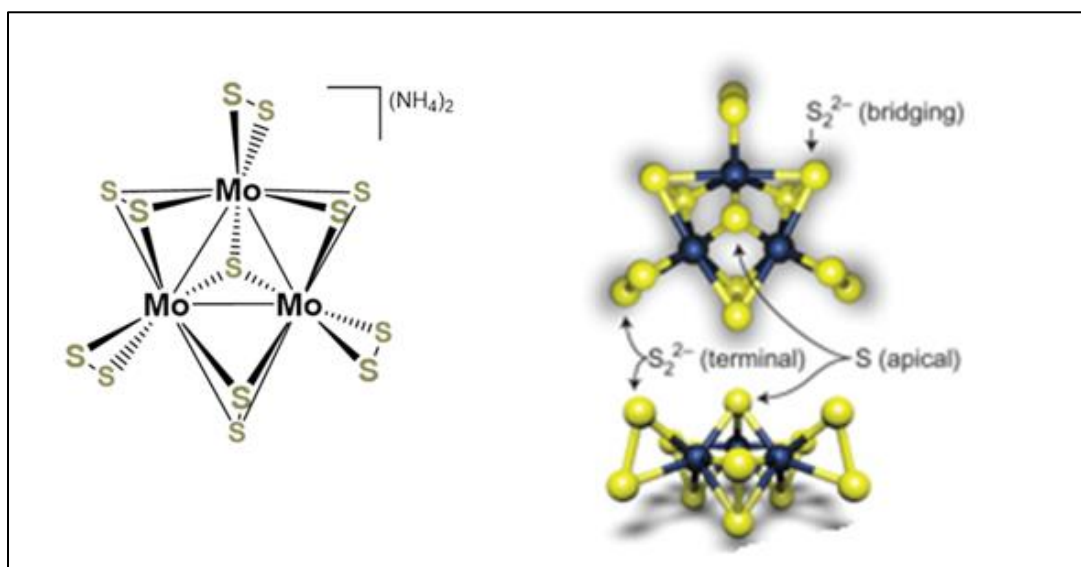


Figure 3.1. $(\text{NH}_4)_2(\text{Mo}_3\text{S}_{13})$ structures. Reproduced with permission from *Nature Chemistry*.

transfer¹⁵. Moreover, MoS₂ has also been studied in photo electrocatalytic water splitting, both as a reduction catalyst and as a photo electrode/catalytic surface¹⁶.

3.1.2 MoSe₂ derivatives in H₂ production

2D layered transitional metal dichalcogenides, MoSe₂ have superior features for attractive catalytic activity through hydrogen evolution reactions. Ni₃Se₄@MoSe₂¹⁷ composites act as an active electro catalyst in hydrogen evolution reactions. MoSe₂@graphene¹⁸ electrocatalyst functionalization having long term electrochemical stability during hydrogen evolution reaction due to that it showed significantly enhance hydrogen evolution reaction activity. Moreover MoSe₂-MoS₂¹⁹ layered heterostructures act as an active electrocatalyst for superior hydrogen evolution reactions.

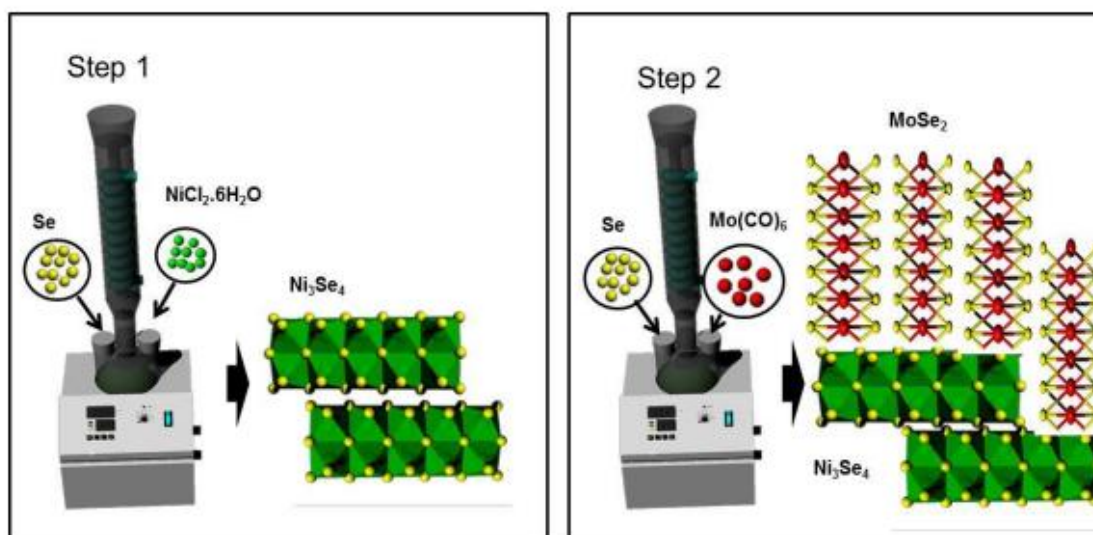


Figure 3.2. Synthesis for Ni₃Se₄@MoSe₂ nanostructures. Reproduced with permission from Applied Sciences.

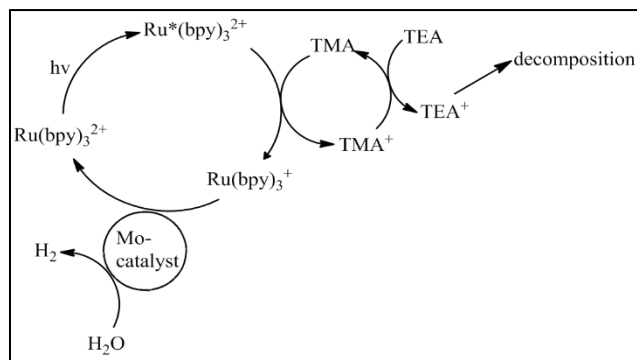
3.1.3 Objective

The objectives of this project are 1) Synthesis of a broad palette of triangular $[\text{Mo}_3(\mu_3\text{-E})(\mu_2\text{-EF})_3]^{4+}$ clusters, which can vary in the chalcogenide core composition (E,F) and with the identity of the ancillary chalcogen donor ligand. All clusters originate from $\text{Mo}(\text{CO})_6$. The supporting ligand can be dithiocarbamate ($\text{R}_2\text{NCS}_2^{1-}$), O- diisopropylidithiophosphate ($(\text{OR})_2\text{PS}_2^{1-}$), dialkyldithiophosphate ($\text{R}_2\text{PS}_2^{1-}$), or diselenocarbamate ($\text{R}_2\text{NCSe}_2^{1-}$). For consistency, R will be maintained as *i*Bu. With differing degrees of activity, these compounds function as homogeneous catalysts for H_2 formation from H_2O under photolysis with a photosensitizer and sacrificial electron donor. 2) Identification of a correlation between photocatalytic activity level and composition of the Mo_3 structure and physical properties of the cluster, such as reduction potentials. 3) Identification of a maximally active $[\text{Mo}_3(\mu_3\text{-E})(\mu_2\text{-EF})_3]^{4+}$ cluster.

3.1.4 Approach

These photocatalytic studies will use a $\text{H}_2\text{O}/\text{MeCN}$ mixture as solvent, $[\text{Ru}(\text{bpy})_3]^{2+}$ as chromophore, Et_3N as sacrificial electron donor and trimethyl aniline (TMA) as electron transfer intermediary (**Scheme 3.1**).

The synthesis of the Mo_3 clusters that are being used in this study proceeds as outlined in (**Scheme 3.2** and **Scheme 3.3**).



Scheme 3.1. Photocatalytic system employed in these studies. Conditions: $[\text{Ru}(\text{bpy})_3]^{2+} = 260 \mu\text{M}$; $[\text{TMA}] = 50 \text{ mM}$; $[\text{TEA}] = 0.4 \text{ M}$; solvent = 1:2:1 THF:MeCN:H₂O, 4 mL total; headspace = 4.7

3.2 Experimental

3.2.1 Analytical, Spectroscopic, and Physical Methods

The UV-vis spectra were recorded at ambient temperature with an Ocean Optics HR2000+ES spectrometer. All NMR spectra were obtained at 25 C with a Bruker 400 MHz spectrometer reported with Me₄Si (0 ppm) as standard. The ESI-MS spectra were recorded on a micrOTOF 11 Bruker Daltonics instrument.. Raman spectra were obtained with a WITec Focus Innovations alpha300 spectrometer. The excitation source was a 532 nm line with a 600 grooves/mm grating. The elemental analyses were performed either by Galbraith Laboratories of Knoxville, TN, or Kolbe Microanalytical Laboratory of Oberhausen, Germany.

Unit cell and refinement data were collected using 1958-9988 selected reflections from the full data set in Tables and, and figures with full atom labeling are presented in Figures.

Electrochemistry measurements were obtained with a AgCl/Ag reference electrode, glassy carbon working electrode, Pt wire counter electrode, [ⁿBu₄N][PF₆] as supporting electrolyte and dry CH₂Cl₂ as solvent.

The photolysis samples were illuminated in a home-built, multiwell photoreactor comprised of an Al cylinder equipped with blue LEDs (Solid Apollo, 24 W, 460 nm) mounted inside the cylinder wall in a uniform, spiral pattern. The actinometry was carried out using the photooxidation of [Ru(bpy)₃]²⁺ by [S₂O₈]²⁻. The 10 mL of photoreaction sample contained 8.5 mL dry MeCN, 1.0 mL H₂O, and 0.5 mL dry THF with concentrations of 0.05 M for *N,N*-trimethylaniline, 260 μM for [Ru(bpy)₃]Cl₂, 0.40 M for Et₃N, and 100 μM for the Mo-based catalysts. The photolysis samples were thoroughly degassed by bubbling with Ar and sealed with screwcaps having PTFE/silicone septa

before irradiation. A 4.7 mL headspace volume was kept for each sample. After irradiation, a 50 μ L sample of gas was extracted and injected into a gas chromatograph (Cow-Mac GC; Molecular Sieve Column, T= 35 0C; Carrier Gas: N₂) for quantitative determination of the H₂ produced. The quantum yield for H₂ production per absorbed photon was measured as $\Phi_{H_2} = 2(\text{moles } H_2 \text{ produced})/(\text{moles photons}) = 2PV_{H_2} / (R \cdot T \cdot I \cdot t)$, where V_{H_2} is the volume of H₂ produced in the cell headspace, P = pressure in the headspace of the photolysis vial, R = gas constant, T = temperature, I = light intensity (quanta /s from actinometry) and t = irradiation time. Turnover numbers (TON) for H₂ production per catalyst were measured as: $TON_{H_2} = (\text{moles } H_2 \text{ produced})/(\text{moles Mo- catalyst}) = PV_{H_2} / (R \cdot T \cdot n_{Mo})$, where n_{Mo} = number of moles of Mo-catalyst in each sample.

3.2.2 Syntheses

3.2.2.1 General Considerations

[NH₄]₂[Mo₃S₁₃], ⁱBu₂NCSSSSCNⁱBu₂ and ⁱBu₂PSSSSPⁱBu₂ were obtained by literature procedures. Solvents for synthesis were dried with a system of drying columns from the Glass Contour Company (CH₂Cl₂, THF, Et₂O). The anhydrous solvents (DMF, 1,2 dichlorobenzene, EtOH) were purchased from commercial sources. All other reagents where commercially available products were used without further purification.

3.2.2.2 K[S₂P(ⁱPrO)₂].

An oven dried two neck 2 L round bottomed flask was equipped with condenser and with an outlet leading to a KOH/H₂O trap with which to neutralize any H₂S gas byproduct. Then 1000 mL of 99% ⁱPrOH were added, and the system was then purged with N₂ gas for

one hour. Then 104.67 g of P₄S₁₀ were added in portions over the course of ~30 min. Initially, the P₄S₁₀ was a pale yellow suspended powder, but over the course of a few hours, it was fully digested to afford a translucent, pale yellow solution. The reaction mixture was stirred for 2 days at ambient temperature and then sparged again with N₂(g) for 30 min and cooled in an ice bath. Portions of K metal that were 0.5 – 1.0 g in size were added under outward N₂ flow over a period of ~1 h. A cream-colored suspension of solid formed during the course of the addition of K metal, during which time the cooling was maintained. After further stirring overnight, the solid product was collected on a large Buchner funnel, washed with cold *i*PrOH followed by cold Et₂O, and dried under vacuum. Yield: 160.23 g, 65.7%. ¹H NMR (400 MHz, CD₃CN-d₂): 4.71 (octet, 1 H, -OCH(CH₃)₂), 1.22 (d, 3 H, -OCH(CH₃)₂), 1.20 (d, 3 H, -OCH(CH₃)₂). ¹³C NMR (400 MHz, CD₃CN-d₂): 118.28, 69.64, 24.11. ³¹P NMR (400 MHz, CD₃CN-d₂): 111.67.

3.2.2.3 (*i*PrO)₂P(=S)SSP(=S)(*O*^{*i*}Pr)₂.

A mixture of K[S₂P(*O*^{*i*}Pr)₂] (10 g, 39.6 mmol) and I₂ (5.0 g, 19.7 mmol) was heated for ~12 h (70 °C) in 150 mL anhydrous EtOH under a N₂ atmosphere. The reaction mixture was cooled to ambient temperature and allowed to stand for one day. Pale yellow crystal and white KI were observed. The remaining EtOH solution was filtered and evaporated (2.21 g) crystal was observed. The crude was washed with DI water and filtered through vacuum (5.51 g) crystal was observed. Yield: 7.72 g, 92%. MP: 85-88 °C. ¹H NMR (400 MHz, CD₂Cl₂-d₂): 4.92 (m, 4 H, -OCH(CH₃)₂), 1.40 (d, 12 H, -OCH(CH₃)₂), 1.38 (d, 12H, -OCH(CH₃)₂). ¹³C NMR (400 MHz, CD₂Cl₂-d₂): 75.21, 75.14, 65.19, 23.93, 23.88, 23.77, 23.72. ³¹P NMR (400 MHz, CD₂Cl₂-d₂): 81.28.

3.2.2.4 *t*Bu₂NC(=Se)SeSeSeC(=S)N^{*t*}Bu₂.

MP: 115-118 °C. ^1H NMR (400 MHz, $\text{CD}_2\text{Cl}_2\text{-d}_2$): 3.86 (d, 4 H, $-\text{CH}_2\text{CH}(\text{CH}_3)_2$), 3.81 (d, 4 H, $-\text{CH}_2\text{CH}(\text{CH}_3)_2$), 2.52 (octet, 4 H, $-\text{CH}_2\text{CH}(\text{CH}_3)_2$), 1.04 (d, 12 H, $-\text{CH}_2\text{CH}(\text{CH}_3)_2$), 0.93 (d, 12 H, $-\text{CH}_2\text{CH}(\text{CH}_3)_2$). ^{13}C NMR (400 MHz, $\text{CD}_2\text{Cl}_2\text{-d}_2$): 204.2, 58, 57.4, 27.7, 27.5, 20.3.

3.2.2.5 $[\text{Mo}_3\text{S}_7(\text{S}_2\text{CN}^i\text{Bu}_2)_3]\text{Cl}$, **[1a]Cl**.

A mixture of $\text{Mo}(\text{CO})_6$ (1.00 g, 3.79 mmol), S powder (0.24 g, 7.58 mmol) and $^i\text{Bu}_2\text{NC}(=\text{S})\text{SSC}(=\text{S})\text{CN}^i\text{Bu}_2$ (1.51 g, 3.71 mmol) was refluxed (170 °C) in 50 mL of anhydrous 1,2-dichlorobenzene for 1.5 h under N_2 atmosphere. The reaction mixture was cooled to room temperature, left to stand for one day, and then reduced to a dark black oily residue under steady stream of air overnight. This oily residue was dissolved in a mixture of 10 mL CH_2Cl_2 and 20 mL Et_2O , and the resulting solution was transferred to a vial that was then loosely covered with Al foil or a cap. After the evaporation of solvent over the course of one week, a black oily residue was again observed. Portions of Et_2O amounting to 30 mL were then used to wash away the black oily material and leave behind an orange crystalline solid at the bottom of the vial (0.9 g). This orange solid was recrystallized by the diffusion of hexanes vapor into a 1,2- $\text{ClCH}_2\text{CH}_2\text{Cl}$ solution. Yield: 0.8 g of orange needles, 68%. ^1H NMR (400 MHz, $\text{CD}_2\text{Cl}_2\text{-d}_2$): 3.66 (d, 6 H, $-\text{CH}_2\text{CH}(\text{CH}_3)_2$), 3.60 (d, 6 H, $-\text{CH}_2\text{CH}(\text{CH}_3)_2$), 2.32 (m, 6 H, $-\text{CH}_2\text{CH}(\text{CH}_3)_2$), 1.00 (d, 18 H, $-\text{CH}_2\text{CH}(\text{CH}_3)_2$), 0.96 (d, 18 H, $-\text{CH}_2\text{CH}(\text{CH}_3)_2$). ^{13}C NMR (400 MHz, $\text{CD}_2\text{Cl}_2\text{-d}_2$): 204.2, 58, 57.4, 27.7, 27.6, 20.3. UV-vis [CH_2Cl_2 , λ_{max} nm (ϵ): ~260, ~284, ~358, ~415. MS (ESI⁺) Calcd for $[\text{C}_{27}\text{H}_{54}\text{Mo}_3\text{N}_3\text{S}_{13}]^+$: m/z 1125.7843; Observed: m/z 1125.7845; Error (δ): 0.21 ppm. Raman (cm^{-1}): 71.6, 103.7, 129.9, 248.2, 265.4, 291.1, 311, 356.4, 390.2, 451.9, 513.1, 535.3.

Anal. Calcd for $C_{27}H_{54}ClMo_3N_3S_{13}$: C, 27.94; H, 4.69; N, 3.62; Cl, 3.05; S, 35.91; C, 27.89; H, 4.71; N, 3.60; Cl, 3.03; S, 35.92.

3.2.2.6 $[Mo_3S_7(S_2CN^iBu_2)_3] I$, [1a]I.

A mixture of $[Mo_3S_7(S_2CN^iBu_2)_3]Cl$ (0.1 g, 0.075 mmol) and 10 NaI (0.11 g, 0.75 mmol) was refluxed overnight (110 °C) in 20 mL anhydrous DMF and 10 mL anhydrous EtOH under a N_2 atmosphere. The reaction mixture was cooled to ambient temperature and then reduced to an orange solid under steady stream of air overnight. Then the crude solid was dissolved in 10 mL of CH_2Cl_2 and filtered. The filtrate was evaporated to an orange solid. Orange crystals were obtained by diffusion of $tBuOMe$ vapor into a concentrated 1,2 $ClCH_2CH_2Cl$ solution of this solid. Yield: 0.085 g, 94%. 1H NMR (400 MHz, $CD_2Cl_2-d_2$): 3.66 (d, 6 H, $-CH_2CH(CH_3)_2$), 3.59 (d, 6 H, $-CH_2CH(CH_3)_2$), 2.32 (m, 6 H, $-CH_2CH(CH_3)_2$), 0.96 (d, 18 H, $-CH_2CH(CH_3)_2$), 0.94 (d, 18 H, $-CH_2CH(CH_3)_2$). ^{13}C NMR (400 MHz, $CD_2Cl_2-d_2$): 204.2, 58, 57.4, 27.7, 27.5, 20.3. UV-vis [CH_2Cl_2 , λ_{max} nm (ϵ): ~263, ~352, ~427. MS (ESI⁺) Calcd for $[C_{27}H_{54}Mo_3N_3S_{13}]^+$: m/z 1125.7843; Observed: m/z 1125.7845 Error (δ): 0.21 ppm. Raman (cm^{-1}): 71.6, 103.7, 129.9, 248.2, 265.4, 291.1, 311, 356.4, 390.2, 451.9, 513.1, 535.3.

3.2.2.7 $Mo_3S_4Se_3(S_2CN^iBu_2)_3SeCN$, [2a]SeCN.

A red solution of $[Mo_3S_7(S_2CN^iBu_2)_3]I$ (0.05 g) in 10 mL CH_2Cl_2 was stirred together with a solution of 4 equivalents of $KSeCN$ (0.023 g) in 5 mL water under a N_2 atmosphere. After 2 days, the organic layer was separated, dried over anhydrous Na_2SO_4 , and

evaporated to dryness to yield [2a]SeCN. Yield: 0.04 g, 74%. A crystalline sample was obtained by diffusing ^tBuOMe into a solution of the compound in 1,2-ClCH₂CH₂Cl. ¹H NMR (400 MHz, CD₂Cl₂-d₂): 3.66 (d, 6 H, -CH₂CH(CH₃)₂), 3.60 (d, 6 H, -CH₂CH(CH₃)₂), 2.28 (m, 6H, -CH₂CH(CH₃)₂), 0.96 (d, 18 H, -CH₂CH(CH₃)₂), 0.94 (d, 18 H, -CH₂CH(CH₃)₂). ¹³C NMR (400 MHz, CD₂Cl₂-d₂): 204.2, 58, 57.1, 27.7, 27.6, 20.3. UV-vis [CH₂Cl₂, λ_{max} nm (ε)]: ~269, ~335, ~434. MS (ESI⁺) Calcd for [C₂₇H₅₄Mo₃N₃S₁₀Se₃]⁺: *m/z* 1265.6206; Observed: *m/z* 1265.6300; Error (δ): 7.45 ppm. Raman (cm⁻¹): 75.7, 93.2, 125.3, 186.1, 257.9, 266.5, 289.4, 340.5, 380.1, 394.1, 441.8, 450.2, 553.

3.2.2.8 [Mo₃Se₇(S₂CN^{*t*}Bu₂)₃]₂Se.

A mixture of Mo(CO)₆ (1.00 g, 3.79 mmol), Se powder (1.2g, 15.2 mmol) and ^tBu₂NC(=S)SSC(=S)N^{*t*}Bu₂ (1.51 g, 3.71 mmol) was refluxed (200-220 °C) in 50 mL anhydrous 1,2- dichlorobenzene for 1.5 h under a N₂ atmosphere. The reaction mixture was cooled to room temperature and then vacuum filtered to remove unreacted Se. The filtrate was reduced to a dark red oily residue under steady stream of air overnight. This residual oily residue was washed with small portions of Et₂O amounting to 30 mL to remove a red oily material. A crude solid residue of [Mo₃Se₇(S₂CN^{*t*}Bu₂)₃]₂Se was observed. Yield: 1.02 g, 70%. ¹H NMR (400 MHz, CD₂Cl₂-d₂): 3.86 (d, 6 H, -CH₂CH(CH₃)₂), 3.82 (d, 6 H, -CH₂CH(CH₃)₂), 3.58 (d, 6 H, -CH₂CH(CH₃)₂), 3.55 (d, 6 H, -CH₂CH(CH₃)₂), 2.32 (m, 12 H, -CH₂CH(CH₃)₂), 0.94 (d, 36 H, -CH₂CH(CH₃)₂), 0.93 (d, 36 H, -CH₂CH(CH₃)₂). ¹³C NMR (400 MHz, CD₂Cl₂-d₂): 204.2, 58.6, 56.4, 27.1, 27.0, 19.8. UV-vis [CH₂Cl₂, λ_{max} nm (ε)]: ~278, ~350, ~428. MS (ESI⁺) Calcd for [C₅₄H₁₀₈Se₁₅Mo₆N₆S₁₂]¹⁺: *m/z* 2985.7233; Observed: *m/z* 2985.7353; Error (δ): 4.01 ppm.

Raman (cm^{-1}): 85.3, 109.6, 135.9, 174.1, 200.1, 235.9, 269.6, 315, 360, 441, 470, 510, 537, 564, 601.8, 669.3.

3.2.2.9 $[\text{Mo}_3\text{Se}_7(\text{S}_2\text{CN}^i\text{Bu}_2)_3]\text{I}$, **[3a]I**.

A mixture of $[\text{Mo}_3\text{Se}_7(\text{S}_2\text{CN}^i\text{Bu}_2)_3]_2\text{Se}$ (1.00 g) and 10 NaI (0.5 g) was refluxed (110 °C) overnight in a mixture of 50 mL anhydrous DMF and 25 mL anhydrous EtOH under a N_2 atmosphere. The reaction mixture was cooled to ambient temperature and then reduced to a red solid under steady stream of air overnight. This crude solid was dissolved in 30 mL of CH_2Cl_2 and filtered. The filtrate was evaporated to again afford a red solid, which was crystallized as red needles by the diffusion of *n*-pentane vapor into a concentrated 1,2- $\text{ClCH}_2\text{CH}_2\text{Cl}$ solution. Yield: 0.44 g (crude), 99%. ^1H NMR (400 MHz, $\text{CD}_2\text{Cl}_2\text{-d}_2$): 3.58 (d, 6 H, $-\text{CH}_2\text{CH}(\text{CH}_3)_2$), 3.55 (d, 6 H, $-\text{CH}_2\text{CH}(\text{CH}_3)_2$), 2.24 (m, 6 H, $-\text{CH}_2\text{CH}(\text{CH}_3)_2$), 0.94 (d, 18 H, $-\text{CH}_2\text{CH}(\text{CH}_3)_2$), 0.88 (d, 18 H, $-\text{CH}_2\text{CH}(\text{CH}_3)_2$). ^{13}C NMR (400 MHz, $\text{CD}_2\text{Cl}_2\text{-d}_2$): 205.2, 57.3, 56.7, 27.6, 27.5, 20.5. UV-vis [CH_2Cl_2 , λ_{max} nm (ϵ): ~284, ~384, ~420. MS (ESI⁺) Calcd for $[\text{C}_{27}\text{H}_{54}\text{Mo}_3\text{N}_3\text{S}_6\text{Se}_7]^+$: m/z 1453.4021; Observed: m/z 1453.4055; Error (δ): 2.36 ppm. Raman (cm^{-1}): 72.8, 107.8, 128.2, 168.8, 203.4, 246, 272.2, 306.5, 332, 354.7, 399.8, 439, 486.5, 553, 580.5.

3.2.2.10 $[\text{Mo}_3\text{Se}_7(\text{Se}_2\text{CN}^i\text{Bu}_2)_3]\text{Cl}$, **[3c]Cl**.

A mixture of $\text{Mo}(\text{CO})_6$ (0.086 g), Se powder (0.1 g) and $^i\text{Bu}_2\text{NCSeSeSeSeSeCN}^i\text{Bu}_2$ (0.2 g) was refluxed (170-180 °C) under N_2 atmosphere in 15 mL of anhydrous 1,2-dichlorobenzene for 1.5 hours. The reaction mixture was cooled to room temperature and then vacuum filtered to remove unreacted Se. The filtrate was reduced to a dark red oily residue under steady stream of air overnight. This residual oily residue was washed with portions of Et_2O amounting to 20 mL to remove a red oily material. The resulting solid

residue was crystallized as orange crystals by diffusion of hexanes vapor into a concentrated 1,2-ClCH₂CH₂Cl solution. Yield: 0.09 g (crude), 70%. ¹H NMR (400 MHz, CD₂Cl₂-d₂): 3.59 (d, 6 H, -CH₂CH(CH₃)₂), 3.55 (d, 6 H, -CH₂CH(CH₃)₂), 2.25 (m, 6 H, -CH₂CH(CH₃)₂), 0.95 (d, 18 H, -CH₂CH(CH₃)₂), 0.91 (d, 18 H, -CH₂CH(CH₃)₂). ¹³C NMR (400 MHz, CD₂Cl₂-d₂): 205.2, 57.1, 56.7, 27.6, 27.5, 20.5. UV-vis [CH₂Cl₂, λ_{max} nm (ε)]: ~278, ~364, ~454. MS (ESI⁺) Calcd for [C₂₇H₅₄Mo₃N₃Se₁₃]⁺: *m/z* 1736.0741; Observed: *m/z* 1736.0253; Error (δ): 29.08 ppm. Raman (cm⁻¹): 80, 100.3, 130.6, 168.8, 214.8, 256.6, 282.3, 319.7, 341.3, 366.7, 403.7, 438.6, 461.7, 494.4, 542.2.

3.2.2.11 [Mo₃Se₇(Se₂CN^{*i*}Bu₂)₃]I, [3c]I.

A mixture of [Mo₃Se₇(Se₂CN^{*i*}Bu₂)₃]Cl (0.0122g) and 10 eq NaI (0.0051 g) was refluxed (110 °C) overnight in a mixture of 10 mL anhydrous DMF and 20 mL anhydrous EtOH under a N₂ atmosphere. The reaction mixture was cooled to room temperature and then reduced to a red solid under steady stream of air overnight. The resulting residual solid was dissolved in 20 mL of CH₂Cl₂ and filtered. Evaporation of the filtrate afforded a red solid. Red needle crystals were obtained by diffusion of hexanes vapor into a concentrated 1,2-ClCH₂CH₂Cl solution. Yield: 0.01 g (crude), 99%. ¹H NMR (400 MHz, CD₂Cl₂-d₂): 3.59 (d, 6 H, -CH₂CH(CH₃)₂), 3.55 (d, 6 H, -CH₂CH(CH₃)₂), 2.25 (m, 6 H, -CH₂CH(CH₃)₂), 0.95 (d, 18 H, -CH₂CH(CH₃)₂), 0.91 (d, 18 H, -CH₂CH(CH₃)₂). ¹³C NMR (400 MHz, CD₂Cl₂-d₂): 205.2, 57.1, 56.7, 27.6, 27.5, 20.5. UV-vis [CH₂Cl₂, λ_{max} nm (ε)]: ~278, ~364, ~454. MS (ESI⁺) Calcd for [C₂₇H₅₄Mo₃N₃Se₁₃]⁺: *m/z* 1736.0741; Observed: *m/z* 1736.0251; Error (δ): 28.08 ppm. Raman (cm⁻¹): 80, 100.3, 130.6, 168.8, 214.8, 256.6, 282.3, 319.7, 341.3, 366.7, 403.7, 438.6, 461.7, 494.4, 542.2.

3.2.2.12. [Mo₃S₇(S₂P^{*i*}Bu₂)₃](S₂P^{*i*}Bu₂), [1e][S₂P^{*i*}Bu₂].

A mixture of Mo(CO)₆ (0.25 g, 3.79 mmol), S powder (0.06 g, 7.58 mmol) and ⁱBu₂PSSSSPⁱBu₂ (0.387g, 3.71 mmol) was refluxed for 5 hours at 140 °C in 20 mL of 1,3,5-triisopropylbenzene under a N₂ atmosphere. The reaction mixture was cooled to room temperature. The resulting yellow-orange precipitate was collected by filtration, washed with Et₂O, and dried. Then the precipitate was purified with hot DCM/methanol, and the solid part was recrystallized by DCM/pentane vapor diffusion (0.2 g). Yield: 65%. ¹H NMR (400 MHz, CD₂Cl₂-d₂): 2.42 (m, 8 H, -CH₂CH(CH₃)₂), 2.14 (d, 8 H, -CH₂CH(CH₃)₂), 2.10 (d, 8 H, -CH₂CH(CH₃)₂), 1.15 (d, 24 H, -CH₂CH(CH₃)₂), 1.11 (d, 24 H, -CH₂CH(CH₃)₂). ¹³C NMR (400 MHz, CD₂Cl₂-d₂): 48.8, 48.4, 46.2, 45.8, 25.1. ³¹P NMR (400 MHz, CD₂Cl₂-d₂): 123.0, 103.8. UV-vis [CH₂Cl₂, λ_{max} nm (ε)]: ~260, ~332, ~420. MS (ESI⁺) Calcd for [C₂₄H₅₄Mo₃P₃S₁₃]⁺: *m/z* 1140.6963; Observed: *m/z* 1140.6968. Error (δ): 0.48 ppm. Raman (cm⁻¹): 84.52, 116.6, 148.56, 160.15, 189.05, 223.6, 235.08, 249.41, 275.14, 332.05, 394.2, 436.3, 497.7, 522.6, 553, 569.5, 619, 660.

3.2.2.13. [Mo₃S₇(S₂PⁱBu₂)₃]I, [1e]I

A mixture of [Mo₃S₇(S₂PⁱBu₂)₃][S₂PⁱBu₂] (0.025 g) and 10 NaI (0.12 g) was refluxed (110 °C) overnight in a mixture of 20 mL anhydrous DMF and 10 mL anhydrous EtOH under a N₂ atmosphere. The reaction mixture was cooled to room temperature, and then the reaction mixture was reduced to an orange solid under steady stream of air overnight. The crude solid residue was dissolved in 10 mL CH₂Cl₂ and filtered. The filtrate was evaporated to afford a red solid. Red crystals were obtained by diffusion of *n*-pentane vapor into a CH₂Cl₂ solution of this solid. Yield: 0.02 g, 99%). ¹H NMR (400 MHz, CD₂Cl₂-d₂): 2.38 (m, 6 H, -CH₂CH(CH₃)₂), 2.14 (d, 6 H, -CH₂CH(CH₃)₂), 2.10 (d, 6 H, -CH₂CH(CH₃)₂), 1.16 (d, 18 H, -CH₂CH(CH₃)₂), 1.14 (d, 18 H, -CH₂CH(CH₃)₂). ¹³C NMR

(400 MHz, CD₂Cl₂-d₂): 48.8, 48.4, 46.2, 45.8, 25.1. ³¹P NMR (400 MHz, CD₂Cl₂-d₂): 102.8. UV-vis [CH₂Cl₂, λ_{max} nm (ε)]: ~238, ~345. MS (ESI⁺) Calcd for [C₂₄H₅₄Mo₃P₃S₁₃]⁺: *m/z* 1140.6963. Observed: *m/z* 1140.6968. Error (δ): 0.48 ppm. Raman (cm⁻¹): 68.7, 115.4, 141.5, 176.3, 239.6, 262.5, 288.2, 356.3, 378.9, 418.3, 449.1, 474.2, 515.9, 612.4, 647.9. Anal. Calcd for C₂₄H₅₄IMo₃P₃S₁₃: C, 22.75; H, 4.30; P, 7.33; S, 33.89. Found: C, 23.01; H, 2.93; P, 7.39; S, 33.41.

3.2.2.14 [Mo₃S₄Se₃(S₂P^{*i*}Bu₂)₃]I, [2e]I.

A red solution of [Mo₃S₇(S₂P^{*i*}Bu₂)₃]I (0.05 g) in 10 mL of CH₂Cl₂ was stirred together with a solution of 4 eq of KSeCN (0.0227 g) in 5 mL water under a N₂ atmosphere. This mixture was gently heated to 50 °C. After 2 days, the organic layer was separated, dried over anhydrous Na₂SO₄, and reduced to dryness to afford the crude product. A crystalline sample was obtained by diffusing *n*-pentane into a concentrated solution of the compound in CH₂Cl₂. Yield: 0.04 g, 74%. ¹H NMR (400 MHz, CD₂Cl₂-d₂): 2.41 (m, 6 H, -CH₂CH(CH₃)₂), 2.14 (d, 6 H, -CH₂CH(CH₃)₂), 2.10 (d, 6 H, -CH₂CH(CH₃)₂), 1.17 (d, 18 H, -CH₂CH(CH₃)₂), 1.15 (d, 18 H, -CH₂CH(CH₃)₂). ¹³C NMR (400 MHz, CD₂Cl₂-d₂): 48.8, 48.4, 46.2, 45.8, 25.1. ³¹P NMR (400 MHz, CD₂Cl₂-d₂): 102.7. UV-vis [CH₂Cl₂, λ_{max} nm (ε)]: ~279, ~345, ~430. MS (ESI⁺) Calcd for [C₂₄H₅₄Mo₃P₃S₁₀Se₃]⁺: *m/z* 1280.5325; Observed: *m/z* 1280.5345. Raman (cm⁻¹): 79.2, 105.5, 149.1, 163.6, 229.8, 304.1, 332.5, 349.5, 397, 422.8, 450.8, 503.7, 550.8, 572.8, 589.3, 646.8, 725.6, 776.8, 841. Anal. Calcd. for C₂₄H₃₆IMo₃P₃S₁₀Se₃: C, 20.48; H, 3.87; P, 6.60; S, 22.77. Found: C, 20.62; H, 2.63; P, 6.67; S, 22.95.

3.2.2.15 [Mo₃Se₇(S₂P^{*i*}Bu₂)₃][S₂P^{*i*}Bu₂], [3e][S₂P^{*i*}Bu₂].

A mixture of Mo(CO)₆ (0.25 g, 3.79 mmol), Se powder (0.3 g, 15.2 mmol) and ⁱBu₂PSSSSPⁱBu₂ (0.387 g, 3.71 mmol) was refluxed for 1.5 hours at 140 °C in 20 mL of anhydrous 1,2-dichlorobenzene under a N₂ atmosphere. The reaction mixture was then cooled to ambient temperature and vacuum filtered to remove unreacted Se. The filtrate was reduced to a dark black oily residue under steady stream of air overnight. This oily residue was dissolved in a mixture of 20 mL Et₂O and 10 mL CH₂Cl₂, and the solution was loosely covered with Al foil or a cap. After the evaporation of the solvent, a black oily residual was obtained. Portions of Et₂O amounting to 30 mL were then used to wash away this dark green oily material and leave behind a red crystalline solid. This red solid was recrystallized by diffusion of *n*-pentane vapor into a CH₂Cl₂ solution. Yield: 0.2 g, 70%. ¹H NMR (400 MHz, CD₂Cl₂-d₂): 2.42 (m, 8 H, -CH₂CH(CH₃)₂), 2.14 (d, 8 H, -CH₂CH(CH₃)₂), 2.09 (d, 8 H, -CH₂CH(CH₃)₂), 1.15 (d, 24 H, -CH₂CH(CH₃)₂), 1.12 (d, 24 H, -CH₂CH(CH₃)₂). ¹³C NMR (400 MHz, CD₂Cl₂-d₂): 48.8, 48.4, 46.2, 45.8, 25.1. ³¹P NMR (400 MHz, CD₂Cl₂-d₂): 123.0, 103.8. UV-vis [CH₂Cl₂, λ_{max} nm (ε)]: ~236, ~277, ~401. MS (ESI⁺) Calcd for [C₂₄H₅₄Mo₃P₃S₆Se₇]⁺: *m/z* 1468.3141; Observed: *m/z* 1468.3058; Error (δ): 5.61 ppm. Raman (cm⁻¹): 116, 163, 197.7, 220.7, 260.8, 357.5, 396.9, 425, 455.8, 492, 553, 599.8, 687.2, 730.5, 797.8, 864.5. Anal. Calcd. for C₃₂H₇₂Mo₃P₄S₈Se₇: C, 22.91; H, 4.33; S, 15.29. Found: C, 22.51; H, 4.26; S, 15.02.

3.2.2.16 [Mo₃Se₇(S₂P^{*i*}Bu₂)₃]**I**, [**3e**]**I**.

A mixture of [Mo₃Se₇(S₂P^{*i*}Bu₂)₃][S₂P^{*i*}Bu₂] (0.025 g) and 10 NaI (0.12 g) was refluxed overnight at 110 °C in a mixture of 20 mL of anhydrous DMF and 10 mL of anhydrous EtOH under a N₂ atmosphere. The reaction mixture was cooled to ambient temperature and then reduced to an orange solid under steady stream of air overnight. This crude solid was

dissolved in 10 mL of CH₂Cl₂ and filtered. The filtrate was evaporated to afford a red solid, which was obtained in crystalline form by diffusion of *n*-pentane vapor into a CH₂Cl₂ solution. Yield: 0.02 g, 99%. ¹H NMR (400 MHz, CD₂Cl₂-d₂): 2.40 (m, 6 H, -CH₂CH(CH₃)₂), 2.11 (d, 6 H, -CH₂CH(CH₃)₂), 2.06 (d, 6 H, -CH₂CH(CH₃)₂), 1.15 (d, 18 H, -CH₂CH(CH₃)₂), 1.10 (d, 18 H, -CH₂CH(CH₃)₂). ¹³C NMR (400 MHz, CD₂Cl₂-d₂): 48.8, 48.4, 46.2, 45.8, 25.1. ³¹P NMR (400 MHz, CD₂Cl₂-d₂): 102.7. UV-vis [CH₂Cl₂, λ_{max} nm (ε)]: ~239, ~282, ~356. MS (ESI⁺) Calcd for [C₂₄H₅₄Mo₃P₃S₆Se₇]⁺: *m/z* 1468.3141; Observed: *m/z* 1468.3058; Error (δ): 5.61 ppm. Raman (cm⁻¹): 75.7, 116.6, 163, 249, 275.1, 332, 382.9, 461, 500.4, 575, 632.7, 670.8, 784.4, 851.2. Anal. Calcd. for C₂₄H₅₄IMo₃P₃S₆Se₇: C, 18.07; H, 3.41; Found: C, 19.55; H, 3.70.

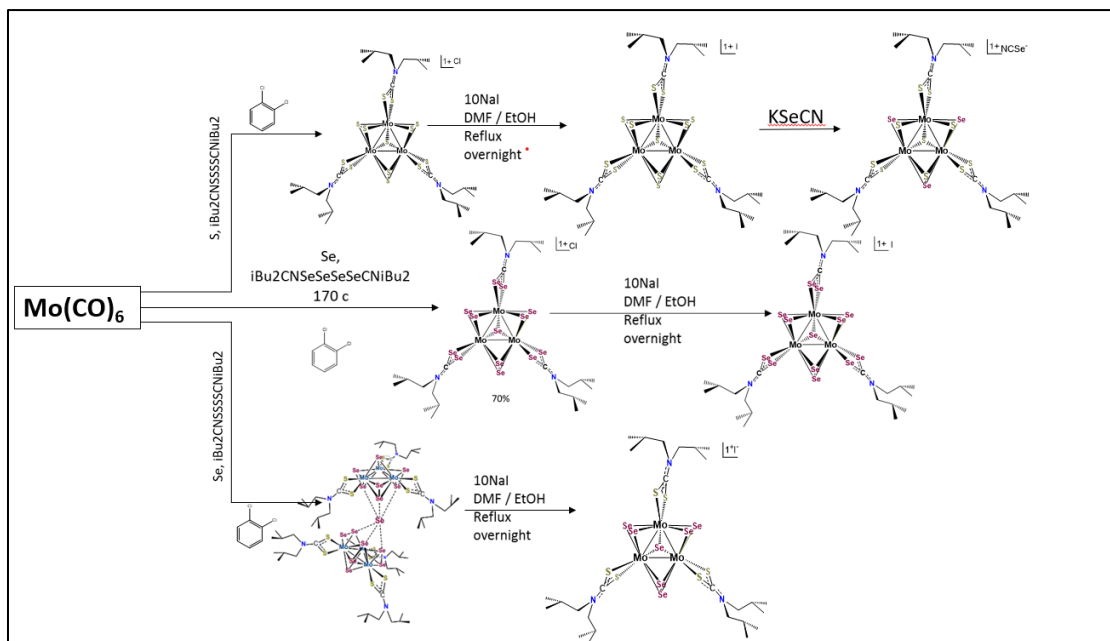
3.2.2.17 [Mo₃Se₇(S₂P(O^{*i*}Pr)₂)₃][S₂P(O^{*i*}Pr)₂], [3f][S₂P(O^{*i*}Pr)₂].

A mixture of Mo(CO)₆ (1.00 g, 3.79 mmol), Se powder (1.2 g, 15.22 mmol) and freshly prepared (^{*i*}PrO)₂P(=S)SSP(=S)(O^{*i*}Pr)₂ (1.6 g, 3.71 mmol) was refluxed for 1.5 hours at (140 °C) in 50 mL of anhydrous 1,2-dichlorobenzene under a N₂ atmosphere. The reaction mixture was cooled to room temperature and then vacuum filtered to remove unreacted Se. The filtrate was reduced to a dark black solid residue under steady stream of air overnight. This residual solid was dissolved in 30 mL of dry Et₂O and slowly evaporated from a vial loosely covered with Al foil or a cap. After one week, crystalline material was collected from the bottom of the vial and washed with portions of dry Et₂O amounting to 30 mL, which removed a black oily material. Yield: 0.8 g (crude), 68%. ¹H NMR (400 MHz, CD₂Cl₂-d₂): 4.86 (m, 8 H, -OCH(CH₃)₂), 1.37 (d, 24 H, -OCH(CH₃)₂), 1.34 (d, 24 H, -OCH(CH₃)₂). ¹³C NMR (400 MHz, CD₂Cl₂-d₂): 74.35, 74.29, 24.09, 24.07, 24.05, 24.03. ³¹P NMR (400 MHz, CD₂Cl₂-d₂): 92.23, 106.4. UV-vis [CH₂Cl₂, λ_{max} nm (ε)]: ~236, ~344,

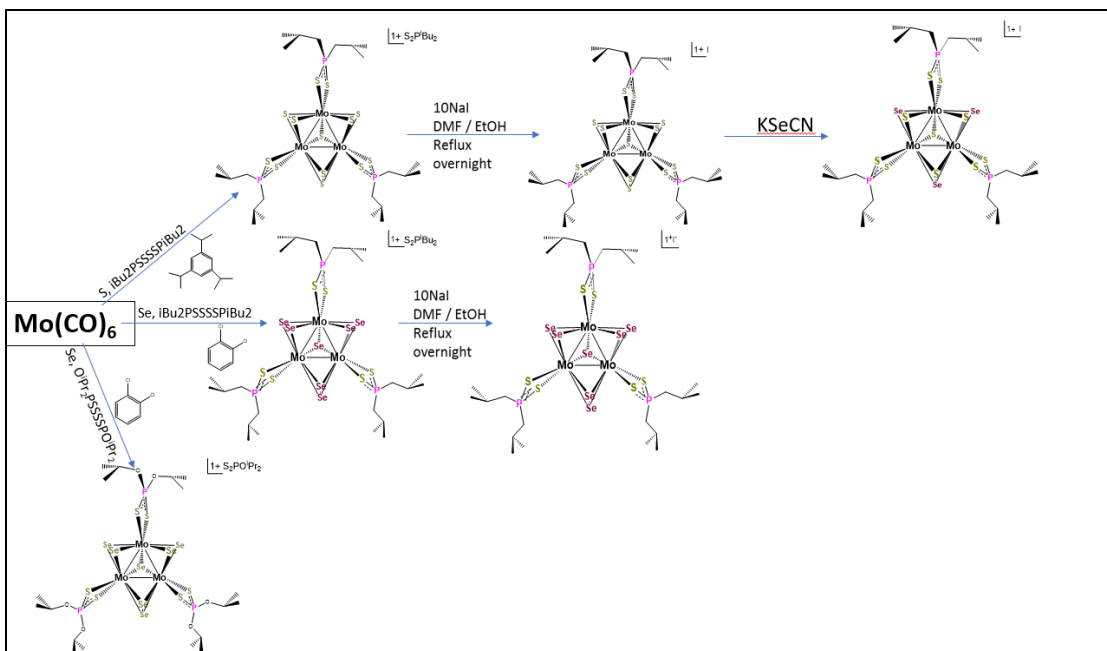
~441. MS (ESI⁺) Calcd for [C₁₈H₄₂O₆Mo₃P₃S₆Se₇]⁺: *m/z* 1152.5717; Observed: *m/z* 1152.5688; Error (δ): 12.04 ppm. Raman (cm⁻¹): 81.3, 103.6, 137.9, 168.1, 184.1, 243.9, 257.8, 301.2, 334.6, 363.9, 383.4, 437.7, 455, 503, 535.5, 571.5, 628.1, 674.9.

3.3 Discussion

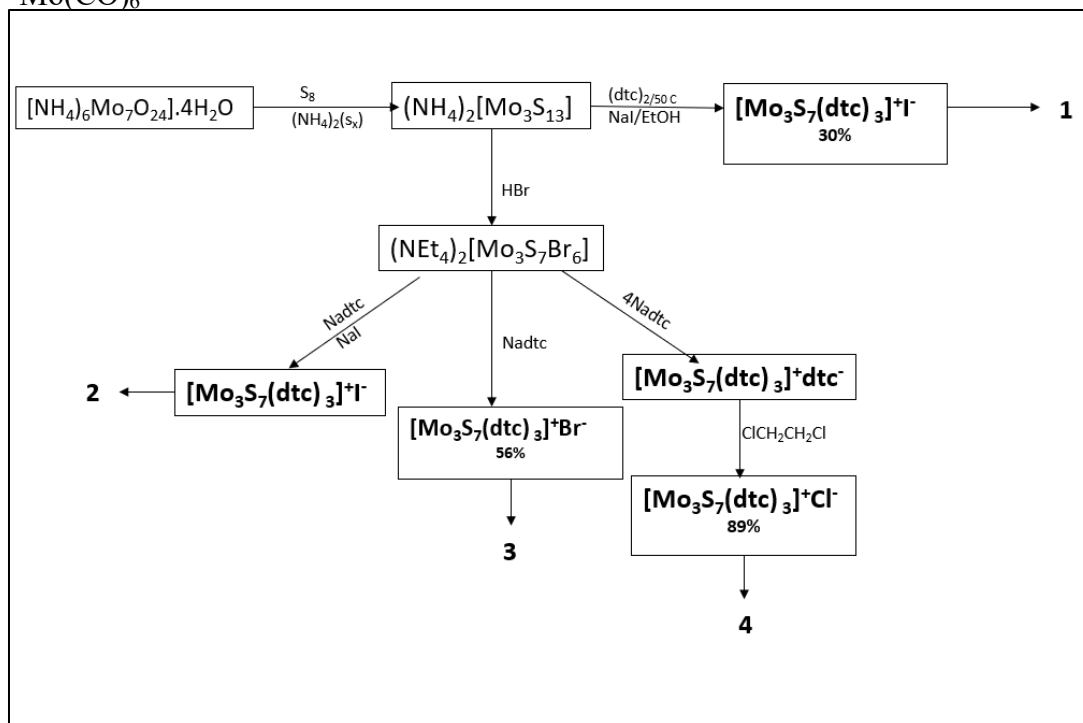
3.3.1 Discussion of Syntheses



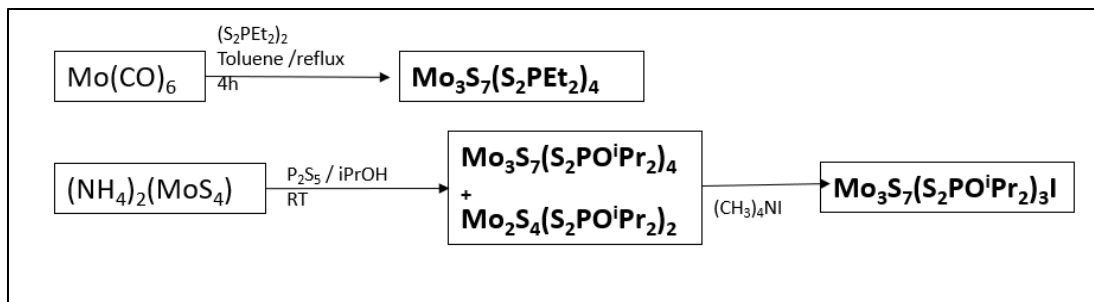
Scheme 3.2. Synthetic routes to $[\text{Mo}_3\text{Q}_7\text{L}_3]^+$ type cluster cations from $\text{Mo}(\text{CO})_6$.



Scheme 3.3. Synthetic routes to $[\text{Mo}_3\text{Q}_7\text{L}_3]^+$ type cluster cations from $\text{Mo}(\text{CO})_6$



Scheme 3.4. Known synthetic routes to $[\text{Mo}_3\text{S}_7\text{L}_3]^+$ type cluster cations from $[\text{Mo}_3\text{S}_{13}]^{2-}$ or $[\text{Mo}_3\text{S}_7\text{Br}_6]^{2-}$.



Scheme 3.5. Known synthetic routes to $[\text{Mo}_3\text{S}_7\text{L}_3]^+$ type cluster cations.

3.3.2 Synthesis of $[\text{Mo}_3\text{S}(\text{S}_2)_3\text{L}_3]^+$ complexes; $\text{L} = (\text{S}_2\text{CN}^i\text{Bu}_2, ^-\text{Se}_2\text{CN}^i\text{Bu}_2, ^-\text{S}_2\text{P}^i\text{Bu}_2, ^-\text{S}_2\text{P}(\text{O}^i\text{Pr})_2)$

Since the first $[\text{Mo}_3\text{S}(\text{S}_2)_3]^{4+}$ cluster core was discovered in 1974²², there are variety of $[\text{Mo}_3\text{S}(\text{S}_2)_3]^{4+}$ complexes and efficient pathways are discovered and have been reported²³⁻³⁰. Especially, a trinuclear remarkable molybdenum complex, $(\text{NH}_4)_2[\text{Mo}_3\text{S}(\text{S}_2)_6]$ ²³, which was discovered in 1980 by Muller, considering it has bridging and terminal disulfide edges, a strong contribution to do this kind of chemistry. After discovery of $(\text{NH}_4)_2[\text{Mo}_3\text{S}(\text{S}_2)_6]$ complex, first $(\text{NEt}_4)_2[\text{Mo}_3\text{S}_7\text{X}_6]$ ²⁸ ($\text{X}=\text{Cl}, \text{Br}$) complex was synthesized by Fedin and coworkers. However, the first cluster with the $[\text{Mo}_3\text{S}(\text{S}_2)_3]^{4+}$ core compound supported by dithiocarbamate ligand was synthesized by Hegetschweiler³¹. Moreover, they reported that they obtained this compound by two methods. One method is that direct oxidation of $(\text{NH}_4)_2[\text{Mo}_3\text{S}(\text{S}_2)_6]$ by dithiocarbamate compound (1) and another method is that nucleophilic substitution of the six Br^- in $(\text{NEt}_4)_2[\text{Mo}_3\text{S}_7\text{X}_6]$ ($\text{X}=\text{Cl}, \text{Br}$) by $\text{Na}(\text{S}_2\text{CNET}_2)$ ligand and NaI was used to form compound (1). Furthermore, in their studies they obtained compound (2) from $(\text{NEt}_4)_2[\text{Mo}_3\text{S}_7\text{X}_6]$ ($\text{X}=\text{Cl}, \text{Br}$) and $\text{Na}(\text{S}_2\text{CNET}_2)$. Around the same time, Fedin and coworkers³² did the experiment between 4 $\text{Na}(\text{S}_2\text{CNET}_2)$ and $(\text{NEt}_4)_2[\text{Mo}_3\text{S}_7\text{X}_6]$ ($\text{X}=\text{Cl}, \text{Br}$) and they obtained $[\text{Mo}_3\text{S}_7(\text{S}_2\text{CNET}_3)]$ (S_2CNET_3) compound.

But it was not characterized by XRD. During the crystallization process of this compound with boiling 1,2 DCE they got $[\text{Mo}_3\text{S}_7(\text{S}_2\text{CNET}_3)] \text{Cl}$ compound (4).

In the case of Mo_3S_7 -cluster dithiophosphinates, Keck et al,1981, reported³³ that reaction of the disulfanes with carbonyl complexes $\text{Mo}(\text{CO})_6$ produced Mo_3S_7 cluster chelate of types $[\text{Mo}_3\text{S}_7(\text{S}_2\text{PET}_3)] (\text{S}_2\text{PET}_3)$ compound. Rong-min et al,1998 reported³⁴ that the molecule structure of the compound of a discrete cluster cation $\text{Mo}_3\text{S}_7(\text{S}_2\text{PO}^i\text{Pr}_2)_4$ and $\text{Mo}_2\text{S}_4(\text{S}_2\text{PO}^i\text{Pr}_2)_2$ were obtained from the reaction between $(\text{NH}_4)_2\{\text{MoS}_4\}$ and $\text{P}_2\text{S}_5^i\text{PrOH}$. Continued Sha-Fang et al, reported³⁵ $[\text{Mo}_3\text{S}_7(\text{S}_2\text{PO}^i\text{Pr}_2)_3] \text{I}$ was prepared by addition of $(\text{CH}_3)_4\text{NI}$ into reaction mixture of $\text{Mo}_3\text{S}_7(\text{S}_2\text{PO}^i\text{Pr}_2)_4$.

Here, we propose a new synthetic route for $[\text{Mo}_3\text{S}_7\text{L}_3]^+$; $\text{L} = (-\text{S}_2\text{CN}^i\text{Bu}_2, -\text{Se}_3\text{CN}^i\text{Bu}_2, -\text{S}_2\text{P}^i\text{Bu}_2, -\text{S}_2\text{P}(\text{O}^i\text{Pr})_2)$ cluster compounds from $\text{Mo}(\text{CO})_6$. One of the features of this study is simply refluxing the mixture of $\text{Mo}(\text{CO})_6$, elemental sulfur and $(-\text{S}_2\text{CN}^i\text{Bu}_2)_2$ or $(\text{S}_2\text{P}^i\text{Bu}_2)_2$ in 1,2 dichlorobenzene at different temperatures. Another feature is that this cheapest method produced high yield within the 1.5 hours of reaction time period. Beginning with $(-\text{S}_2\text{CN}^i\text{Bu}_2)_2$ ligand produced direct $[\text{Mo}_3\text{S}_7(\text{S}_2\text{CN}^i\text{Bu}_2)_3] \text{Cl}$ cluster at 170 C temperature and then NaI addition produced $[\text{Mo}_3\text{S}_7(\text{S}_2\text{CN}^i\text{Bu}_2)_3] \text{I}$ (94%). In the high temperature (220-240 C), $[\text{Mo}_3\text{S}_7(\text{S}_2\text{CN}^i\text{Bu}_2)_3] \text{S}_2\text{CN}^i\text{Bu}_2$ was formed. But this is not characterized by X-ray analysis but confirmed with $^1\text{H-NMR}$. Followed by addition of NaI proved that it formed $[\text{Mo}_3\text{S}_7(\text{S}_2\text{CN}^i\text{Bu}_2)_3] \text{I}$ cluster. The reaction with triseleno carbamate ($i\text{Bu}_2\text{NCS}_2$) Se at 170 C, its dimer compound and solid elemental Se were observed.

The reaction with disulfanes ($i\text{Bu}_2\text{PS}_2$)₂ at 140 C in 1,2 dichlorobenzene produced dimer type $\text{Mo}_2\text{S}_4(\text{S}_2\text{P}^i\text{Bu}_2)_2$ clusters rather than Mo_3S_7 type clusters, whereas non-polar solvent like 1,3,5 triisopropylbenzene produced $[\text{Mo}_3\text{S}_7(\text{S}_2\text{P}^i\text{Bu}_2)_3] \text{S}_2\text{P}^i\text{Bu}_2$ type clusters.

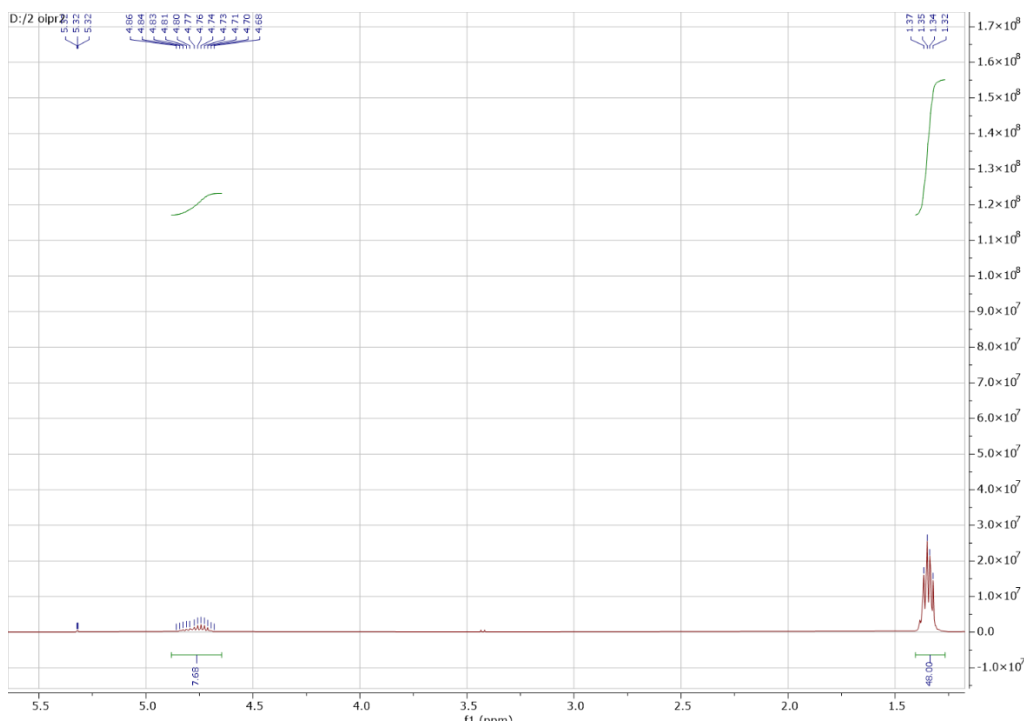


Figure 3.4. ^1H NMR spectrum of complex $[\text{Mo}_3\text{S}_7(\text{S}_2\text{P}(\text{O}^i\text{Pr})_2)_3][\text{S}_2\text{P}(\text{O}^i\text{Pr})_2]$.

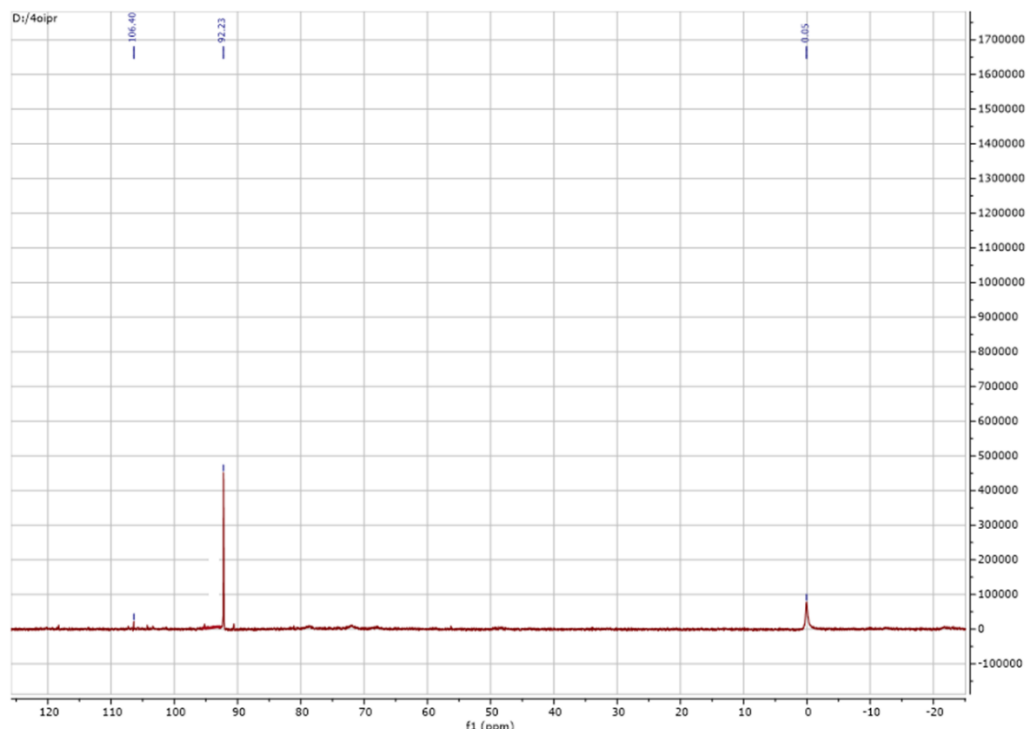
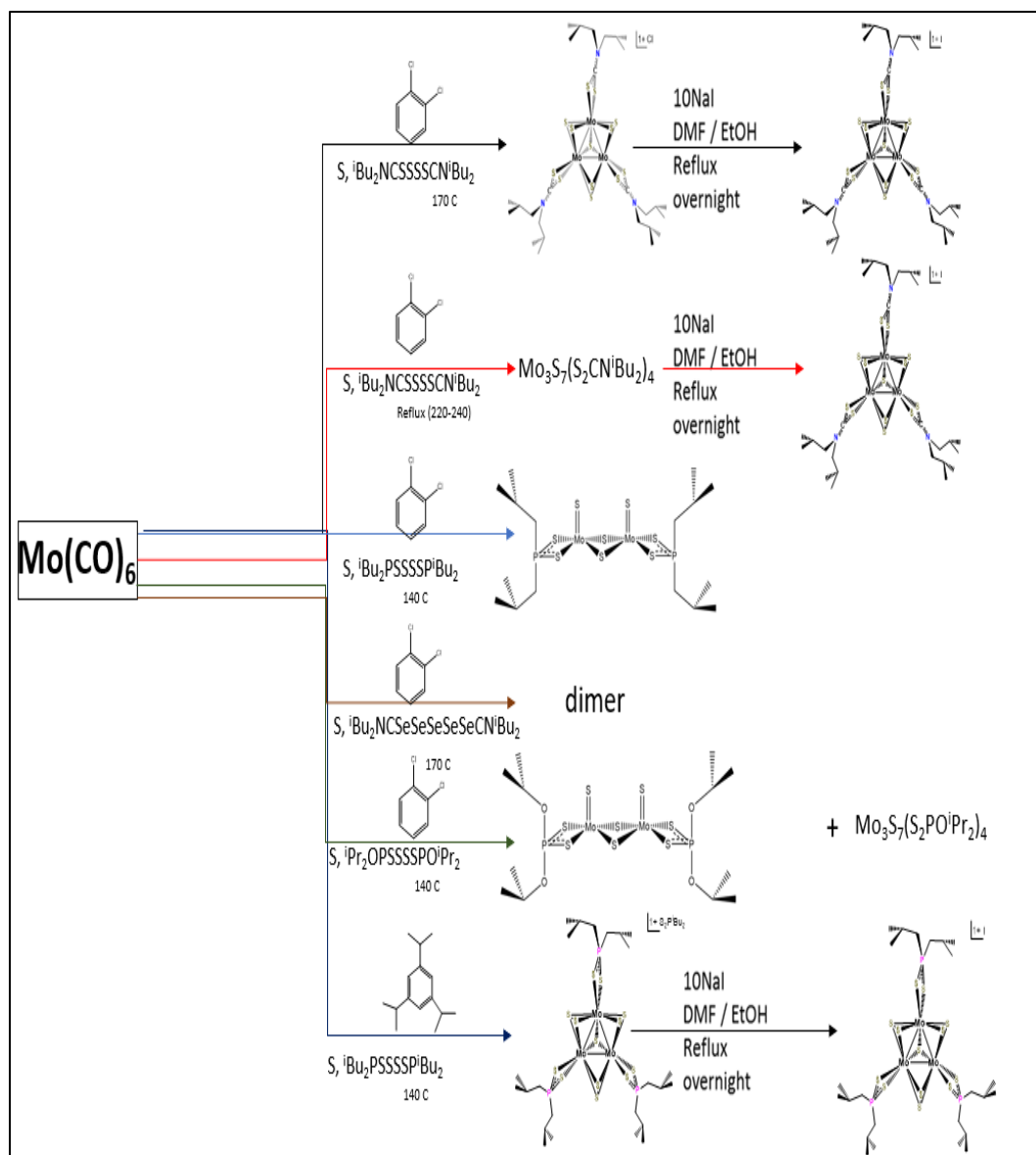


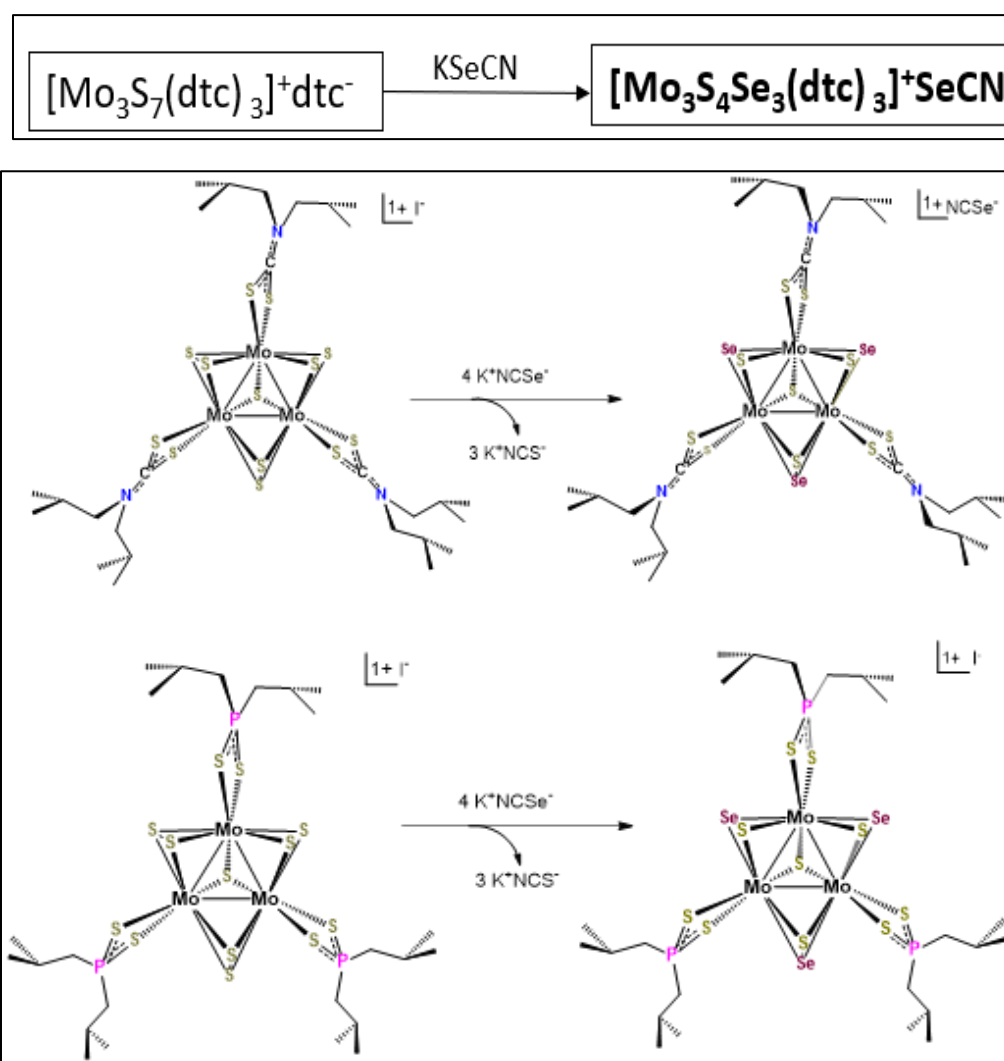
Figure 3.5. ^{31}P NMR spectrum of complex $[\text{Mo}_3\text{S}_7(\text{S}_2\text{P}(\text{O}^i\text{Pr})_2)_3][\text{S}_2\text{P}(\text{O}^i\text{Pr})_2]$.



Scheme 3.6. Synthetic routes to $[\text{Mo}_3\text{S}_7\text{L}_3]^+$ type cluster cations from $\text{Mo}(\text{CO})_6$.

3.3.3 Synthesis of $[\text{Mo}_3\text{S}_4\text{Se}_3\text{L}_3]^+$; $\text{L} = (-\text{S}_2\text{CN}^i\text{Bu}_2, -\text{S}_2\text{P}^i\text{Bu}_2)$ complexes

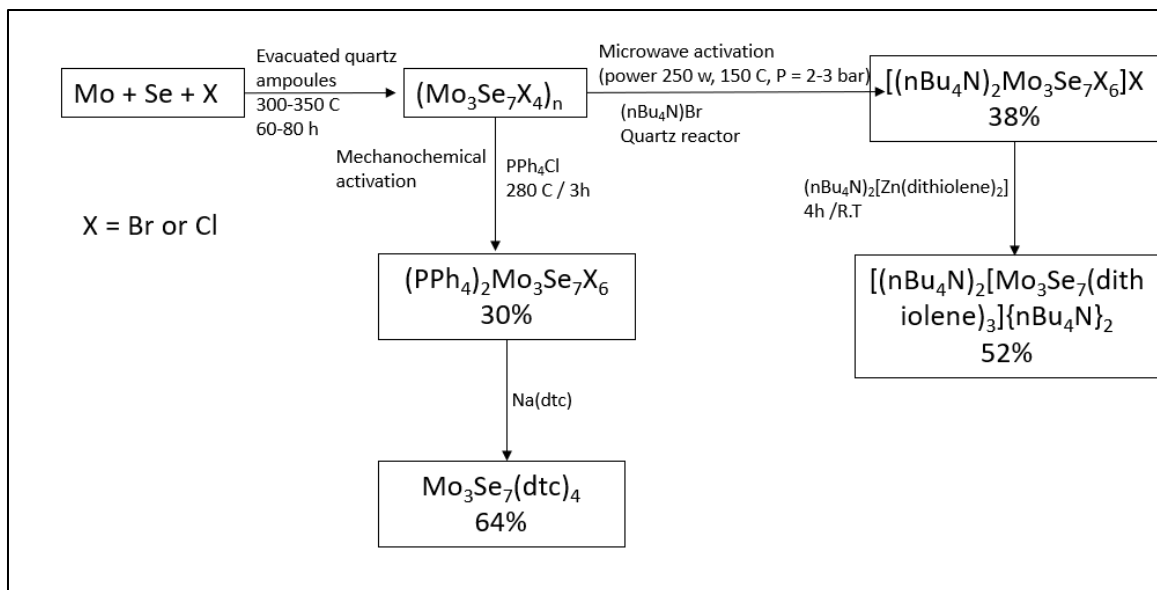
The formation of $[\text{Mo}_3\text{S}_4\text{Se}_3(\text{S}_2\text{CNET}_2)_3] \text{SeCN}$ has been reported³⁶ from $[\text{Mo}_3\text{S}_7(\text{S}_2\text{CNET}_2)_3] \text{S}_2\text{CNET}_2$. The same literature procedure was used for compound $[\text{Mo}_3\text{S}_7(\text{S}_2\text{CN}^i\text{Bu}_2)_3] \text{I}$ to form $[\text{Mo}_3\text{S}_4\text{Se}_3(\text{S}_2\text{CN}^i\text{Bu}_2)_3] \text{SeCN}$. However, for dithiophosphate compounds $[\text{Mo}_3\text{S}_7(\text{S}_2\text{P}^i\text{Bu}_2)_3] \text{I}$ this procedure was applied but the starting material was observed so it was modified with warming the mixture at 50 C for 2 days then $[\text{Mo}_3\text{S}_4\text{Se}_3(\text{S}_2\text{P}^i\text{Bu}_2)_3] \text{I}$ was observed.



Scheme 3.7. Synthetic routes to $[\text{Mo}_3\text{S}_4\text{Se}_3\text{L}_3]^+$ type cluster cations.

3.3.4 Synthesis of $[\text{Mo}_3\text{Se}(\text{Se}_2)_3\text{L}_3]^{4+}$; $\text{L} = (-\text{S}_2\text{CN}^i\text{Bu}_2, -\text{Se}_2\text{CN}^i\text{Bu}_2, -\text{S}_2\text{P}^i\text{Bu}_2, -\text{S}_2\text{P}(\text{O}^i\text{Pr})_2)$ complexes.

As we previously discussed, the discovery of a largest number of the synthesis have been obtained for $[\text{Mo}_3\text{S}(\text{S}_2)_3]^{4+}$ complexes. Particularly different synthetic methods for $[\text{Mo}_3\text{S}(\text{S}_2)_3]^{4+}$ complexes and $[\text{Mo}_3\text{S}_4\text{Se}_3]^{4+}$ complexes have been developed. Moreover, Di cluster compound joint with central chalcogen atom $[\text{Mo}_3\text{S}_7(\text{S}_2\text{CNEt}_2)_3]_2\text{S}^{37}$ have been developed. Most of the work in this area of specifically built polymeric metal sulfide species has been studied. However, the reports of analogs for selenides such as $[\text{Mo}_3\text{Se}(\text{Se}_2)_3]^{4+}$ have been rarely studied. The initial $[\text{Mo}_3\text{Se}(\text{Se}_2)_3]^{4+}$ core compound of $[\text{Mo}_{12}\text{Se}_{56}]^{12-}$ ³⁸ was obtained from metallic Mo and K_2Se_4 in H_2O and it was structurally characterized. Fedin and coworkers developed³⁹ a new method for $[\text{Mo}_3\text{Se}(\text{Se}_2)_3]^{4+}$ complexes from polymeric material $[\text{Mo}_3\text{Se}_7\text{X}_4]_n$ ($\text{X}=\text{Cl}$ or Br) by mechanochemical activation. Furthermore, they discovered another method⁴⁰ for $[\text{Mo}_3\text{Se}_7\text{X}_6]^{2-}$ complexes from polymeric material $[\text{Mo}_3\text{Se}_7\text{X}_4]_n$ by heating. They obtained the first $[\text{Mo}_3\text{Se}(\text{Se}_2)_3]^{4+}$ cluster core supported by dithiocarbamate compounds ($[\text{Mo}_3\text{Se}_7(\text{S}_2\text{CNEt}_2)_3] \text{S}_2\text{CNEt}_2$) from reaction between $[\text{Mo}_3\text{Se}_7\text{X}_6]^{2-}$ and $\text{Na}(\text{S}_2\text{CNEt}_2)$ ligand. The same $[\text{Mo}_3\text{Se}(\text{Se}_2)_3]^{4+}$ cluster supported with dithiocarbamate compounds joint with central Se atom $[\text{Mo}_3\text{Se}_7(\text{S}_2\text{CNEt}_2)_3]_2\text{Se}$ type complex was synthesized by Almond and coworkers⁴¹ from by heating of $\text{Mo}(\text{CO})_6$, elemental Se and $(\text{Et}_2\text{CNS}_2)_2$ in 1,2 dichlorobenzene for 1.5 hours. Gushchin et al⁴² recently reported that, $(^n\text{Bu}_4\text{N})_2\text{Mo}_3\text{Se}_7\text{X}_6]X$ ($\text{X}=\text{Cl}$ or Br) was made by microwave activation of polymeric $\text{Mo}_3\text{Se}_7\text{Br}_4$ and $(^n\text{Bu}_4\text{N})\text{Br}$ and they obtained $(^n\text{Bu}_4\text{N})_2[\text{Mo}_3\text{Se}_7(\text{dithiolene})_3] ^n\text{Bu}_4\text{N}$.



Scheme 3.8. Known synthetic routes to $[\text{Mo}_3\text{Se}_7\text{L}_3]^+$ type cluster cations.

Here in, we propose one of the efficient, cheapest, and a new method for synthesis of $[\text{Mo}_3\text{Se}(\text{Se}_2)_3\text{L}_3]^+$; $\text{L} = (-\text{S}_2\text{CN}^i\text{Bu}_2, -\text{Se}_3\text{CN}^i\text{Bu}_2, -\text{S}_2\text{P}^i\text{Bu}_2, -\text{S}_2\text{P}(\text{O}^i\text{Pr})_2)$ analogs from $\text{Mo}(\text{CO})_6$, elemental Se and $(-\text{S}_2\text{CN}^i\text{Bu}_2)_2$ or $(\text{S}_2\text{P}^i\text{Bu}_2)_2$ in 1,2 dichlorobenzene by simply refluxing at different temperatures for 1.5 hours. This method produced high yield within the short period of time compared with other expensive previously developed methods.

Beginning with $\text{Mo}(\text{CO})_6$, elemental Se and $(^i\text{Bu}_2\text{NCS}_2)_2$ was heated (220 C) under reflux in 1,2 dichlorobenzene for 1.5 hours as previously reported⁴¹ dicluster $[\text{Mo}_3\text{Se}_7(\text{S}_2\text{CN}^i\text{Bu}_2)_3]_2\text{Se}$ was formed. Then it was treated with NaI and formed $[\text{Mo}_3\text{Se}_7(\text{S}_2\text{CN}^i\text{Bu}_2)_3] \text{I}$ cluster. On the other hand, when this reaction mixture was heated at 170 C under reflux, $[\text{Mo}_3\text{Se}_7(\text{S}_2\text{CN}^i\text{Bu}_2)_3] \text{Cl}$ or $[\text{Mo}_3\text{Se}_7(\text{S}_2\text{CN}^i\text{Bu}_2)_3] (\text{S}_2\text{CN}^i\text{Bu}_2)$ formed but this was not characterized by XRD, ESI-MS proved its identity of this compound. Then followed by addition of NaI, $[\text{Mo}_3\text{Se}_7(\text{S}_2\text{CN}^i\text{Bu}_2)_3] \text{I}$ was observed. The same method was applied for $(^i\text{Bu}_2\text{NCS}_2)_2\text{Se}$ triselenocarbamate ligand,

$[\text{Mo}_3\text{Se}_7(\text{Se}_2\text{CN}^i\text{Bu}_2)_3]$ Cl and $[\text{Mo}_3\text{Se}_7(\text{Se}_2\text{CN}^i\text{Bu}_2)_3]$ I were observed. But at 240 C dimer was observed.

For disulfanes ($i\text{Bu}_2\text{PS}_2$)₂, and (($i\text{PrO}$)₂PS₂)₂ the temperature was kept at 140 °C, $\text{Mo}_3\text{Se}_7(\text{S}_2\text{P}(\text{O}^i\text{Pr})_2)_4$ and $\text{Mo}_3\text{Se}_7(\text{S}_2\text{P}^i\text{Bu}_2)_4$ were observed. Followed by NaI addition produced its $\text{Mo}_3\text{Se}_7(\text{S}_2\text{P}^i\text{Bu}_2)_3\text{I}$ cluster.

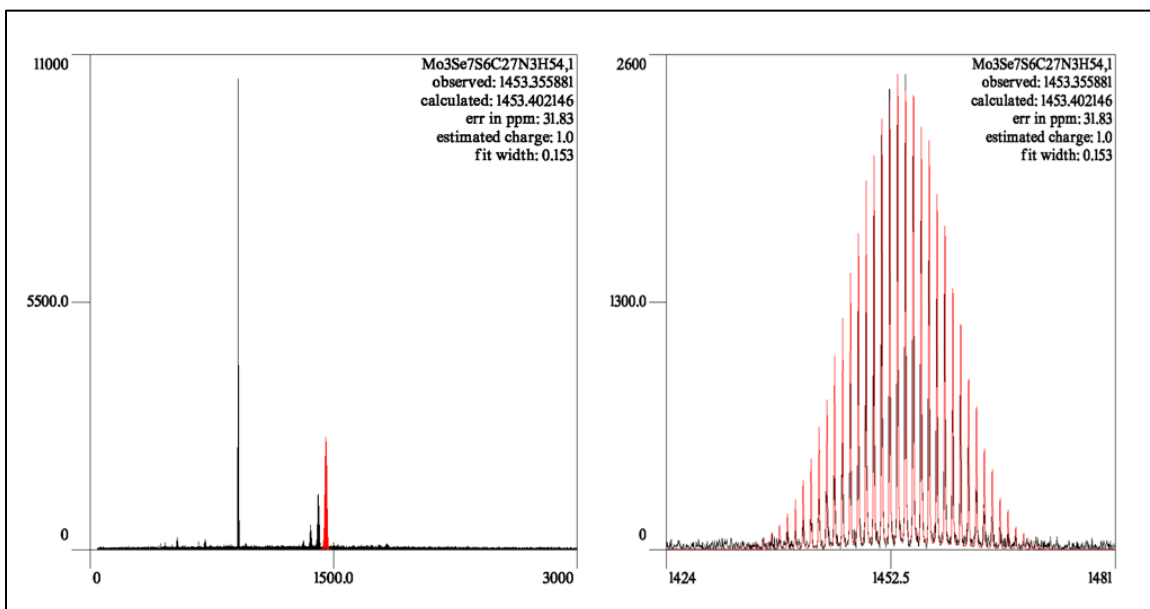
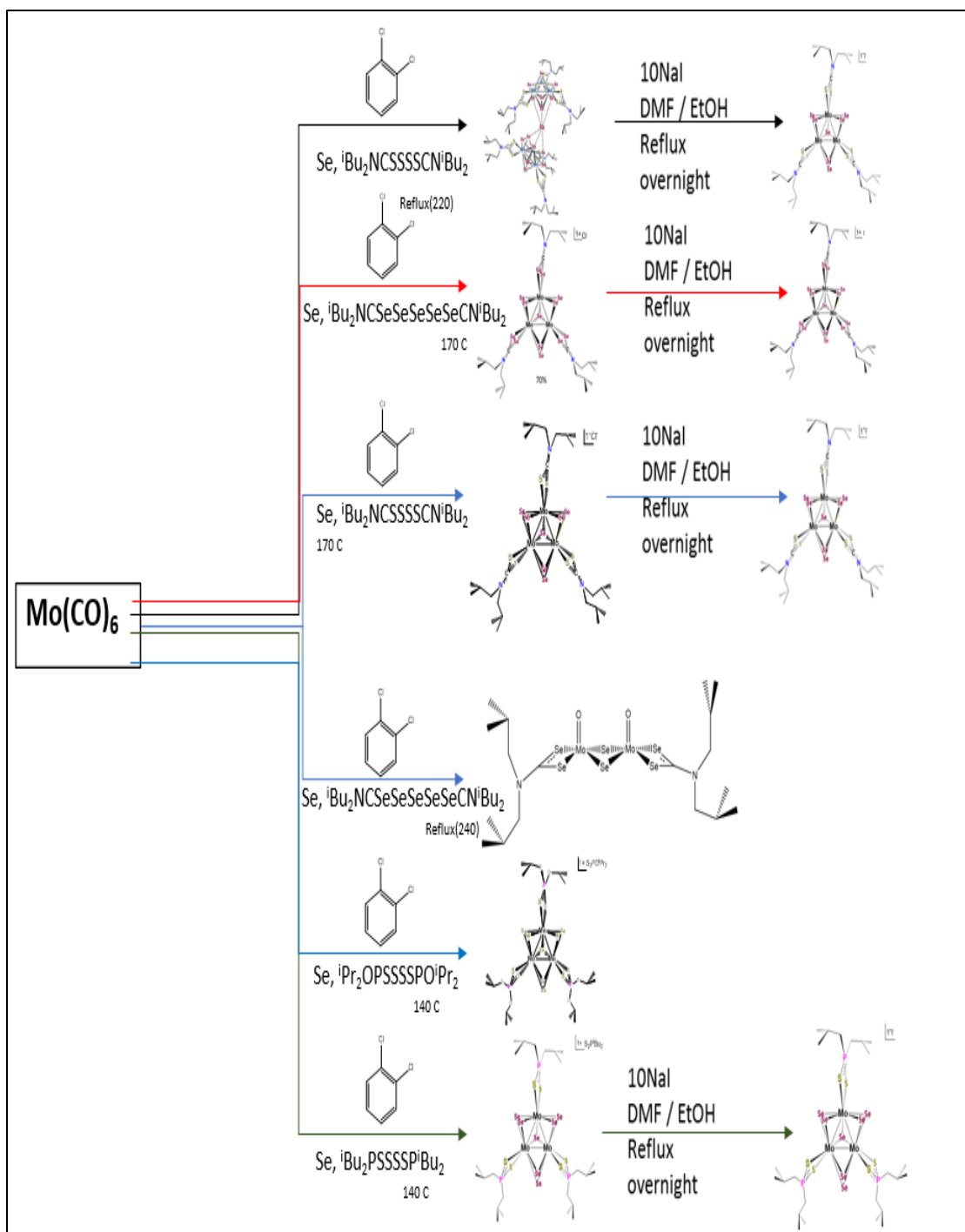


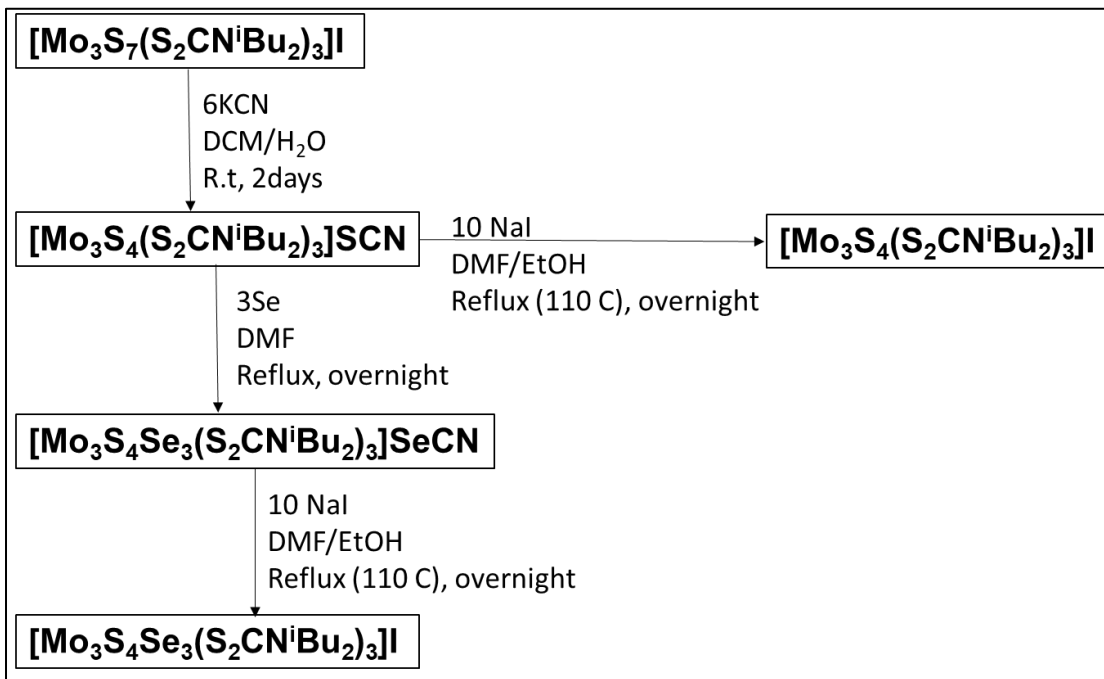
Figure 3.6. ESI-MS spectrum of complex $[\text{Mo}_3\text{Se}_7(\text{S}_2\text{CN}^i\text{Bu}_2)_3]^+$ during the reaction at 170 °C.



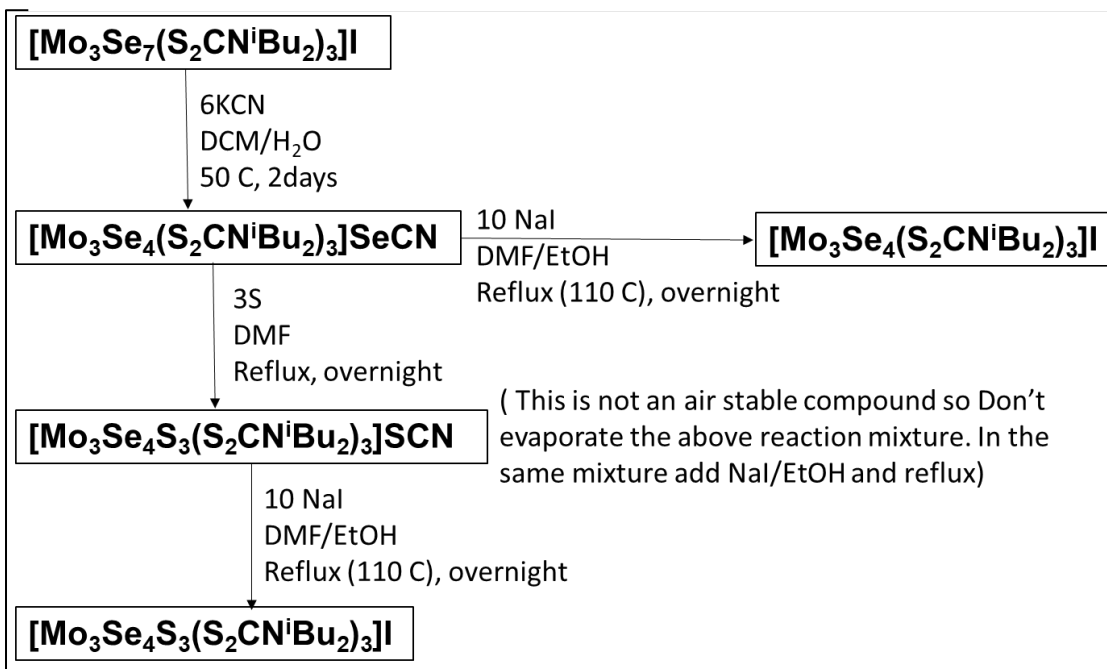
Scheme 3.9. Synthetic routes to $[\text{Mo}_3\text{Se}_7\text{L}_3]^+$ type cluster cations from $\text{Mo}(\text{CO})_6$.

3.3.5 Future work

1) Synthesis of $[\text{Mo}_3\text{S}_4\text{Se}_3\text{L}_3]^+$ and $[\text{Mo}_3\text{Se}_4\text{S}_3\text{L}_3]^+$; $\text{L} = (-\text{S}_2\text{CN}^i\text{Bu}_2, -\text{Se}_2\text{CN}^i\text{Bu}_2, -\text{S}_2\text{P}^i\text{Bu}_2)$ complexes can be achieved by developed new synthetic routes as illustrated in (Scheme 3.10 and Scheme 3.11).



Scheme 3.10. New synthetic routes to $[\text{Mo}_3\text{S}_4\text{Se}_3\text{L}_3]^+$ type cluster cations.



Scheme 3.11. New synthetic routes to $[\text{Mo}_3\text{Se}_4\text{S}_3\text{L}_3]^+$ type cluster cations.

- 2) Try to make $[\text{Mo}_3\text{Te}_7\text{L}_3] +$; $\text{L} = (-\text{S}_2\text{CN}^i\text{Bu}_2, -\text{Se}_2\text{CN}^i\text{Bu}_2, -\text{S}_2\text{P}^i\text{Bu}_2)$ complexes by developed new synthetic route as illustrated in (**Scheme 3.9**) at high temperatures (240 C or above).
- 3) Synthesis of $[\text{Mo}_3\text{S}_7\text{L}_3] \text{Br}$; $\text{L} = (-\text{S}_2\text{CN}^i\text{Bu}_2, -\text{Se}_2\text{CN}^i\text{Bu}_2)$ complexes by developed new synthetic route as illustrated in (**Scheme 3.6**) with 1,2 dibromobenzene lieu of 1,2 dichlorobenzene.
- 4) Similar new synthetic route as illustrated in (**Scheme 3.6**) can be implemented to other metal carbonyls such as $(\text{Co}_2(\text{CO})_8, \text{V}(\text{CO})_6, \text{Cr}(\text{CO})_6, \text{Fe}(\text{CO})_5, \text{Ni}(\text{CO})_5)$ etc)

3.4 Discussion of Crystal Structures

The crystal structure of bis(*O,O'*-di-isopropylphosphorothionyl)disulfide, which is the disulfide form of the *O,O'*-di-isopropyldithiophosphate salt, has been previously reported by others.⁴³ The unit cell found is the same as that observed earlier (Table 3.1), but the quality of the data obtained here, as manifested by final R-factors (Table 3.1) and the low uncertainties in bond parameters, is appreciably improved over the data reported earlier. The compound crystallizes on an inversion center that coincides with the S1–S1A midpoint (Figure 3.7), which has a length of 2.1106(3) Å as consistent with its single bond character.

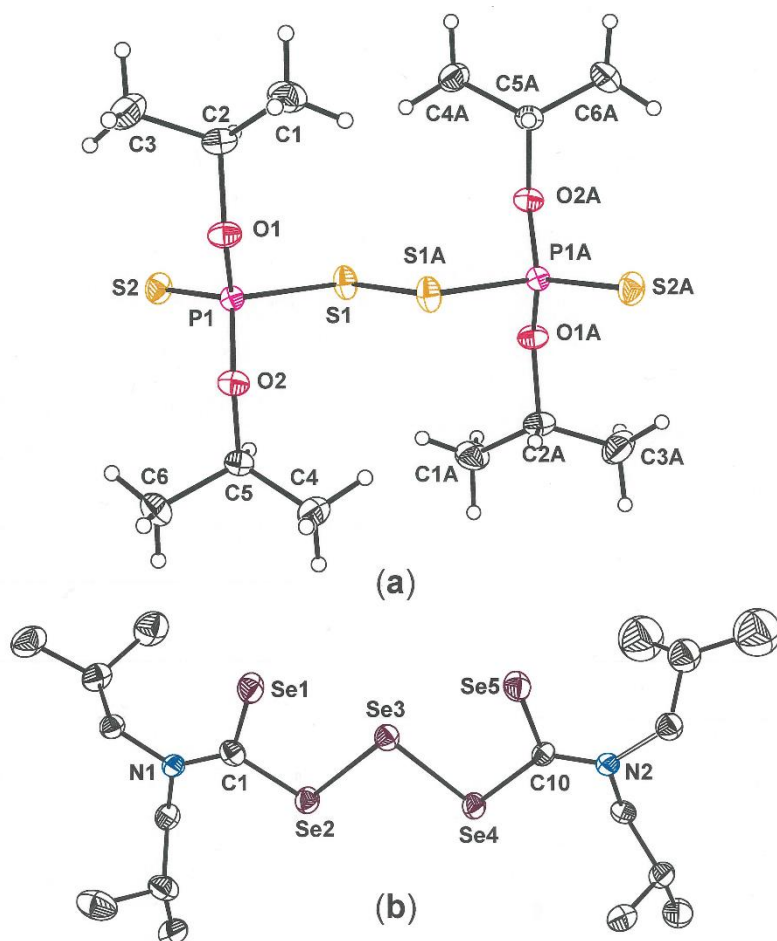
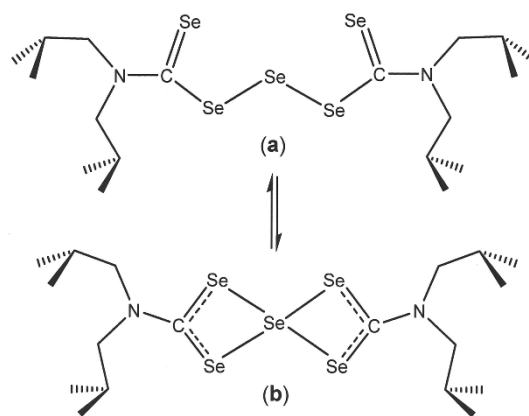


Figure 3.7. Thermal ellipsoid plots (50%) for bis(*O,O'*-di-isopropylphosphorothionyl)disulfide (a), and bis[[bis(2-methylpropyl)amino]selenoxomethyl] triselenide (b). All H atoms are omitted for clarity.

The terminal phosphorus bond (P1–S2) has a length of 1.9205(2), which is consistent with its ylid character and contrasts with the P1–S1 single bond length of 2.0822(3) Å. Related compounds that have been structurally characterized are those Me,⁴⁴ Np,⁴⁴ Cy,⁴⁵ Ph,⁴⁶ and *p*-tolyl⁴⁷ in place of *i*Pr.

Bis[[bis(2-methylpropyl)amino]selenoxomethyl] triselenide, although not the intended diselenide, nevertheless serves as a source of the corresponding diselenocarbamate ligand when use in the same fashion as tetraalkyl thiuram disulfides (**Figure 3.7, (b)**). This compound has been previously prepared and identified as being, on the basis of ⁷⁷Se NMR, in solution equilibrium between an open chain form ((a) in **Scheme 3.12**) and a chelating form ((b) in **Scheme 3.12**).⁴⁷ The Se2–Se(3) and Se3–Se4 bond distances are 2.4674(12) Å and 2.4642(13) Å, respectively, which are similar to the 2.446 Å and 2.479 Å distance reported for the analogous compound reported with Et groups. The Se1⋯Se3 and Se5⋯Se3 distances are appreciable longer at 2.8309(13) Å and 2.7999(13) Å, respectively; indicating that chelation of the central Se atom, to the extent that such description is appropriate, is weak and readily gives way to the linear triselenide structure. However, the crystallographic van der Waals radius reported for selenium is 1.9 Å, well beyond half the Se1⋯Se3 and Se5⋯Se3 separations. This fact argues that the interactions are both real bonding interactions and non-negligible in degree.



Scheme 3.12. Proposed solution equilibrium for $i\text{Bu}_2\text{NC}(\text{Se})\text{SeSeSeC}(\text{Se})\text{N}^i\text{Bu}_2$, as deduced by ⁷⁷Se NMR.

Table 3.1. Crystal and refinement data for bis(O,O'-di-isopropylphosphorothionyl)disulfide, and bis[[bis(2-methylpropyl)amino]selenoxomethyl] triselenide.

compound	(ⁱ PrO) ₂ P(S)SSP(S)(O ⁱ Pr) ₂	^t Bu ₂ NC(Se)SeSeSeC(Se)N ⁱ Bu ₂
structure code	JPD1268	JPD1141
formula	C ₁₂ H ₂₈ O ₄ P ₂ S ₄	C ₁₈ H ₃₆ N ₂ Se ₅
FW	426.52	675.29
temperature, K	150	150
wavelength, Å	0.71073	0.71073
2θ range, deg.	2.442 – 38.450	4.606 – 58.542
crystal system	triclinic	monoclinic
space group	<i>P</i> -1	<i>P</i> 2 ₁ / <i>n</i>
<i>a</i> , Å	8.1001(8)	12.6525(11)
<i>b</i> , Å	8.3522(8)	11.7435(11)
<i>c</i> , Å	8.4745(8)	18.2297(15)
<i>α</i> , deg.	97.731(4)	90
<i>β</i> , deg.	111.085(3)	106.629(3)
<i>γ</i> , deg.	94.678(4)	90
volume, Å ³	524.82(9)	2595.4(4)
<i>Z</i>	1	4
density, g/cm ³	1.350	1.728
<i>μ</i> , mm ⁻¹	0.616	7.062
F(000)	11552	1312
crystal size	0.248 x 0.273 x 0.563	0.128 x 0.286 x 0.361
color, habit	colorless block	orange block
limiting indices, <i>h</i>	-15 ≤ <i>h</i> ≤ 15	-17 ≤ <i>h</i> ≤ 16
limiting indices, <i>k</i>	-15 ≤ <i>k</i> ≤ 15	0 ≤ <i>k</i> ≤ 16
limiting indices, <i>l</i>	-16 ≤ <i>l</i> ≤ 16	0 ≤ <i>l</i> ≤ 25
reflections collected	40335	16311
independent data	7197	16311
restraints	0	12
parameters refined	104	247
GooF ^a	1.063	1.040
R1, ^{b,c} wR2 ^{d,c}	0.0253, 0.0673	0.0727, 0.1540
R1, ^{b,e} wR2 ^{d,e}	0.0318, 0.0710	0.1042, 0.1704
largest diff. peak, e·Å ⁻³	0.395	1.306
largest diff. hole, e·Å ⁻³	-0.216	-1.396

^aGooF = {Σ[w(F_o² - F_c²)²]/(n - p)}^{1/2}, where n = number of reflections and p is the total number of parameters refined; ^bR1 = Σ||F_o| - |F_c||/Σ|F_o|; ^cR indices for data cut off at I > 2σ(I); ^dwR2 = {Σ[w(F_o² - F_c²)²]/Σw(F_o²)²}^{1/2}; w = 1/[σ²(F_o²) + (xP)² + yP], where P = (F_o² + 2F_c²)/3; ^eR indices for all data.

Table 3.2. Crystal and refinement data for structurally characterized Mo₃ and Mo₂ compounds.

compound	[Mo ₃ S ₄ Se ₃ (S ₂ CN ^t Bu ₂) ₃] ⁺	[Mo ₃ S ₇ (S ₂ P ^t Bu ₂) ₃] ⁺	[Mo ₃ Se ₇ (S ₂ P(O ^t Pr) ₂) ₃] ⁺
counteranion	[SeCN] ⁻	[I] ⁻	[S ₂ P(O ^t Pr) ₂] ⁻
structure code	JPD1002	JPD839	JPD1296
compound abbrev.	[2a]SeCN	[1e]I	[3f][S ₂ P(O ^t Pr) ₂]
solvent	¹ / ₂ (DCE)· ¹ / ₂ ^t BuOMe	-	¹ / ₄ Et ₂ O
formula	C _{31.50} H ₆₂ ClMo ₃ N ₄ O _{0.50} S ₁₀ Se ₄	C ₂₄ H ₅₄ IMo ₃ P ₃ S ₁₃	C ₂₅ H _{58.50} Mo ₃ O _{8.25} P ₄ S ₈ Se ₇
FW	1464.56	1267.08	1712.11
temperature, K	150	100	150
wavelength, Å	0.71073	0.71073	0.71073
2θ range, deg.	2.442 – 38.450	2.746 – 57.662	4.458 – 53.034
crystal system	tetragonal	orthorhombic	triclinic
space group	<i>I</i> 4 ₁ / <i>a</i>	<i>Pna</i> 2 ₁	<i>P</i> -1
<i>a</i> , Å	35.378(4)	11.5814(18)	13.7582(4)
<i>b</i> , Å	35.378(4)	23.552(4)	14.3562(4)
<i>c</i> , Å	18.903(2)	19.102(3)	16.1940(5)
<i>α</i> , deg.	90	90	72.260(2)
<i>β</i> , deg.	90	90	72.906(2)
<i>γ</i> , deg.	90	90	68.909(2)
volume, Å ³	23659(6)	5210.2(14)	2780.59(15)
<i>Z</i>	16	4	2
density, g/cm ³	1.645	1.615	2.045
μ, mm ⁻¹	3.512	1.934	5.701
F(000)	11552	2520	1653
crystal size	0.150 x 0.150 x 0.200	0.084 x 0.212 x 0.273	0.139 x 0.173 x 0.326
color, habit	red-orange block	orange plate	orange plate
limiting indices, <i>h</i>	-32 ≤ <i>h</i> ≤ 32	-15 ≤ <i>h</i> ≤ 15	-17 ≤ <i>h</i> ≤ 17
limiting indices, <i>k</i>	-32 ≤ <i>k</i> ≤ 32	-31 ≤ <i>k</i> ≤ 30	-17 ≤ <i>k</i> ≤ 18
limiting indices, <i>l</i>	-17 ≤ <i>l</i> ≤ 17	-25 ≤ <i>l</i> ≤ 25	-20 ≤ <i>l</i> ≤ 20
reflections collected	48575	47648	105771
independent data	4894	13014	11504
restraints	22	1	5
parameters refined	513	410	517
GooF ^a	1.130	1.005	1.036
R1, ^{b,c} wR2 ^{d,e}	0.0455, 0.1263	0.0356, 0.0804	0.0650, 0.1461
R1, ^{b,e} wR2 ^{d,e}	0.0581, 0.1378	0.0455, 0.0839	0.1035, 0.1771
largest diff. peak, e·Å ⁻³	1.183	1.005	2.125
largest diff. hole, e·Å ⁻³	-0.499	-0.566	-2.154

^aGooF = {Σ[w(F_o² - F_c²)²]/(n - p)}^{1/2}, where n = number of reflections and p is the total number of parameters refined; ^bR1 = Σ||F_o - F_c||/Σ|F_o|; ^cR indices for data cut off at I > 2σ(I); ^dwR2 = {Σ[w(F_o² - F_c²)²]/Σw(F_o²)²}^{1/2}; w = 1/[σ²(F_o²) + (xP)² + yP], where P = (F_o² + 2F_c²)/3; ^eR indices for all data.

Table 3.2., Cont'd. Crystal and refinement data for structurally characterized Mo₃ and Mo₂ compounds.

compound	[Mo ₃ S ₄ Se ₃ (S ₂ CN ^t Bu ₂) ₃] ⁺	[Mo ₃ Se ₇ (S ₂ CN ^t Bu ₂) ₃] ⁺	[Mo ₃ Se ₇ (Se ₂ CN ^t Bu ₂) ₃] ⁺
counteranion	[I] ⁻	[I] ⁻	[I] ⁻
structure code	JPD1097	JPD1172	JPD1375
compound abbrev.	[2a]I	[3a]I	[3c]I
solvent	1/2(C ₅ H ₁₀)	1/6(DCE)·1/3(C ₅ H ₁₀)	-
formula	C _{26.50} H ₆₀ IMo ₃ P ₃ S ₁₀ Se ₃	C ₂₉ H _{54.67} Cl _{0.33} Mo ₃ N ₃ S ₆ Se ₇	C ₂₇ H ₅₄ IMo ₃ N ₃ Se ₁₃
FW	1443.85	1617.04	1861.93
temperature, K	150	156	150
wavelength, Å	0.71073	0.71073	0.71073
2θ range, deg.	4.234 – 54.498	2.500 - 59.290	3.576 – 52.888
crystal system	monoclinic	monoclinic	monoclinic
space group	C2/c	P2 ₁ /c	P2 ₁ /c
a, Å	32.047(3)	27.7223(12)	28.1698(14)
b, Å	17.7330(14)	13.5820(4)	13.6823(7)
c, Å	20.1100(15)	40.7503(11)	41.079(2)
α, deg.	90	90	90
β, deg.	106.950(2)	90.917(1)	90.876(1)
γ, deg.	90	90	90
volume, Å ³	10931.9(15)	15341.5(8)	15831.3(14)
Z	8	12	12
density, g/cm ³	1.755	2.100	2.344
μ, mm ⁻¹	3.729	6.597	10.276
F(000)	5640	9220	10296
crystal size	0.060 x 0.206 x 0.217	0.312 x 0.406 x 0.503	0.022 x 0.145 x 0.364
color, habit	orange plate	thick red-orange plate	yellow plate
limiting indices, h	-41 ≤ h ≤ 41	-38 ≤ h ≤ 38	-35 ≤ h ≤ 35
limiting indices, k	-22 ≤ k ≤ 22	-18 ≤ k ≤ 18	-17 ≤ k ≤ 17
limiting indices, l	-25 ≤ l ≤ 25	-56 ≤ l ≤ 56	-51 ≤ l ≤ 51
reflections collected	144302	1076082	285209
independent data	12155	43161	32504
restraints	101	0	0
parameters refined	465	1329	1290
GooF ^a	1.072	1.080	1.019
R1, ^{b,c} wR2 ^{d,e}	0.0638, 0.1794	0.0566, 0.1495	0.0519, 0.0935
R1, ^{b,e} wR2 ^{d,e}	0.0877, 0.2066	0.0695, 0.1615	0.1003, 0.116
largest diff. peak, e·Å ⁻³	1.791	2.620	1.344
largest diff. hole, e·Å ⁻³	-2.021	-5.018	-1.641

^aGooF = {Σ[w(F_o² - F_c²)]/(n - p)}^{1/2}, where n = number of reflections and p is the total number of parameters refined; ^bR1 = Σ||F_o| - |F_c||/Σ|F_o|; ^cR indices for data cut off at I > 2σ(I); ^dwR2 = {Σ[w(F_o² - F_c²)²]/Σw(F_o²)²}^{1/2}; w = 1/[σ²(F_o²) + (xP)² + yP], where P = (F_o² + 2F_c²)/3; ^eR indices for all data.

Table 3.2., Cont'd. Crystal and refinement data for structurally characterized Mo₃ and Mo₂ compounds

compound	[Mo ₃ Se ₇ (S ₂ P(O ⁱ Pr) ₂) ₃] ⁺	[(ⁱ Bu ₂ NCS ₂)Mo(O)(μ-S)] ₂	[(ⁱ PrO) ₂ PS ₂)Mo(S)(μ-S)] ₂
counteranion	[S ₂ P(O ⁱ Pr) ₂] ⁻	-	-
structure code	JPD1296	JPD1106	JPD1309
compound abbrev.	[3f] [S ₂ P(O ⁱ Pr) ₂]	4	5
solvent	¹ / ₄ Et ₂ O	-	-
formula	C ₂₅ H _{58.50} Mo ₃ O _{8.25} P ₄ S ₈ Se ₇	C ₁₈ H ₃₆ Mo ₂ N ₂ O ₂ S ₆	C ₁₂ H ₂₈ Mo ₂ O ₄ P ₂ S ₈
FW	1712.11	696.73	746.64
temperature, K	150	150	150
wavelength, Å	0.71073	0.71073	0.71073
2θ range, deg.	4.458 – 53.034	2.336 – 46.604	4.760 – 52.856
crystal system	triclinic	monoclinic	monoclinic
space group	<i>P</i> -1	<i>P</i> 2 ₁ / <i>c</i>	<i>P</i> 2 ₁ / <i>c</i>
<i>a</i> , Å	13.7582(4)	18.7482(8)	12.6795(5)
<i>b</i> , Å	14.3562(4)	9.6344(4)	13.8455(6)
<i>c</i> , Å	16.1940(5)	16.9043(7)	16.1584(6)
<i>α</i> , deg.	72.260(2)	90	90
<i>β</i> , deg.	72.906(2)	111.590(1)	101.481(1)
<i>γ</i> , deg.	68.909(2)	90	90
volume, Å ³	2780.59(15)	2839.2(2)	2779.91(19)
<i>Z</i>	2	4	4
density, g/cm ³	2.045	1.630	1.784
μ, mm ⁻¹	5.701	1.342	1.635
F(000)	1653	1416	1496
crystal size	0.139 x 0.173 x 0.326	0.051 x 0.062 x 0.252	0.009 x 0.189 x 0.357
color, habit	orange plate	yellow column	brown plate
limiting indices, <i>h</i>	-17 ≤ <i>h</i> ≤ 17	-20 ≤ <i>h</i> ≤ 20	-15 ≤ <i>h</i> ≤ 15
limiting indices, <i>k</i>	-17 ≤ <i>k</i> ≤ 18	-10 ≤ <i>k</i> ≤ 10	-17 ≤ <i>k</i> ≤ 17
limiting indices, <i>l</i>	-20 ≤ <i>l</i> ≤ 20	-18 ≤ <i>l</i> ≤ 18	-20 ≤ <i>l</i> ≤ 20
reflections collected	105771	65330	88748
independent data	11504	4109	5684
restraints	5	0	0
parameters refined	517	279	261
Goof ^a	1.036	1.175	1.018
R1, ^{b,c} wR2 ^{d,c}	0.0650, 0.1461	0.0476, 0.0931	0.0230, 0.0574
R1, ^{b,e} wR2 ^{d,e}	0.1035, 0.1771	0.0595, 0.0973	0.0345, 0.0642
abs. struct. param	-	-	-
largest diff. peak, e ⁻ Å ⁻³	2.125	0.831	0.439
largest diff. hole, e ⁻ Å ⁻³	-2.154	-0.472	-0.343

^aGoof = {Σ[w(F_o² - F_c²)²]/(n - p)}^{1/2}, where n = number of reflections and p is the total number of parameters refined; ^bR1 = Σ||F_o| - |F_c||/Σ|F_o|; ^cR indices for data cut off at I > 2σ(I); ^dwR2 = {Σ[w(F_o² - F_c²)²]/Σw(F_o²)²}^{1/2}; w = 1/[σ²(F_o²) + (xP)² + yP], where P = (F_o² + 2F_c²)/3; ^eR indices for all data.

Table 3.2., Cont'd. Crystal and refinement data for structurally characterized Mo₃ and Mo₂ compounds.

compound	[(^t Bu ₂ NCSe ₂)Mo(O)(μ-Se)] ₂
counteranion	-
structure code	JPD1293
compound abbrev.	6
solvent	-
formula	C ₁₈ H ₃₆ Mo ₂ N ₂ O ₂ Se ₆
FW	978.13
temperature, K	273
wavelength, Å	0.71073
2θ range, deg.	4.544 – 61.106
crystal system	monoclinic
space group	<i>Cc</i>
<i>a</i> , Å	11.3342(6)
<i>b</i> , Å	17.9266(10)
<i>c</i> , Å	14.5595(8)
<i>α</i> , deg.	90
<i>β</i> , deg.	95.7698(19)
<i>γ</i> , deg.	90
volume, Å ³	2943.3(3)
<i>Z</i>	4
density, g/cm ³	2.207
<i>μ</i> , mm ⁻¹	8.289
F(000)	1848
crystal size	0.090 x 0.221 x 0.286
color, habit	yellow block
limiting indices, <i>h</i>	-16 ≤ <i>h</i> ≤ 16
limiting indices, <i>k</i>	-25 ≤ <i>k</i> ≤ 25
limiting indices, <i>l</i>	-20 ≤ <i>l</i> ≤ 20
reflections collected	29564
independent data	8643
restraints	2
parameters refined	280
GooF ^a	1.054
R1, ^{b,c} wR2 ^{d,c}	0.0356, 0.0818
R1, ^{b,e} wR2 ^{d,e}	0.0435, 0.0876
abs. struct. param	0.049(10)
largest diff. peak, e ⁻ Å ⁻³	1.568
largest diff. hole, e ⁻ Å ⁻³	-1.037

^aGooF = {Σ[w(F_o² - F_c²)²]/(n - p)}^{1/2}, where n = number of reflections and p is the total number of parameters refined; ^bR1 = Σ||F_o|| - |F_c||/Σ|F_o||; ^cR indices for data cut off at I > 2σ(I); ^dwR2 = {Σ[w(F_o² - F_c²)²]/Σw(F_o²)²}^{1/2}; w = 1/[σ²(F_o²) + (xP)² + yP], where P = (F_o² + 2F_c²)/3; ^eR indices for all data.

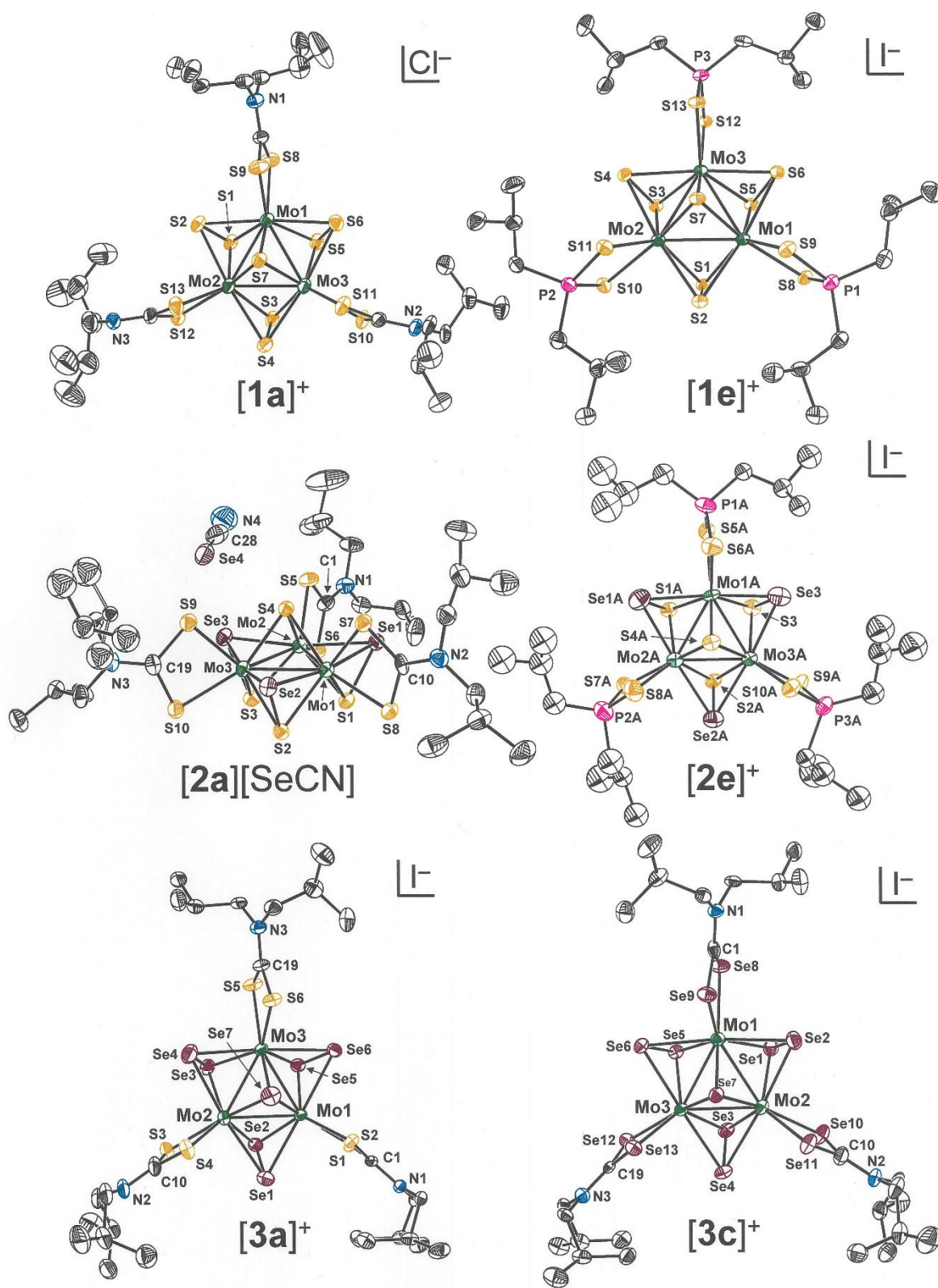


Figure 3.8. Thermal ellipsoid plots (50%) of $[1a]^+$, $[1e]^+$, $[2a][SeCN]$, $[2e]^+$, $[3a]^+$, and $[3c]^+$. For clarity, all H atoms are omitted, and any disorder is edited to show only one of two parts.

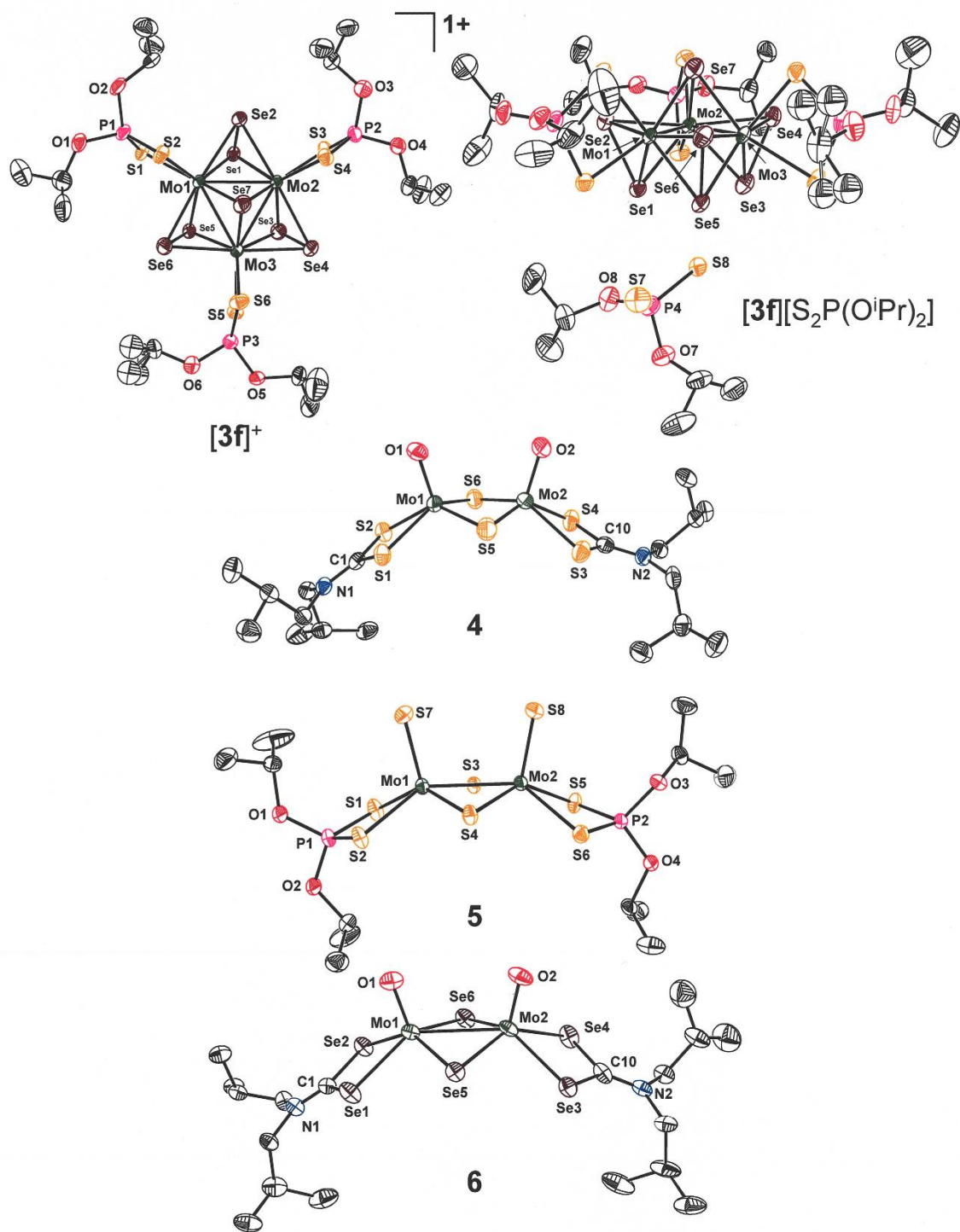


Figure 3.9. Thermal ellipsoid plots (50%) of $[3f]^+$, **4**, **5**, and **6**. For clarity, all H atoms are omitted, and any disorder is edited to show only one of two parts.

The isostructural clusters illustrated in **Figures 3.8 and 3.9** are defined by an equilateral triangle of Mo^{IV} ions that are joined by a single chalcogenide dianion, either S^{2-} or Se^{2-} ($\mu_3\text{Q}^{2-}$), in a μ_3 -bridging mode and by three identical dichalcogenide ligands, either S_2^{2-} , Se_2^{2-} or SeS^{2-} , that are situated at the midpoints of the intermetal vectors. These dichalcogenide ligands are asymmetrically positioned such that one atom is within the M_3 plane (Q_{eq}) while other (Q_{ax}) is held somewhat below the M_3 plane on the side opposite the $\mu_3\text{Q}^{2-}$ ligand (**Figure 3.10**). The chemical lability that distinguishes the Q_{eq} atom from the Q_{ax} atom and enables formation of the complexes with mixed dichalcogenide SeS^{2-} is reflected in $\text{M}-\text{Q}_{\text{eq}}$ bond lengths that are $\sim 0.06 - 0.08 \text{ \AA}$ longer than the $\text{M}-\text{Q}_{\text{ax}}$ interatomic distances (**Table 3.3**). Excision of the Q_{eq} atoms produces $[\text{M}_3\text{S}_4]^{4+}$ voided cubanes that provide ingress to a broad range of homo- and heterometallic cubanes. Completing the coordination sphere at each metal ion is a dithiocarbamate, diselenocarbamate, or dithiophosphate ligand (**Figure 3.10**), whose three-atom chelate is oriented with near orthogonality to the M_3 plane (*cf* θ , **Table 3.3**). A tighter binding of the $\mu_3\text{Q}^{2-}$ atom to M than the Q_{ax} atom is revealed in $\text{M}-\mu_3\text{Q}$ bond lengths that are $\sim 0.03-0.04 \text{ \AA}$ shorter than the corresponding $\text{M}-\text{Q}_{\text{ax}}$ values (**Table 3.3**) and additionally manifested by a *trans* influence upon the chelating ligand that renders its chelation modestly asymmetric. The $\text{M}-\text{E}_{\text{anti}}$ bond lengths consistently exceed the $\text{M}-\text{E}_{\text{syn}}$ bond lengths by $\sim 0.03 \text{ \AA}$, a difference that is significant within the resolution of the data. In all instances, the soft counteranion to the cluster is ensconced in close proximity (**Table 3.3**)

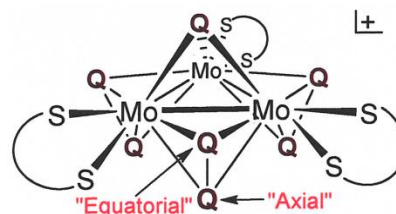


Figure 3.10. Illustration of the distinction between equatorial and axial positions in bridging dichalcogenide ligands.

Table 3.3. Selected interatomic distances (Å) and angles (deg.) for triangular M₃ cations. Averaged values^a are presented for distances and angles that are chemically identical.

	[1a]Cl ^f	[1e]I	[2a][SeCN]	[3a]I ^{g,h,i,j}	[3c]I ^{g,h,i,k}	[4a]I ^{j,l,m}
M–M ^b	2.7129[3]	2.7285[5]	2.7278[8]	2.7950[3]	2.7718[4]	2.7092[4]
M–μ ₃ Q	2.3745[7]	2.3775[9]	2.370[2]	2.4718[4]	2.5052[4]	2.393[1]
M–Q _{ax}	2.4068[5]	2.4075[7]	2.421[1]	2.5416[2]	2.5472[3]	2.418[1]
M–Q _{eq}	2.4854[5]	2.4867[7]	2.6063[6]	2.6006[2]	2.6100[3]	2.496[1]
Q–Q	2.051[1]	2.053[1]	2.229[2]	2.3158[4]	2.3271[5]	2.068[2]
M–E _{dte,syn} ^c	2.4674[7]	2.5126[9]	2.469[2]	2.4846[4]	2.6053[4]	2.471[1]
M–E _{dte,anti} ^d	2.5141[7]	2.536[1]	2.527[2]	2.5227[6]	2.6425[4]	2.507[1]
M–μ ₃ Q–M	69.68[2]	70.03[2]	70.28[5]	67.79[1]	67.18[1]	68.96[3]
M–Q _{ax} –M	68.61[2]	69.04[2]	68.58[5]	65.69[1]	65.92[1]	68.15[3]
M–Q _{eq} –M	66.15[2]	66.54[2]	63.11[2]	64.02[1]	64.15[1]	65.73[3]
Q _{ax} –M–Q _{ax}	84.44[2]	84.31[3]	83.79[6]	83.11[1]	83.05[1]	85.02[4]
Q _{eq} –M–Q _{eq}	171.40[3]	171.05[3]	168.96[3]	167.21[1]	166.94[2]	171.06[4]
Q _{eq} –M–Q _{ax}	49.54[2]	49.58[2]	52.48[3]	53.52[1]	53.63[1]	49.75[3]
μ ₃ Q–M–Q _{ax}	110.30[2]	109.95[2]	110.10[4]	112.63[1]	112.80[1]	110.79[3]
μ ₃ Q–M–Q _{eq}	85.73[2]	85.56[2]	84.35[3]	84.05[1]	83.84[1]	85.53[3]
θ ^e	87.1[1]	87.67[5]	87.4[2]	88.2[1]	88.0[1]	88.8[2]

^aFor averaged values, uncertainties are determined using the general formula for error propagation as described by Taylor⁴⁵ and are enclosed with square brackets; ^bM = metal; ^cM–E bond length for dichalcogenocarbamate atom or ⁻S₂PⁱBu₂ sulfur atom on the same side of the M₃ plane as the μ₃S ligand; ^dM–E bond length for dichalcogenocarbamate atom or ⁻S₂PⁱBu₂ sulfur atom on the opposite side of the M₃ plane as the μ₃S ligand; ^eθ = Angle between M₃ plane and E₂C or S₂P plane of chelating ligand; ^fValues are averaged across 2 independent clusters in the asymmetric unit; ^gValues are averaged across 3 independent clusters in the asymmetric unit; ^hM = Mo; ⁱQ = Se; ^jE = S; ^kE = Se; ^lM = W; ^mQ = S.

to the Q_{ax} atoms of the bridging Q_{eq}–Q_{ax} ligands, which bear a distinctive electrophilic character that has been noted early in the elucidation of these clusters and their properties.

3.5 Electrochemistry

3.5.1 Cyclic Voltammetry and Differential Pulse Voltammetry

The laboratory experiment for electrochemistry will introduce cyclic voltammetry. This is one of the rapid and powerful methods for characterizing the electrochemical behavior of

compounds can provide information as to whether they can be electrochemically oxidized or reduced.

To analyze the electrochemical behavior of Mo_3S_7 , $\text{Mo}_3\text{S}_4\text{Se}_3$ & Mo_3Se_7 complexes cyclic voltammetry was used. Here, there are 3 standard electrode setups that were used. Pt wire (Auxiliary or counter electrode (CE)), Ag/AgCl reference electrode (RE) and glassy carbon working electrode (WE). DCM was used as a solvent (7ml) and $[\text{Bu}_4\text{N}] [\text{PF}_6]$ was used as electrolyte. For each experiment 100 mVs^{-1} scan rate was carried out.

For the differential pulse voltammetry measurements, here the same experimental set up was carried out like cyclic voltammetry. The potential was scanned only in the negative, cathode directions.

3.5.1.1 $[\text{Mo}_3\text{S}_7(\text{S}_2\text{CN}^i\text{Bu}_2)_3] \text{I}$

Cyclic voltammetry measurements for $[\text{Mo}_3\text{S}_7(\text{S}_2\text{CN}^i\text{Bu}_2)_3] \text{I}$, the whole window shows 3 reductions peaks followed by two irreversible oxidations peaks. Moreover, the third reduction is reversible with an $E_{1/2} = -1.22\text{V}$.

DPV measurements show its all reductions within the 0 to -1.6V window. It showed four reductions with its reversible third reduction at $E_{1/2} = -1.12\text{V}$

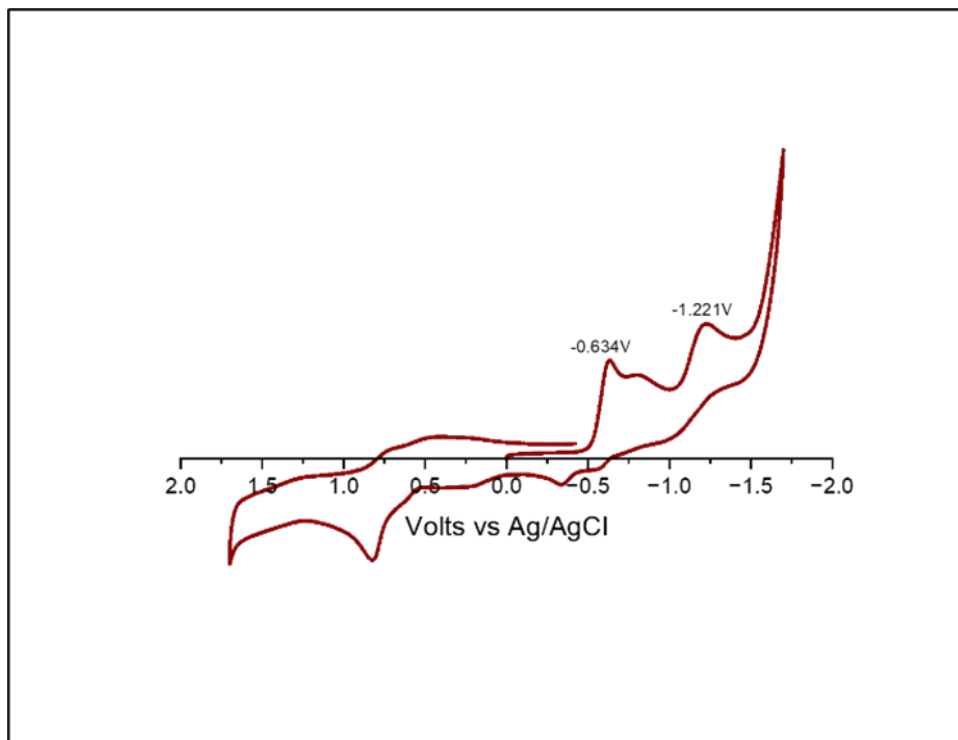


Figure 3.11. The whole CV window for $[\text{Mo}_3\text{S}_7(\text{S}_2\text{CN}^i\text{Bu}_2)_3]\text{I}$ in DCM.

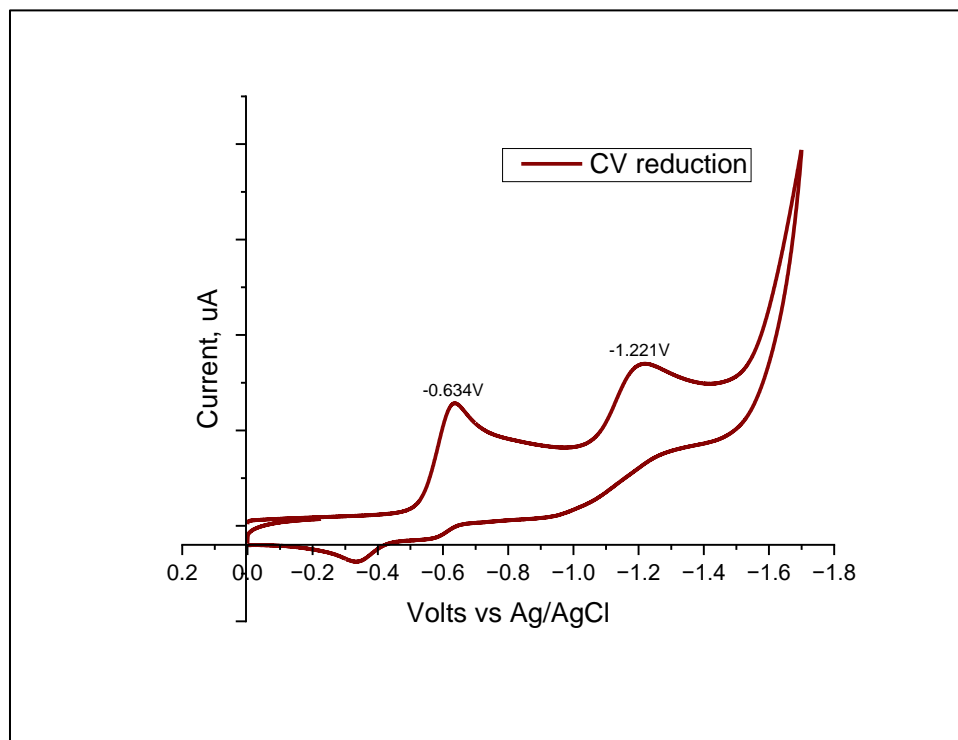


Figure 3.12. Reductive CV data for $[\text{Mo}_3\text{S}_7(\text{S}_2\text{CN}^i\text{Bu}_2)_3]\text{I}$ in DCM.

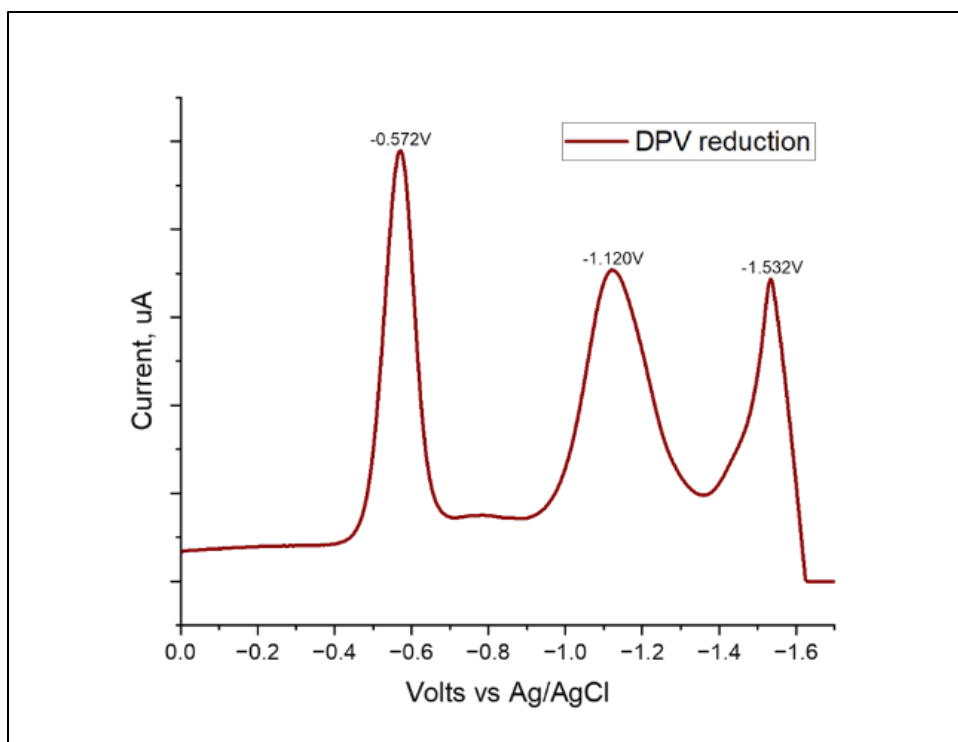


Figure 3.13. Reduction peak potentials for $[\text{Mo}_3\text{S}_7(\text{S}_2\text{CN}^i\text{Bu}_2)_3]\text{I}$ by DPV.

3.5.1.2 $[\text{Mo}_3\text{S}_7(\text{S}_2\text{CN}^i\text{Bu}_2)_3]\text{Cl}$

A similar pattern was observed like $[\text{Mo}_3\text{S}_7(\text{S}_2\text{CN}^i\text{Bu}_2)_3]\text{I}$. here also third reduction is reversible reduction with an $E_{1/2} = -1.224\text{V}$.

Again, DPV window shows four reductions with its third reduction was reversible reduction at $E_{1/2} = -1.12\text{V}$.

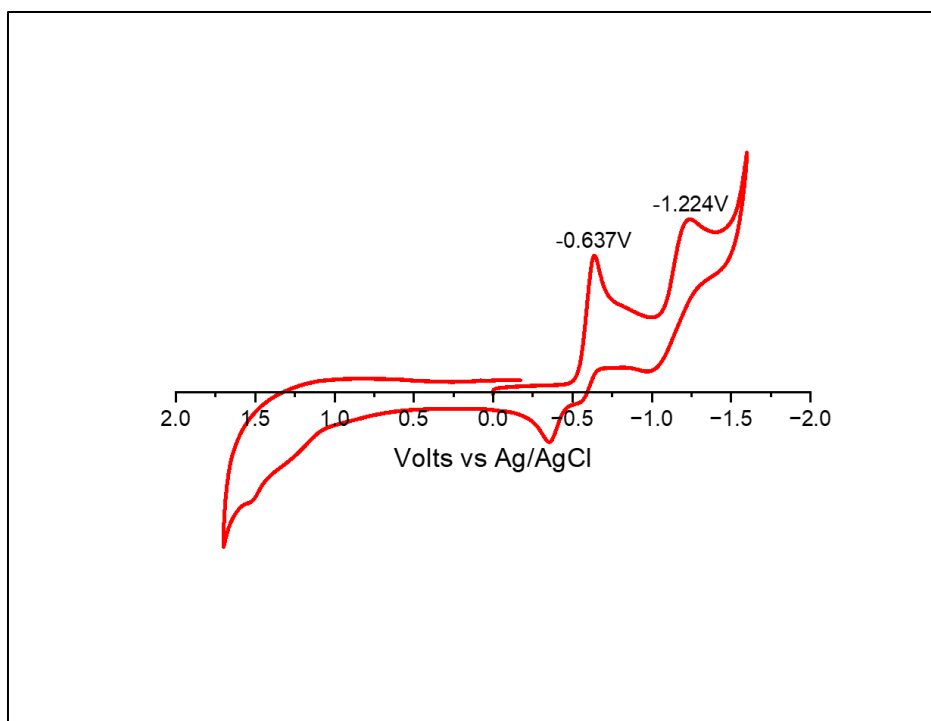


Figure 3.14. The whole CV window for $[\text{Mo}_3\text{S}_7(\text{S}_2\text{CN}^t\text{Bu}_2)_3]\text{Cl}$ in DCM

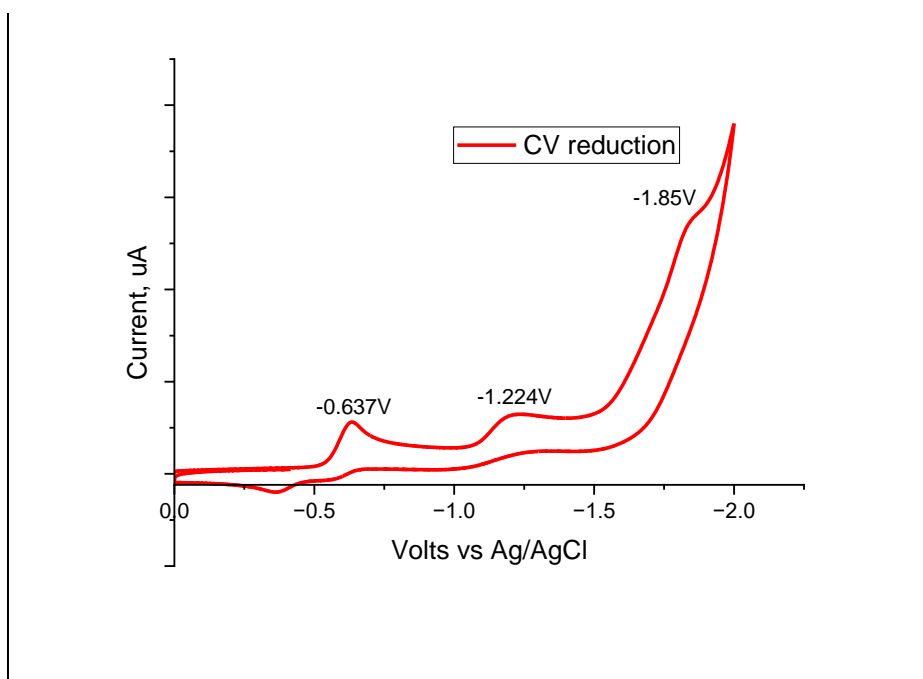


Figure 3.15. Reductive CV data for $[\text{Mo}_3\text{S}_7(\text{S}_2\text{CN}^t\text{Bu}_2)_3]\text{Cl}$ in DCM.

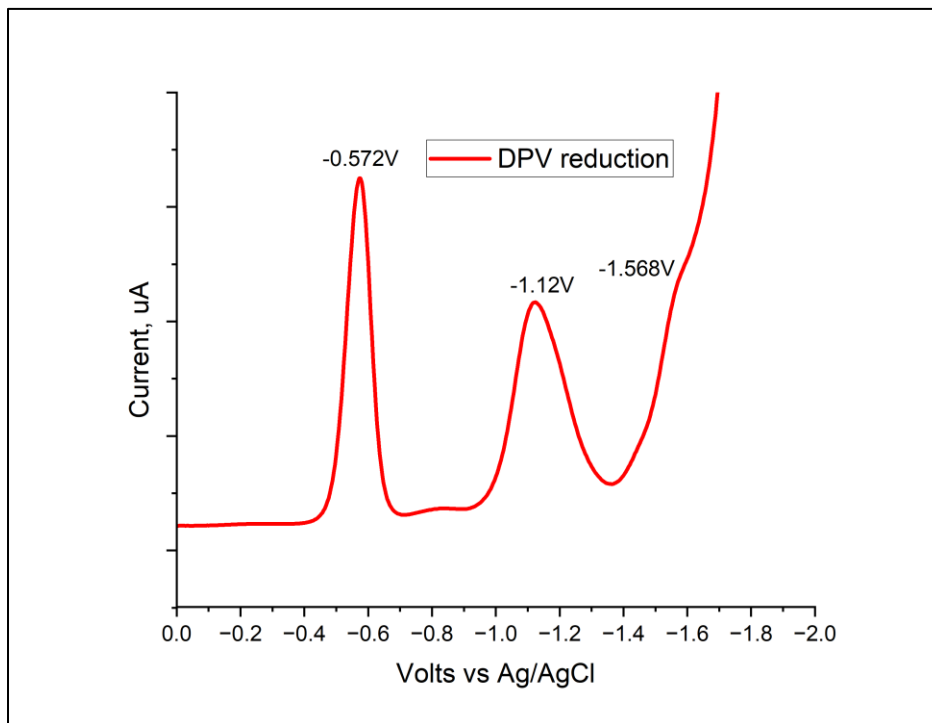


Figure 3.16. Reduction peak potentials for $[\text{Mo}_3\text{S}_7(\text{S}_2\text{CN}^i\text{Bu}_2)_3]\text{Cl}$ by DPV.

3.5.1.3 $[\text{Mo}_3\text{S}_4\text{Se}_3(\text{S}_2\text{CN}^i\text{Bu}_2)_3]\text{SeCN}$

This compound shows a complex CV with multiple reductions peaks followed by one irreversible oxidation. Here the sixth reduction shows reversibility with an $E_{1/2} = -1.52\text{V}$. In the DPV measurements. The first peak and sixth peak show its maximum, whereas in between peaks shows smaller peaks. Here at sixth position $E_{1/2} = -1.412\text{V}$ reversible reduction was observed.

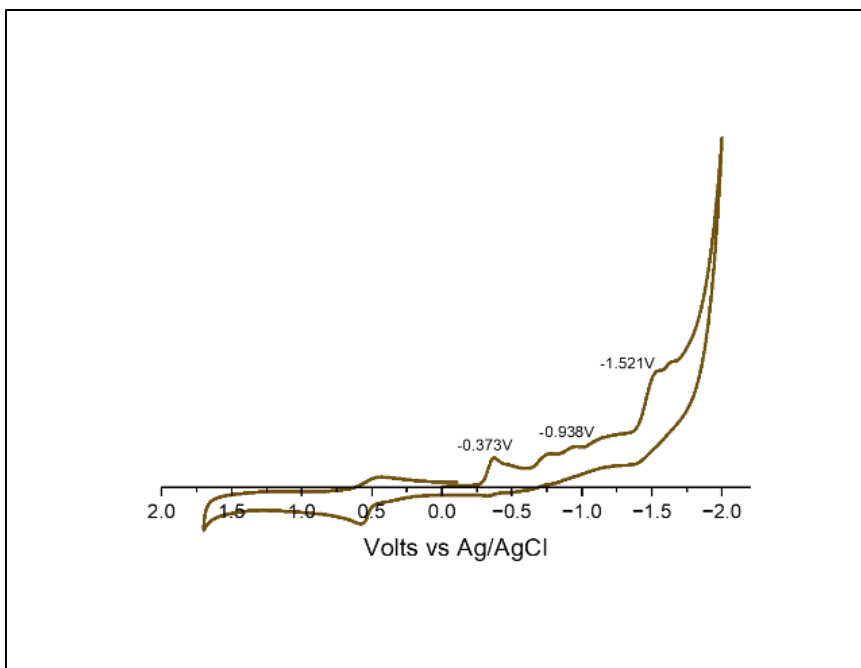


Figure 3.17. The whole CV window for $[\text{Mo}_3\text{S}_4\text{Se}_3(\text{S}_2\text{CN}^i\text{Bu}_2)_3]\text{SeCN}$ in DCM

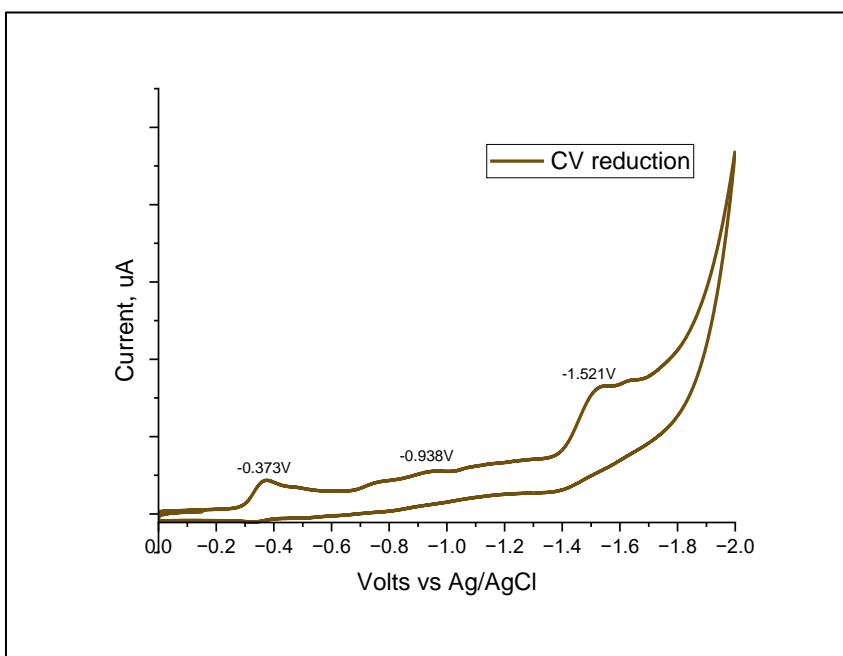


Figure 3.18. Reductive CV data for $[\text{Mo}_3\text{S}_4\text{Se}_3(\text{S}_2\text{CN}^i\text{Bu}_2)_3]\text{SeCN}$ in DCM.

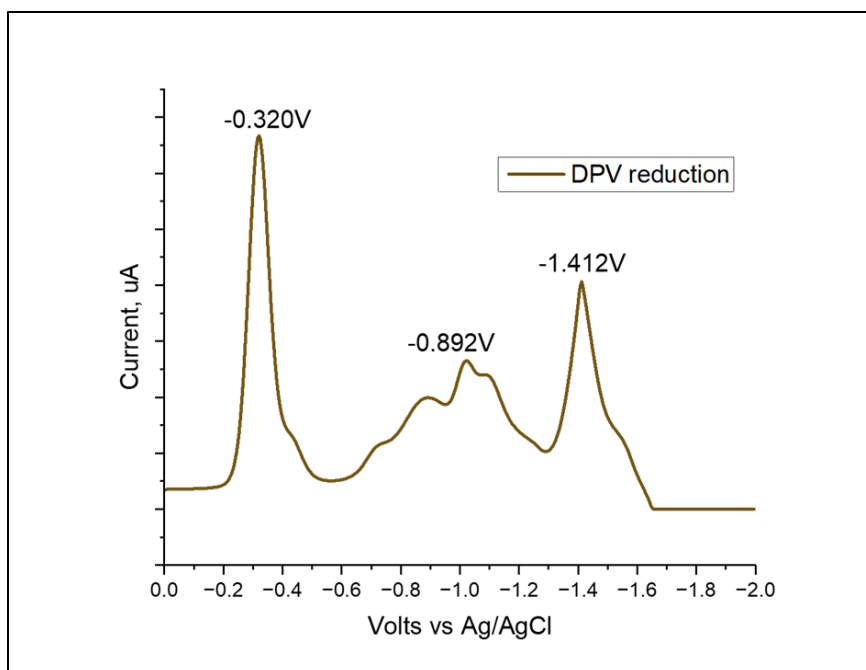


Figure 3.19. Reduction peak potentials for $[\text{Mo}_3\text{S}_4\text{Se}_3(\text{S}_2\text{CN}^i\text{Bu}_2)_3]\text{SeCN}$ by DPV.

3.5.1.4 $[\text{Mo}_3\text{Se}_7(\text{S}_2\text{CN}^i\text{Bu}_2)_3] \text{I}$

This compound also shows complex CV with multiple reductions peaks followed by four irreversible oxidations. This shows similarity third reduction reversibility like $[\text{Mo}_3\text{S}_7(\text{S}_2\text{CN}^i\text{Bu}_2)_3] \text{I}$ with an $E_{1/2} = -1.040\text{V}$.

In the DPV window, there are five reductions observed. However, very sharp peak third reduction at $E_{1/2} = -0.960\text{V}$ was a reversible peak.

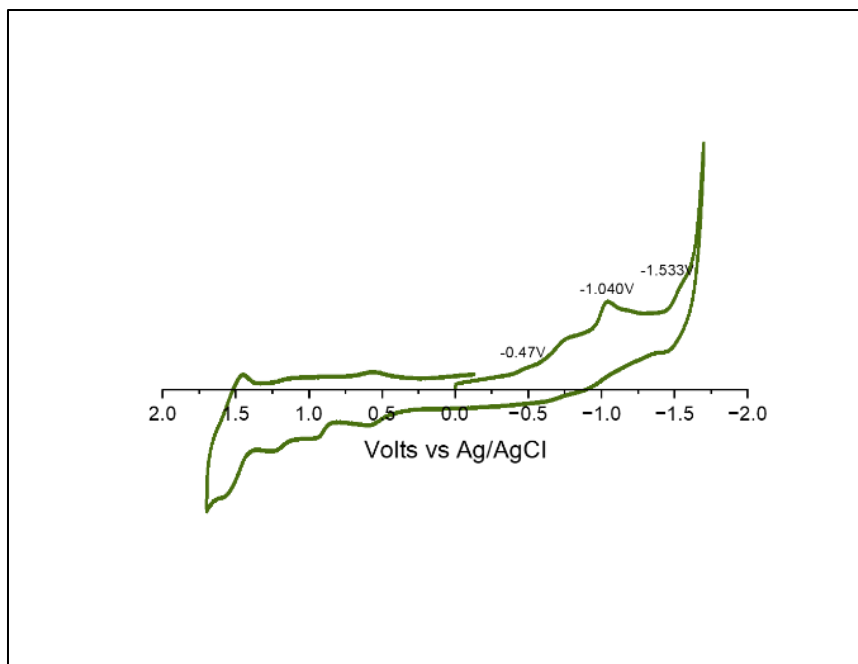


Figure 3.20. The whole CV window for $[\text{Mo}_3\text{Se}_7(\text{S}_2\text{CN}^i\text{Bu}_2)_3]\text{I}$ in DCM

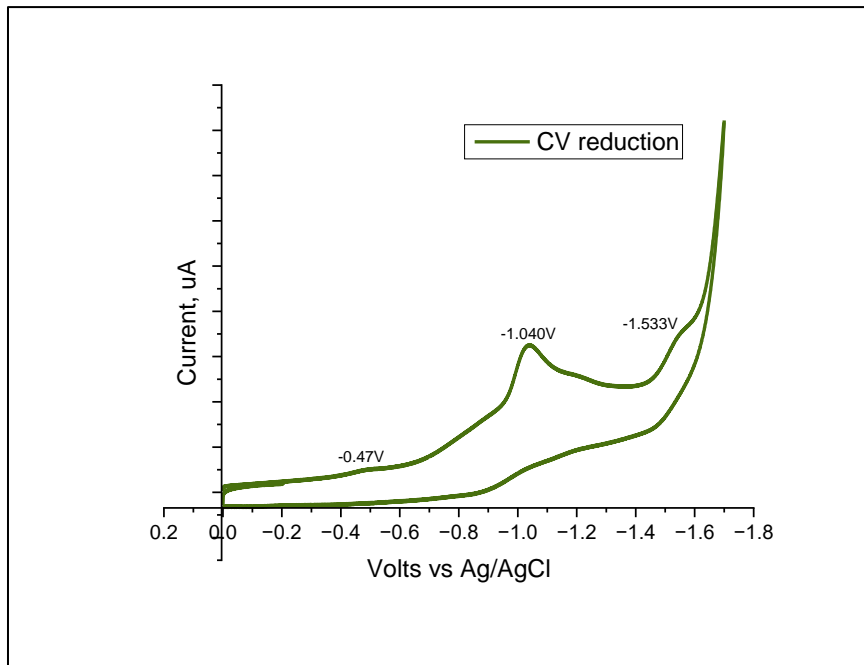


Figure 3.21. Reductive CV data for $[\text{Mo}_3\text{Se}_7(\text{S}_2\text{CN}^i\text{Bu}_2)_3]\text{I}$ in DCM.

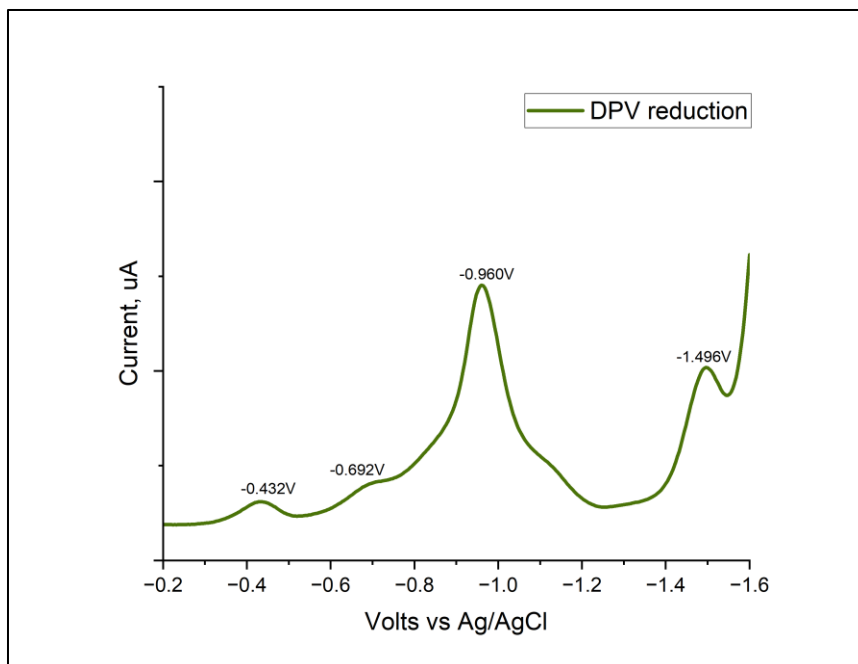


Figure 3.22. Reduction peak potentials for $[\text{Mo}_3\text{Se}_7(\text{S}_2\text{CN}^i\text{Bu}_2)_3]\text{I}$ by DPV.

3.5.1.5 $[\text{Mo}_3\text{Se}_7(\text{Se}_2\text{CN}^i\text{Bu}_2)_3]\text{I}$

Similar reduction pattern like $[\text{Mo}_3\text{S}_7(\text{S}_2\text{CN}^i\text{Bu}_2)_3]\text{I}$ was observed. However, here fourth reduction shows reversibility with an $E_{1/2} = -1.103\text{ V}$.

Here, in the DPV reductions, although there are three smaller reductions peaks in the whole window, the broad peak with an $E_{1/2} = -1.052\text{ V}$ was a reversible peak.

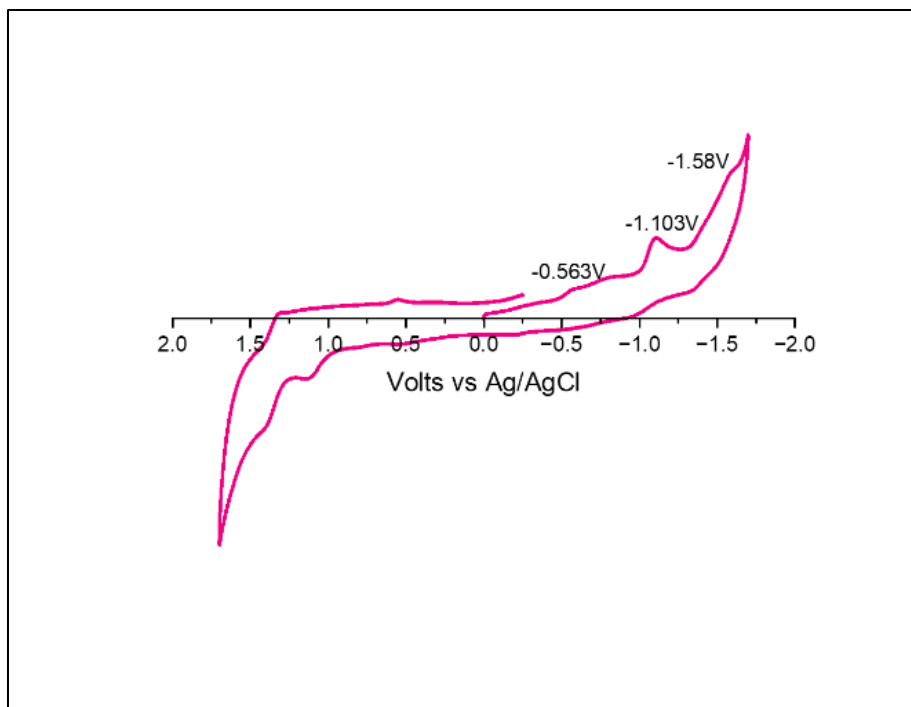


Figure 3.23. The whole CV window for $[\text{Mo}_3\text{Se}_7(\text{Se}_2\text{CN}^i\text{Bu}_2)_3]\text{I}$ in DCM

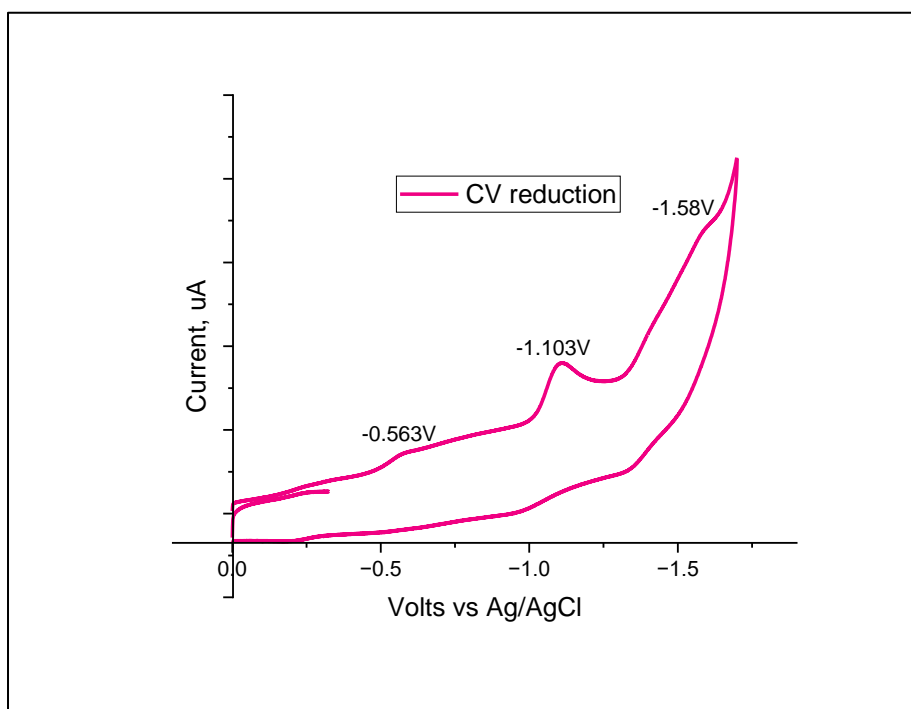


Figure 3.24. Reductive CV data for $[\text{Mo}_3\text{Se}_7(\text{Se}_2\text{CN}^i\text{Bu}_2)_3]\text{I}$ in DCM.

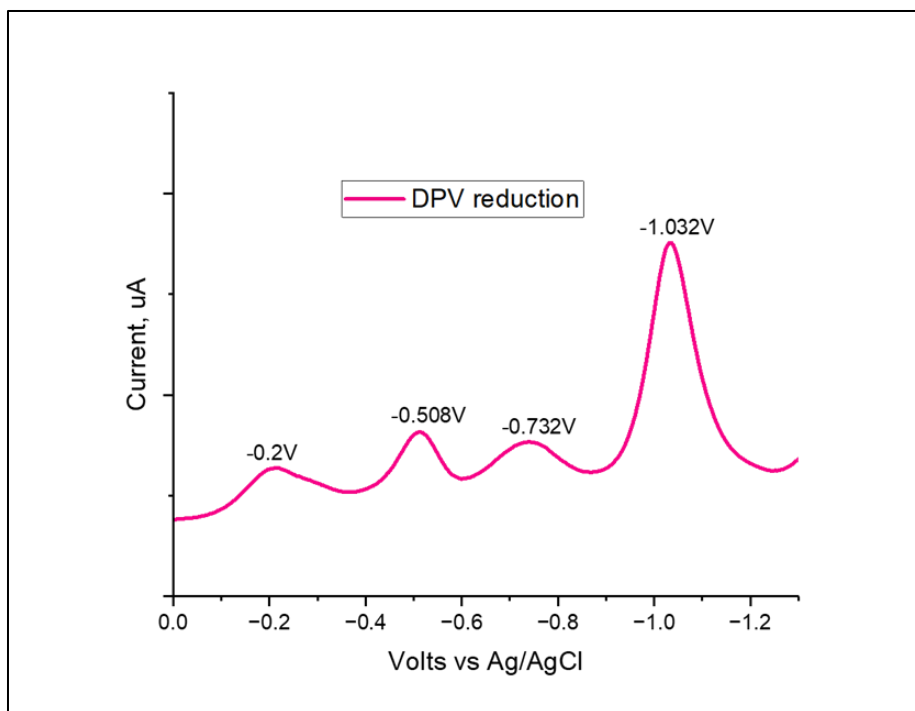


Figure 3.25. Reduction peak potentials for $[\text{Mo}_3\text{Se}_7(\text{Se}_2\text{CN}^i\text{Bu}_2)_3]\text{I}$ by DPV.

3.5.1.6 $[\text{Mo}_3\text{S}_7(\text{S}_2\text{P}^i\text{Bu}_2)_3]\text{I}$

In the whole CV window, there were three reduction peaks followed by one oxidation peak being observed. Here the second reduction peak shows reversibility with an $E_{1/2} = -0.979\text{ V}$.

In the DPV window, the maxima peak at $E_{1/2} = -0.888\text{ V}$ shows reversibility.

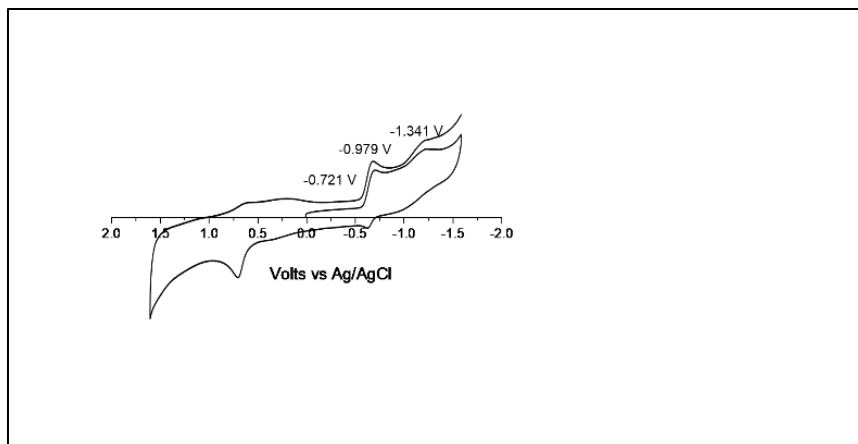


Figure 3.26. The whole CV window for $[\text{Mo}_3\text{S}_7(\text{S}_2\text{P}^i\text{Bu}_2)_3]\text{I}$ in DCM

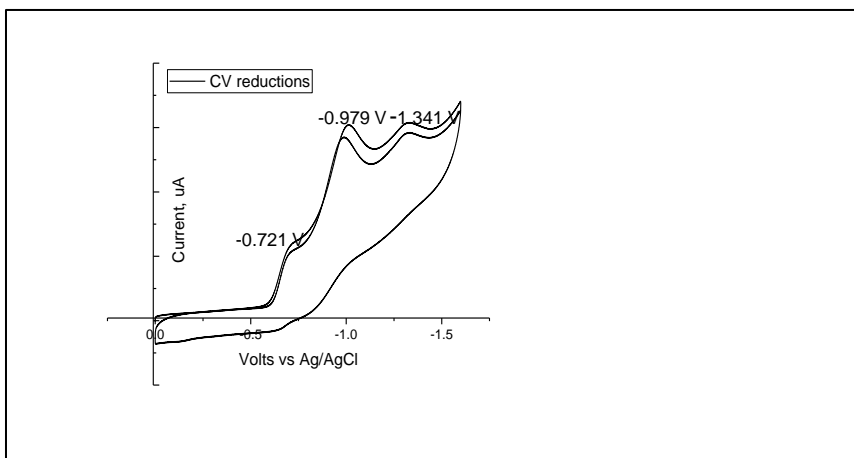


Figure 3.27. Reductive CV data for $[\text{Mo}_3\text{S}_7(\text{S}_2\text{P}^i\text{Bu}_2)_3]\text{I}$ in DCM.

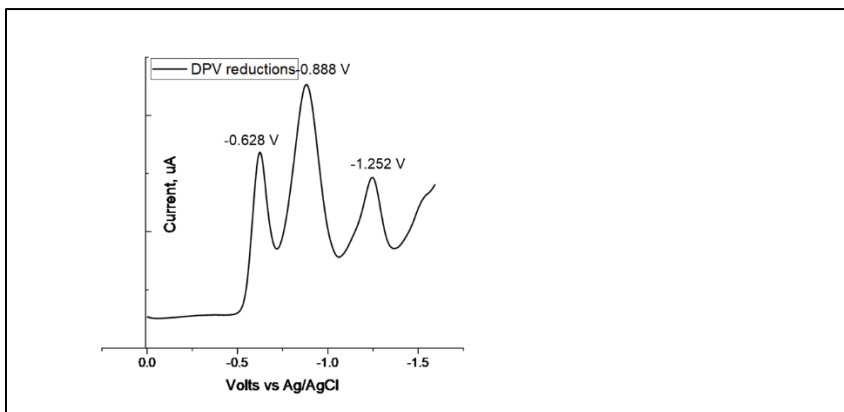


Figure 3.28. Reduction peak potentials for $[\text{Mo}_3\text{S}_7(\text{S}_2\text{P}^i\text{Bu}_2)_3]\text{I}$ by DPV.

3.5.1.7 $[\text{Mo}_3\text{S}_4\text{Se}_3(\text{S}_2\text{P}^i\text{Bu}_2)_3]\text{I}$

The whole CV window shows complex CV with multiple reductions peaks like $[\text{Mo}_3\text{S}_4\text{Se}_3(\text{S}_2\text{CN}^i\text{Bu}_2)_3]\text{SeCN}$ compound. Followed by two irreversible oxidations. A reversible reduction pattern was observed at $E_{1/2} = -1.03\text{V}$, it was the fourth reduction.

When scanning the DPV. The reversible peak was formed at $E_{1/2} = -0.912\text{V}$ with multiple reductions.

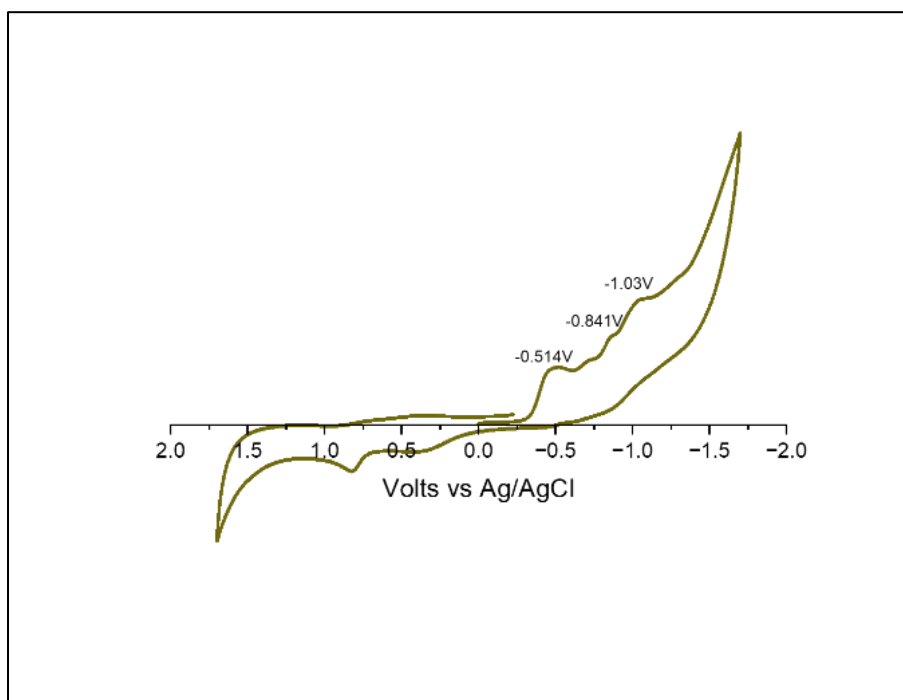


Figure 3.29. The whole CV window for $[\text{Mo}_3\text{S}_4\text{Se}_3(\text{S}_2\text{P}^i\text{Bu}_2)_3]\text{I}$ in DCM

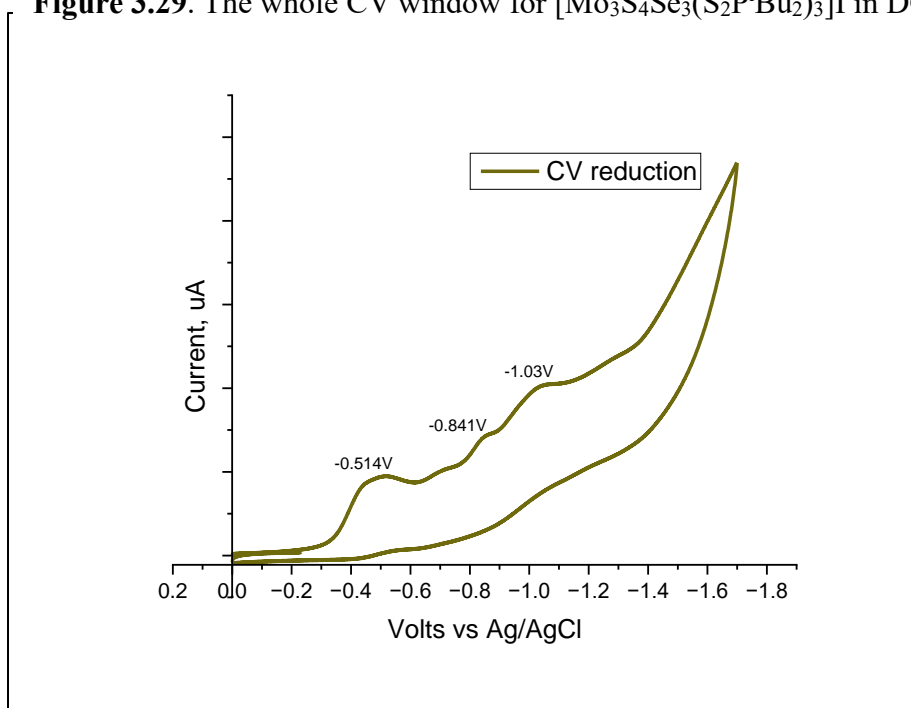


Figure 3.30. Reductive CV data for $[\text{Mo}_3\text{S}_4\text{Se}_3(\text{S}_2\text{P}^i\text{Bu}_2)_3]\text{I}$ in DCM.

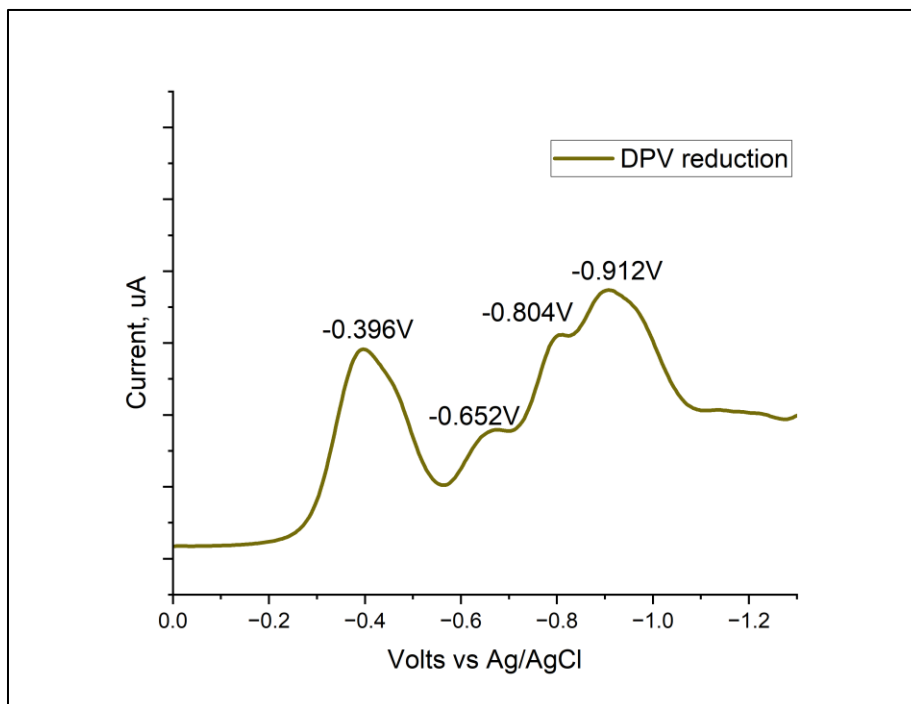


Figure 3.31. Reduction peak potentials for $[\text{Mo}_3\text{S}_4\text{Se}_3(\text{S}_2\text{P}^i\text{Bu}_2)_3]\text{I}$ by DPV.

3.5.1.8 $[\text{Mo}_3\text{Se}_7(\text{S}_2\text{P}^i\text{Bu}_2)_3]\text{I}$

This compound reduction pattern was like $[\text{Mo}_3\text{Se}_7(\text{S}_2\text{CN}^i\text{Bu}_2)_3]\text{I}$ with complex CV with multiple reductions peaks followed by three irreversible oxidations. Here reversible reduction peak was observed at $E_{1/2} = -0.976\text{V}$.

In the DPV measurements, the third reduction peak with $E_{1/2} = -0.942\text{V}$ was a reversible peak.

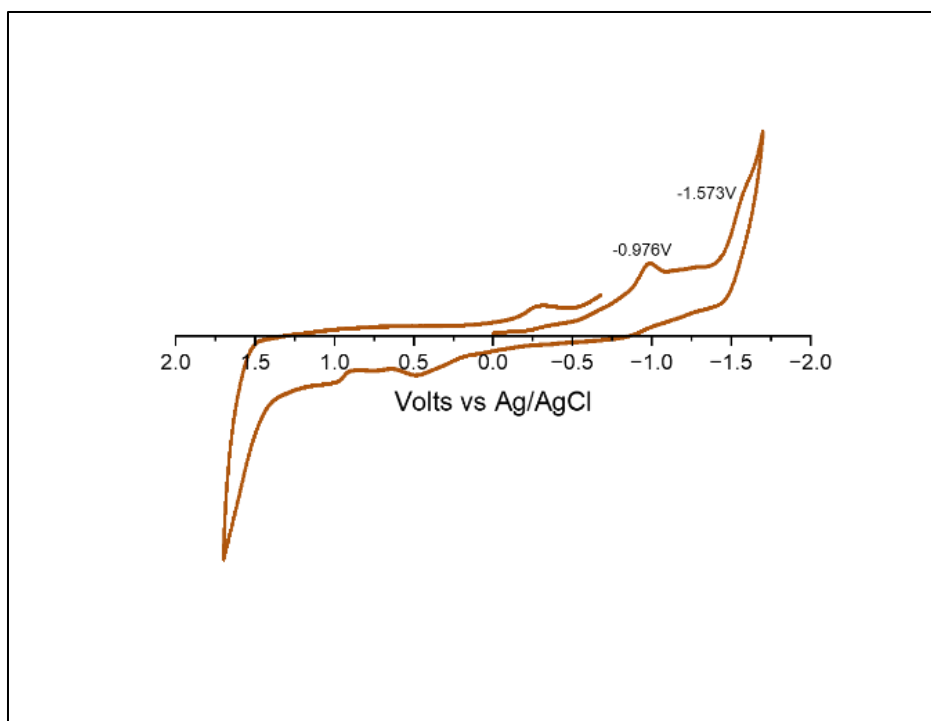


Figure 3.32. The whole CV window for $[\text{Mo}_3\text{Se}_7(\text{S}_2\text{P}^i\text{Bu}_2)_3]\text{I}$ in DCM.

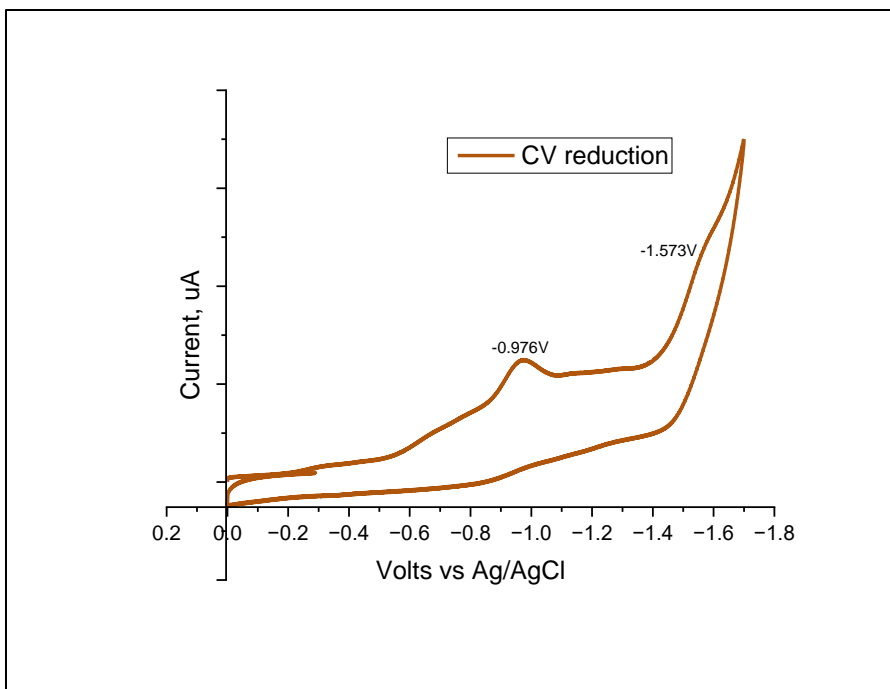


Figure 3.33. Reductive CV data for [Mo₃Se₇(S₂PⁱBu₂)₃]I in DCM.

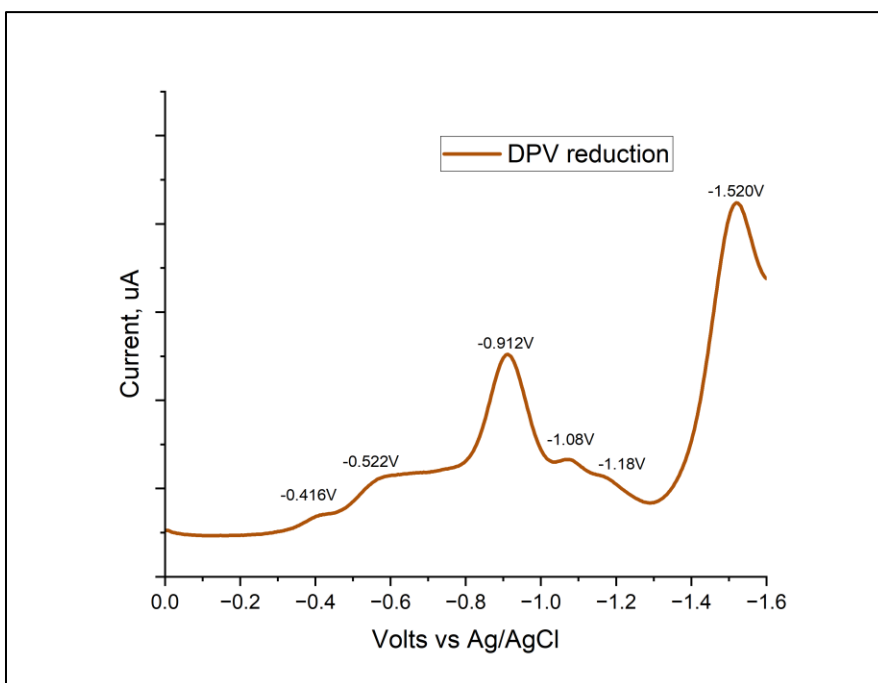


Figure 3.34. Reduction peak potentials for [Mo₃Se₇(S₂PⁱBu₂)₃]I by DPV.

3.5.1.9 $[\text{Mo}_3\text{Se}_7(\text{S}_2\text{P}(\text{O}^i\text{Pr})_2)_3] (\text{S}_2\text{P}(\text{O}^i\text{Pr})_2)$

When scanning the whole CV window, multiple reductions peaks were observed. Here at $E_{1/2} = -0.859\text{V}$ reversible reduction peak was observed. It was a third reduction.

In DPV, there are five reductions peaks were obtained. However, the third reduction peak was a reversible reduction peak with an $E_{1/2} = -0.796\text{V}$.

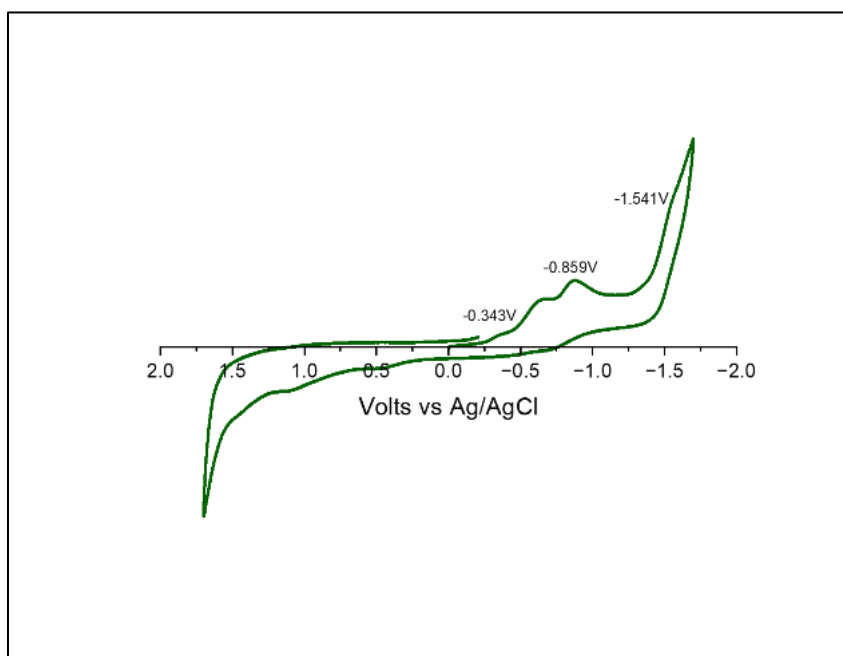


Figure 3.35. The whole CV window for $[\text{Mo}_3\text{Se}_7(\text{S}_2\text{P}(\text{O}^i\text{Pr})_2)_3] (\text{S}_2\text{P}(\text{O}^i\text{Pr})_2)$ in DCM

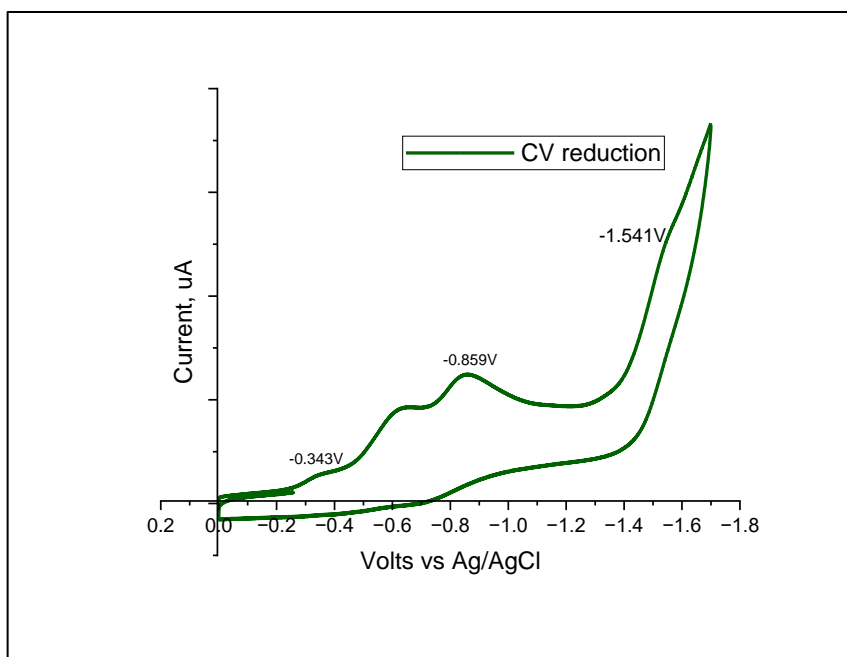


Figure 3.36. Reductive CV data for $[\text{Mo}_3\text{Se}_7(\text{S}_2\text{P}(\text{O}^i\text{Pr})_2)_3]$ ($\text{S}_2\text{P}(\text{O}^i\text{Pr})_2$) in DCM

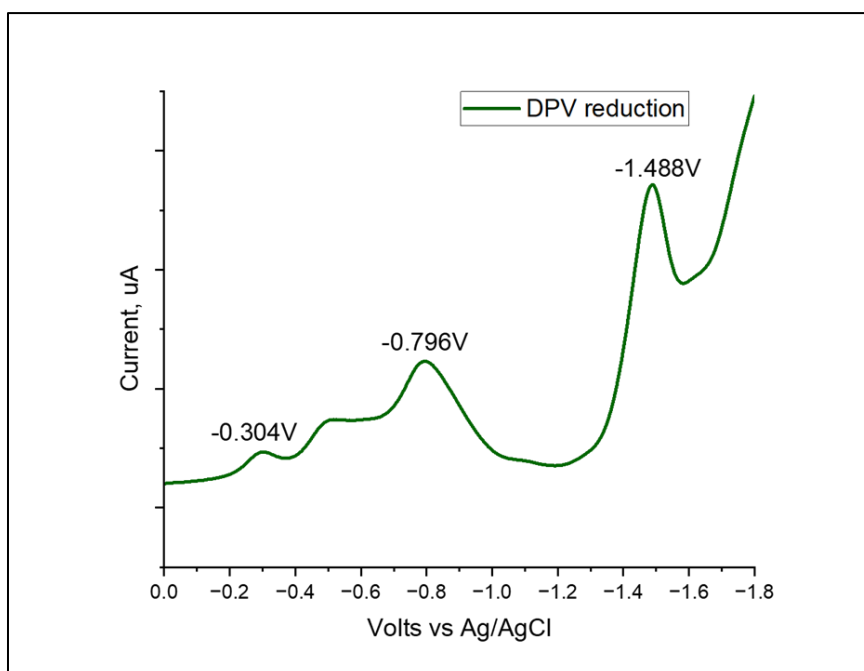


Figure 3.37. Reduction peak potentials for $[\text{Mo}_3\text{Se}_7(\text{S}_2\text{P}(\text{O}^i\text{Pr})_2)_3]$ ($\text{S}_2\text{P}(\text{O}^i\text{Pr})_2$) by DPV.

Table 3.4. Comparison of first reduction potential for all clusters.

Compound	CV $E_{1/2}$	DPV $E_{1/2}$	Reduction type
[Mo ₃ S ₇ (S ₂ CN ⁱ Bu ₂) ₃] I	-0.634V	-0.572V	1st
[Mo ₃ S ₇ (S ₂ CN ⁱ Bu ₂) ₃] Cl	-0.637V	-0.572V	1st
[Mo ₃ S ₄ Se ₃ (S ₂ CN ⁱ Bu ₂) ₃] SeCN	-0.373V	-0.320V	1st
[Mo ₃ Se ₇ (S ₂ CN ⁱ Bu ₂) ₃] I	-0.470V	-0.432V	1st
[Mo ₃ Se ₇ (Se ₂ CN ⁱ Bu ₂) ₃] I		-0.2V	1st
[Mo ₃ S ₇ (S ₂ P ⁱ Bu ₂) ₃] I	-0.721V	-0.628V	1st
[Mo ₃ S ₄ Se ₃ (S ₂ P ⁱ Bu ₂) ₃] I	-0.514V	-0.396V	1st
[Mo ₃ Se ₇ (S ₂ P ⁱ Bu ₂) ₃] I		-0.416V	1st
[Mo ₃ Se ₇ (S ₂ PO ⁱ Pr ₂) ₃] (S ₂ PO ⁱ Pr ₂)	-0.343V	-0.304V	1st

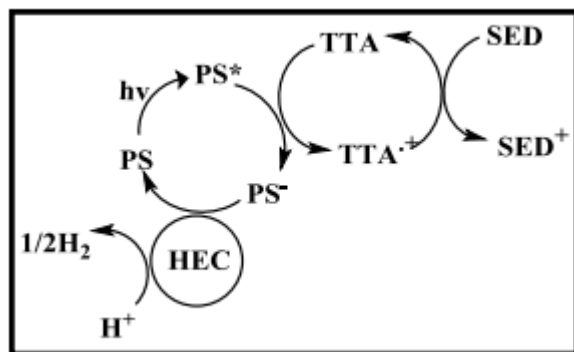
Table 3.5. Comparison of reversible reduction between CV and DPV.

Compound	CV $E_{1/2}$	DPV $E_{1/2}$	Reduction type
[Mo ₃ S ₇ (S ₂ CN ⁱ Bu ₂) ₃] I	-1.221V	-1.12V	3rd
[Mo ₃ S ₇ (S ₂ CN ⁱ Bu ₂) ₃] Cl	-1.224V	-1.12V	3rd
[Mo ₃ S ₄ Se ₃ (S ₂ CN ⁱ Bu ₂) ₃] SeCN	-1.521V	-1.412V	5th
[Mo ₃ Se ₇ (S ₂ CN ⁱ Bu ₂) ₃] I	-1.04V	-0.990V	3rd
[Mo ₃ Se ₇ (Se ₂ CN ⁱ Bu ₂) ₃] I	-1.103V	-1.032V	4th
[Mo ₃ S ₇ (S ₂ P ⁱ Bu ₂) ₃] I	-0.979V	-0.888V	2nd
[Mo ₃ S ₄ Se ₃ (S ₂ P ⁱ Bu ₂) ₃] I	-1.03V	-0.912V	4th
[Mo ₃ Se ₇ (S ₂ P ⁱ Bu ₂) ₃] I	-0.976V	-0.912V	3rd
[Mo ₃ Se ₇ (S ₂ PO ⁱ Pr ₂) ₃] (S ₂ PO ⁱ Pr ₂)	-0.859V	-0.796V	3rd

3.6 Photolysis

3.6.1 Previous findings

The initial design and development of the multistep component systems for Mo_3S_7 coordinate with dithiocarbamate catalyst's work was done by Dr. Bing Shan.⁴⁹ In this work they used reductive quenchers such as (TTA) or the more soluble (TMA). Here the excited state of photosensitizer (PS^*) was reduced by (PS^-) by quencher (TTA). Then this (PS^-) was reacted with (HEC) then H^+ from H_2 . Here sacrificial electron donor acts to complete the cycle and to form its original state of quencher (TTA).



Scheme 3.13. Four component photosystem using reductive quenching.

Initially $[\text{Mo}_3\text{S}_{13}]^{2-}$ was tested in this system. The results showed that it produced over 80 TON hydrogen within the 3 hours of time by using only 26 M catalyst. Due to its anionic nature and poor solubility, it shows modest activity. So, to observe its changes in this photosystem, they made cationic catalyst $[\text{Mo}_3\text{S}_7(\text{S}_2\text{CNET}_3)]\text{I}$. This was tested. The maximum TON was observed at concentration of 50M catalyst. They carried out MALDI-*Ms* experiment with photolysis to find out its changes during the time interval. They obtained conversion from $[\text{Mo}_3\text{S}_7(\text{S}_2\text{CNET}_2)_3]^+$ (peak A at 957 m/z) to $[\text{Mo}_3\text{S}_4(\text{S}_2\text{CNET}_2)_3]$

⁺ (species B at 861 m/z) within the 3 min time interval. So, they concluded that $[\text{Mo}_3\text{S}_7(\text{S}_2\text{CNEt})_3]^+$ I act as a precatalyst in this photo system.

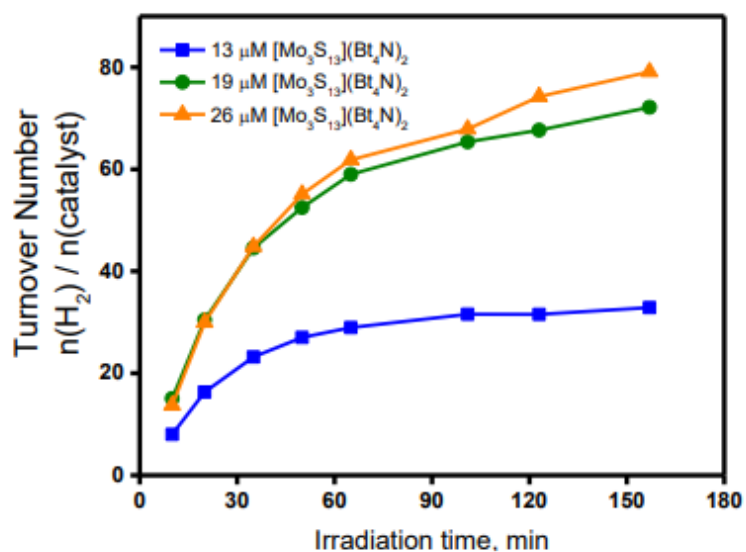


Figure 3.38. TON for the $[\text{NBu}_4]_2[\text{Mo}_3\text{S}_{13}]$ catalyst at various concentrations

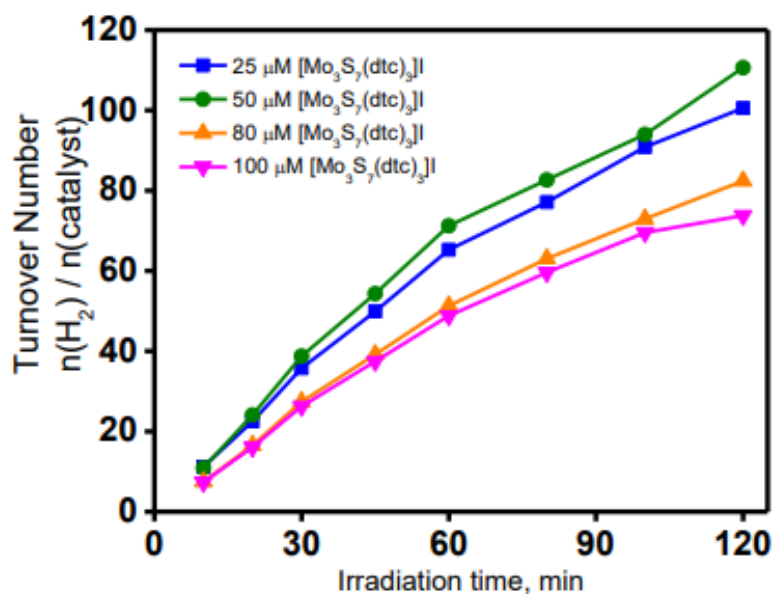


Figure 3.39. TON for the $[\text{Mo}_3\text{S}_7(\text{S}_2\text{CNEt}_3)_3]^+$ catalyst at various concentrations.

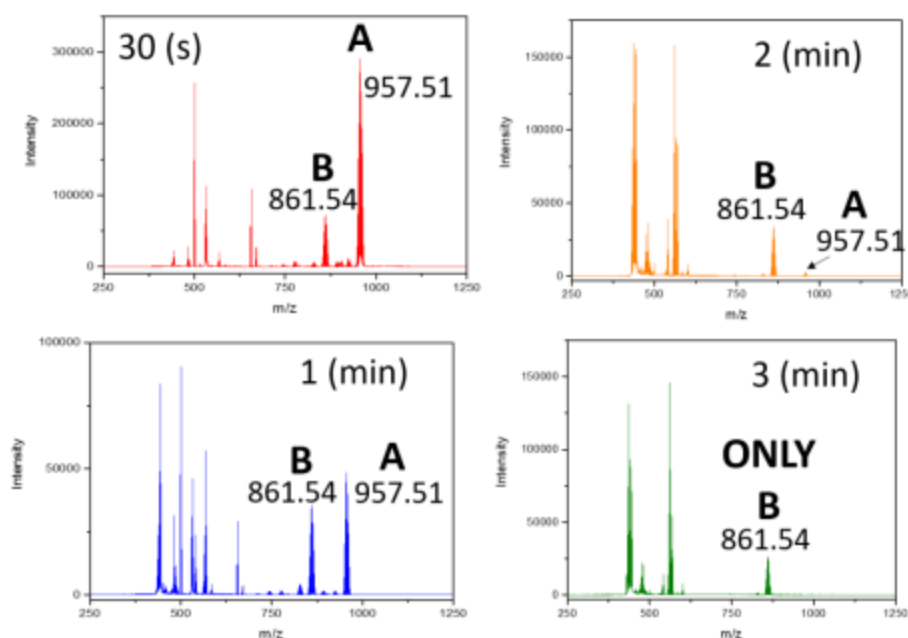


Figure 3.40. MALDI-MS experiment during photolysis of $[\text{Mo}_3\text{S}_7(\text{S}_2\text{CNEt}_2)_3]^+$.

The continuation of this work was carried out by Dr. Fontenot as part of her dissertation.⁵⁰ She measured the hydrogen evolution ability for $[\text{Mo}_3\text{S}_7(\text{S}_2\text{CNR}_2)_3]$ I, $[\text{Mo}_3\text{S}_4(\text{S}_2\text{CNR}_2)_3]$ I, and $[\text{Mo}_3\text{S}_4(\text{S}_2\text{CNR}_2)_4]$ clusters. Among these three types of catalysts, $[\text{Mo}_3\text{S}_7(\text{S}_2\text{CNR}_2)_3]$ I produced more hydrogen in this photosystem. Moreover, there are three types of $[\text{Mo}_3\text{S}_7(\text{S}_2\text{CNR}_2)_3]$ I: R= Me, Et, ⁱBu clusters were made and tested through in this photosystem. More soluble ⁱBu type clusters ($[\text{Mo}_3\text{S}_7(\text{S}_2\text{CN}^i\text{Bu}_2)_3]$ I) act as a maximally active catalyst in this photosystem. It produced over 300 TON hydrogen within 3 hours. Investigated which concentration of this catalyst produced more hydrogen in this system.

They found that 100 μM catalyst produced maximum hydrogen than other concentrations.

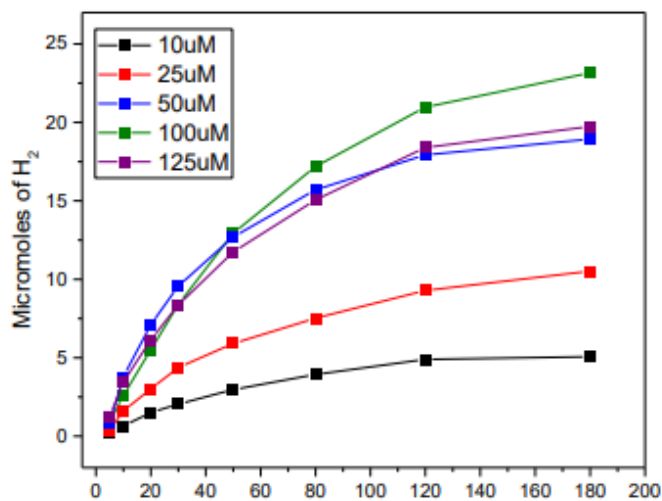


Figure 3.41. Hydrogen production at various concentrations of $[\text{Mo}_3\text{S}_7(\text{S}_2\text{CN}^t\text{Bu}_2)_3]^+$.

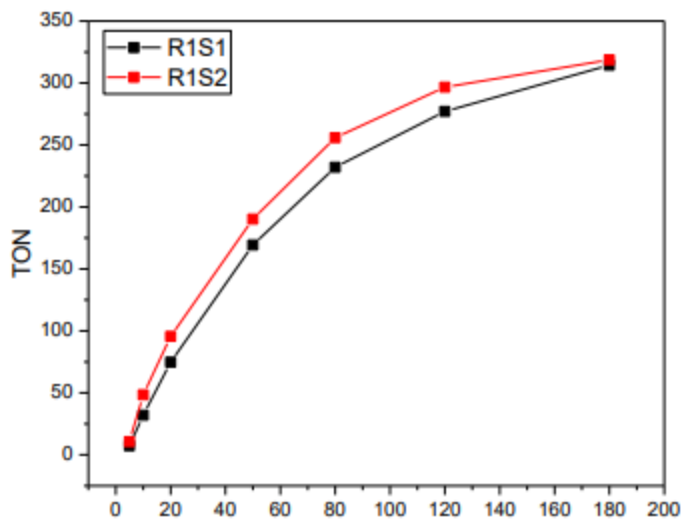


Figure 3.42. Turnover number during 3-hour photolysis of $[\text{Mo}_3\text{S}_7(\text{S}_2\text{CN}^t\text{Bu}_2)_3]^+$.

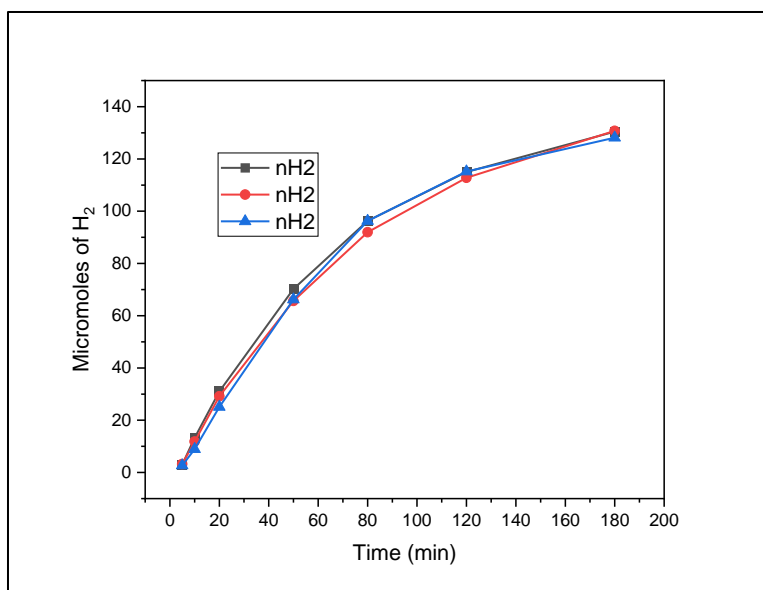


Figure 3.43. Micromoles of hydrogen during 3-hour photolysis of $[\text{Mo}_3\text{S}_7(\text{S}_2\text{CN}^i\text{Bu}_2)_3]^+\Gamma^-$.

From previous conclusions, my work was started. In my work, broad synthesis of $[\text{Mo}_3\text{Q}_7\text{L}_3]^+$; Q = (S or Se), L = ($-\text{S}_2\text{CN}^i\text{Bu}_2$, $-\text{Se}_2\text{CN}^i\text{Bu}_2$, $-\text{S}_2\text{P}^i\text{Bu}_2$, $-\text{S}_2\text{P}(\text{O}^i\text{Pr})_2$) clusters were made to investigate hydrogen evolution activity in this photosystem. Here, especially ^iBu or O^iPr type of clusters were made to increase the solubility of the catalyst in MeCN / H_2O solvent set and 100 μM catalyst was used for permanent factor to find out maximally active catalyst.

The photolysis samples were illuminated in a home-built, multi-well photoreactor comprised of an Al cylinder equipped with blue LEDs (Solid Apollo, 24 W, 460 nm) mounted inside the cylinder wall in a uniform, spiral pattern. The Actinometry was carried out using the photooxidation of $[\text{Ru}(\text{bpy})_3]^{2+}$ by $[\text{S}_2\text{O}_8]^{2-}$. The 4 ml of photoreaction sample contained 8.5 mL dry MeCN, 1.0 mL H_2O , and 0.5 mL dry THF with concentrations of 0.05 M for N,N-trimethylaniline, 260 μM for $[\text{Ru}(\text{bpy})_3]\text{Cl}_2$, 0.40 M for Et_3N , and 100 μM for the Mo-based catalysts. The photolysis samples were thoroughly

degassed by bubbling with Ar and sealed with screwcaps having PTFE/silicone septa, before irradiation. The 4.7 mL headspace volume was kept for each sample. After irradiation, a 50 μ L sample of gas was extracted and injected into a gas chromatograph (Cow-Mac GC; Molecular Sieve Column, T= 35 0C; Carrier Gas: N₂) for quantitative determination of the H₂ produced. The quantum yield for H₂ production per absorbed photon was measured as $\Phi_{H_2} = 2(\text{moles H}_2 \text{ produced})/(\text{moles photons}) = 2PV_{H_2} / (R \cdot T \cdot I \cdot t)$, where V_{H_2} is the volume of H₂ produced in the cell headspace, P = pressure in the headspace of the photolysis vial, R = gas constant, T = temperature, I = light intensity (quanta /s from actinometry) and t = irradiation time. Turnover numbers (TON) for H₂ production per catalyst were measured as: $TON_{H_2} = (\text{moles H}_2 \text{ produced})/(\text{moles Mo-catalyst}) = PV_{H_2} / (R \cdot T \cdot n_{Mo})$, where nMo = number of moles of Mo-catalyst in each sample.

3.6.2 Results

3.6.2.1 Photolysis of [Mo₃S₄Se₃(S₂CNⁱBu₂)₃] SeCN

The same conditions ((100 μ M) Catalyst in 9:1 MeCN: H₂O, 260 μ M [Ru(bpy)₃]²⁺, 0.05 M TMA, and 0.4M Et₃N) were used as previously they used for [Mo₃S₇(S₂CNⁱBu₂)₃] I cluster. Although it has anionic effect, it shows median activity in hydrogen production. It produced 228 TON hydrogen whereas [Mo₃S₇(S₂CNⁱBu₂)₃] I produced 314 TON in a 3-hour photolysis. This apparently shows that, when its equatorial S was changed with high molar mass Se, decreases in hydrogen evolution activity in this photosystem.

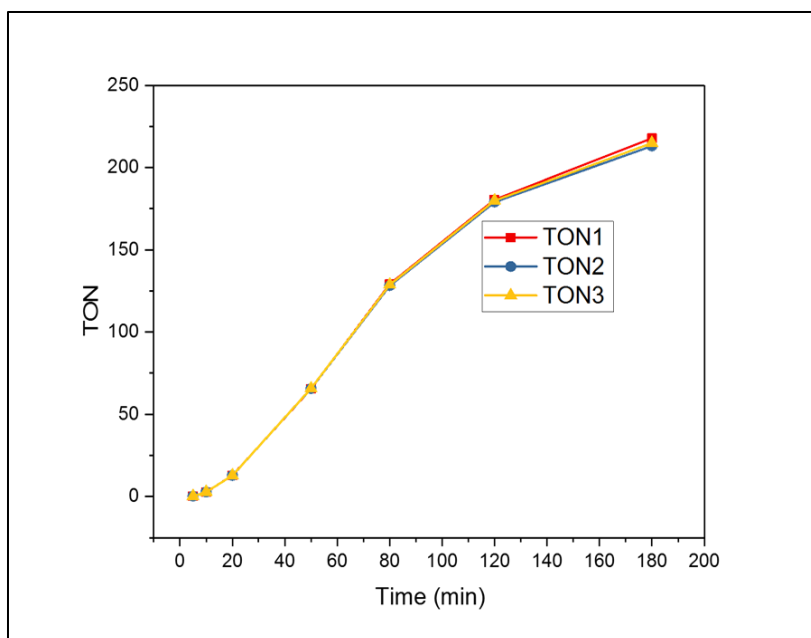


Figure 3.44. Turnover number during 3-hour photolysis of $[\text{Mo}_3\text{S}_4\text{Se}_3(\text{S}_2\text{CN}^i\text{Bu}_2)_3] \text{SeCN}$

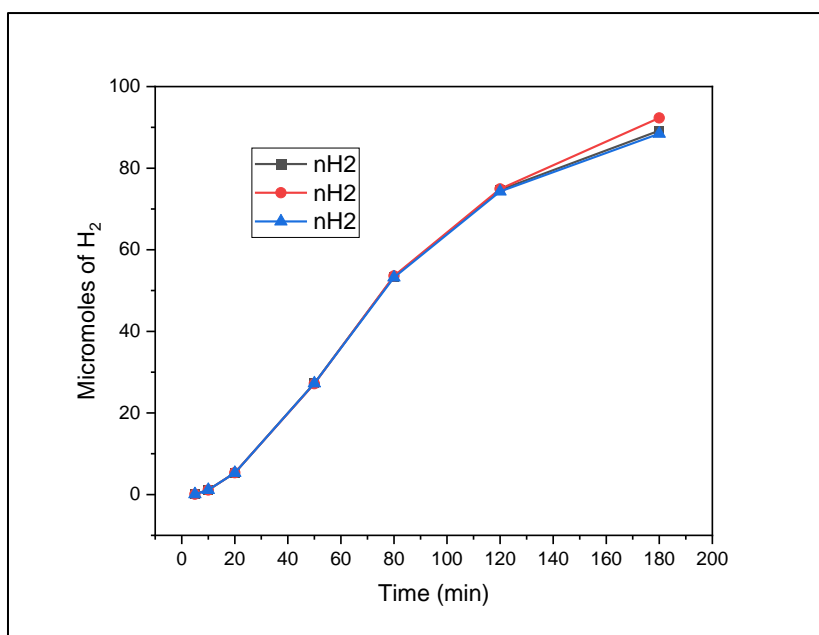


Figure 3.45. Micromoles of hydrogen during 3-hour photolysis of $[\text{Mo}_3\text{S}_4\text{Se}_3(\text{S}_2\text{CN}^i\text{Bu}_2)_3] \text{SeCN}$.

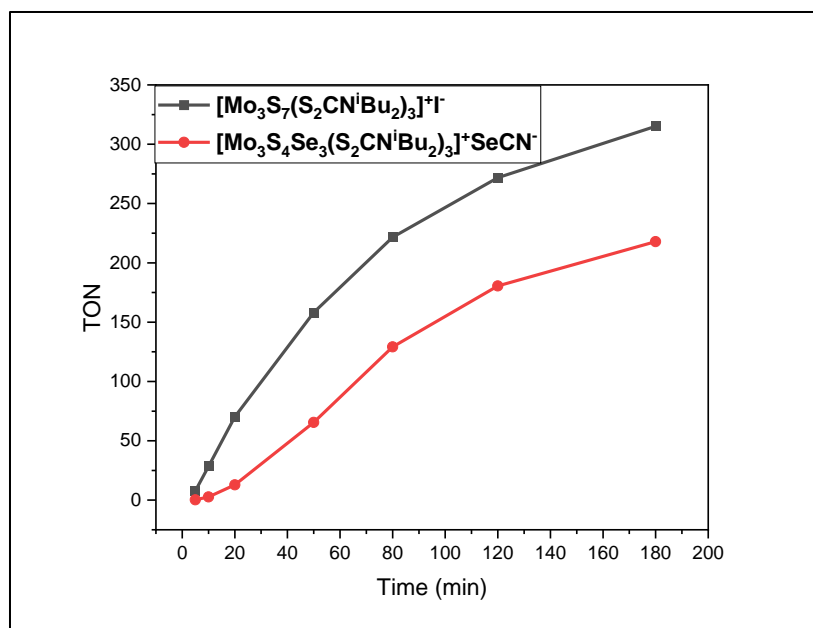


Figure 3.46. photolysis measurement comparing $[\text{Mo}_3\text{S}_7(\text{S}_2\text{CN}^i\text{Bu}_2)_3]^+\text{I}^-$, versus $[\text{Mo}_3\text{S}_4\text{Se}_3(\text{S}_2\text{CN}^i\text{Bu}_2)_3]^+\text{SeCN}^-$

3.6.2.2 Photolysis of $[\text{Mo}_3\text{Se}_7(\text{S}_2\text{CN}^i\text{Bu}_2)_3]^+\text{I}^-$

As this cluster compound has higher molar mass Se atoms in equatorial, axial, and apical positions, this shows less solubility in organic solvents. So, 0.5 ml THF was used to dissolve this cluster. Here 8.5 ml MeCN, 1.0 ml H_2O and 0.5 ml THF were used as solvent. Other remaining conditions (100 μM) Catalyst in 8.5:1:0.5 MeCN: H_2O :THF, 260 μM $[\text{Ru}(\text{bpy})_3]^{2+}$, 0.05 M TMA, and 0.4M Et_3N are maintained same like previous photolysis. Due to its poor solubility, it showed modest hydrogen evolution reactivity in this photosystem. It produced 80 TON hydrogen in a 3-hour period. This is four times lower than $[\text{Mo}_3\text{S}_7(\text{S}_2\text{CN}^i\text{Bu}_2)_3]^+\text{I}^-$ cluster hydrogen evolution reactivity.

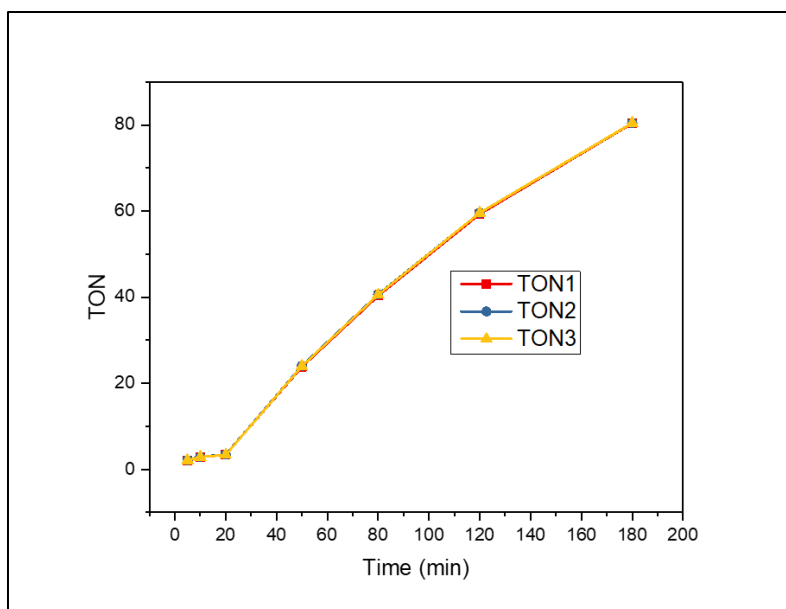


Figure 3.47. Turnover number during 3-hour photolysis of $[\text{Mo}_3\text{Se}_7(\text{S}_2\text{CN}^i\text{Bu}_2)_3] + \text{I}$

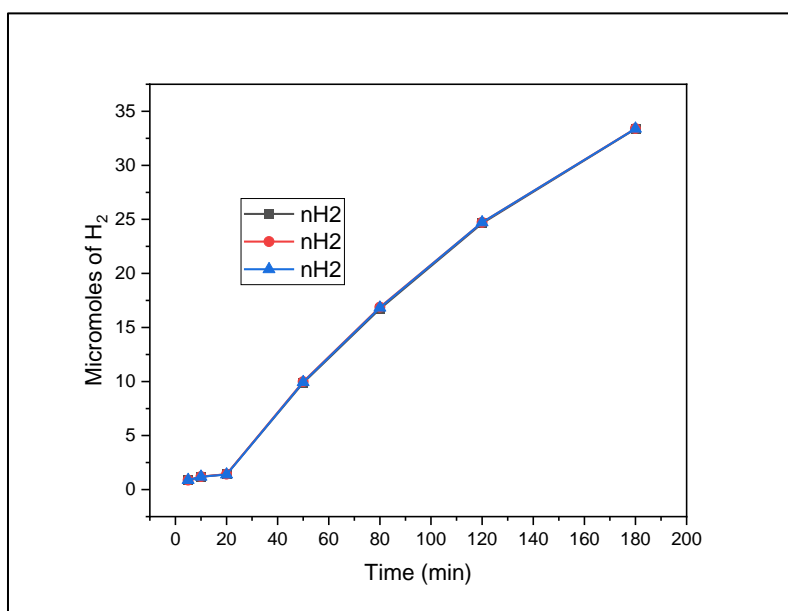


Figure 3.48. Micromoles of hydrogen during 3-hour photolysis of $[\text{Mo}_3\text{Se}_7(\text{S}_2\text{CN}^i\text{Bu}_2)_3] + \text{I}$

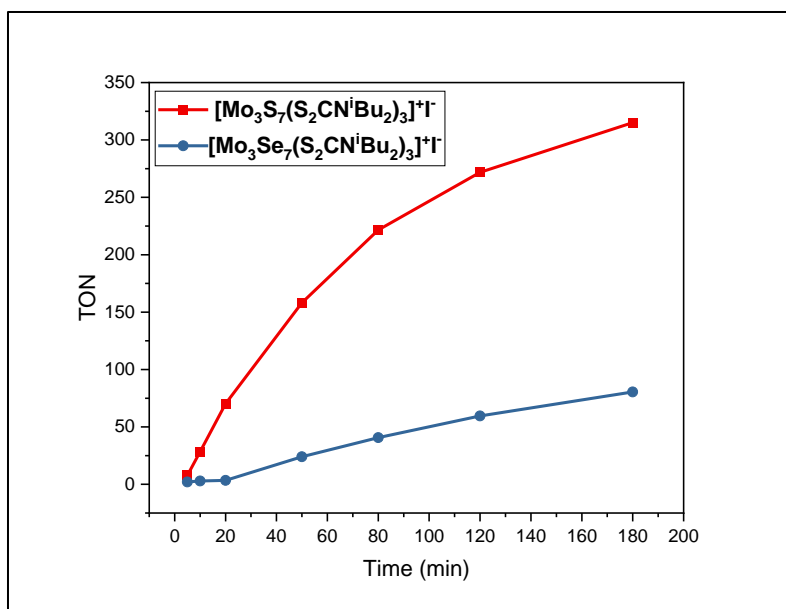


Figure 3.49. Photolysis measurement comparing $[\text{Mo}_3\text{S}_7(\text{S}_2\text{CN}^i\text{Bu}_2)_3]^+\text{I}^-$, versus $[\text{Mo}_3\text{Se}_7(\text{S}_2\text{CN}^i\text{Bu}_2)_3]^+\text{I}^-$

3.6.2.3 Photolysis of $[\text{Mo}_3\text{Se}_7(\text{Se}_2\text{CN}^i\text{Bu}_2)_3]^+\text{I}^-$

As previously mentioned about solubility, this cluster having Se atom in all positions, was insoluble in MeCN:H₂O = 9:1 solvent set. So above compound parameters were used for this cluster (100 μM) Catalyst in 8.5:1.0:0.5 MeCN: H₂O:THF, 260 μM $[\text{Ru}(\text{bpy})_3]^{2+}$, 0.05 M TMA, and 0.4M Et₃N in the photosystem. When the ligand position was changed from (S₂CNⁱBu₂)₃ to (Se₂CNⁱBu₂)₃, it produced 100 TON hydrogen. This number is 20 TON higher than $[\text{Mo}_3\text{Se}_7(\text{S}_2\text{CN}^i\text{Bu}_2)_3]^+\text{I}^-$ compound produced in this photosystem. So external factors also affect its hydrogen production activity not only its equatorial and axial positions.

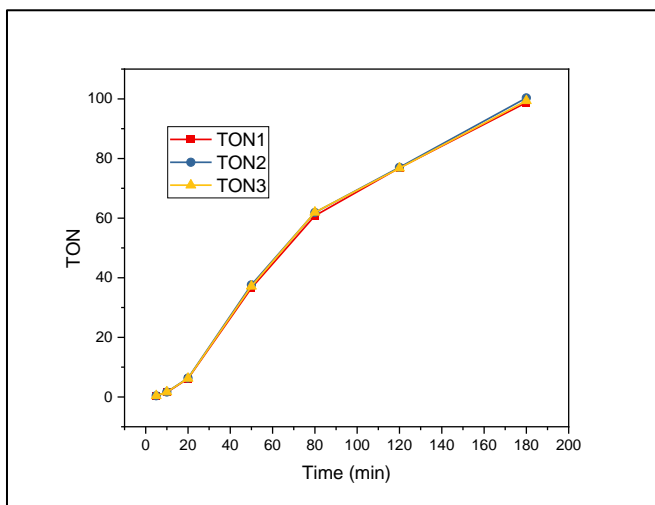


Figure 3.50. Turnover number during 3-hour photolysis of $[\text{Mo}_3\text{Se}_7(\text{Se}_2\text{CN}^i\text{Bu}_2)_3] + \text{I}$

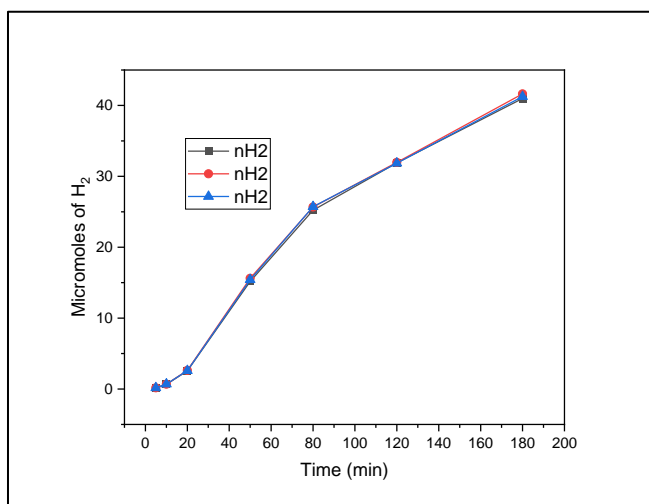


Figure 3.51. Micromoles of hydrogen during 3-hour photolysis of $[\text{Mo}_3\text{Se}_7(\text{Se}_2\text{CN}^i\text{Bu}_2)_3] + \text{I}$

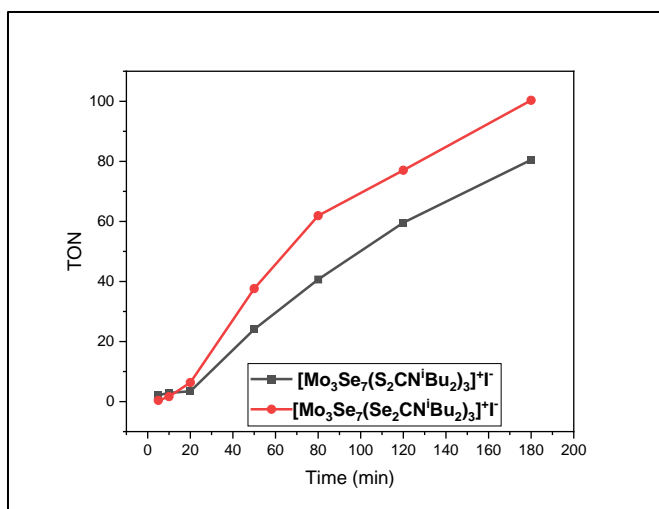


Figure 3.52. photolysis measurement comparing $[\text{Mo}_3\text{Se}_7(\text{S}_2\text{CN}^i\text{Bu}_2)_3]^+\text{I}$ versus $[\text{Mo}_3\text{Se}_7(\text{Se}_2\text{CN}^i\text{Bu}_2)_3]^+\text{I}$.

Here within the same Mo_3S_7 core cluster, like $[\text{Mo}_3\text{S}_7(\text{S}_2\text{CN}^i\text{Bu}_2)_3]^+\text{I}$ only external ligand part was changed from $(\text{S}_2\text{CN}^i\text{Bu}_2)_3$ to $(\text{S}_2\text{P}^i\text{Bu}_2)_3$. However same conditions (100 μM) Catalyst in 9:1 MeCN: H_2O , 260 μM $[\text{Ru}(\text{bpy})_3]^{2+}$, 0.05 M TMA, and 0.4M Et_3N were applied like $[\text{Mo}_3\text{S}_7(\text{S}_2\text{CN}^i\text{Bu}_2)_3]^+\text{I}$, particularly, same solvent set were applied, it dissolved like $[\text{Mo}_3\text{S}_7(\text{S}_2\text{CN}^i\text{Bu}_2)_3]^+\text{I}$, it showed modest hydrogen evolution reaction activity was observed. It produced about 78 TON hydrogen in a 3-hour period. Compared with $[\text{Mo}_3\text{S}_7(\text{S}_2\text{CN}^i\text{Bu}_2)_3]^+\text{I}$ cluster it produced 4 times less hydrogen evolution reaction activity. This compound produced the same amount of hydrogen as $[\text{Mo}_3\text{Se}_7(\text{S}_2\text{CN}^i\text{Bu}_2)_3]^+\text{I}$.

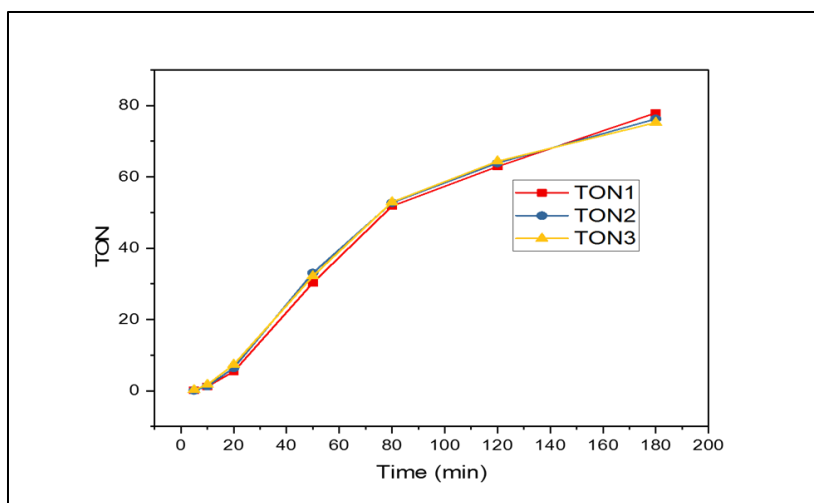


Figure 3.53. Turnover number during 3-hour photolysis of $[\text{Mo}_3\text{S}_7(\text{S}_2\text{P}^i\text{Bu}_2)_3] + \text{I}$

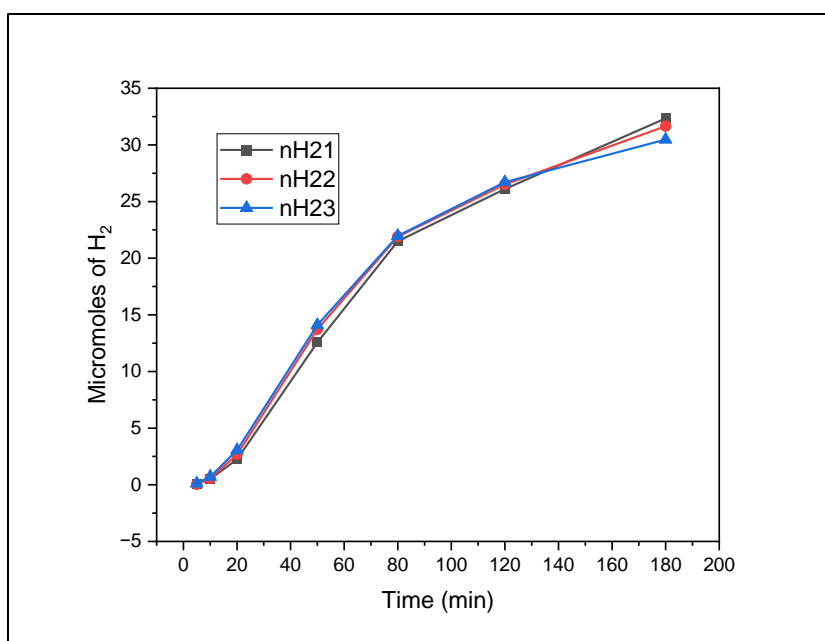


Figure 3.54. Micromoles of hydrogen during 3-hour photolysis of $[\text{Mo}_3\text{S}_7(\text{S}_2\text{P}^i\text{Bu}_2)_3] + \text{I}$

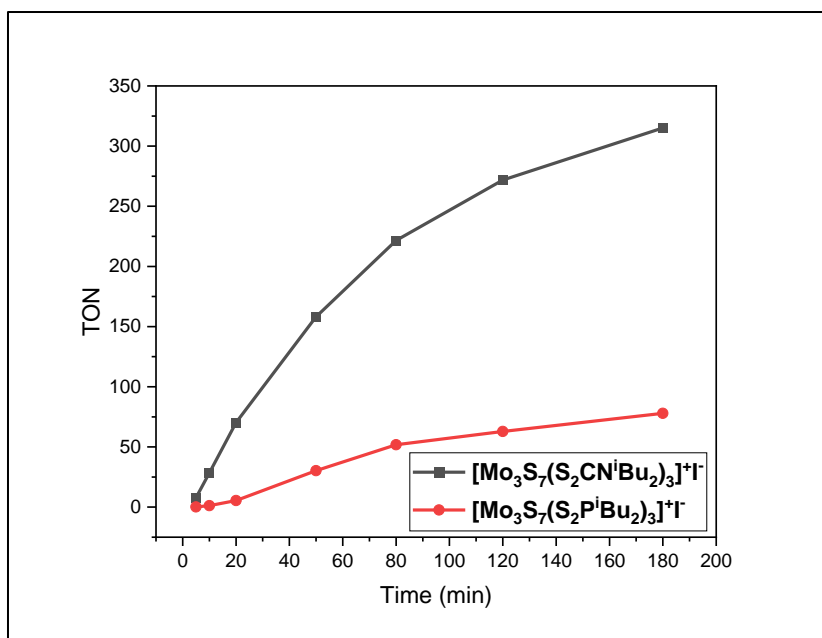


Figure 3.55. photolysis measurement comparing $[\text{Mo}_3\text{S}_7(\text{S}_2\text{CN}^i\text{Bu}_2)_3]^+\text{I}^-$, versus $[\text{Mo}_3\text{S}_7(\text{S}_2\text{P}^i\text{Bu}_2)_3]^+\text{I}^-$.

3.6.2.5 Photolysis of $[\text{Mo}_3\text{S}_4\text{Se}_3(\text{S}_2\text{P}^i\text{Bu}_2)_3]^+\text{I}^-$

When Se was substituted instead of S atom, similar decreasing behavior was observed like dithiocarbamate compounds. Even though similar reaction conditions (100 μM) Catalyst in 9:1 MeCN: H_2O , 260 μM $[\text{Ru}(\text{bpy})_3]^{2+}$, 0.05 M TMA, and 0.4 M Et_3N were applied like $[\text{Mo}_3\text{S}_7(\text{S}_2\text{P}^i\text{Bu}_2)_3]^+\text{I}^-$, it produced 65 TON hydrogen. Not a very drastic difference between $[\text{Mo}_3\text{S}_4\text{Se}_3(\text{S}_2\text{P}^i\text{Bu}_2)_3]^+\text{I}^-$ and $[\text{Mo}_3\text{S}_7(\text{S}_2\text{P}^i\text{Bu}_2)_3]^+\text{I}^-$ in hydrogen production in this system was observed. Only 15 TON differentiates both compounds.

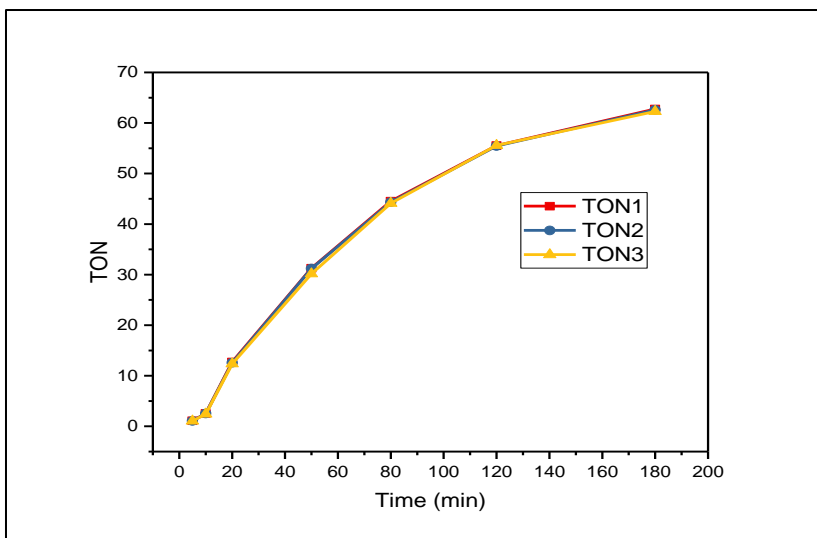


Figure 3.56. Turnover number during 3-hour photolysis of $[\text{Mo}_3\text{S}_4\text{Se}_3(\text{S}_2\text{P}^i\text{Bu}_2)_3]^+\text{I}^-$.

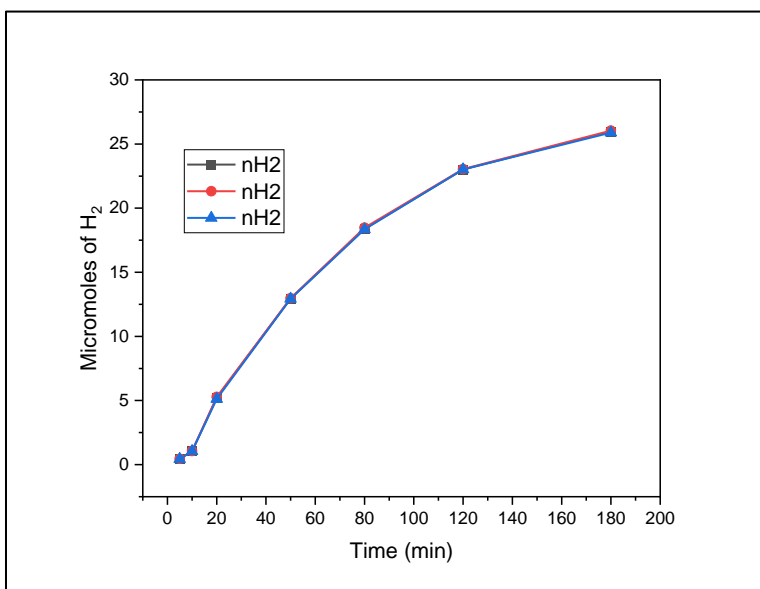


Figure 3.57. Micromoles of hydrogen during 3-hour photolysis of $[\text{Mo}_3\text{S}_4\text{Se}_3(\text{S}_2\text{P}^i\text{Bu}_2)_3]^+\text{I}^-$.

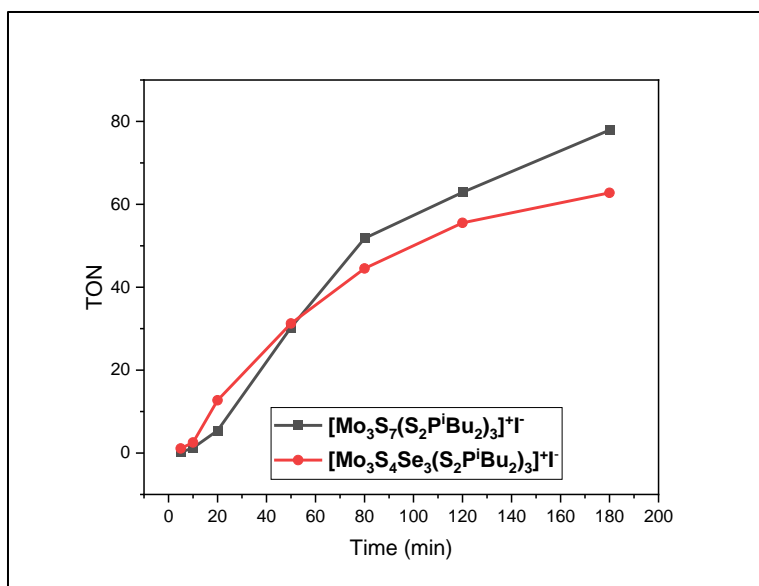


Figure 3.58. Photolysis measurement comparing $[\text{Mo}_3\text{S}_7(\text{S}_2\text{P}^i\text{Bu}_2)_3]\text{I}^-$, versus $[\text{Mo}_3\text{S}_4\text{Se}_3(\text{S}_2\text{P}^i\text{Bu}_2)_3]\text{I}^-$.

3.6.2.6 Photolysis of $[\text{Mo}_3\text{Se}_7(\text{S}_2\text{P}^i\text{Bu}_2)_3]\text{I}^-$

The same photolysis conditions (100 μM) Catalyst in 8.5:1.0:0.5 MeCN: H_2O :THF, 260 μM $[\text{Ru}(\text{bpy})_3]^{2+}$, 0.05 M TMA, and 0.4M Et_3N used, except for the change in the solvent set, were applied in measuring the hydrogen evolution reaction activity of $[\text{Mo}_3\text{Se}_7(\text{S}_2\text{P}^i\text{Bu}_2)_3]\text{I}^-$. As mentioned earlier, the solvent was changed to have 3 components, THF, MeCN, and H_2O . Again, a similar pattern was observed like dithiocarbamate compounds, but here the same amount of TON was reduced from $[\text{Mo}_3\text{S}_4\text{Se}_3(\text{S}_2\text{P}^i\text{Bu}_2)_3]\text{I}^-$. It produced 50 TON hydrogen. The difference between all 3 compounds was the same. In this case, all 3 are the same type and there is no anion effect like dithiocarbamate

compounds. Compared with Mo_3S_7 core cluster with dithiocarbamate compounds act as very active catalyst than Mo_3S_7 coordinated with dithiophosphate clusters in this photosystem.

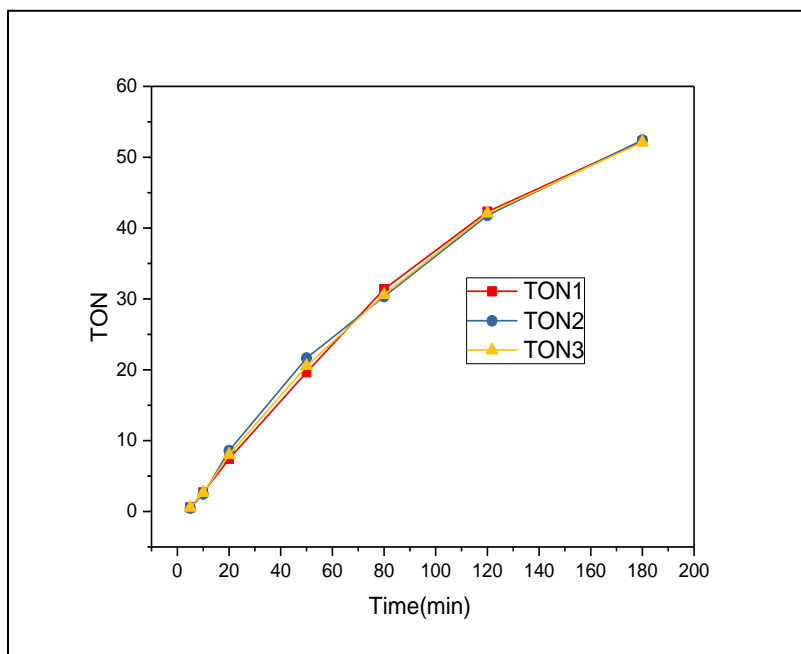


Figure 3.59. Turnover number during 3-hour photolysis of $[\text{Mo}_3\text{Se}_7(\text{S}_2\text{P}^i\text{Bu}_2)_3]\text{I}$.

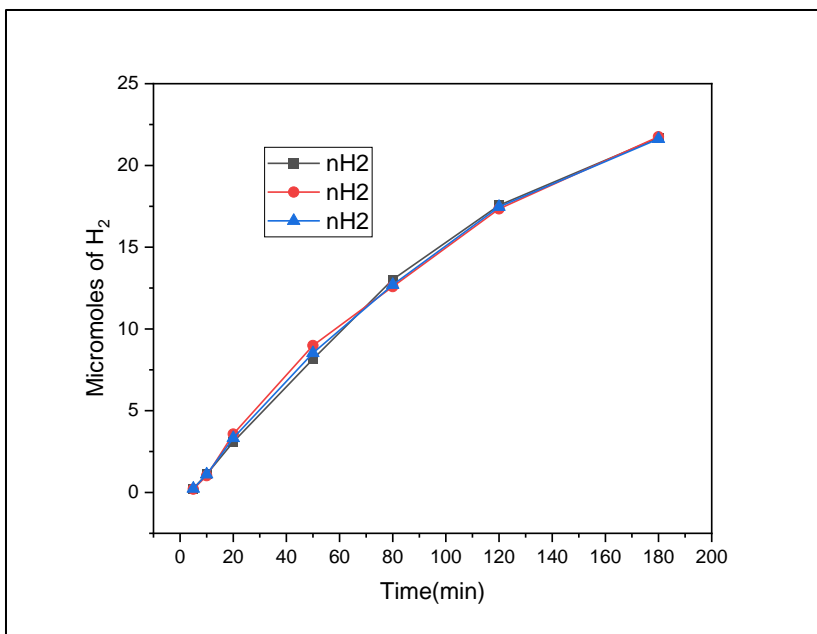


Figure 3.60. Micromoles of hydrogen during 3-hour photolysis of $[\text{Mo}_3\text{Se}_7(\text{S}_2\text{P}^i\text{Bu}_2)_3]\text{I}$.

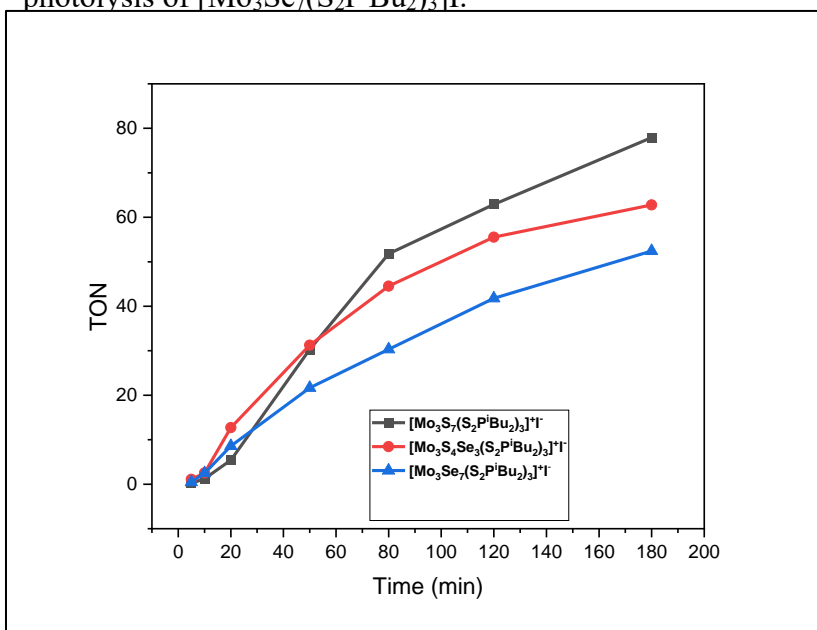


Figure 3.61. photolysis measurement comparing $[\text{Mo}_3\text{S}_7(\text{S}_2\text{P}^i\text{Bu}_2)_3]\text{I}$, versus $[\text{Mo}_3\text{S}_4\text{Se}_3(\text{S}_2\text{P}^i\text{Bu}_2)_3]\text{I}$ and $[\text{Mo}_3\text{Se}_7(\text{S}_2\text{P}^i\text{Bu}_2)_3]\text{I}$.

3.6.2.7 Photolysis of $[\text{Mo}_3\text{Se}_7(\text{S}_2\text{P}(\text{O}^i\text{Bu})_2)_3] (\text{S}_2\text{P}(\text{O}^i\text{Bu})_2)_2$

As this compound is like a polar compound, the same solvent set was applied MeCN: H₂O = 9:1. Moreover, same conditions (100 μM) Catalyst in 9:1 MeCN:H₂O, 260 μM $[\text{Ru}(\text{bpy})_3]^{2+}$, 0.05 M TMA, and 0.4 M Et₃N were applied to find out its hydrogen evolution reaction activity. Although, this compound has different anion than previous compounds, within the 3-hour photolysis this produced only 38 TON hydrogen.

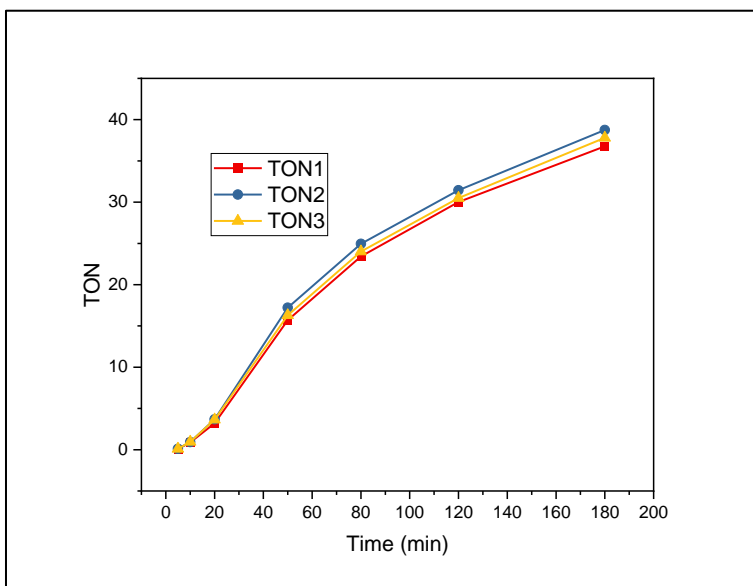


Figure 3.62. Turnover number during 3-hour photolysis of $[\text{Mo}_3\text{Se}_7(\text{S}_2\text{P}(\text{iPrO})_2)_3] (\text{S}_2\text{P}(\text{iPrO})_2)_2$

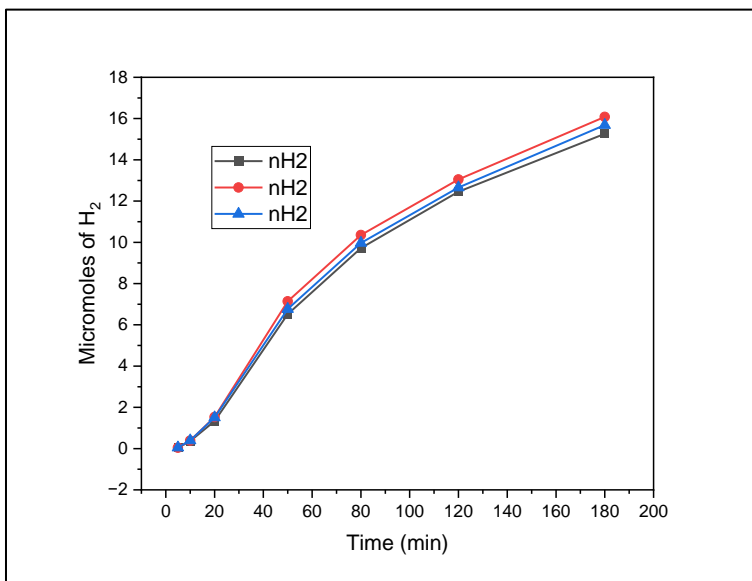


Figure 3.63. Micromoles of hydrogen during 3-hour photolysis of $[\text{Mo}_3\text{Se}_7(\text{S}_2\text{P}(\text{iPrO})_2)_3] (\text{S}_2\text{P}(\text{iPrO})_2)$

3.6.2.8 Anion effect between $[\text{Mo}_3\text{S}_7(\text{S}_2\text{CN}^i\text{Bu}_2)_3]$ I and $[\text{Mo}_3\text{S}_7(\text{S}_2\text{CN}^i\text{Bu}_2)_3]$ Cl

When Mo_3S_7 core cluster coordinated with dithiocarbamate compound was changed in the anion factor from I^- to very strong electronegativity Cl^- atom, it showed very drastic difference in hydrogen evolution reaction activity and its solubility. $[\text{Mo}_3\text{S}_7(\text{S}_2\text{CN}^i\text{Bu}_2)_3]$ Cl compound having higher solubility in organic solvents, especially in MeCN, it immediately dissolves in MeCN without any sonication than $[\text{Mo}_3\text{S}_7(\text{S}_2\text{CN}^i\text{Bu}_2)_3]$ I. Even though, its dissolving ability in MeCN higher than $[\text{Mo}_3\text{S}_7(\text{S}_2\text{CN}^i\text{Bu}_2)_3]$ I, the same 100 μM catalyst was used and same other photolysis conditions (100 μM) Catalyst in 9:1 MeCN: H_2O , 260 μM $[\text{Ru}(\text{bpy})_3]^{2+}$, 0.05 M TMA, and 0.4 M Et_3N were implemented to measuring HER activity in this system. Surprisingly, it surpassed the previous record 300 TON hydrogen in 50 minutes, and it produced the highest TON hydrogen in this photolysis

system. This is one of the maximally active catalysts in the multicomponent system. 220 micromoles of hydrogen were observed within the 3-hour photolysis and over 500 TON produced. Compared with $[\text{Mo}_3\text{S}_7(\text{S}_2\text{CN}^i\text{Bu}_2)_3]$ I, its value was 1.6 times higher than $[\text{Mo}_3\text{S}_7(\text{S}_2\text{CN}^i\text{Bu}_2)_3]$ I cluster produced in photosystem. This is apparently shown that this is the maximally active catalyst in this photosystem.

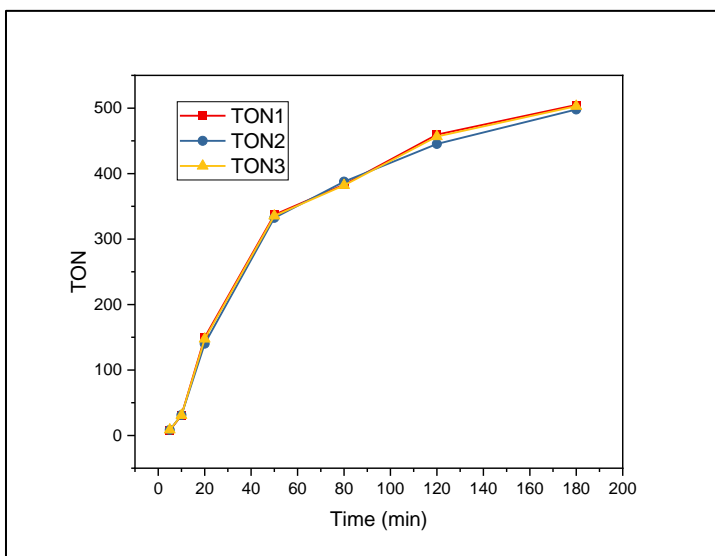


Figure 3.64. Turnover number during 3-hour photolysis of $[\text{Mo}_3\text{S}_7(\text{S}_2\text{CN}^i\text{Bu}_2)_3]$ Cl

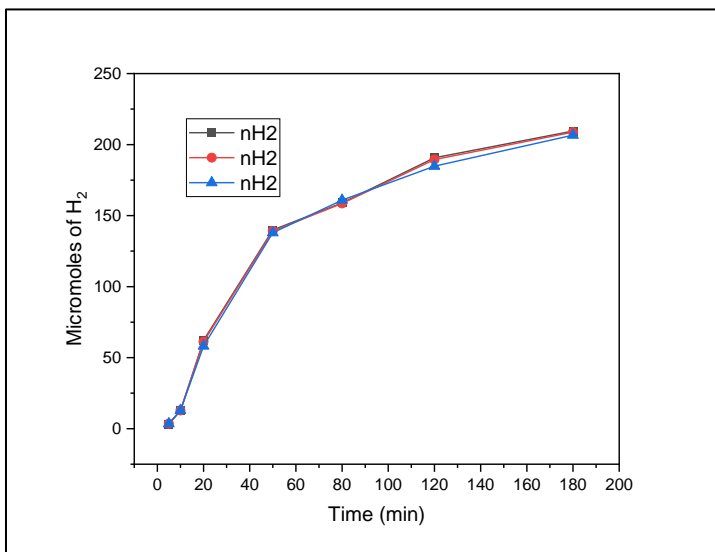


Figure 3.65. Micromoles of hydrogen during 3-hour photolysis of $[\text{Mo}_3\text{S}_7(\text{S}_2\text{CN}^i\text{Bu}_2)_3]$ Cl

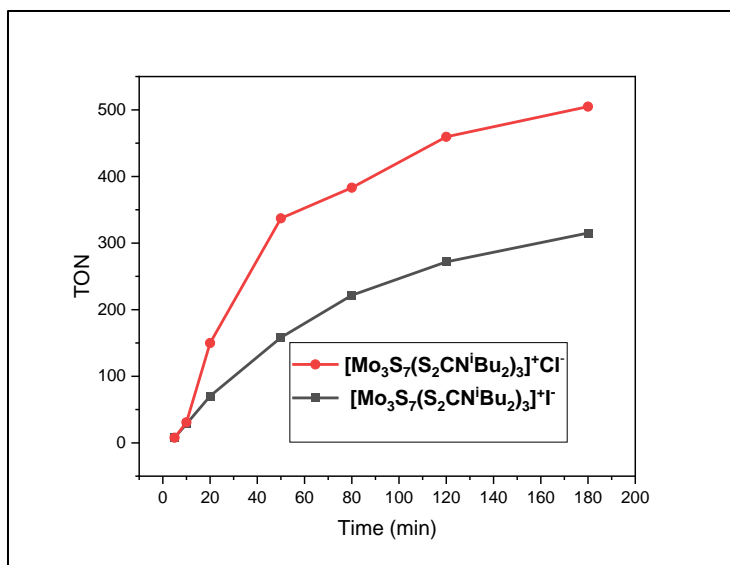


Figure 3.66. photolysis measurement comparing $[\text{Mo}_3\text{S}_7(\text{S}_2\text{CN}^i\text{Bu}_2)_3]^+\text{I}^-$, versus $[\text{Mo}_3\text{S}_7(\text{S}_2\text{CN}^i\text{Bu}_2)_3]^+\text{Cl}^-$.

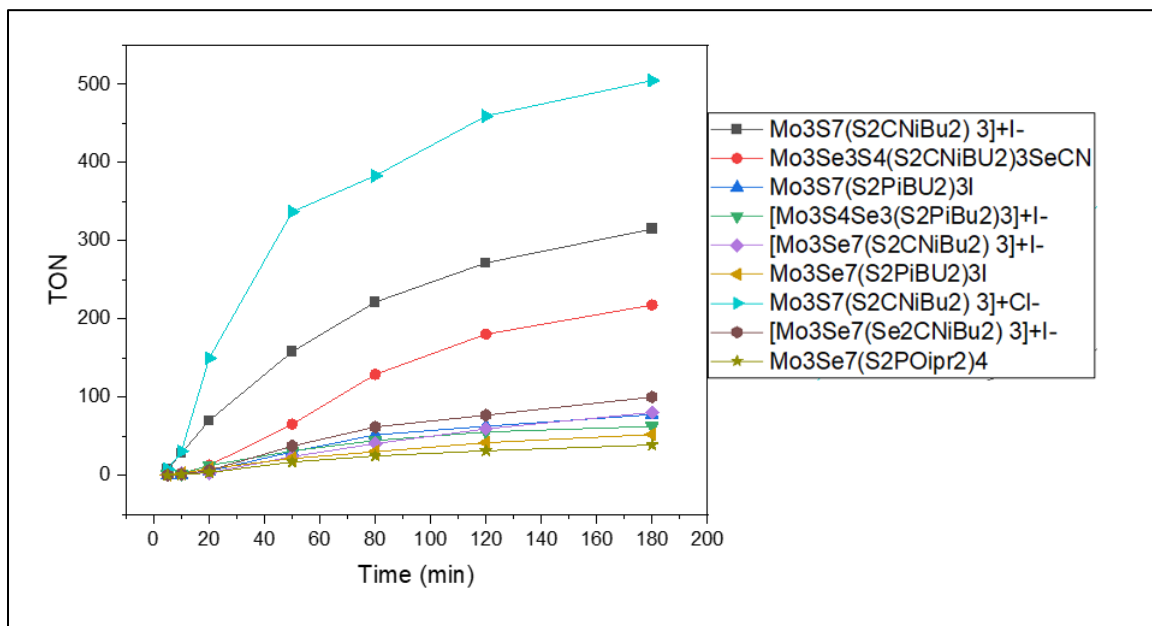


Figure 3.67. Comparison of all clusters.

3.7 Conclusion

Preparation of broad $[\text{Mo}_3\text{Q}_7\text{L}_3]^+$ complexes; $\text{L} = (-\text{S}_2\text{CN}^i\text{Bu}_2, -\text{Se}_2\text{CN}^i\text{Bu}_2, -\text{S}_2\text{PiBu}_2, -\text{S}_2\text{P}(\text{O}^i\text{Pr})_2)$ $\text{Q} = (\text{S} \text{ or } \text{Se})$ was achieved by developed new methods. Although, synthesis of $[\text{Mo}_3\text{S}_7\text{L}_3]^+$ clusters having several methods, we developed a new method from $\text{Mo}(\text{CO})_6$ that helps us to find out maximally active catalyst in our photosystem. However, for selenium analogs $[\text{Mo}_3\text{Se}_7\text{L}_3]^+$, there was only one method that was previously developed. As we developed one of the efficient pathways for $[\text{Mo}_3\text{Se}_7\text{L}_3]^+$ clusters, we were able to make almost all types of $[\text{Mo}_3\text{Se}_7\text{L}_3]^+$ clusters. Even from triseleno carbamate $(\text{Se}_2\text{CN}^i\text{Bu}_2)$ Se ligand, $[\text{Mo}_3\text{Se}_7(\text{Se}_2\text{CN}^i\text{Bu}_2)_3]$ I compound was made by using that method.

As we successfully made all $[\text{Mo}_3\text{Q}_7\text{L}_3]^+$ clusters, to learn what effects these differing compositions of molybdenum complexes as hydrogen evolution catalyst in a photosystem was achieved. Previous work by Dr. Fontenot provided a clear idea and proposed insight for ways to carryout effective photocatalytic activity in this photosystem.

Synthesis and analysis of broad varieties of the catalysts helped to explain their differing compositions directly correlated with photocatalytic activity in this photosystem. Moreover, it provided a clear analysis to figure out and design a most active catalyst particularly for our photosystem. There were 4 different ligands $\text{L} = (-\text{S}_2\text{CN}^i\text{Bu}_2, -\text{Se}_2\text{CN}^i\text{Bu}_2, -\text{S}_2\text{P}^i\text{Bu}_2, -\text{S}_2\text{P}(\text{O}^i\text{Pr})_2)$ catalysts tested in this photosystem, $(-\text{S}_2\text{CN}^i\text{Bu}_2)$ ligand precursors produced more hydrogen than $(-\text{S}_2\text{P}^i\text{Bu}_2)$ ligand precursors.

The studies of insight compositions of these clusters in this photosystem clearly addressed that $[\text{Mo}_3\text{S}_7(\text{S}_2\text{CN}^i\text{Bu}_2)_3]$ I clusters are active than $[\text{Mo}_3\text{S}_4\text{Se}_3(\text{S}_2\text{CN}^i\text{Bu}_2)_3]$ SeCN and

$[\text{Mo}_3\text{Se}_7(\text{S}_2\text{CN}^i\text{Bu}_2)_3]$ I. Even though, the choice of solvent (MeCN:H₂O =9:1) was same for both $[\text{Mo}_3\text{S}_7(\text{S}_2\text{CN}^i\text{Bu}_2)_3]$ I and $[\text{Mo}_3\text{S}_4\text{Se}_3(\text{S}_2\text{CN}^i\text{Bu}_2)_3]$ SeCN clusters, $[\text{Mo}_3\text{S}_7(\text{S}_2\text{CN}^i\text{Bu}_2)_3]$ I act as a active catalyst in this photosystem. Comparatively, $[\text{Mo}_3\text{Se}_7(\text{S}_2\text{CN}^i\text{Bu}_2)_3]$ I cluster having less solubility in this solvent system.

Another category composition anion effect provided an interesting and important thoughts to resolve many of the problems in the homogeneous systems. Here solubility is a very important factor as previously Dr. Fontenot provided to enhance the hydrogen production in this photosystem. The solubility difference between $[\text{Mo}_3\text{S}_7(\text{S}_2\text{CN}^i\text{Bu}_2)_3]$ I and $[\text{Mo}_3\text{S}_7(\text{S}_2\text{CN}^i\text{Bu}_2)_3]$ Cl, the $[\text{Mo}_3\text{S}_7(\text{S}_2\text{CN}^i\text{Bu}_2)_3]$ Cl is readily soluble in MeCN than $[\text{Mo}_3\text{S}_7(\text{S}_2\text{CN}^i\text{Bu}_2)_3]$ I and due to electronegativity behavior of Cl⁻ is higher than I⁻, $[\text{Mo}_3\text{S}_7(\text{S}_2\text{CN}^i\text{Bu}_2)_3]$ Cl become more positive than $[\text{Mo}_3\text{S}_7(\text{S}_2\text{CN}^i\text{Bu}_2)_3]$ I.

The making of a new catalyst with more soluble behavior, $[\text{Mo}_3\text{S}_7(\text{S}_2\text{CN}^i\text{Bu}_2)_3]\text{Cl}$, made a new path to enhance the hydrogen within the 3-hours time. The new catalyst, $[\text{Mo}_3\text{S}_7(\text{S}_2\text{CN}^i\text{Bu}_2)_3]$ Cl from new method that resulted produced much greatest activity with highest TONs. Among all types of clusters, $[\text{Mo}_3\text{S}_7(\text{S}_2\text{CN}^i\text{Bu}_2)_3]$ + clusters proved again that it is an active catalyst in homogeneous systems. Particularly, $[\text{Mo}_3\text{S}_7(\text{S}_2\text{CN}^i\text{Bu}_2)_3]\text{Cl}$ catalyst is a maximally active catalyst in the photosystem.

3.8 References

- [1] C.D. Giovanni, A. Reyes-Carmona, A. Coursier, S. Nowak, J. Grenèche, H. Lecoq, L. Mouton, J. Rozière, D. Jones, J. Peron, M. Giraud, C. Tard, Low-cost nanostructured iron sulfide electrocatalysts for PEM water electrolysis, *ACS Catal.* (2016), 6, 2626–2631.
- [2] J. Kibsgaard, T.F. Jaramillo, F. Besenbacher, Building an appropriate active-site motif into a hydrogen-evolution catalyst with thiomolybdate $[\text{Mo}_3\text{S}_{13}]^{2-}$ clusters, *Nat. Chem.* (2014), 6, 248–253.
- [3] Z. Qin, Y. Chen, Z. Huang, J. Su, Z. Diao, L. Guo, Composition-dependent catalytic activities of noble-metal-free NiS/Ni₃S₄ for hydrogen evolution reaction, *J. Phys. Chem.* (2016), C 120, 14581–14589.
- [4] N. Jiang, L. Bogoev, M. Popova, S. Gul, J. Yano, Y. Sun, Electrodeposited nickelsulfide films as competent hydrogen evolution catalysts in neutral water, *J. Mater. Chem.* (2014), 2, 19407–19414.
- [5] J.O. Bockris, A.K.N. Reddy, A. K. N. Modern Electrochemistry, Springer Private Limited, New York, 2014.
- [6] J.K. Norskov, C.H. Christensen, Toward efficient hydrogen production at surfaces, *Science*, (2006), 312, 1322–1323.

- [7] D.Y. Chung, J.W. Han, D.H. Lim, J.H. Jo, S.J. Yoo, H. Lee, Y.E. Sung, Structure dependent active sites of Ni_xS_y as an electrocatalyst for hydrogen evolution reaction, *Nanoscale* (2015), 7, 5157–5163.
- [8] C.G. Morales-Guio, S.D. Tilley, H. Vrubel, M. Gratzel, X. Hu, Hydrogen evolution from a Copper(I) oxide photocathode coated with an amorphous molybdenum sulphide catalyst, *Nat. Commun.* (2014), 5 (3059) 1–7.
- [9] J.D. Benck, Z. Chen, L.Y. Kuritzky, A.J. Forman, T.F. Jaramillo, Amorphous molybdenum sulfide catalysts for electrochemical hydrogen production: insights into the origin of their catalytic activity, *ACS Catal.* (2012), 2, 1916–1923.
- [10] M.A. Lukowski, A.S. Daniel, F. Meng, A. Forticaux, L. Li, S. Jin, Enhanced hydrogen evolution catalysis from chemically exfoliated metallic MoS₂ nanosheets, *J. Am. Chem. Soc.* (2013), 135, 10274–10277.
- [11] T.R. Cook, D.K. Dogutan, S.Y. Reece, Y. Surendranath, T.S. Teets, D.G. Nocera, Solar energy supply and storage for the legacy and nonlegacy worlds, *Chem. Rev.* (2010), 110, 6474–6502.
- [12] J. Wang, W. Cui, Q. Liu, Z. Xing, A.M. Asiri, X. Sun, Recent progress in cobaltbased

heterogeneous catalysts for electrochemical water splitting, *Adv. Mater.* (2016) ,28, 215–230.

[13] Angelici, R. J. Hydrodesulfurization and Hydrodenitrogenation. In *Encyclopedia of Inorganic Chemistry*; King, R. B., Ed.; Wiley: New York, 1994; Vol. 3, pp 1433– 1443.

[14] Smil, V. *Enriching the Earth*; MIT Press: Cambridge, MA, 2001.

[15] B. Hinnemann, P.G. Moses, J. Bonde, K.P. Jørgensen, J.H. Nielsen, S. Horch, I. Chorkendorff, J.K. Nørskov, Biomimetic hydrogen evolution: MoS₂ nanoparticles as catalyst for hydrogen evolution, *J. Am. Chem. Soc.* (2005), 127, 5308–5309.

[16] Laursen, A. B.; Kegnæs, S.; Dahl, S.; Chorkendorff, I. Molybdenum Sulfides—Efficient and Viable Materials for Electro- and Photoelectrocatalytic Hydrogen Evolution. *Energy Environ. Sci.* 2012, 5, 5577– 5591.

[17] Guo, W.; Le, Q.V.; Do, H.H.; Hasani, A.; Tekalgne, M.; Bae, S.-R.; Lee, T.H.; Jang, H.W.; Ahn, S.H.; Kim, S.Y. Ni₃Se₄@MoSe₂ Composites for Hydrogen Evolution Reaction. *Appl. Sci.* 2019, 9, 5035. <https://doi.org/10.3390/app9235035>.

[18] Bui, H.T.; Lam, N.D.; Linh, D.C.; Mai, N.T.; Chang, H.; Han, S.-H.; Oanh, V.T.K.; Pham, A.T.; Patil, S.A.; Tung, N.T.; et al. Escalating Catalytic Activity for Hydrogen Evolution Reaction on MoSe₂@Graphene Functionalization. *Nanomaterials* 2023, 13, 2139. <https://doi.org/10.3390/nano131421>.

[19] Jing Yang, Jixin Zhu, Jingsan Xu, Chao Zhang, and Tianxi Liu *ACS Applied Materials & Interfaces* **2017**, 9 (51), 44550-44559 DOI: 10.1021/acsami.7b15854.

[20] Fontenot., P. R.; Shan., B.; Wang., B.; Simpson., S.; Raguathan., G.; Green., A. F.; Obanda., A.; Hunt., L. N.; Hammer., N. I.; Webster., C. E.; Mague., J. T.; Schmehl., R. S.; Donahue, J. P. Photocatalytic H₂ Evolution by Homogeneous Molybdenum Sulfide Clusters Supported by Ditiocarbamate Ligands. *Inorg. Chem.* **2019**, 58, 16458-16474.

[21] W. Kuchen, K. Strolenberg, *J. Metten Chem. Ber.*, (**1963**), 96, p. 1733.

[22] Marcoll,J.;Rabenau,A.;Mootz,D.;Wunderlich,H.*Rev.Chim.Miner.***1974**,11,607.

[23]Muller,A.;Pohl,S.;Dartmann,M.;Cohen,J.P.;Benett,J.M.;Kirchner,R.M.*Z.Naturforsch.***1979**,34B,434.

[24] Meyer,B.; Wunderlich,H. *Z.Naturforsch.***1982**,37B,1437.

[25] Maoyu,B.S.;Jinling,H.;Jiayi,L.*ActaCrystallogr.***1984**,C40,759.

[26]Halbert,T.R.;McGaully,K.;Pan,W.H.;Scernuszewicz,R.S.;Stiefel,E.I.*J.Am.Chem.Soc.***1984**,106,1849.

[27]Klingelhofer,P.;Mflller,U.;Friebel,C.;Pebler,J.*Z.Anorg.Ailg.Chem.***1986**,543,22.

[28] Fedin, V.P.; Sokolov, M.N.; Mironov, Y.V.; Kolesov, B.A.; Tkachev, S.V.; Fedorov, V.Y. *Inorg. Chim. Acta* **1990**, 167, 39.

[29] Hegetschweiler, K.; Keller, T.; Zimmermann, H.; Schneider, W.; Schmalke, H.; Dubler, E. *Inorg. Chim. Acta* **1990**, 169, 235.

[30] (a) Muller, A.; Reinsch, U. *Angew. Chem.* 1980, 92, 69. (b) Keck, H.; Kuchen, W.; Mathow, J.; Wunderlich, H. *Angew. Chem.* 1982, 94, 927. (c) Cotton, F.A.; Llusar, R.; Marler, D.O.; Schwotzer, W. *Inorg. Chim. Acta* **1985**, 102, L25.

[31] Heinrich Zimmermann, Kaspar Hegetschweiler, Thomas Keller, Volker Gramlich, Helmut W. Schmalke, Walter Petter, and Walter Schneider *Inorganic Chemistry* **1991** 30 (23), 4336-4341 DOI: 10.1021/ic00023a010.

[32] V.P. Fedin, M.N. Sokolov, O.A. Geras'ko, A.V. Virovets, N.V. Podberezskaya, V.Ye. Fedorov, *Inorg. Chim. Acta* (**1992**), 192, 153.

[33] Keck, H., Kuchen, W., Mathow, J., Meyer, B., Mottz, D. & Wunderlich, H.. *Angew. Chem. Int. Ed. Engl.* (**1981**), 20, 975-976.

[34] Yu, R. M.; Lu, S. F.; Huang, X. Y.; Wu, Q. J.; Huang, J. Q. *Chin. J. Struct. Chem.* **1998**, 17(2), 137.

[35] LU, S. F., SUN, F. X., ZHU, Y. B., PENG, Y., LIANG, Y. C., LI, J. Q., ... & LU, C. Z. (2005). Synthesis, structural characterization and properties of a series of trinuclear molybdenum-sulfur cluster compounds. *Acta Chimica Sinica*, **1979**, 63(21).

[36] V.P. Fedin, Y.V. Mironov, A.V. Virovets, N.V. Podberezskaya, V.Y. Fedorov, *Polyhedron* (**1992**), 11, 1959.

[37] M.D. Meienberger, K. Hegetschweiler, H. Rüeggli, V. Gramlich, *Inorg. Chim. Acta* (**1993**), 213, 157.

[38] Liao Ju-Hsiou and M. G. Kanatzidis, *J. Am. Chem. Soc.*, (**1990**), 112, 7400.

[39] V. P. Fedin, M. N. Sokolov, K. G. Myakishev, O. A. Gevas'ko, V. Ye. Fedorov and J. Macielik, *Polyhedron* (**1991**) in press.

[40] Fedin, V. P.; Sokolov, M. N.; Geras'ko, O. A.; Virovets, A. V.; Podberezskaya, N. V. Fedorov, V. Ye. *Inorg. Chim. Acta* **1991**, 187, 81.

[41] Almond, M. J., Drew, M. G. B., Redman, H., & Rice, D. A. A new simple synthetic route to M_3Se_7 (M=Mo or W) core containing complexes: crystal structure and characterisation of $[M_3(\mu_3-Se)(\mu-Se_2)_3(dtc)_3]_2Se$. *Polyhedron* **2000**, 19(20-21), 2127–2133. [https://doi.org/10.1016/S0277-5387\(00\)00515-5](https://doi.org/10.1016/S0277-5387(00)00515-5).

[42] Gushchin, A. L.; Llusar, R.; Vicent, C.; Abramov, P. A.; Gómez-García, C. J. Mo_3Q_7 (Q = S, Se) Clusters Containing Dithiolate/Diselenolate Ligands: Synthesis, Structures, and

Their Use as Precursors of Magnetic Single-Component Molecular Conductors. *Eur. J. Inorg. Chem.* **2013**, 2615-2622. <https://doi.org/10.1002/ejic.201201532>.

[43] Lawton, S. L. The Crystal and Molecular Structure of Bis(O,O'-diisopropylphosphorothionyl) Disulfide, $[(i-C_3H_7O)_2PS_2]_2$. *Inorg. Chem.* **1970**, 9, 2269-2274.

[44] Potrzebowski, M. J. Reibenspies, J. H.; Zhong, Z. X-Ray and ^{31}P CP MAS NMR Studies of Bis(Dialkoxythiophosphoryl) Disulfides. *Heterat. Chem.* **1993**, 2, 455-460.

[45] Ivanov, A. V.; Korneeva, E. V.; Lutsenko, I. A.; Gerasimenko, A. V.; Antzutkin, O. N.; Larsson, A.-C.; Sergienko, V. I. A Fixation Mode of Gold from Solutions Using Heterogeneous Reaction of Cadmium Dicyclohexyl Dithiophosphate with $H[AuCl_4]$. Structural and (^{13}C , ^{31}P) CP/MAS NMR Studies and Thermal Behaviour of Crystalline Polymeric Gold(I) Dicyclohexyl Dithiophosphate and Bis(dicyclohexylthiophosphoryl) Disulphide. *J. Mol. Struct.* **2013**, 1034, 152-161.

[46] Gallacher, A. C.; Pinkerton, A. A. Structures of the Bis(diarythiophosphoryl) Disulfides $[Ph_2P(S)]_2S_2$ and $[(PhO)_2P(S)]_2S_2$ and the Question of P-S π Bonding. *Acta Crystallogr., Sect. C* **1993**, 49, 1793-1796.

[47] Gurnani, C.; Maheshwari, S.; Ratnani, R.; Drake, J. E. Crystal Structure of Bis[*O,O'*-di(*p*-tolyl)thiophosphoryl]disulfide, [(*p*-MeC₆H₄O)₂PS₂]₂. *Anal. Sci.: X-Ray Struct. Anal. Online* **2008**, *24*, x197-x198.

[48] Mazaki, Y.; Kobayashi, K. Structure and Intramolecular Dynamics of Bis(diisobutylselenocarbamoyl) Triselenide as Identified in Solution by the ⁷⁷Se NMR Spectroscopy. *Tetrahedron Lett.* **1989**, *30*(21), 2813-2816.

[49] Shan, B. Photoinduced Electron Transfer Systems For Generation Of Strong Reductants / Oxidants And Their Applications In Solar Fuel Generation:: Tulane University Theses and Dissertations Archive, Tulane University.

[50] Fontenot, P. Synthesis, Characterization and Photocatalytic – Activity Of Homogeneous Molybdenum Sulfide Complexes Serving Hydrogen Evolution Catalyts: Tulane University Theses and Dissertations Archive, Tulane University.

Chapter 4

Synthesis of a Phosphonate-Substituted Dithiocarbamate Ligand for Surface Immobilization of Mo₃ Sulfide Catalysts

4.1 Introduction

As noted in Chapter 3, we have shown that clusters of the type $[\text{Mo}_3\text{S}_7(\text{S}_2\text{CN}^i\text{Bu}_2)_3]^+$, which are derived from $\text{Mo}(\text{CO})_6$, are precursors to fairly active homogeneous catalysts for H_2 formation under photolysis. Thus far, no method has been developed for surface attachment of discrete molybdenum sulfide clusters to electrode surfaces via covalent bonds. Here, we propose the chemical immobilization of $[\text{Mo}_3\text{S}_7(\text{S}_2\text{CNR}_2)_3]^+$ onto a Cu_2O photocathode surface. When chemically tethered to an electrode surface, a well-defined small molecule redox catalyst can enjoy the kinetic advantage of restricted proximity to the source of reducing equivalents. The methyl phosphate functional group, $(\text{HO})_2\text{P}(\text{O})\text{CH}_2-$,

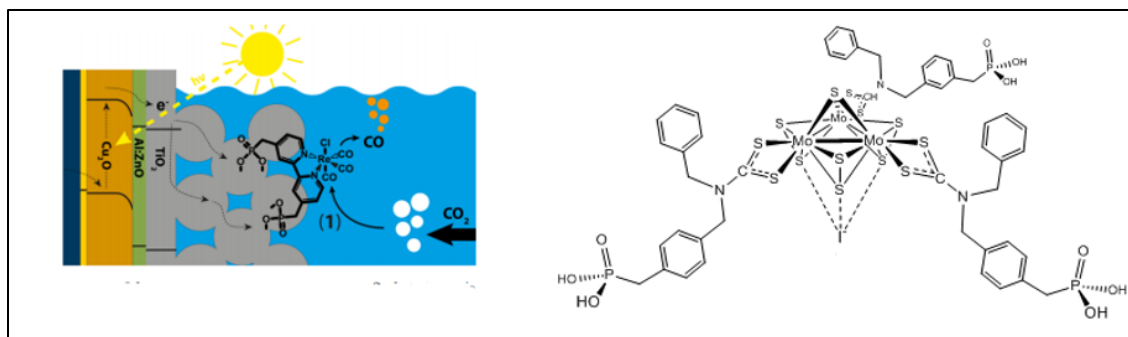
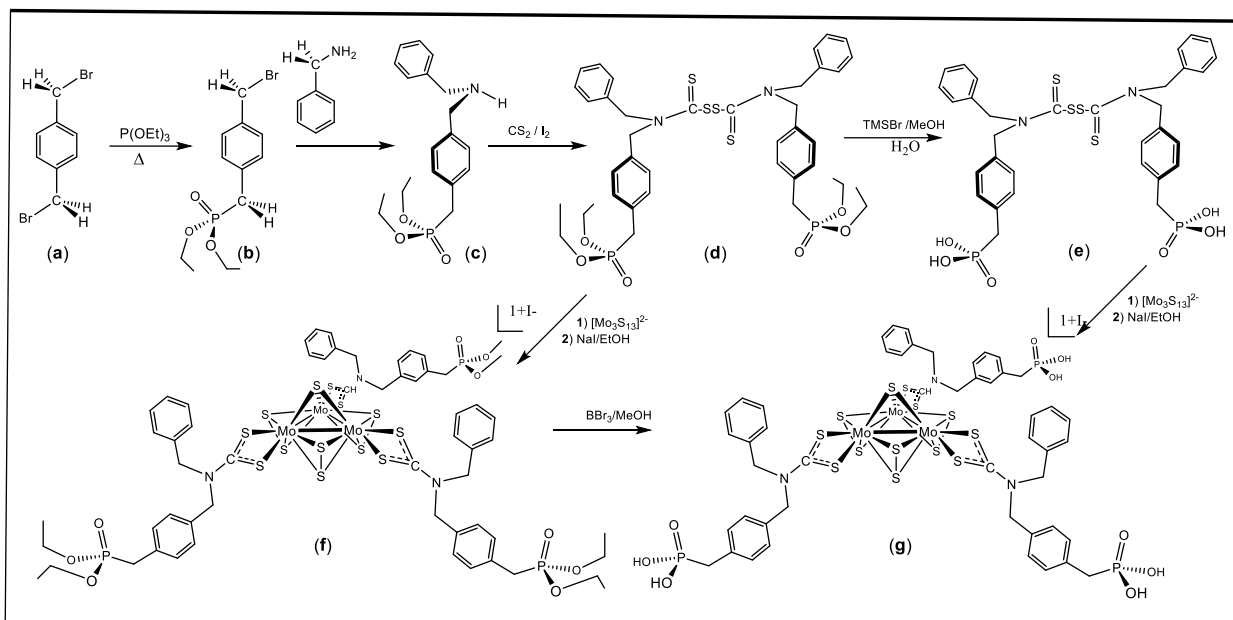


Figure 4.1. (Left) A Re catalysts for CO_2 reduction immobilized onto a Cu_2O photocathode by a bipyridyl ligand functionalized with phosphate groups. Reproduced with permission from American Chemical Society. (Right) A proposed $[\text{Mo}_3\text{S}_7]^{4+}$ cluster functionalized with a phosphonate-substituted dithiocarbamate ligand.



Scheme 4.1. A proposed synthesis of an asymmetric phosphate-substituted dithiocarbamate ligand for surface immobilization.

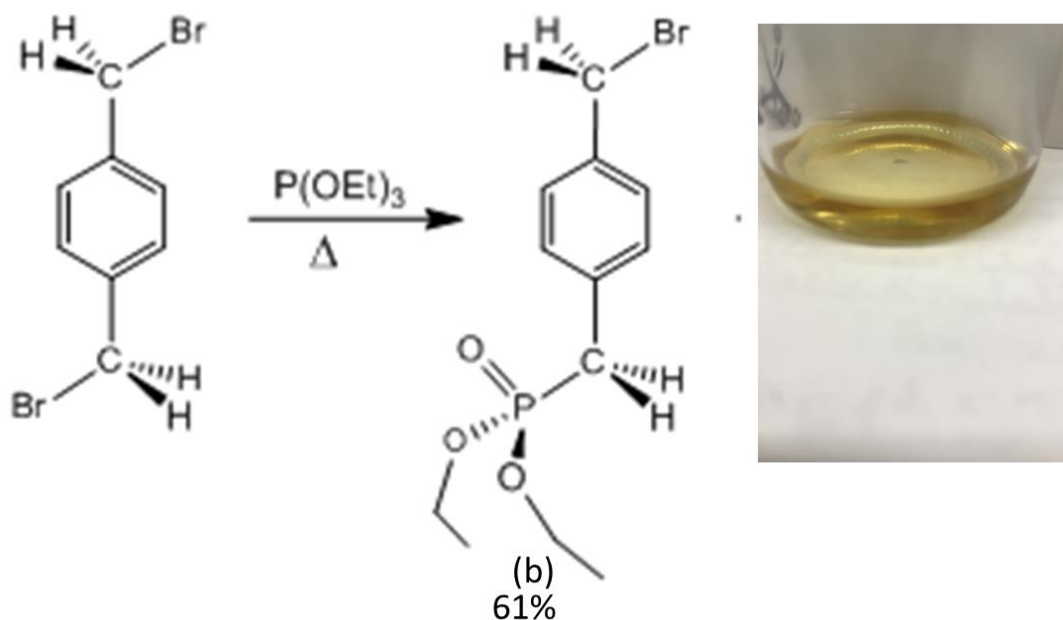
has been incorporated into 2,2'-bipyridine¹ (**Figure 4.1**, left) and 1,10 phenanthroline² ligands for the tethering of a metal complex to an oxide surface and is therefore a well-vetted choice as anchoring unit.

4.2 Physical Methods and General Considerations

All NMR spectra were obtained at 25 C with a Bruker-400 MHz spectrometer with a δ (ppm) scale and TMS (= 0 ppm) as an internal standard. The ESI-MS spectra were recorded on a microTOF 11 Bruker Daltonics instrument. Solvents for synthesis were dried with a system of drying columns from the Glass Contour Company (CH_2Cl_2 , THF, Et_2O). The anhydrous solvents (DMF, EtOH) were purchased from commercial sources. All other reagents where commercially available products were used without further purification.

4.3 Result and Discussion

Herein, a synthesis procedure for the surface-tethering of a $[\text{Mo}_3\text{S}_7(\text{S}_2\text{CN}^i\text{Bu}_2)_3]^+$ type cluster is described (**Scheme 4.1**). Beginning with commercially available 1,4-bis(bromoethyl)benzene ((**a**), **Scheme 4.1**), a Michaelis-Arbuzov condensation followed by $\text{S}_{\text{N}}2$ reaction with benzyl amine and triethylamine (base) produces the asymmetric dibenzyl amine shown as (**c**) in **Scheme 4.1**. Treatment of (**c**) with carbon disulfide followed by a typical oxidation protocol for tetrathium disulfide synthesis should yield (**d**). Dealkylation of phosphonate (**d**) with TMSBr , MeOH and water is intended to produce phosphonic acid (**e**). Compound (**e**) would serve as an immediate precursor to an *N,N*-dialkyldithiocarbamate ligand when introduced to $[\text{Mo}_3\text{S}_{13}]^{2-}$ complex (**g**).



Scheme 4.2. Synthesis of diethyl *P*-[[4-(bromomethyl)phenyl]methyl]phosphonate, which is targeted as precursor to phosphate-substituted-dithiocarbamate.

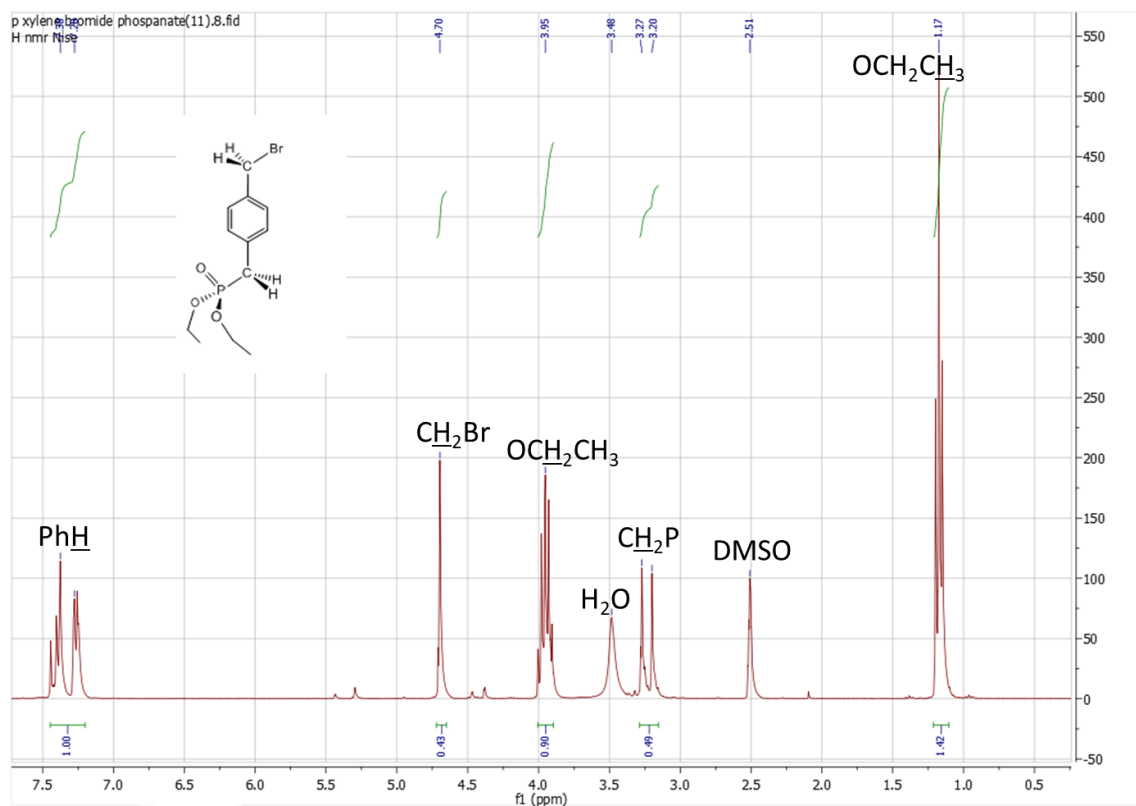
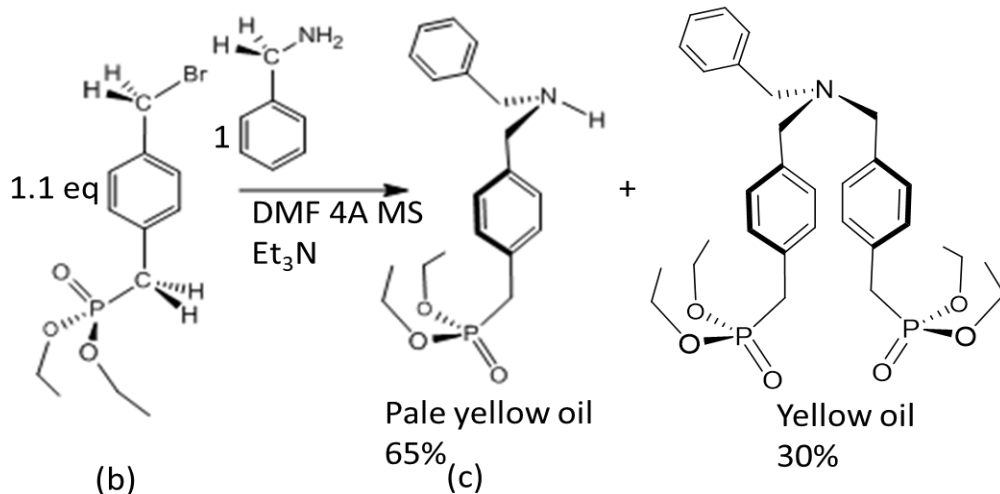


Figure 4.2. ^1H NMR spectrum in CDCl_3 of diethyl *P*-[[4-(bromomethyl)phenyl]methyl]phosphonate.

Compound (**b**)³ was prepared by refluxing commercially available *p*-xylene dibromide with 1 equivalent of triethylphosphite at 80-90°C for 3 hours. The remaining triethylphosphite was then removed by vacuum distillation. A small quantity of MeOH was added to the mixture, and unreacted *p*-xylene dibromide was then separated by filtration. Then the remaining oily material was purified by silica column chromatography (3:7/EtOAc:hexanes) to afford (**b**) in **Scheme 4.2** as a pale yellow oil (61%), as gauged by ^1H NMR spectroscopy (**Figure 4.2**).

In the next step (**Scheme 4.3**), compound (**b**) (2.35 g) was treated with 1 equivalent of benzyl amine (0.79 mL) in the presence of 1 equivalent of NEt_3 (1 mL), activated powered



Scheme 4.3. Synthesis of diethyl [[4-[(phenylmethyl)amino]methyl]phenyl]methyl] phosphonate, (c).

4 Å activated powdered molecular sieves (1 g)(optional) and dry DMF (30 mL) at 20-25°C for one day. The solids were separated by filtration and washed with EtOAc. The crude product collected from the filtrate was purified by silica column chromatography (EtOAc:EtOH /9.9:0.1). Before the crude product mixture was loaded onto the column, 4 drops of NEt₃ were used to wash the silica (3 times) to prevent the amine from sticking to the silica. Compound (c) was obtained as a pale-yellow oil (65%) and separated from the tertiary amine (30%), which was also a yellow oil. Initial analysis of the reaction mixture by mass spectrometry showed the presence of both components, and mass spectrometry and ¹H NMR and ³¹P NMR spectroscopy of the purified compounds confirmed their identities (**Figures 4.3-4.8**).

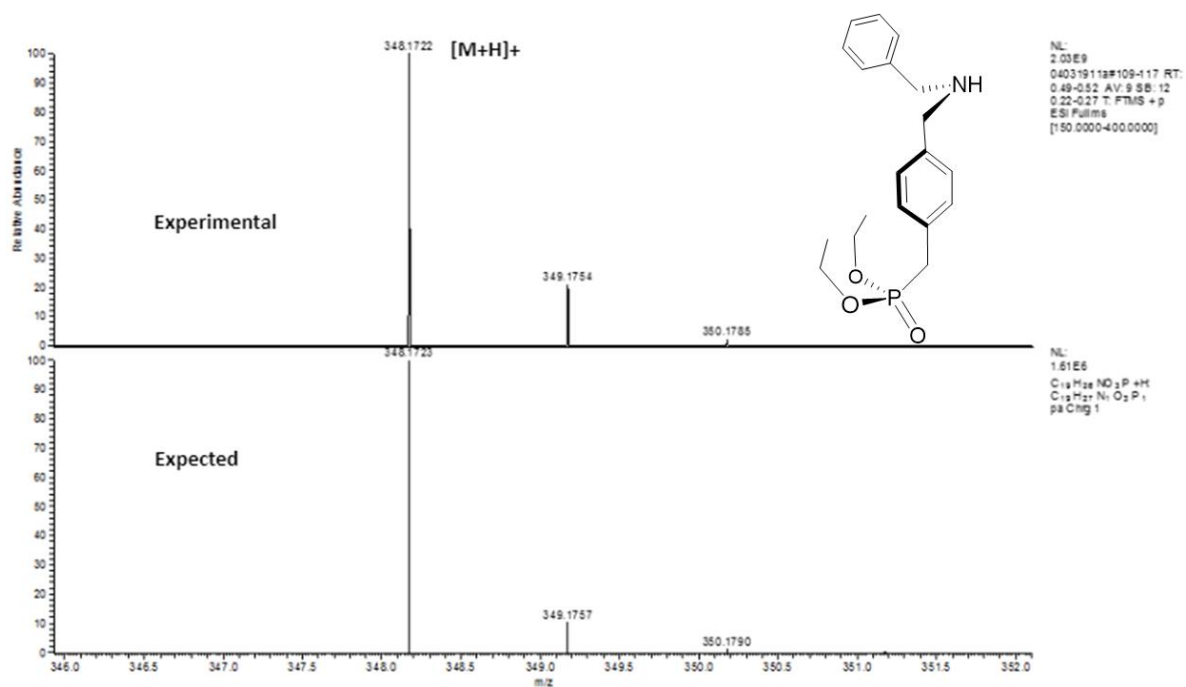


Figure 4.3. ESI mass spectrum of diethyl [[4-[(phenylmethyl)amino]methyl]phenyl]methyl] phosphate (c).

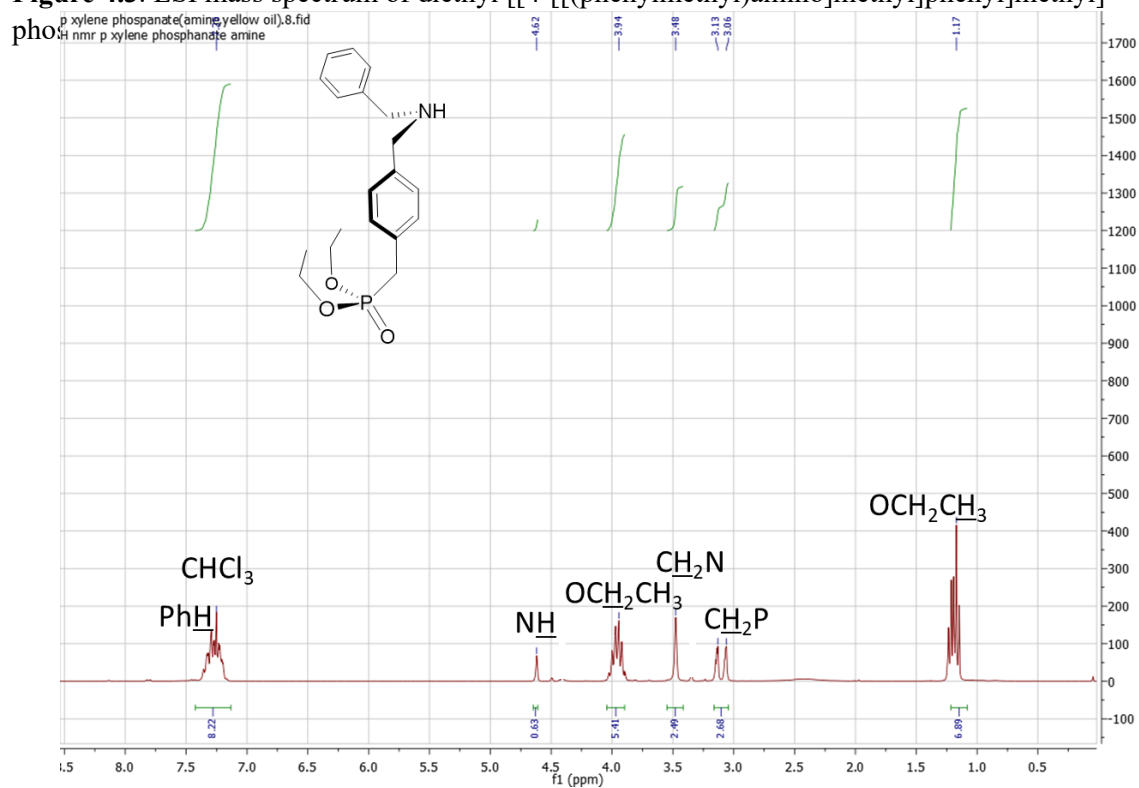


Figure 4.4. ^1H NMR spectrum of diethyl [[4-[(phenylmethyl)amino]methyl]phenyl]methyl] phosphate, (c).

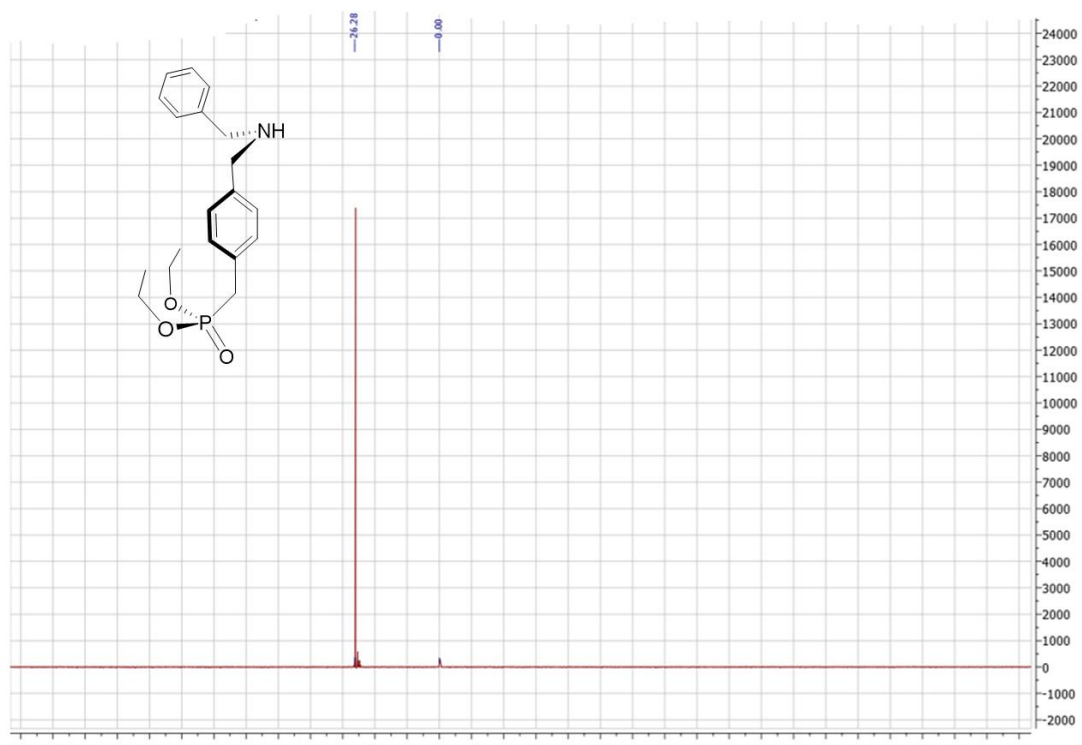


Figure 4.5. ^{31}P NMR spectrum of diethyl [[4-[(phenylmethyl)amino]methyl]phenyl]methyl]phosphonate, (c).

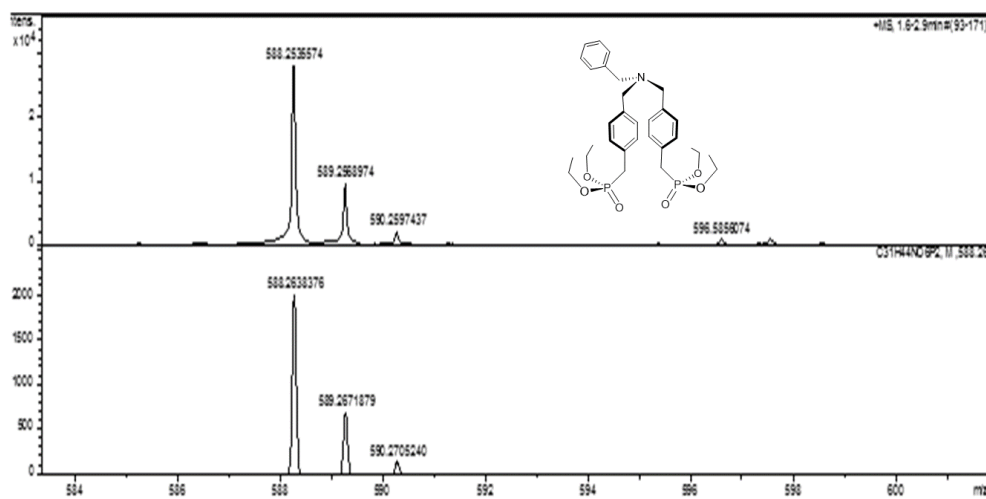


Figure 4.6. ESI mass spectrum of bis([benzyl-4-methyl]diethylphosphonate) benzylamine.

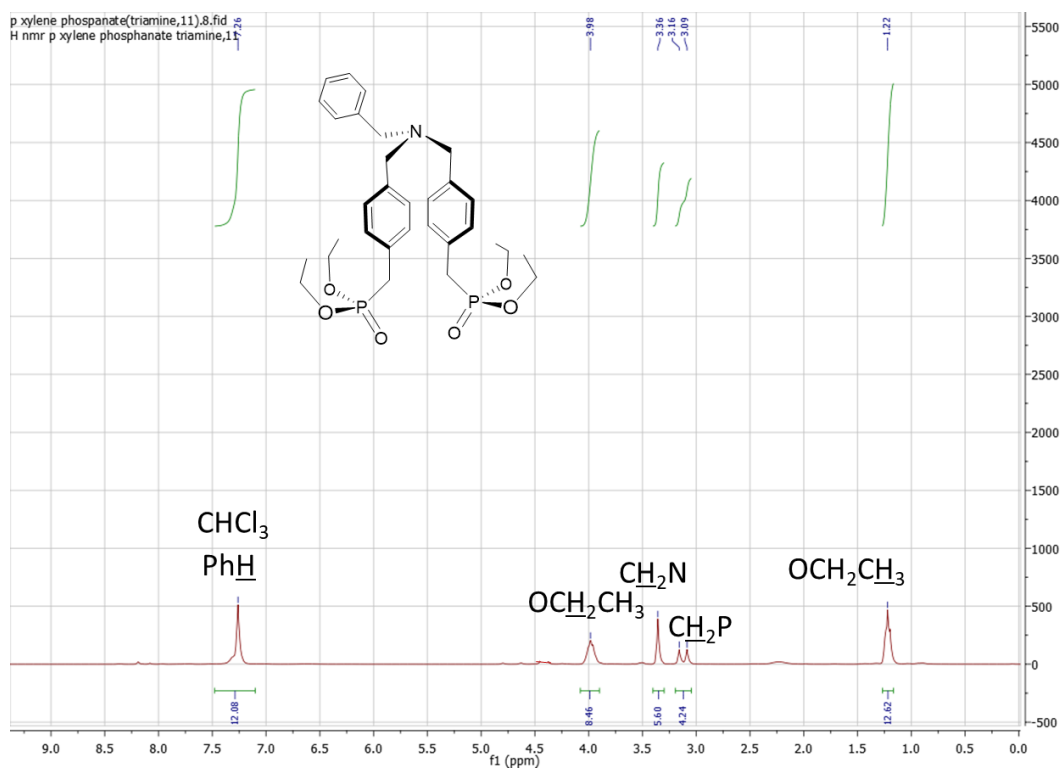


Figure 4.7. ¹H NMR spectrum of bis([benzyl-4-methyl]diethylphosphonate) benzylamine.

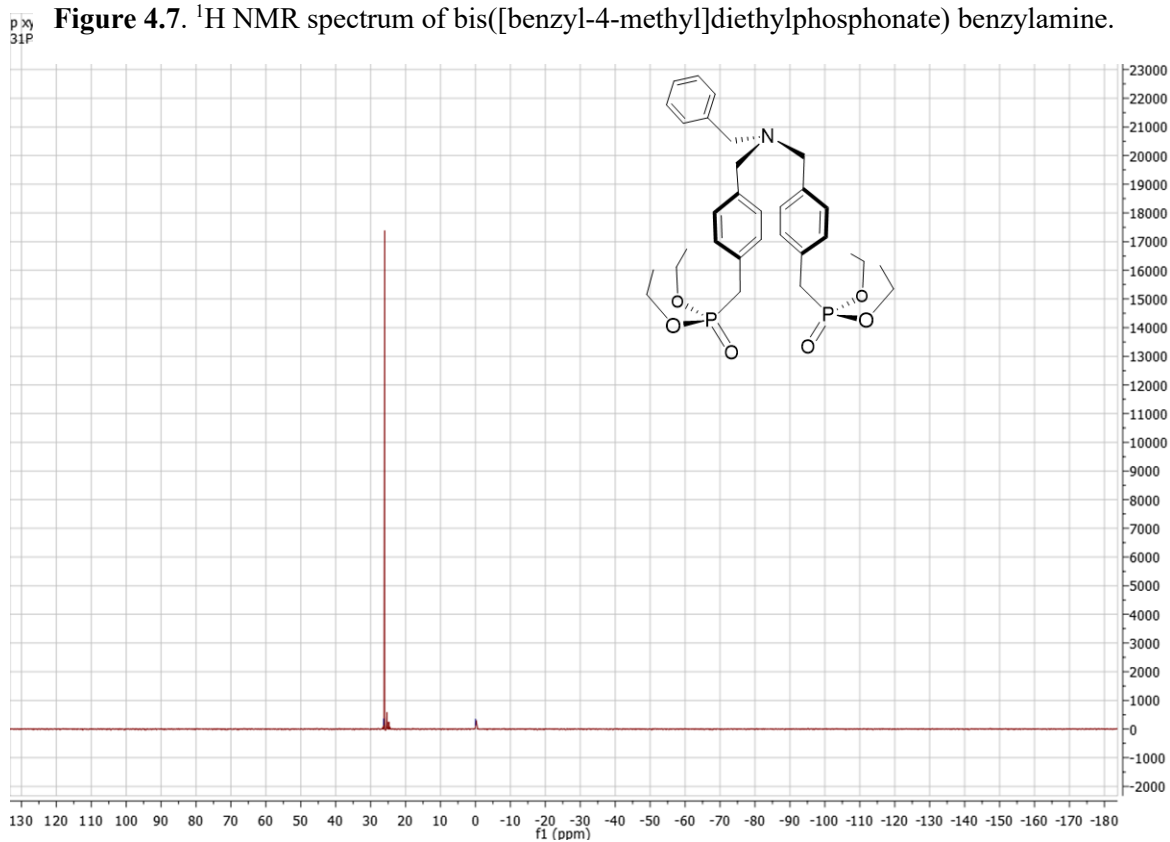
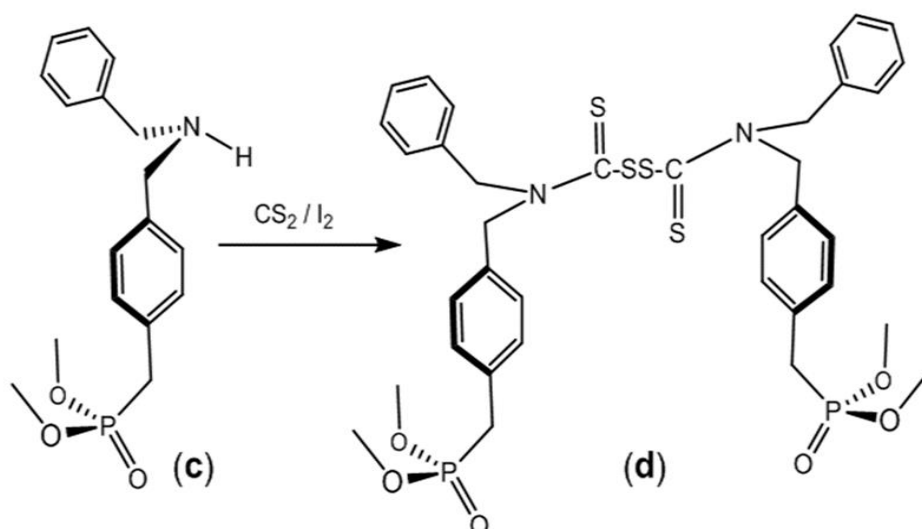


Figure 4.8. ³¹P NMR spectrum of bis([benzyl-4-methyl]diethylphosphonate) benzylamine.



Scheme 4.4. Synthesis of tetrathiuram disulfide (d).

2 equivalents of compound (c) (0.4 g) and 1 equivalent of carbon disulfide (0.044 g, 0.04 mL) were mixed in 20 mL of absolute EtOH. This mixture was stirred for 1 h at ambient temperature, and the solution was then refluxed at 90 °C under a N₂ atmosphere. Half an equivalent of solid I₂ (0.07 g) was added to the reaction mixture, and stirring was continued overnight. The mixture was cooled to room temperature, and the solvent was removed under reduced pressure to afford an oily residue. This residue was extracted with EtOAc (3 x 10 mL) and filtered through paper. A yellow oil was obtained upon removal of the solvent. The identity of the product obtained from the reaction illustrated in **Scheme 4.4** was assessed by NMR spectroscopy (**Figure 4.9**).

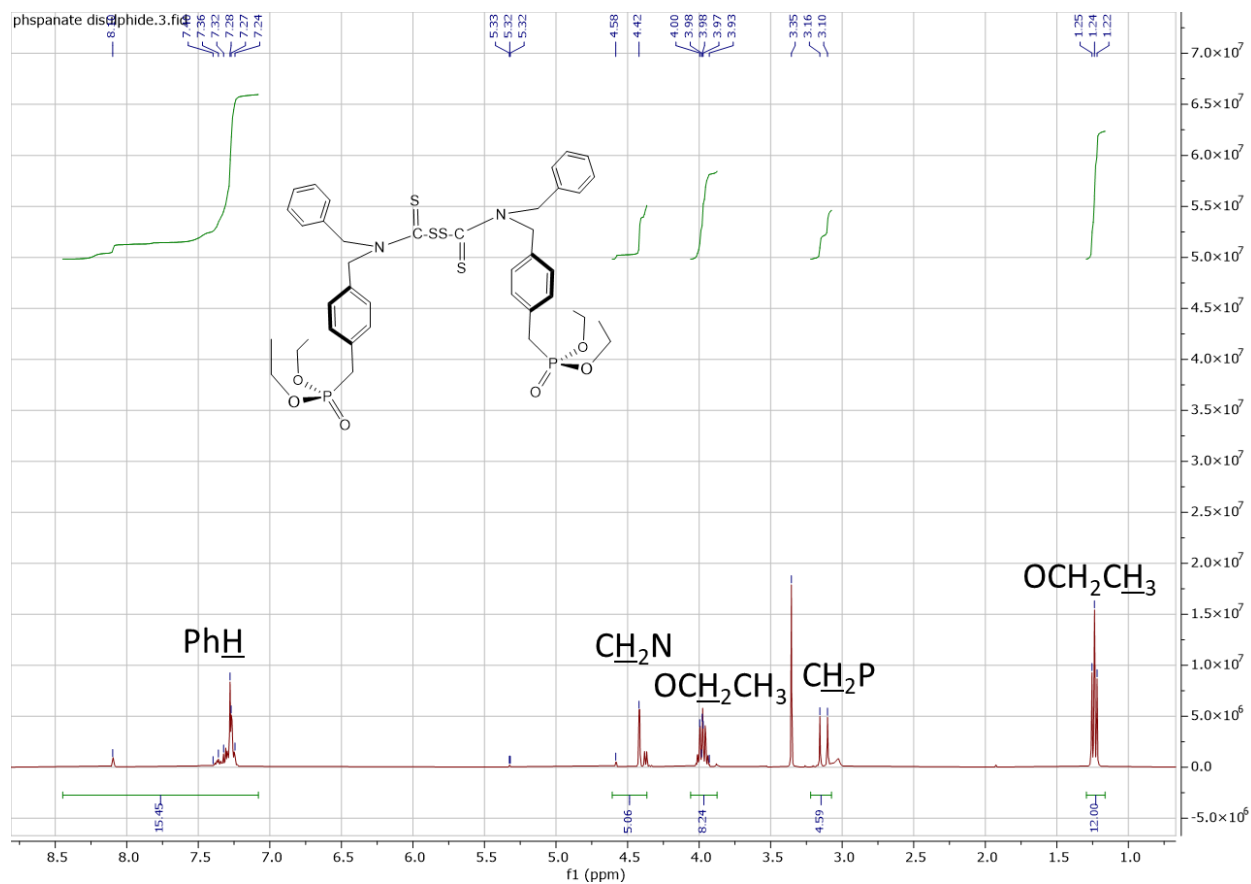
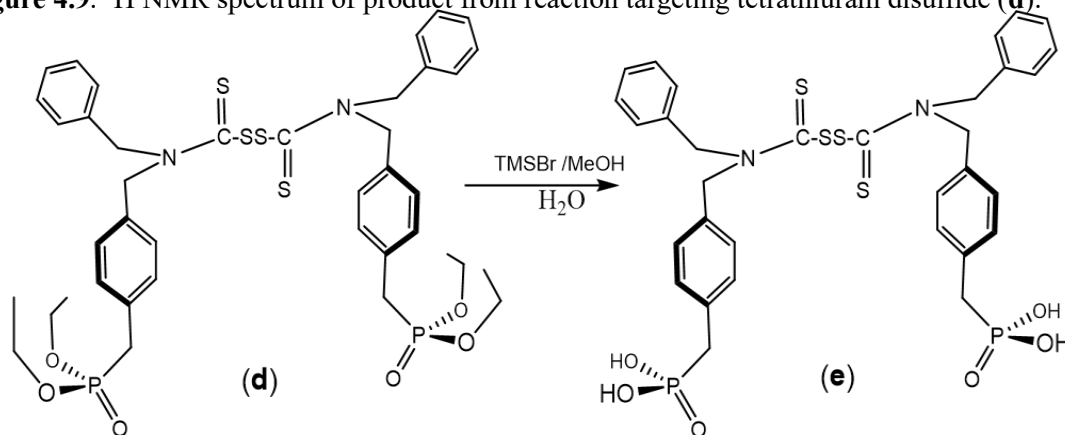


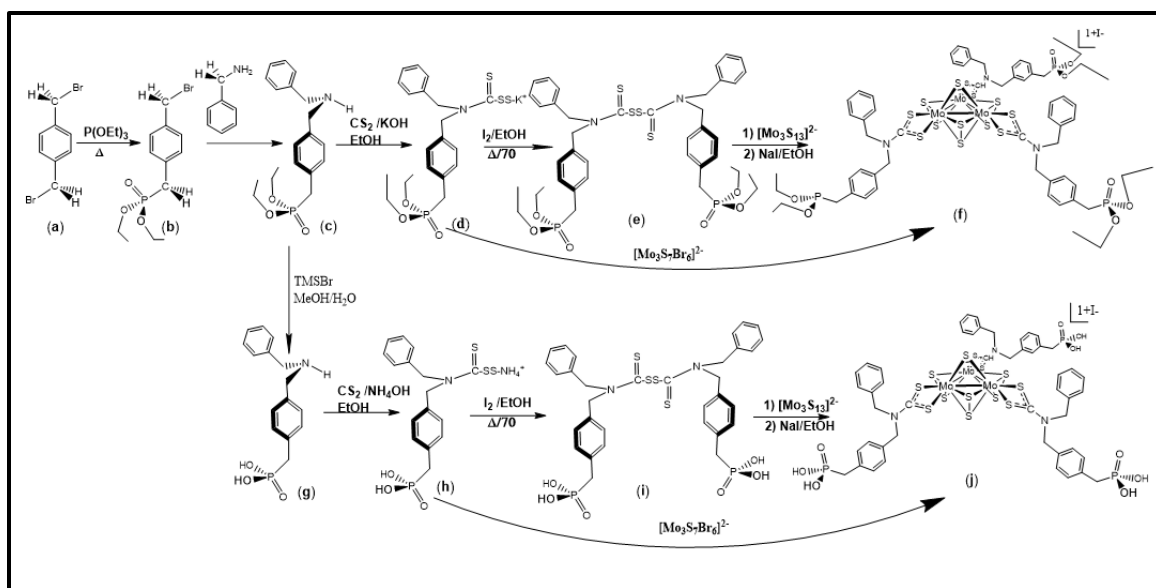
Figure 4.9. ¹H NMR spectrum of product from reaction targeting tetrathuram disulfide (**d**).



Scheme 4.5. Synthesis targeting tetrathuram disulfide (**e**).

One equivalent of the compound presumed to be (d) (0.3785 g) was added to a round bottom flask with 15 mL of dry CH₂Cl₂. The reaction mixture was stirred for 15 minutes. Then 6 equivalents of Me₃SiBr (0.355 mL) were added, and it was sealed with a greased

stopper. Stirring of the reaction was continued overnight at room temperature, and the solvent was then removed under reduced pressure. A yellow oily material was observed. Water and methanol were added. The flask was sealed with rubber septum, and a needle was inserted to vent any pressure build-up of volatiles. Then it was allowed to stir at room temperature overnight. A pale yellow solution was observed. The solvent was then evaporated overnight under a steady stream of air. The crude residue was washed with EtOAc to remove a yellow oily material and leave behind a white crude solid. This white crude solid was recrystallized from MeCN to afford white needle crystals.



Scheme 4.6. Alternative synthetic route to Mo₃ cluster

4.4 Future Work

The targeted synthesis of cluster (j) might be accomplished by an alternate route that involves reaction between the dithiocarbamate salt (h) and [Mo₃S₇Br₆]²⁻, as illustrated in **Scheme 4.6**. If cluster (j) can be accessed, then its homogeneous catalytic activity will be

assessed, and samples of it will be provided to Prof. Shanlin Pan, a collaborator at the University of Alabama, who will undertake photoelectrocatalytic studies of the cluster immobilized onto a Cu₂O electrode.

4.5 References

- (1) Schreier, M. Luo, J.; Gao, P.; Moehl, T.; Mayer, M. T.; Grätzel, M. Covalent Immobilization of a Molecular Catalyst on Cu₂O Photocathodes for CO₂ Reduction. *J. Am. Chem. Soc.* **2016**, *138*(6), 1938-1946.
- (2) Mitrofanov, A.; Brandès, S.; Herbst, F.; Rigolet, S.; Bessmertnykh-Lemeune, A.; Beletskaya, I. Immobilization of Copper Complexes with (1,10-Phenanthroline)phosphonates on Titania Supports for Sustainable Catalysts. *J. Mater. Chem. A* **2017**, *5*, 12216-12235.
- (3) Garbay-Jaureguiberry, C.; McCort-Tranchepain, I.; Barbe, B.; Ficheux, D.; Roques, B. P. Improved Synthesis of [p-Phosphono and p-Sulfo]methylphenylalanine. Resolution of [p-Phosphono-, p-Sulfo, and p-Carboxy and p-N-Hydroxycarboxamido]methylphenylalanine. *Tetrahedron: Asymmetry* **1992**, *3*(5), 637-650.
- (4) Yang, T.; Lin, C.; Fu, H.; Jiang, Y.; Zhao, Y., An Efficient Method for Synthesis of 4-(Phosphonomethyl)benzene Derivatives Under Solvent-Free Conditions. *Synth. Commun.* **2004**, *34*(6), 1017-1022.

Appendices

Supporting Spectra and Crystallographic Data

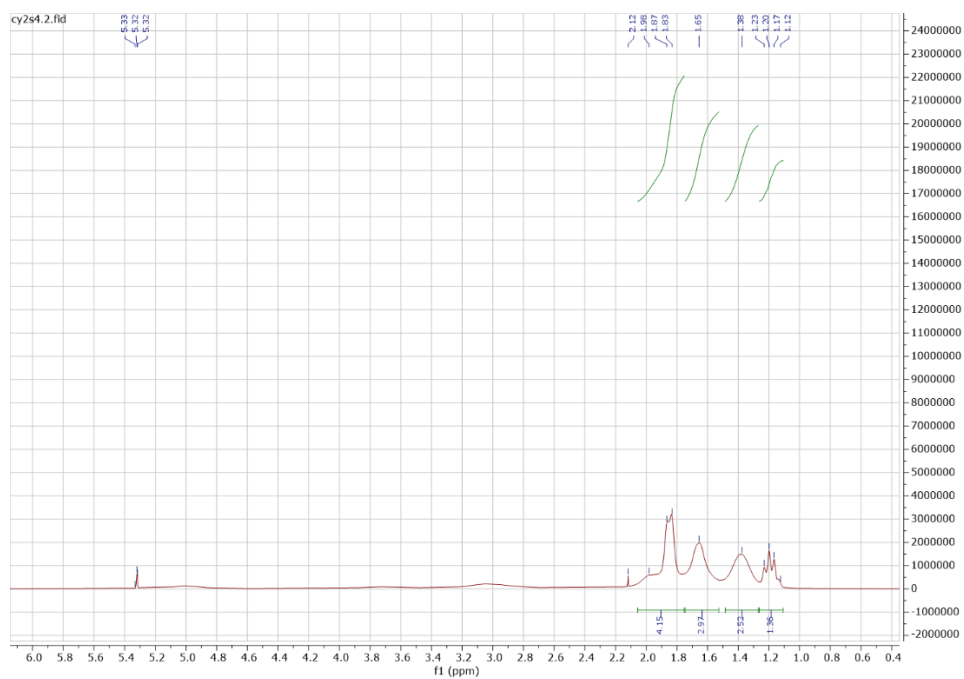


Figure B-3 ^1H NMR spectrum of complex $\text{Cy}_2\text{NCSSSSCNCy}_2$ in Chapter 2

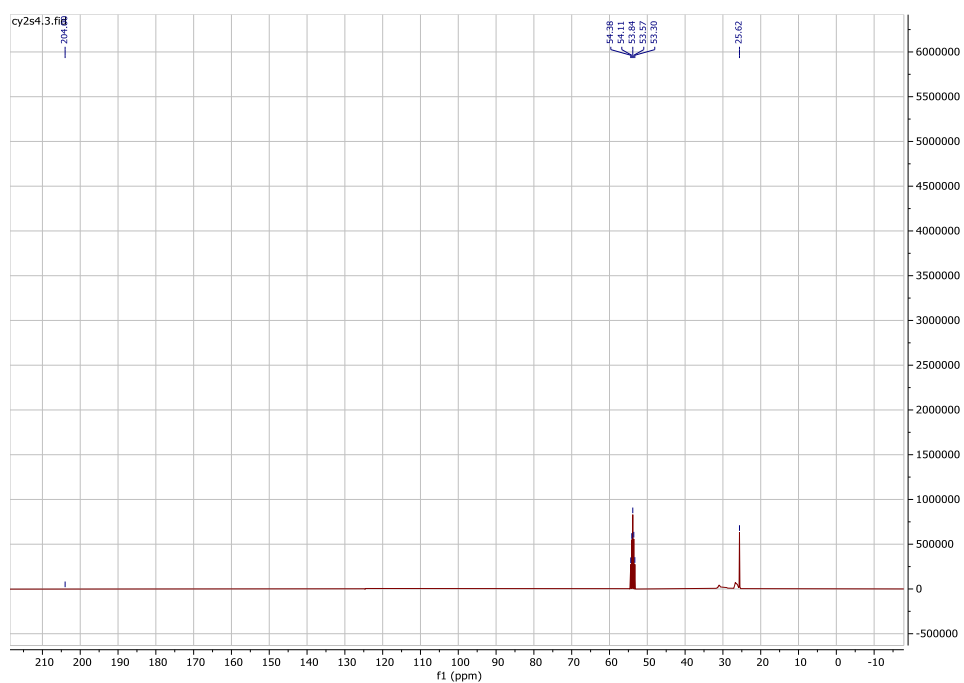


Figure B-2 ^{13}C NMR spectrum of complex $\text{Cy}_2\text{NCSSSSCNCy}_2$ in Chapter 2

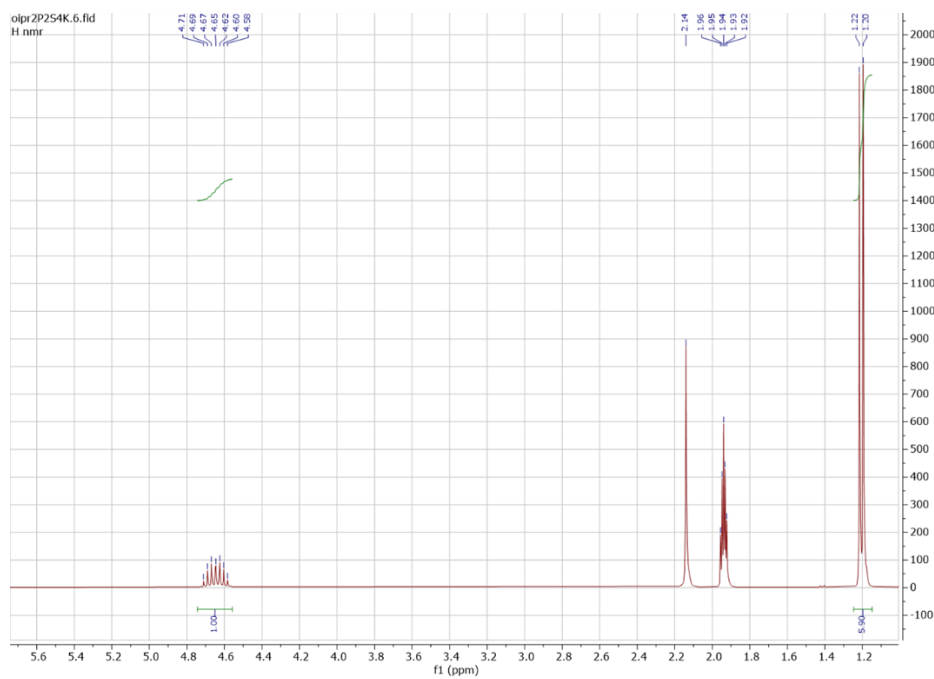


Figure C-4 ^1H NMR spectrum of complex $\text{K}[\text{S}_2\text{P}(\text{iPrO})_2]$ in Chapter 3

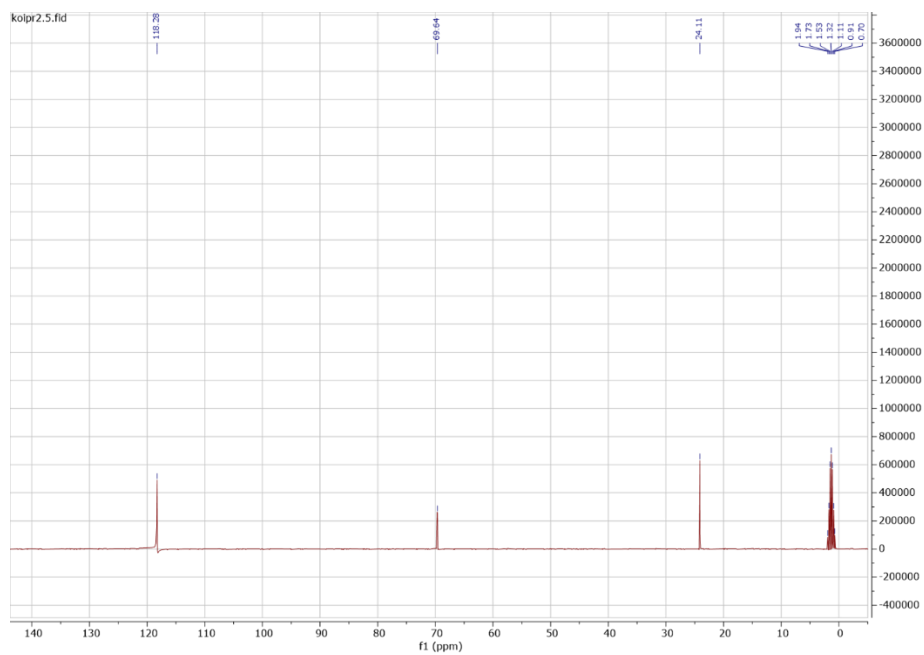


Figure C-5 ^{13}C NMR spectrum of complex $\text{K}[\text{S}_2\text{P}(\text{iPrO})_2]$ in Chapter 3

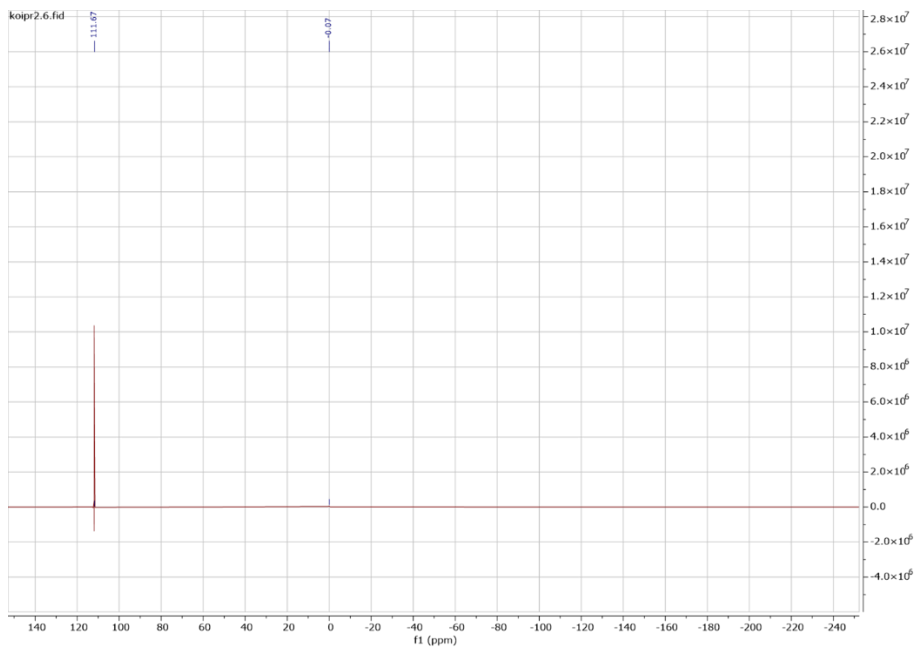


Figure C-6 ^{31}P NMR spectrum of complex $\text{K}[\text{S}_2\text{P}(\text{iPrO})_2]$ in Chapter 3

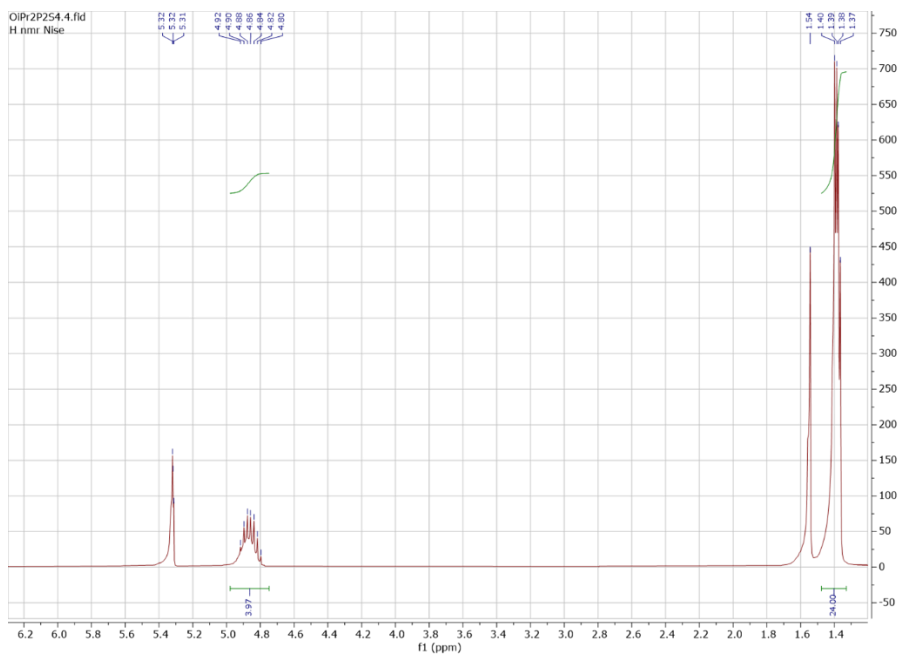


Figure C-4 ^1H NMR spectrum of complex $(\text{iPrO})_2\text{P}(=\text{S})\text{SSP}(=\text{S})(\text{O}^i\text{Pr})_2$ in Chapter 3

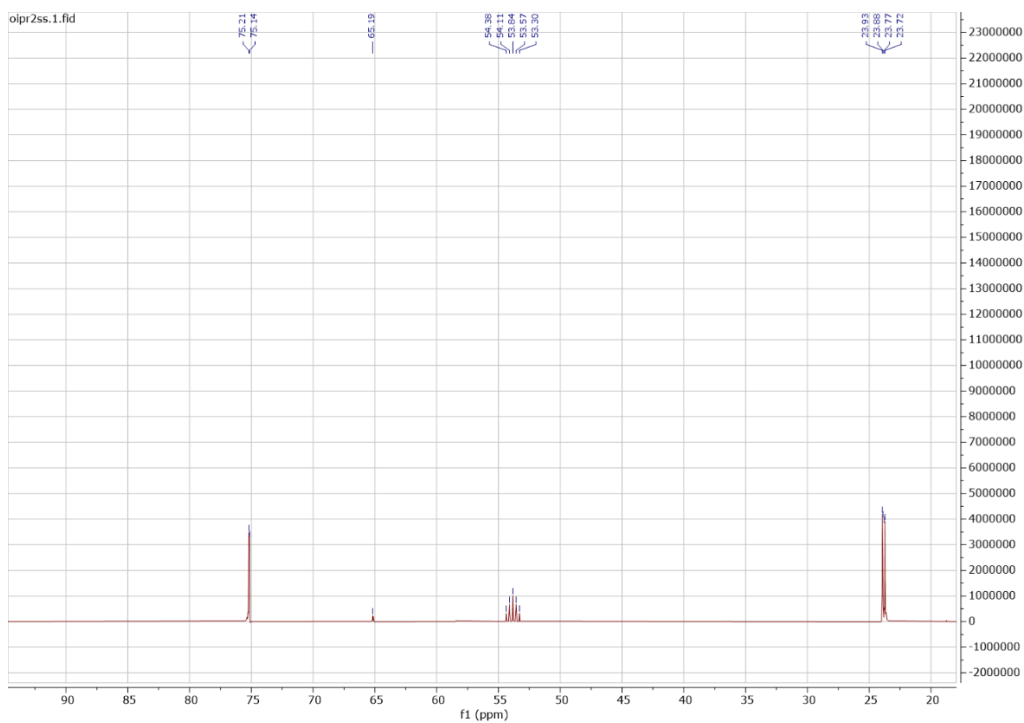


Figure C-5 ^{13}C NMR spectrum of complex $(i\text{PrO})_2\text{P}(=\text{S})\text{SSP}(=\text{S})(\text{O}^i\text{Pr})_2$ in Chapter 3

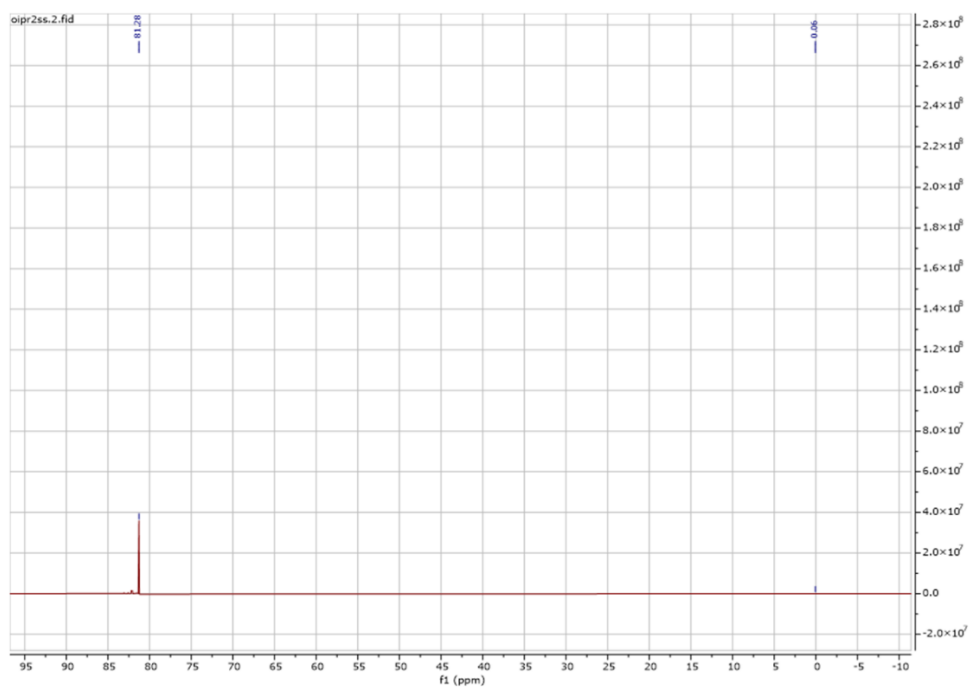


Figure C-6 ^{31}P NMR spectrum of complex $(i\text{PrO})_2\text{P}(=\text{S})\text{SSP}(=\text{S})(\text{O}^i\text{Pr})_2$ in Chapter 3

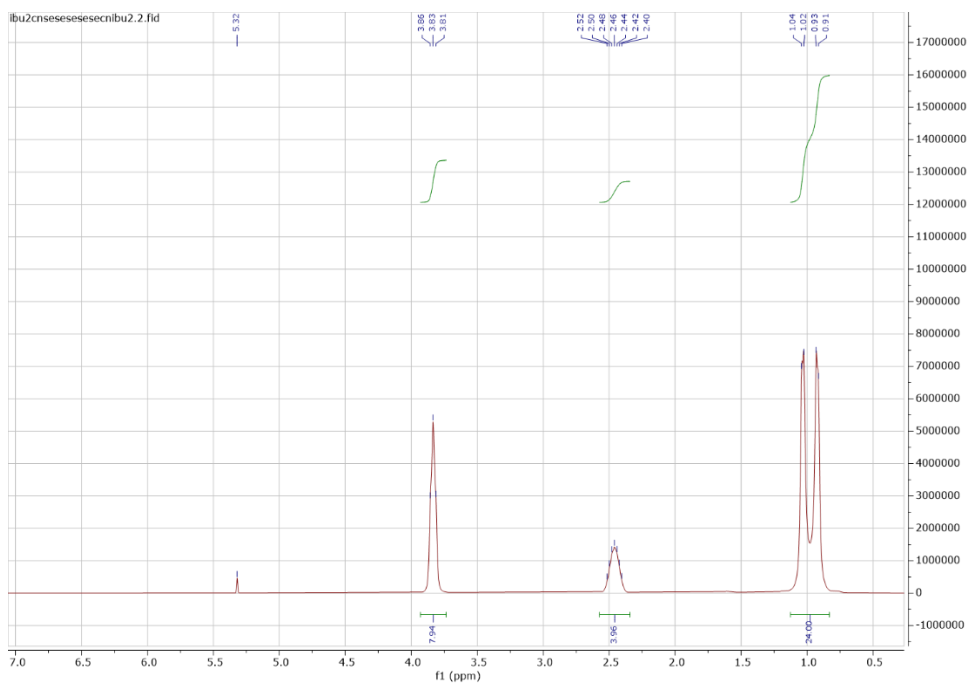


Figure C-7 ^1H NMR spectrum of complex $i\text{Bu}_2\text{NC}(=\text{Se})\text{SeSeSeC}(=\text{S})\text{N}^i\text{Bu}_2$ in Chapter 3

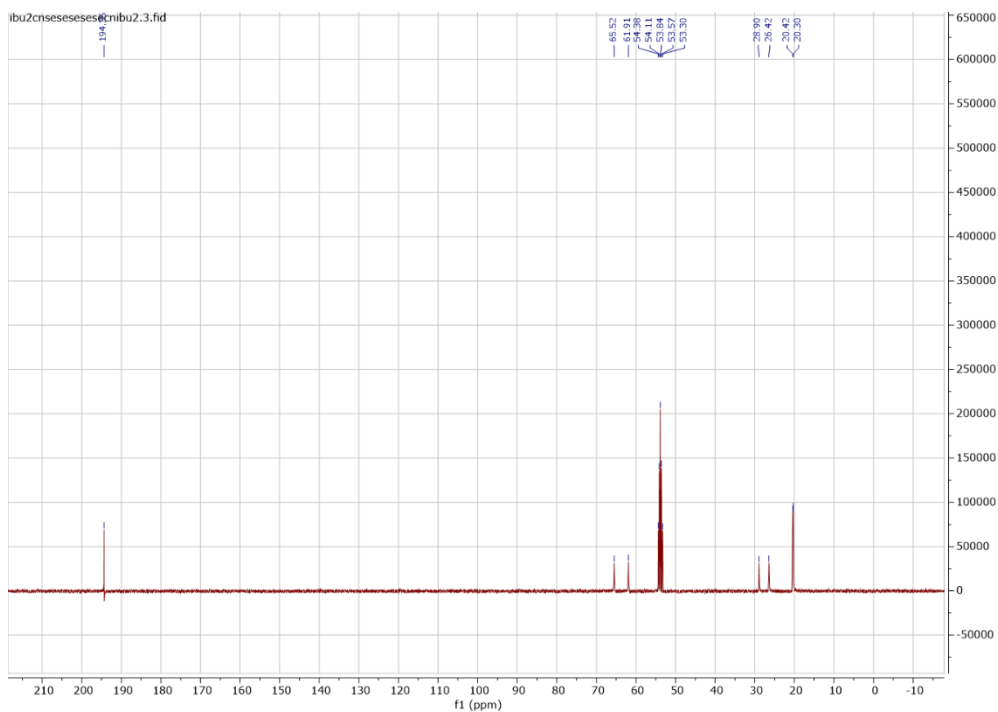


Figure C-8 ^{13}C NMR spectrum of complex $i\text{Bu}_2\text{NC}(=\text{Se})\text{SeSeSeC}(=\text{S})\text{N}^i\text{Bu}_2$ in Chapter 3

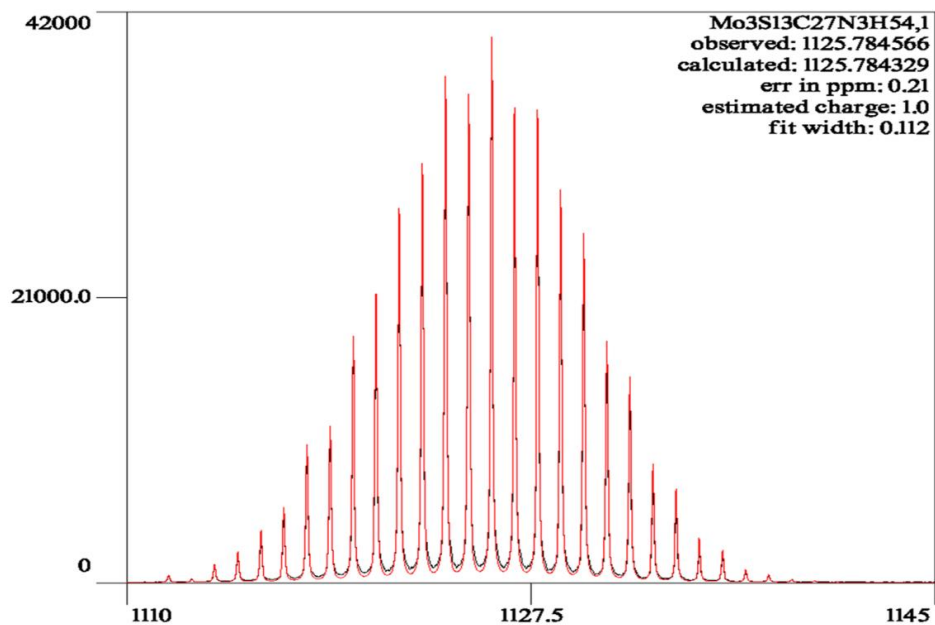


Figure C-9 ESI-MS spectrum of complex $[\text{Mo}_3\text{S}_7(\text{S}_2\text{CN}^i\text{Bu}_2)_3] \text{I}$ in Chapter 3

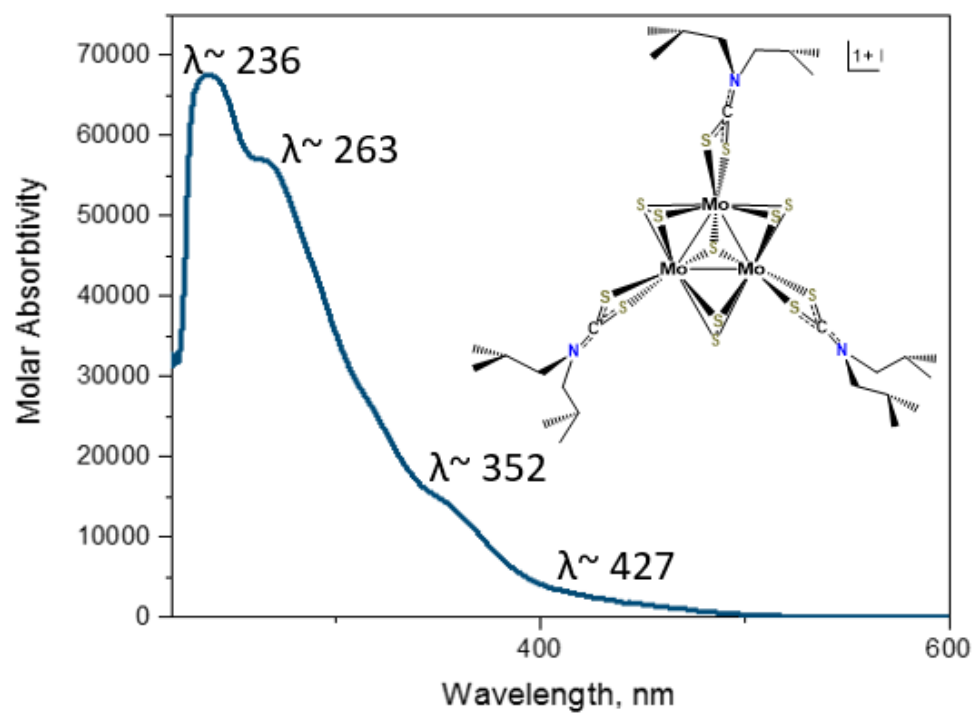


Figure C-10 UV-VIS spectrum of complex $[\text{Mo}_3\text{S}_7(\text{S}_2\text{CN}^i\text{Bu}_2)_3] \text{I}$ in Chapter 3

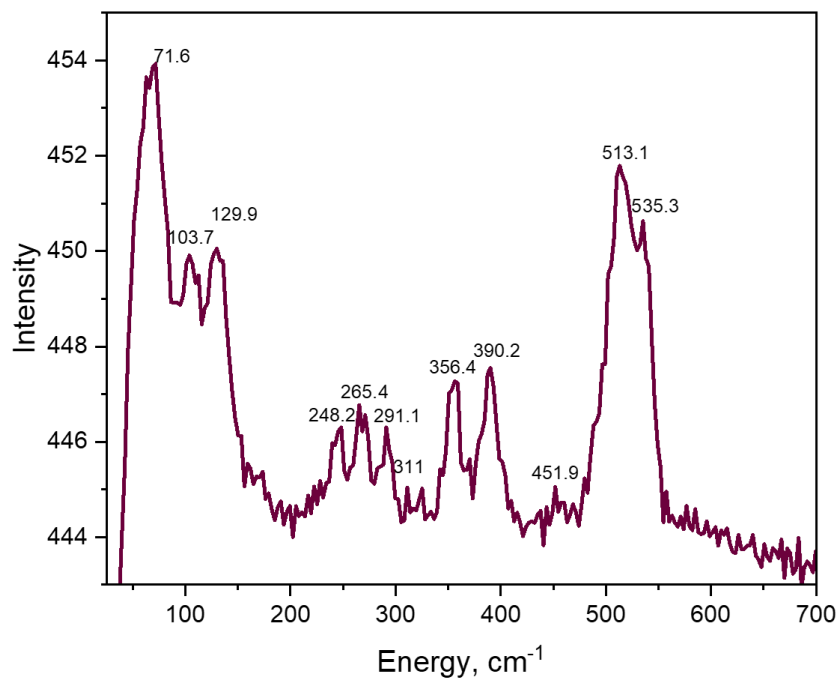


Figure C-11 Raman spectrum of complex $[\text{Mo}_3\text{S}_7(\text{S}_2\text{CN}^t\text{Bu}_2)_3]$ I in Chapter 3

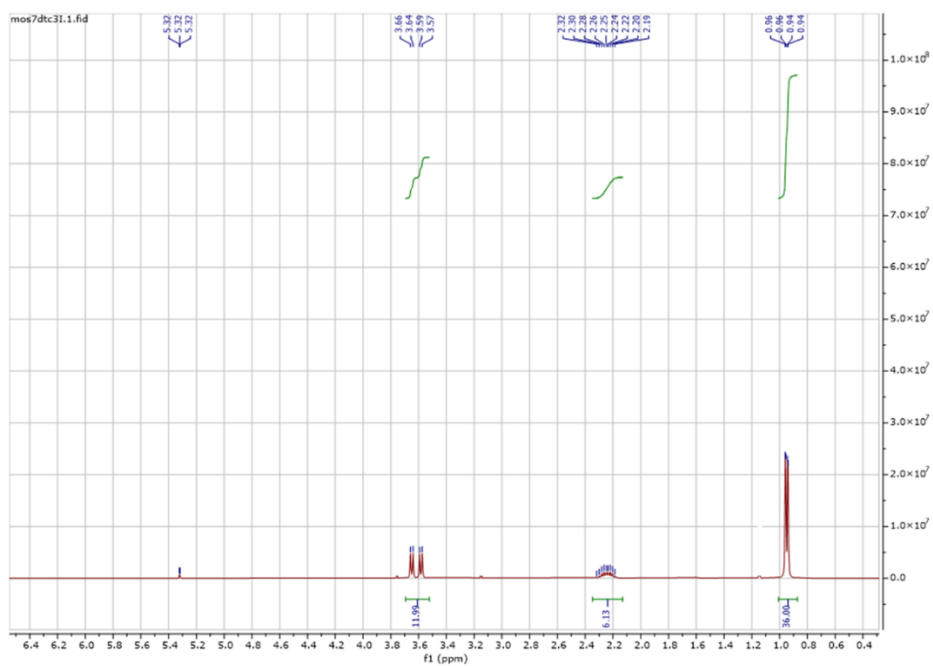


Figure C-12 ^1H NMR spectrum of complex $[\text{Mo}_3\text{S}_7(\text{S}_2\text{CN}^t\text{Bu}_2)_3]$ I in Chapter 3

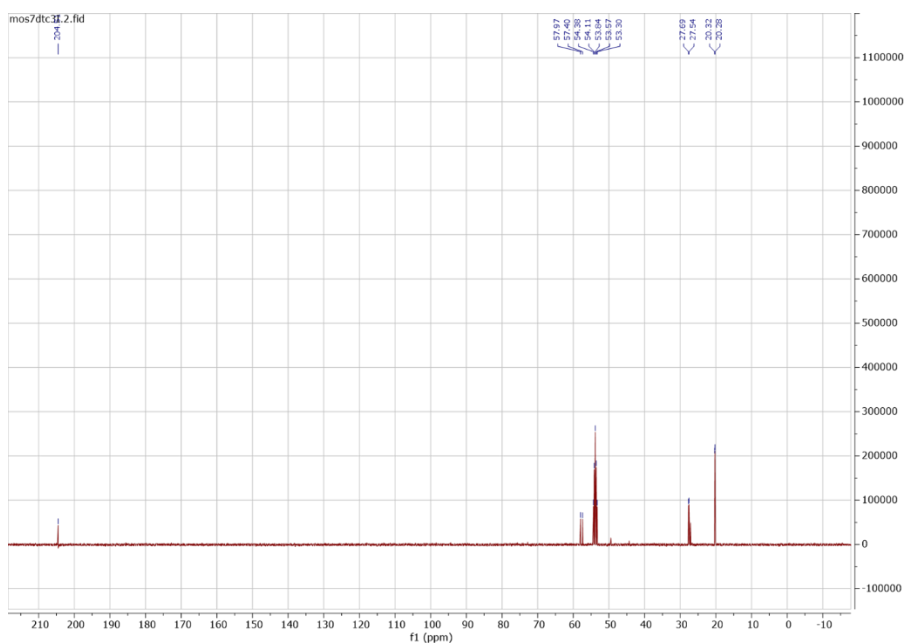


Figure C-13 ¹³C NMR spectrum of complex [Mo₃S₇(S₂CN^{*i*}Bu₂)₃] I in Chapter 3

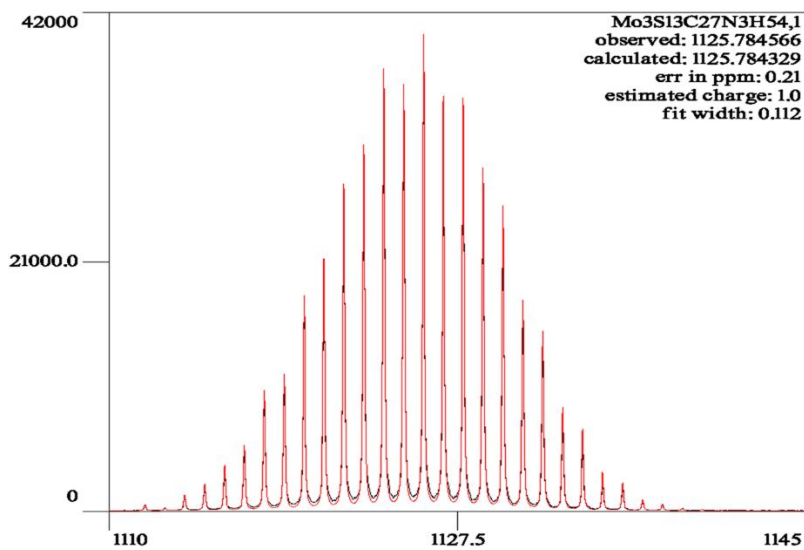


Figure C-14 ESI-MS spectrum of complex [Mo₃S₇(S₂CN^{*i*}Bu₂)₃] Cl in Chapter 3

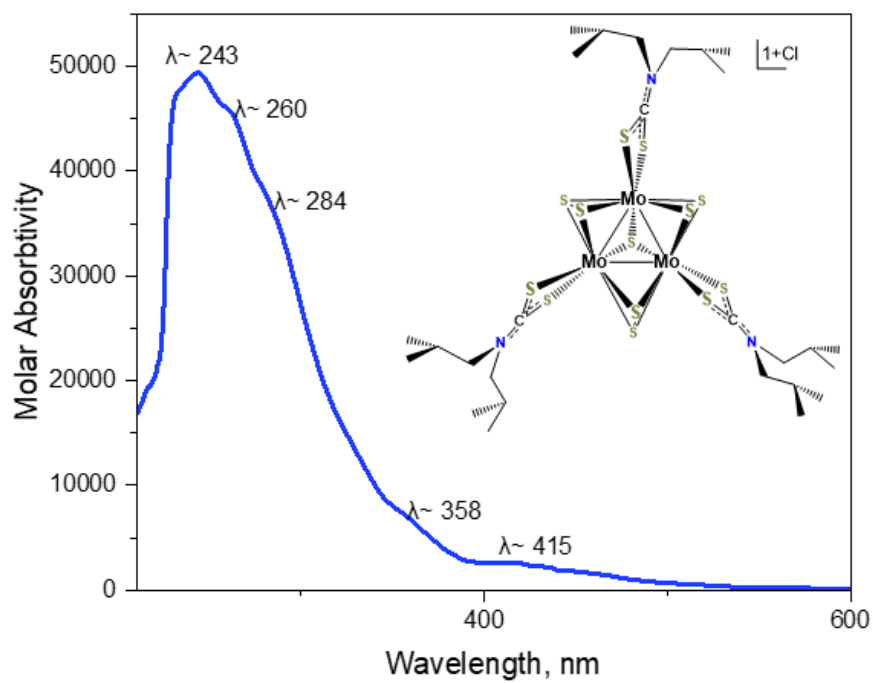


Figure C-15 UV-VIS spectrum of complex $[Mo_3S_7(S_2CN^iBu_2)_3] Cl$ in Chapter 3

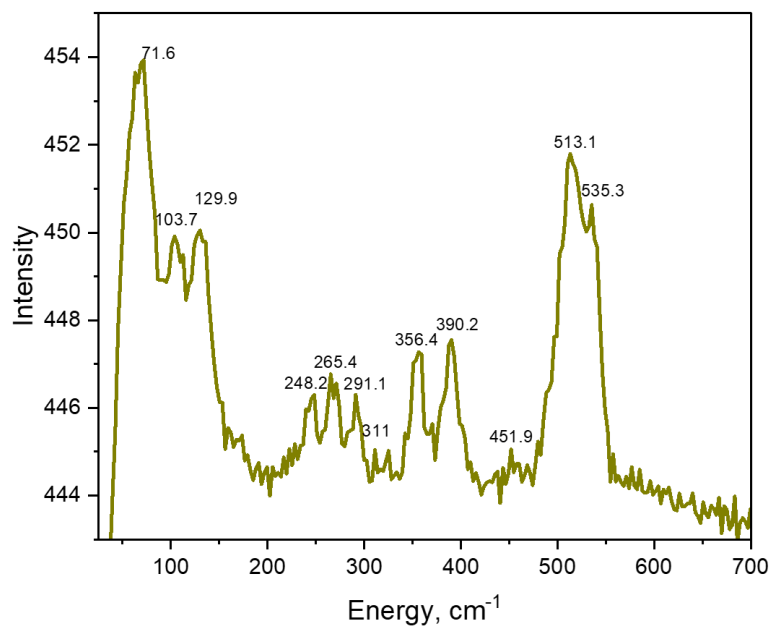


Figure C-16 Raman spectrum of complex $[\text{Mo}_3\text{S}_7(\text{S}_2\text{CN}^t\text{Bu}_2)_3] \text{Cl}$ in Chapter 3

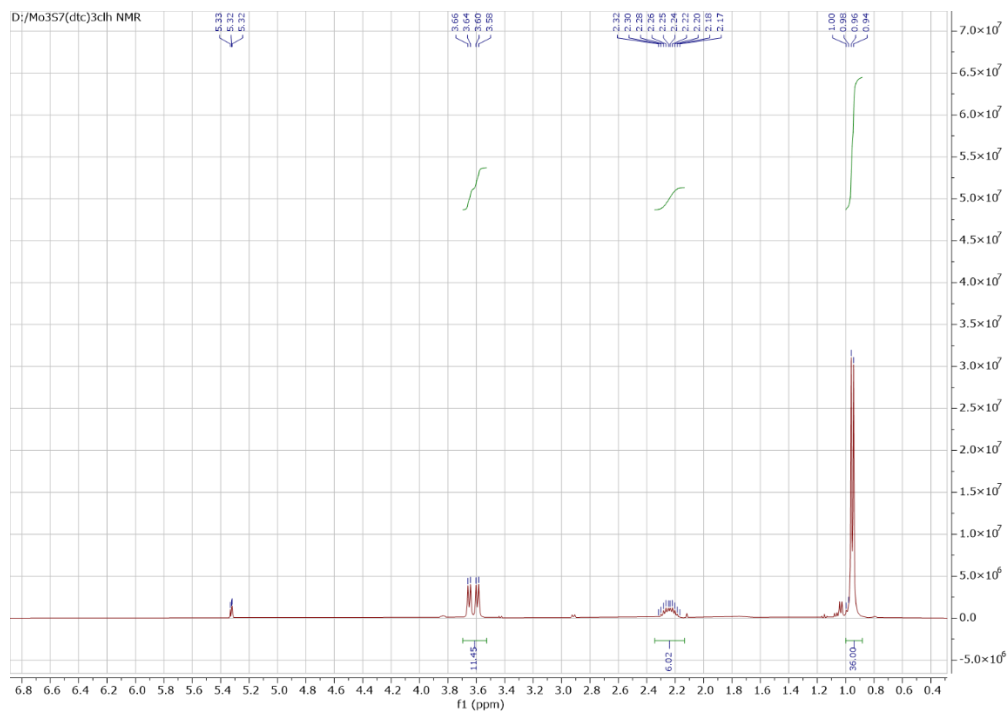


Figure C-17 ^1H NMR spectrum of complex $[\text{Mo}_3\text{S}_7(\text{S}_2\text{CN}^t\text{Bu}_2)_3] \text{Cl}$ in Chapter 3

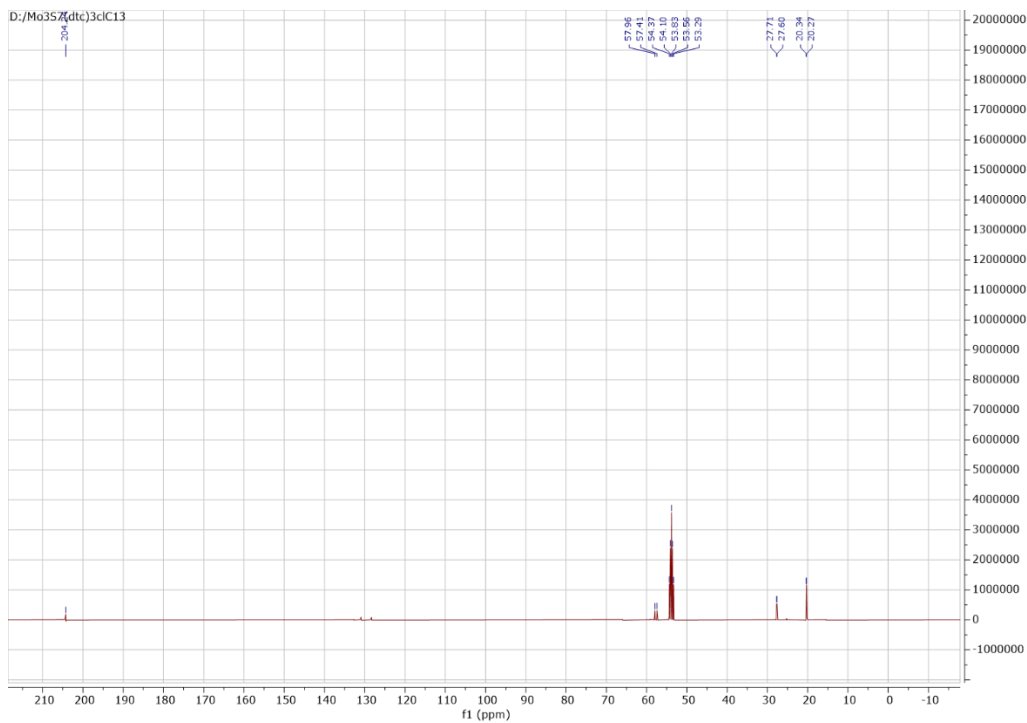


Figure C-18 ^{13}C NMR spectrum of complex $[\text{Mo}_3\text{S}_7(\text{S}_2\text{CN}^i\text{Bu}_2)_3] \text{Cl}$ in Chapter 3

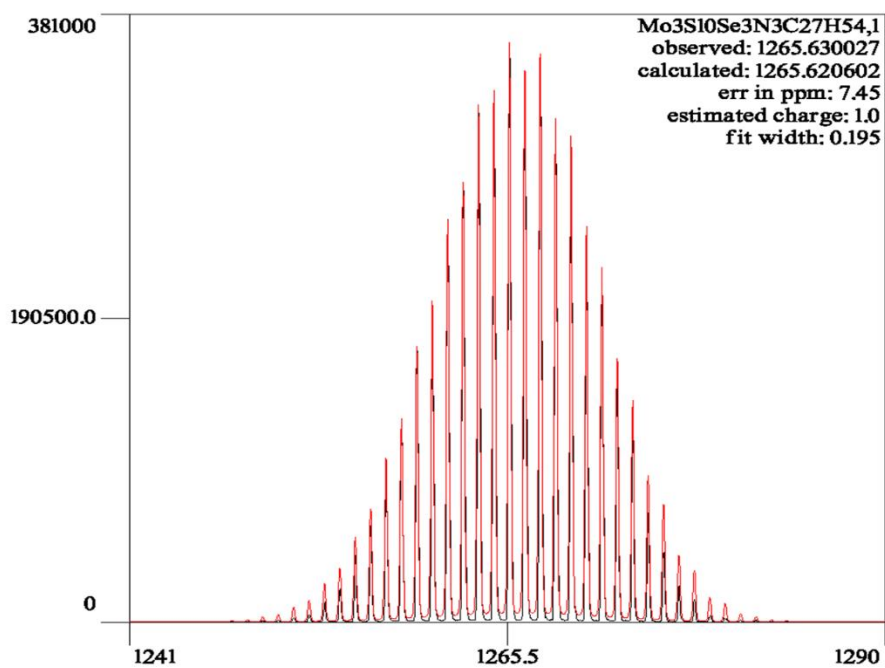


Figure C-19 ESI-MS spectrum of complex $[\text{Mo}_3\text{S}_7(\text{S}_2\text{CN}^i\text{Bu}_2)_3] \text{SeCN}$ in Chapter 3

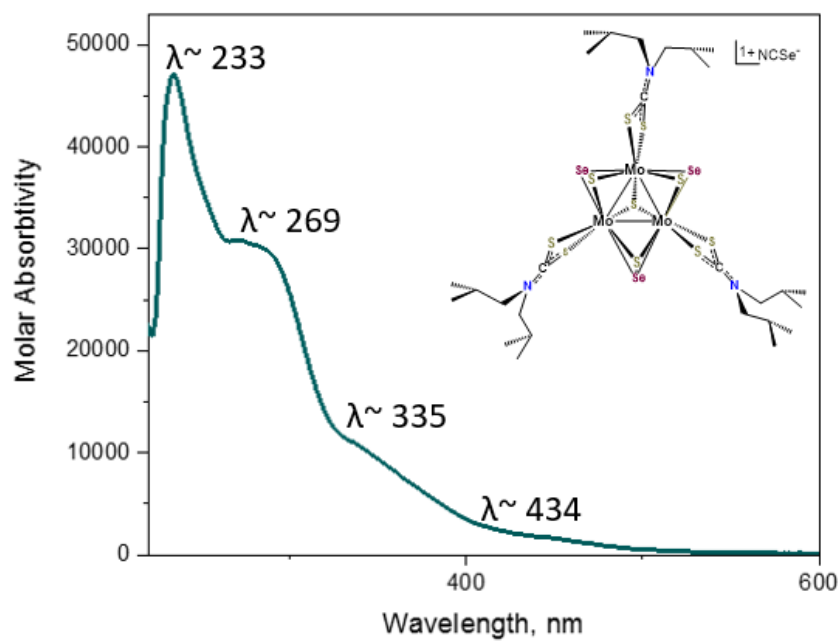


Figure C-20 UV-VIS spectrum of complex $[Mo_3S_7(S_2CN^iBu_2)_3] SeCN$ in Chapter 3

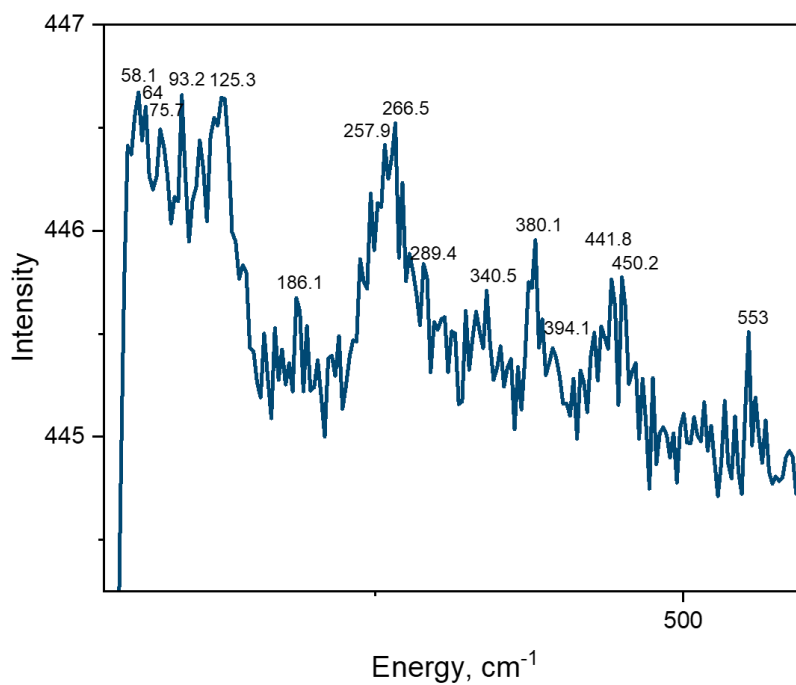


Figure C-21 Raman spectrum of complex $[Mo_3S_7(S_2CN^iBu_2)_3] SeCN$ in Chapter 3

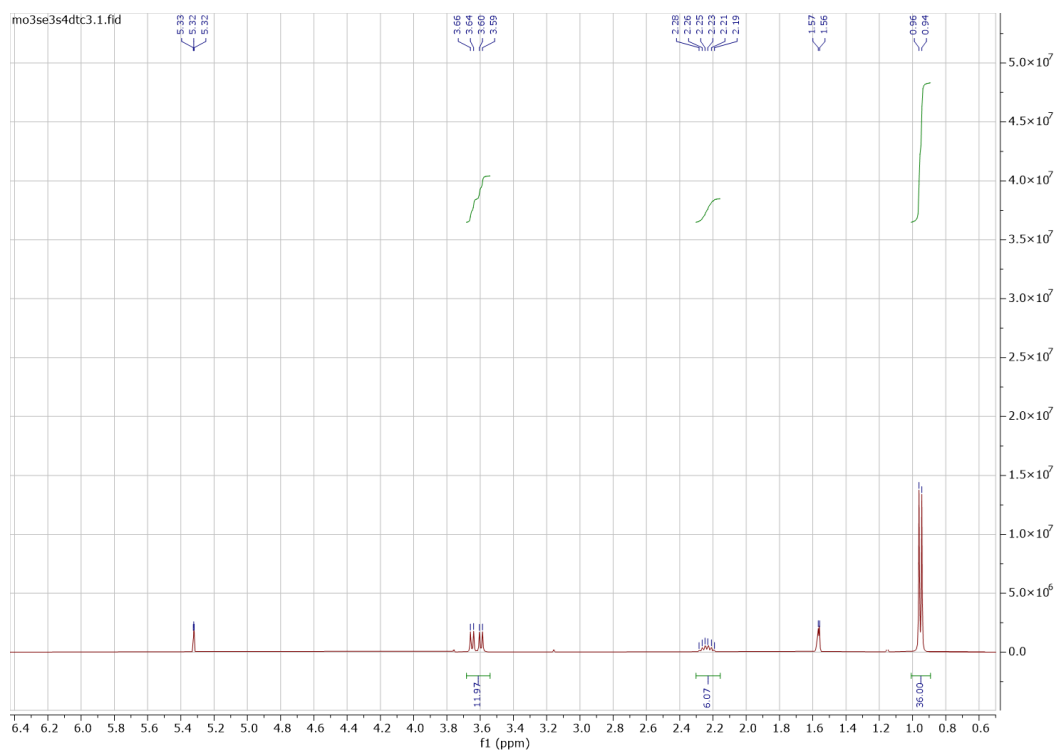


Figure C-22 ^1H NMR spectrum of complex $[\text{Mo}_3\text{S}_7(\text{S}_2\text{CN}^i\text{Bu}_2)_3] \text{SeCN}$ in Chapter 3

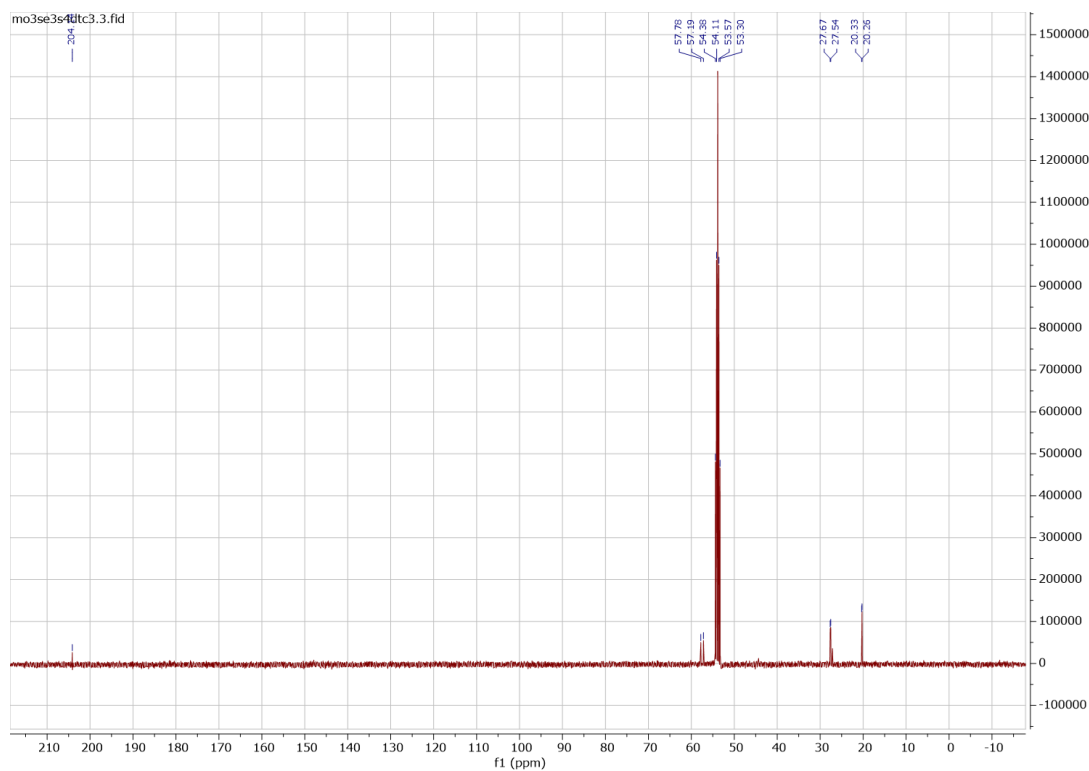


Figure C-23 ^{13}C NMR spectrum of complex $[\text{Mo}_3\text{S}_7(\text{S}_2\text{CN}^i\text{Bu}_2)_3] \text{SeCN}$ in Chapter 3

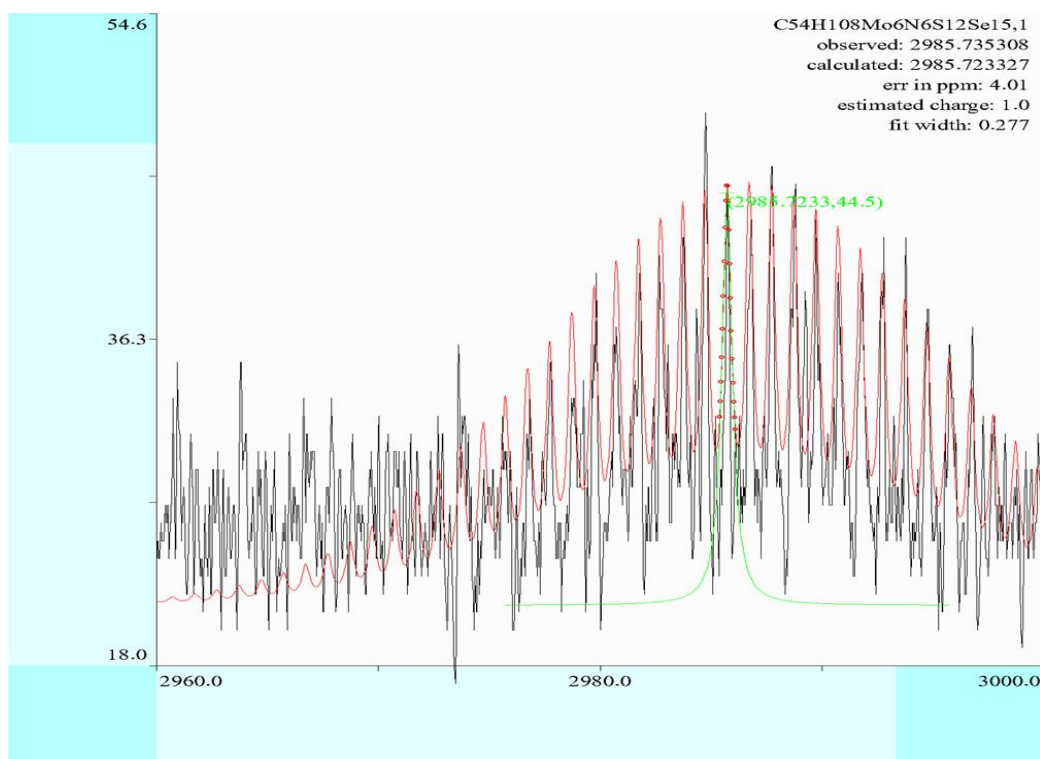


Figure C-24 ESI-MS spectrum of complex $[\text{Mo}_3\text{S}_7(\text{S}_2\text{CN}^t\text{Bu}_2)_3]_2\text{Se}$ in Chapter 3

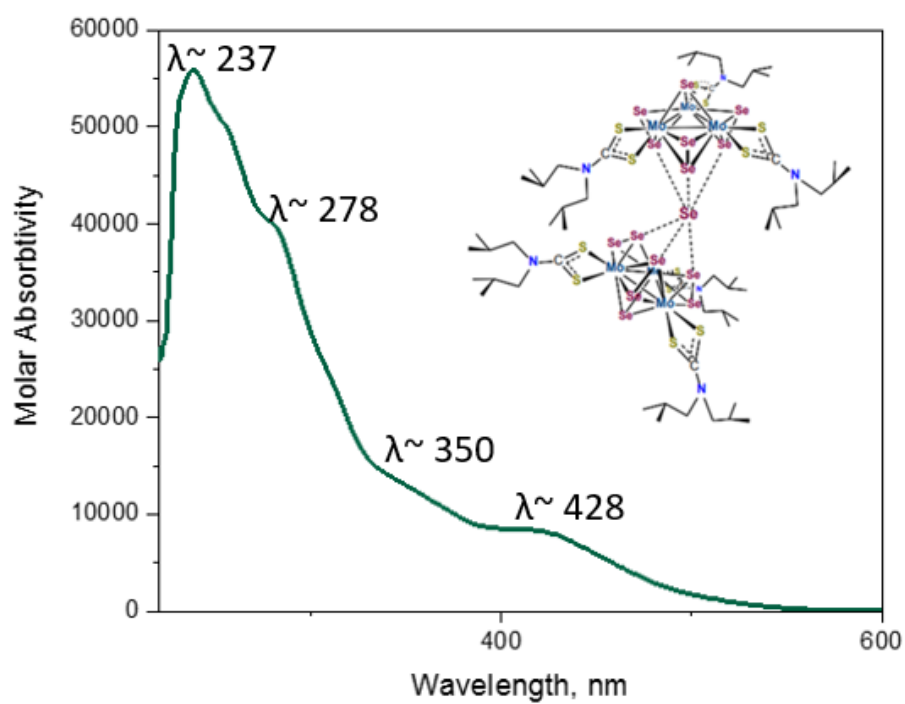


Figure C-25 UV-VIS spectrum of complex $[\text{Mo}_3\text{S}_7(\text{S}_2\text{CN}^t\text{Bu}_2)_3]_2\text{Se}$ in Chapter 3

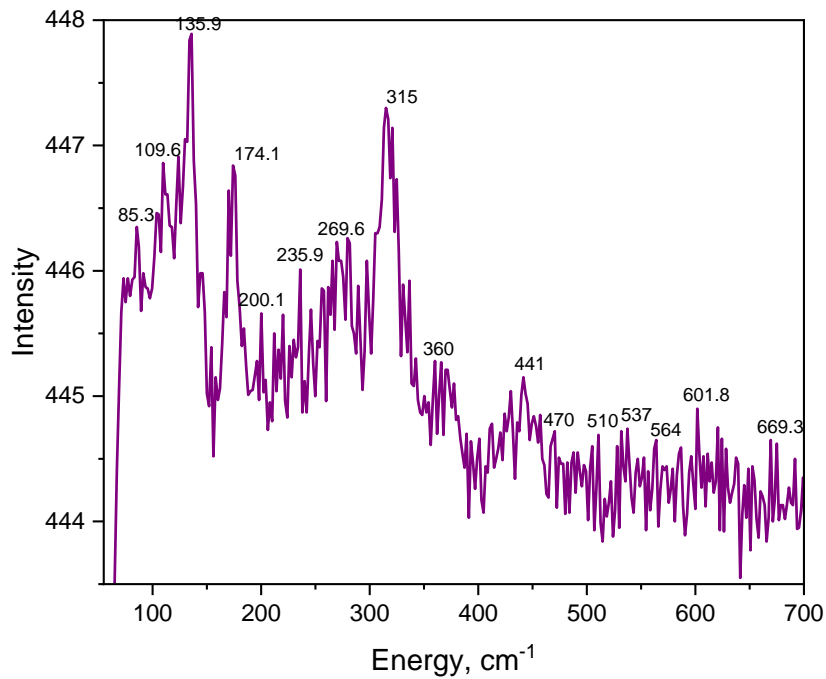


Figure C-26 Raman spectrum of complex $[\text{Mo}_3\text{S}_7(\text{S}_2\text{CN}^t\text{Bu}_2)_3]_2\text{Se}$ in Chapter 3

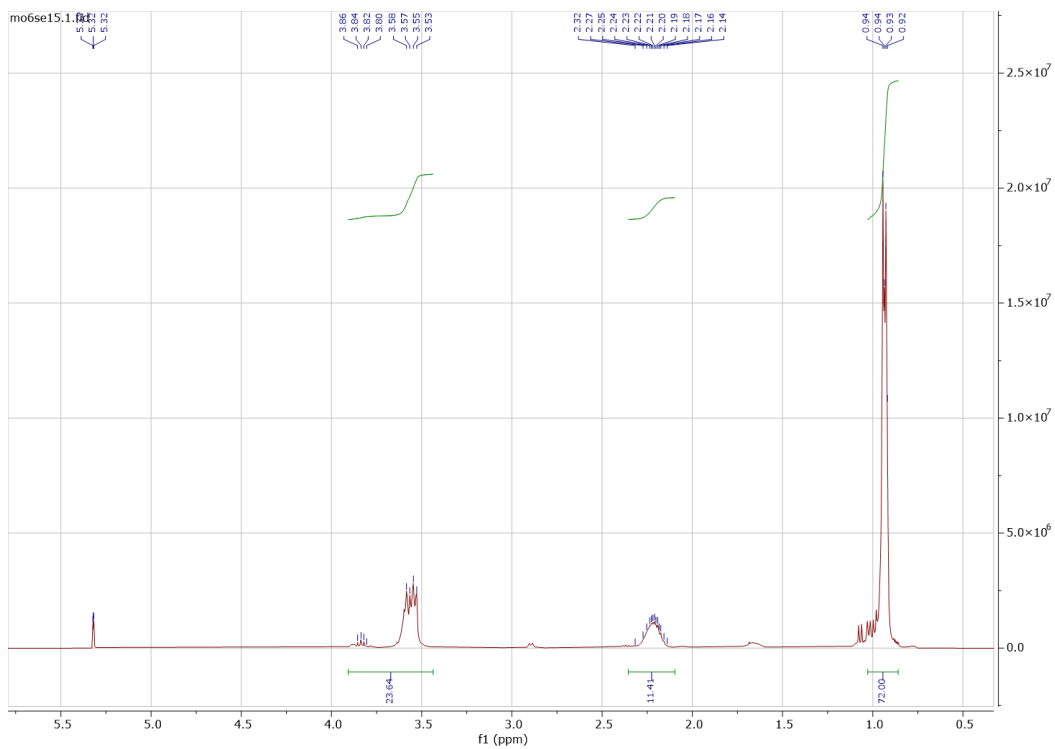


Figure C-27 ^1H NMR spectrum of complex $[\text{Mo}_3\text{S}_7(\text{S}_2\text{CN}^i\text{Bu}_2)_3]_2\text{Se}$ in Chapter 3

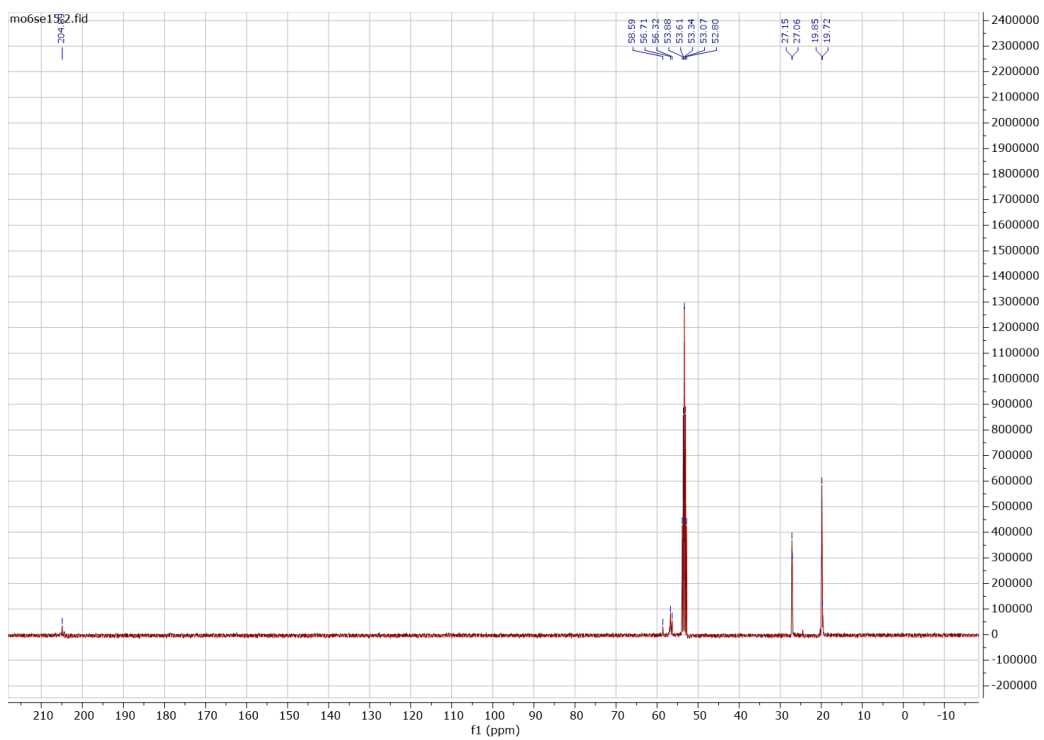


Figure C-28 ^{13}C NMR spectrum of complex $[\text{Mo}_3\text{S}_7(\text{S}_2\text{CN}^i\text{Bu}_2)_3]_2\text{Se}$ in Chapter 3

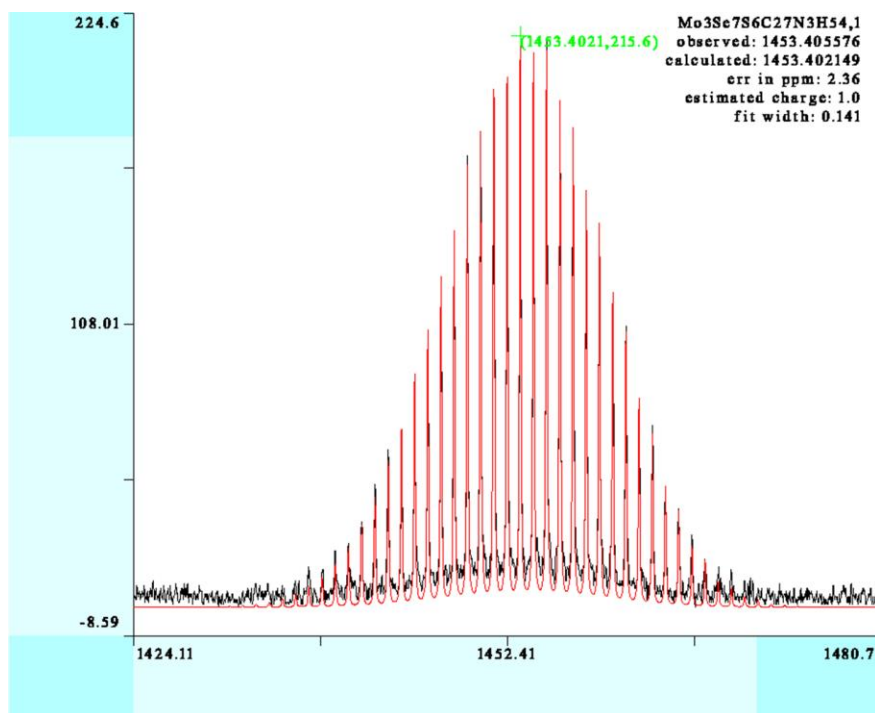


Figure C-29 ESI-MS spectrum of complex $[\text{Mo}_3\text{Se}_7(\text{S}_2\text{CN}'\text{Bu}_2)_3]$ I in Chapter 3

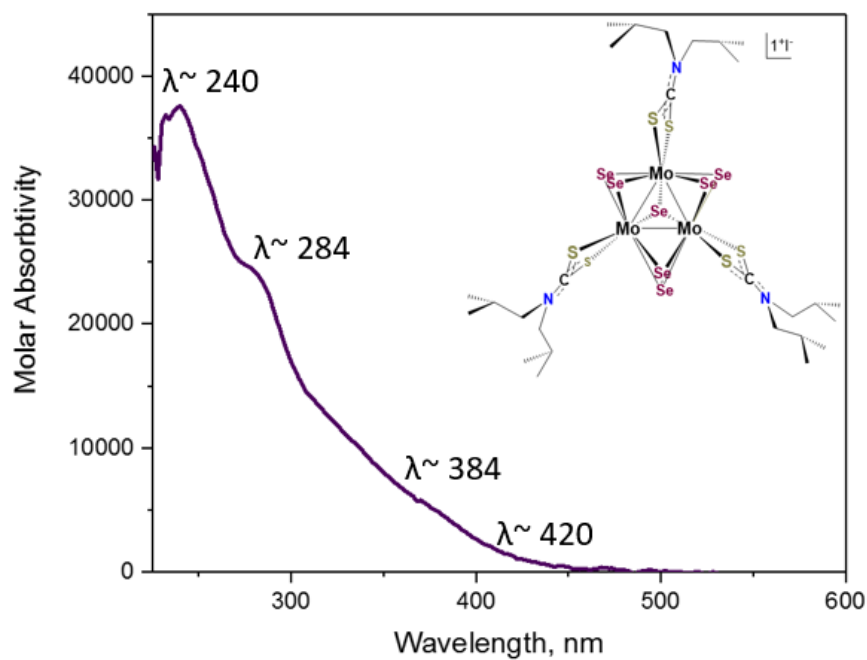


Figure C-30 UV-VIS spectrum of complex $[\text{Mo}_3\text{Se}_7(\text{S}_2\text{CN}'\text{Bu}_2)_3]$ I in Chapter 3

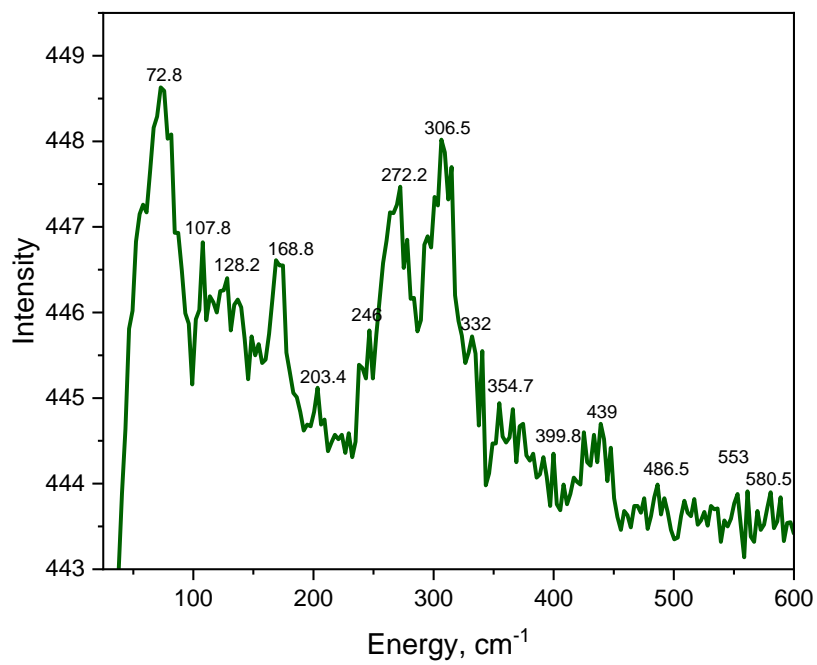


Figure C-31 Raman spectrum of complex $[\text{Mo}_3\text{Se}_7(\text{S}_2\text{CN}^i\text{Bu}_2)_3]$ I in Chapter 3

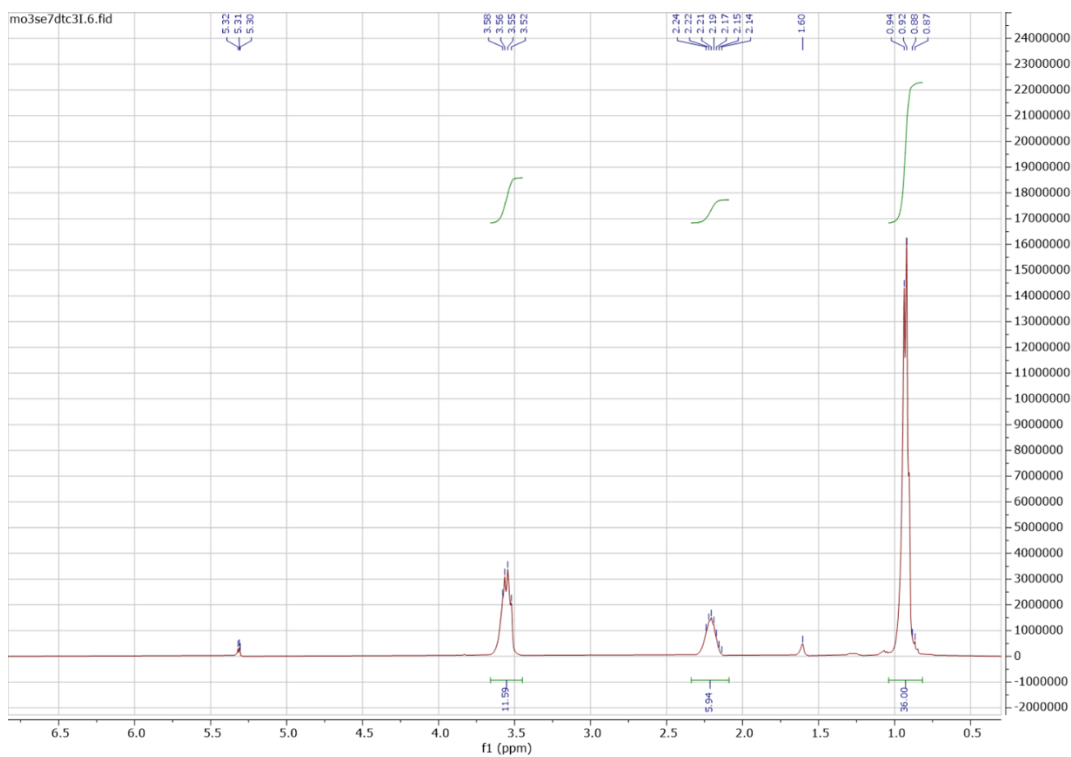


Figure C-32 ^1H NMR spectrum of complex $[\text{Mo}_3\text{Se}_7(\text{S}_2\text{CN}^i\text{Bu}_2)_3] \text{I}$ in Chapter 3

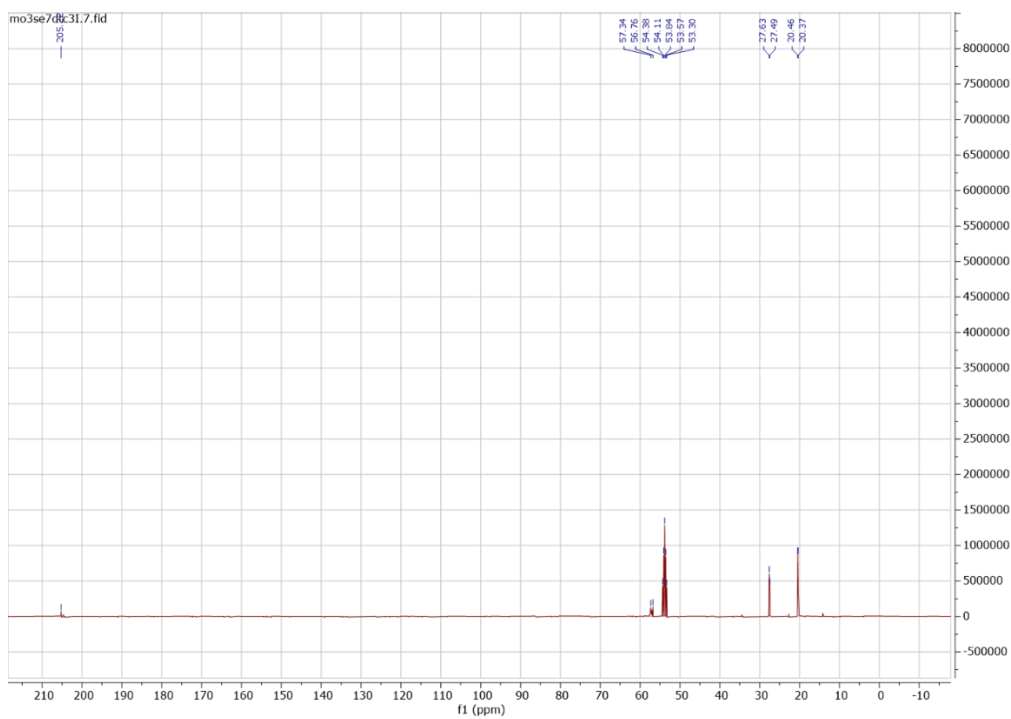


Figure C-33 ^{13}C NMR spectrum of complex $[\text{Mo}_3\text{Se}_7(\text{S}_2\text{CN}^i\text{Bu}_2)_3] \text{I}$ in Chapter 3

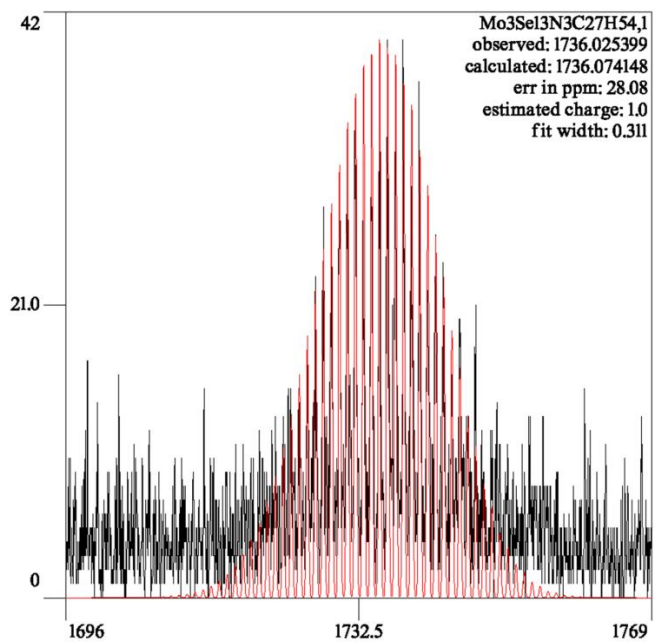


Figure C-34 ESI-MS spectrum of complex $[\text{Mo}_3\text{Se}_7(\text{Se}_2\text{CN}^i\text{Bu}_2)_3] \text{Cl}$ in Chapter 3

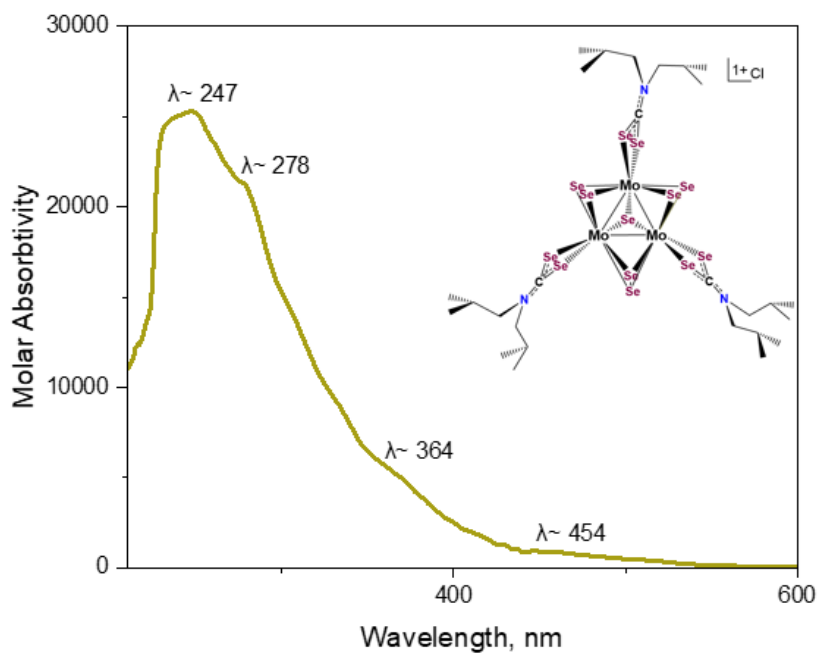


Figure C-35 UV-VIS spectrum of complex $[\text{Mo}_3\text{Se}_7(\text{Se}_2\text{CN}^i\text{Bu}_2)_3] \text{Cl}$ in Chapter 3

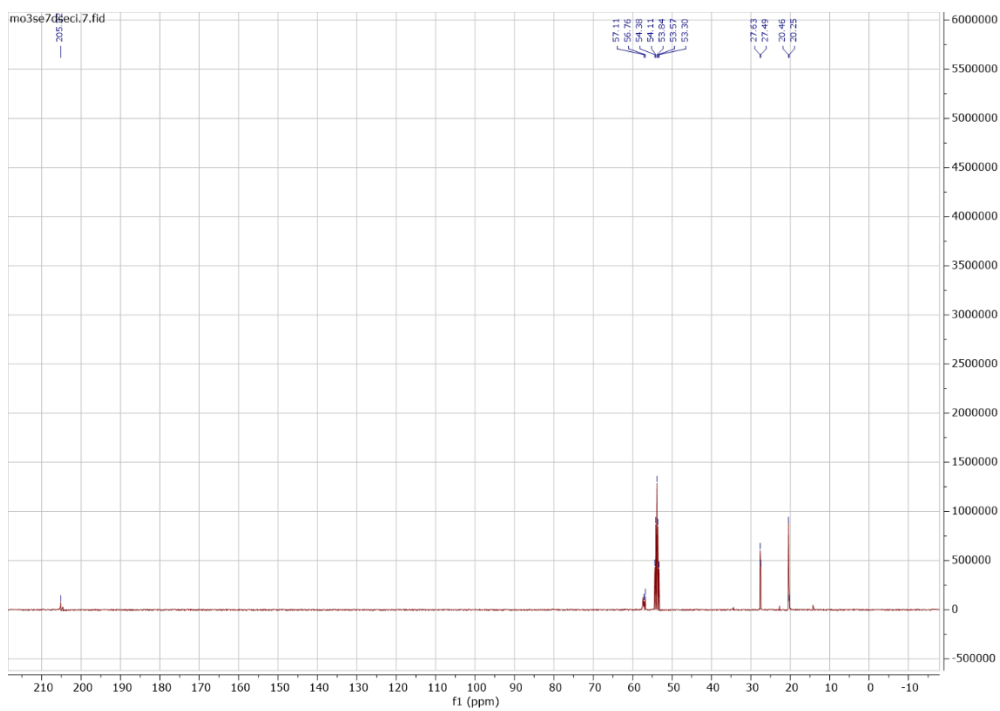


Figure C-38 ^{13}C NMR spectrum of complex $[\text{Mo}_3\text{Se}_7(\text{Se}_2\text{CN}^t\text{Bu}_2)_3] \text{Cl}$ in Chapter 3

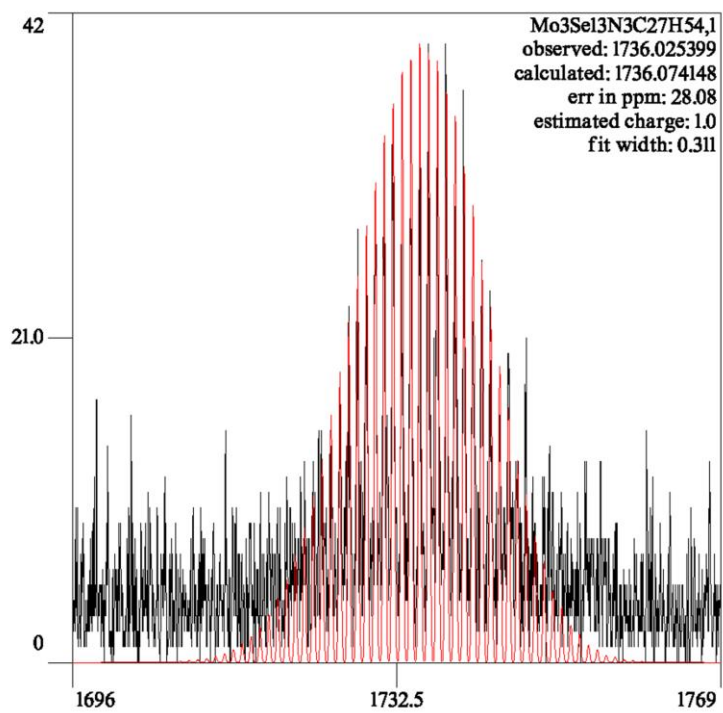


Figure C-39 ESI-MS spectrum of complex $[\text{Mo}_3\text{Se}_7(\text{Se}_2\text{CN}^t\text{Bu}_2)_3] \text{I}$ in Chapter 3

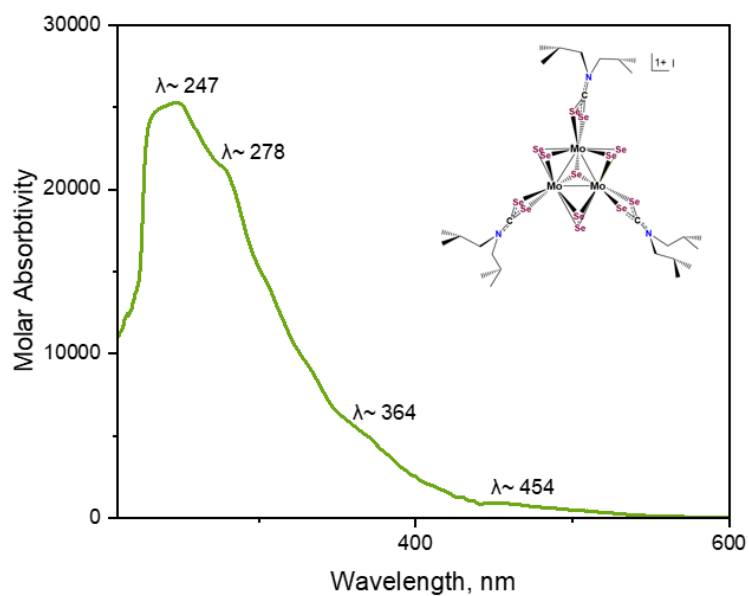


Figure C-40 UV-VIS spectrum of complex $[\text{Mo}_3\text{Se}_7(\text{Se}_2\text{CN}^i\text{Bu}_2)_3] \text{I}$ in Chapter

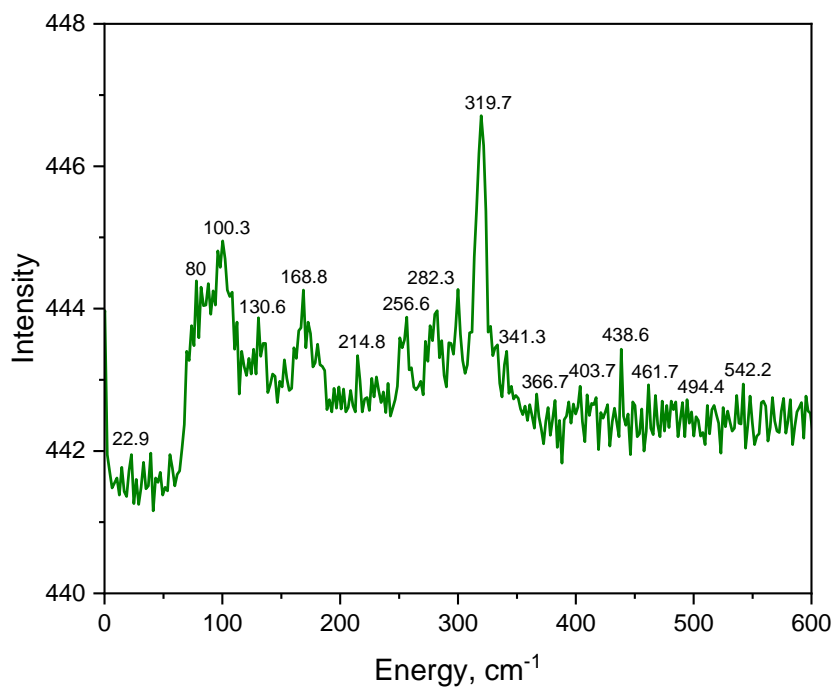


Figure C-41 Raman spectrum of complex $[\text{Mo}_3\text{Se}_7(\text{Se}_2\text{CN}^i\text{Bu}_2)_3] \text{I}$ in Chapter 3

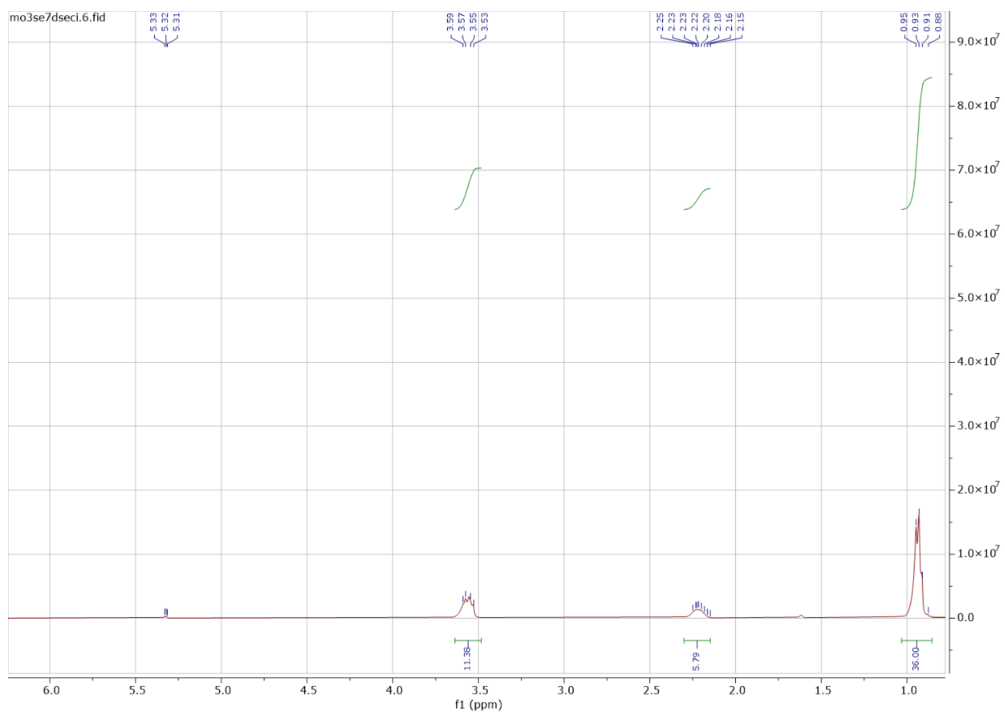


Figure C-42 ^1H NMR spectrum of complex $[\text{Mo}_3\text{Se}_7(\text{Se}_2\text{CN}^i\text{Bu}_2)_3]$ I in Chapter 3

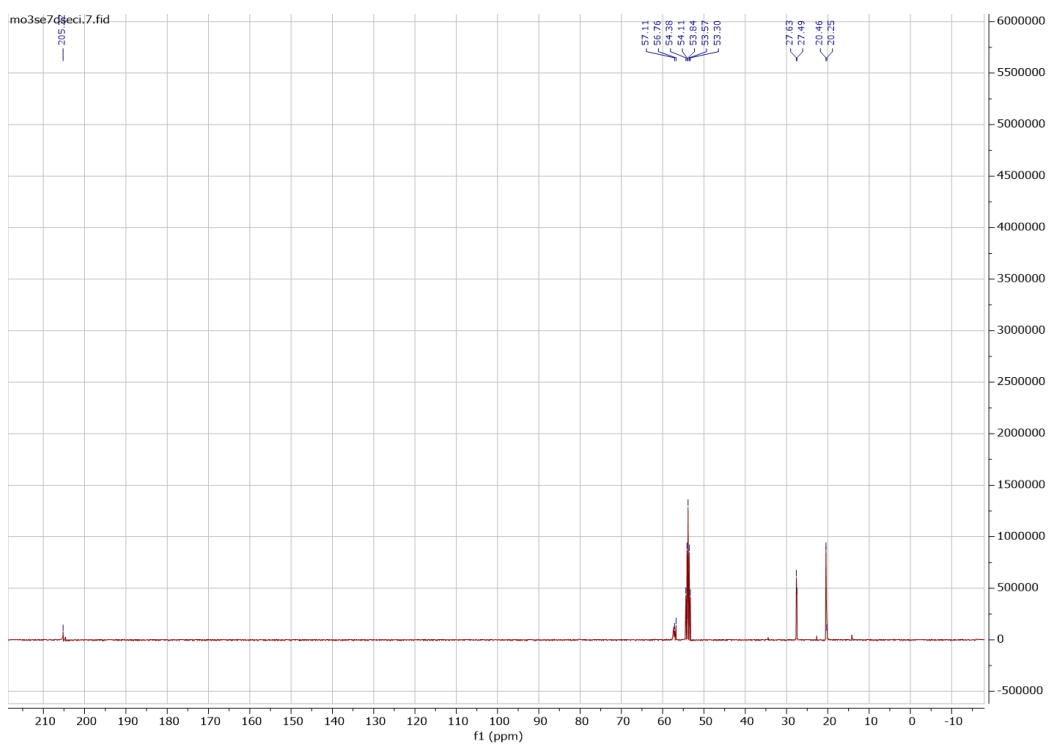


Figure C-43 ^{13}C NMR spectrum of complex $[\text{Mo}_3\text{Se}_7(\text{Se}_2\text{CN}^i\text{Bu}_2)_3]$ I in Chapter 3

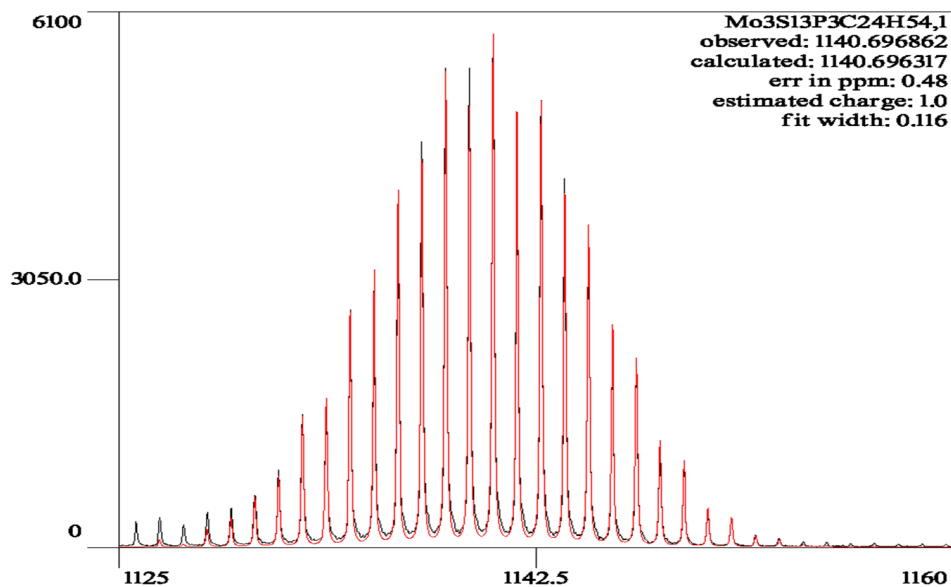


Figure C-44 ESI-MS spectrum of complex $[\text{Mo}_3\text{S}_7(\text{S}_2\text{P}^i\text{Bu}_2)_3](\text{S}_2\text{P}^i\text{Bu}_2)$ in Chapter 3

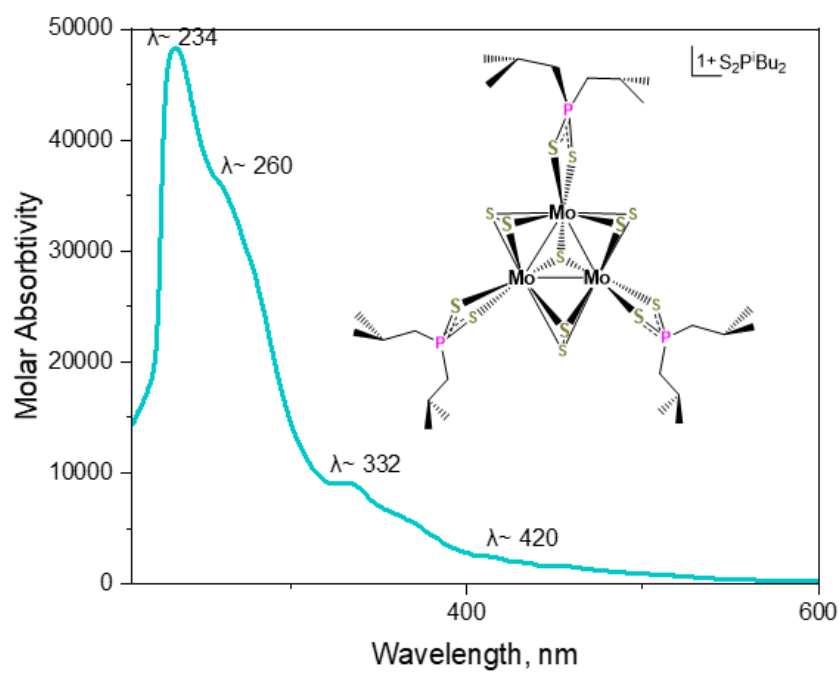


Figure C-45 UV-VIS spectrum of complex $[\text{Mo}_3\text{S}_7(\text{S}_2\text{P}^i\text{Bu}_2)_3](\text{S}_2\text{P}^i\text{Bu}_2)$ in Chapter 3

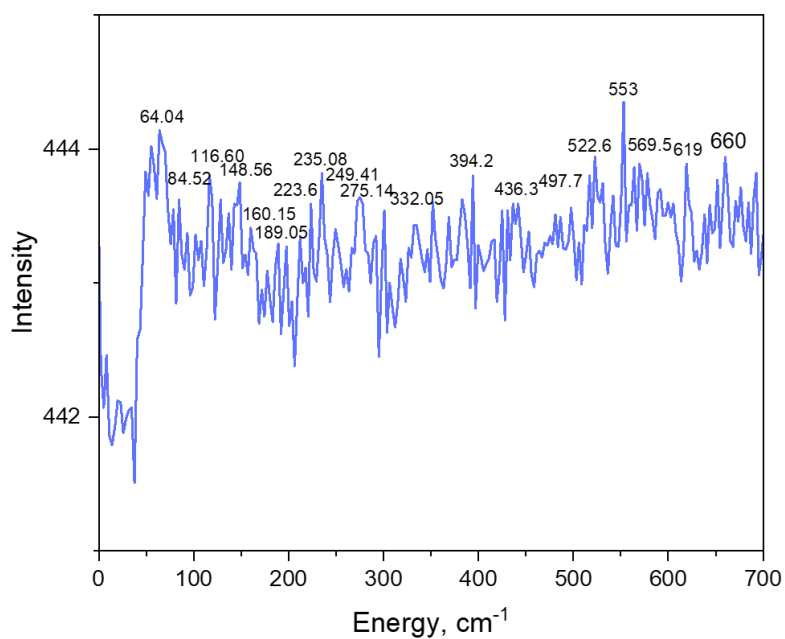


Figure C-46 Raman spectrum of complex $[\text{Mo}_3\text{S}_7(\text{S}_2\text{P}^i\text{Bu}_2)_3] (\text{S}_2\text{P}^i\text{Bu}_2)$ in Chapter 3

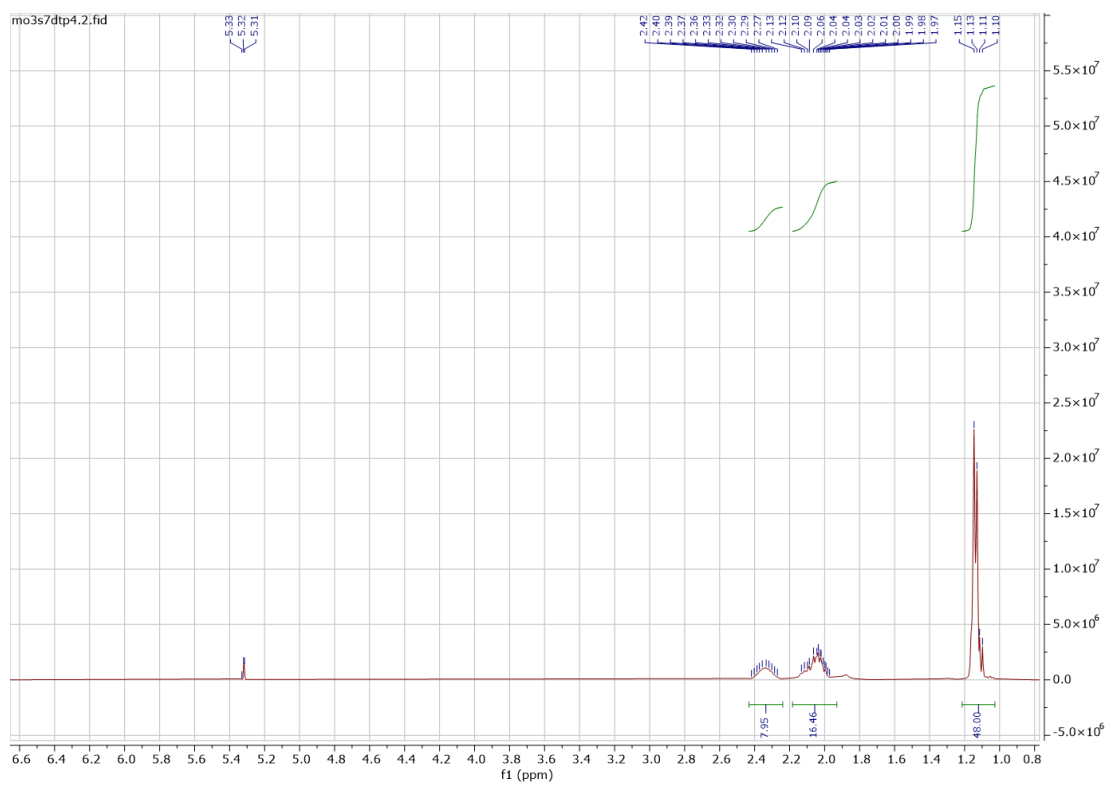


Figure C-47 ^1H NMR spectrum of complex $[\text{Mo}_3\text{S}_7(\text{S}_2\text{P}^i\text{Bu}_2)_3] (\text{S}_2\text{P}^i\text{Bu}_2)$ in Chapter 3

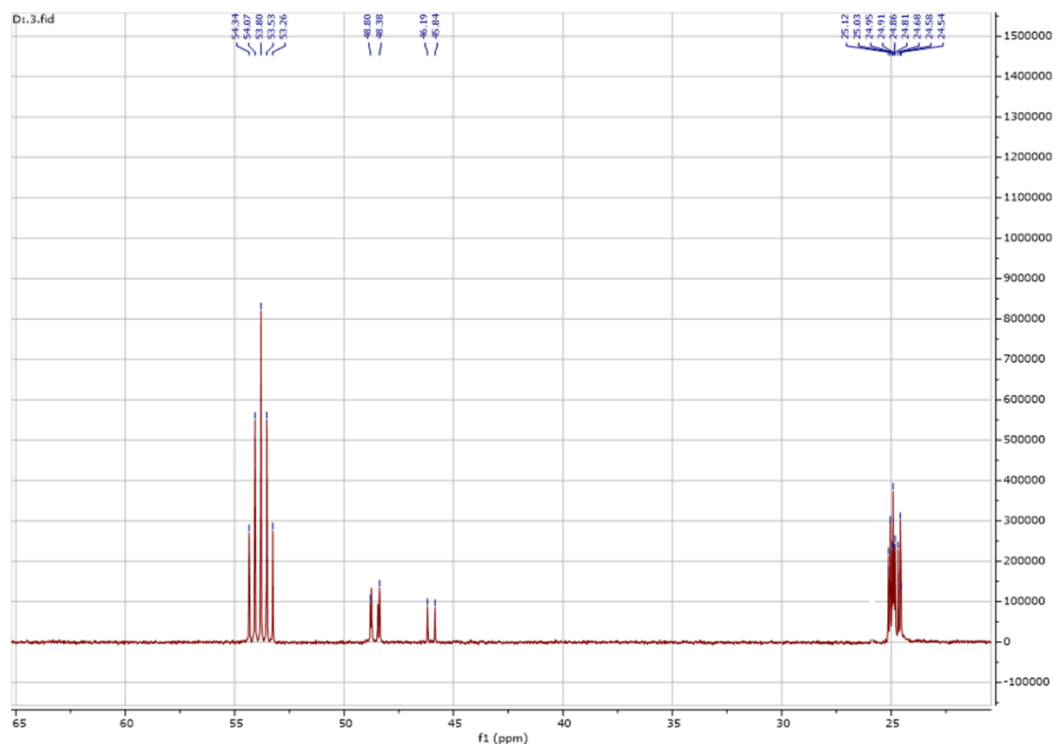


Figure C-48 ^{13}C NMR spectrum of complex $[\text{Mo}_3\text{S}_7(\text{S}_2\text{P}^i\text{Bu}_2)_3](\text{S}_2\text{P}^i\text{Bu}_2)$ in Chapter 3

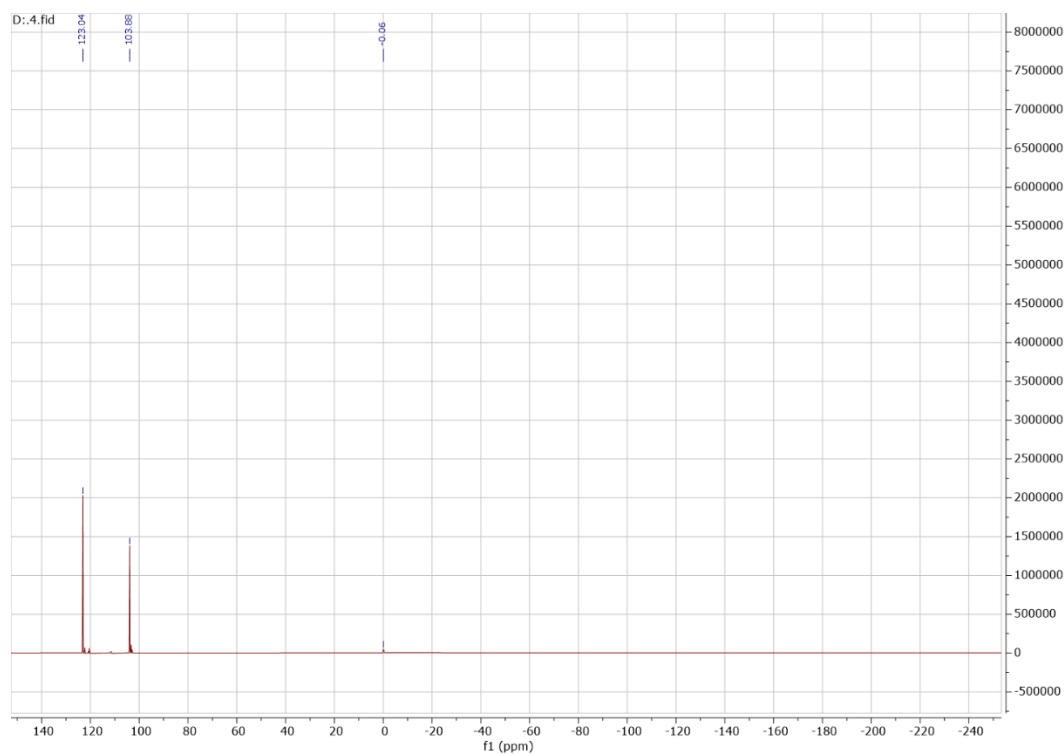


Figure C-49 ^{31}P NMR spectrum of complex $[\text{Mo}_3\text{S}_7(\text{S}_2\text{P}^i\text{Bu}_2)_3](\text{S}_2\text{P}^i\text{Bu}_2)$ in Chapter 3

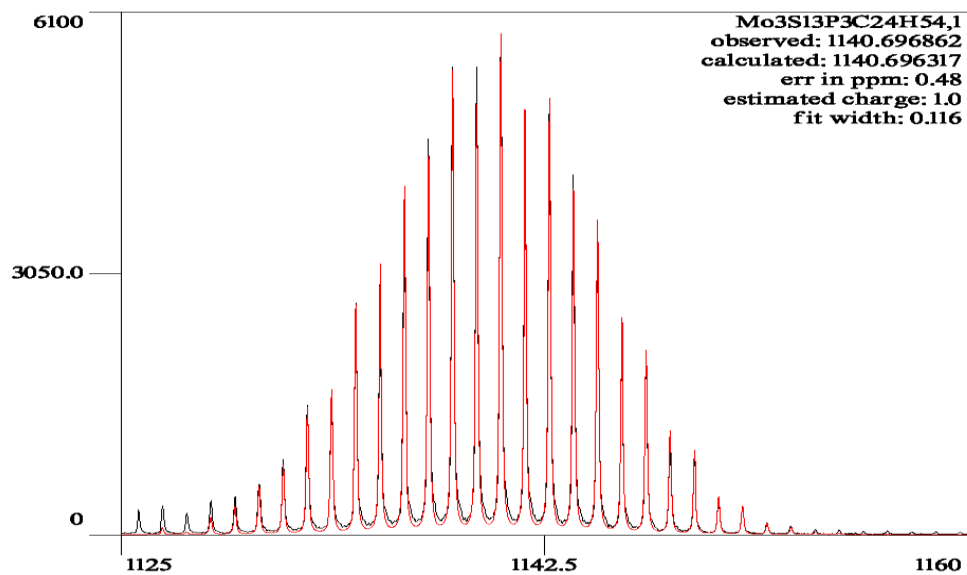


Figure C-50 ESI-MS spectrum of complex $[\text{Mo}_3\text{S}_7(\text{S}_2\text{P}^i\text{Bu}_2)_3] \text{I}$ in Chapter 3

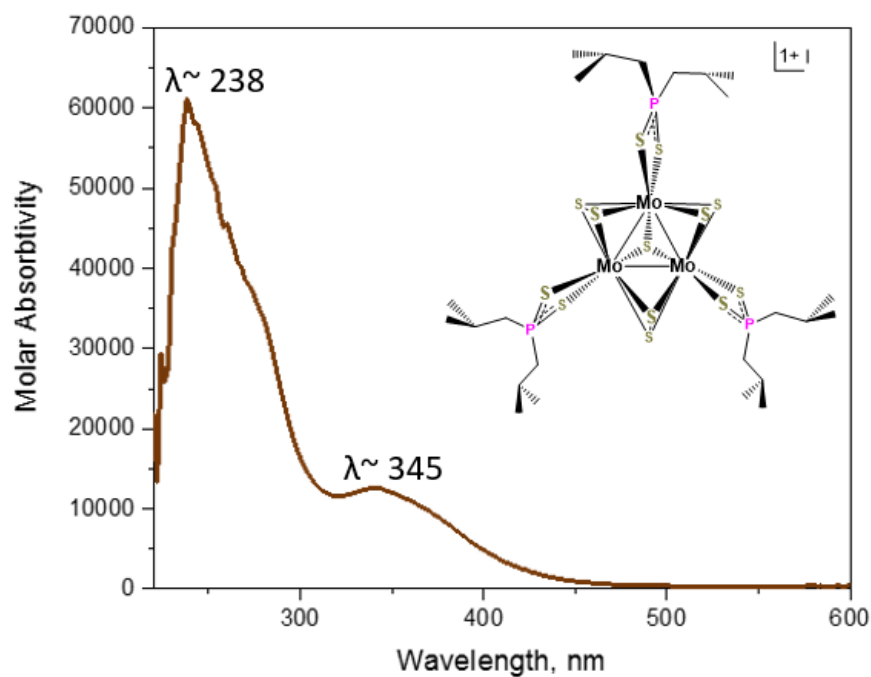


Figure C-51 UV-VIS spectrum of complex $[\text{Mo}_3\text{S}_7(\text{S}_2\text{P}^i\text{Bu}_2)_3] \text{I}$ in Chapter 3

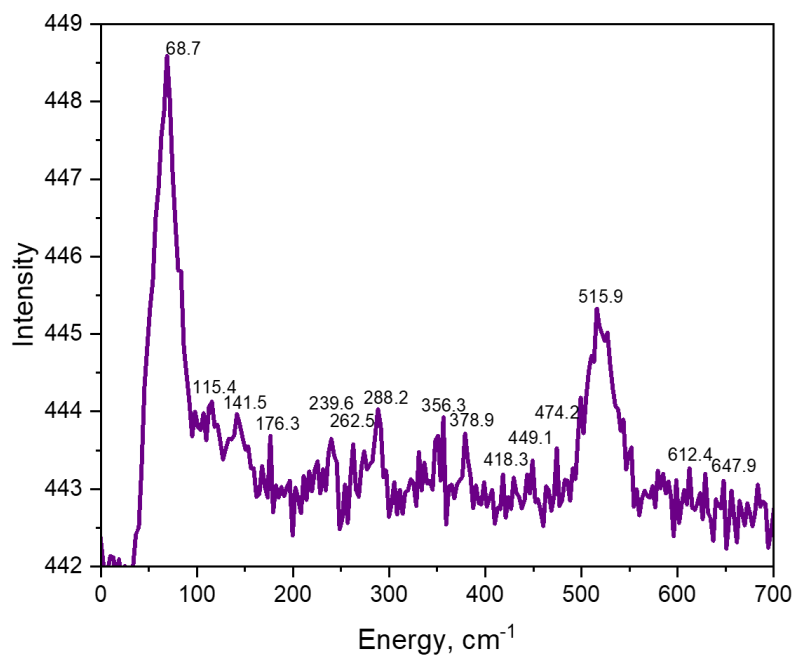


Figure C-52 Raman spectrum of complex $[\text{Mo}_3\text{S}_7(\text{S}_2\text{P}^i\text{Bu}_2)_3] \text{I}$ in Chapter 3

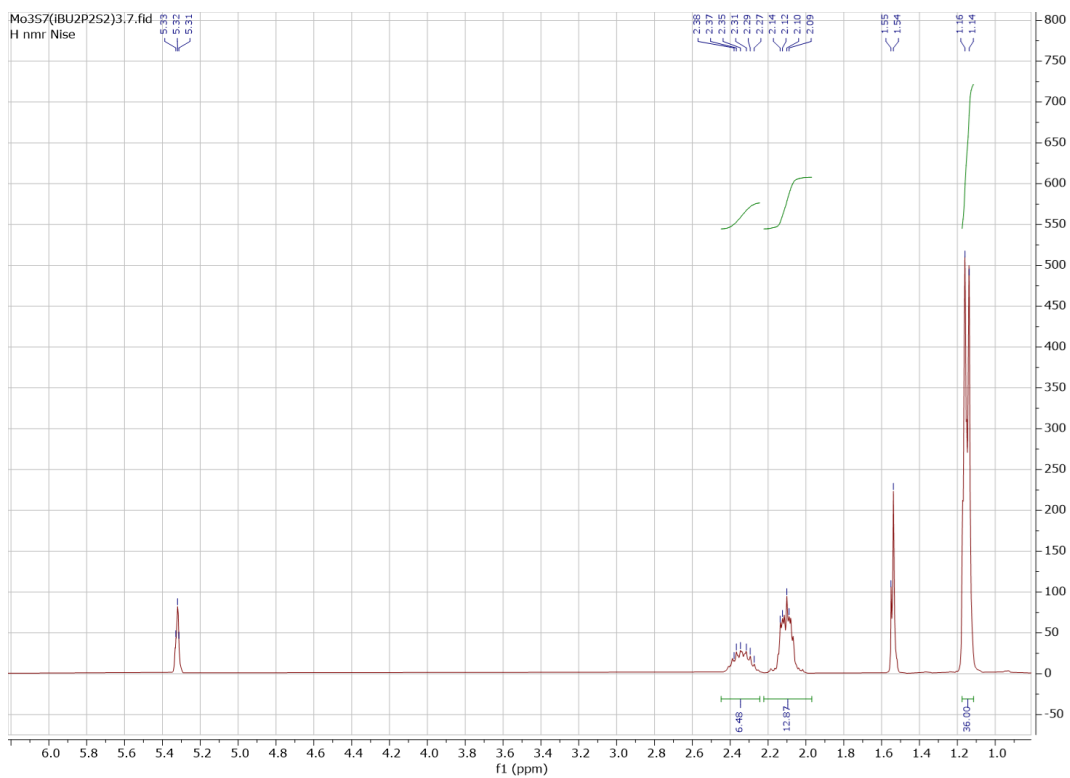


Figure C-53 ^1H NMR spectrum of complex $[\text{Mo}_3\text{S}_7(\text{S}_2\text{P}^i\text{Bu}_2)_3]$ I in Chapter 3

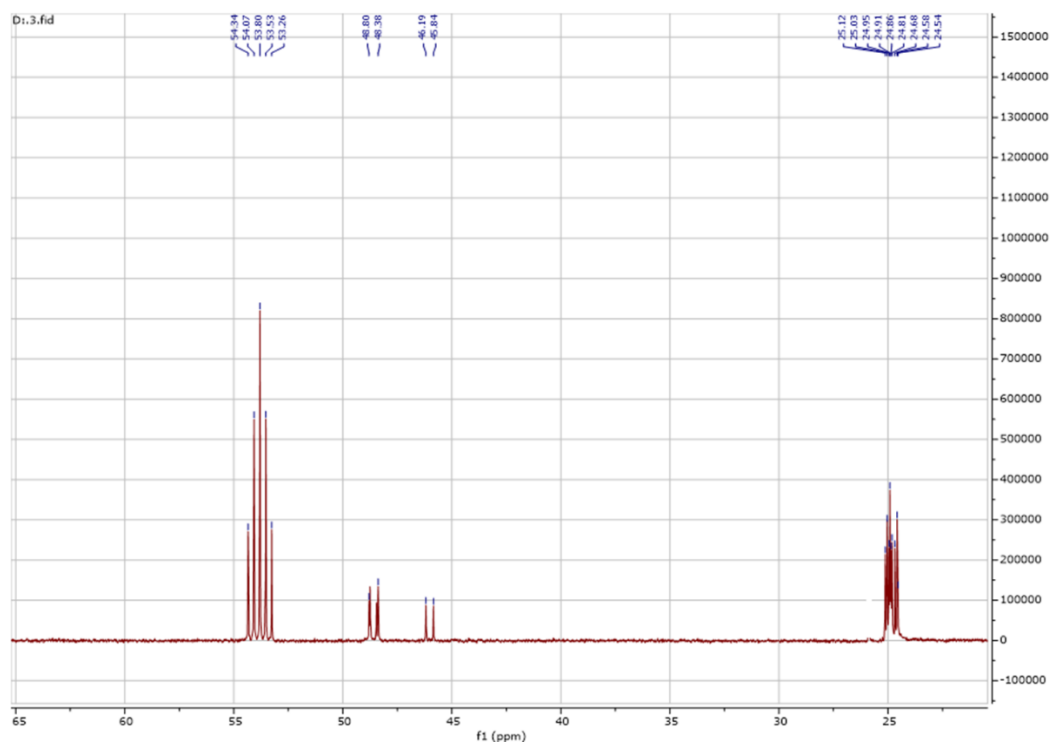


Figure C-54 ^{13}C NMR spectrum of complex $[\text{Mo}_3\text{S}_7(\text{S}_2\text{P}^i\text{Bu}_2)_3]$ I in Chapter 3

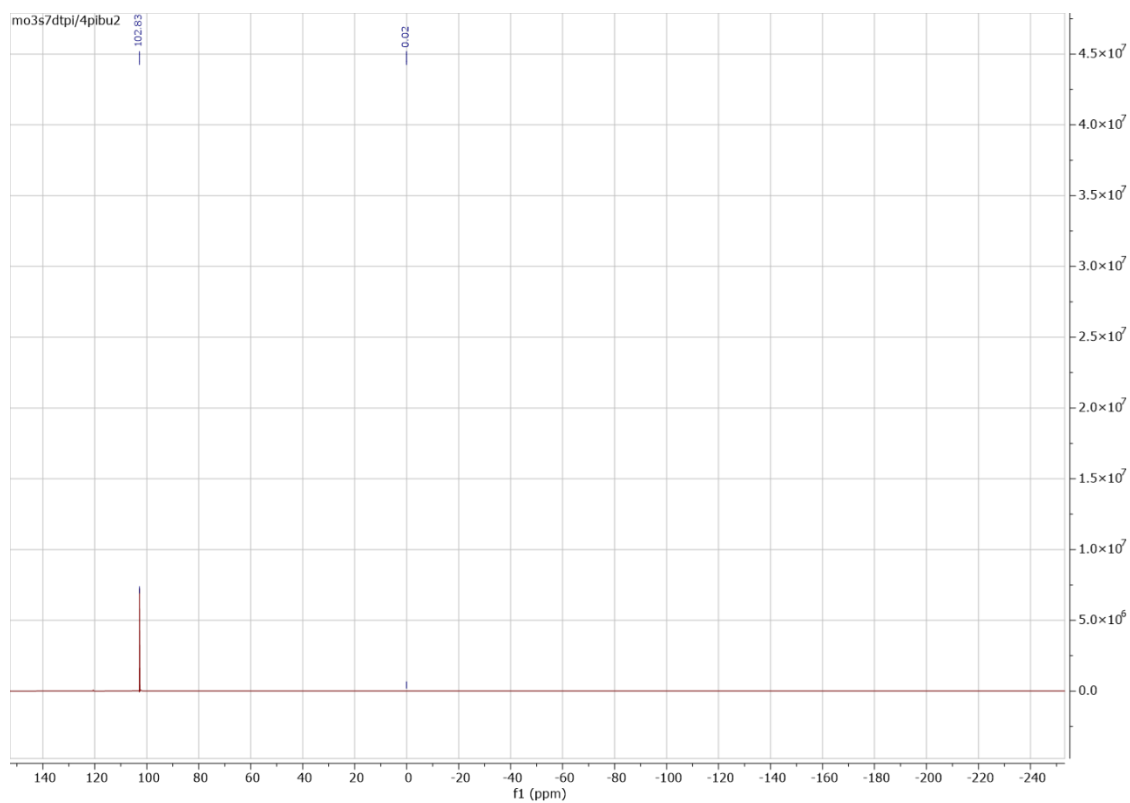


Figure C-55 ^{31}P NMR spectrum of complex $[\text{Mo}_3\text{S}_7(\text{S}_2\text{P}^i\text{Bu}_2)_3]$ I in Chapter 3

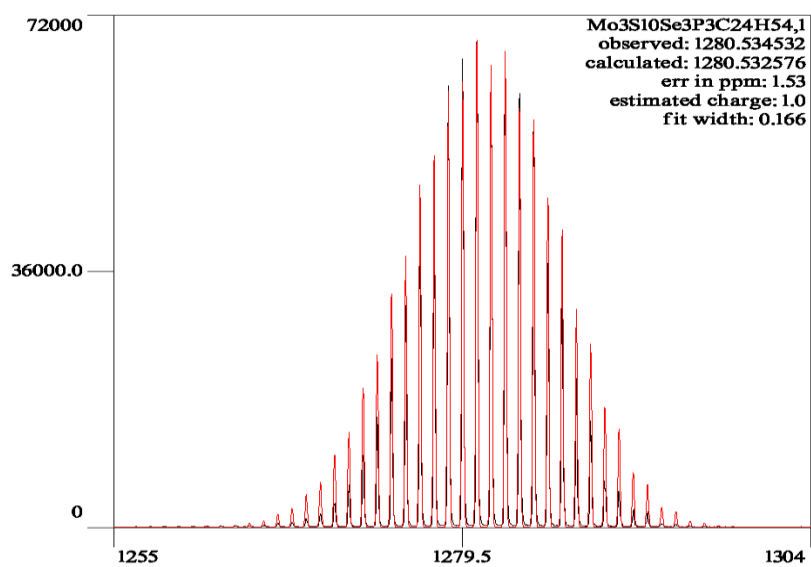


Figure C-56 ESI-MS spectrum of complex $[\text{Mo}_3\text{S}_4\text{Se}_3(\text{S}_2\text{P}^i\text{Bu}_2)_3]$ I in Chapter 3

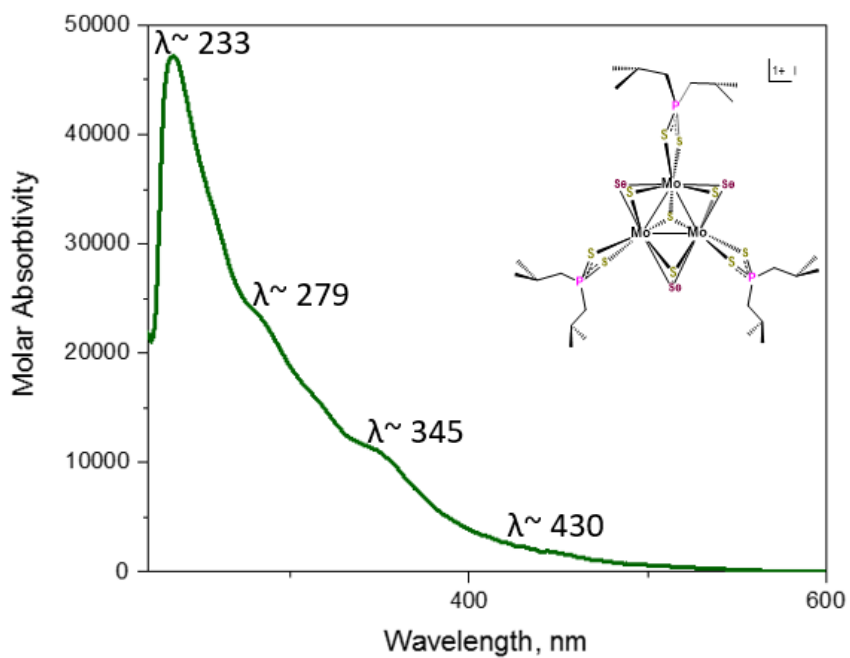


Figure C-57 UV-VIS spectrum of complex $[\text{Mo}_3\text{S}_4\text{Se}_3(\text{S}_2\text{P}^i\text{Bu}_2)_3] \text{I}$ in Chapter 3

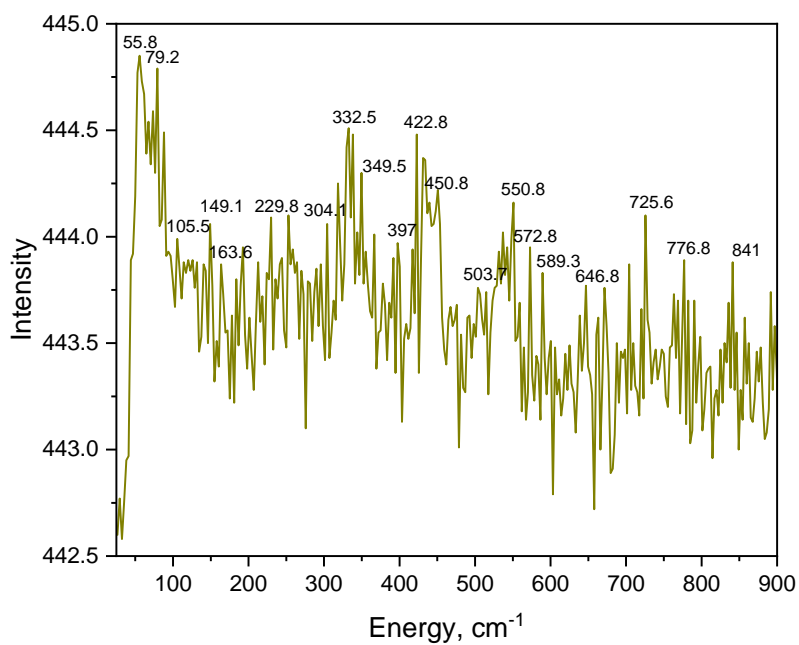


Figure C-58 Raman spectrum of complex $[\text{Mo}_3\text{S}_4\text{Se}_3(\text{S}_2\text{P}^i\text{Bu}_2)_3] \text{I}$ in Chapter 3

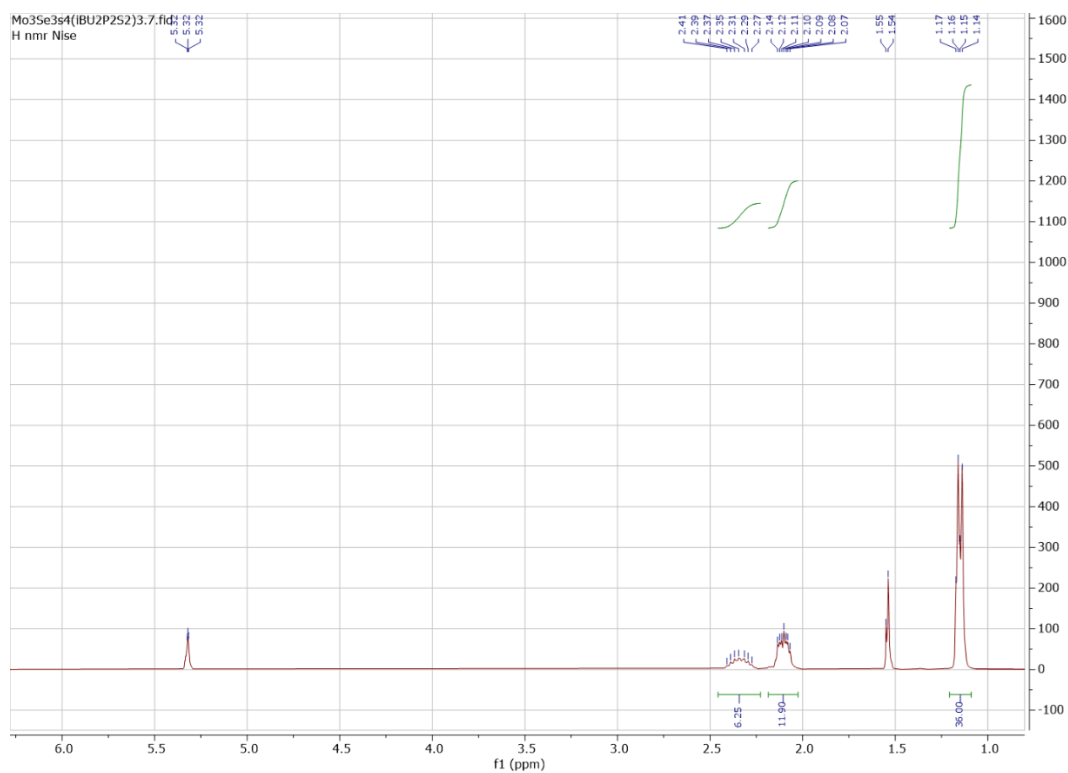


Figure C-59 ^1H NMR spectrum of complex $[\text{Mo}_3\text{S}_4\text{Se}_3(\text{S}_2\text{P}^i\text{Bu}_2)_3] \text{I}$ in Chapter 3

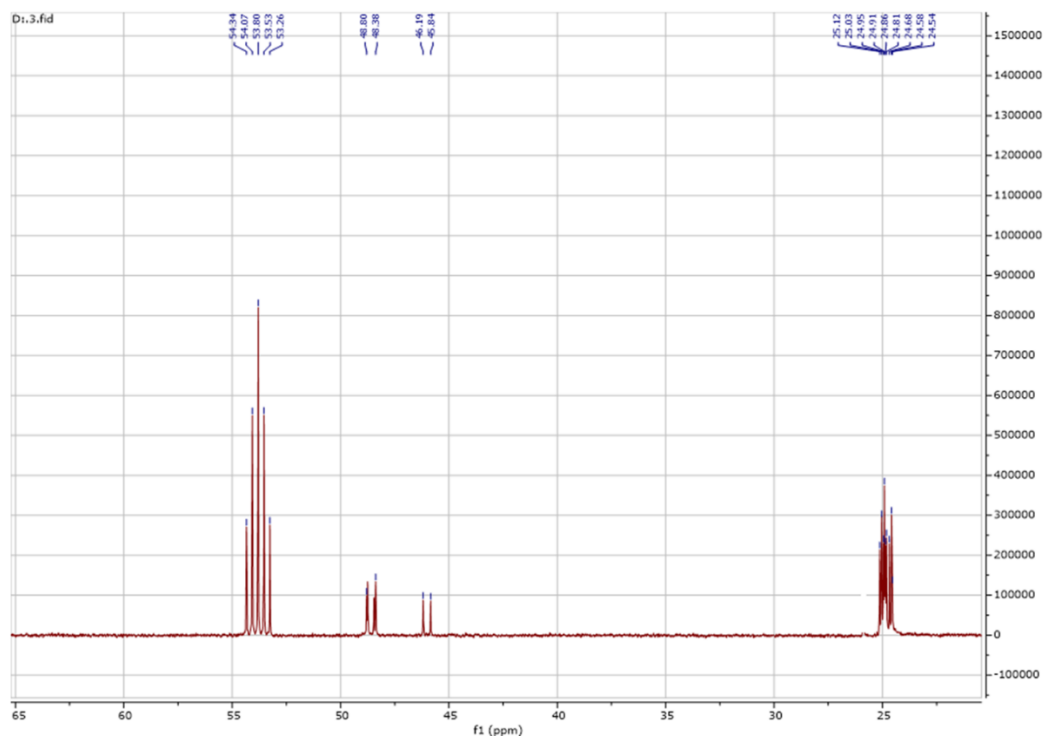


Figure C-60 ^{13}C NMR spectrum of complex $[\text{Mo}_3\text{S}_4\text{Se}_3(\text{S}_2\text{P}^i\text{Bu}_2)_3] \text{I}$ in Chapter 3

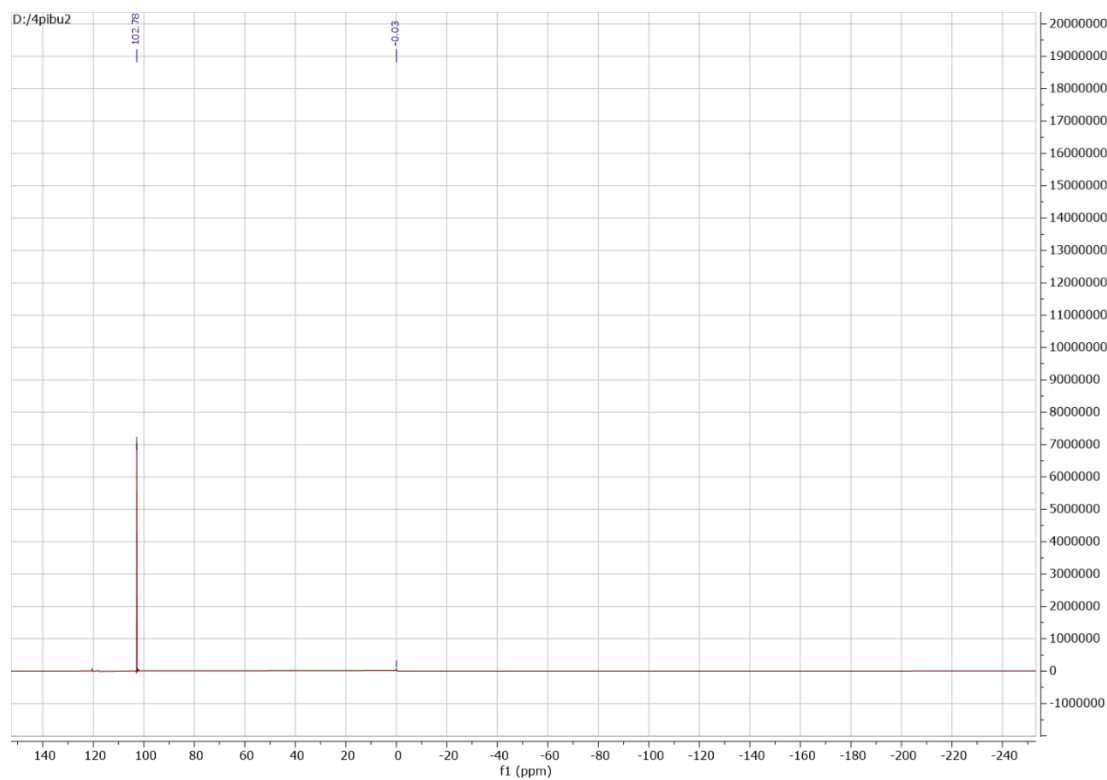


Figure C-61 ^{31}P NMR spectrum of complex $[\text{Mo}_3\text{S}_4\text{Se}_3(\text{S}_2\text{P}^i\text{Bu}_2)_3] \text{I}$ in Chapter 3

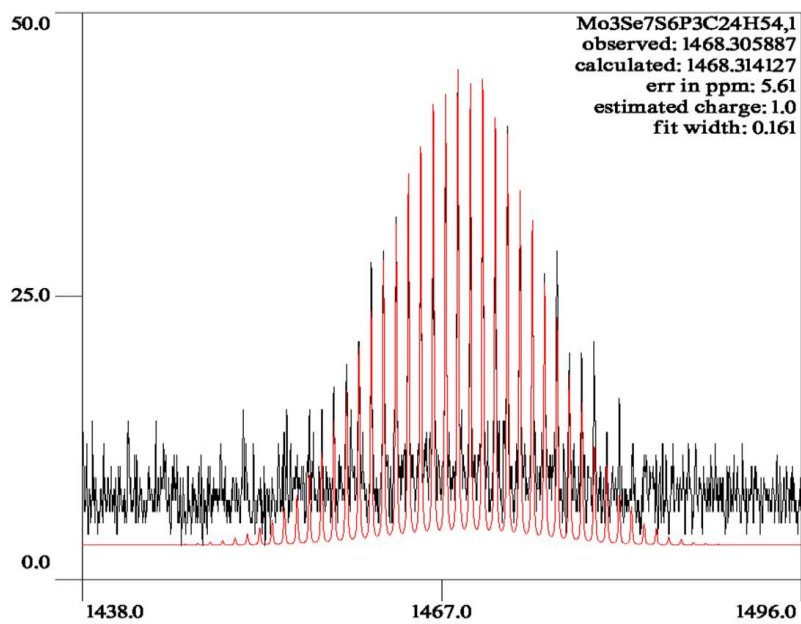


Figure C-62 ESI-MS spectrum of complex $[\text{Mo}_3\text{Se}_7(\text{S}_2\text{P}^i\text{Bu}_2)_3](\text{S}_2\text{P}^i\text{Bu}_2)$ in Chapter 3

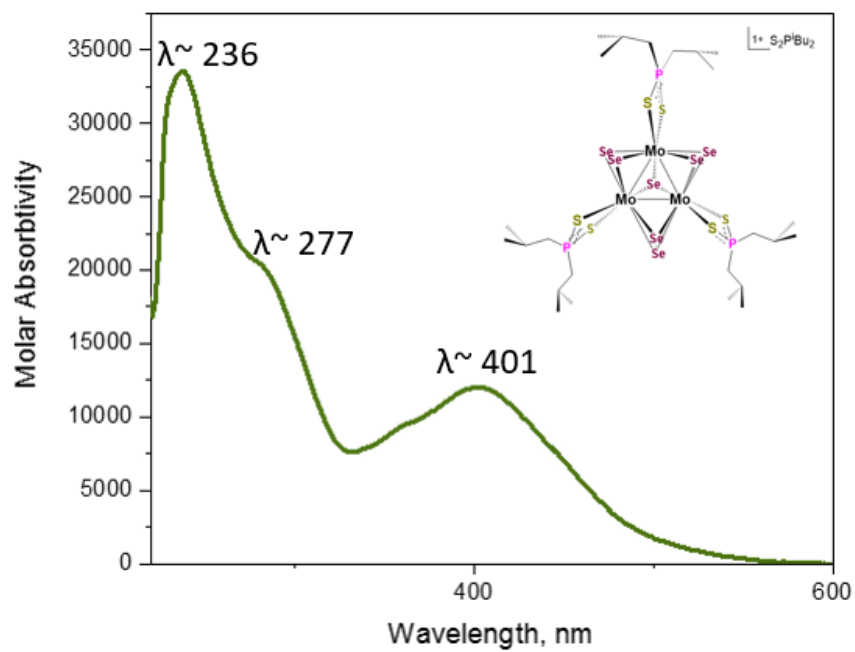


Figure C-63 UV-VIS spectrum of complex $[\text{Mo}_3\text{Se}_7(\text{S}_2\text{P}^i\text{Bu}_2)_3](\text{S}_2\text{P}^i\text{Bu}_2)$ in Chapter 3

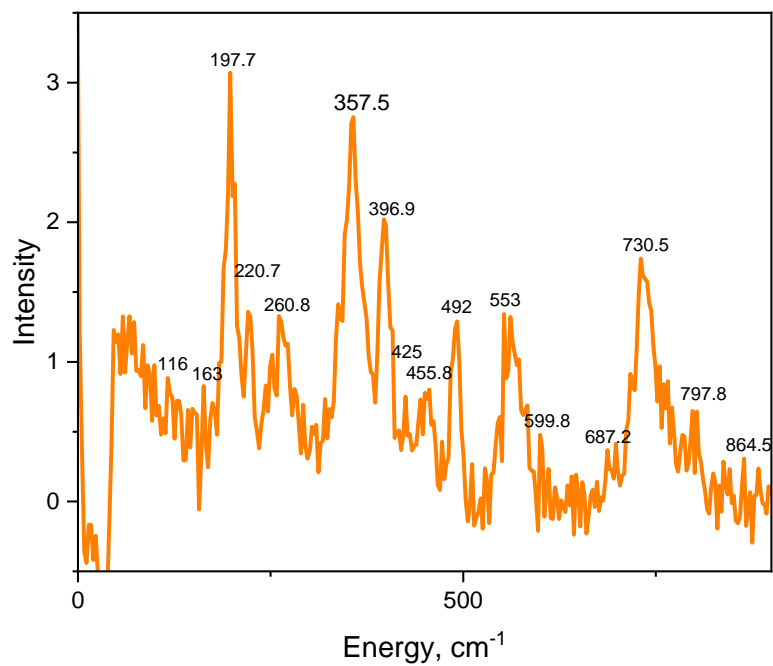


Figure C-64 Raman spectrum of complex $[\text{Mo}_3\text{Se}_7(\text{S}_2\text{P}^i\text{Bu}_2)_3](\text{S}_2\text{P}^i\text{Bu}_2)$ in Chapter 3

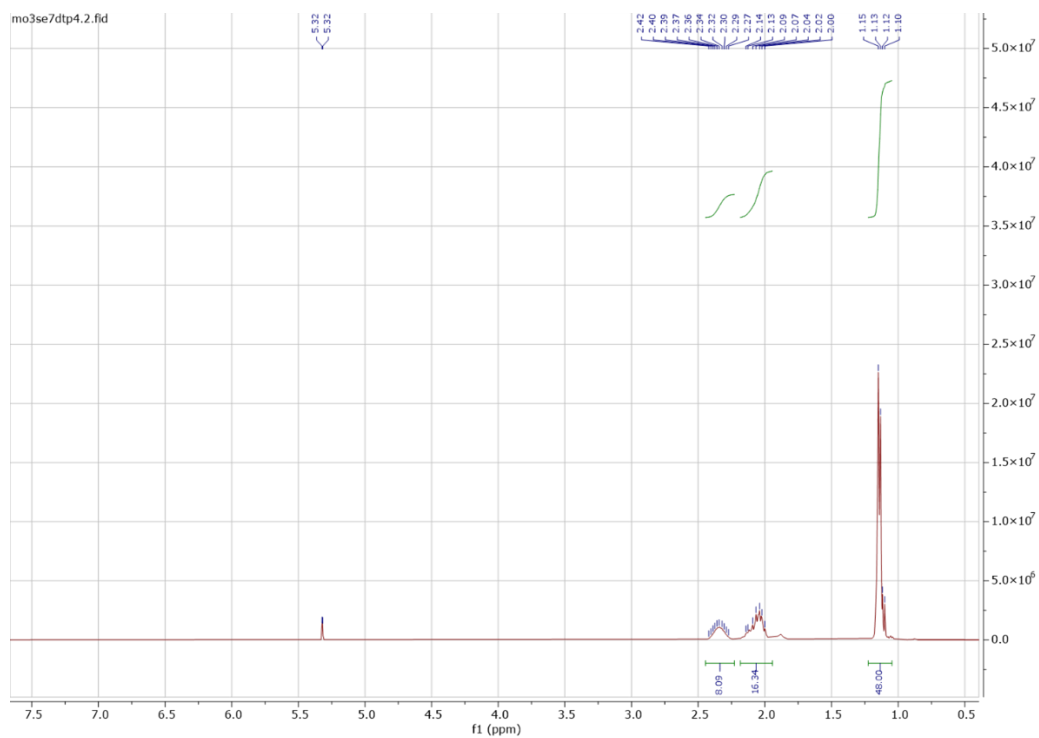


Figure C-65 ^1H NMR spectrum of complex $[\text{Mo}_3\text{Se}_7(\text{S}_2\text{P}^i\text{Bu}_2)_3](\text{S}_2\text{P}^i\text{Bu}_2)$ in Chapter 3

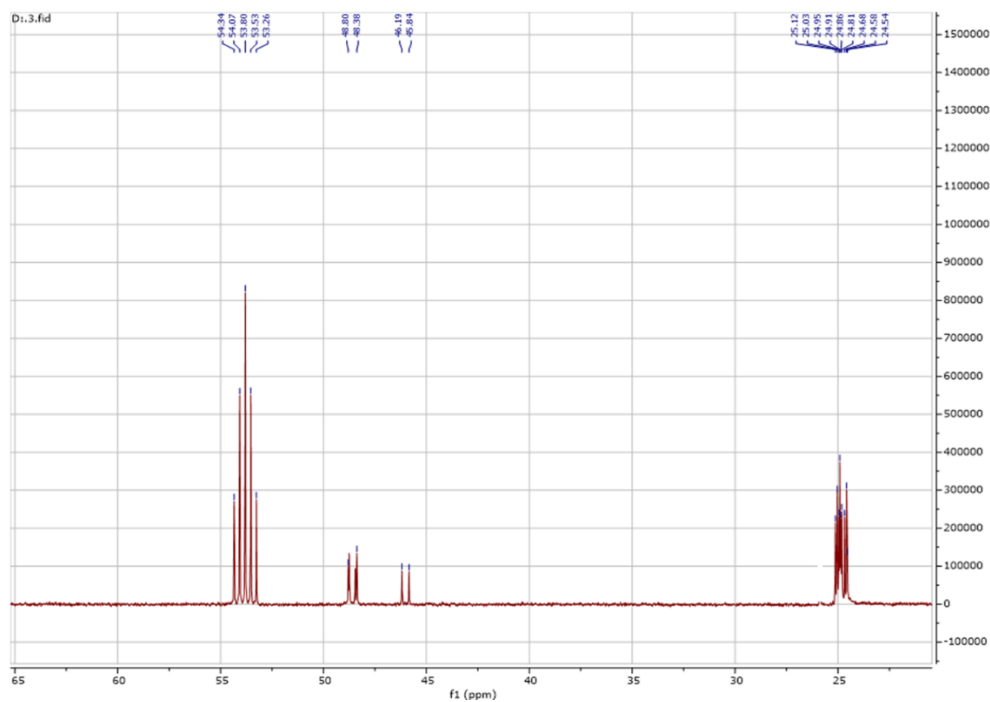


Figure C-66 ^{13}C NMR spectrum of complex $[\text{Mo}_3\text{Se}_7(\text{S}_2\text{P}^i\text{Bu}_2)_3](\text{S}_2\text{P}^i\text{Bu}_2)$ in Chapter 3

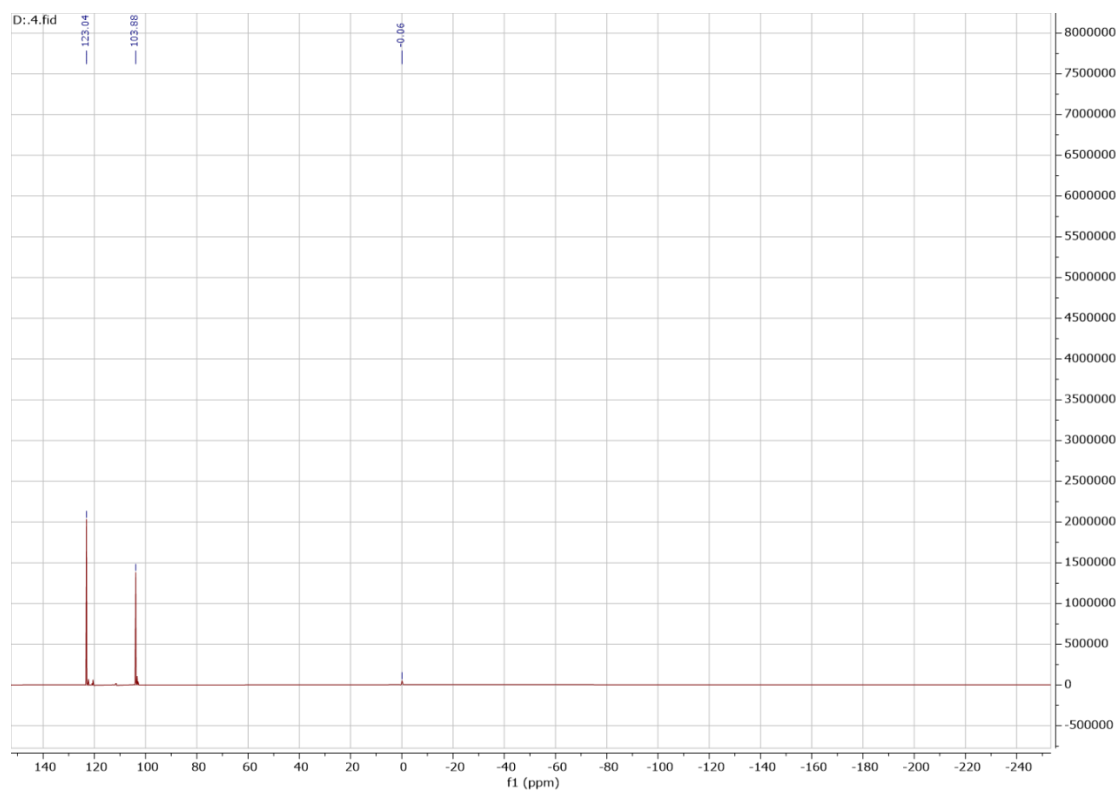


Figure C-67 ^{31}P NMR spectrum of complex $[\text{Mo}_3\text{Se}_7(\text{S}_2\text{P}^i\text{Bu}_2)_3](\text{S}_2\text{P}^i\text{Bu}_2)$ in Chapter 3

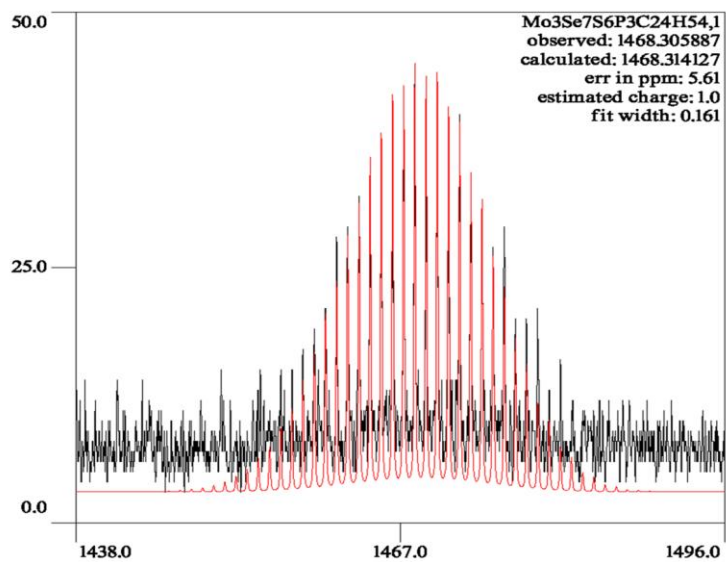


Figure C-68 ESI-MS spectrum of complex $[\text{Mo}_3\text{Se}_7(\text{S}_2\text{P}^i\text{Bu}_2)_3] \text{I}$ in Chapter 3

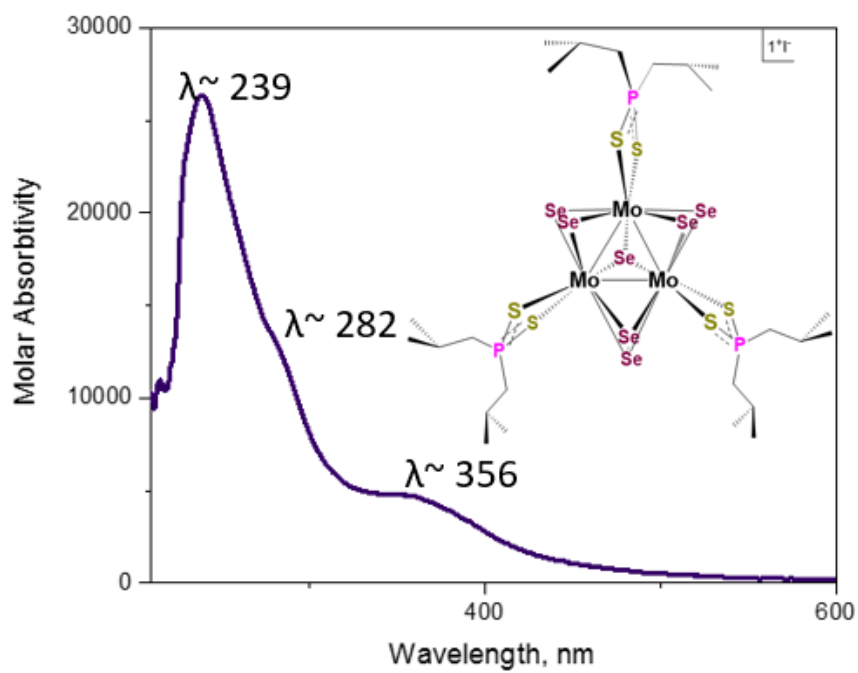


Figure C-69 UV-VIS spectrum of complex $[\text{Mo}_3\text{Se}_7(\text{S}_2\text{P}^i\text{Bu}_2)_3] \text{I}$ in Chapter 3

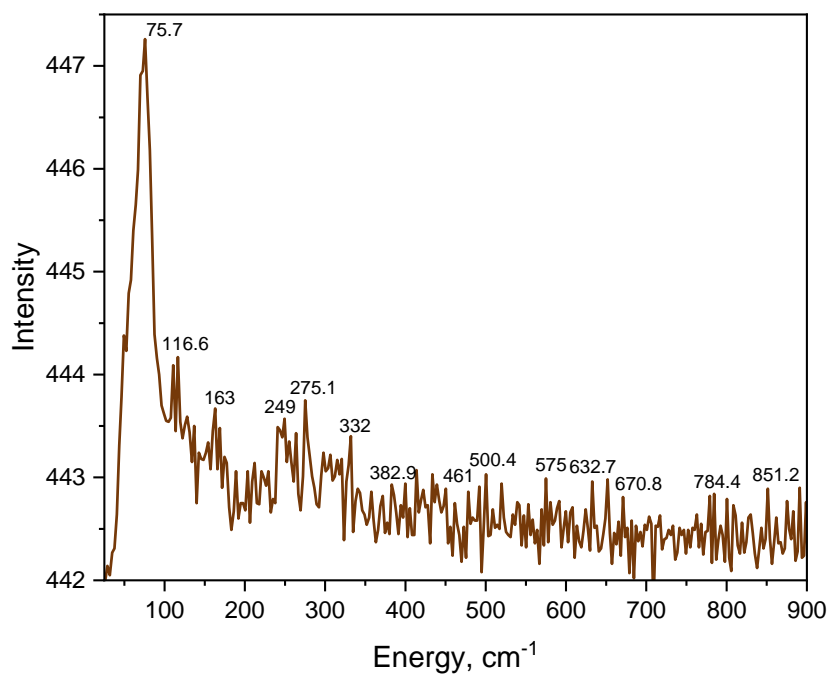


Figure C-70 Raman spectrum of complex $[\text{Mo}_3\text{Se}_7(\text{S}_2\text{P}^i\text{Bu}_2)_3] \text{I}$ in Chapter 3

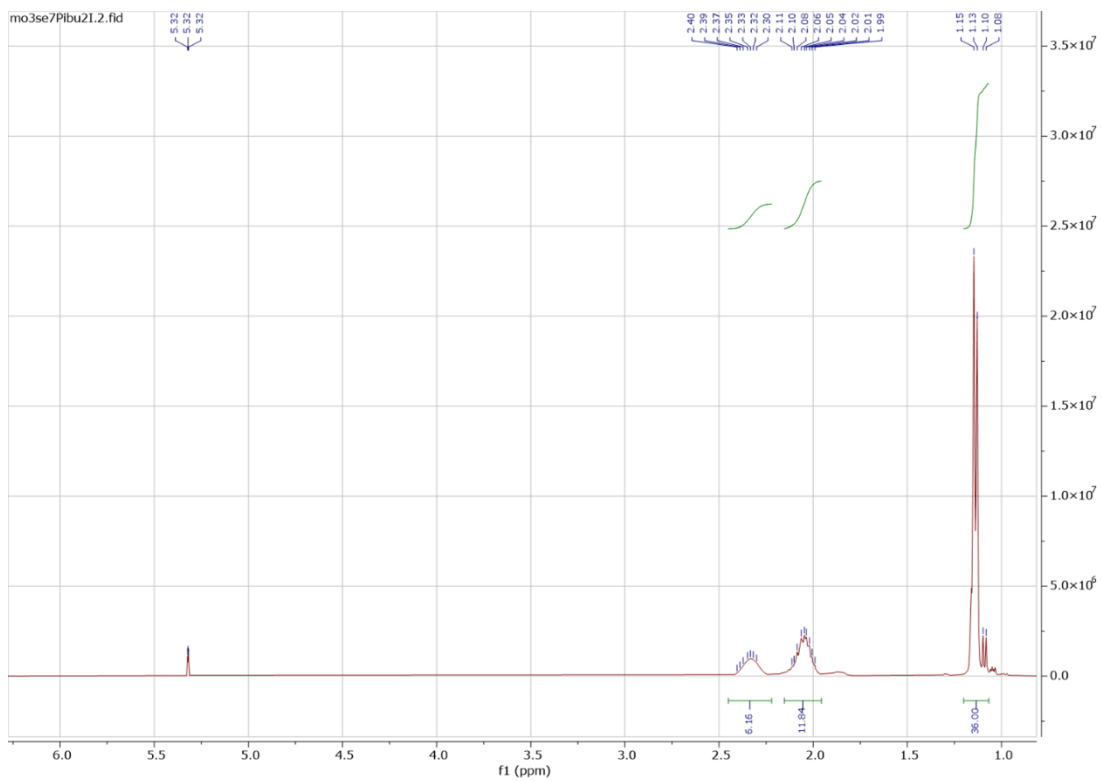


Figure C-71 ^1H NMR spectrum of complex $[\text{Mo}_3\text{Se}_7(\text{S}_2\text{P}'\text{Bu}_2)_3]$ I in Chapter 3

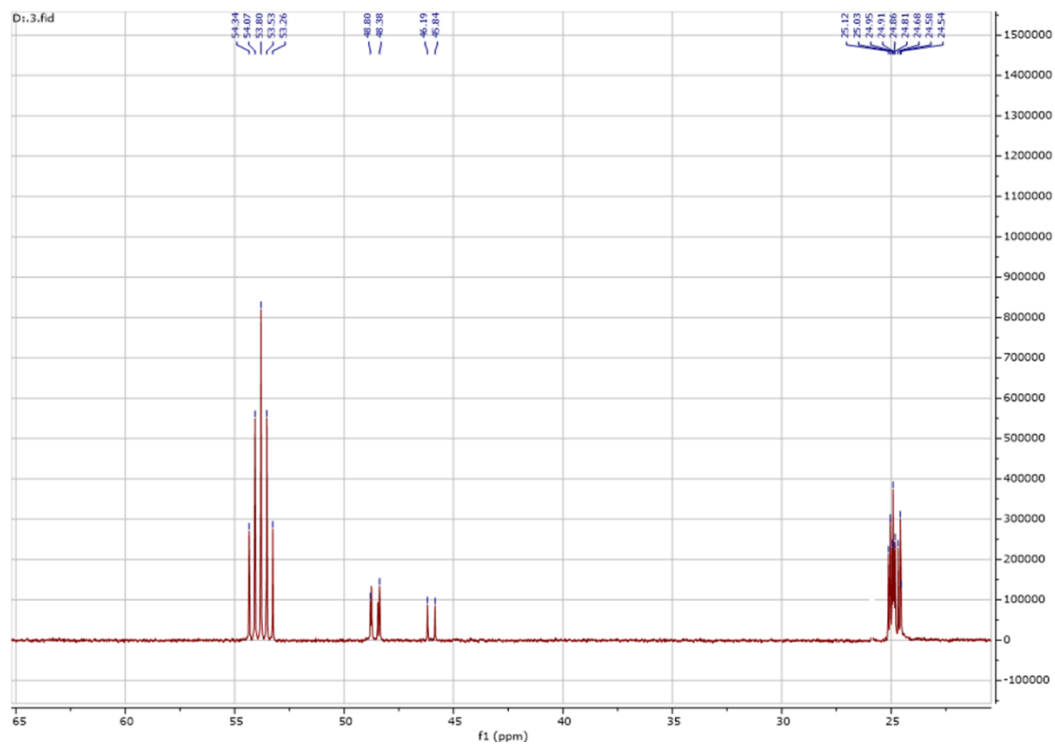


Figure C-72 ^{13}C NMR spectrum of complex $[\text{Mo}_3\text{Se}_7(\text{S}_2\text{P}^i\text{Bu}_2)_3] \text{I}$ in Chapter 3

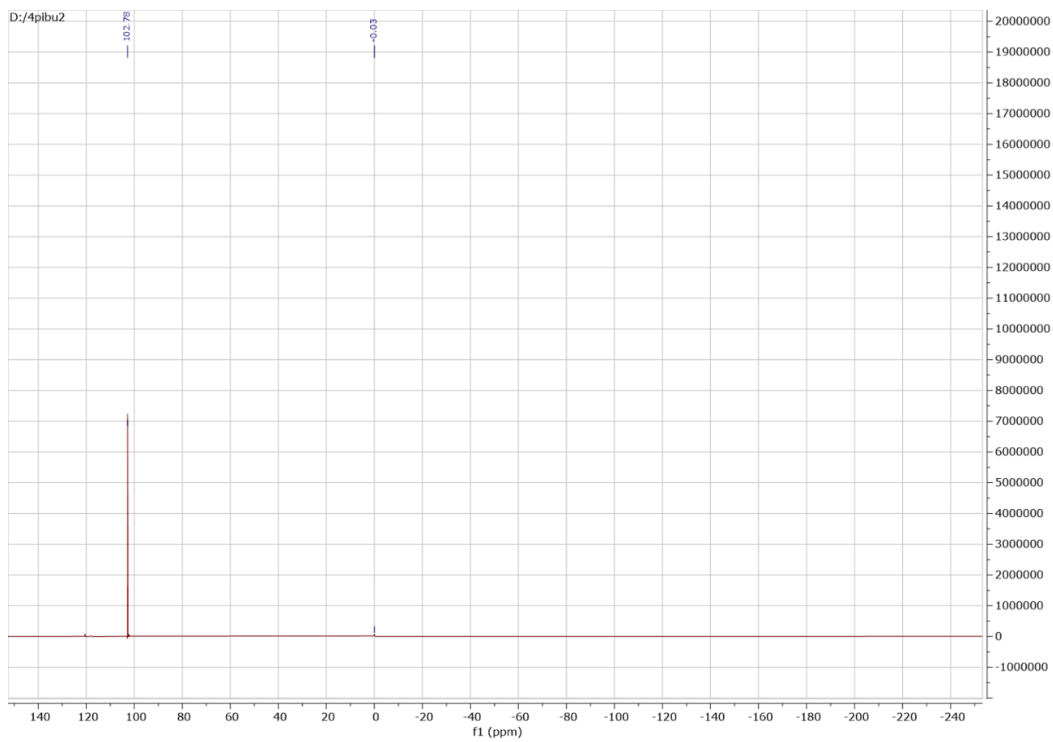


Figure C-73 ^1H NMR spectrum of complex $[\text{Mo}_3\text{Se}_7(\text{S}_2\text{P}^i\text{Bu}_2)_3] \text{I}$ in Chapter

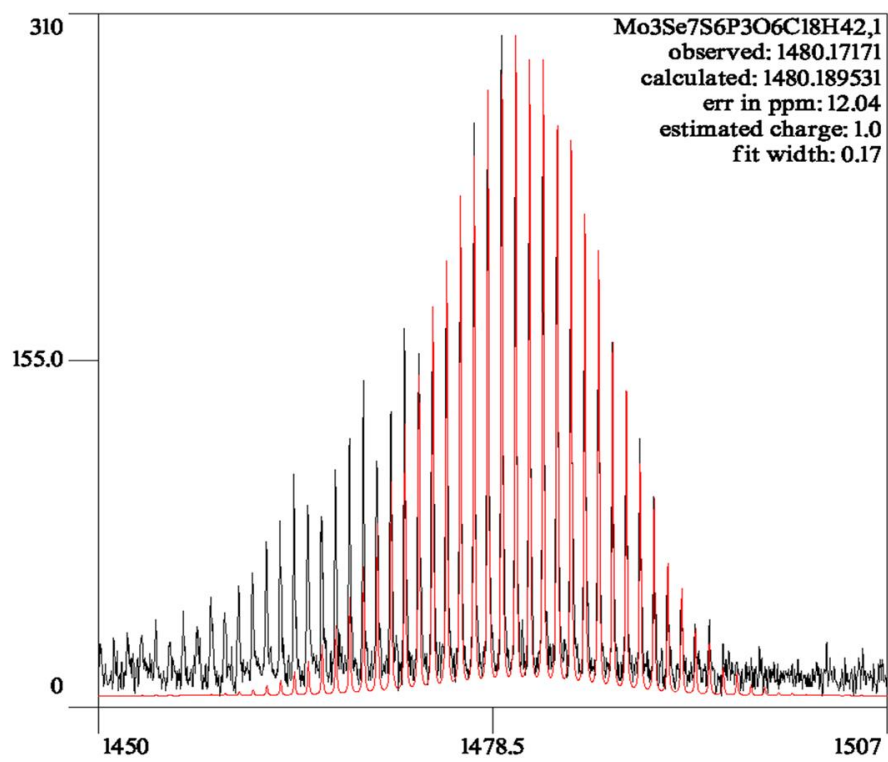


Figure C-74 ESI-MS spectrum of complex $[\text{Mo}_3\text{S}_7((\text{S}_2\text{P}(\text{iPrO})_2)_3)] (\text{S}_2\text{P}(\text{iPrO})_2)$ Chapt

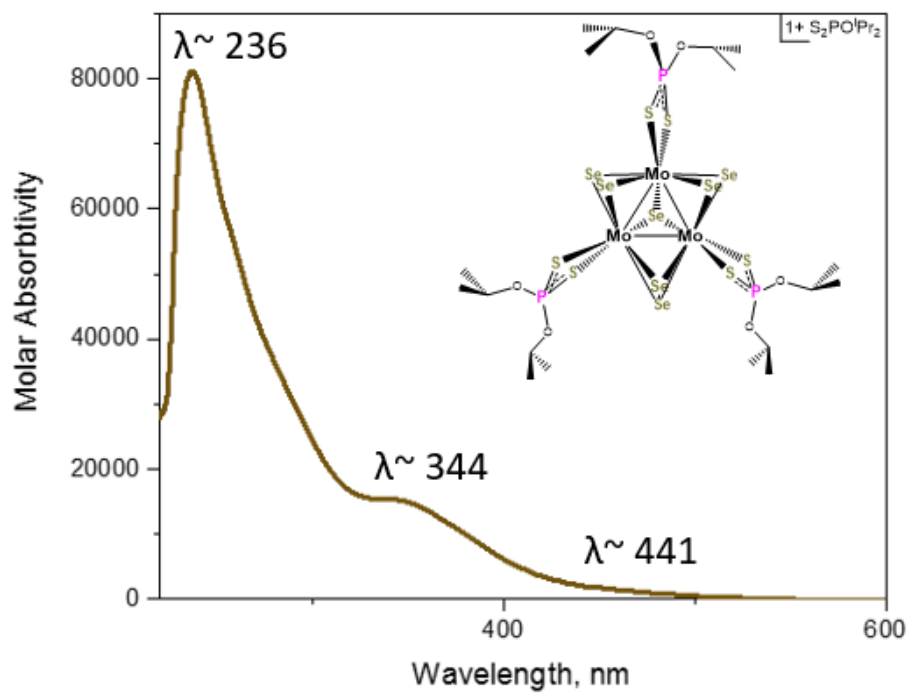


Figure C-75 UV-VIS spectrum of complex $[\text{Mo}_3\text{S}_7((\text{S}_2\text{P}(\text{iPrO})_2)_3)] (\text{S}_2\text{P}(\text{iPrO})_2)$ in Chapter 3

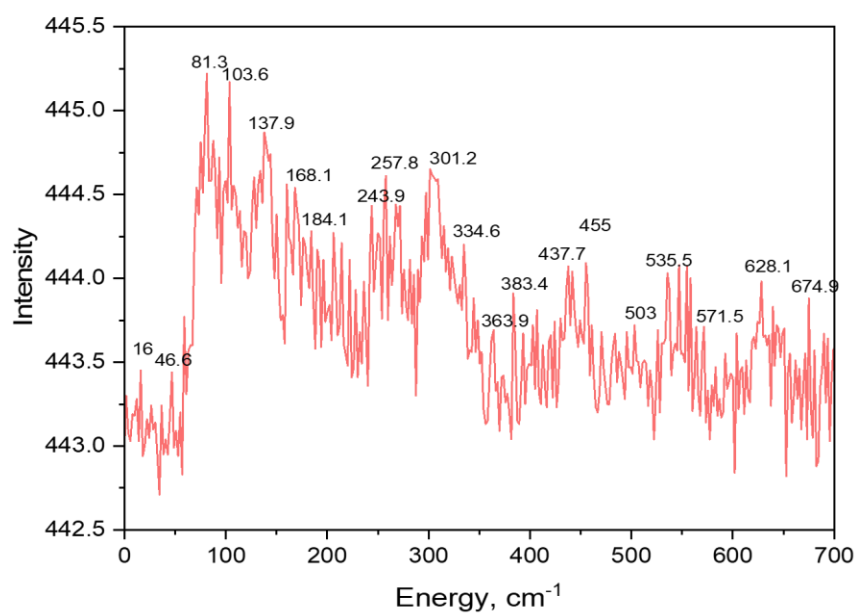


Figure C-76 Raman spectrum of complex $[\text{Mo}_3\text{S}_7((\text{S}_2\text{P}(\text{iPrO})_2)_3)(\text{S}_2\text{P}(\text{iPrO})_2)]$ in Chapter 3

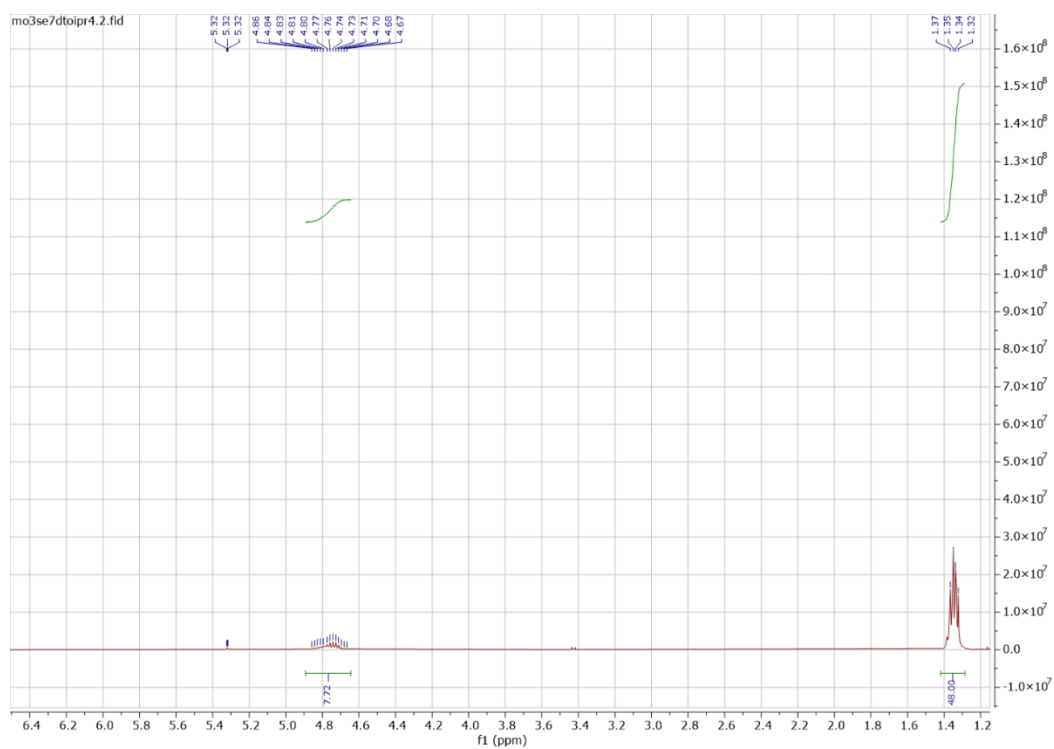


Figure C-77 ^1H NMR spectrum of complex $[\text{Mo}_3\text{S}_7((\text{S}_2\text{P}(\text{iPrO})_2)_3)(\text{S}_2\text{P}(\text{iPrO})_2)]$ in Chapter 3

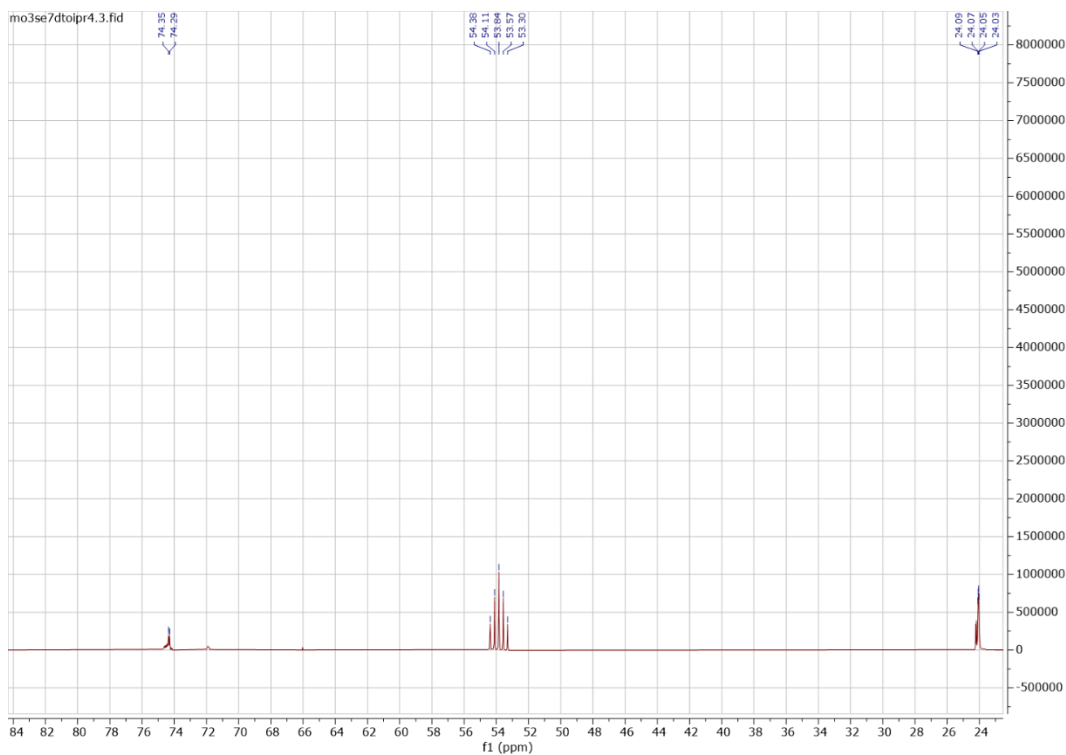


Figure C-78 ^{13}C NMR spectrum of complex $[\text{Mo}_3\text{S}_7((\text{S}_2\text{P}(\text{iPrO})_2)_3)(\text{S}_2\text{P}(\text{iPrO})_2)]$ in Chapter 3

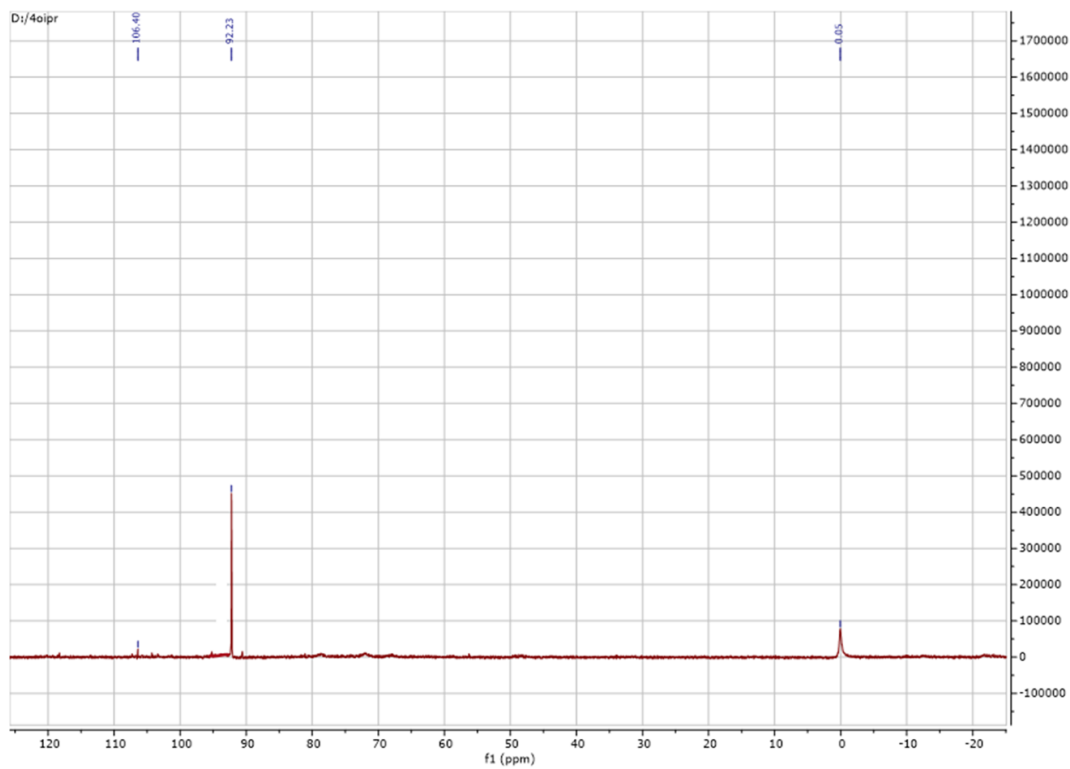


Figure C-79 ^{31}P NMR spectrum of complex $[\text{Mo}_3\text{S}_7((\text{S}_2\text{P}(\text{iPrO})_2)_3)(\text{S}_2\text{P}(\text{iPrO})_2)]$ in Chapter 3

Structure Determination Summary



Thermal ellipsoid plot is drawn at the 30% level. All H atoms are omitted for clarity.

Table A.1. Crystal Data and Structure Refinement for $\text{Cy}_2\text{NC}(\text{S})\text{SSC}(\text{S})\text{NCy}_2$

Identification code	JPD926_0m_a	
Empirical formula	$\text{C}_{26}\text{H}_{44}\text{N}_2\text{S}_4$	
Formula weight	512.87	
Temperature	298(2) K	
Wavelength	0.71073 Å	
Crystal system	Triclinic	
Space group	$P\bar{1}$	
Unit cell dimensions	$a = 12.8612(11)$ Å	$\alpha = 109.9650(10)^\circ$
	$b = 13.1642(11)$ Å	$\beta = 97.9220(10)^\circ$

Volume	$c = 18.3871(16) \text{ \AA}$	$\gamma = 90.4460(10)^\circ$
Z	$2893.0(4) \text{ \AA}^3$	
Density (calculated)	4	
Absorption coefficient	1.178 g/cm^3	
F(000)	0.345 mm^{-1}	
Crystal size	1112	
θ range for data collection	$0.397 \times 0.357 \times 0.083 \text{ mm}^3$	
Index ranges	$1.667 \text{ to } 25.725^\circ$	
Reflections collected	$-15 \leq h \leq 15, -16 \leq k \leq 15, -22 \leq l \leq 22$	
Independent reflections	22600	
Completeness to $\theta = 25.242^\circ$	10898 [R(int) = 0.0582]	
Absorption correction	99.2 %	
Refinement method	None	
Data / restraints / parameters	Full-matrix least-squares on F^2	
Goodness-of-fit on F^2	10898 / 12 / 557	
Final R indices [$I > 2\sigma(I)$]	0.965	
R indices (all data)	R1 = 0.0536, wR2 = 0.0680	
Extinction coefficient	R1 = 0.1276, wR2 = 0.0716	
Largest diff. peak and hole	n/a	
	$0.339 \text{ and } -0.331 \text{ e} \cdot \text{\AA}^{-3}$	

Table A.2. Atomic coordinates ($\times 10^4$) and equivalent isotropic displacement parameters ($\text{\AA}^2 \times 10^3$) for $\text{C}_{27}\text{H}_{20}\text{N}_4\text{S}_8$. $U(\text{eq})$ is defined as one third of the trace of the orthogonalized U^{ij} tensor.

Atom	x	y	z	U(eq)
S(1)	6808(1)	2656(1)	1984(1)	64(1)
S(2)	5945(1)	2310(1)	3322(1)	72(1)
S(3)	5303(1)	3680(1)	3306(1)	75(1)
S(4)	3973(1)	2003(1)	1948(1)	78(1)
S(5)	-1107(1)	7709(1)	2056(1)	67(1)
S(6)	329(1)	7374(1)	3386(1)	67(1)
S(7)	972(1)	8705(1)	3307(1)	69(1)
S(8)	1696(1)	6959(1)	1973(1)	77(1)
N(1)	7473(2)	1222(2)	2662(2)	43(1)
N(2)	3514(2)	4081(2)	2578(2)	55(1)
N(3)	-1441(2)	6193(2)	2689(2)	44(1)
N(4)	2456(2)	9019(2)	2533(2)	59(1)
C(1)	7582(3)	874(3)	3349(2)	50(1)
C(2)	8705(3)	855(3)	3699(2)	71(1)
C(3)	8759(3)	602(4)	4445(2)	92(1)
C(4)	8192(4)	-454(4)	4305(2)	100(2)
C(5)	7053(3)	-482(3)	3934(3)	95(2)
C(6)	6976(3)	-191(3)	3187(2)	65(1)
C(7)	8040(2)	589(3)	2016(2)	46(1)
C(8)	9021(2)	1214(3)	1953(2)	64(1)
C(9)	9626(3)	439(3)	1349(2)	77(1)
C(10)	8937(3)	-91(3)	570(2)	82(1)
C(11)	7972(3)	-679(3)	653(2)	72(1)
C(12)	7369(2)	68(3)	1251(2)	59(1)
C(13)	6847(2)	2010(3)	2598(2)	46(1)
C(14)	4138(2)	3255(3)	2549(2)	54(1)
C(15)	2664(3)	4008(3)	1946(3)	70(1)
C(16)	2932(3)	3849(3)	1168(2)	85(1)
C(17)	2040(3)	3944(3)	584(2)	84(1)
C(18)	1038(3)	3343(4)	592(3)	109(2)
C(19)	769(3)	3490(3)	1363(3)	82(1)
C(20)	1670(3)	3381(3)	1946(2)	68(1)
C(21)	3659(3)	5128(3)	3244(2)	67(1)
C(22)	4224(3)	5990(3)	3063(2)	66(1)
C(23)	4435(3)	7010(3)	3758(3)	100(2)
C(24)	3545(4)	7354(3)	4203(3)	110(2)
C(25)	3015(3)	6468(4)	4367(2)	93(2)
C(26)	2758(3)	5499(3)	3657(2)	94(2)
C(27)	-2271(2)	5583(3)	2048(2)	45(1)

Table A.2, Cont'd. Atomic coordinates ($\times 10^4$) and equivalent isotropic displacement parameters ($\text{\AA}^2 \times 10^3$) for $\text{Cy}_2\text{NC(S)SSC(S)NCy}_2$. $U(\text{eq})$ is defined as one third of the trace of the orthogonalized U^{ij} tensor.

Atom	x	y	z	U(eq)
C(28)	-1905(2)	5112(3)	1263(2)	55(1)
C(29)	-2739(3)	4364(3)	659(2)	73(1)
C(30)	-3758(3)	4924(3)	595(2)	78(1)
C(31)	-4122(3)	5407(3)	1396(2)	70(1)
C(32)	-3279(2)	6189(3)	1997(2)	61(1)
C(33)	-1206(2)	5744(3)	3323(2)	48(1)
C(34)	-653(2)	4691(3)	3064(2)	59(1)
C(35)	-354(3)	4294(3)	3743(2)	77(1)
C(36)	-1300(3)	4207(3)	4137(2)	79(1)
C(37)	-1831(3)	5259(3)	4390(2)	75(1)
C(38)	-2161(2)	5645(3)	3701(2)	62(1)
C(39)	-860(2)	7042(3)	2653(2)	45(1)
C(40)	1810(2)	8213(3)	2547(2)	49(1)
C(41A)	2590(6)	10136(5)	3303(5)	48(2)
C(42A)	1962(7)	10933(7)	3141(6)	45(3)
C(43A)	2072(7)	12007(7)	3818(6)	84(3)
C(44A)	3098(6)	12385(6)	4153(5)	75(3)
C(45A)	3822(6)	11233(8)	4310(5)	64(3)
C(46A)	3729(6)	10519(7)	3615(4)	69(3)
C(41B)	2711(7)	10023(8)	2971(7)	44(3)
C(42B)	1876(11)	10949(12)	2928(9)	89(6)
C(43B)	2256(11)	11979(9)	3549(8)	83(5)
C(44B)	2881(11)	12013(12)	4376(7)	107(5)
C(45B)	3597(10)	11643(10)	4353(7)	67(4)
C(46B)	3301(8)	10076(8)	3774(5)	60(4)
C(47A)	3095(6)	9042(10)	2006(6)	62(3)
C(48A)	2496(6)	8739(9)	1156(4)	61(3)
C(49A)	3335(10)	8827(10)	544(7)	77(4)
C(50A)	4175(7)	8289(10)	608(5)	83(3)
C(51A)	4788(6)	8540(9)	1455(6)	61(3)
C(52A)	4122(7)	8492(7)	1914(6)	51(3)
C(47B)	2988(7)	8633(11)	1721(8)	47(3)
C(48B)	2758(9)	9291(12)	1234(6)	68(4)
C(49B)	3093(12)	8977(14)	586(10)	95(7)
C(50B)	4480(9)	8846(13)	736(7)	94(4)
C(51B)	4621(9)	8132(11)	1165(9)	75(4)
C(52B)	4078(10)	8360(11)	2081(8)	73(5)

Table A.3. Bond lengths (Å) for $\text{Cy}_2\text{NC}(\text{S})\text{SSC}(\text{S})\text{NCy}_2$. Symmetry transformations used to generate equivalent atoms:

S(1)-C(13)	1.625(3)	C(7)-H(7)	0.9800
S(2)-C(13)	1.830(3)	C(8)-C(9)	1.535(4)
S(2)-S(3)	1.9980(12)	C(8)-H(8A)	0.9700
S(3)-C(14)	1.837(3)	C(8)-H(8B)	0.9700
S(4)-C(14)	1.633(3)	C(9)-C(10)	1.511(4)
S(5)-C(39)	1.626(3)	C(9)-H(9A)	0.9700
S(6)-C(39)	1.834(3)	C(9)-H(9B)	0.9700
S(6)-S(7)	1.9905(12)	C(10)-C(11)	1.510(4)
S(7)-C(40)	1.828(3)	C(10)-H(10A)	0.9700
S(8)-C(40)	1.620(3)	C(10)-H(10B)	0.9700
N(1)-C(13)	1.345(3)	C(11)-C(12)	1.512(4)
N(1)-C(1)	1.474(3)	C(11)-H(11A)	0.9700
N(1)-C(7)	1.486(3)	C(11)-H(11B)	0.9700
N(2)-C(14)	1.348(4)	C(12)-H(12A)	0.9700
N(2)-C(15)	1.458(4)	C(12)-H(12B)	0.9700
N(2)-C(21)	1.489(4)	C(15)-C(16)	1.463(4)
N(3)-C(39)	1.365(3)	C(15)-C(20)	1.517(4)
N(3)-C(33)	1.475(3)	C(15)-H(15)	0.9800
N(3)-C(27)	1.473(3)	C(16)-C(17)	1.496(4)
N(4)-C(41B)	1.302(10)	C(16)-H(16A)	0.9700
N(4)-C(40)	1.352(3)	C(16)-H(16B)	0.9700
N(4)-C(47A)	1.361(8)	C(17)-C(18)	1.511(4)
N(4)-C(41A)	1.644(8)	C(17)-H(17A)	0.9700
N(4)-C(47B)	1.651(11)	C(17)-H(17B)	0.9700
C(1)-C(2)	1.502(4)	C(18)-C(19)	1.455(4)
C(1)-C(6)	1.515(4)	C(18)-H(18A)	0.9700
C(1)-H(1)	0.9800	C(18)-H(18B)	0.9700
C(2)-C(3)	1.510(4)	C(19)-C(20)	1.508(4)
C(2)-H(2A)	0.9700	C(19)-H(19A)	0.9700
C(2)-H(2B)	0.9700	C(19)-H(19B)	0.9700
C(3)-C(4)	1.490(5)	C(20)-H(20A)	0.9700
C(3)-H(3A)	0.9700	C(20)-H(20B)	0.9700
C(3)-H(3B)	0.9700	C(21)-C(26)	1.468(4)
C(4)-C(5)	1.523(4)	C(21)-C(22)	1.496(4)
C(4)-H(4A)	0.9700	C(21)-H(21)	0.9800
C(4)-H(4B)	0.9700	C(22)-C(23)	1.496(4)
C(5)-C(6)	1.538(4)	C(22)-H(22A)	0.9700
C(5)-H(5A)	0.9700	C(22)-H(22B)	0.9700
C(5)-H(5B)	0.9700	C(23)-C(24)	1.483(5)
C(6)-H(6A)	0.9700	C(23)-H(23A)	0.9700
C(6)-H(6B)	0.9700	C(23)-H(23B)	0.9700
C(7)-C(12)	1.480(4)	C(24)-C(25)	1.482(5)
C(7)-C(8)	1.540(4)	C(24)-H(24A)	0.97

Table A.3, Cont'd. Bond lengths (Å) for $\text{Cy}_2\text{NC}(\text{S})\text{SSC}(\text{S})\text{NCy}_2$. Symmetry transformations used to generate equivalent atoms:

C(24)-H(24B)	0.9700	C(42A)-C(43A)	1.522(11)
C(25)-C(26)	1.477(4)	C(42A)-H(42A)	0.9700
C(25)-H(25A)	0.9700	C(42A)-H(42B)	0.9700
C(25)-H(25B)	0.9700	C(43A)-C(44A)	1.387(12)
C(26)-H(26A)	0.9700	C(43A)-H(43A)	0.9700
C(26)-H(26B)	0.9700	C(43A)-H(43B)	0.9700
C(27)-C(28)	1.506(4)	C(44A)-C(45A)	1.869(13)
C(27)-C(32)	1.536(4)	C(44A)-H(44A)	0.9700
C(27)-H(27)	0.9800	C(44A)-H(44B)	0.9700
C(28)-C(29)	1.504(4)	C(45A)-C(46A)	1.291(9)
C(28)-H(28A)	0.9700	C(45A)-H(45A)	0.9700
C(28)-H(28B)	0.9700	C(45A)-H(45B)	0.9700
C(29)-C(30)	1.519(4)	C(46A)-H(46A)	0.9700
C(29)-H(29A)	0.9700	C(46A)-H(46B)	0.9700
C(29)-H(29B)	0.9700	C(41B)-C(46B)	1.542(15)
C(30)-C(31)	1.532(4)	C(41B)-C(42B)	1.646(17)
C(30)-H(30A)	0.9700	C(41B)-H(41B)	0.9800
C(30)-H(30B)	0.9700	C(42B)-C(43B)	1.470(17)
C(31)-C(32)	1.527(4)	C(42B)-H(42C)	0.9700
C(31)-H(31A)	0.9700	C(42B)-H(42D)	0.9700
C(31)-H(31B)	0.9700	C(43B)-C(44B)	1.61(2)
C(32)-H(32A)	0.9700	C(43B)-H(43C)	0.9700
C(32)-H(32B)	0.9700	C(43B)-H(43D)	0.9700
C(33)-C(38)	1.517(4)	C(44B)-C(45B)	1.044(14)
C(33)-C(34)	1.520(4)	C(44B)-H(44C)	0.9700
C(33)-H(33)	0.9800	C(44B)-H(44D)	0.9700
C(34)-C(35)	1.515(4)	C(45B)-C(46B)	1.978(17)
C(34)-H(34A)	0.9700	C(45B)-H(45C)	0.9700
C(34)-H(34B)	0.9700	C(45B)-H(45D)	0.9700
C(35)-C(36)	1.521(4)	C(46B)-H(46C)	0.9700
C(35)-H(35A)	0.9700	C(46B)-H(46D)	0.9700
C(35)-H(35B)	0.9700	C(47A)-C(52A)	1.513(12)
C(36)-C(37)	1.505(4)	C(47A)-C(48A)	1.560(14)
C(36)-H(36A)	0.9700	C(47A)-H(47A)	0.9800
C(36)-H(36B)	0.9700	C(48A)-C(49A)	1.693(14)
C(37)-C(38)	1.530(4)	C(48A)-H(48A)	0.9700
C(37)-H(37A)	0.9700	C(48A)-H(48B)	0.9700
C(37)-H(37B)	0.9700	C(49A)-C(50A)	1.309(12)
C(38)-H(38A)	0.9700	C(49A)-H(49A)	0.9700
C(38)-H(38B)	0.9700	C(49A)-H(49B)	0.9700
C(41A)-C(42A)	1.416(10)	C(50A)-C(51A)	1.569(14)
C(41A)-C(46A)	1.513(10)	C(50A)-H(50A)	0.9700
C(41A)-H(41A)	0.9800	C(50A)-H(50B)	0.9700

Table A.3, Cont'd. Bond lengths (Å) for $\text{Cy}_2\text{NC}(\text{S})\text{SSC}(\text{S})\text{NCy}_2$. Symmetry transformations used to generate equivalent atoms:

C(51A)-C(52A)	1.299(11)
C(51A)-H(51A)	0.9700
C(51A)-H(51B)	0.9700
C(52A)-H(52A)	0.9700
C(52A)-H(52B)	0.9700
C(47B)-C(48B)	1.448(15)
C(47B)-C(52B)	1.565(16)
C(47B)-H(47B)	0.9800
C(48B)-C(49B)	1.259(17)
C(48B)-H(48C)	0.9700
C(48B)-H(48D)	0.9700
C(49B)-C(50B)	1.79(2)
C(49B)-H(49C)	0.9700
C(49B)-H(49D)	0.9700
C(50B)-C(51B)	1.416(17)
C(50B)-H(50C)	0.9700
C(50B)-H(50D)	0.9700
C(51B)-C(52B)	1.84(2)
C(51B)-H(51C)	0.9700
C(51B)-H(51D)	0.9700
C(52B)-H(52C)	0.9700
C(52B)-H(52D)	0.9700

Table A.4. Bond angles (deg.) for $\text{Cy}_2\text{NC}(\text{S})\text{SSC}(\text{S})\text{NCy}_2$. Symmetry transformations used to generate equivalent atoms:

C(13)-S(2)-S(3)	105.50(11)	C(6)-C(5)-H(5A)	109.3
C(14)-S(3)-S(2)	105.38(12)	C(4)-C(5)-H(5B)	109.3
C(39)-S(6)-S(7)	104.31(12)	C(6)-C(5)-H(5B)	109.3
C(40)-S(7)-S(6)	104.87(12)	H(5A)-C(5)-H(5B)	108.0
C(13)-N(1)-C(1)	122.5(3)	C(1)-C(6)-C(5)	110.6(3)
C(13)-N(1)-C(7)	121.9(3)	C(1)-C(6)-H(6A)	109.5
C(1)-N(1)-C(7)	115.4(2)	C(5)-C(6)-H(6A)	109.5
C(14)-N(2)-C(15)	121.7(3)	C(1)-C(6)-H(6B)	109.5
C(14)-N(2)-C(21)	122.4(3)	C(5)-C(6)-H(6B)	109.5
C(15)-N(2)-C(21)	115.9(3)	H(6A)-C(6)-H(6B)	108.1
C(39)-N(3)-C(33)	122.6(3)	C(12)-C(7)-N(1)	115.0(3)
C(39)-N(3)-C(27)	121.8(3)	C(12)-C(7)-C(8)	112.6(3)
C(33)-N(3)-C(27)	115.2(2)	N(1)-C(7)-C(8)	113.0(3)
C(41B)-N(4)-C(40)	136.2(6)	C(12)-C(7)-H(7)	105.0
C(40)-N(4)-C(47A)	130.6(6)	N(1)-C(7)-H(7)	105.0
C(40)-N(4)-C(41A)	116.6(4)	C(8)-C(7)-H(7)	105.0
C(40)-N(4)-C(47B)	110.3(5)	C(9)-C(8)-C(7)	108.6(3)
N(1)-C(1)-C(2)	113.5(3)	C(9)-C(8)-H(8A)	110.0
N(1)-C(1)-C(6)	112.5(3)	C(7)-C(8)-H(8A)	110.0
C(2)-C(1)-C(6)	111.5(3)	C(9)-C(8)-H(8B)	110.0
N(1)-C(1)-H(1)	106.3	C(7)-C(8)-H(8B)	110.0
C(2)-C(1)-H(1)	106.3	H(8A)-C(8)-H(8B)	108.4
C(6)-C(1)-H(1)	106.3	C(10)-C(9)-C(8)	111.9(3)
C(1)-C(2)-C(3)	110.7(3)	C(10)-C(9)-H(9A)	109.2
C(1)-C(2)-H(2A)	109.5	C(8)-C(9)-H(9A)	109.2
C(3)-C(2)-H(2A)	109.5	C(10)-C(9)-H(9B)	109.2
C(1)-C(2)-H(2B)	109.5	C(8)-C(9)-H(9B)	109.2
C(3)-C(2)-H(2B)	109.5	H(9A)-C(9)-H(9B)	107.9
H(2A)-C(2)-H(2B)	108.1	C(9)-C(10)-C(11)	111.6(3)
C(4)-C(3)-C(2)	111.4(3)	C(9)-C(10)-H(10A)	109.3
C(4)-C(3)-H(3A)	109.4	C(11)-C(10)-H(10A)	109.3
C(2)-C(3)-H(3A)	109.4	C(9)-C(10)-H(10B)	109.3
C(4)-C(3)-H(3B)	109.4	C(11)-C(10)-H(10B)	109.3
C(2)-C(3)-H(3B)	109.4	H(10A)-C(10)-H(10B)	108.0
H(3A)-C(3)-H(3B)	108.0	C(10)-C(11)-C(12)	111.0(3)
C(3)-C(4)-C(5)	111.5(3)	C(10)-C(11)-H(11A)	109.4
C(3)-C(4)-H(4A)	109.3	C(12)-C(11)-H(11A)	109.4
C(5)-C(4)-H(4A)	109.3	C(10)-C(11)-H(11B)	109.4
C(3)-C(4)-H(4B)	109.3	C(12)-C(11)-H(11B)	109.4
C(5)-C(4)-H(4B)	109.3	H(11A)-C(11)-H(11B)	108.0
H(4A)-C(4)-H(4B)	108.0	C(7)-C(12)-C(11)	112.0(3)
C(4)-C(5)-C(6)	111.5(3)	C(7)-C(12)-H(12A)	109.2
C(4)-C(5)-H(5A)	109.3	C(11)-C(12)-H(12A)	109.2

Table A.4, Cont'd. Bond angles (deg.) for $\text{Cy}_2\text{NC}(\text{S})\text{SSC}(\text{S})\text{NCy}_2$. Symmetry transformations used to generate equivalent atoms:

C(7)-C(12)-H(12B)	109.2	C(15)-C(20)-H(20B)	109.2
C(11)-C(12)-H(12B)	109.2	H(20A)-C(20)-H(20B)	107.9
H(12A)-C(12)-H(12B)	107.9	C(26)-C(21)-N(2)	117.6(3)
N(1)-C(13)-S(1)	128.8(2)	C(26)-C(21)-C(22)	114.2(3)
N(1)-C(13)-S(2)	110.7(2)	N(2)-C(21)-C(22)	112.4(3)
S(1)-C(13)-S(2)	120.50(19)	C(26)-C(21)-H(21)	103.4
N(2)-C(14)-S(4)	128.5(3)	N(2)-C(21)-H(21)	103.4
N(2)-C(14)-S(3)	111.6(3)	C(22)-C(21)-H(21)	103.4
S(4)-C(14)-S(3)	119.9(2)	C(23)-C(22)-C(21)	111.7(3)
N(2)-C(15)-C(16)	118.4(3)	C(23)-C(22)-H(22A)	109.3
N(2)-C(15)-C(20)	115.0(3)	C(21)-C(22)-H(22A)	109.3
C(16)-C(15)-C(20)	114.6(3)	C(23)-C(22)-H(22B)	109.3
N(2)-C(15)-H(15)	101.7	C(21)-C(22)-H(22B)	109.3
C(16)-C(15)-H(15)	101.7	H(22A)-C(22)-H(22B)	107.9
C(20)-C(15)-H(15)	101.7	C(24)-C(23)-C(22)	115.4(4)
C(15)-C(16)-C(17)	114.9(3)	C(24)-C(23)-H(23A)	108.4
C(15)-C(16)-H(16A)	108.6	C(22)-C(23)-H(23A)	108.4
C(17)-C(16)-H(16A)	108.6	C(24)-C(23)-H(23B)	108.4
C(15)-C(16)-H(16B)	108.6	C(22)-C(23)-H(23B)	108.4
C(17)-C(16)-H(16B)	108.6	H(23A)-C(23)-H(23B)	107.5
H(16A)-C(16)-H(16B)	107.5	C(23)-C(24)-C(25)	114.0(4)
C(16)-C(17)-C(18)	112.9(3)	C(23)-C(24)-H(24A)	108.7
C(16)-C(17)-H(17A)	109.0	C(25)-C(24)-H(24A)	108.7
C(18)-C(17)-H(17A)	109.0	C(23)-C(24)-H(24B)	108.7
C(16)-C(17)-H(17B)	109.0	C(25)-C(24)-H(24B)	108.7
C(18)-C(17)-H(17B)	109.0	H(24A)-C(24)-H(24B)	107.6
H(17A)-C(17)-H(17B)	107.8	C(26)-C(25)-C(24)	111.8(4)
C(19)-C(18)-C(17)	115.6(3)	C(26)-C(25)-H(25A)	109.3
C(19)-C(18)-H(18A)	108.4	C(24)-C(25)-H(25A)	109.3
C(17)-C(18)-H(18A)	108.4	C(26)-C(25)-H(25B)	109.3
C(19)-C(18)-H(18B)	108.4	C(24)-C(25)-H(25B)	109.3
C(17)-C(18)-H(18B)	108.4	H(25A)-C(25)-H(25B)	107.9
H(18A)-C(18)-H(18B)	107.4	C(21)-C(26)-C(25)	113.5(4)
C(18)-C(19)-C(20)	114.5(3)	C(21)-C(26)-H(26A)	108.9
C(18)-C(19)-H(19A)	108.6	C(25)-C(26)-H(26A)	108.9
C(20)-C(19)-H(19A)	108.6	C(21)-C(26)-H(26B)	108.9
C(18)-C(19)-H(19B)	108.6	C(25)-C(26)-H(26B)	108.9
C(20)-C(19)-H(19B)	108.6	H(26A)-C(26)-H(26B)	107.7
H(19A)-C(19)-H(19B)	107.6	N(3)-C(27)-C(28)	114.3(3)
C(19)-C(20)-C(15)	112.3(3)	N(3)-C(27)-C(32)	114.1(3)
C(19)-C(20)-H(20A)	109.2	C(28)-C(27)-C(32)	111.8(3)
C(15)-C(20)-H(20A)	109.2	N(3)-C(27)-H(27)	105.2
C(19)-C(20)-H(20B)	109.2	C(28)-C(27)-H(27)	105.2

Table A.4, Cont'd. Bond angles (deg.) for $\text{Cy}_2\text{NC}(\text{S})\text{SSC}(\text{S})\text{NCy}_2$. Symmetry transformations used to generate equivalent atoms:

C(32)-C(27)-H(27)	105.2	C(34)-C(35)-C(36)	111.4(3)
C(29)-C(28)-C(27)	112.0(3)	C(34)-C(35)-H(35A)	109.3
C(29)-C(28)-H(28A)	109.2	C(36)-C(35)-H(35A)	109.3
C(27)-C(28)-H(28A)	109.2	C(34)-C(35)-H(35B)	109.3
C(29)-C(28)-H(28B)	109.2	C(36)-C(35)-H(35B)	109.3
C(27)-C(28)-H(28B)	109.2	H(35A)-C(35)-H(35B)	108.0
H(28A)-C(28)-H(28B)	107.9	C(37)-C(36)-C(35)	111.7(3)
C(28)-C(29)-C(30)	111.3(3)	C(37)-C(36)-H(36A)	109.3
C(28)-C(29)-H(29A)	109.4	C(35)-C(36)-H(36A)	109.3
C(30)-C(29)-H(29A)	109.4	C(37)-C(36)-H(36B)	109.3
C(28)-C(29)-H(29B)	109.4	C(35)-C(36)-H(36B)	109.3
C(30)-C(29)-H(29B)	109.4	H(36A)-C(36)-H(36B)	107.9
H(29A)-C(29)-H(29B)	108.0	C(36)-C(37)-C(38)	111.3(3)
C(29)-C(30)-C(31)	111.0(3)	C(36)-C(37)-H(37A)	109.4
C(29)-C(30)-H(30A)	109.4	C(38)-C(37)-H(37A)	109.4
C(31)-C(30)-H(30A)	109.4	C(36)-C(37)-H(37B)	109.4
C(29)-C(30)-H(30B)	109.4	C(38)-C(37)-H(37B)	109.4
C(31)-C(30)-H(30B)	109.4	H(37A)-C(37)-H(37B)	108.0
H(30A)-C(30)-H(30B)	108.0	C(33)-C(38)-C(37)	109.4(3)
C(32)-C(31)-C(30)	111.7(3)	C(33)-C(38)-H(38A)	109.8
C(32)-C(31)-H(31A)	109.3	C(37)-C(38)-H(38A)	109.8
C(30)-C(31)-H(31A)	109.3	C(33)-C(38)-H(38B)	109.8
C(32)-C(31)-H(31B)	109.3	C(37)-C(38)-H(38B)	109.8
C(30)-C(31)-H(31B)	109.3	H(38A)-C(38)-H(38B)	108.2
H(31A)-C(31)-H(31B)	107.9	N(3)-C(39)-S(5)	127.9(2)
C(31)-C(32)-C(27)	108.4(3)	N(3)-C(39)-S(6)	111.0(2)
C(31)-C(32)-H(32A)	110.0	S(5)-C(39)-S(6)	121.12(19)
C(27)-C(32)-H(32A)	110.0	N(4)-C(40)-S(8)	127.9(3)
C(31)-C(32)-H(32B)	110.0	N(4)-C(40)-S(7)	111.5(2)
C(27)-C(32)-H(32B)	110.0	S(8)-C(40)-S(7)	120.6(2)
H(32A)-C(32)-H(32B)	108.4	C(42A)-C(41A)-C(46A)	113.8(7)
N(3)-C(33)-C(38)	112.8(3)	C(42A)-C(41A)-N(4)	110.0(7)
N(3)-C(33)-C(34)	112.2(3)	C(46A)-C(41A)-N(4)	112.6(6)
C(38)-C(33)-C(34)	112.4(3)	C(42A)-C(41A)-H(41A)	106.6
N(3)-C(33)-H(33)	106.3	C(46A)-C(41A)-H(41A)	106.6
C(38)-C(33)-H(33)	106.3	N(4)-C(41A)-H(41A)	106.6
C(34)-C(33)-H(33)	106.3	C(41A)-C(42A)-C(43A)	113.1(8)
C(35)-C(34)-C(33)	110.8(3)	C(41A)-C(42A)-H(42A)	109.0
C(35)-C(34)-H(34A)	109.5	C(43A)-C(42A)-H(42A)	109.0
C(33)-C(34)-H(34A)	109.5	C(41A)-C(42A)-H(42B)	109.0
C(35)-C(34)-H(34B)	109.5	C(43A)-C(42A)-H(42B)	109.0
C(33)-C(34)-H(34B)	109.5	H(42A)-C(42A)-H(42B)	107.8
H(34A)-C(34)-H(34B)	108.1	C(44A)-C(43A)-C(42A)	115.1(7)

Table A.4, Cont'd. Bond angles (deg.) for $\text{Cy}_2\text{NC(S)SSC(S)NCy}_2$. Symmetry transformations used to generate equivalent atoms:

C(44A)-C(43A)-H(43A)	108.5	C(43B)-C(44B)-H(44C)	108.4
C(42A)-C(43A)-H(43A)	108.5	C(45B)-C(44B)-H(44D)	108.4
C(44A)-C(43A)-H(43B)	108.5	C(43B)-C(44B)-H(44D)	108.4
C(42A)-C(43A)-H(43B)	108.5	H(44C)-C(44B)-H(44D)	107.5
H(43A)-C(43A)-H(43B)	107.5	C(44B)-C(45B)-C(46B)	108.0(13)
C(43A)-C(44A)-C(45A)	108.0(7)	C(44B)-C(45B)-H(45C)	110.1
C(43A)-C(44A)-H(44A)	110.1	C(46B)-C(45B)-H(45C)	110.1
C(45A)-C(44A)-H(44A)	110.1	C(44B)-C(45B)-H(45D)	110.1
C(43A)-C(44A)-H(44B)	110.1	C(46B)-C(45B)-H(45D)	110.1
C(45A)-C(44A)-H(44B)	110.1	H(45C)-C(45B)-H(45D)	108.4
H(44A)-C(44A)-H(44B)	108.4	C(41B)-C(46B)-C(45B)	104.0(8)
C(46A)-C(45A)-C(44A)	103.2(7)	C(41B)-C(46B)-H(46C)	111.0
C(46A)-C(45A)-H(45A)	111.1	C(45B)-C(46B)-H(46C)	111.0
C(44A)-C(45A)-H(45A)	111.1	C(41B)-C(46B)-H(46D)	111.0
C(46A)-C(45A)-H(45B)	111.1	C(45B)-C(46B)-H(46D)	111.0
C(44A)-C(45A)-H(45B)	111.1	H(46C)-C(46B)-H(46D)	109.0
H(45A)-C(45A)-H(45B)	109.1	N(4)-C(47A)-C(52A)	125.2(7)
C(45A)-C(46A)-C(41A)	110.9(8)	N(4)-C(47A)-C(48A)	113.0(7)
C(45A)-C(46A)-H(46A)	109.4	C(52A)-C(47A)-C(48A)	104.9(9)
C(41A)-C(46A)-H(46A)	109.4	N(4)-C(47A)-H(47A)	103.8
C(45A)-C(46A)-H(46B)	109.4	C(52A)-C(47A)-H(47A)	103.8
C(41A)-C(46A)-H(46B)	109.4	C(48A)-C(47A)-H(47A)	103.8
H(46A)-C(46A)-H(46B)	108.0	C(47A)-C(48A)-C(49A)	110.1(7)
N(4)-C(41B)-C(46B)	110.0(8)	C(47A)-C(48A)-H(48A)	109.6
N(4)-C(41B)-C(42B)	118.6(8)	C(49A)-C(48A)-H(48A)	109.6
C(46B)-C(41B)-C(42B)	119.2(10)	C(47A)-C(48A)-H(48B)	109.6
N(4)-C(41B)-H(41B)	101.8	C(49A)-C(48A)-H(48B)	109.6
C(46B)-C(41B)-H(41B)	101.8	H(48A)-C(48A)-H(48B)	108.2
C(42B)-C(41B)-H(41B)	101.8	C(50A)-C(49A)-C(48A)	111.9(10)
C(43B)-C(42B)-C(41B)	108.8(10)	C(50A)-C(49A)-H(49A)	109.2
C(43B)-C(42B)-H(42C)	109.9	C(48A)-C(49A)-H(49A)	109.2
C(41B)-C(42B)-H(42C)	109.9	C(50A)-C(49A)-H(49B)	109.2
C(43B)-C(42B)-H(42D)	109.9	C(48A)-C(49A)-H(49B)	109.2
C(41B)-C(42B)-H(42D)	109.9	H(49A)-C(49A)-H(49B)	107.9
H(42C)-C(42B)-H(42D)	108.3	C(49A)-C(50A)-C(51A)	116.7(9)
C(42B)-C(43B)-C(44B)	121.4(11)	C(49A)-C(50A)-H(50A)	108.1
C(42B)-C(43B)-H(43C)	107.0	C(51A)-C(50A)-H(50A)	108.1
C(44B)-C(43B)-H(43C)	107.0	C(49A)-C(50A)-H(50B)	108.1
C(42B)-C(43B)-H(43D)	107.0	C(51A)-C(50A)-H(50B)	108.1
C(44B)-C(43B)-H(43D)	107.0	H(50A)-C(50A)-H(50B)	107.3
H(43C)-C(43B)-H(43D)	106.7	C(52A)-C(51A)-C(50A)	108.6(9)
C(45B)-C(44B)-C(43B)	115.5(14)	C(52A)-C(51A)-H(51A)	110.0
C(45B)-C(44B)-H(44C)	108.4	C(50A)-C(51A)-H(51A)	110.0

Table A.4, Cont'd. Bond angles (deg.) for $\text{Cy}_2\text{NC}(\text{S})\text{SSC}(\text{S})\text{NCy}_2$. Symmetry transformations used to generate equivalent atoms:

C(52A)-C(51A)-H(51B)	110.0	C(51B)-C(52B)-H(52D)	113.3
C(50A)-C(51A)-H(51B)	110.0	H(52C)-C(52B)-H(52D)	110.6
H(51A)-C(51A)-H(51B)	108.3		
C(51A)-C(52A)-C(47A)	127.6(9)		
C(51A)-C(52A)-H(52A)	105.4		
C(47A)-C(52A)-H(52A)	105.4		
C(51A)-C(52A)-H(52B)	105.4		
C(47A)-C(52A)-H(52B)	105.4		
H(52A)-C(52A)-H(52B)	106.0		
C(48B)-C(47B)-C(52B)	129.3(9)		
C(48B)-C(47B)-N(4)	114.6(8)		
C(52B)-C(47B)-N(4)	97.1(9)		
C(48B)-C(47B)-H(47B)	104.5		
C(52B)-C(47B)-H(47B)	104.5		
N(4)-C(47B)-H(47B)	104.5		
C(49B)-C(48B)-C(47B)	116.3(13)		
C(49B)-C(48B)-H(48C)	108.2		
C(47B)-C(48B)-H(48C)	108.2		
C(49B)-C(48B)-H(48D)	108.2		
C(47B)-C(48B)-H(48D)	108.2		
H(48C)-C(48B)-H(48D)	107.4		
C(48B)-C(49B)-C(50B)	109.8(13)		
C(48B)-C(49B)-H(49C)	109.7		
C(50B)-C(49B)-H(49C)	109.7		
C(48B)-C(49B)-H(49D)	109.7		
C(50B)-C(49B)-H(49D)	109.7		
H(49C)-C(49B)-H(49D)	108.2		
C(51B)-C(50B)-C(49B)	104.9(11)		
C(51B)-C(50B)-H(50C)	110.8		
C(49B)-C(50B)-H(50C)	110.8		
C(51B)-C(50B)-H(50D)	110.8		
C(49B)-C(50B)-H(50D)	110.8		
H(50C)-C(50B)-H(50D)	108.8		
C(50B)-C(51B)-C(52B)	122.6(10)		
C(50B)-C(51B)-H(51C)	106.7		
C(52B)-C(51B)-H(51C)	106.7		
C(50B)-C(51B)-H(51D)	106.7		
C(52B)-C(51B)-H(51D)	106.7		
H(51C)-C(51B)-H(51D)	106.6		
C(47B)-C(52B)-C(51B)	92.0(10)		
C(47B)-C(52B)-H(52C)	113.3		
C(51B)-C(52B)-H(52C)	113.3		
C(47B)-C(52B)-H(52D)	113.3		

Table A.5. Anisotropic displacement parameters ($\text{\AA}^2 \times 10^3$) for $\text{Cy}_2\text{NC(S)SSC(S)NCy}_2$. The anisotropic displacement factor exponent takes the form: $-2\pi^2[h^2a^*U^{11} + \dots + 2hka^*b^*U^{12}]$.

Atom	U^{11}	U^{22}	U^{33}	U^{23}	U^{13}	U^{12}
S(1)	60(1)	63(1)	88(1)	45(1)	16(1)	13(1)
S(2)	56(1)	85(1)	94(1)	49(1)	32(1)	35(1)
S(3)	49(1)	60(1)	105(1)	18(1)	6(1)	19(1)
S(4)	65(1)	46(1)	115(1)	16(1)	15(1)	6(1)
S(5)	58(1)	62(1)	95(1)	45(1)	7(1)	-1(1)
S(6)	47(1)	72(1)	87(1)	38(1)	-1(1)	-16(1)
S(7)	56(1)	51(1)	94(1)	12(1)	24(1)	-11(1)
S(8)	72(1)	48(1)	105(1)	15(1)	20(1)	2(1)
N(1)	38(2)	44(2)	56(2)	25(2)	18(2)	12(1)
N(2)	33(2)	50(2)	89(3)	33(2)	9(2)	11(2)
N(3)	35(2)	47(2)	53(2)	24(2)	2(2)	-4(1)
N(4)	48(2)	48(2)	91(3)	32(2)	21(2)	-1(2)
C(1)	48(3)	52(3)	60(3)	27(2)	21(2)	23(2)
C(2)	66(3)	80(3)	75(3)	41(3)	0(2)	9(2)
C(3)	90(4)	105(4)	81(4)	36(3)	2(3)	37(3)
C(4)	134(5)	116(4)	83(4)	65(3)	40(3)	59(4)
C(5)	105(4)	94(4)	115(4)	65(3)	36(3)	14(3)
C(6)	62(3)	74(3)	71(3)	37(3)	23(2)	13(2)
C(7)	50(2)	38(2)	59(3)	22(2)	22(2)	12(2)
C(8)	40(2)	70(3)	81(3)	21(2)	21(2)	4(2)
C(9)	53(3)	79(3)	109(4)	31(3)	43(3)	8(2)
C(10)	85(3)	94(4)	72(4)	23(3)	38(3)	8(3)
C(11)	71(3)	65(3)	79(3)	19(3)	23(2)	5(2)
C(12)	49(2)	59(3)	64(3)	12(2)	15(2)	-8(2)
C(13)	34(2)	47(2)	57(3)	18(2)	10(2)	7(2)
C(14)	34(2)	48(3)	76(3)	18(2)	5(2)	0(2)
C(15)	50(3)	84(3)	94(4)	56(3)	1(3)	0(2)
C(16)	66(3)	112(4)	78(4)	35(3)	12(3)	-22(3)
C(17)	91(4)	86(3)	81(4)	33(3)	16(3)	0(3)
C(18)	81(4)	135(5)	85(4)	12(3)	-3(3)	-10(3)
C(19)	54(3)	96(4)	99(4)	36(3)	8(3)	4(2)
C(20)	42(3)	71(3)	96(3)	34(3)	18(2)	3(2)
C(21)	58(3)	38(3)	102(4)	13(3)	26(3)	23(2)
C(22)	57(3)	55(3)	81(3)	14(3)	15(2)	-9(2)
C(23)	119(4)	51(3)	108(4)	2(3)	11(3)	-6(3)
C(24)	95(4)	76(4)	121(5)	-15(3)	15(3)	9(3)
C(25)	101(4)	94(4)	83(4)	20(3)	40(3)	36(3)
C(26)	88(4)	90(4)	102(4)	16(3)	49(3)	-5(3)
C(27)	40(2)	44(2)	47(3)	13(2)	-4(2)	-10(2)

Table A.5, Cont'd. Anisotropic displacement parameters ($\text{\AA}^2 \times 10^3$) for $\text{Cy}_2\text{NC(S)SSC(S)NCy}_2$. The anisotropic displacement factor exponent takes the form: $-2\pi^2[h^2a^{*2}U^{11} + \dots + 2hka^*b^*U^{12}]$.

Atom	U^{11}	U^{22}	U^{33}	U^{23}	U^{13}	U^{12}
C(28)	47(2)	55(3)	61(3)	21(2)	-1(2)	5(2)
C(29)	82(3)	67(3)	69(3)	26(3)	3(3)	-6(3)
C(30)	56(3)	92(3)	79(4)	32(3)	-18(3)	-12(2)
C(31)	40(3)	81(3)	96(4)	41(3)	1(3)	2(2)
C(32)	31(2)	67(3)	86(3)	28(2)	4(2)	2(2)
C(33)	38(2)	48(3)	56(3)	20(2)	-2(2)	-10(2)
C(34)	49(2)	62(3)	68(3)	26(2)	7(2)	9(2)
C(35)	71(3)	71(3)	93(4)	42(3)	-10(3)	4(2)
C(36)	94(4)	74(3)	74(3)	40(3)	-8(3)	-9(3)
C(37)	89(3)	81(3)	67(3)	35(3)	24(2)	-4(3)
C(38)	57(3)	62(3)	79(3)	31(2)	30(2)	5(2)

Table A.6. Hydrogen coordinates ($\times 10^4$) and isotropic displacement parameters ($\text{\AA}^2 \times 10^3$) for $\text{Cy}_2\text{NC}(\text{S})\text{SSC}(\text{S})\text{NCy}_2$.

H atom	x	y	z	U(eq)
H(1)	7260	1420	3750	60
H(2A)	9066	1553	3810	85
H(2B)	9057	311	3327	85
H(3A)	9489	580	4656	110
H(3B)	8450	1173	4829	110
H(4A)	8211	-575	4798	120
H(4B)	8547	-1033	3963	120
H(5A)	6673	26	4307	114
H(5B)	6727	-1201	3807	114
H(6A)	7258	-760	2784	78
H(6B)	6244	-136	2998	78
H(7)	8314	-12	2171	56
H(8A)	8812	1820	1791	77
H(8B)	9465	1494	2458	77
H(9A)	10218	838	1277	93
H(9B)	9901	-116	1546	93
H(10A)	9337	-599	214	98
H(10B)	8722	458	347	98
H(11A)	8182	-1288	812	86
H(11B)	7521	-960	151	86
H(12A)	7084	623	1058	71
H(12B)	6785	-343	1321	71
H(15)	2440	4753	2102	85
H(16A)	3203	3137	966	102
H(16B)	3492	4378	1219	102
H(17A)	2239	3661	65	101
H(17B)	1910	4703	694	101
H(18A)	462	3572	296	131
H(18B)	1100	2576	324	131
H(19A)	207	2961	1308	99
H(19B)	502	4203	1571	99
H(20A)	1809	2622	1821	81
H(20B)	1471	3642	2465	81
H(21)	4168	4976	3637	81
H(22A)	4885	5731	2895	80
H(22B)	3803	6142	2636	80
H(23A)	5029	6916	4111	120
H(23B)	4636	7589	3582	120
H(24A)	3031	7658	3910	132
H(24B)	3803	7921	4696	132

Table A.6, Cont'd. Hydrogen coordinates ($\times 10^4$) and isotropic displacement parameters ($\text{\AA}^2 \times 10^3$) for $\text{Cy}_2\text{NC(S)SSC(S)NCy}_2$.

H atom	x	y	z	U(eq)
H(25A)	3471	6278	4761	111
H(25B)	2374	6719	4575	111
H(26A)	2487	4917	3802	113
H(26B)	2206	5658	3303	113
H(27)	-2479	4957	2180	55
H(28A)	-1715	5696	1089	66
H(28B)	-1283	4717	1316	66
H(29A)	-2866	3732	798	88
H(29B)	-2493	4122	155	88
H(30A)	-4298	4406	237	94
H(30B)	-3655	5495	386	94
H(31A)	-4755	5786	1343	85
H(31B)	-4291	4826	1581	85
H(32A)	-3515	6454	2504	74
H(32B)	-3144	6804	1839	74
H(33)	-705	6268	3731	57
H(34A)	-1114	4146	2651	71
H(34B)	-25	4804	2857	71
H(35A)	183	4791	4123	92
H(35B)	-63	3590	3554	92
H(36A)	-1799	3644	3776	94
H(36B)	-1073	4001	4590	94
H(37A)	-1355	5805	4790	91
H(37B)	-2448	5164	4616	91
H(38A)	-2686	5133	3320	74
H(38B)	-2467	6342	3883	74
H(41A)	2305	9961	3716	58
H(42A)	1231	10666	3016	54
H(42B)	2157	11053	2684	54
H(43A)	1734	12548	3634	101
H(43B)	1697	11928	4221	101
H(44A)	3103	12968	4649	90
H(44B)	3432	12658	3810	90
H(45A)	4555	11450	4523	77
H(45B)	3505	10958	4660	77
H(46A)	4137	9907	3628	82
H(46B)	4008	10830	3268	82
H(41B)	3281	10204	2725	52
H(42C)	1817	11033	2421	107
H(42D)	1186	10728	2998	107

Table A.6, Cont'd. Hydrogen coordinates ($\times 10^4$) and isotropic displacement parameters ($\text{\AA}^2 \times 10^3$) for $\text{Cy}_2\text{NC(S)SSC(S)NCy}_2$.

H atom	x	y	z	U(eq)
H(43C)	1649	12409	3658	99
H(43D)	2708	12354	3329	99
H(44C)	3011	12764	4715	128
H(44D)	2431	11666	4616	128
H(45C)	3952	11760	4878	80
H(45D)	4047	11949	4089	80
H(46C)	3948	9702	3716	73
H(46D)	2867	9755	4039	73
H(47A)	3303	9812	2154	75
H(48A)	1936	9226	1147	74
H(48B)	2182	8007	982	74
H(49A)	2977	8543	9	92
H(49B)	3545	9582	660	92
H(50A)	4656	8432	288	99
H(50B)	3968	7522	392	99
H(51A)	5315	8017	1451	73
H(51B)	5140	9256	1641	73
H(52A)	4524	8726	2436	62
H(52B)	3939	7727	1780	62
H(47B)	2633	7925	1410	57
H(48C)	2001	9327	1136	81
H(48D)	3053	10020	1528	81
H(49C)	2937	9495	322	114
H(49D)	2743	8284	257	114
H(50C)	4740	8548	240	113
H(50D)	4846	9543	1030	113
H(51C)	5374	8085	1285	90
H(51D)	4345	7422	809	90
H(52C)	4044	7717	2223	88
H(52D)	4433	8964	2517	88

Table A.7. Crystal Data and Structure Refinement for $\text{Cy}_2\text{NC}(\text{S})\text{SSC}(\text{S})\text{NCy}_2$, Monoclinic Polymorph

Identification code	JPD1425_0m_a	
Empirical formula	$\text{C}_{26}\text{H}_{44}\text{N}_2\text{S}_4$	
Formula weight	512.87	
Temperature	150(2) K	
Wavelength	1.54178 Å	
Crystal system	monoclinic	
Space group	$P2_1/m$	
Unit cell dimensions	$a = 10.3672(3)$ Å	$\alpha = 90^\circ$
	$b = 13.2293(3)$ Å	$\beta = 109.5180(10)^\circ$
	$c = 10.6033(2)$ Å	$\gamma = 90^\circ$
Volume	$1370.68(6)$ Å ³	
Z	2	
Density (calculated)	1.243 g/cm ³	
Absorption coefficient	3.296 mm ⁻¹	
F(000)	556	
Crystal size	0.290 x 0.103 x 0.093 mm ³	
θ range for data collection	4.53 to 72.28°	
Index ranges	$-11 \leq h \leq 12, -16 \leq k \leq 16, -13 \leq l \leq 13$	
Reflections collected	27733	
Independent reflections	2745 [R(int) = 0.0323]	
Completeness to $\theta = 72.28^\circ$	97.1%	
Absorption correction	Semi-empirical from equivalents	
Max. and min. transmission	0.75 and 0.61	
Refinement method	Full-matrix least-squares on F^2	
Data / restraints / parameters	2745 / 483 / 282	
Goodness-of-fit on F^2	1.097	
Final R indices [$I > 2\sigma(I)$]	R1 = 0.0347, wR2 = 0.0946	
R indices (all data)	R1 = 0.0356, wR2 = 0.0954	
Extinction coefficient	n/a	
Largest diff. peak and hole	0.217 and -0.189 e·Å ⁻³	

Table A.8. Atomic coordinates ($\times 10^4$) and equivalent isotropic displacement parameters ($\text{\AA}^2 \times 10^3$) for monoclinic $\text{C}_{12}\text{H}_{10}\text{N}_2\text{S}_2$. $U(\text{eq})$ is defined as one third of the trace of the orthogonalized U^{ij} tensor.

Atom	x	y	z	$U(\text{eq})$
S(1)	4972(1)	2478(3)	1415(1)	49(1)
S(2)	7530(1)	2735(1)	3236(1)	53(1)
S(3)	8865(1)	3312(1)	4994(1)	47(1)
S(4)	9139(1)	1057(1)	5371(1)	49(1)
C(10)	9720(2)	2190(2)	5919(2)	41(1)
C(5)	5754(2)	2614(12)	3069(2)	35(2)
C(2)	3141(7)	1428(6)	3163(13)	59(2)
C(3)	1639(7)	1345(5)	3047(9)	81(2)
C(4)	813(3)	2231(4)	2309(4)	82(3)
C(2A)	2898(8)	3338(7)	3042(13)	60(2)
C(3A)	1395(8)	3231(6)	2961(10)	80(2)
C(7)	5711(7)	3534(7)	6086(7)	51(1)
C(8)	6683(5)	3659(4)	7527(5)	63(1)
C(9)	6681(4)	2731(4)	8353(3)	74(2)
C(7A)	6075(8)	1642(7)	6281(8)	62(2)
C(8A)	7022(6)	1788(5)	7709(5)	73(1)
N(1)	5227(1)	2500	4040(1)	40(1)
C(1)	3717(2)	2500	3783(2)	53(1)
C(6)	6083(2)	2500	5468(2)	52(1)
N(2)	10792(2)	2500	7023(2)	45(1)
C(11A)	11278(5)	3483(4)	7419(5)	50(1)
C(12A)	11190(6)	3739(5)	8798(7)	51(1)
C(13A)	11664(7)	4829(6)	9151(8)	67(2)
C(14A)	13102(5)	4991(4)	9147(4)	53(1)
C(15A)	13157(7)	4734(5)	7763(5)	63(2)
C(16A)	12711(6)	3646(5)	7372(6)	57(1)
C(11B)	11612(5)	3375(3)	7900(5)	43(1)
C(12B)	10852(6)	3991(4)	8642(6)	46(1)
C(13B)	11807(8)	4717(6)	9624(6)	63(2)
C(14B)	12619(6)	5350(4)	8995(6)	75(1)
C(15B)	13402(5)	4732(5)	8283(7)	63(1)
C(16B)	12423(5)	4032(4)	7260(5)	51(1)

Table A.9. Bond lengths (Å) for monoclinic $\text{Cy}_2\text{NC(S)SSC(S)NCy}_2$. Symmetry transformations used to generate equivalent atoms: #1 $x, -y + \frac{1}{2}, z$.

S(1)-C(5)	1.678(3)	C(6)-H(1AA)	0.94(3)
S(2)-C(5)	1.797(3)	N(2)-C(11A)#1	1.407(5)
S(2)-S(3)	2.0613(10)	N(2)-C(11A)	1.407(5)
S(3)-C(10)	1.835(2)	N(2)-C(11B)	1.549(5)
S(4)-C(10)	1.647(2)	N(2)-C(11B)#1	1.549(5)
C(10)-N(2)	1.380(3)	C(11A)-C(16A)	1.519(7)
C(5)-N(1)	1.326(3)	C(11A)-C(12A)	1.532(8)
C(2)-C(3)	1.525(9)	C(11A)-H(11A)	1.0000
C(2)-C(1)	1.593(8)	C(12A)-C(13A)	1.529(9)
C(2)-H(2A)	0.9900	C(12A)-H(12A)	0.9900
C(2)-H(2B)	0.9900	C(12A)-H(12B)	0.9900
C(3)-C(4)	1.507(7)	C(13A)-C(14A)	1.508(8)
C(3)-H(3A)	0.9900	C(13A)-H(13A)	0.9900
C(3)-H(3B)	0.9900	C(13A)-H(13B)	0.9900
C(4)-C(3A)	1.521(7)	C(14A)-C(15A)	1.526(7)
C(4)-H(4A)	0.9900	C(14A)-H(14A)	0.9900
C(4)-H(4B)	0.9900	C(14A)-H(14B)	0.9900
C(2A)-C(1)	1.456(9)	C(15A)-C(16A)	1.526(8)
C(2A)-C(3A)	1.538(9)	C(15A)-H(15A)	0.9900
C(2A)-H(2AA)	0.9900	C(15A)-H(15B)	0.9900
C(2A)-H(2AB)	0.9900	C(16A)-H(16A)	0.9900
C(3A)-H(3AA)	0.9900	C(16A)-H(16B)	0.9900
C(3A)-H(3AB)	0.9900	C(11B)-C(16B)	1.518(6)
C(7)-C(8)	1.533(7)	C(11B)-C(12B)	1.522(6)
C(7)-C(6)	1.618(7)	C(11B)-H(11B)	1.0000
C(7)-H(7A)	0.9900	C(12B)-C(13B)	1.516(8)
C(7)-H(7B)	0.9900	C(12B)-H(12C)	0.9900
C(8)-C(9)	1.508(7)	C(12B)-H(12D)	0.9900
C(8)-H(8A)	0.9900	C(13B)-C(14B)	1.493(8)
C(8)-H(8B)	0.9900	C(13B)-H(13C)	0.9900
C(9)-C(8A)	1.519(7)	C(13B)-H(13D)	0.9900
C(9)-H(9A)	0.9900	C(14B)-C(15B)	1.518(7)
C(9)-H(9B)	0.9900	C(14B)-H(14C)	0.9900
C(7A)-C(6)	1.426(8)	C(14B)-H(14D)	0.9900
C(7A)-C(8A)	1.517(7)	C(15B)-C(16B)	1.526(7)
C(7A)-H(7AA)	0.9900	C(15B)-H(15C)	0.9900
C(7A)-H(7AB)	0.9900	C(15B)-H(15D)	0.9900
C(8A)-H(8AA)	0.9900	C(16B)-H(16C)	0.9900
C(8A)-H(8AB)	0.9900	C(16B)-H(16D)	0.9900
N(1)-C(6)	1.477(2)		
N(1)-C(1)	1.496(2)		
C(1)-H(1)	0.98(3)		

Table A.10. Bond angles (deg.) for monoclinic $\text{Cy}_2\text{NC(S)SSC(S)NCy}_2$. Symmetry transformations used to generate equivalent atoms: Symmetry transformations used to generate equivalent atoms: #1 $x, -y + \frac{1}{2}, z$.

C(5)-S(2)-S(3)	118.6(2)	C(6)-C(7)-H(7B)	109.8
C(10)-S(3)-S(2)	104.05(9)	H(7A)-C(7)-H(7B)	108.3
N(2)-C(10)-S(4)	131.74(16)	C(9)-C(8)-C(7)	111.3(5)
N(2)-C(10)-S(3)	108.75(14)	C(9)-C(8)-H(8A)	109.4
S(4)-C(10)-S(3)	119.52(14)	C(7)-C(8)-H(8A)	109.4
N(1)-C(5)-S(1)	128.2(3)	C(9)-C(8)-H(8B)	109.4
N(1)-C(5)-S(2)	127.47(16)	C(7)-C(8)-H(8B)	109.4
S(1)-C(5)-S(2)	103.51(12)	H(8A)-C(8)-H(8B)	108.0
C(3)-C(2)-C(1)	109.3(7)	C(8)-C(9)-C(8A)	111.2(3)
C(3)-C(2)-H(2A)	109.8	C(8)-C(9)-H(9A)	109.4
C(1)-C(2)-H(2A)	109.8	C(8A)-C(9)-H(9A)	109.4
C(3)-C(2)-H(2B)	109.8	C(8)-C(9)-H(9B)	109.4
C(1)-C(2)-H(2B)	109.8	C(8A)-C(9)-H(9B)	109.4
H(2A)-C(2)-H(2B)	108.3	H(9A)-C(9)-H(9B)	108.0
C(4)-C(3)-C(2)	111.9(6)	C(6)-C(7A)-C(8A)	111.7(5)
C(4)-C(3)-H(3A)	109.2	C(6)-C(7A)-H(7AA)	109.3
C(2)-C(3)-H(3A)	109.2	C(8A)-C(7A)-H(7AA)	109.3
C(4)-C(3)-H(3B)	109.2	C(6)-C(7A)-H(7AB)	109.3
C(2)-C(3)-H(3B)	109.2	C(8A)-C(7A)-H(7AB)	109.3
H(3A)-C(3)-H(3B)	107.9	H(7AA)-C(7A)-H(7AB)	107.9
C(3)-C(4)-C(3A)	111.7(3)	C(7A)-C(8A)-C(9)	112.5(6)
C(3)-C(4)-H(4A)	109.3	C(7A)-C(8A)-H(8AA)	109.1
C(3A)-C(4)-H(4A)	109.3	C(9)-C(8A)-H(8AA)	109.1
C(3)-C(4)-H(4B)	109.3	C(7A)-C(8A)-H(8AB)	109.1
C(3A)-C(4)-H(4B)	109.3	C(9)-C(8A)-H(8AB)	109.1
H(4A)-C(4)-H(4B)	107.9	H(8AA)-C(8A)-H(8AB)	107.8
C(1)-C(2A)-C(3A)	111.0(7)	C(5)-N(1)-C(6)	122.26(16)
C(1)-C(2A)-H(2AA)	109.4	C(5)-N(1)-C(1)	122.42(17)
C(3A)-C(2A)-H(2AA)	109.4	C(6)-N(1)-C(1)	114.85(15)
C(1)-C(2A)-H(2AB)	109.4	C(2A)-C(1)-N(1)	119.0(4)
C(3A)-C(2A)-H(2AB)	109.4	C(2A)-C(1)-C(2)	112.6(3)
H(2AA)-C(2A)-H(2AB)	108.0	N(1)-C(1)-C(2)	107.5(3)
C(4)-C(3A)-C(2A)	110.3(6)	C(2A)-C(1)-H(1)	107.6(12)
C(4)-C(3A)-H(3AA)	109.6	N(1)-C(1)-H(1)	103.9(18)
C(2A)-C(3A)-H(3AA)	109.6	C(2)-C(1)-H(1)	105.1(8)
C(4)-C(3A)-H(3AB)	109.6	C(7A)-C(6)-N(1)	119.8(3)
C(2A)-C(3A)-H(3AB)	109.6	C(7A)-C(6)-C(7)	112.2(2)
H(3AA)-C(3A)-H(3AB)	108.1	N(1)-C(6)-C(7)	105.8(2)
C(8)-C(7)-C(6)	109.2(4)	C(7A)-C(6)-H(1AA)	103.3(11)
C(8)-C(7)-H(7A)	109.8	N(1)-C(6)-H(1AA)	102.7(17)
C(6)-C(7)-H(7A)	109.8	C(7)-C(6)-H(1AA)	112.9(8)
C(8)-C(7)-H(7B)	109.8	C(10)-N(2)-C(11A)#1	94.9(2)

Table A.10, Cont'd. Bond angles (deg.) for monoclinic $\text{Cy}_2\text{NC}(\text{S})\text{SSC}(\text{S})\text{NCy}_2$. Symmetry transformations used to generate equivalent atoms: #1 $x, -y + \frac{1}{2}, z$.

C(10)-N(2)-C(11A)	129.4(2)	C(16B)-C(11B)-C(12B)	112.6(4)
C(11A)#1-N(2)-C(11A)	135.1(4)	C(16B)-C(11B)-N(2)	115.7(3)
C(10)-N(2)-C(11B)#1	114.3(2)	C(12B)-C(11B)-N(2)	115.8(4)
C(11A)#1-N(2)-C(11B)#1	19.97(17)	C(16B)-C(11B)-H(11B)	103.5
C(11A)-N(2)-C(11B)#1	116.2(4)	C(12B)-C(11B)-H(11B)	103.5
C(11B)-N(2)-C(11B)#1	96.7(4)	N(2)-C(11B)-H(11B)	103.5
N(2)-C(11A)-C(16A)	112.2(4)	C(13B)-C(12B)-C(11B)	111.3(5)
N(2)-C(11A)-C(12A)	111.1(4)	C(13B)-C(12B)-H(12C)	109.4
C(16A)-C(11A)-C(12A)	111.7(5)	C(11B)-C(12B)-H(12C)	109.4
N(2)-C(11A)-H(11A)	107.1	C(13B)-C(12B)-H(12D)	109.4
C(16A)-C(11A)-H(11A)	107.1	C(11B)-C(12B)-H(12D)	109.4
C(12A)-C(11A)-H(11A)	107.1	H(12C)-C(12B)-H(12D)	108.0
C(13A)-C(12A)-C(11A)	109.1(6)	C(14B)-C(13B)-C(12B)	112.6(5)
C(13A)-C(12A)-H(12A)	109.9	C(14B)-C(13B)-H(13C)	109.1
C(11A)-C(12A)-H(12A)	109.9	C(12B)-C(13B)-H(13C)	109.1
C(13A)-C(12A)-H(12B)	109.9	C(14B)-C(13B)-H(13D)	109.1
C(11A)-C(12A)-H(12B)	109.9	C(12B)-C(13B)-H(13D)	109.1
H(12A)-C(12A)-H(12B)	108.3	H(13C)-C(13B)-H(13D)	107.8
C(14A)-C(13A)-C(12A)	111.7(6)	C(13B)-C(14B)-C(15B)	113.3(6)
C(14A)-C(13A)-H(13A)	109.3	C(13B)-C(14B)-H(14C)	108.9
C(12A)-C(13A)-H(13A)	109.3	C(15B)-C(14B)-H(14C)	108.9
C(14A)-C(13A)-H(13B)	109.3	C(13B)-C(14B)-H(14D)	108.9
C(12A)-C(13A)-H(13B)	109.3	C(15B)-C(14B)-H(14D)	108.9
H(13A)-C(13A)-H(13B)	107.9	H(14C)-C(14B)-H(14D)	107.7
C(13A)-C(14A)-C(15A)	109.0(5)	C(14B)-C(15B)-C(16B)	110.0(4)
C(13A)-C(14A)-H(14A)	109.9	C(14B)-C(15B)-H(15C)	109.7
C(15A)-C(14A)-H(14A)	109.9	C(16B)-C(15B)-H(15C)	109.7
C(13A)-C(14A)-H(14B)	109.9	C(14B)-C(15B)-H(15D)	109.7
C(15A)-C(14A)-H(14B)	109.9	C(16B)-C(15B)-H(15D)	109.7
H(14A)-C(14A)-H(14B)	108.3	H(15C)-C(15B)-H(15D)	108.2
C(14A)-C(15A)-C(16A)	111.5(5)	C(11B)-C(16B)-C(15B)	111.4(5)
C(14A)-C(15A)-H(15A)	109.3	C(11B)-C(16B)-H(16C)	109.3
C(16A)-C(15A)-H(15A)	109.3	C(15B)-C(16B)-H(16C)	109.3
C(14A)-C(15A)-H(15B)	109.3	C(11B)-C(16B)-H(16D)	109.3
C(16A)-C(15A)-H(15B)	109.3	C(15B)-C(16B)-H(16D)	109.3
H(15A)-C(15A)-H(15B)	108.0	H(16C)-C(16B)-H(16D)	108.0
C(11A)-C(16A)-C(15A)	109.7(5)		
C(11A)-C(16A)-H(16A)	109.7		
C(15A)-C(16A)-H(16A)	109.7		
C(11A)-C(16A)-H(16B)	109.7		
C(15A)-C(16A)-H(16B)	109.7		
H(16A)-C(16A)-H(16B)	108.2		

Table A.11. Anisotropic displacement parameters ($\text{\AA}^2 \times 10^3$) for monoclinic $\text{Cy}_2\text{NC}(\text{S})\text{SSC}(\text{S})\text{NCy}_2$. The anisotropic displacement factor exponent takes the form: $-2\pi^2[h^2a^*U^{11} + \dots + 2hka^*b^*U^{12}]$.

Atom	U^{11}	U^{22}	U^{33}	U^{23}	U^{13}	U^{12}
S(1)	34(1)	68(1)	39(1)	-15(1)	5(1)	1(1)
S(2)	30(1)	83(1)	40(1)	11(1)	6(1)	-8(1)
S(3)	32(1)	52(1)	48(1)	9(1)	1(1)	-7(1)
S(4)	42(1)	51(1)	46(1)	-6(1)	6(1)	-7(1)
C(10)	32(1)	50(2)	40(1)	2(1)	11(1)	-3(1)
C(5)	31(1)	27(6)	43(1)	2(1)	5(1)	-1(1)
C(2)	34(3)	75(4)	64(3)	-4(3)	11(3)	-21(3)
C(3)	44(3)	126(5)	73(4)	-24(4)	19(3)	-35(3)
C(4)	31(1)	143(8)	69(2)	-33(3)	15(1)	-15(2)
C(2A)	37(3)	79(4)	59(3)	-5(3)	9(2)	2(2)
C(3A)	33(2)	129(6)	75(3)	-26(4)	16(2)	3(3)
C(7)	36(3)	74(3)	37(2)	-12(2)	6(2)	-3(2)
C(8)	45(2)	91(3)	52(2)	-15(2)	14(2)	-2(2)
C(9)	55(2)	120(7)	42(1)	0(2)	11(1)	7(2)
C(7A)	45(4)	80(4)	56(3)	10(2)	11(2)	13(3)
C(8A)	62(3)	105(4)	44(2)	18(3)	8(2)	16(3)
N(1)	29(1)	49(1)	40(1)	0	6(1)	0
C(1)	30(1)	79(1)	48(1)	0	10(1)	0
C(6)	31(1)	82(1)	40(1)	0	8(1)	0
N(2)	30(1)	61(1)	40(1)	0	4(1)	0
C(11A)	41(2)	53(2)	47(3)	7(2)	2(2)	0(2)
C(12A)	27(2)	55(3)	69(3)	-14(2)	12(2)	-3(2)
C(13A)	43(2)	64(3)	81(5)	-20(3)	4(3)	7(2)
C(14A)	39(2)	46(2)	62(2)	2(2)	1(2)	-3(1)
C(15A)	57(3)	68(2)	51(3)	10(2)	1(2)	-18(2)
C(16A)	51(3)	65(3)	57(2)	-6(2)	23(2)	-18(2)
C(11B)	37(2)	45(2)	47(2)	3(2)	12(2)	-1(1)
C(12B)	40(3)	52(3)	49(2)	-3(2)	17(2)	0(2)
C(13B)	59(3)	69(3)	60(3)	-20(2)	19(3)	-15(2)
C(14B)	61(3)	66(3)	100(3)	-24(2)	29(3)	-22(2)
C(15B)	38(2)	64(2)	80(4)	-2(3)	12(3)	-16(2)
C(16B)	37(2)	60(3)	58(2)	4(2)	20(1)	1(2)

Table A.12. Hydrogen coordinates ($\times 10^4$) and isotropic displacement parameters ($\text{\AA}^2 \times 10^3$) for monoclinic $\text{C}_{12}\text{H}_{16}\text{N}_2\text{O}_2\text{S}_2$.

H atom	x	y	z	U(eq)
H(2A)	3234	1356	2268	71
H(2B)	3674	882	3744	71
H(3A)	1254	713	2570	97
H(3B)	1569	1309	3955	97
H(4A)	-143	2163	2292	98
H(4B)	804	2227	1372	98
H(2AA)	2950	3355	2127	72
H(2AB)	3272	3982	3490	72
H(3AA)	1333	3263	3871	96
H(3AB)	853	3796	2431	96
H(7A)	5803	4118	5539	61
H(7B)	4752	3508	6075	61
H(8A)	7622	3784	7520	76
H(8B)	6399	4253	7939	76
H(9A)	5768	2652	8448	88
H(9B)	7362	2816	9259	88
H(7AA)	6365	1037	5896	74
H(7AB)	5132	1524	6281	74
H(8AA)	7977	1836	7714	87
H(8AB)	6959	1190	8246	87
H(1)	3640(30)	2500	4680(30)	80
H(1AA)	6980(30)	2500	5430(30)	78
H(11A)	10658	3961	6763	60
H(12A)	10236	3661	8784	61
H(12B)	11778	3273	9479	61
H(13A)	11035	5293	8497	80
H(13B)	11624	4994	10049	80
H(14A)	13745	4554	9829	63
H(14B)	13376	5704	9368	63
H(15A)	14103	4830	7759	76
H(15B)	12552	5201	7095	76
H(16A)	12721	3509	6457	68
H(16B)	13356	3174	7996	68
H(11B)	12336	3019	8634	52
H(12C)	10107	4377	7988	56
H(12D)	10434	3529	9130	56
H(13C)	11262	5166	9999	75
H(13D)	12442	4327	10372	75
H(14C)	13277	5764	9697	90
H(14D)	11993	5817	8344	90

Table A.12, Cont'd. Hydrogen coordinates ($\times 10^4$) and isotropic displacement parameters ($\text{\AA}^2 \times 10^3$) for monoclinic $\text{Cy}_2\text{NC}(\text{S})\text{SSC}(\text{S})\text{NCy}_2$.

H atom	x	y	z	U(eq)
H(15C)	14115	4326	8945	75
H(15D)	13859	5190	7826	75
H(16C)	11783	4442	6539	61
H(16D)	12952	3595	6852	61

Table A.13. Crystal Data and Structure Refinement for $\text{Cy}_2\text{NC}(\text{S})\text{S}_4\text{C}(\text{S})\text{NCy}_2$.

Identification code	jpd864_4a_a	
Empirical formula	$\text{C}_{26}\text{H}_{44}\text{N}_2\text{S}_6$	
Formula weight	576.99	
Temperature	150(2) K	
Wavelength	1.54178 Å	
Crystal system	monoclinic	
Space group	$C2/c$	
Unit cell dimensions	$a = 28.1464(15)$ Å	$\alpha = 90^\circ$
	$b = 9.2015(5)$ Å	$\beta = 105.848(2)^\circ$
	$c = 12.0265(6)$ Å	$\gamma = 90^\circ$
Volume	$2996.3(3)$ Å ³	
Z	4	
Density (calculated)	1.279 g/cm ³	
Absorption coefficient	4.343 mm ⁻¹	
F(000)	1240	
Crystal size	0.183 x 0.143 x 0.026 mm ³	
θ range for data collection	3.264 to 72.253°	
Index ranges	$-14 \leq h \leq 14$, $-10 \leq k \leq 10$, $16 \leq l \leq -33$	
Reflections collected	17752	
Independent reflections	2731 [R(int) = 0.0637]	
Completeness to $\theta = 68.000^\circ$	93.5 %	
Absorption correction	Semi-empirical from equivalents	
Max. and min. transmission	0.90 and 0.50	
Refinement method	Full-matrix least-squares on F^2	
Data / restraints / parameters	2731 / 0 / 242	
Goodness-of-fit on F^2	1.043	
Final R indices [I > 2 σ (I)]	R1 = 0.0575, wR2 = 0.1398	
R indices (all data)	R1 = 0.0767, wR2 = 0.1489	
Extinction coefficient	n/a	
Largest diff. peak and hole	0.394 and -0.515 e \cdot Å ⁻³	

Table A.14. Atomic coordinates ($\times 10^4$) and equivalent isotropic displacement parameters ($\text{\AA}^2 \times 10^3$) for $\text{C}_{13}\text{H}_2\text{N}_2\text{S}_4$. $U(\text{eq})$ is defined as one third of the trace of the orthogonalized U^{ij} tensor.

Atom	x	y	z	U(eq)
S(1)	4098(1)	10506(1)	3397(1)	38(1)
S(2)	4771(1)	7926(1)	4025(1)	32(1)
S(3)	5162(1)	9391(1)	3383(1)	37(1)
N(1)	3891(1)	8093(3)	4441(3)	29(1)
C(1)	4193(1)	8878(4)	3982(3)	28(1)
C(2)	3397(1)	8619(5)	4481(4)	36(1)
C(3)	3410(2)	9972(4)	5206(4)	36(1)
C(4)	2887(2)	10387(6)	5244(5)	59(1)
C(5)	2540(2)	10515(7)	4058(6)	73(2)
C(6)	2518(2)	9126(7)	3361(5)	61(1)
C(7)	3035(2)	8694(5)	3292(4)	45(1)
C(8)	4025(1)	6629(4)	4958(3)	33(1)
C(9)	4121(2)	6628(5)	6263(4)	45(1)
C(10)	4290(2)	5132(6)	6767(5)	52(1)
C(11)	3931(2)	3953(5)	6200(5)	55(1)
C(12)	3831(2)	3965(5)	4902(5)	59(1)
C(13)	3665(2)	5444(4)	4379(4)	45(1)

Table A.15. Bond lengths (Å) for $\text{Cy}_2\text{NC}(\text{S})\text{S}_4\text{C}(\text{S})\text{NCy}_2$. Symmetry transformations used to generate equivalent atoms: #1 $-x + 1, y, -z + 1/2$.

S(1)-C(1)	1.646(4)
S(2)-C(1)	1.836(4)
S(2)-S(3)	2.0216(13)
S(3)-S(3)#1	2.069(2)
N(1)-C(1)	1.345(5)
N(1)-C(2)	1.486(4)
N(1)-C(8)	1.488(5)
C(2)-C(7)	1.513(6)
C(2)-C(3)	1.514(6)
C(2)-H(2)	1.01(4)
C(3)-C(4)	1.535(6)
C(3)-H(3A)	0.99(6)
C(3)-H(3B)	1.00(5)
C(4)-C(5)	1.497(9)
C(4)-H(4A)	1.10(6)
C(4)-H(4B)	0.97(6)
C(5)-C(6)	1.520(9)
C(5)-H(5A)	1.01(5)
C(5)-H(5B)	1.12(8)
C(6)-C(7)	1.532(7)
C(6)-H(6A)	0.96(6)
C(6)-H(6B)	1.05(6)
C(7)-H(7A)	1.00(5)
C(7)-H(7B)	1.06(5)
C(8)-C(9)	1.519(6)
C(8)-C(13)	1.522(6)
C(8)-H(8)	1.01(4)
C(9)-C(10)	1.527(6)
C(9)-H(9A)	0.97(5)
C(9)-H(9B)	0.86(4)
C(10)-C(11)	1.513(7)
C(10)-H(10A)	1.09(8)
C(10)-H(10B)	0.84(5)
C(11)-C(12)	1.510(8)
C(11)-H(11B)	0.97(6)
C(11)-H(11A)	1.07(6)
C(12)-C(13)	1.519(6)
C(12)-H(12A)	0.93(6)
C(12)-H(12B)	0.92(5)
C(13)-H(13A)	1.05(5)
C(13)-H(13B)	0.95(5)

Table A.16. Bond angles (deg.) for $\text{Cy}_2\text{NC}(\text{S})\text{S}_4\text{C}(\text{S})\text{NCy}_2$. Symmetry transformations used to generate equivalent atoms: #1 $-x + 1, y, -z + 1/2$.

C(1)-S(2)-S(3)	103.96(13)	H(7A)-C(7)-H(7B)	121(4)
S(2)-S(3)-S(3)#1	105.02(6)	N(1)-C(8)-C(9)	112.7(3)
C(1)-N(1)-C(2)	122.8(3)	N(1)-C(8)-C(13)	113.3(3)
C(1)-N(1)-C(8)	122.7(3)	C(9)-C(8)-C(13)	112.3(4)
C(2)-N(1)-C(8)	114.5(3)	N(1)-C(8)-H(8)	108(2)
N(1)-C(1)-S(1)	128.1(3)	C(9)-C(8)-H(8)	104(2)
N(1)-C(1)-S(2)	112.8(3)	C(13)-C(8)-H(8)	105(2)
S(1)-C(1)-S(2)	119.1(2)	C(8)-C(9)-C(10)	111.0(4)
N(1)-C(2)-C(7)	112.2(3)	C(8)-C(9)-H(9A)	109(3)
N(1)-C(2)-C(3)	114.2(3)	C(10)-C(9)-H(9A)	108(3)
C(7)-C(2)-C(3)	114.3(4)	C(8)-C(9)-H(9B)	97(3)
N(1)-C(2)-H(2)	107(2)	C(10)-C(9)-H(9B)	113(3)
C(7)-C(2)-H(2)	104(2)	H(9A)-C(9)-H(9B)	118(4)
C(3)-C(2)-H(2)	104(3)	C(11)-C(10)-C(9)	111.7(4)
C(2)-C(3)-C(4)	110.4(4)	C(11)-C(10)-H(10A)	113(4)
C(2)-C(3)-H(3A)	111(3)	C(9)-C(10)-H(10A)	115(4)
C(4)-C(3)-H(3A)	109(3)	C(11)-C(10)-H(10B)	109(3)
C(2)-C(3)-H(3B)	112(3)	C(9)-C(10)-H(10B)	107(3)
C(4)-C(3)-H(3B)	108(3)	H(10A)-C(10)-H(10B)	100(5)
H(3A)-C(3)-H(3B)	105(4)	C(12)-C(11)-C(10)	112.0(4)
C(5)-C(4)-C(3)	111.9(4)	C(12)-C(11)-H(11B)	104(3)
C(5)-C(4)-H(4A)	104(3)	C(10)-C(11)-H(11B)	113(3)
C(3)-C(4)-H(4A)	109(3)	C(12)-C(11)-H(11A)	113(3)
C(5)-C(4)-H(4B)	105(3)	C(10)-C(11)-H(11A)	106(3)
C(3)-C(4)-H(4B)	106(3)	H(11B)-C(11)-H(11A)	109(4)
H(4A)-C(4)-H(4B)	119(5)	C(11)-C(12)-C(13)	112.6(4)
C(4)-C(5)-C(6)	112.1(4)	C(11)-C(12)-H(12A)	115(4)
C(4)-C(5)-H(5A)	106(3)	C(13)-C(12)-H(12A)	103(4)
C(6)-C(5)-H(5A)	108(3)	C(11)-C(12)-H(12B)	107(3)
C(4)-C(5)-H(5B)	115(4)	C(13)-C(12)-H(12B)	102(3)
C(6)-C(5)-H(5B)	103(4)	H(12A)-C(12)-H(12B)	118(5)
H(5A)-C(5)-H(5B)	114(5)	C(12)-C(13)-C(8)	111.2(4)
C(5)-C(6)-C(7)	110.6(4)	C(12)-C(13)-H(13A)	112(3)
C(5)-C(6)-H(6A)	107(4)	C(8)-C(13)-H(13A)	110(3)
C(7)-C(6)-H(6A)	112(3)	C(12)-C(13)-H(13B)	111(3)
C(5)-C(6)-H(6B)	115(3)	C(8)-C(13)-H(13B)	104(3)
C(7)-C(6)-H(6B)	108(3)	H(13A)-C(13)-H(13B)	108(4)
H(6A)-C(6)-H(6B)	104(4)		
C(2)-C(7)-C(6)	111.4(4)		
C(2)-C(7)-H(7A)	103(3)		
C(6)-C(7)-H(7A)	107(2)		
C(2)-C(7)-H(7B)	106(3)		
C(6)-C(7)-H(7B)	108(2)		

Table A.17. Anisotropic displacement parameters ($\text{\AA}^2 \times 10^3$) for $\text{Cy}_2\text{NC(S)S}_4\text{C(S)NCy}_2$. The anisotropic displacement factor exponent takes the form: $-2\pi^2[h^2a^*U^{11} + \dots + 2hka^*b^*U^{12}]$.

Atom	U^{11}	U^{22}	U^{33}	U^{23}	U^{13}	U^{12}
S(1)	46(1)	29(1)	41(1)	6(1)	16(1)	4(1)
S(2)	31(1)	32(1)	34(1)	0(1)	12(1)	2(1)
S(3)	34(1)	40(1)	38(1)	-6(1)	15(1)	-9(1)
N(1)	29(2)	23(2)	35(2)	-3(1)	12(1)	2(1)
C(1)	33(2)	21(2)	30(2)	-4(1)	8(1)	0(1)
C(2)	26(2)	39(2)	46(2)	-1(2)	12(2)	5(2)
C(3)	45(2)	26(2)	42(2)	5(2)	18(2)	7(2)
C(4)	62(3)	48(3)	77(4)	3(3)	35(3)	19(2)
C(5)	52(3)	78(4)	91(4)	18(3)	21(3)	35(3)
C(6)	34(2)	67(4)	72(4)	20(3)	-1(2)	1(2)
C(7)	43(2)	40(3)	44(2)	3(2)	0(2)	2(2)
C(8)	37(2)	22(2)	41(2)	2(2)	12(2)	0(2)
C(9)	47(3)	35(2)	46(3)	4(2)	3(2)	0(2)
C(10)	42(3)	50(3)	57(3)	18(2)	0(2)	0(2)
C(11)	57(3)	32(2)	72(3)	17(2)	8(2)	5(2)
C(12)	65(3)	25(2)	82(4)	-2(2)	13(3)	-1(2)
C(13)	64(3)	25(2)	43(3)	-3(2)	7(2)	1(2)

K,GTRDAXVNM

Table A.18. Hydrogen coordinates ($\times 10^4$) and isotropic displacement parameters ($\text{\AA}^2 \times 10^3$) for $\text{Cy}_2\text{NC}(\text{S})\text{S}_4\text{C}(\text{S})\text{NCy}_2$.

H atom	x	y	z	U(eq)
H(2)	3252(16)	7850(50)	4890(40)	43(12)
H(3A)	3620(20)	9830(60)	6010(50)	68(16)
H(3B)	3557(19)	10820(60)	4900(50)	62(15)
H(4A)	2730(20)	9510(70)	5660(50)	90(20)
H(4B)	2910(19)	11360(70)	5560(50)	70(17)
H(5A)	2201(19)	10670(50)	4180(40)	53(14)
H(5B)	2650(30)	11350(90)	3490(70)	130(30)
H(6A)	2370(20)	8390(70)	3730(50)	71(17)
H(6B)	2290(20)	9170(60)	2520(50)	76(18)
H(7A)	3013(15)	7660(50)	3030(40)	41(12)
H(7B)	3165(17)	9520(50)	2840(40)	48(13)
H(8)	4351(15)	6340(50)	4830(40)	37(11)
H(9A)	3820(20)	6870(60)	6450(50)	64(16)
H(9B)	4354(16)	7270(50)	6410(40)	35(11)
H(10A)	4400(30)	5080(80)	7710(70)	120(30)
H(10B)	4564(17)	4970(50)	6640(40)	39(13)
H(11B)	4060(20)	2990(60)	6420(50)	72(17)
H(11A)	3610(20)	4110(60)	6490(50)	70(16)
H(12A)	3570(20)	3360(60)	4510(50)	70(17)
H(12B)	4130(20)	3860(60)	4740(50)	60(16)
H(13A)	3310(20)	5710(60)	4430(50)	68(16)
H(13B)	3664(17)	5480(50)	3590(50)	50(13)

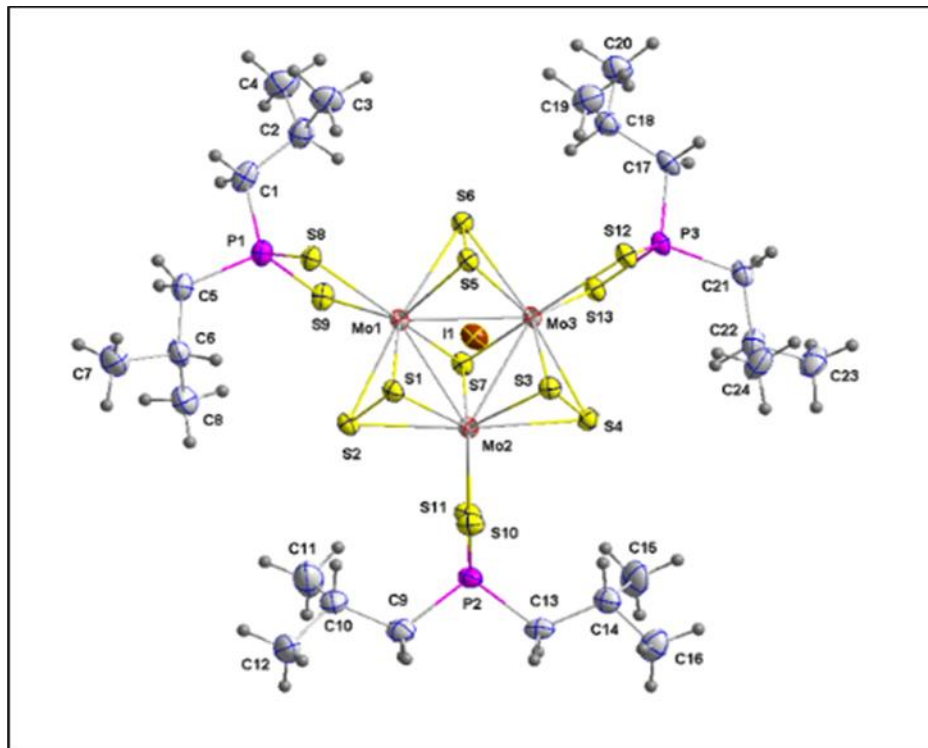


Table A.19. Crystal Data and Structure Refinement for $[\text{Mo}_3(\mu_2\text{-S}_2)_3(\mu_3\text{-S})(\text{S}_2\text{P}^i\text{Bu}_2)_3]$.

Identification code	jpd839_0m_a_sq	
Empirical formula	$\text{C}_{24}\text{H}_{54}\text{IMo}_3\text{P}_3\text{S}_{13}$	
Formula weight	1267.08	
Temperature	100(2) K	
Wavelength	0.71073 Å	
Crystal system	orthorhombic	
Space group	$Pna2_1$	
Unit cell dimensions	$a = 11.5814(18)$ Å	$\alpha = 90^\circ$
	$b = 23.552(4)$ Å	$\beta = 90^\circ$
	$c = 19.102(3)$ Å	$\gamma = 90^\circ$
Volume	$5210.2(14)$ Å ³	
Z	4	
Density (calculated)	1.615 g/cm ³	
Absorption coefficient	1.934 mm ⁻¹	
F(000)	2520	
Crystal size	0.273 x 0.212 x 0.084 mm ³	
θ range for data collection	1.373 to 28.831°	
Index ranges	$-15 \leq h \leq 15, -31 \leq k \leq 30, -25 \leq l \leq 25$	
Reflections collected	47648	
Independent reflections	13014 [R(int) = 0.0454]	
Completeness to $\theta = 28.500^\circ$	99.3 %	
Absorption correction	Semi-empirical from equivalents	
Max. and min. transmission	0.74 and 0.61	

Table A.19, Cont'd. Crystal Data and Structure Refinement for $[\text{Mo}_3(\mu_2\text{-S}_2)_3(\mu_3\text{-S})(\text{S}_2\text{P}^i\text{Bu}_2)_3]$.

Refinement method	Full-matrix least-squares on F^2
Data / restraints / parameters	13014 / 1 / 410
Goodness-of-fit on F^2	1.005
Final R indices [$I > 2\sigma(I)$]	R1 = 0.0356, wR2 = 0.0804
R indices (all data)	R1 = 0.0455, wR2 = 0.0839
Absolute structure parameter	0.483(18)
Extinction coefficient	n/a
Largest diff. peak and hole	1.332 and -0.566 e $\cdot\text{\AA}^{-3}$

Table A.20. Atomic coordinates ($\times 10^4$) and equivalent isotropic displacement parameters ($\text{\AA}^2 \times 10^3$) for $[\text{Mo}_3(\mu_2\text{-S}_2)_3(\mu_3\text{-S})(\text{S}_2\text{P}^i\text{Bu}_2)_3]$. $U(\text{eq})$ is defined as one third of the trace of the orthogonalized U^{ij} tensor.

Atom	x	y	z	U(eq)
I(1)	608(1)	3658(1)	5251(1)	28(1)
Mo(1)	7933(1)	4846(1)	4234(1)	17(1)
Mo(2)	7844(1)	5010(1)	5644(1)	18(1)
Mo(3)	6730(1)	4106(1)	5058(1)	17(1)
S(1)	9602(1)	4909(1)	4980(1)	20(1)
S(2)	8809(1)	5678(1)	4829(1)	22(1)
S(3)	8179(1)	4032(1)	5957(1)	20(1)
S(4)	6637(1)	4336(1)	6327(1)	22(1)
S(5)	8278(1)	3840(1)	4285(1)	20(1)
S(6)	6787(1)	4041(1)	3755(1)	21(1)
S(7)	6236(1)	5075(1)	4875(1)	20(1)
S(8)	9349(1)	4776(1)	3224(1)	21(1)
S(9)	7082(1)	5527(1)	3366(1)	24(1)
S(10)	9218(1)	5244(1)	6633(1)	24(1)
S(11)	6831(1)	5825(1)	6245(1)	25(1)
S(12)	6499(1)	3040(1)	5219(1)	22(1)
S(13)	4579(1)	4000(1)	5041(1)	22(1)
P(1)	8423(1)	5372(1)	2704(1)	23(1)
P(2)	8140(2)	5866(1)	6950(1)	24(1)
P(3)	4765(1)	3146(1)	5172(1)	21(1)
C(1)	7830(6)	5182(3)	1866(4)	30(2)
C(2)	7020(6)	4677(3)	1824(4)	34(2)
C(3)	7651(7)	4101(3)	1809(4)	39(2)
C(4)	6224(7)	4731(4)	1179(4)	42(2)
C(5)	9364(6)	5966(3)	2508(4)	28(2)
C(6)	9982(7)	6247(3)	3110(4)	33(2)
C(7)	11117(7)	6506(4)	2827(5)	46(2)
C(8)	9257(7)	6695(3)	3464(4)	42(2)
C(9)	8895(6)	6546(3)	6972(4)	33(2)
C(10)	9418(7)	6755(3)	6285(4)	36(2)
C(11)	8534(8)	7042(4)	5804(5)	56(2)
C(12)	10414(7)	7157(4)	6448(5)	44(2)
C(13)	7695(5)	5765(3)	7849(4)	27(1)
C(14)	7152(6)	5198(3)	8050(4)	31(2)
C(15)	5848(7)	5187(4)	7923(5)	52(2)
C(16)	7408(7)	5044(4)	8807(5)	41(2)
C(17)	4057(5)	2766(3)	4469(4)	24(1)
C(18)	4389(5)	2909(3)	3718(4)	28(2)
C(19)	5507(6)	2610(4)	3503(4)	41(2)

Table A.20, Cont'd. Atomic coordinates ($\times 10^4$) and equivalent isotropic displacement parameters ($\text{\AA}^2 \times 10^3$) for $[\text{Mo}_3(\mu_2\text{-S}_2)_3(\mu_3\text{-S})(\text{S}_2\text{P}^i\text{Bu}_2)_3]$. $U(\text{eq})$ is defined as one third of the trace of the orthogonalized U^{ij} tensor.

Atom	x	y	z	$U(\text{eq})$
C(20)	3418(6)	2743(3)	3225(4)	37(2)
C(21)	4007(6)	2895(3)	5940(4)	27(2)
C(22)	4248(6)	3186(3)	6639(4)	33(2)
C(23)	3238(7)	3099(4)	7126(4)	41(2)
C(24)	5375(7)	2983(4)	6980(4)	45(2)

Table A.21. Bond lengths (Å) for $[\text{Mo}_3(\mu_2\text{-S}_2)_3(\mu_3\text{-S})(\text{S}_2\text{P}^i\text{Bu}_2)_3]$. Symmetry transformations used to generate equivalent atoms:

Mo(1)-S(7)	2.3776(16)	C(2)-C(4)	1.545(10)
Mo(1)-S(5)	2.4041(16)	C(2)-H(2)	1.0000
Mo(1)-S(1)	2.4071(16)	C(3)-H(3A)	0.9800
Mo(1)-S(2)	2.4829(17)	C(3)-H(3B)	0.9800
Mo(1)-S(6)	2.4892(17)	C(3)-H(3C)	0.9800
Mo(1)-S(9)	2.5081(17)	C(4)-H(4A)	0.9800
Mo(1)-S(8)	2.5364(17)	C(4)-H(4B)	0.9800
Mo(1)-Mo(2)	2.7239(9)	C(4)-H(4C)	0.9800
Mo(1)-Mo(3)	2.7309(8)	C(5)-C(6)	1.508(11)
Mo(2)-S(7)	2.3765(16)	C(5)-H(5A)	0.9900
Mo(2)-S(1)	2.4106(16)	C(5)-H(5B)	0.9900
Mo(2)-S(3)	2.4107(16)	C(6)-C(8)	1.508(11)
Mo(2)-S(2)	2.4802(17)	C(6)-C(7)	1.547(11)
Mo(2)-S(4)	2.4862(16)	C(6)-H(6)	1.0000
Mo(2)-S(11)	2.5260(17)	C(7)-H(7A)	0.9800
Mo(2)-S(10)	2.5299(17)	C(7)-H(7B)	0.9800
Mo(2)-Mo(3)	2.7306(8)	C(7)-H(7C)	0.9800
Mo(3)-S(7)	2.3784(16)	C(8)-H(8A)	0.9800
Mo(3)-S(5)	2.4047(16)	C(8)-H(8B)	0.9800
Mo(3)-S(3)	2.4076(16)	C(8)-H(8C)	0.9800
Mo(3)-S(4)	2.4870(17)	C(9)-C(10)	1.527(10)
Mo(3)-S(6)	2.4947(17)	C(9)-H(9A)	0.9900
Mo(3)-S(13)	2.5038(15)	C(9)-H(9B)	0.9900
Mo(3)-S(12)	2.5428(16)	C(10)-C(12)	1.524(10)
S(1)-S(2)	2.053(2)	C(10)-C(11)	1.533(11)
S(3)-S(4)	2.049(2)	C(10)-H(10)	1.0000
S(5)-S(6)	2.058(2)	C(11)-H(11A)	0.9800
S(8)-P(1)	2.028(2)	C(11)-H(11B)	0.9800
S(9)-P(1)	2.037(2)	C(11)-H(11C)	0.9800
S(10)-P(2)	2.018(2)	C(12)-H(12A)	0.9800
S(11)-P(2)	2.030(2)	C(12)-H(12B)	0.9800
S(12)-P(3)	2.026(2)	C(12)-H(12C)	0.9800
S(13)-P(3)	2.037(2)	C(13)-C(14)	1.527(10)
P(1)-C(1)	1.799(7)	C(13)-H(13A)	0.9900
P(1)-C(5)	1.811(7)	C(13)-H(13B)	0.9900
P(2)-C(13)	1.808(7)	C(14)-C(16)	1.519(11)
P(2)-C(9)	1.826(7)	C(14)-C(15)	1.530(10)
P(3)-C(21)	1.809(7)	C(14)-H(14)	1.0000
P(3)-C(17)	1.810(7)	C(15)-H(15A)	0.9800
C(1)-C(2)	1.518(10)	C(15)-H(15B)	0.9800
C(1)-H(1A)	0.9900	C(15)-H(15C)	0.9800
C(1)-H(1B)	0.9900	C(16)-H(16A)	0.9800
C(2)-C(3)	1.540(11)	C(16)-H(16B)	0.9800

Table A.21, Cont'd. Bond lengths (Å) for $[\text{Mo}_3(\mu_2\text{-S}_2)_3(\mu_3\text{-S})(\text{S}_2\text{P}^i\text{Bu}_2)_3]$. Symmetry transformations used to generate equivalent atoms:

C(16)-H(16C)	0.9800
C(17)-C(18)	1.523(10)
C(17)-H(17A)	0.9900
C(17)-H(17B)	0.9900
C(18)-C(20)	1.518(10)
C(18)-C(19)	1.530(10)
C(18)-H(18)	1.0000
C(19)-H(19A)	0.9800
C(19)-H(19B)	0.9800
C(19)-H(19C)	0.9800
C(20)-H(20A)	0.9800
C(20)-H(20B)	0.9800
C(20)-H(20C)	0.9800
C(21)-C(22)	1.528(10)
C(21)-H(21A)	0.9900
C(21)-H(21B)	0.9900
C(22)-C(23)	1.508(10)
C(22)-C(24)	1.534(10)
C(22)-H(22)	1.0000
C(23)-H(23A)	0.9800
C(23)-H(23B)	0.9800
C(23)-H(23C)	0.9800
C(24)-H(24A)	0.9800
C(24)-H(24B)	0.9800
C(24)-H(24C)	0.9800

Table A.22. Bond angles (deg.) for $[\text{Mo}_3(\mu_2\text{-S}_2)_3(\mu_3\text{-S})(\text{S}_2\text{P}^i\text{Bu}_2)_3]$. Symmetry transformations used to generate equivalent atoms:

S(7)-Mo(1)-S(5)	109.85(6)	S(1)-Mo(2)-S(4)	133.46(6)
S(7)-Mo(1)-S(1)	110.15(6)	S(3)-Mo(2)-S(4)	49.45(5)
S(5)-Mo(1)-S(1)	84.43(5)	S(2)-Mo(2)-S(4)	171.26(6)
S(7)-Mo(1)-S(2)	85.57(5)	S(7)-Mo(2)-S(11)	82.42(6)
S(5)-Mo(1)-S(2)	133.74(6)	S(1)-Mo(2)-S(11)	134.97(6)
S(1)-Mo(1)-S(2)	49.61(5)	S(3)-Mo(2)-S(11)	133.48(6)
S(7)-Mo(1)-S(6)	85.48(5)	S(2)-Mo(2)-S(11)	90.71(6)
S(5)-Mo(1)-S(6)	49.69(5)	S(4)-Mo(2)-S(11)	89.19(6)
S(1)-Mo(1)-S(6)	133.88(6)	S(7)-Mo(2)-S(10)	160.08(6)
S(2)-Mo(1)-S(6)	171.02(5)	S(1)-Mo(2)-S(10)	83.30(6)
S(7)-Mo(1)-S(9)	82.56(6)	S(3)-Mo(2)-S(10)	85.48(6)
S(5)-Mo(1)-S(9)	136.26(6)	S(2)-Mo(2)-S(10)	92.74(6)
S(1)-Mo(1)-S(9)	131.90(6)	S(4)-Mo(2)-S(10)	95.77(6)
S(2)-Mo(1)-S(9)	87.59(6)	S(11)-Mo(2)-S(10)	77.75(6)
S(6)-Mo(1)-S(9)	91.99(6)	S(7)-Mo(2)-Mo(1)	55.06(4)
S(7)-Mo(1)-S(8)	160.19(6)	S(1)-Mo(2)-Mo(1)	55.51(4)
S(5)-Mo(1)-S(8)	81.91(6)	S(3)-Mo(2)-Mo(1)	95.95(4)
S(1)-Mo(1)-S(8)	86.29(6)	S(2)-Mo(2)-Mo(1)	56.76(4)
S(2)-Mo(1)-S(8)	97.78(6)	S(4)-Mo(2)-Mo(1)	116.72(4)
S(6)-Mo(1)-S(8)	90.90(6)	S(11)-Mo(2)-Mo(1)	125.09(5)
S(9)-Mo(1)-S(8)	78.10(5)	S(10)-Mo(2)-Mo(1)	138.22(4)
S(7)-Mo(1)-Mo(2)	55.03(4)	S(7)-Mo(2)-Mo(3)	54.98(4)
S(5)-Mo(1)-Mo(2)	96.07(4)	S(1)-Mo(2)-Mo(3)	96.09(4)
S(1)-Mo(1)-Mo(2)	55.63(4)	S(3)-Mo(2)-Mo(3)	55.43(4)
S(2)-Mo(1)-Mo(2)	56.67(4)	S(2)-Mo(2)-Mo(3)	116.76(5)
S(6)-Mo(1)-Mo(2)	116.84(4)	S(4)-Mo(2)-Mo(3)	56.71(4)
S(9)-Mo(1)-Mo(2)	123.21(5)	S(11)-Mo(2)-Mo(3)	124.03(4)
S(8)-Mo(1)-Mo(2)	141.78(4)	S(10)-Mo(2)-Mo(3)	140.61(5)
S(7)-Mo(1)-Mo(3)	54.97(4)	Mo(1)-Mo(2)-Mo(3)	60.09(2)
S(5)-Mo(1)-Mo(3)	55.41(4)	S(7)-Mo(3)-S(5)	109.80(6)
S(1)-Mo(1)-Mo(3)	96.16(4)	S(7)-Mo(3)-S(3)	109.95(6)
S(2)-Mo(1)-Mo(3)	116.65(4)	S(5)-Mo(3)-S(3)	84.25(6)
S(6)-Mo(1)-Mo(3)	56.87(4)	S(7)-Mo(3)-S(4)	85.62(6)
S(9)-Mo(1)-Mo(3)	126.05(4)	S(5)-Mo(3)-S(4)	133.43(5)
S(8)-Mo(1)-Mo(3)	136.58(4)	S(3)-Mo(3)-S(4)	49.48(5)
Mo(2)-Mo(1)-Mo(3)	60.08(2)	S(7)-Mo(3)-S(6)	85.34(6)
S(7)-Mo(2)-S(1)	110.06(6)	S(5)-Mo(3)-S(6)	49.62(5)
S(7)-Mo(2)-S(3)	109.90(6)	S(3)-Mo(3)-S(6)	133.58(5)
S(1)-Mo(2)-S(3)	84.26(6)	S(4)-Mo(3)-S(6)	170.88(6)
S(7)-Mo(2)-S(2)	85.65(6)	S(7)-Mo(3)-S(13)	81.63(5)
S(1)-Mo(2)-S(2)	49.60(5)	S(5)-Mo(3)-S(13)	135.06(6)
S(3)-Mo(2)-S(2)	133.59(6)	S(3)-Mo(3)-S(13)	134.06(6)
S(7)-Mo(2)-S(4)	85.67(6)	S(4)-Mo(3)-S(13)	89.48(6)

Table A.22, Cont'd. Bond angles (deg.) for $[\text{Mo}_3(\mu_2\text{-S}_2)_3(\mu_3\text{-S})(\text{S}_2\text{P}^i\text{Bu}_2)_3]$. Symmetry transformations used to generate equivalent atoms:

S(6)-Mo(3)-S(13)	90.40(5)	P(1)-S(8)-Mo(1)	89.17(7)
S(7)-Mo(3)-S(12)	159.97(5)	P(1)-S(9)-Mo(1)	89.76(7)
S(5)-Mo(3)-S(12)	84.05(5)	P(2)-S(10)-Mo(2)	89.59(8)
S(3)-Mo(3)-S(12)	85.18(5)	P(2)-S(11)-Mo(2)	89.44(7)
S(4)-Mo(3)-S(12)	95.28(6)	P(3)-S(12)-Mo(3)	88.69(7)
S(6)-Mo(3)-S(12)	93.62(6)	P(3)-S(13)-Mo(3)	89.53(7)
S(13)-Mo(3)-S(12)	78.37(5)	C(1)-P(1)-C(5)	103.7(3)
S(7)-Mo(3)-Mo(2)	54.92(4)	C(1)-P(1)-S(8)	117.8(3)
S(5)-Mo(3)-Mo(2)	95.88(4)	C(5)-P(1)-S(8)	108.5(2)
S(3)-Mo(3)-Mo(2)	55.53(4)	C(1)-P(1)-S(9)	107.8(2)
S(4)-Mo(3)-Mo(2)	56.68(4)	C(5)-P(1)-S(9)	116.7(3)
S(6)-Mo(3)-Mo(2)	116.41(4)	S(8)-P(1)-S(9)	102.89(10)
S(13)-Mo(3)-Mo(2)	123.58(4)	C(13)-P(2)-C(9)	103.3(3)
S(12)-Mo(3)-Mo(2)	140.35(4)	C(13)-P(2)-S(10)	111.5(2)
S(7)-Mo(3)-Mo(1)	54.94(4)	C(9)-P(2)-S(10)	110.4(2)
S(5)-Mo(3)-Mo(1)	55.38(4)	C(13)-P(2)-S(11)	114.3(2)
S(3)-Mo(3)-Mo(1)	95.84(4)	C(9)-P(2)-S(11)	114.5(3)
S(4)-Mo(3)-Mo(1)	116.44(4)	S(10)-P(2)-S(11)	103.22(10)
S(6)-Mo(3)-Mo(1)	56.68(4)	C(21)-P(3)-C(17)	102.7(3)
S(13)-Mo(3)-Mo(1)	124.31(4)	C(21)-P(3)-S(12)	113.9(2)
S(12)-Mo(3)-Mo(1)	138.91(4)	C(17)-P(3)-S(12)	114.9(2)
Mo(2)-Mo(3)-Mo(1)	59.83(2)	C(21)-P(3)-S(13)	111.8(2)
S(2)-S(1)-Mo(1)	67.12(6)	C(17)-P(3)-S(13)	110.4(2)
S(2)-S(1)-Mo(2)	66.96(6)	S(12)-P(3)-S(13)	103.41(9)
Mo(1)-S(1)-Mo(2)	68.86(4)	C(2)-C(1)-P(1)	118.6(5)
S(1)-S(2)-Mo(2)	63.43(6)	C(2)-C(1)-H(1A)	107.7
S(1)-S(2)-Mo(1)	63.27(6)	P(1)-C(1)-H(1A)	107.7
Mo(2)-S(2)-Mo(1)	66.57(4)	C(2)-C(1)-H(1B)	107.7
S(4)-S(3)-Mo(3)	67.28(6)	P(1)-C(1)-H(1B)	107.7
S(4)-S(3)-Mo(2)	67.19(6)	H(1A)-C(1)-H(1B)	107.1
Mo(3)-S(3)-Mo(2)	69.04(4)	C(1)-C(2)-C(3)	113.4(6)
S(3)-S(4)-Mo(2)	63.35(6)	C(1)-C(2)-C(4)	110.2(6)
S(3)-S(4)-Mo(3)	63.25(6)	C(3)-C(2)-C(4)	110.0(7)
Mo(2)-S(4)-Mo(3)	66.61(4)	C(1)-C(2)-H(2)	107.7
S(6)-S(5)-Mo(1)	67.31(6)	C(3)-C(2)-H(2)	107.7
S(6)-S(5)-Mo(3)	67.46(6)	C(4)-C(2)-H(2)	107.7
Mo(1)-S(5)-Mo(3)	69.21(4)	C(2)-C(3)-H(3A)	109.5
S(5)-S(6)-Mo(1)	63.00(6)	C(2)-C(3)-H(3B)	109.5
S(5)-S(6)-Mo(3)	62.91(6)	H(3A)-C(3)-H(3B)	109.5
Mo(1)-S(6)-Mo(3)	66.45(4)	C(2)-C(3)-H(3C)	109.5
Mo(2)-S(7)-Mo(1)	69.91(4)	H(3A)-C(3)-H(3C)	109.5
Mo(2)-S(7)-Mo(3)	70.10(4)	H(3B)-C(3)-H(3C)	109.5
Mo(1)-S(7)-Mo(3)	70.09(4)	C(2)-C(4)-H(4A)	109.5

Table A.22, Cont'd. Bond angles (deg.) for $[\text{Mo}_3(\mu_2\text{-S}_2)_3(\mu_3\text{-S})(\text{S}_2\text{P}^i\text{Bu}_2)_3]$. Symmetry transformations used to generate equivalent atoms:

C(2)-C(4)-H(4B)	109.5	H(11A)-C(11)-H(11B)	109.5
H(4A)-C(4)-H(4B)	109.5	C(10)-C(11)-H(11C)	109.5
C(2)-C(4)-H(4C)	109.5	H(11A)-C(11)-H(11C)	109.5
H(4A)-C(4)-H(4C)	109.5	H(11B)-C(11)-H(11C)	109.5
H(4B)-C(4)-H(4C)	109.5	C(10)-C(12)-H(12A)	109.5
C(6)-C(5)-P(1)	117.8(5)	C(10)-C(12)-H(12B)	109.5
C(6)-C(5)-H(5A)	107.9	H(12A)-C(12)-H(12B)	109.5
P(1)-C(5)-H(5A)	107.9	C(10)-C(12)-H(12C)	109.5
C(6)-C(5)-H(5B)	107.9	H(12A)-C(12)-H(12C)	109.5
P(1)-C(5)-H(5B)	107.9	H(12B)-C(12)-H(12C)	109.5
H(5A)-C(5)-H(5B)	107.2	C(14)-C(13)-P(2)	118.1(5)
C(8)-C(6)-C(5)	112.6(7)	C(14)-C(13)-H(13A)	107.8
C(8)-C(6)-C(7)	110.7(6)	P(2)-C(13)-H(13A)	107.8
C(5)-C(6)-C(7)	108.0(6)	C(14)-C(13)-H(13B)	107.8
C(8)-C(6)-H(6)	108.5	P(2)-C(13)-H(13B)	107.8
C(5)-C(6)-H(6)	108.5	H(13A)-C(13)-H(13B)	107.1
C(7)-C(6)-H(6)	108.5	C(16)-C(14)-C(13)	111.6(6)
C(6)-C(7)-H(7A)	109.5	C(16)-C(14)-C(15)	109.8(6)
C(6)-C(7)-H(7B)	109.5	C(13)-C(14)-C(15)	112.4(6)
H(7A)-C(7)-H(7B)	109.5	C(16)-C(14)-H(14)	107.6
C(6)-C(7)-H(7C)	109.5	C(13)-C(14)-H(14)	107.6
H(7A)-C(7)-H(7C)	109.5	C(15)-C(14)-H(14)	107.6
H(7B)-C(7)-H(7C)	109.5	C(14)-C(15)-H(15A)	109.5
C(6)-C(8)-H(8A)	109.5	C(14)-C(15)-H(15B)	109.5
C(6)-C(8)-H(8B)	109.5	H(15A)-C(15)-H(15B)	109.5
H(8A)-C(8)-H(8B)	109.5	C(14)-C(15)-H(15C)	109.5
C(6)-C(8)-H(8C)	109.5	H(15A)-C(15)-H(15C)	109.5
H(8A)-C(8)-H(8C)	109.5	H(15B)-C(15)-H(15C)	109.5
H(8B)-C(8)-H(8C)	109.5	C(14)-C(16)-H(16A)	109.5
C(10)-C(9)-P(2)	116.9(5)	C(14)-C(16)-H(16B)	109.5
C(10)-C(9)-H(9A)	108.1	H(16A)-C(16)-H(16B)	109.5
P(2)-C(9)-H(9A)	108.1	C(14)-C(16)-H(16C)	109.5
C(10)-C(9)-H(9B)	108.1	H(16A)-C(16)-H(16C)	109.5
P(2)-C(9)-H(9B)	108.1	H(16B)-C(16)-H(16C)	109.5
H(9A)-C(9)-H(9B)	107.3	C(18)-C(17)-P(3)	118.4(4)
C(12)-C(10)-C(9)	108.9(6)	C(18)-C(17)-H(17A)	107.7
C(12)-C(10)-C(11)	110.7(7)	P(3)-C(17)-H(17A)	107.7
C(9)-C(10)-C(11)	113.1(7)	C(18)-C(17)-H(17B)	107.7
C(12)-C(10)-H(10)	108.0	P(3)-C(17)-H(17B)	107.7
C(9)-C(10)-H(10)	108.0	H(17A)-C(17)-H(17B)	107.1
C(11)-C(10)-H(10)	108.0	C(20)-C(18)-C(17)	109.9(5)
C(10)-C(11)-H(11A)	109.5	C(20)-C(18)-C(19)	110.0(6)
C(10)-C(11)-H(11B)	109.5	C(17)-C(18)-C(19)	111.4(6)

Table A.22, Cont'd. Bond angles (deg.) for $[\text{Mo}_3(\mu_2\text{-S}_2)_3(\mu_3\text{-S})(\text{S}_2\text{P}^i\text{Bu}_2)_3]$. Symmetry transformations used to generate equivalent atoms:

C(20)-C(18)-H(18)	108.5
C(17)-C(18)-H(18)	108.5
C(19)-C(18)-H(18)	108.5
C(18)-C(19)-H(19A)	109.5
C(18)-C(19)-H(19B)	109.5
H(19A)-C(19)-H(19B)	109.5
C(18)-C(19)-H(19C)	109.5
H(19A)-C(19)-H(19C)	109.5
H(19B)-C(19)-H(19C)	109.5
C(18)-C(20)-H(20A)	109.5
C(18)-C(20)-H(20B)	109.5
H(20A)-C(20)-H(20B)	109.5
C(18)-C(20)-H(20C)	109.5
H(20A)-C(20)-H(20C)	109.5
H(20B)-C(20)-H(20C)	109.5
C(22)-C(21)-P(3)	118.2(5)
C(22)-C(21)-H(21A)	107.8
P(3)-C(21)-H(21A)	107.8
C(22)-C(21)-H(21B)	107.8
P(3)-C(21)-H(21B)	107.8
H(21A)-C(21)-H(21B)	107.1
C(23)-C(22)-C(21)	109.5(6)
C(23)-C(22)-C(24)	110.9(6)
C(21)-C(22)-C(24)	112.7(6)
C(23)-C(22)-H(22)	107.9
C(21)-C(22)-H(22)	107.9
C(24)-C(22)-H(22)	107.9
C(22)-C(23)-H(23A)	109.5
C(22)-C(23)-H(23B)	109.5
H(23A)-C(23)-H(23B)	109.5
C(22)-C(23)-H(23C)	109.5
H(23A)-C(23)-H(23C)	109.5
H(23B)-C(23)-H(23C)	109.5
C(22)-C(24)-H(24A)	109.5
C(22)-C(24)-H(24B)	109.5
H(24A)-C(24)-H(24B)	109.5
C(22)-C(24)-H(24C)	109.5
H(24A)-C(24)-H(24C)	109.5
H(24B)-C(24)-H(24C)	109.5

Table A.23. Anisotropic displacement parameters ($\text{\AA}^2 \times 10^3$) for $[\text{Mo}_3(\mu_2\text{-S}_2)_3(\mu_3\text{-S})(\text{S}_2\text{P}^i\text{Bu}_2)_3]$. The anisotropic displacement factor exponent takes the form: $-2\pi^2[h^2a^*{}^2U^{11} + \dots + 2hka^*b^*U^{12}]$

Atom	U^{11}	U^{22}	U^{33}	U^{23}	U^{13}	U^{12}
I(1)	19(1)	26(1)	40(1)	-1(1)	-2(1)	3(1)
Mo(1)	12(1)	18(1)	21(1)	2(1)	0(1)	0(1)
Mo(2)	12(1)	20(1)	22(1)	-1(1)	1(1)	1(1)
Mo(3)	12(1)	18(1)	21(1)	1(1)	0(1)	0(1)
S(1)	13(1)	23(1)	25(1)	-2(1)	1(1)	-1(1)
S(2)	19(1)	19(1)	28(1)	0(1)	1(1)	-1(1)
S(3)	15(1)	22(1)	23(1)	2(1)	-1(1)	1(1)
S(4)	17(1)	27(1)	21(1)	1(1)	2(1)	-1(1)
S(5)	14(1)	20(1)	24(1)	0(1)	1(1)	1(1)
S(6)	15(1)	26(1)	22(1)	0(1)	-1(1)	0(1)
S(7)	12(1)	21(1)	26(1)	1(1)	0(1)	1(1)
S(8)	15(1)	26(1)	23(1)	4(1)	3(1)	2(1)
S(9)	18(1)	27(1)	28(1)	6(1)	2(1)	5(1)
S(10)	14(1)	32(1)	27(1)	-6(1)	-2(1)	3(1)
S(11)	18(1)	25(1)	32(1)	-6(1)	1(1)	2(1)
S(12)	14(1)	19(1)	31(1)	2(1)	-1(1)	1(1)
S(13)	13(1)	21(1)	31(1)	2(1)	0(1)	-1(1)
P(1)	19(1)	26(1)	25(1)	5(1)	1(1)	2(1)
P(2)	20(1)	25(1)	28(1)	-6(1)	2(1)	-1(1)
P(3)	14(1)	20(1)	28(1)	2(1)	1(1)	-1(1)
C(1)	21(3)	42(4)	26(4)	9(3)	1(3)	8(3)
C(2)	31(4)	42(4)	31(4)	9(3)	-2(3)	-1(3)
C(3)	31(4)	45(5)	41(5)	-2(4)	-12(3)	-1(3)
C(4)	34(4)	53(5)	40(4)	0(4)	-10(4)	2(4)
C(5)	27(4)	28(4)	28(3)	7(3)	2(3)	2(3)
C(6)	34(4)	27(3)	37(4)	6(3)	-1(3)	-8(3)
C(7)	42(5)	47(5)	49(5)	-3(4)	2(4)	-12(4)
C(8)	53(5)	31(4)	43(5)	3(4)	3(4)	-6(4)
C(9)	29(4)	34(4)	36(4)	-9(3)	6(3)	0(3)
C(10)	44(5)	31(4)	32(4)	-5(3)	8(3)	-1(3)
C(11)	57(6)	55(6)	55(6)	13(5)	-5(4)	-13(5)
C(12)	42(5)	48(5)	42(5)	-2(4)	5(4)	-16(4)
C(13)	17(3)	33(4)	30(4)	-11(3)	0(3)	3(3)
C(14)	22(3)	35(4)	37(4)	-6(3)	3(3)	-1(3)
C(15)	29(4)	73(6)	53(6)	7(5)	5(4)	-16(4)
C(16)	31(4)	53(5)	40(5)	2(4)	5(4)	2(4)
C(17)	15(3)	20(3)	38(4)	1(3)	-5(3)	-3(2)
C(18)	23(3)	28(4)	32(4)	-2(3)	1(3)	-2(3)
C(19)	31(4)	53(5)	40(5)	-5(4)	0(3)	0(4)

Table A.23, Cont'd. Anisotropic displacement parameters ($\text{\AA}^2 \times 10^3$) for $[\text{Mo}_3(\mu_2\text{-S}_2)_3(\mu_3\text{-S})(\text{S}_2\text{P}^i\text{Bu}_2)_3]$. The anisotropic displacement factor exponent takes the form: $-2\pi^2[h^2a^{*2}U^{11} + \dots + 2hka^*b^*U^{12}]$

Atom	U^{11}	U^{22}	U^{33}	U^{23}	U^{13}	U^{12}
C(20)	32(4)	39(4)	39(4)	2(4)	-5(3)	-1(3)
C(21)	24(3)	20(3)	36(4)	1(3)	8(3)	-1(3)
C(22)	34(4)	31(4)	33(4)	7(3)	5(3)	-1(3)
C(23)	46(5)	42(5)	36(4)	0(4)	15(4)	9(4)
C(24)	35(4)	70(6)	29(4)	7(4)	3(3)	-6(4)

Table A.24. Hydrogen coordinates ($\times 10^4$) and isotropic displacement parameters ($\text{\AA}^2 \times 10^3$) for $[\text{Mo}_3(\mu_2\text{-S}_2)_3(\mu_3\text{-S})(\text{S}_2\text{P}^i\text{Bu}_2)_3]$.

H atom	x	y	z	U(eq)
H(1A)	7411	5517	1683	35
H(1B)	8483	5109	1544	35
H(2)	6519	4683	2251	41
H(3A)	7086	3793	1848	58
H(3B)	8192	4081	2203	58
H(3C)	8076	4064	1368	58
H(4A)	6686	4699	751	63
H(4B)	5836	5101	1188	63
H(4C)	5644	4428	1188	63
H(5A)	9954	5833	2171	33
H(5B)	8898	6259	2267	33
H(6)	10182	5949	3463	39
H(7A)	11662	6201	2716	69
H(7B)	11454	6756	3182	69
H(7C)	10953	6726	2402	69
H(8A)	9170	7021	3151	64
H(8B)	9635	6816	3898	64
H(8C)	8494	6538	3572	64
H(9A)	8347	6838	7140	40
H(9B)	9523	6519	7322	40
H(10)	9740	6419	6031	43
H(11A)	8919	7173	5377	84
H(11B)	8189	7367	6047	84
H(11C)	7927	6770	5681	84
H(12A)	10766	7286	6010	66
H(12B)	10993	6958	6730	66
H(12C)	10122	7485	6709	66
H(13A)	8381	5824	8150	32
H(13B)	7135	6069	7965	32
H(14)	7508	4898	7747	38
H(15A)	5691	5263	7428	78
H(15B)	5476	5477	8212	78
H(15C)	5543	4812	8048	78
H(16A)	8224	4942	8854	62
H(16B)	6926	4722	8947	62
H(16C)	7238	5371	9108	62
H(17A)	4199	2356	4541	29
H(17B)	3215	2828	4518	29
H(18)	4511	3328	3682	33
H(19A)	5694	2707	3017	62

Table A.24, Cont'd. Hydrogen coordinates ($\times 10^4$) and isotropic displacement parameters ($\text{\AA}^2 \times 10^3$) for $[\text{Mo}_3(\mu_2\text{-S}_2)_3(\mu_3\text{-S})(\text{S}_2\text{P}^i\text{Bu}_2)_3]$.

H atom	x	y	z	U(eq)
H(19B)	5406	2198	3545	62
H(19C)	6137	2733	3810	62
H(20A)	3627	2847	2744	55
H(20B)	2710	2942	3360	55
H(20C)	3291	2332	3252	55
H(21A)	3168	2926	5846	32
H(21B)	4184	2486	5996	32
H(22)	4322	3603	6549	39
H(23A)	2520	3196	6882	62
H(23B)	3327	3342	7538	62
H(23C)	3210	2700	7273	62
H(24A)	5328	2574	7069	67
H(24B)	5492	3185	7423	67
H(24C)	6024	3062	6665	67

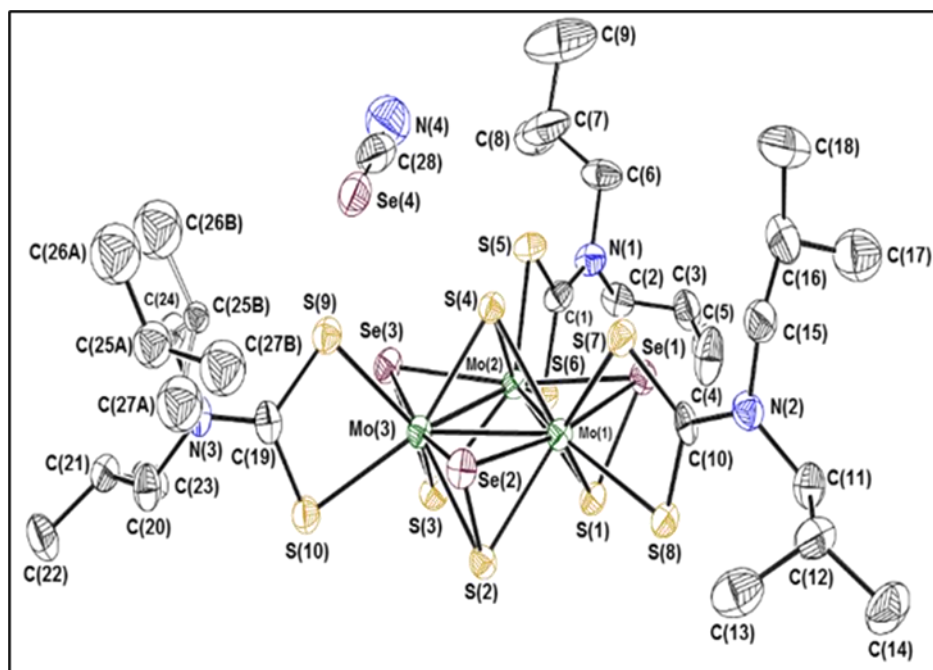


Table A.25. Crystal Data and Structure Refinement for $[\text{Mo}_3(\mu_3\text{-S})(\mu\text{-S})\text{Se}_3(\text{S}_2\text{CN}^t\text{Bu})_3][\text{SeCN}] \cdot \frac{1}{2}\text{ClCH}_2\text{CH}_2\text{Cl} \cdot \frac{1}{2}^t\text{BuOMe}$.

Identification code	JPD1002_0m_a	
Empirical formula	$\text{C}_{31.50}\text{H}_{62}\text{Cl}\text{Mo}_3\text{N}_4\text{O}_{0.50}\text{S}_{10}\text{Se}_4$	
Formula weight	1464.56	
Temperature	150(2) K	
Wavelength	0.71073 Å	
Crystal system	Tetragonal	
Space group	$I4_1/a$	
Unit cell dimensions	$a = 35.378(4)$ Å	$\alpha = 90^\circ$
	$b = 35.378(4)$ Å	$\beta = 90^\circ$
	$c = 18.903(2)$ Å	$\gamma = 90^\circ$
Volume	$23659(6)$ Å ³	
Z	16	
Density (calculated)	1.645 g/cm ³	
Absorption coefficient	3.512 mm ⁻¹	
F(000)	11552	
Crystal size	0.200 x 0.150 x 0.150 mm ³	
θ range for data collection	1.221 to 19.225°	
Index ranges	$-32 \leq h \leq 32, -32 \leq k \leq 32, -17 \leq l \leq 17$	
Reflections collected	48575	
Independent reflections	4894 [R(int) = 0.0791]	
Completeness to $\theta = 19.225^\circ$	99.2 %	
Absorption correction	Semi-empirical from equivalents	
Max. and min. transmission	0.621 and 0.403	

Table A.25, Cont'd. Crystal Data and Structure Refinement for $[\text{Mo}_3(\mu_3\text{-S})(\mu\text{-SSe})_3(\text{S}_2\text{CN}^t\text{Bu}_2)_3][\text{SeCN}] \cdot \frac{1}{2}\text{ClCH}_2\text{CH}_2\text{Cl} \cdot \frac{1}{2}^t\text{BuOMe}$.

Refinement method	Full-matrix least-squares on F^2
Data / restraints / parameters	4894 / 22 / 513
Goodness-of-fit on F^2	1.130
Final R indices [$I > 2\sigma(I)$]	R1 = 0.0455, wR2 = 0.1263
R indices (all data)	R1 = 0.0581, wR2 = 0.1378
Extinction coefficient	n/a
Largest diff. peak and hole	1.183 and -0.499 e $\cdot\text{\AA}^{-3}$

Table A.26. Atomic coordinates ($\times 10^4$) and equivalent isotropic displacement parameters ($\text{\AA}^2 \times 10^3$) for $[\text{Mo}_3(\mu_3\text{-S})(\mu\text{-SSe})_3(\text{S}_2\text{CN}^i\text{Bu}_2)_3][\text{SeCN}] \cdot \frac{1}{2}\text{ClCH}_2\text{CH}_2\text{Cl} \cdot \frac{1}{2}\text{BuOMe}$. $U(\text{eq})$ is defined as one third of the trace of the orthogonalized U^{ij} tensor.

Atom	x	y	z	U(eq)
Mo(1)	720(1)	5247(1)	5611(1)	24(1)
Mo(3)	1229(1)	4998(1)	4638(1)	24(1)
Mo(2)	952(1)	5715(1)	4542(1)	23(1)
Se(1)	498(1)	5950(1)	5545(1)	29(1)
Se(2)	1485(1)	5479(1)	3706(1)	29(1)
Se(3)	1065(1)	4604(1)	5759(1)	31(1)
Se(4)	1704(1)	4741(1)	6691(1)	54(1)
S(1)	300(1)	5544(1)	4762(1)	26(1)
S(2)	898(1)	5249(1)	3615(1)	27(1)
S(3)	632(1)	4692(1)	4888(2)	28(1)
S(4)	1342(1)	5486(1)	5467(1)	24(1)
S(5)	832(1)	5361(1)	6883(2)	34(1)
S(6)	140(1)	5066(1)	6316(2)	31(1)
S(7)	1329(1)	6297(1)	4668(2)	30(1)
S(8)	696(1)	6227(1)	3738(2)	29(1)
S(9)	1896(1)	4831(1)	4868(2)	31(1)
S(10)	1411(1)	4431(1)	3907(2)	33(1)
N(1)	183(3)	5373(3)	7621(5)	37(3)
N(2)	1062(2)	6883(3)	3961(5)	31(2)
N(3)	2138(3)	4237(2)	4126(5)	30(2)
N(4)	1374(4)	4651(4)	8080(8)	89(4)
C(1)	361(3)	5274(3)	7025(6)	32(3)
C(2)	-224(3)	5332(3)	7719(6)	37(3)
C(3)	-444(4)	5700(3)	7653(7)	49(4)
C(4)	-393(4)	5883(4)	6940(7)	66(4)
C(5)	-857(3)	5625(4)	7821(7)	57(4)
C(6)	403(3)	5557(4)	8196(6)	49(4)
C(7)	620(4)	5279(5)	8662(8)	75(5)
C(8)	372(4)	5036(4)	9097(7)	71(4)
C(9)	885(5)	5517(6)	9143(9)	127(8)
C(10)	1031(3)	6517(3)	4095(5)	26(3)
C(11)	791(3)	7085(3)	3486(6)	35(3)
C(12)	961(3)	7192(3)	2778(6)	42(3)
C(13)	1083(4)	6848(4)	2348(6)	56(4)
C(14)	675(4)	7431(4)	2376(7)	61(4)
C(15)	1372(3)	7104(3)	4269(6)	38(3)
C(16)	1324(4)	7203(3)	5051(7)	47(4)
C(17)	989(4)	7453(4)	5188(7)	68(4)
C(18)	1686(4)	7384(4)	5315(8)	80(5)
C(19)	1855(3)	4467(3)	4272(6)	29(3)
C(20)	2097(3)	3908(3)	3660(6)	37(3)
C(21)	2056(3)	3538(3)	4049(6)	38(3)
C(22)	2103(4)	3207(3)	3545(6)	48(4)

Table A.26, Cont'd. Atomic coordinates ($\times 10^4$) and equivalent isotropic displacement parameters ($\text{\AA}^2 \times 10^3$) for $[\text{Mo}_3(\mu_3\text{-S})(\mu\text{-SSe})_3(\text{S}_2\text{CN}^i\text{Bu}_2)_3][\text{SeCN}] \cdot \frac{1}{2}\text{ClCH}_2\text{CH}_2\text{Cl} \cdot \frac{1}{2}\text{BuOMe}$. $U(\text{eq})$ is defined as one third of the trace of the orthogonalized U^{ij} tensor.

Atom	x	y	z	U(eq)
C(23)	1680(4)	3509(3)	4434(6)	47(3)
C(24)	2520(3)	4306(3)	4396(6)	38(3)
C(25A)	2790(6)	4469(8)	3854(12)	46(8)
C(26A)	3179(7)	4506(9)	4177(15)	77(9)
C(27A)	2654(6)	4835(8)	3586(14)	65(8)
C(25B)	2717(9)	4666(11)	4080(20)	21(12)
C(27B)	2723(12)	4652(14)	3280(30)	62(16)
C(26B)	3114(14)	4697(16)	4370(30)	73(16)
C(28)	1498(4)	4691(4)	7489(10)	62(4)
Cl(1)	-1011(2)	6522(2)	10677(4)	75(2)
Cl(2)	-1137(2)	5735(2)	9659(5)	88(3)
C(29)	-1130(7)	6074(6)	10915(13)	46(7)
C(30)	-1397(7)	5846(7)	10391(12)	47(7)
O(1A)	-580(1)	5849(1)	9748(2)	117(16)
C(31A)	-909(1)	6007(1)	10098(1)	90(20)
C(32A)	-1160(1)	5665(1)	10300(2)	250(70)
C(33A)	-848(1)	6255(1)	10763(1)	270(80)
C(34A)	-1116(1)	6244(1)	9528(1)	130(30)
C(35)	-233(1)	6046(2)	9916(5)	159(18)
O(1B)	216(1)	6160(1)	9602(2)	89(13)
C(31B)	363(1)	6542(1)	9630(1)	53(14)
C(32B)	525(1)	6592(1)	10385(1)	50(14)
C(33B)	90(1)	6874(1)	9472(2)	160(40)
C(34B)	693(1)	6554(1)	9092(1)	140(30)

Table A.27. Bond lengths (Å) for $[\text{Mo}_3(\mu_3\text{-S})(\mu\text{-SSe})_3(\text{S}_2\text{CN}^i\text{Bu}_2)_3][\text{SeCN}]\cdot\frac{1}{2}\text{ClCH}_2\text{CH}_2\text{Cl}\cdot\frac{1}{2}\text{BuOMe}$. Symmetry transformations used to generate equivalent atoms:

Mo(1)-S(4)	2.373(3)	C(2)-H(2B)	0.9900
Mo(1)-S(3)	2.413(3)	C(3)-C(4)	1.506(17)
Mo(1)-S(1)	2.428(3)	C(3)-C(5)	1.519(17)
Mo(1)-S(5)	2.471(3)	C(3)-H(3)	1.0000
Mo(1)-S(6)	2.530(3)	C(4)-H(4A)	0.9800
Mo(1)-Se(3)	2.5959(15)	C(4)-H(4B)	0.9800
Mo(1)-Se(1)	2.6116(14)	C(4)-H(4C)	0.9800
Mo(1)-Mo(3)	2.7205(13)	C(5)-H(5A)	0.9800
Mo(1)-Mo(2)	2.7374(13)	C(5)-H(5B)	0.9800
Mo(3)-S(4)	2.365(3)	C(5)-H(5C)	0.9800
Mo(3)-S(3)	2.421(3)	C(6)-C(7)	1.528(19)
Mo(3)-S(2)	2.429(3)	C(6)-H(6A)	0.9900
Mo(3)-S(9)	2.469(3)	C(6)-H(6B)	0.9900
Mo(3)-S(10)	2.518(3)	C(7)-C(8)	1.477(19)
Mo(3)-Se(3)	2.6014(14)	C(7)-C(9)	1.55(2)
Mo(3)-Se(2)	2.6098(14)	C(7)-H(7)	1.0000
Mo(3)-Mo(2)	2.7256(13)	C(8)-H(8A)	0.9800
Mo(2)-S(4)	2.372(3)	C(8)-H(8B)	0.9800
Mo(2)-S(2)	2.414(3)	C(8)-H(8C)	0.9800
Mo(2)-S(1)	2.420(3)	C(9)-H(9A)	0.9800
Mo(2)-S(7)	2.467(3)	C(9)-H(9B)	0.9800
Mo(2)-S(8)	2.532(3)	C(9)-H(9C)	0.9800
Mo(2)-Se(2)	2.5991(14)	C(11)-C(12)	1.514(16)
Mo(2)-Se(1)	2.6201(14)	C(11)-H(11A)	0.9900
Se(1)-S(1)	2.178(3)	C(11)-H(11B)	0.9900
Se(2)-S(2)	2.237(3)	C(12)-C(14)	1.520(16)
Se(3)-S(3)	2.271(3)	C(12)-C(13)	1.527(17)
Se(4)-C(28)	1.684(19)	C(12)-H(12)	1.0000
S(5)-C(1)	1.713(12)	C(13)-H(13A)	0.9800
S(6)-C(1)	1.718(12)	C(13)-H(13B)	0.9800
S(7)-C(10)	1.702(11)	C(13)-H(13C)	0.9800
S(8)-C(10)	1.710(11)	C(14)-H(14A)	0.9800
S(9)-C(19)	1.718(12)	C(14)-H(14B)	0.9800
S(10)-C(19)	1.722(12)	C(14)-H(14C)	0.9800
N(1)-C(1)	1.338(13)	C(15)-C(16)	1.529(16)
N(1)-C(2)	1.459(14)	C(15)-H(15A)	0.9900
N(1)-C(6)	1.487(14)	C(15)-H(15B)	0.9900
N(2)-C(10)	1.322(12)	C(16)-C(17)	1.502(17)
N(2)-C(15)	1.469(14)	C(16)-C(18)	1.517(18)
N(2)-C(11)	1.496(14)	C(16)-H(16)	1.0000
N(3)-C(19)	1.318(13)	C(17)-H(17A)	0.9800
N(3)-C(20)	1.465(14)	C(17)-H(17B)	0.9800
N(3)-C(24)	1.466(13)	C(17)-H(17C)	0.9800
N(4)-C(28)	1.207(19)	C(18)-H(18A)	0.9800
C(2)-C(3)	1.522(16)	C(18)-H(18B)	0.9800
C(2)-H(2A)	0.9900	C(18)-H(18C)	0.9800

Table A.27, Cont'd. Bond lengths (Å) for $[\text{Mo}_3(\mu_3\text{-S})(\mu\text{-SSe})_3(\text{S}_2\text{CN}^t\text{Bu}_2)_3][\text{SeCN}]\cdot\frac{1}{2}\text{ClCH}_2\text{CH}_2\text{Cl}\cdot\frac{1}{2}\text{BuOMe}$. Symmetry transformations used to generate equivalent atoms:

C(20)-C(21)	1.507(15)	C(20)-H(20A)	0.9900
C(20)-H(20B)	0.9900	C(32A)-H(32B)	0.9800
C(21)-C(22)	1.520(15)	C(32A)-H(32C)	0.9800
C(21)-C(23)	1.521(16)	C(33A)-H(33A)	0.9800
C(21)-H(21)	1.0000	C(33A)-H(33B)	0.9800
C(22)-H(22A)	0.9800	C(33A)-H(33C)	0.9800
C(22)-H(22B)	0.9800	C(34A)-H(34A)	0.9800
C(22)-H(22C)	0.9800	C(34A)-H(34B)	0.9800
C(23)-H(23A)	0.9800	C(34A)-H(34C)	0.9800
C(23)-H(23B)	0.9800	C(35)-H(35A)	0.9800
C(23)-H(23C)	0.9800	C(35)-H(35B)	0.9800
C(24)-C(25A)	1.52(2)	C(35)-H(35C)	0.9800
C(24)-C(25B)	1.57(3)	O(1B)-C(31B)	1.44889(19)
C(24)-H(24A)	0.9900	C(31B)-C(33B)	1.5488(2)
C(24)-H(24B)	0.9900	C(31B)-C(32B)	1.54899(18)
C(25A)-C(27A)	1.47(4)	C(31B)-C(34B)	1.54899(17)
C(25A)-C(26A)	1.51(3)	C(32B)-H(32D)	0.9800
C(25A)-H(25A)	1.0000	C(32B)-H(32E)	0.9800
C(26A)-H(26A)	0.9800	C(32B)-H(32F)	0.9800
C(26A)-H(26B)	0.9800	C(33B)-H(33D)	0.9800
C(26A)-H(26C)	0.9800	C(33B)-H(33E)	0.9800
C(27A)-H(27A)	0.9800	C(33B)-H(33F)	0.9800
C(27A)-H(27B)	0.9800	C(34B)-H(34D)	0.9800
C(27A)-H(27C)	0.9800	C(34B)-H(34E)	0.9800
C(25B)-C(26B)	1.51(5)	C(34B)-H(34F)	0.9800
C(25B)-C(27B)	1.53(8)		
C(25B)-H(25B)	1.0000		
C(27B)-H(27D)	0.9800		
C(27B)-H(27E)	0.9800		
C(27B)-H(27F)	0.9800		
C(26B)-H(26D)	0.9800		
C(26B)-H(26E)	0.9800		
C(26B)-H(26F)	0.9800		
Cl(1)-C(29)	1.70(2)		
Cl(2)-C(30)	1.71(3)		
C(29)-C(30)	1.59(3)		
C(29)-H(29A)	0.9900		
C(29)-H(29B)	0.9900		
C(30)-H(30A)	0.9900		
C(30)-H(30B)	0.9900		
O(1A)-C(31A)	1.44889(17)		
O(1A)-C(35)	1.4500(2)		
C(31A)-C(32A)	1.54899(19)		
C(31A)-C(33A)	1.54882(18)		
C(31A)-C(34A)	1.54899(16)		
C(32A)-H(32A)	0.9800		

Table A.28. Bond angles (deg.) for $[\text{Mo}_3(\mu_3\text{-S})(\mu\text{-SSe})_3(\text{S}_2\text{CN}^i\text{Bu}_2)_3][\text{SeCN}]\cdot\frac{1}{2}\text{ClCH}_2\text{CH}_2\text{Cl}\cdot\frac{1}{2}\text{BuOMe}$. Symmetry transformations used to generate equivalent atoms:

S(4)-Mo(1)-S(3)	110.18(10)	S(4)-Mo(3)-Se(3)	83.60(7)
S(4)-Mo(1)-S(1)	109.78(10)	S(3)-Mo(3)-Se(3)	53.62(7)
S(3)-Mo(1)-S(1)	84.19(10)	S(2)-Mo(3)-Se(3)	137.42(8)
S(4)-Mo(1)-S(5)	84.53(10)	S(9)-Mo(3)-Se(3)	86.63(8)
S(3)-Mo(1)-S(5)	134.89(10)	S(10)-Mo(3)-Se(3)	94.43(8)
S(1)-Mo(1)-S(5)	132.09(10)	S(4)-Mo(3)-Se(2)	85.04(7)
S(4)-Mo(1)-S(6)	154.51(10)	S(3)-Mo(3)-Se(2)	136.51(8)
S(3)-Mo(1)-S(6)	89.34(10)	S(2)-Mo(3)-Se(2)	52.56(7)
S(1)-Mo(1)-S(6)	87.74(9)	S(9)-Mo(3)-Se(2)	86.79(8)
S(5)-Mo(1)-S(6)	69.99(9)	S(10)-Mo(3)-Se(2)	93.44(8)
S(4)-Mo(1)-Se(3)	83.57(7)	Se(3)-Mo(3)-Se(2)	167.40(5)
S(3)-Mo(1)-Se(3)	53.78(7)	S(4)-Mo(3)-Mo(1)	55.09(7)
S(1)-Mo(1)-Se(3)	137.64(8)	S(3)-Mo(3)-Mo(1)	55.60(7)
S(5)-Mo(1)-Se(3)	87.91(8)	S(2)-Mo(3)-Mo(1)	95.77(7)
S(6)-Mo(1)-Se(3)	95.96(8)	S(9)-Mo(3)-Mo(1)	126.21(8)
S(4)-Mo(1)-Se(1)	86.26(7)	S(10)-Mo(3)-Mo(1)	142.88(8)
S(3)-Mo(1)-Se(1)	135.17(8)	Se(3)-Mo(3)-Mo(1)	58.34(4)
S(1)-Mo(1)-Se(1)	51.06(7)	Se(2)-Mo(3)-Mo(1)	118.35(4)
S(5)-Mo(1)-Se(1)	86.45(8)	S(4)-Mo(3)-Mo(2)	54.99(7)
S(6)-Mo(1)-Se(1)	91.20(8)	S(3)-Mo(3)-Mo(2)	96.58(7)
Se(3)-Mo(1)-Se(1)	168.79(5)	S(2)-Mo(3)-Mo(2)	55.48(7)
S(4)-Mo(1)-Mo(3)	54.81(7)	S(9)-Mo(3)-Mo(2)	125.37(8)
S(3)-Mo(1)-Mo(3)	55.91(7)	S(10)-Mo(3)-Mo(2)	142.77(8)
S(1)-Mo(1)-Mo(3)	95.69(7)	Se(3)-Mo(3)-Mo(2)	118.18(5)
S(5)-Mo(1)-Mo(3)	127.24(8)	Se(2)-Mo(3)-Mo(2)	58.26(4)
S(6)-Mo(1)-Mo(3)	144.30(8)	Mo(1)-Mo(3)-Mo(2)	60.35(3)
Se(3)-Mo(1)-Mo(3)	58.53(4)	S(4)-Mo(2)-S(2)	110.34(10)
Se(1)-Mo(1)-Mo(3)	118.39(4)	S(4)-Mo(2)-S(1)	110.07(10)
S(4)-Mo(1)-Mo(2)	54.74(7)	S(2)-Mo(2)-S(1)	83.08(10)
S(3)-Mo(1)-Mo(2)	96.47(8)	S(4)-Mo(2)-S(7)	84.17(9)
S(1)-Mo(1)-Mo(2)	55.49(7)	S(2)-Mo(2)-S(7)	133.09(10)
S(5)-Mo(1)-Mo(2)	124.85(8)	S(1)-Mo(2)-S(7)	135.08(10)
S(6)-Mo(1)-Mo(2)	141.67(8)	S(4)-Mo(2)-S(8)	153.60(10)
Se(3)-Mo(1)-Mo(2)	117.94(5)	S(2)-Mo(2)-S(8)	91.41(9)
Se(1)-Mo(1)-Mo(2)	58.60(4)	S(1)-Mo(2)-S(8)	86.60(9)
Mo(3)-Mo(1)-Mo(2)	59.92(3)	S(7)-Mo(2)-S(8)	69.81(9)
S(4)-Mo(3)-S(3)	110.15(10)	S(4)-Mo(2)-Se(2)	85.14(7)
S(4)-Mo(3)-S(2)	110.05(10)	S(2)-Mo(2)-Se(2)	52.85(7)
S(3)-Mo(3)-S(2)	84.11(10)	S(1)-Mo(2)-Se(2)	135.74(8)
S(4)-Mo(3)-S(9)	84.09(10)	S(7)-Mo(2)-Se(2)	86.20(8)
S(3)-Mo(3)-S(9)	133.78(10)	S(8)-Mo(2)-Se(2)	97.17(7)
S(2)-Mo(3)-S(9)	133.50(10)	S(4)-Mo(2)-Se(1)	86.08(7)
S(4)-Mo(3)-S(10)	154.35(10)	S(2)-Mo(2)-Se(1)	133.97(8)
S(3)-Mo(3)-S(10)	88.48(10)	S(1)-Mo(2)-Se(1)	51.02(7)
S(2)-Mo(3)-S(10)	88.68(10)	S(7)-Mo(2)-Se(1)	89.83(8)
S(9)-Mo(3)-S(10)	70.26(9)	S(8)-Mo(2)-Se(1)	89.33(7)

Table A.28, Cont'd. Bond angles (deg.) for $[\text{Mo}_3(\mu_3\text{-S})(\mu\text{-SSe})_3(\text{S}_2\text{CN}^i\text{Bu}_2)_3][[\text{SeCN}]\cdot\frac{1}{2}\text{ClCH}_2\text{CH}_2\text{Cl}\cdot\frac{1}{2}\text{BuOMe}]$. Symmetry transformations used to generate equivalent atoms:

Se(2)-Mo(2)-Se(1)	170.69(5)	S(4)-Mo(2)-Mo(3)	54.75(7)
S(2)-Mo(2)-Mo(3)	56.01(7)	C(10)-N(2)-C(11)	122.0(9)
S(1)-Mo(2)-Mo(3)	95.74(7)	C(15)-N(2)-C(11)	117.5(9)
S(7)-Mo(2)-Mo(3)	125.10(7)	C(19)-N(3)-C(20)	122.7(9)
S(8)-Mo(2)-Mo(3)	146.55(8)	C(19)-N(3)-C(24)	121.5(9)
Se(2)-Mo(2)-Mo(3)	58.64(4)	C(20)-N(3)-C(24)	115.7(9)
Se(1)-Mo(2)-Mo(3)	117.90(4)	N(1)-C(1)-S(5)	122.9(8)
S(4)-Mo(2)-Mo(1)	54.77(7)	N(1)-C(1)-S(6)	123.6(8)
S(2)-Mo(2)-Mo(1)	95.69(7)	S(5)-C(1)-S(6)	113.5(7)
S(1)-Mo(2)-Mo(1)	55.75(7)	N(1)-C(2)-C(3)	114.1(10)
S(7)-Mo(2)-Mo(1)	126.56(8)	N(1)-C(2)-H(2A)	108.7
S(8)-Mo(2)-Mo(1)	140.23(7)	C(3)-C(2)-H(2A)	108.7
Se(2)-Mo(2)-Mo(1)	118.12(4)	N(1)-C(2)-H(2B)	108.7
Se(1)-Mo(2)-Mo(1)	58.30(4)	C(3)-C(2)-H(2B)	108.7
Mo(3)-Mo(2)-Mo(1)	59.73(3)	H(2A)-C(2)-H(2B)	107.6
S(1)-Se(1)-Mo(1)	60.10(8)	C(4)-C(3)-C(5)	112.1(11)
S(1)-Se(1)-Mo(2)	59.74(8)	C(4)-C(3)-C(2)	112.4(10)
Mo(1)-Se(1)-Mo(2)	63.10(4)	C(5)-C(3)-C(2)	109.1(10)
S(2)-Se(2)-Mo(2)	59.32(8)	C(4)-C(3)-H(3)	107.7
S(2)-Se(2)-Mo(3)	59.56(8)	C(5)-C(3)-H(3)	107.7
Mo(2)-Se(2)-Mo(3)	63.10(4)	C(2)-C(3)-H(3)	107.7
S(3)-Se(3)-Mo(1)	58.98(8)	C(3)-C(4)-H(4A)	109.5
S(3)-Se(3)-Mo(3)	59.13(7)	C(3)-C(4)-H(4B)	109.5
Mo(1)-Se(3)-Mo(3)	63.13(4)	H(4A)-C(4)-H(4B)	109.5
Se(1)-S(1)-Mo(2)	69.24(8)	C(3)-C(4)-H(4C)	109.5
Se(1)-S(1)-Mo(1)	68.84(8)	H(4A)-C(4)-H(4C)	109.5
Mo(2)-S(1)-Mo(1)	68.76(8)	H(4B)-C(4)-H(4C)	109.5
Se(2)-S(2)-Mo(2)	67.83(8)	C(3)-C(5)-H(5A)	109.5
Se(2)-S(2)-Mo(3)	67.88(8)	C(3)-C(5)-H(5B)	109.5
Mo(2)-S(2)-Mo(3)	68.50(8)	H(5A)-C(5)-H(5B)	109.5
Se(3)-S(3)-Mo(1)	67.23(8)	C(3)-C(5)-H(5C)	109.5
Se(3)-S(3)-Mo(3)	67.24(8)	H(5A)-C(5)-H(5C)	109.5
Mo(1)-S(3)-Mo(3)	68.49(8)	H(5B)-C(5)-H(5C)	109.5
Mo(3)-S(4)-Mo(2)	70.27(8)	N(1)-C(6)-C(7)	113.6(11)
Mo(3)-S(4)-Mo(1)	70.10(8)	N(1)-C(6)-H(6A)	108.8
Mo(2)-S(4)-Mo(1)	70.48(8)	C(7)-C(6)-H(6A)	108.8
C(1)-S(5)-Mo(1)	88.2(4)	N(1)-C(6)-H(6B)	108.8
C(1)-S(6)-Mo(1)	86.1(4)	C(7)-C(6)-H(6B)	108.8
C(10)-S(7)-Mo(2)	89.1(4)	H(6A)-C(6)-H(6B)	107.7
C(10)-S(8)-Mo(2)	86.8(4)	C(8)-C(7)-C(6)	113.3(12)
C(19)-S(9)-Mo(3)	89.2(4)	C(8)-C(7)-C(9)	110.4(12)
C(19)-S(10)-Mo(3)	87.5(4)	C(6)-C(7)-C(9)	106.9(14)
C(1)-N(1)-C(2)	123.1(9)	C(8)-C(7)-H(7)	108.7
C(1)-N(1)-C(6)	119.0(9)	C(6)-C(7)-H(7)	108.7
C(2)-N(1)-C(6)	117.8(9)	C(9)-C(7)-H(7)	108.7
C(10)-N(2)-C(15)	120.5(9)	C(7)-C(8)-H(8A)	109.5

Table A.28, Cont'd. Bond angles (deg.) for $[\text{Mo}_3(\mu_3\text{-S})(\mu\text{-SSe})_3(\text{S}_2\text{CN}^-\text{Bu}_2)_3][\text{SeCN}]\cdot\frac{1}{2}\text{ClCH}_2\text{CH}_2\text{Cl}\cdot\frac{1}{2}\text{BuOMe}$. Symmetry transformations used to generate equivalent atoms:

C(7)-C(8)-H(8B)	109.5	C(7)-C(8)-H(8C)	109.5
H(8A)-C(8)-H(8B)	109.5	H(8A)-C(8)-H(8C)	109.5
H(8B)-C(8)-H(8C)	109.5	C(18)-C(16)-H(16)	108.0
C(7)-C(9)-H(9A)	109.5	C(15)-C(16)-H(16)	108.0
C(7)-C(9)-H(9B)	109.5	C(16)-C(17)-H(17A)	109.5
H(9A)-C(9)-H(9B)	109.5	C(16)-C(17)-H(17B)	109.5
C(7)-C(9)-H(9C)	109.5	H(17A)-C(17)-H(17B)	109.5
H(9A)-C(9)-H(9C)	109.5	C(16)-C(17)-H(17C)	109.5
H(9B)-C(9)-H(9C)	109.5	H(17A)-C(17)-H(17C)	109.5
N(2)-C(10)-S(7)	121.3(8)	H(17B)-C(17)-H(17C)	109.5
N(2)-C(10)-S(8)	124.7(8)	C(16)-C(18)-H(18A)	109.5
S(7)-C(10)-S(8)	114.0(6)	C(16)-C(18)-H(18B)	109.5
N(2)-C(11)-C(12)	113.3(9)	H(18A)-C(18)-H(18B)	109.5
N(2)-C(11)-H(11A)	108.9	C(16)-C(18)-H(18C)	109.5
C(12)-C(11)-H(11A)	108.9	H(18A)-C(18)-H(18C)	109.5
N(2)-C(11)-H(11B)	108.9	H(18B)-C(18)-H(18C)	109.5
C(12)-C(11)-H(11B)	108.9	N(3)-C(19)-S(9)	122.5(9)
H(11A)-C(11)-H(11B)	107.7	N(3)-C(19)-S(10)	124.4(8)
C(11)-C(12)-C(14)	108.5(10)	S(9)-C(19)-S(10)	113.1(7)
C(11)-C(12)-C(13)	112.5(9)	N(3)-C(20)-C(21)	114.0(9)
C(14)-C(12)-C(13)	111.5(10)	N(3)-C(20)-H(20A)	108.8
C(11)-C(12)-H(12)	108.1	C(21)-C(20)-H(20A)	108.8
C(14)-C(12)-H(12)	108.1	N(3)-C(20)-H(20B)	108.8
C(13)-C(12)-H(12)	108.1	C(21)-C(20)-H(20B)	108.8
C(12)-C(13)-H(13A)	109.5	H(20A)-C(20)-H(20B)	107.7
C(12)-C(13)-H(13B)	109.5	C(20)-C(21)-C(22)	110.7(10)
H(13A)-C(13)-H(13B)	109.5	C(20)-C(21)-C(23)	112.1(9)
C(12)-C(13)-H(13C)	109.5	C(22)-C(21)-C(23)	110.2(10)
H(13A)-C(13)-H(13C)	109.5	C(20)-C(21)-H(21)	107.9
H(13B)-C(13)-H(13C)	109.5	C(22)-C(21)-H(21)	107.9
C(12)-C(14)-H(14A)	109.5	C(23)-C(21)-H(21)	107.9
C(12)-C(14)-H(14B)	109.5	C(21)-C(22)-H(22A)	109.5
H(14A)-C(14)-H(14B)	109.5	C(21)-C(22)-H(22B)	109.5
C(12)-C(14)-H(14C)	109.5	H(22A)-C(22)-H(22B)	109.5
H(14A)-C(14)-H(14C)	109.5	C(21)-C(22)-H(22C)	109.5
H(14B)-C(14)-H(14C)	109.5	H(22A)-C(22)-H(22C)	109.5
N(2)-C(15)-C(16)	115.0(10)	H(22B)-C(22)-H(22C)	109.5
N(2)-C(15)-H(15A)	108.5	C(21)-C(23)-H(23A)	109.5
C(16)-C(15)-H(15A)	108.5	C(21)-C(23)-H(23B)	109.5
N(2)-C(15)-H(15B)	108.5	H(23A)-C(23)-H(23B)	109.5
C(16)-C(15)-H(15B)	108.5	C(21)-C(23)-H(23C)	109.5
H(15A)-C(15)-H(15B)	107.5	H(23A)-C(23)-H(23C)	109.5
C(17)-C(16)-C(18)	111.1(11)	H(23B)-C(23)-H(23C)	109.5
C(17)-C(16)-C(15)	112.9(11)	N(3)-C(24)-C(25A)	114.2(11)
C(18)-C(16)-C(15)	108.7(11)	N(3)-C(24)-C(25B)	114.5(14)
C(17)-C(16)-H(16)	108.0	N(3)-C(24)-H(24A)	108.7

Table A.28, Cont'd. Bond angles (deg.) for $[\text{Mo}_3(\mu_3\text{-S})(\mu\text{-SSe})_3(\text{S}_2\text{CN}^i\text{Bu}_2)_3][\text{SeCN}]\cdot\frac{1}{2}\text{ClCH}_2\text{CH}_2\text{Cl}\cdot\frac{1}{2}\text{BuOMe}$. Symmetry transformations used to generate equivalent atoms:

C(25A)-C(24)-H(24A)	108.7	H(24A)-C(24)-H(24B)	107.6
N(3)-C(24)-H(24B)	108.7	C(27A)-C(25A)-C(26A)	111.2(19)
C(25A)-C(24)-H(24B)	108.7	C(27A)-C(25A)-C(24)	111(2)
C(26A)-C(25A)-C(24)	109.5(17)	Cl(2)-C(30)-H(30A)	110.2
C(27A)-C(25A)-H(25A)	108.3	C(29)-C(30)-H(30B)	110.2
C(26A)-C(25A)-H(25A)	108.3	Cl(2)-C(30)-H(30B)	110.2
C(24)-C(25A)-H(25A)	108.3	H(30A)-C(30)-H(30B)	108.5
C(25A)-C(26A)-H(26A)	109.5	C(31A)-O(1A)-C(35)	113.191(12)
C(25A)-C(26A)-H(26B)	109.5	O(1A)-C(31A)-C(32A)	105.711(10)
H(26A)-C(26A)-H(26B)	109.5	O(1A)-C(31A)-C(33A)	118.57(3)
C(25A)-C(26A)-H(26C)	109.5	C(32A)-C(31A)-C(33A)	108.839(12)
H(26A)-C(26A)-H(26C)	109.5	O(1A)-C(31A)-C(34A)	105.711(12)
H(26B)-C(26A)-H(26C)	109.5	C(32A)-C(31A)-C(34A)	108.825(10)
C(25A)-C(27A)-H(27A)	109.5	C(33A)-C(31A)-C(34A)	108.839(13)
C(25A)-C(27A)-H(27B)	109.5	C(31A)-C(32A)-H(32A)	109.5
H(27A)-C(27A)-H(27B)	109.5	C(31A)-C(32A)-H(32B)	109.5
C(25A)-C(27A)-H(27C)	109.5	H(32A)-C(32A)-H(32B)	109.5
H(27A)-C(27A)-H(27C)	109.5	C(31A)-C(32A)-H(32C)	109.5
H(27B)-C(27A)-H(27C)	109.5	H(32A)-C(32A)-H(32C)	109.5
C(26B)-C(25B)-C(27B)	110(3)	H(32B)-C(32A)-H(32C)	109.5
C(26B)-C(25B)-C(24)	110(3)	C(31A)-C(33A)-H(33A)	109.5
C(27B)-C(25B)-C(24)	111(3)	C(31A)-C(33A)-H(33B)	109.5
C(26B)-C(25B)-H(25B)	108.7	H(33A)-C(33A)-H(33B)	109.5
C(27B)-C(25B)-H(25B)	108.7	C(31A)-C(33A)-H(33C)	109.5
C(24)-C(25B)-H(25B)	108.7	H(33A)-C(33A)-H(33C)	109.5
C(25B)-C(27B)-H(27D)	109.5	H(33B)-C(33A)-H(33C)	109.5
C(25B)-C(27B)-H(27E)	109.5	C(31A)-C(34A)-H(34A)	109.5
H(27D)-C(27B)-H(27E)	109.5	C(31A)-C(34A)-H(34B)	109.5
C(25B)-C(27B)-H(27F)	109.5	H(34A)-C(34A)-H(34B)	109.5
H(27D)-C(27B)-H(27F)	109.5	C(31A)-C(34A)-H(34C)	109.5
H(27E)-C(27B)-H(27F)	109.5	H(34A)-C(34A)-H(34C)	109.5
C(25B)-C(26B)-H(26D)	109.5	H(34B)-C(34A)-H(34C)	109.5
C(25B)-C(26B)-H(26E)	109.5	O(1A)-C(35)-H(35A)	109.5
H(26D)-C(26B)-H(26E)	109.5	O(1A)-C(35)-H(35B)	109.5
C(25B)-C(26B)-H(26F)	109.5	H(35A)-C(35)-H(35B)	109.5
H(26D)-C(26B)-H(26F)	109.5	O(1A)-C(35)-H(35C)	109.5
H(26E)-C(26B)-H(26F)	109.5	H(35A)-C(35)-H(35C)	109.5
N(4)-C(28)-Se(4)	175.6(14)	H(35B)-C(35)-H(35C)	109.5
C(30)-C(29)-Cl(1)	117.1(17)	O(1B)-C(31B)-C(33B)	118.57(3)
C(30)-C(29)-H(29A)	108.0	O(1B)-C(31B)-C(32B)	105.711(11)
Cl(1)-C(29)-H(29A)	108.0	C(33B)-C(31B)-C(32B)	108.839(10)
C(30)-C(29)-H(29B)	108.0	O(1B)-C(31B)-C(34B)	105.711(10)
Cl(1)-C(29)-H(29B)	108.0	C(33B)-C(31B)-C(34B)	108.839(11)
H(29A)-C(29)-H(29B)	107.3	C(32B)-C(31B)-C(34B)	108.826(13)
C(29)-C(30)-Cl(2)	107.6(17)	C(31B)-C(32B)-H(32D)	109.5
C(29)-C(30)-H(30A)	110.2	C(31B)-C(32B)-H(32E)	109.5

Table A.28, Cont'd. Bond angles (deg.) for $[\text{Mo}_3(\mu_3\text{-S})(\mu\text{-SSe})_3(\text{S}_2\text{CN}^i\text{Bu}_2)_3][\text{SeCN}]\cdot\frac{1}{2}\text{ClCH}_2\text{CH}_2\text{Cl}\cdot\frac{1}{2}\text{BuOMe}$. Symmetry transformations used to generate equivalent atoms:

H(32D)-C(32B)-H(32E)	109.5
C(31B)-C(32B)-H(32F)	109.5
H(32D)-C(32B)-H(32F)	109.5
H(32E)-C(32B)-H(32F)	109.5
C(31B)-C(33B)-H(33D)	109.5
C(31B)-C(33B)-H(33E)	109.5
H(33D)-C(33B)-H(33E)	109.5
C(31B)-C(33B)-H(33F)	109.5
H(33D)-C(33B)-H(33F)	109.5
H(33E)-C(33B)-H(33F)	109.5
C(31B)-C(34B)-H(34D)	109.5
C(31B)-C(34B)-H(34E)	109.5
H(34D)-C(34B)-H(34E)	109.5
C(31B)-C(34B)-H(34F)	109.5
H(34D)-C(34B)-H(34F)	109.5
H(34E)-C(34B)-H(34F)	109.5

Table A.29. Anisotropic displacement parameters ($\text{\AA}^2 \times 10^3$) for $[\text{Mo}_3(\mu_3\text{-S})(\mu\text{-SSe})_3(\text{S}_2\text{CN}^i\text{Bu}_2)_3][\text{SeCN}] \cdot \frac{1}{2}\text{ClCH}_2\text{CH}_2\text{Cl} \cdot \frac{1}{2}\text{BuOMe}$. The anisotropic displacement factor exponent takes the form: $-2\pi^2[h^2 a^{*2}U^{11} + \dots + 2hka^*b^*U^{12}]$.

Atom	U^{11}	U^{22}	U^{33}	U^{23}	U^{13}	U^{12}
Mo(1)	23(1)	25(1)	24(1)	3(1)	0(1)	-2(1)
Mo(3)	22(1)	22(1)	28(1)	2(1)	1(1)	-1(1)
Mo(2)	22(1)	23(1)	24(1)	2(1)	0(1)	-1(1)
Se(1)	28(1)	30(1)	30(1)	0(1)	0(1)	3(1)
Se(2)	28(1)	30(1)	30(1)	4(1)	5(1)	0(1)
Se(3)	29(1)	28(1)	36(1)	8(1)	-1(1)	-1(1)
Se(4)	43(1)	39(1)	78(1)	3(1)	-14(1)	1(1)
S(1)	21(2)	29(2)	28(2)	4(1)	1(1)	0(1)
S(2)	31(2)	24(2)	26(2)	1(1)	1(1)	-1(1)
S(3)	24(2)	29(2)	32(2)	1(1)	1(1)	-4(1)
S(4)	21(2)	23(2)	29(2)	2(1)	-2(1)	-2(1)
S(5)	28(2)	45(2)	29(2)	2(2)	-3(1)	-8(2)
S(6)	29(2)	40(2)	24(2)	1(1)	2(1)	-4(1)
S(7)	28(2)	25(2)	36(2)	4(1)	-4(1)	-2(1)
S(8)	27(2)	29(2)	31(2)	4(1)	-4(1)	1(1)
S(9)	25(2)	29(2)	39(2)	0(2)	-2(1)	-1(1)
S(10)	31(2)	28(2)	40(2)	-3(2)	-2(2)	2(1)
N(1)	31(7)	47(7)	32(7)	-1(5)	1(6)	-2(5)
N(2)	31(6)	27(7)	36(6)	-2(5)	-1(5)	-4(5)
N(3)	27(7)	23(6)	39(6)	0(5)	6(5)	4(5)
N(4)	111(12)	76(10)	80(11)	6(9)	-17(10)	-1(8)
C(1)	32(7)	41(8)	23(8)	7(6)	1(6)	1(6)
C(2)	34(8)	49(9)	28(7)	-2(6)	12(6)	-8(7)
C(3)	52(10)	41(9)	55(10)	-10(7)	3(7)	9(7)
C(4)	73(11)	52(10)	74(11)	23(8)	20(8)	20(8)
C(5)	47(10)	59(9)	63(10)	-1(8)	4(7)	10(7)
C(6)	38(8)	81(10)	28(8)	-16(8)	4(7)	-10(8)
C(7)	47(10)	137(15)	42(9)	-11(10)	-13(9)	5(10)
C(8)	74(11)	95(12)	46(9)	3(9)	-12(9)	-2(9)
C(9)	70(12)	240(30)	69(12)	14(14)	-10(10)	-60(15)
C(10)	37(7)	10(7)	30(7)	5(5)	11(6)	-2(5)
C(11)	32(7)	34(7)	39(8)	2(6)	7(7)	3(6)
C(12)	44(8)	34(8)	47(9)	14(7)	-15(7)	-18(6)
C(13)	53(9)	84(11)	32(8)	8(8)	4(7)	-2(8)
C(14)	76(10)	46(9)	59(9)	25(7)	-22(8)	-9(8)
C(15)	49(8)	30(7)	33(8)	4(6)	-2(6)	1(6)
C(16)	54(9)	35(8)	53(10)	-9(7)	2(7)	3(7)
C(17)	74(11)	79(11)	51(9)	-4(8)	3(8)	-1(9)
C(18)	77(12)	87(12)	77(11)	-32(10)	-31(9)	-2(9)
C(19)	33(8)	21(7)	33(7)	6(6)	11(6)	-1(6)
C(20)	44(8)	26(8)	40(8)	8(7)	9(6)	8(6)
C(21)	40(8)	37(8)	36(8)	0(7)	-4(6)	10(6)
C(22)	68(10)	32(8)	44(8)	-6(7)	8(7)	7(7)

Table A.29, Cont'd. Anisotropic displacement parameters ($\text{\AA}^2 \times 10^3$) for $[\text{Mo}_3(\mu_3\text{-S})(\mu\text{-SSe})_3(\text{S}_2\text{CN}^i\text{Bu}_2)_3][\text{SeCN}] \cdot \frac{1}{2}\text{ClCH}_2\text{CH}_2\text{Cl} \cdot \frac{1}{2}^i\text{BuOMe}$. The anisotropic displacement factor exponent takes the form: $-2\pi^2[h^2 a^{*2}U^{11} + \dots + 2hka^*b^*U^{12}]$.

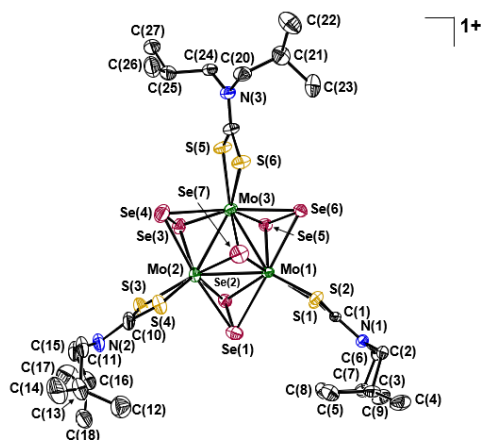
Atom	U^{11}	U^{22}	U^{33}	U^{23}	U^{13}	U^{12}
C(23)	65(10)	40(8)	37(8)	-8(6)	-1(7)	-6(7)
C(24)	26(8)	40(8)	48(8)	5(6)	0(6)	1(6)
C(28)	66(11)	40(9)	81(13)	14(9)	-33(10)	-10(7)

Table A.30. Hydrogen coordinates ($\times 10^4$) and isotropic displacement parameters ($\text{\AA}^2 \times 10^3$) for $[\text{Mo}_3(\mu_3\text{-S})(\mu\text{-SSe})_3(\text{S}_2\text{CN}^t\text{Bu}_2)_3][\text{SeCN}] \cdot \frac{1}{2}\text{ClCH}_2\text{CH}_2\text{Cl} \cdot \frac{1}{2}^t\text{BuOMe}$.

H atom	x	y	z	U(eq)
H(2A)	-271	5223	8194	44
H(2B)	-321	5150	7364	44
H(3)	-344	5878	8018	59
H(4A)	-471	5706	6568	100
H(4B)	-127	5950	6874	100
H(4C)	-549	6112	6914	100
H(5A)	-994	5866	7838	85
H(5B)	-877	5498	8280	85
H(5C)	-967	5464	7452	85
H(6A)	227	5704	8497	59
H(6B)	585	5737	7983	59
H(7)	778	5113	8352	90
H(8A)	229	5194	9430	107
H(8B)	526	4854	9360	107
H(8C)	195	4900	8789	107
H(9A)	739	5624	9535	190
H(9B)	998	5721	8866	190
H(9C)	1086	5354	9332	190
H(11A)	702	7317	3726	42
H(11B)	568	6921	3404	42
H(12)	1189	7351	2869	50
H(13A)	859	6702	2208	84
H(13B)	1250	6689	2636	84
H(13C)	1219	6931	1924	84
H(14A)	446	7282	2290	91
H(14B)	785	7510	1923	91
H(14C)	611	7655	2656	91
H(15A)	1398	7342	3997	45
H(15B)	1610	6960	4211	45
H(16)	1286	6962	5318	57
H(17A)	980	7518	5692	102
H(17B)	757	7320	5056	102
H(17C)	1012	7685	4907	102
H(18A)	1741	7610	5031	121
H(18B)	1895	7204	5271	121
H(18C)	1656	7457	5812	121
H(20A)	2321	3893	3348	44
H(20B)	1872	3946	3356	44
H(21)	2262	3524	4410	45
H(22A)	1890	3200	3214	72
H(22B)	2111	2971	3816	72
H(22C)	2339	3236	3279	72
H(23A)	1636	3740	4708	71
H(23B)	1685	3291	4755	71

Table A.30, Cont'd. Hydrogen coordinates ($\times 10^4$) and isotropic displacement parameters ($\text{\AA}^2 \times 10^3$) for $[\text{Mo}_3(\mu_3\text{-S})(\mu\text{-SSe})_3(\text{S}_2\text{CN}^i\text{Bu}_2)_3][\text{SeCN}]\cdot\frac{1}{2}\text{ClCH}_2\text{CH}_2\text{Cl}\cdot\frac{1}{2}\text{BuOMe}$.

H atom	x	y	z	U(eq)
H(23C)	1475	3477	4089	71
H(24A)	2625	4065	4575	46
H(24B)	2503	4483	4801	46
H(25A)	2806	4289	3447	56
H(26A)	3262	4258	4351	116
H(26B)	3357	4597	3818	116
H(26C)	3170	4685	4571	116
H(27A)	2407	4800	3362	97
H(27B)	2834	4933	3238	97
H(27C)	2631	5013	3980	97
H(25B)	2571	4895	4235	25
H(27D)	2917	4472	3121	93
H(27E)	2782	4904	3091	93
H(27F)	2475	4571	3103	93
H(26D)	3106	4706	4888	109
H(26E)	3261	4477	4219	109
H(26F)	3232	4928	4189	109
H(29A)	-894	5927	10976	55
H(29B)	-1256	6085	11382	55
H(30A)	-1618	6003	10257	56
H(30B)	-1490	5613	10622	56
H(32A)	-1388	5755	10540	369
H(32B)	-1231	5527	9871	369
H(32C)	-1019	5497	10616	369
H(33A)	-1093	6342	10941	410
H(33B)	-720	6107	11130	410
H(33C)	-692	6474	10639	410
H(34A)	-1342	6359	9735	195
H(34B)	-947	6443	9355	195
H(34C)	-1189	6080	9134	195
H(35A)	-22	5927	9666	239
H(35B)	-254	6311	9769	239
H(35C)	-188	6034	10427	239
H(32D)	629	6847	10436	75
H(32E)	323	6554	10733	75
H(32F)	725	6405	10465	75
H(33D)	228	7114	9510	246
H(33E)	-11	6848	8992	246
H(33F)	-118	6872	9813	246
H(34D)	804	6807	9087	207
H(34E)	886	6369	9230	207
H(34F)	598	6492	8619	207



The thermal ellipsoid plot is drawn at the 50% level. All H atoms are omitted for clarity.

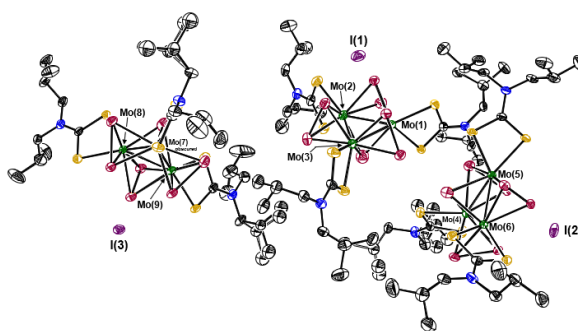


Table A.31. Crystal Data and Structure Refinement for $[\text{Mo}_3\text{Se}_7(\text{S}_2\text{CN}^t\text{Bu}_2)_3]\text{I} \cdot \frac{1}{6}(\text{ClCH}_2\text{CH}_2\text{Cl}) \cdot \frac{1}{3}(\text{C}_5\text{H}_{10})$.

Identification code	JPD1172_0m_a	
Empirical formula	$\text{C}_{29}\text{H}_{54.67}\text{Cl}_{0.33}\text{IMo}_3\text{N}_3\text{S}_6\text{Se}_7$	
Formula weight	1617.04	
Temperature	156(2) K	
Wavelength	0.71073 Å	
Crystal system	Monoclinic	
Space group	$P2_1/c$	
Unit cell dimensions	$a = 27.7223(8)$ Å	$\alpha = 90^\circ$
	$b = 13.5820(4)$ Å	$\beta = 90.9170(10)^\circ$
	$c = 40.7503(11)$ Å	$\gamma = 90^\circ$
Volume	$15341.5(8)$ Å ³	
Z	12	
Density (calculated)	2.100 g/cm ³	
Absorption coefficient	6.597 mm ⁻¹	
F(000)	9220	
Crystal size	0.503 x 0.406 x 0.312 mm ³	
θ range for data collection	1.250 to 29.645°	
Index ranges	$-38 \leq h \leq 38, -18 \leq k \leq 18, -56 \leq l \leq 56$	

Table A.31, Cont'd. Crystal Data and Structure Refinement for $[\text{Mo}_3\text{Se}_7(\text{S}_2\text{CN}^i\text{Bu}_2)_3]\text{I} \cdot \frac{1}{6}(\text{ClCH}_2\text{CH}_2\text{Cl}) \cdot \frac{1}{3}(\text{C}_5\text{H}_{10})$.

Reflections collected	1076082
Independent reflections	43161 [R(int) = 0.0626]
Completeness to $\theta = 25.242^\circ$	99.9 %
Absorption correction	Semi-empirical from equivalents
Refinement method	Full-matrix least-squares on F^2
Data / restraints / parameters	43161 / 0 / 1329
Goodness-of-fit on F^2	1.080
Final R indices [I > 2 σ (I)]	R1 = 0.0566, wR2 = 0.1495
R indices (all data)	R1 = 0.0695, wR2 = 0.1615
Extinction coefficient	n/a
Largest diff. peak and hole	2.620 and -5.018 e $\cdot\text{\AA}^{-3}$

Table A.32. Atomic coordinates ($\times 10^4$) and equivalent isotropic displacement parameters ($\text{\AA}^2 \times 10^3$) for $[\text{Mo}_3\text{Se}_7(\text{S}_2\text{CN}^i\text{Bu}_2)_3]\text{I} \cdot \frac{1}{6}(\text{ClCH}_2\text{CH}_2\text{Cl}) \cdot \frac{1}{3}(\text{C}_5\text{H}_{10})$. $U(\text{eq})$ is defined as one third of the trace of the orthogonalized U^{ij} tensor.

Atom	x	y	z	U(eq)
I(1)	2677(1)	11202(1)	4110(1)	45(1)
I(2)	1097(1)	6070(1)	1473(1)	36(1)
I(3)	4890(1)	3212(1)	6236(1)	29(1)
Mo(1)	1528(1)	8847(1)	3782(1)	19(1)
Mo(2)	1619(1)	8843(1)	4456(1)	25(1)
Mo(3)	2283(1)	7862(1)	4078(1)	23(1)
Mo(4)	1698(1)	6087(1)	2528(1)	15(1)
Mo(5)	2063(1)	7742(1)	2221(1)	15(1)
Mo(6)	2480(1)	5936(1)	2120(1)	15(1)
Mo(7)	4553(1)	6521(1)	6046(1)	19(1)
Mo(8)	4206(1)	6037(1)	6656(1)	19(1)
Mo(9)	3679(1)	5564(1)	6099(1)	20(1)
Se(1)	1596(1)	10418(1)	4120(1)	29(1)
Se(2)	871(1)	9582(1)	4154(1)	37(1)
Se(3)	2517(1)	9191(1)	4492(1)	33(1)
Se(4)	2276(1)	7696(1)	4714(1)	43(1)
Se(5)	2406(1)	9248(1)	3666(1)	27(1)
Se(6)	2124(1)	7786(1)	3444(1)	27(1)
Se(7)	1432(1)	7360(1)	4124(1)	49(1)
Se(8)	1192(1)	7194(1)	2158(1)	22(1)
Se(9)	1398(1)	7857(1)	2664(1)	26(1)
Se(10)	2142(1)	6990(1)	1654(1)	22(1)
Se(11)	2854(1)	7539(1)	1891(1)	25(1)
Se(12)	1705(1)	4974(1)	2025(1)	23(1)
Se(13)	2179(1)	4457(1)	2466(1)	29(1)
Se(14)	2500(1)	6805(1)	2650(1)	37(1)
Se(15)	5023(1)	5467(1)	6455(1)	24(1)
Se(16)	4971(1)	7127(1)	6580(1)	30(1)
Se(17)	4377(1)	4877(1)	5773(1)	26(1)
Se(18)	3988(1)	6223(1)	5543(1)	34(1)
Se(19)	3952(1)	4286(1)	6515(1)	25(1)
Se(20)	3337(1)	5318(1)	6685(1)	28(1)
Se(21)	3828(1)	7277(1)	6286(1)	42(1)
S(1)	1282(1)	9911(1)	3305(1)	25(1)
S(2)	853(1)	8068(1)	3473(1)	23(1)
S(3)	1538(1)	9976(2)	4941(1)	37(1)
S(4)	1042(1)	8143(2)	4858(1)	36(1)
S(5)	3171(1)	7479(1)	4055(1)	35(1)
S(6)	2407(1)	6056(1)	4037(1)	32(1)

Table A.32, Cont'd. Atomic coordinates ($\times 10^4$) and equivalent isotropic displacement parameters ($\text{\AA}^2 \times 10^3$) for $[\text{Mo}_3\text{Se}_7(\text{S}_2\text{CN}^i\text{Bu}_2)_3]\text{I} \cdot \frac{1}{6}(\text{ClCH}_2\text{CH}_2\text{Cl}) \cdot \frac{1}{3}(\text{C}_5\text{H}_{10})$. $U(\text{eq})$ is defined as one third of the trace of the orthogonalized U^{ij} tensor.

Atom	x	y	z	U(eq)
S(7)	924(1)	5229(1)	2683(1)	26(1)
S(8)	1697(1)	5727(1)	3128(1)	22(1)
S(9)	1827(1)	9311(1)	1927(1)	24(1)
S(10)	2452(1)	9183(1)	2492(1)	25(1)
S(11)	2881(1)	4924(1)	1683(1)	25(1)
S(12)	3294(1)	5428(1)	2310(1)	24(1)
S(13)	5324(1)	6595(1)	5724(1)	26(1)
S(14)	4676(1)	8197(1)	5815(1)	28(1)
S(15)	4434(1)	5350(1)	7212(1)	25(1)
S(16)	3971(1)	7205(1)	7095(1)	24(1)
S(17)	3173(1)	4230(1)	5832(1)	28(1)
S(18)	2872(1)	6224(1)	5942(1)	29(1)
N(1)	444(2)	9299(4)	3028(1)	21(1)
N(2)	913(3)	9311(5)	5389(2)	35(2)
N(3)	3348(2)	5535(5)	4054(2)	31(1)
N(4)	897(2)	4798(5)	3327(2)	25(1)
N(5)	2193(2)	10919(4)	2223(2)	26(1)
N(6)	3743(2)	4226(4)	1890(2)	26(1)
N(7)	5507(2)	8412(4)	5488(2)	26(1)
N(8)	4100(2)	6470(4)	7704(1)	24(1)
N(9)	2308(2)	4904(5)	5626(2)	27(1)
C(1)	806(2)	9116(5)	3238(2)	20(1)
C(2)	66(2)	8544(5)	2961(2)	24(1)
C(3)	-412(2)	8721(5)	3130(2)	28(1)
C(4)	-776(3)	7962(7)	3000(3)	42(2)
C(5)	-368(3)	8660(7)	3504(2)	37(2)
C(6)	438(3)	10190(5)	2825(2)	25(1)
C(7)	113(3)	11025(6)	2954(2)	31(2)
C(8)	249(4)	11367(6)	3296(2)	42(2)
C(9)	144(3)	11868(7)	2707(2)	41(2)
C(10)	1135(3)	9168(6)	5103(2)	36(2)
C(11)	670(4)	8505(7)	5558(2)	39(2)
C(12)	136(4)	8659(8)	5618(2)	45(2)
C(13)	-157(5)	8729(9)	5301(3)	58(3)
C(14)	-44(5)	7790(10)	5822(3)	64(3)
C(15)	1048(4)	10186(7)	5591(2)	41(2)
C(16)	831(4)	11178(7)	5479(2)	42(2)
C(17)	1125(5)	12001(9)	5640(4)	69(3)
C(18)	302(4)	11276(8)	5558(2)	49(2)

Table A.32, Cont'd. Atomic coordinates ($\times 10^4$) and equivalent isotropic displacement parameters ($\text{\AA}^2 \times 10^3$) for $[\text{Mo}_3\text{Se}_7(\text{S}_2\text{CN}^i\text{Bu}_2)_3]\text{I} \cdot \frac{1}{6}(\text{ClCH}_2\text{CH}_2\text{Cl}) \cdot \frac{1}{3}(\text{C}_5\text{H}_{10})$. $U(\text{eq})$ is defined as one third of the trace of the orthogonalized U^{ij} tensor.

Atom	x	y	z	U(eq)
C(19)	3026(3)	6251(5)	4042(2)	29(1)
C(20)	3233(3)	4506(6)	3982(2)	34(2)
C(21)	3365(3)	4224(6)	3632(2)	41(2)
C(22)	3432(5)	3137(8)	3602(3)	61(3)
C(23)	2985(4)	4603(8)	3381(2)	49(2)
C(24)	3850(3)	5751(6)	4154(2)	31(2)
C(25)	3899(3)	5863(7)	4529(2)	38(2)
C(26)	3683(4)	5024(8)	4716(2)	48(2)
C(27)	4433(3)	6016(7)	4619(2)	39(2)
C(28)	1134(2)	5195(5)	3085(2)	22(1)
C(29)	425(3)	4320(6)	3266(2)	34(2)
C(30A)	3(5)	5091(10)	3254(3)	40(3)
C(31A)	-64(6)	5680(12)	3580(4)	51(3)
C(32A)	-466(6)	4545(13)	3155(4)	53(3)
C(30B)	9(11)	4670(20)	3418(8)	40(3)
C(31B)	-39(13)	5700(30)	3348(9)	51(3)
C(32B)	-447(14)	4120(30)	3287(10)	53(3)
C(33)	1097(3)	4763(6)	3663(2)	32(2)
C(34A)	1204(8)	3764(15)	3786(5)	39(3)
C(35A)	1584(9)	3292(19)	3580(6)	53(3)
C(36A)	1380(10)	3827(19)	4152(6)	52(4)
C(34B)	1465(6)	3891(12)	3716(4)	39(3)
C(35B)	1287(8)	2929(15)	3620(5)	53(3)
C(36B)	1630(8)	3869(16)	4090(5)	52(4)
C(37)	2163(2)	9941(5)	2214(2)	24(1)
C(38)	1946(3)	11536(5)	1975(2)	28(1)
C(39)	2228(3)	11677(6)	1660(2)	36(2)
C(40)	2728(4)	12101(7)	1722(3)	49(2)
C(41)	1935(5)	12370(8)	1434(3)	59(3)
C(42)	2442(3)	11413(5)	2495(2)	33(2)
C(43)	2153(4)	11460(6)	2810(2)	41(2)
C(44)	2435(5)	12032(8)	3067(3)	63(3)
C(45)	1651(4)	11888(7)	2752(2)	45(2)
C(46)	3358(2)	4782(5)	1951(2)	24(1)
C(47)	3819(3)	3823(6)	1561(2)	31(2)
C(48)	4044(3)	4577(6)	1331(2)	38(2)
C(49)	4539(4)	4889(9)	1447(3)	59(3)
C(50)	4051(5)	4157(8)	984(2)	55(3)
C(51)	4108(3)	4056(6)	2148(2)	31(2)

Table A.32, Cont'd. Atomic coordinates ($\times 10^4$) and equivalent isotropic displacement parameters ($\text{\AA}^2 \times 10^3$) for $[\text{Mo}_3\text{Se}_7(\text{S}_2\text{CN}^i\text{Bu}_2)_3]\text{I} \cdot \frac{1}{6}(\text{ClCH}_2\text{CH}_2\text{Cl}) \cdot \frac{1}{3}(\text{C}_5\text{H}_{10})$. $U(\text{eq})$ is defined as one third of the trace of the orthogonalized U^{ij} tensor.

Atom	x	y	z	U(eq)
C(52)	3952(4)	3316(7)	2402(2)	46(2)
C(53)	3917(5)	2314(8)	2266(3)	64(3)
C(54)	4306(5)	3377(11)	2698(3)	75(4)
C(55)	5214(2)	7823(5)	5653(2)	26(1)
C(56)	5957(3)	8051(6)	5346(2)	31(2)
C(57)	5927(4)	8028(8)	4967(3)	51(2)
C(58)	5530(5)	7370(11)	4841(3)	67(3)
C(59)	6436(5)	7713(12)	4850(4)	83(5)
C(60)	5390(3)	9454(5)	5437(2)	32(2)
C(61A)	5776(5)	10182(10)	5583(3)	38(2)
C(62A)	5598(7)	11261(14)	5503(5)	58(4)
C(63A)	5883(8)	10039(15)	5926(5)	62(4)
C(61B)	5546(10)	10070(20)	5735(7)	38(2)
C(62B)	5399(14)	11160(30)	5634(10)	58(4)
C(63B)	6095(15)	10020(30)	5815(10)	62(4)
C(64)	4160(2)	6358(5)	7384(2)	22(1)
C(65)	4289(3)	5729(6)	7934(2)	28(1)
C(66)	3943(4)	4876(7)	7994(3)	47(2)
C(67)	3487(4)	5143(11)	8155(4)	71(4)
C(68)	4224(5)	4106(9)	8190(4)	77(4)
C(69)	3860(3)	7325(6)	7839(2)	29(2)
C(70)	4202(3)	8021(7)	8021(2)	38(2)
C(71)	3913(4)	8814(8)	8184(3)	56(3)
C(72)	4560(4)	8466(9)	7793(3)	62(3)
C(73)	2728(2)	5084(6)	5780(2)	26(1)
C(74)	2209(3)	3954(6)	5473(2)	32(2)
C(75A)	2422(7)	4010(20)	5102(5)	32(2)
C(76A)	2276(10)	3010(20)	4961(7)	54(4)
C(77A)	2267(10)	4840(30)	4905(7)	52(4)
C(75B)	2413(7)	3728(18)	5152(5)	32(2)
C(76B)	2273(9)	2700(20)	5030(7)	54(4)
C(77B)	2275(9)	4480(20)	4897(6)	52(4)
C(78)	1926(3)	5650(7)	5624(2)	38(2)
C(79)	1642(3)	5681(9)	5944(3)	56(3)
C(80)	1301(5)	6547(11)	5934(6)	119(8)
C(81)	1383(4)	4750(10)	6018(3)	65(3)
C(82)	3568(11)	16030(20)	222(8)	69(7)
C(83)	3621(10)	16440(20)	136(7)	62(6)
C(84)	3310(11)	16460(20)	409(8)	65(7)

Table A.32, Cont'd. Atomic coordinates ($\times 10^4$) and equivalent isotropic displacement parameters ($\text{\AA}^2 \times 10^3$) for $[\text{Mo}_3\text{Se}_7(\text{S}_2\text{CN}^i\text{Bu}_2)_3]\text{I} \cdot \frac{1}{6}(\text{ClCH}_2\text{CH}_2\text{Cl}) \cdot \frac{1}{3}(\text{C}_5\text{H}_{10})$. $U(\text{eq})$ is defined as one third of the trace of the orthogonalized U^{ij} tensor.

Atom	x	y	z	U(eq)
C(85)	3190(20)	16170(50)	478(16)	150(20)
C(86)	2960(9)	15488(19)	475(6)	57(5)
C(87)	2615(11)	15550(20)	762(7)	74(7)
C(88)	2294(13)	15950(30)	822(9)	89(9)
C(89)	2095(9)	16394(18)	696(6)	57(5)
C(90)	2393(14)	14720(30)	836(10)	101(11)
C(91)	2654(13)	13650(30)	793(9)	94(10)
C(92)	458(14)	5830(30)	4599(10)	101(11)
C(93)	858(15)	5450(30)	4775(11)	112(12)
Cl(1)	125(6)	5191(12)	4402(4)	151(5)
Cl(2)	850(5)	4372(10)	4991(3)	126(4)

Table A.33. Bond lengths (Å) for $[\text{Mo}_3\text{Se}_7(\text{S}_2\text{CN}^i\text{Bu}_2)_3]\text{I} \cdot \frac{1}{6}(\text{ClCH}_2\text{CH}_2\text{Cl}) \cdot \frac{1}{3}(\text{C}_5\text{H}_{10})$. Symmetry transformations used to generate equivalent atoms:

Mo(1)-Se(7)	2.4699(13)	Mo(6)-S(11)	2.5217(17)
Mo(1)-S(2)	2.4772(17)	Mo(6)-Se(12)	2.5393(8)
Mo(1)-S(1)	2.5103(18)	Mo(6)-Se(10)	2.5445(8)
Mo(1)-Se(5)	2.5450(9)	Mo(6)-Se(11)	2.5934(8)
Mo(1)-Se(1)	2.5456(9)	Mo(6)-Se(13)	2.5978(9)
Mo(1)-Se(2)	2.5881(10)	Mo(7)-Se(21)	2.4731(11)
Mo(1)-Se(6)	2.6027(9)	Mo(7)-S(14)	2.4878(19)
Mo(1)-Mo(3)	2.7451(8)	Mo(7)-S(13)	2.5272(18)
Mo(1)-Mo(2)	2.7523(8)	Mo(7)-Se(17)	2.5388(9)
Mo(2)-Se(7)	2.4753(13)	Mo(7)-Se(15)	2.5420(9)
Mo(2)-S(4)	2.494(2)	Mo(7)-Se(16)	2.5867(9)
Mo(2)-S(3)	2.518(2)	Mo(7)-Se(18)	2.5896(10)
Mo(2)-Se(3)	2.5357(10)	Mo(7)-Mo(8)	2.7601(8)
Mo(2)-Se(1)	2.5401(10)	Mo(7)-Mo(9)	2.7604(8)
Mo(2)-Se(2)	2.5970(11)	Mo(8)-Se(21)	2.4830(12)
Mo(2)-Se(4)	2.6063(11)	Mo(8)-S(16)	2.4866(17)
Mo(2)-Mo(3)	2.7617(9)	Mo(8)-S(15)	2.5220(18)
Mo(3)-Se(7)	2.4670(13)	Mo(8)-Se(15)	2.5411(8)
Mo(3)-S(6)	2.483(2)	Mo(8)-Se(19)	2.5433(9)
Mo(3)-S(5)	2.5195(19)	Mo(8)-Se(20)	2.6044(9)
Mo(3)-Se(3)	2.5473(10)	Mo(8)-Se(16)	2.6079(9)
Mo(3)-Se(5)	2.5489(10)	Mo(8)-Mo(9)	2.7550(7)
Mo(3)-Se(4)	2.6039(11)	Mo(9)-Se(21)	2.4793(11)
Mo(3)-Se(6)	2.6156(10)	Mo(9)-S(18)	2.4850(18)
Mo(4)-Se(14)	2.4700(10)	Mo(9)-S(17)	2.5280(17)
Mo(4)-S(8)	2.4900(16)	Mo(9)-Se(19)	2.5333(9)
Mo(4)-S(7)	2.5317(17)	Mo(9)-Se(17)	2.5423(9)
Mo(4)-Se(8)	2.5386(8)	Mo(9)-Se(18)	2.5949(10)
Mo(4)-Se(12)	2.5496(8)	Mo(9)-Se(20)	2.6062(9)
Mo(4)-Se(13)	2.5998(9)	Se(1)-Se(2)	2.3143(12)
Mo(4)-Se(9)	2.6059(9)	Se(3)-Se(4)	2.3254(13)
Mo(4)-Mo(6)	2.7603(7)	Se(5)-Se(6)	2.3130(10)
Mo(4)-Mo(5)	2.7712(7)	Se(8)-Se(9)	2.3146(10)
Mo(5)-Se(14)	2.4665(10)	Se(10)-Se(11)	2.3070(9)
Mo(5)-S(10)	2.4855(16)	Se(12)-Se(13)	2.3182(10)
Mo(5)-S(9)	2.5263(16)	Se(15)-Se(16)	2.3170(10)
Mo(5)-Se(8)	2.5350(8)	Se(17)-Se(18)	2.3127(12)
Mo(5)-Se(10)	2.5380(8)	Se(19)-Se(20)	2.3204(10)
Mo(5)-Se(9)	2.6049(9)	S(1)-C(1)	1.722(7)
Mo(5)-Se(11)	2.6063(9)	S(2)-C(1)	1.720(7)
Mo(5)-Mo(6)	2.7450(7)	S(3)-C(10)	1.707(9)
Mo(6)-Se(14)	2.4618(10)	S(4)-C(10)	1.731(8)
Mo(6)-S(12)	2.4724(17)	S(5)-C(19)	1.715(8)

Table A.33, Cont'd. Bond lengths (Å) for $[\text{Mo}_3\text{Se}_7(\text{S}_2\text{CN}^i\text{Bu}_2)_3]\text{I} \cdot \frac{1}{6}(\text{ClCH}_2\text{CH}_2\text{Cl}) \cdot \frac{1}{3}(\text{C}_5\text{H}_{10})$. Symmetry transformations used to generate equivalent atoms:

S(6)-C(19)	1.734(8)	C(2)-H(2B)	0.9900
S(7)-C(28)	1.729(7)	C(3)-C(5)	1.528(11)
S(8)-C(28)	1.726(7)	C(3)-C(4)	1.532(11)
S(9)-C(37)	1.714(7)	C(3)-H(3)	1.0000
S(10)-C(37)	1.718(7)	C(4)-H(4A)	0.9800
S(11)-C(46)	1.711(7)	C(4)-H(4B)	0.9800
S(12)-C(46)	1.717(7)	C(4)-H(4C)	0.9800
S(13)-C(55)	1.720(7)	C(5)-H(5A)	0.9800
S(14)-C(55)	1.719(7)	C(5)-H(5B)	0.9800
S(15)-C(64)	1.719(7)	C(5)-H(5C)	0.9800
S(16)-C(64)	1.721(7)	C(6)-C(7)	1.548(10)
S(17)-C(73)	1.705(7)	C(6)-H(6A)	0.9900
S(18)-C(73)	1.727(7)	C(6)-H(6B)	0.9900
N(1)-C(1)	1.331(8)	C(7)-C(8)	1.512(12)
N(1)-C(6)	1.465(9)	C(7)-C(9)	1.527(11)
N(1)-C(2)	1.489(8)	C(7)-H(7)	1.0000
N(2)-C(10)	1.341(10)	C(8)-H(8A)	0.9800
N(2)-C(11)	1.464(11)	C(8)-H(8B)	0.9800
N(2)-C(15)	1.489(11)	C(8)-H(8C)	0.9800
N(3)-C(19)	1.322(9)	C(9)-H(9A)	0.9800
N(3)-C(20)	1.462(10)	C(9)-H(9B)	0.9800
N(3)-C(24)	1.472(10)	C(9)-H(9C)	0.9800
N(4)-C(28)	1.310(8)	C(11)-C(12)	1.517(14)
N(4)-C(33)	1.470(9)	C(11)-H(11A)	0.9900
N(4)-C(29)	1.478(9)	C(11)-H(11B)	0.9900
N(5)-C(37)	1.332(8)	C(12)-C(13)	1.518(15)
N(5)-C(42)	1.460(9)	C(12)-C(14)	1.532(15)
N(5)-C(38)	1.474(9)	C(12)-H(12)	1.0000
N(6)-C(46)	1.335(9)	C(13)-H(13A)	0.9800
N(6)-C(51)	1.466(10)	C(13)-H(13B)	0.9800
N(6)-C(47)	1.466(10)	C(13)-H(13C)	0.9800
N(7)-C(55)	1.329(9)	C(14)-H(14A)	0.9800
N(7)-C(60)	1.465(9)	C(14)-H(14B)	0.9800
N(7)-C(56)	1.469(9)	C(14)-H(14C)	0.9800
N(8)-C(64)	1.326(8)	C(15)-C(16)	1.541(13)
N(8)-C(69)	1.454(9)	C(15)-H(15A)	0.9900
N(8)-C(65)	1.467(9)	C(15)-H(15B)	0.9900
N(9)-C(73)	1.335(9)	C(16)-C(18)	1.513(14)
N(9)-C(74)	1.457(9)	C(16)-C(17)	1.524(15)
N(9)-C(78)	1.466(10)	C(16)-H(16)	1.0000
C(2)-C(3)	1.520(10)	C(17)-H(17A)	0.9800
C(2)-H(2A)	0.9900	C(17)-H(17B)	0.9800

Table A.33, Cont'd. Bond lengths (Å) for $[\text{Mo}_3\text{Se}_7(\text{S}_2\text{CN}^i\text{Bu}_2)_3]\text{I} \cdot \frac{1}{6}(\text{ClCH}_2\text{CH}_2\text{Cl}) \cdot \frac{1}{3}(\text{C}_5\text{H}_{10})$. Symmetry transformations used to generate equivalent atoms:

C(17)-H(17C)	0.9800	C(30B)-C(32B)	1.56(5)
C(18)-H(18A)	0.9800	C(30B)-H(30B)	1.0000
C(18)-H(18B)	0.9800	C(31B)-H(31D)	0.9800
C(18)-H(18C)	0.9800	C(31B)-H(31E)	0.9800
C(20)-C(21)	1.529(13)	C(31B)-H(31F)	0.9800
C(20)-H(20A)	0.9900	C(32B)-H(32D)	0.9800
C(20)-H(20B)	0.9900	C(32B)-H(32E)	0.9800
C(21)-C(22)	1.493(14)	C(32B)-H(32F)	0.9800
C(21)-C(23)	1.544(13)	C(33)-C(34A)	1.47(2)
C(21)-H(21)	1.0000	C(33)-C(34B)	1.576(19)
C(22)-H(22A)	0.9800	C(33)-H(33A)	0.9900
C(22)-H(22B)	0.9800	C(33)-H(33B)	0.9900
C(22)-H(22C)	0.9800	C(34A)-C(35A)	1.50(3)
C(23)-H(23A)	0.9800	C(34A)-C(36A)	1.56(3)
C(23)-H(23B)	0.9800	C(34A)-H(34A)	1.0000
C(23)-H(23C)	0.9800	C(35A)-H(35A)	0.9800
C(24)-C(25)	1.537(12)	C(35A)-H(35B)	0.9800
C(24)-H(24A)	0.9900	C(35A)-H(35C)	0.9800
C(24)-H(24B)	0.9900	C(36A)-H(36A)	0.9800
C(25)-C(26)	1.502(14)	C(36A)-H(36B)	0.9800
C(25)-C(27)	1.534(12)	C(36A)-H(36C)	0.9800
C(25)-H(25)	1.0000	C(34B)-C(35B)	1.45(3)
C(26)-H(26A)	0.9800	C(34B)-C(36B)	1.58(3)
C(26)-H(26B)	0.9800	C(34B)-H(34B)	1.0000
C(26)-H(26C)	0.9800	C(35B)-H(35D)	0.9800
C(27)-H(27A)	0.9800	C(35B)-H(35E)	0.9800
C(27)-H(27B)	0.9800	C(35B)-H(35F)	0.9800
C(27)-H(27C)	0.9800	C(36B)-H(36D)	0.9800
C(29)-C(30B)	1.40(3)	C(36B)-H(36E)	0.9800
C(29)-C(30A)	1.571(16)	C(36B)-H(36F)	0.9800
C(29)-H(29A)	0.9900	C(38)-C(39)	1.526(11)
C(29)-H(29B)	0.9900	C(38)-H(38A)	0.9900
C(30A)-C(32A)	1.55(2)	C(38)-H(38B)	0.9900
C(30A)-C(31A)	1.56(2)	C(39)-C(40)	1.520(13)
C(30A)-H(30A)	1.0000	C(39)-C(41)	1.538(13)
C(31A)-H(31A)	0.9800	C(39)-H(39)	1.0000
C(31A)-H(31B)	0.9800	C(40)-H(40A)	0.9800
C(31A)-H(31C)	0.9800	C(40)-H(40B)	0.9800
C(32A)-H(32A)	0.9800	C(40)-H(40C)	0.9800
C(32A)-H(32B)	0.9800	C(41)-H(41A)	0.9800
C(32A)-H(32C)	0.9800	C(41)-H(41B)	0.9800
C(30B)-C(31B)	1.44(5)	C(41)-H(41C)	0.9800

Table A.33, Cont'd. Bond lengths (Å) for $[\text{Mo}_3\text{Se}_7(\text{S}_2\text{CN}^i\text{Bu}_2)_3]\text{I} \cdot \frac{1}{6}(\text{ClCH}_2\text{CH}_2\text{Cl}) \cdot \frac{1}{3}(\text{C}_5\text{H}_{10})$. Symmetry transformations used to generate equivalent atoms:

C(42)-C(43)	1.526(13)	C(58)-H(58A)	0.9800
C(42)-H(42A)	0.9900	C(58)-H(58B)	0.9800
C(42)-H(42B)	0.9900	C(58)-H(58C)	0.9800
C(43)-C(44)	1.509(13)	C(59)-H(59A)	0.9800
C(43)-C(45)	1.525(14)	C(59)-H(59B)	0.9800
C(43)-H(43)	1.0000	C(59)-H(59C)	0.9800
C(44)-H(44A)	0.9800	C(60)-C(61B)	1.53(3)
C(44)-H(44B)	0.9800	C(60)-C(61A)	1.569(15)
C(44)-H(44C)	0.9800	C(60)-H(60A)	0.9900
C(45)-H(45A)	0.9800	C(60)-H(60B)	0.9900
C(45)-H(45B)	0.9800	C(61A)-C(63A)	1.44(2)
C(45)-H(45C)	0.9800	C(61A)-C(62A)	1.58(2)
C(47)-C(48)	1.528(11)	C(61A)-H(61A)	1.0000
C(47)-H(47A)	0.9900	C(62A)-H(62A)	0.9800
C(47)-H(47B)	0.9900	C(62A)-H(62B)	0.9800
C(48)-C(49)	1.506(15)	C(62A)-H(62C)	0.9800
C(48)-C(50)	1.525(13)	C(63A)-H(63A)	0.9800
C(48)-H(48)	1.0000	C(63A)-H(63B)	0.9800
C(49)-H(49A)	0.9800	C(63A)-H(63C)	0.9800
C(49)-H(49B)	0.9800	C(61B)-C(63B)	1.55(5)
C(49)-H(49C)	0.9800	C(61B)-C(62B)	1.59(5)
C(50)-H(50A)	0.9800	C(61B)-H(61B)	1.0000
C(50)-H(50B)	0.9800	C(62B)-H(62D)	0.9800
C(50)-H(50C)	0.9800	C(62B)-H(62E)	0.9800
C(51)-C(52)	1.512(13)	C(62B)-H(62F)	0.9800
C(51)-H(51A)	0.9900	C(63B)-H(63D)	0.9800
C(51)-H(51B)	0.9900	C(63B)-H(63E)	0.9800
C(52)-C(53)	1.471(15)	C(63B)-H(63F)	0.9800
C(52)-C(54)	1.547(15)	C(65)-C(66)	1.526(12)
C(52)-H(52A)	1.0000	C(65)-H(65A)	0.9900
C(53)-H(53A)	0.9800	C(65)-H(65B)	0.9900
C(53)-H(53B)	0.9800	C(66)-C(67)	1.479(16)
C(53)-H(53C)	0.9800	C(66)-C(68)	1.522(15)
C(54)-H(54A)	0.9800	C(66)-H(66)	1.0000
C(54)-H(54B)	0.9800	C(67)-H(67A)	0.9800
C(54)-H(54C)	0.9800	C(67)-H(67B)	0.9800
C(56)-C(57)	1.544(13)	C(67)-H(67C)	0.9800
C(56)-H(56A)	0.9900	C(68)-H(68A)	0.9800
C(56)-H(56B)	0.9900	C(68)-H(68B)	0.9800
C(57)-C(58)	1.503(18)	C(68)-H(68C)	0.9800
C(57)-C(59)	1.556(15)	C(69)-C(70)	1.521(10)
C(57)-H(57)	1.0000	C(69)-H(69A)	0.9900

Table A.33, Cont'd. Bond lengths (Å) for $[\text{Mo}_3\text{Se}_7(\text{S}_2\text{CN}^i\text{Bu}_2)_3]\text{I} \cdot \frac{1}{6}(\text{ClCH}_2\text{CH}_2\text{Cl}) \cdot \frac{1}{3}(\text{C}_5\text{H}_{10})$. Symmetry transformations used to generate equivalent atoms:

C(69)-H(69B)	0.9900	C(70)-H(70)	1.0000
C(70)-C(72)	1.496(15)	C(71)-H(71A)	0.9800
C(70)-C(71)	1.503(12)	C(71)-H(71B)	0.9800
C(71)-H(71C)	0.9800	C(82)-C(84)	1.21(4)
C(72)-H(72A)	0.9800	C(82)-C(85)	1.51(7)
C(72)-H(72B)	0.9800	C(83)-C(84)	1.42(4)
C(72)-H(72C)	0.9800	C(83)-C(85)	1.89(7)
C(74)-C(75B)	1.47(2)	C(84)-C(85)	0.59(7)
C(74)-C(75A)	1.63(2)	C(84)-C(86)	1.66(4)
C(74)-H(74A)	0.9900	C(85)-C(86)	1.13(6)
C(74)-H(74B)	0.9900	C(86)-C(87)	1.53(4)
C(75A)-C(77A)	1.44(3)	C(87)-C(88)	1.08(4)
C(75A)-C(76A)	1.52(3)	C(87)-C(90)	1.32(5)
C(75A)-H(75A)	1.0000	C(87)-C(89)	1.86(4)
C(76A)-H(76A)	0.9800	C(88)-C(89)	0.96(4)
C(76A)-H(76B)	0.9800	C(88)-C(90)	1.70(5)
C(76A)-H(76C)	0.9800	C(90)-C(91)	1.64(5)
C(77A)-H(77A)	0.9800	C(92)-C(93)	1.40(5)
C(77A)-H(77B)	0.9800	C(92)-Cl(1)	1.49(4)
C(77A)-H(77C)	0.9800	C(92)-H(92A)	0.9900
C(75B)-C(77B)	1.51(3)	C(92)-H(92B)	0.9900
C(75B)-C(76B)	1.52(3)	C(93)-Cl(2)	1.71(4)
C(75B)-H(75B)	1.0000	C(93)-H(93A)	0.9900
C(76B)-H(76D)	0.9800	C(93)-H(93B)	0.9900
C(76B)-H(76E)	0.9800		
C(76B)-H(76F)	0.9800		
C(77B)-H(77D)	0.9800		
C(77B)-H(77E)	0.9800		
C(77B)-H(77F)	0.9800		
C(78)-C(79)	1.537(15)		
C(78)-H(78A)	0.9900		
C(78)-H(78B)	0.9900		
C(79)-C(81)	1.487(18)		
C(79)-C(80)	1.509(16)		
C(79)-H(79)	1.0000		
C(80)-H(80A)	0.9800		
C(80)-H(80B)	0.9800		
C(80)-H(80C)	0.9800		
C(81)-H(81A)	0.9800		
C(81)-H(81B)	0.9800		
C(81)-H(81C)	0.9800		
C(82)-C(83)	0.68(3)		

Table A.34. Bond angles (deg.) for $[\text{Mo}_3\text{Se}_7(\text{S}_2\text{CN}^i\text{Bu}_2)_3]\text{I} \cdot \frac{1}{6}(\text{ClCH}_2\text{CH}_2\text{Cl}) \cdot \frac{1}{3}(\text{C}_5\text{H}_{10})$. Symmetry transformations used to generate equivalent atoms:

Se(7)-Mo(1)-S(2)	81.38(5)	S(4)-Mo(2)-Se(1)	131.53(6)
Se(7)-Mo(1)-S(1)	151.31(5)	S(3)-Mo(2)-Se(1)	84.59(6)
S(2)-Mo(1)-S(1)	69.94(6)	Se(3)-Mo(2)-Se(1)	83.74(3)
Se(7)-Mo(1)-Se(5)	113.15(4)	Se(7)-Mo(2)-Se(2)	84.05(4)
S(2)-Mo(1)-Se(5)	135.52(5)	S(4)-Mo(2)-Se(2)	86.70(6)
S(1)-Mo(1)-Se(5)	88.94(5)	S(3)-Mo(2)-Se(2)	93.17(6)
Se(7)-Mo(1)-Se(1)	112.82(4)	Se(3)-Mo(2)-Se(2)	137.01(4)
S(2)-Mo(1)-Se(1)	132.97(5)	Se(1)-Mo(2)-Se(2)	53.54(3)
S(1)-Mo(1)-Se(1)	87.32(5)	Se(7)-Mo(2)-Se(4)	82.75(4)
Se(5)-Mo(1)-Se(1)	81.90(3)	S(4)-Mo(2)-Se(4)	87.63(6)
Se(7)-Mo(1)-Se(2)	84.34(4)	S(3)-Mo(2)-Se(4)	96.82(6)
S(2)-Mo(1)-Se(2)	85.91(5)	Se(3)-Mo(2)-Se(4)	53.75(3)
S(1)-Mo(1)-Se(2)	92.61(5)	Se(1)-Mo(2)-Se(4)	137.13(4)
Se(5)-Mo(1)-Se(2)	135.28(3)	Se(2)-Mo(2)-Se(4)	166.02(4)
Se(1)-Mo(1)-Se(2)	53.58(3)	Se(7)-Mo(2)-Mo(1)	56.09(3)
Se(7)-Mo(1)-Se(6)	85.53(3)	S(4)-Mo(2)-Mo(1)	127.26(6)
S(2)-Mo(1)-Se(6)	88.55(5)	S(3)-Mo(2)-Mo(1)	140.69(6)
S(1)-Mo(1)-Se(6)	94.31(5)	Se(3)-Mo(2)-Mo(1)	97.55(3)
Se(5)-Mo(1)-Se(6)	53.39(3)	Se(1)-Mo(2)-Mo(1)	57.33(2)
Se(1)-Mo(1)-Se(6)	135.16(3)	Se(2)-Mo(2)-Mo(1)	57.78(3)
Se(2)-Mo(1)-Se(6)	169.09(4)	Se(4)-Mo(2)-Mo(1)	117.15(3)
Se(7)-Mo(1)-Mo(3)	56.17(3)	Se(7)-Mo(2)-Mo(1)	55.89(3)
S(2)-Mo(1)-Mo(3)	125.42(5)	S(4)-Mo(2)-Mo(3)	128.48(6)
S(1)-Mo(1)-Mo(3)	144.78(5)	S(3)-Mo(2)-Mo(3)	143.25(6)
Se(5)-Mo(1)-Mo(3)	57.46(2)	Se(3)-Mo(2)-Mo(3)	57.29(3)
Se(1)-Mo(1)-Mo(3)	97.04(3)	Se(1)-Mo(2)-Mo(3)	96.75(3)
Se(2)-Mo(1)-Mo(3)	118.06(3)	Se(2)-Mo(2)-Mo(3)	117.15(3)
Se(6)-Mo(1)-Mo(3)	58.49(2)	Se(4)-Mo(2)-Mo(3)	57.95(3)
Se(7)-Mo(1)-Mo(2)	56.28(3)	Mo(1)-Mo(2)-Mo(3)	59.72(2)
S(2)-Mo(1)-Mo(2)	124.25(5)	Se(7)-Mo(3)-S(6)	82.31(5)
S(1)-Mo(1)-Mo(2)	142.53(5)	Se(7)-Mo(3)-S(5)	151.93(6)
Se(5)-Mo(1)-Mo(2)	96.54(3)	S(6)-Mo(3)-S(5)	69.92(6)
Se(1)-Mo(1)-Mo(2)	57.14(2)	Se(7)-Mo(3)-Se(3)	112.25(4)
Se(2)-Mo(1)-Mo(2)	58.10(3)	S(6)-Mo(3)-Se(3)	135.25(6)
Se(6)-Mo(1)-Mo(2)	118.60(3)	S(5)-Mo(3)-Se(3)	86.14(6)
Mo(3)-Mo(1)-Mo(2)	60.31(2)	Se(7)-Mo(3)-Se(5)	113.11(4)
Se(7)-Mo(2)-S(4)	85.24(6)	S(6)-Mo(3)-Se(5)	131.72(6)
Se(7)-Mo(2)-S(3)	154.85(6)	S(5)-Mo(3)-Se(5)	89.28(6)
S(4)-Mo(2)-S(3)	69.63(7)	Se(3)-Mo(3)-Se(5)	82.98(3)
Se(7)-Mo(2)-Se(3)	112.36(4)	Se(7)-Mo(3)-Se(4)	82.96(4)
S(4)-Mo(2)-Se(3)	132.24(6)	S(6)-Mo(3)-Se(4)	89.11(6)
S(3)-Mo(2)-Se(3)	86.58(6)	S(5)-Mo(3)-Se(4)	92.40(6)
Se(7)-Mo(2)-Se(1)	112.83(4)	Se(3)-Mo(3)-Se(4)	53.66(3)

Table A.34, Cont'd. Bond angles (deg.) for $[\text{Mo}_3\text{Se}_7(\text{S}_2\text{CN}^i\text{Bu}_2)_3]\text{I} \cdot \frac{1}{6}(\text{ClCH}_2\text{CH}_2\text{Cl}) \cdot \frac{1}{3}(\text{C}_5\text{H}_{10})$. Symmetry transformations used to generate equivalent atoms:

Se(5)-Mo(3)-Se(4)	136.32(4)	Se(13)-Mo(4)-Se(9)	166.57(3)
Se(7)-Mo(3)-Se(6)	85.31(3)	Se(14)-Mo(4)-Mo(6)	55.82(3)
S(6)-Mo(3)-Se(6)	85.19(6)	S(8)-Mo(4)-Mo(6)	126.12(4)
S(5)-Mo(3)-Se(6)	96.01(6)	S(7)-Mo(4)-Mo(6)	142.43(5)
Se(3)-Mo(3)-Se(6)	135.99(4)	Se(8)-Mo(4)-Mo(6)	96.75(2)
Se(5)-Mo(3)-Se(6)	53.20(3)	Se(12)-Mo(4)-Mo(6)	56.97(2)
Se(4)-Mo(3)-Se(6)	167.55(4)	Se(13)-Mo(4)-Mo(6)	57.89(2)
Se(7)-Mo(3)-Mo(1)	56.27(3)	Se(9)-Mo(4)-Mo(6)	116.92(3)
S(6)-Mo(3)-Mo(1)	123.87(5)	Se(14)-Mo(4)-Mo(5)	55.79(3)
S(5)-Mo(3)-Mo(1)	145.36(6)	S(8)-Mo(4)-Mo(5)	127.52(4)
Se(3)-Mo(3)-Mo(1)	97.45(3)	S(7)-Mo(4)-Mo(5)	143.38(5)
Se(5)-Mo(3)-Mo(1)	57.32(2)	Se(8)-Mo(4)-Mo(5)	56.83(2)
Se(4)-Mo(3)-Mo(1)	117.49(3)	Se(12)-Mo(4)-Mo(5)	96.28(2)
Se(6)-Mo(3)-Mo(1)	58.03(2)	Se(13)-Mo(4)-Mo(5)	117.06(3)
Se(7)-Mo(3)-Mo(2)	56.17(3)	Se(9)-Mo(4)-Mo(5)	57.85(2)
S(6)-Mo(3)-Mo(2)	127.47(6)	Mo(6)-Mo(4)-Mo(5)	59.505(18)
S(5)-Mo(3)-Mo(2)	141.34(6)	Se(14)-Mo(5)-S(10)	83.44(5)
Se(3)-Mo(3)-Mo(2)	56.89(3)	Se(14)-Mo(5)-S(9)	153.17(5)
Se(5)-Mo(3)-Mo(2)	96.22(3)	S(10)-Mo(5)-S(9)	69.73(5)
Se(4)-Mo(3)-Mo(2)	58.03(3)	Se(14)-Mo(5)-Se(8)	112.16(3)
Se(6)-Mo(3)-Mo(2)	117.80(3)	S(10)-Mo(5)-Se(8)	132.99(5)
Mo(1)-Mo(3)-Mo(2)	59.97(2)	S(9)-Mo(5)-Se(8)	87.77(4)
Se(14)-Mo(4)-S(8)	84.00(4)	Se(14)-Mo(5)-Se(10)	112.91(3)
Se(14)-Mo(4)-S(7)	153.59(5)	S(10)-Mo(5)-Se(10)	132.68(5)
S(8)-Mo(4)-S(7)	69.59(5)	S(9)-Mo(5)-Se(10)	86.15(5)
Se(14)-Mo(4)-Se(8)	111.92(3)	Se(8)-Mo(5)-Se(10)	83.47(3)
S(8)-Mo(4)-Se(8)	133.67(5)	Se(14)-Mo(5)-Se(9)	83.34(3)
S(7)-Mo(4)-Se(8)	87.57(5)	S(10)-Mo(5)-Se(9)	87.19(5)
Se(14)-Mo(4)-Se(12)	112.22(3)	S(9)-Mo(5)-Se(9)	95.64(5)
S(8)-Mo(4)-Se(12)	132.28(5)	Se(8)-Mo(5)-Se(9)	53.51(2)
S(7)-Mo(4)-Se(12)	86.79(5)	Se(10)-Mo(5)-Se(9)	136.71(3)
Se(8)-Mo(4)-Se(12)	83.29(3)	Se(14)-Mo(5)-Se(11)	84.47(3)
Se(14)-Mo(4)-Se(13)	83.96(3)	S(10)-Mo(5)-Se(11)	87.09(5)
S(8)-Mo(4)-Se(13)	86.43(5)	S(9)-Mo(5)-Se(11)	93.26(5)
S(7)-Mo(4)-Se(13)	94.04(5)	Se(8)-Mo(5)-Se(11)	136.47(3)
Se(8)-Mo(4)-Se(13)	136.50(3)	Se(10)-Mo(5)-Se(11)	53.27(2)
Se(12)-Mo(4)-Se(13)	53.50(3)	Se(9)-Mo(5)-Se(11)	167.05(3)
Se(14)-Mo(4)-Se(9)	83.25(3)	Se(14)-Mo(5)-Mo(6)	56.07(3)
S(8)-Mo(4)-Se(9)	88.17(5)	S(10)-Mo(5)-Mo(6)	126.09(4)
S(7)-Mo(4)-Se(9)	95.58(5)	S(9)-Mo(5)-Mo(6)	142.09(5)
Se(8)-Mo(4)-Se(9)	53.46(2)	Se(8)-Mo(5)-Mo(6)	97.22(2)
Se(12)-Mo(4)-Se(9)	136.41(3)	Se(10)-Mo(5)-Mo(6)	57.43(2)

Table A.34, Cont'd. Bond angles (deg.) for $[\text{Mo}_3\text{Se}_7(\text{S}_2\text{CN}^i\text{Bu}_2)_3]\cdot\frac{1}{6}(\text{ClCH}_2\text{CH}_2\text{Cl})\cdot\frac{1}{3}(\text{C}_5\text{H}_{10})$. Symmetry transformations used to generate equivalent atoms:

Se(9)-Mo(5)-Mo(6)	117.50(3)	Se(11)-Mo(5)-Mo(6)	57.91(2)
Se(14)-Mo(5)-Mo(4)	55.91(2)	Se(11)-Mo(6)-Mo(4)	118.50(3)
S(10)-Mo(5)-Mo(4)	126.60(5)	Se(13)-Mo(6)-Mo(4)	57.96(2)
S(9)-Mo(5)-Mo(4)	143.66(5)	Mo(5)-Mo(6)-Mo(4)	60.446(18)
Se(8)-Mo(5)-Mo(4)	56.95(2)	Se(21)-Mo(7)-S(14)	83.49(5)
Se(10)-Mo(5)-Mo(4)	97.06(2)	Se(21)-Mo(7)-S(13)	152.69(5)
Se(9)-Mo(5)-Mo(4)	57.89(2)	S(14)-Mo(7)-S(13)	69.28(6)
Se(11)-Mo(5)-Mo(4)	117.65(3)	Se(21)-Mo(7)-Se(17)	112.74(3)
Mo(6)-Mo(5)-Mo(4)	60.049(18)	S(14)-Mo(7)-Se(17)	131.79(5)
Se(14)-Mo(6)-S(12)	81.48(5)	S(13)-Mo(7)-Se(17)	88.05(5)
Se(14)-Mo(6)-S(11)	151.26(5)	Se(21)-Mo(7)-Se(15)	112.70(4)
S(12)-Mo(6)-S(11)	69.98(6)	S(14)-Mo(7)-Se(15)	133.72(5)
Se(14)-Mo(6)-Se(12)	112.85(3)	S(13)-Mo(7)-Se(15)	86.17(5)
S(12)-Mo(6)-Se(12)	132.10(5)	Se(17)-Mo(7)-Se(15)	83.36(3)
S(11)-Mo(6)-Se(12)	89.62(5)	Se(21)-Mo(7)-Se(16)	83.76(3)
Se(14)-Mo(6)-Se(10)	112.85(3)	S(14)-Mo(7)-Se(16)	87.98(5)
S(12)-Mo(6)-Se(10)	135.50(5)	S(13)-Mo(7)-Se(16)	93.02(5)
S(11)-Mo(6)-Se(10)	86.59(4)	Se(17)-Mo(7)-Se(16)	136.81(3)
Se(12)-Mo(6)-Se(10)	82.81(3)	Se(15)-Mo(7)-Se(16)	53.71(3)
Se(14)-Mo(6)-Se(11)	84.84(3)	Se(21)-Mo(7)-Se(18)	83.85(3)
S(12)-Mo(6)-Se(11)	88.76(5)	S(14)-Mo(7)-Se(18)	85.96(5)
S(11)-Mo(6)-Se(11)	91.11(5)	S(13)-Mo(7)-Se(18)	95.83(5)
Se(12)-Mo(6)-Se(11)	136.00(3)	Se(17)-Mo(7)-Se(18)	53.60(3)
Se(10)-Mo(6)-Se(11)	53.35(2)	Se(15)-Mo(7)-Se(18)	136.70(3)
Se(14)-Mo(6)-Se(13)	84.17(3)	Se(16)-Mo(7)-Se(18)	166.74(3)
S(12)-Mo(6)-Se(13)	85.08(5)	Se(21)-Mo(7)-Mo(8)	56.33(3)
S(11)-Mo(6)-Se(13)	96.33(5)	S(14)-Mo(7)-Mo(8)	127.57(5)
Se(12)-Mo(6)-Se(13)	53.63(3)	S(13)-Mo(7)-Mo(8)	141.83(5)
Se(10)-Mo(6)-Se(13)	136.22(3)	Se(17)-Mo(7)-Mo(8)	96.76(3)
Se(11)-Mo(6)-Se(13)	168.08(3)	Se(15)-Mo(7)-Mo(8)	57.10(2)
Se(14)-Mo(6)-Mo(5)	56.23(3)	Se(16)-Mo(7)-Mo(8)	58.28(2)
S(12)-Mo(6)-Mo(5)	125.97(4)	Se(18)-Mo(7)-Mo(8)	117.44(3)
S(11)-Mo(6)-Mo(5)	141.62(5)	Se(21)-Mo(7)-Mo(9)	56.23(3)
Se(12)-Mo(6)-Mo(5)	97.18(2)	S(14)-Mo(7)-Mo(9)	125.90(5)
Se(10)-Mo(6)-Mo(5)	57.20(2)	S(13)-Mo(7)-Mo(9)	144.11(5)
Se(11)-Mo(6)-Mo(5)	58.36(2)	Se(17)-Mo(7)-Mo(9)	57.15(2)
Se(13)-Mo(6)-Mo(5)	118.06(3)	Se(15)-Mo(7)-Mo(9)	97.13(3)
Se(14)-Mo(6)-Mo(4)	56.11(3)	Se(16)-Mo(7)-Mo(9)	117.72(3)
S(12)-Mo(6)-Mo(4)	123.65(5)	Se(18)-Mo(7)-Mo(9)	57.92(3)
S(11)-Mo(6)-Mo(4)	145.65(5)	Mo(8)-Mo(7)-Mo(9)	59.874(19)
Se(12)-Mo(6)-Mo(4)	57.33(2)	Se(21)-Mo(8)-S(16)	83.76(5)
Se(10)-Mo(6)-Mo(4)	97.18(2)	Se(21)-Mo(8)-S(15)	153.44(5)

Table A.34, Cont'd. Bond angles (deg.) for $[\text{Mo}_3\text{Se}_7(\text{S}_2\text{CN}^i\text{Bu}_2)_3]\cdot\frac{1}{6}(\text{ClCH}_2\text{CH}_2\text{Cl})\cdot\frac{1}{3}(\text{C}_5\text{H}_{10})$. Symmetry transformations used to generate equivalent atoms:

S(16)-Mo(8)-S(15)	69.76(6)	Se(21)-Mo(8)-Se(15)	112.40(3)
S(16)-Mo(8)-Se(15)	132.26(5)	S(15)-Mo(8)-Se(15)	88.05(5)
Se(21)-Mo(8)-Se(19)	112.58(3)	Se(21)-Mo(9)-Se(18)	83.61(3)
S(16)-Mo(8)-Se(19)	133.12(5)	S(18)-Mo(9)-Se(18)	87.64(6)
S(15)-Mo(8)-Se(19)	85.47(5)	S(17)-Mo(9)-Se(18)	93.41(5)
Se(15)-Mo(8)-Se(19)	83.54(3)	Se(19)-Mo(9)-Se(18)	136.18(3)
Se(21)-Mo(8)-Se(20)	84.26(3)	Se(17)-Mo(9)-Se(18)	53.50(3)
S(16)-Mo(8)-Se(20)	87.25(5)	Se(21)-Mo(9)-Se(20)	84.30(3)
S(15)-Mo(8)-Se(20)	92.16(5)	S(18)-Mo(9)-Se(20)	86.77(5)
Se(15)-Mo(8)-Se(20)	136.89(3)	S(17)-Mo(9)-Se(20)	95.48(5)
Se(19)-Mo(8)-Se(20)	53.57(2)	Se(19)-Mo(9)-Se(20)	53.66(3)
Se(21)-Mo(8)-Se(16)	83.12(3)	Se(17)-Mo(9)-Se(20)	136.32(3)
S(16)-Mo(8)-Se(16)	86.93(5)	Se(18)-Mo(9)-Se(20)	167.19(3)
S(15)-Mo(8)-Se(16)	97.13(5)	Se(21)-Mo(9)-Mo(8)	56.34(3)
Se(15)-Mo(8)-Se(16)	53.47(3)	S(18)-Mo(9)-Mo(8)	126.30(5)
Se(19)-Mo(8)-Se(16)	136.64(3)	S(17)-Mo(9)-Mo(8)	143.65(5)
Se(20)-Mo(8)-Se(16)	166.61(3)	Se(19)-Mo(9)-Mo(8)	57.31(2)
Se(21)-Mo(8)-Mo(9)	56.21(3)	Se(17)-Mo(9)-Mo(8)	96.81(3)
S(16)-Mo(8)-Mo(9)	126.82(4)	Se(18)-Mo(9)-Mo(8)	117.44(3)
S(15)-Mo(8)-Mo(9)	140.86(5)	Se(20)-Mo(9)-Mo(8)	58.05(2)
Se(15)-Mo(8)-Mo(9)	97.29(3)	Se(21)-Mo(9)-Mo(7)	56.02(3)
Se(19)-Mo(8)-Mo(9)	56.96(2)	S(18)-Mo(9)-Mo(7)	126.68(5)
Se(20)-Mo(8)-Mo(9)	58.11(2)	S(17)-Mo(9)-Mo(7)	141.72(5)
Se(16)-Mo(8)-Mo(9)	117.17(3)	Se(19)-Mo(9)-Mo(7)	97.05(3)
Se(21)-Mo(8)-Mo(7)	55.99(3)	Se(17)-Mo(9)-Mo(7)	57.03(2)
S(16)-Mo(8)-Mo(7)	126.57(5)	Se(18)-Mo(9)-Mo(7)	57.74(2)
S(15)-Mo(8)-Mo(7)	144.34(5)	Se(20)-Mo(9)-Mo(7)	117.74(3)
Se(15)-Mo(8)-Mo(7)	57.13(2)	Mo(8)-Mo(9)-Mo(7)	60.06(2)
Se(19)-Mo(8)-Mo(7)	96.82(3)	Se(2)-Se(1)-Mo(2)	64.49(3)
Se(20)-Mo(8)-Mo(7)	117.81(3)	Se(2)-Se(1)-Mo(1)	64.15(3)
Se(16)-Mo(8)-Mo(7)	57.53(2)	Mo(2)-Se(1)-Mo(1)	65.53(3)
Mo(9)-Mo(8)-Mo(7)	60.07(2)	Se(1)-Se(2)-Mo(1)	62.27(3)
Se(21)-Mo(9)-S(18)	83.39(5)	Se(1)-Se(2)-Mo(2)	61.97(3)
Se(21)-Mo(9)-S(17)	153.24(5)	Mo(1)-Se(2)-Mo(2)	64.12(3)
S(18)-Mo(9)-S(17)	69.90(6)	Se(4)-Se(3)-Mo(2)	64.68(3)
Se(21)-Mo(9)-Se(19)	113.05(3)	Se(4)-Se(3)-Mo(3)	64.42(3)
S(18)-Mo(9)-Se(19)	132.65(6)	Mo(2)-Se(3)-Mo(3)	65.82(3)
S(17)-Mo(9)-Se(19)	87.40(5)	Se(3)-Se(4)-Mo(3)	61.93(3)
Se(21)-Mo(9)-Se(17)	112.40(3)	Se(3)-Se(4)-Mo(2)	61.57(3)
S(18)-Mo(9)-Se(17)	133.39(6)	Mo(3)-Se(4)-Mo(2)	64.02(3)
S(17)-Mo(9)-Se(17)	86.13(5)	Se(6)-Se(5)-Mo(1)	64.59(3)
Se(19)-Mo(9)-Se(17)	82.93(3)	Se(6)-Se(5)-Mo(3)	64.88(3)

Table A.34, Cont'd. Bond angles (deg.) for $[\text{Mo}_3\text{Se}_7(\text{S}_2\text{CN}^i\text{Bu}_2)_3]\text{I} \cdot \frac{1}{6}(\text{ClCH}_2\text{CH}_2\text{Cl}) \cdot \frac{1}{3}(\text{C}_5\text{H}_{10})$. Symmetry transformations used to generate equivalent atoms:

Mo(1)-Se(5)-Mo(3)	65.22(2)	Se(5)-Se(6)-Mo(1)	62.03(3)
Se(5)-Se(6)-Mo(3)	61.93(3)	Mo(3)-Se(7)-Mo(1)	67.57(3)
Mo(1)-Se(6)-Mo(3)	63.48(2)	Mo(3)-Se(7)-Mo(2)	67.94(4)
Mo(1)-Se(7)-Mo(2)	67.64(4)	Mo(8)-Se(20)-Mo(9)	63.84(2)
Se(9)-Se(8)-Mo(5)	64.79(3)	Mo(7)-Se(21)-Mo(9)	67.75(3)
Se(9)-Se(8)-Mo(4)	64.76(3)	Mo(7)-Se(21)-Mo(8)	67.68(3)
Mo(5)-Se(8)-Mo(4)	66.21(2)	Mo(9)-Se(21)-Mo(8)	67.45(3)
Se(8)-Se(9)-Mo(5)	61.70(3)	C(1)-S(1)-Mo(1)	87.7(2)
Se(8)-Se(9)-Mo(4)	61.78(3)	C(1)-S(2)-Mo(1)	88.9(2)
Mo(5)-Se(9)-Mo(4)	64.26(2)	C(10)-S(3)-Mo(2)	88.7(3)
Se(11)-Se(10)-Mo(5)	64.88(3)	C(10)-S(4)-Mo(2)	89.0(3)
Se(11)-Se(10)-Mo(6)	64.41(3)	C(19)-S(5)-Mo(3)	88.4(2)
Mo(5)-Se(10)-Mo(6)	65.38(2)	C(19)-S(6)-Mo(3)	89.2(3)
Se(10)-Se(11)-Mo(6)	62.24(3)	C(28)-S(7)-Mo(4)	88.4(2)
Se(10)-Se(11)-Mo(5)	61.85(3)	C(28)-S(8)-Mo(4)	89.9(2)
Mo(6)-Se(11)-Mo(5)	63.73(2)	C(37)-S(9)-Mo(5)	87.9(2)
Se(13)-Se(12)-Mo(6)	64.47(3)	C(37)-S(10)-Mo(5)	89.1(2)
Se(13)-Se(12)-Mo(4)	64.36(3)	C(46)-S(11)-Mo(6)	87.5(2)
Mo(6)-Se(12)-Mo(4)	65.69(2)	C(46)-S(12)-Mo(6)	89.0(2)
Se(12)-Se(13)-Mo(6)	61.89(3)	C(55)-S(13)-Mo(7)	88.7(2)
Se(12)-Se(13)-Mo(4)	62.14(3)	C(55)-S(14)-Mo(7)	90.0(3)
Mo(6)-Se(13)-Mo(4)	64.16(2)	C(64)-S(15)-Mo(8)	88.0(2)
Mo(6)-Se(14)-Mo(5)	67.70(3)	C(64)-S(16)-Mo(8)	89.1(2)
Mo(6)-Se(14)-Mo(4)	68.07(3)	C(73)-S(17)-Mo(9)	87.8(2)
Mo(5)-Se(14)-Mo(4)	68.30(3)	C(73)-S(18)-Mo(9)	88.7(2)
Se(16)-Se(15)-Mo(8)	64.74(3)	C(1)-N(1)-C(6)	121.2(6)
Se(16)-Se(15)-Mo(7)	64.13(3)	C(1)-N(1)-C(2)	120.6(6)
Mo(8)-Se(15)-Mo(7)	65.78(2)	C(6)-N(1)-C(2)	117.7(5)
Se(15)-Se(16)-Mo(7)	62.16(3)	C(10)-N(2)-C(11)	121.4(7)
Se(15)-Se(16)-Mo(8)	61.79(3)	C(10)-N(2)-C(15)	118.8(7)
Mo(7)-Se(16)-Mo(8)	64.19(2)	C(11)-N(2)-C(15)	116.8(6)
Se(18)-Se(17)-Mo(7)	64.32(3)	C(19)-N(3)-C(20)	123.5(7)
Se(18)-Se(17)-Mo(9)	64.41(3)	C(19)-N(3)-C(24)	119.9(7)
Mo(7)-Se(17)-Mo(9)	65.81(2)	C(20)-N(3)-C(24)	116.6(6)
Se(17)-Se(18)-Mo(7)	62.08(3)	C(28)-N(4)-C(33)	121.9(6)
Se(17)-Se(18)-Mo(9)	62.09(3)	C(28)-N(4)-C(29)	120.6(6)
Mo(7)-Se(18)-Mo(9)	64.34(3)	C(33)-N(4)-C(29)	117.5(6)
Se(20)-Se(19)-Mo(9)	64.78(3)	C(37)-N(5)-C(42)	120.5(6)
Se(20)-Se(19)-Mo(8)	64.56(3)	C(37)-N(5)-C(38)	121.3(6)
Mo(9)-Se(19)-Mo(8)	65.73(2)	C(42)-N(5)-C(38)	118.0(6)
Se(19)-Se(20)-Mo(8)	61.87(3)	C(46)-N(6)-C(51)	119.9(6)
Se(19)-Se(20)-Mo(9)	61.57(3)	C(46)-N(6)-C(47)	120.6(6)

Table A.34, Cont'd. Bond angles (deg.) for $[\text{Mo}_3\text{Se}_7(\text{S}_2\text{CN}^i\text{Bu}_2)_3]\text{I} \cdot \frac{1}{6}(\text{ClCH}_2\text{CH}_2\text{Cl}) \cdot \frac{1}{3}(\text{C}_5\text{H}_{10})$. Symmetry transformations used to generate equivalent atoms:

C(51)-N(6)-C(47)	119.4(6)	C(55)-N(7)-C(60)	121.2(6)
C(55)-N(7)-C(56)	121.8(6)	C(64)-N(8)-C(65)	120.2(6)
C(60)-N(7)-C(56)	117.0(6)	C(69)-N(8)-C(65)	117.7(6)
C(64)-N(8)-C(69)	122.1(6)	C(73)-N(9)-C(74)	121.4(6)
C(73)-N(9)-C(78)	120.0(6)	C(8)-C(7)-H(7)	108.4
C(74)-N(9)-C(78)	118.6(6)	C(9)-C(7)-H(7)	108.4
N(1)-C(1)-S(2)	124.2(5)	C(6)-C(7)-H(7)	108.4
N(1)-C(1)-S(1)	123.5(5)	C(7)-C(8)-H(8A)	109.5
S(2)-C(1)-S(1)	112.3(4)	C(7)-C(8)-H(8B)	109.5
N(1)-C(2)-C(3)	115.1(6)	H(8A)-C(8)-H(8B)	109.5
N(1)-C(2)-H(2A)	108.5	C(7)-C(8)-H(8C)	109.5
C(3)-C(2)-H(2A)	108.5	H(8A)-C(8)-H(8C)	109.5
N(1)-C(2)-H(2B)	108.5	H(8B)-C(8)-H(8C)	109.5
C(3)-C(2)-H(2B)	108.5	C(7)-C(9)-H(9A)	109.5
H(2A)-C(2)-H(2B)	107.5	C(7)-C(9)-H(9B)	109.5
C(2)-C(3)-C(5)	112.7(6)	H(9A)-C(9)-H(9B)	109.5
C(2)-C(3)-C(4)	108.2(6)	C(7)-C(9)-H(9C)	109.5
C(5)-C(3)-C(4)	110.5(7)	H(9A)-C(9)-H(9C)	109.5
C(2)-C(3)-H(3)	108.4	H(9B)-C(9)-H(9C)	109.5
C(5)-C(3)-H(3)	108.4	N(2)-C(10)-S(3)	123.7(7)
C(4)-C(3)-H(3)	108.4	N(2)-C(10)-S(4)	123.6(7)
C(3)-C(4)-H(4A)	109.5	S(3)-C(10)-S(4)	112.7(5)
C(3)-C(4)-H(4B)	109.5	N(2)-C(11)-C(12)	115.5(8)
H(4A)-C(4)-H(4B)	109.5	N(2)-C(11)-H(11A)	108.4
C(3)-C(4)-H(4C)	109.5	C(12)-C(11)-H(11A)	108.4
H(4A)-C(4)-H(4C)	109.5	N(2)-C(11)-H(11B)	108.4
H(4B)-C(4)-H(4C)	109.5	C(12)-C(11)-H(11B)	108.4
C(3)-C(5)-H(5A)	109.5	H(11A)-C(11)-H(11B)	107.5
C(3)-C(5)-H(5B)	109.5	C(11)-C(12)-C(13)	112.4(8)
H(5A)-C(5)-H(5B)	109.5	C(11)-C(12)-C(14)	107.9(9)
C(3)-C(5)-H(5C)	109.5	C(13)-C(12)-C(14)	109.6(10)
H(5A)-C(5)-H(5C)	109.5	C(11)-C(12)-H(12)	109.0
H(5B)-C(5)-H(5C)	109.5	C(13)-C(12)-H(12)	109.0
N(1)-C(6)-C(7)	114.5(6)	C(14)-C(12)-H(12)	109.0
N(1)-C(6)-H(6A)	108.6	C(12)-C(13)-H(13A)	109.5
C(7)-C(6)-H(6A)	108.6	C(12)-C(13)-H(13B)	109.5
N(1)-C(6)-H(6B)	108.6	H(13A)-C(13)-H(13B)	109.5
C(7)-C(6)-H(6B)	108.6	C(12)-C(13)-H(13C)	109.5
H(6A)-C(6)-H(6B)	107.6	H(13A)-C(13)-H(13C)	109.5
C(8)-C(7)-C(9)	111.2(7)	H(13B)-C(13)-H(13C)	109.5
C(8)-C(7)-C(6)	113.5(6)	C(12)-C(14)-H(14A)	109.5
C(9)-C(7)-C(6)	106.6(7)	C(12)-C(14)-H(14B)	109.5

Table A.34, Cont'd. Bond angles (deg.) for $[\text{Mo}_3\text{Se}_7(\text{S}_2\text{CN}^i\text{Bu}_2)_3]\text{I} \cdot \frac{1}{6}(\text{ClCH}_2\text{CH}_2\text{Cl}) \cdot \frac{1}{3}(\text{C}_5\text{H}_{10})$. Symmetry transformations used to generate equivalent atoms:

H(14A)-C(14)-H(14B)	109.5	C(12)-C(14)-H(14C)	109.5
H(14A)-C(14)-H(14C)	109.5	C(16)-C(15)-H(15A)	108.2
H(14B)-C(14)-H(14C)	109.5	N(2)-C(15)-H(15B)	108.2
N(2)-C(15)-C(16)	116.2(7)	C(16)-C(15)-H(15B)	108.2
N(2)-C(15)-H(15A)	108.2	H(15A)-C(15)-H(15B)	107.4
C(18)-C(16)-C(17)	110.9(9)	H(22A)-C(22)-H(22C)	109.5
C(18)-C(16)-C(15)	112.8(8)	H(22B)-C(22)-H(22C)	109.5
C(17)-C(16)-C(15)	108.2(9)	C(21)-C(23)-H(23A)	109.5
C(18)-C(16)-H(16)	108.3	C(21)-C(23)-H(23B)	109.5
C(17)-C(16)-H(16)	108.3	H(23A)-C(23)-H(23B)	109.5
C(15)-C(16)-H(16)	108.3	C(21)-C(23)-H(23C)	109.5
C(16)-C(17)-H(17A)	109.5	H(23A)-C(23)-H(23C)	109.5
C(16)-C(17)-H(17B)	109.5	H(23B)-C(23)-H(23C)	109.5
H(17A)-C(17)-H(17B)	109.5	N(3)-C(24)-C(25)	111.3(6)
C(16)-C(17)-H(17C)	109.5	N(3)-C(24)-H(24A)	109.4
H(17A)-C(17)-H(17C)	109.5	C(25)-C(24)-H(24A)	109.4
H(17B)-C(17)-H(17C)	109.5	N(3)-C(24)-H(24B)	109.4
C(16)-C(18)-H(18A)	109.5	C(25)-C(24)-H(24B)	109.4
C(16)-C(18)-H(18B)	109.5	H(24A)-C(24)-H(24B)	108.0
H(18A)-C(18)-H(18B)	109.5	C(26)-C(25)-C(27)	111.8(8)
C(16)-C(18)-H(18C)	109.5	C(26)-C(25)-C(24)	113.6(8)
H(18A)-C(18)-H(18C)	109.5	C(27)-C(25)-C(24)	108.7(7)
H(18B)-C(18)-H(18C)	109.5	C(26)-C(25)-H(25)	107.5
N(3)-C(19)-S(5)	123.8(6)	C(27)-C(25)-H(25)	107.5
N(3)-C(19)-S(6)	123.7(6)	C(24)-C(25)-H(25)	107.5
S(5)-C(19)-S(6)	112.4(4)	C(25)-C(26)-H(26A)	109.5
N(3)-C(20)-C(21)	111.9(7)	C(25)-C(26)-H(26B)	109.5
N(3)-C(20)-H(20A)	109.2	H(26A)-C(26)-H(26B)	109.5
C(21)-C(20)-H(20A)	109.2	C(25)-C(26)-H(26C)	109.5
N(3)-C(20)-H(20B)	109.2	H(26A)-C(26)-H(26C)	109.5
C(21)-C(20)-H(20B)	109.2	H(26B)-C(26)-H(26C)	109.5
H(20A)-C(20)-H(20B)	107.9	C(25)-C(27)-H(27A)	109.5
C(22)-C(21)-C(20)	110.7(8)	C(25)-C(27)-H(27B)	109.5
C(22)-C(21)-C(23)	111.2(9)	H(27A)-C(27)-H(27B)	109.5
C(20)-C(21)-C(23)	111.3(8)	C(25)-C(27)-H(27C)	109.5
C(22)-C(21)-H(21)	107.8	H(27A)-C(27)-H(27C)	109.5
C(20)-C(21)-H(21)	107.8	H(27B)-C(27)-H(27C)	109.5
C(23)-C(21)-H(21)	107.8	N(4)-C(28)-S(8)	124.0(5)
C(21)-C(22)-H(22A)	109.5	N(4)-C(28)-S(7)	123.9(5)
C(21)-C(22)-H(22B)	109.5	S(8)-C(28)-S(7)	112.1(3)
H(22A)-C(22)-H(22B)	109.5	C(30B)-C(29)-N(4)	120.6(14)
C(21)-C(22)-H(22C)	109.5	N(4)-C(29)-C(30A)	111.7(8)

Table A.34, Cont'd. Bond angles (deg.) for $[\text{Mo}_3\text{Se}_7(\text{S}_2\text{CN}^i\text{Bu}_2)_3]\text{I} \cdot \frac{1}{6}(\text{ClCH}_2\text{CH}_2\text{Cl}) \cdot \frac{1}{3}(\text{C}_5\text{H}_{10})$. Symmetry transformations used to generate equivalent atoms:

N(4)-C(29)-H(29A)	109.3	C(30A)-C(29)-H(29A)	109.3
N(4)-C(29)-H(29B)	109.3	N(4)-C(33)-H(33A)	108.6
C(30A)-C(29)-H(29B)	109.3	C(34A)-C(33)-H(33A)	108.6
H(29A)-C(29)-H(29B)	108.0	N(4)-C(33)-H(33B)	108.6
C(32A)-C(30A)-C(31A)	110.8(12)	C(34A)-C(33)-H(33B)	108.6
C(32A)-C(30A)-C(29)	108.1(11)	H(33A)-C(33)-H(33B)	107.6
C(31A)-C(30A)-C(29)	114.5(11)	C(33)-C(34A)-C(35A)	109.9(17)
C(32A)-C(30A)-H(30A)	107.7	C(33)-C(34A)-C(36A)	109.4(16)
C(31A)-C(30A)-H(30A)	107.7	C(35A)-C(34A)-C(36A)	110.3(19)
C(29)-C(30A)-H(30A)	107.7	C(33)-C(34A)-H(34A)	109.1
C(30A)-C(31A)-H(31A)	109.5C(30A)-	C(35A)-C(34A)-H(34A)	109.1
C(31A)-H(31B)	109.5	C(36A)-C(34A)-H(34A)	109.1
H(31A)-C(31A)-H(31B)	109.5	C(34A)-C(35A)-H(35A)	109.5
C(30A)-C(31A)-H(31C)	109.5	C(34A)-C(35A)-H(35B)	109.5
H(31A)-C(31A)-H(31C)	109.5	H(35A)-C(35A)-H(35B)	109.5
H(31B)-C(31A)-H(31C)	109.5	C(34A)-C(35A)-H(35C)	109.5
C(30A)-C(32A)-H(32A)	109.5	H(35A)-C(35A)-H(35C)	109.5
C(30A)-C(32A)-H(32B)	109.5	H(35B)-C(35A)-H(35C)	109.5
H(32A)-C(32A)-H(32B)	109.5	C(34A)-C(36A)-H(36A)	109.5
C(30A)-C(32A)-H(32C)	109.5	C(34A)-C(36A)-H(36B)	109.5
H(32A)-C(32A)-H(32C)	109.5	H(36A)-C(36A)-H(36B)	109.5
H(32B)-C(32A)-H(32C)	109.5	C(34A)-C(36A)-H(36C)	109.5
C(29)-C(30B)-C(31B)	109(3)	H(36A)-C(36A)-H(36C)	109.5
C(29)-C(30B)-C(32B)	111(2)	H(36B)-C(36A)-H(36C)	109.5
C(31B)-C(30B)-C(32B)	109(3)	C(35B)-C(34B)-C(33)	115.0(14)
C(29)-C(30B)-H(30B)	109.4	C(35B)-C(34B)-C(36B)	109.6(15)
C(31B)-C(30B)-H(30B)	109.4	C(33)-C(34B)-C(36B)	108.8(13)
C(32B)-C(30B)-H(30B)	109.4	C(35B)-C(34B)-H(34B)	107.7
C(30B)-C(31B)-H(31D)	109.5	C(33)-C(34B)-H(34B)	107.7
C(30B)-C(31B)-H(31E)	109.5	C(36B)-C(34B)-H(34B)	107.7
H(31D)-C(31B)-H(31E)	109.5	C(34B)-C(35B)-H(35D)	109.5
C(30B)-C(31B)-H(31F)	109.5	C(34B)-C(35B)-H(35E)	109.5
H(31D)-C(31B)-H(31F)	109.5	H(35D)-C(35B)-H(35E)	109.5
H(31E)-C(31B)-H(31F)	109.5	C(34B)-C(35B)-H(35F)	109.5
C(30B)-C(32B)-H(32D)	109.5	H(35D)-C(35B)-H(35F)	109.5
C(30B)-C(32B)-H(32E)	109.5	H(35E)-C(35B)-H(35F)	109.5
H(32D)-C(32B)-H(32E)	109.5	C(34B)-C(36B)-H(36D)	109.5
C(30B)-C(32B)-H(32F)	109.5	C(34B)-C(36B)-H(36E)	109.5
H(32D)-C(32B)-H(32F)	109.5	H(36D)-C(36B)-H(36E)	109.5
H(32E)-C(32B)-H(32F)	109.5	C(34B)-C(36B)-H(36F)	109.5
N(4)-C(33)-C(34A)	114.7(10)	H(36D)-C(36B)-H(36F)	109.5
N(4)-C(33)-C(34B)	112.7(8)	H(36E)-C(36B)-H(36F)	109.5

Table A.34, Cont'd. Bond angles (deg.) for $[\text{Mo}_3\text{Se}_7(\text{S}_2\text{CN}^i\text{Bu}_2)_3]\cdot\frac{1}{6}(\text{ClCH}_2\text{CH}_2\text{Cl})\cdot\frac{1}{3}(\text{C}_5\text{H}_{10})$. Symmetry transformations used to generate equivalent atoms:

N(5)-C(37)-S(9)	123.4(5)	N(5)-C(37)-S(10)	123.5(5)
S(9)-C(37)-S(10)	113.2(4)	H(38A)-C(38)-H(38B)	107.6
N(5)-C(38)-C(39)	114.2(6)	C(40)-C(39)-C(38)	112.7(8)
N(5)-C(38)-H(38A)	108.7	C(40)-C(39)-C(41)	109.9(8)
C(39)-C(38)-H(38A)	108.7	C(38)-C(39)-C(41)	107.9(7)
N(5)-C(38)-H(38B)	108.7	C(40)-C(39)-H(39)	108.8
C(39)-C(38)-H(38B)	108.7	C(38)-C(39)-H(39)	108.8
C(41)-C(39)-H(39)	108.8	H(45A)-C(45)-H(45C)	109.5
C(39)-C(40)-H(40A)	109.5	H(45B)-C(45)-H(45C)	109.5
C(39)-C(40)-H(40B)	109.5	N(6)-C(46)-S(11)	123.9(6)
H(40A)-C(40)-H(40B)	109.5	N(6)-C(46)-S(12)	122.8(6)
C(39)-C(40)-H(40C)	109.5	S(11)-C(46)-S(12)	113.3(4)
H(40A)-C(40)-H(40C)	109.5	N(6)-C(47)-C(48)	112.1(7)
H(40B)-C(40)-H(40C)	109.5	N(6)-C(47)-H(47A)	109.2
C(39)-C(41)-H(41A)	109.5	C(48)-C(47)-H(47A)	109.2
C(39)-C(41)-H(41B)	109.5	N(6)-C(47)-H(47B)	109.2
H(41A)-C(41)-H(41B)	109.5	C(48)-C(47)-H(47B)	109.2
C(39)-C(41)-H(41C)	109.5	H(47A)-C(47)-H(47B)	107.9
H(41A)-C(41)-H(41C)	109.5	C(49)-C(48)-C(50)	111.8(9)
H(41B)-C(41)-H(41C)	109.5	C(49)-C(48)-C(47)	112.0(7)
N(5)-C(42)-C(43)	114.2(7)	C(50)-C(48)-C(47)	109.2(8)
N(5)-C(42)-H(42A)	108.7	C(49)-C(48)-H(48)	107.9
C(43)-C(42)-H(42A)	108.7	C(50)-C(48)-H(48)	107.9
N(5)-C(42)-H(42B)	108.7	C(47)-C(48)-H(48)	107.9
C(43)-C(42)-H(42B)	108.7	C(48)-C(49)-H(49A)	109.5
H(42A)-C(42)-H(42B)	107.6	C(48)-C(49)-H(49B)	109.5
C(44)-C(43)-C(45)	111.9(8)	H(49A)-C(49)-H(49B)	109.5
C(44)-C(43)-C(42)	109.3(9)	C(48)-C(49)-H(49C)	109.5
C(45)-C(43)-C(42)	112.0(7)	H(49A)-C(49)-H(49C)	109.5
C(44)-C(43)-H(43)	107.8	H(49B)-C(49)-H(49C)	109.5
C(45)-C(43)-H(43)	107.8	C(48)-C(50)-H(50A)	109.5
C(42)-C(43)-H(43)	107.8	C(48)-C(50)-H(50B)	109.5
C(43)-C(44)-H(44A)	109.5	H(50A)-C(50)-H(50B)	109.5
C(43)-C(44)-H(44B)	109.5	C(48)-C(50)-H(50C)	109.5
H(44A)-C(44)-H(44B)	109.5	H(50A)-C(50)-H(50C)	109.5
C(43)-C(44)-H(44C)	109.5	H(50B)-C(50)-H(50C)	109.5
H(44A)-C(44)-H(44C)	109.5	N(6)-C(51)-C(52)	113.2(7)
H(44B)-C(44)-H(44C)	109.5	N(6)-C(51)-H(51A)	108.9
C(43)-C(45)-H(45A)	109.5	C(52)-C(51)-H(51A)	108.9
C(43)-C(45)-H(45B)	109.5	N(6)-C(51)-H(51B)	108.9
H(45A)-C(45)-H(45B)	109.5	C(52)-C(51)-H(51B)	108.9
C(43)-C(45)-H(45C)	109.5	H(51A)-C(51)-H(51B)	107.7

Table A.34, Cont'd. Bond angles (deg.) for $[\text{Mo}_3\text{Se}_7(\text{S}_2\text{CN}^i\text{Bu}_2)_3]\text{I} \cdot \frac{1}{6}(\text{ClCH}_2\text{CH}_2\text{Cl}) \cdot \frac{1}{3}(\text{C}_5\text{H}_{10})$. Symmetry transformations used to generate equivalent atoms:

C(53)-C(52)-C(51)	112.0(9)	C(53)-C(52)-C(54)	112.4(10)
C(51)-C(52)-C(54)	108.2(9)	C(52)-C(53)-H(53C)	109.5
C(53)-C(52)-H(52A)	108.0	H(53A)-C(53)-H(53C)	109.5
C(51)-C(52)-H(52A)	108.0	H(53B)-C(53)-H(53C)	109.5
C(54)-C(52)-H(52A)	108.0	C(52)-C(54)-H(54A)	109.5
C(52)-C(53)-H(53A)	109.5	C(52)-C(54)-H(54B)	109.5
C(52)-C(53)-H(53B)	109.5	H(54A)-C(54)-H(54B)	109.5
H(53A)-C(53)-H(53B)	109.5	C(52)-C(54)-H(54C)	109.5
H(54A)-C(54)-H(54C)	109.5	C(61A)-C(60)-H(60B)	108.8
H(54B)-C(54)-H(54C)	109.5	H(60A)-C(60)-H(60B)	107.7
N(7)-C(55)-S(14)	123.9(5)	C(63A)-C(61A)-C(60)	114.4(13)
N(7)-C(55)-S(13)	124.1(5)	C(63A)-C(61A)-C(62A)	112.7(14)
S(14)-C(55)-S(13)	112.0(4)	C(60)-C(61A)-C(62A)	107.3(11)
N(7)-C(56)-C(57)	111.6(7)	C(63A)-C(61A)-H(61A)	107.4
N(7)-C(56)-H(56A)	109.3	C(60)-C(61A)-H(61A)	107.4
C(57)-C(56)-H(56A)	109.3	C(62A)-C(61A)-H(61A)	107.4
N(7)-C(56)-H(56B)	109.3	C(61A)-C(62A)-H(62A)	109.5
C(57)-C(56)-H(56B)	109.3	C(61A)-C(62A)-H(62B)	109.5
H(56A)-C(56)-H(56B)	108.0	H(62A)-C(62A)-H(62B)	109.5
C(58)-C(57)-C(56)	112.5(8)	C(61A)-C(62A)-H(62C)	109.5
C(58)-C(57)-C(59)	113.2(11)	H(62A)-C(62A)-H(62C)	109.5
C(56)-C(57)-C(59)	106.1(9)	H(62B)-C(62A)-H(62C)	109.5
C(58)-C(57)-H(57)	108.3	C(61A)-C(63A)-H(63A)	109.5
C(56)-C(57)-H(57)	108.3	C(61A)-C(63A)-H(63B)	109.5
C(59)-C(57)-H(57)	108.3	H(63A)-C(63A)-H(63B)	109.5
C(57)-C(58)-H(58A)	109.5	C(61A)-C(63A)-H(63C)	109.5
C(57)-C(58)-H(58B)	109.5	H(63A)-C(63A)-H(63C)	109.5
H(58A)-C(58)-H(58B)	109.5	H(63B)-C(63A)-H(63C)	109.5
C(57)-C(58)-H(58C)	109.5	C(60)-C(61B)-C(63B)	114(2)
H(58A)-C(58)-H(58C)	109.5	C(60)-C(61B)-C(62B)	104(2)
H(58B)-C(58)-H(58C)	109.5	C(63B)-C(61B)-C(62B)	110(3)
C(57)-C(59)-H(59A)	109.5	C(60)-C(61B)-H(61B)	109.7
C(57)-C(59)-H(59B)	109.5	C(63B)-C(61B)-H(61B)	109.7
H(59A)-C(59)-H(59B)	109.5	C(62B)-C(61B)-H(61B)	109.7
C(57)-C(59)-H(59C)	109.5	C(61B)-C(62B)-H(62D)	109.5
H(59A)-C(59)-H(59C)	109.5	C(61B)-C(62B)-H(62E)	109.5
H(59B)-C(59)-H(59C)	109.5	H(62D)-C(62B)-H(62E)	109.5
N(7)-C(60)-C(61B)	110.7(12)	C(61B)-C(62B)-H(62F)	109.5
N(7)-C(60)-C(61A)	114.0(8)	H(62D)-C(62B)-H(62F)	109.5
N(7)-C(60)-H(60A)	108.8	H(62E)-C(62B)-H(62F)	109.5
C(61A)-C(60)-H(60A)	108.8	C(61B)-C(63B)-H(63D)	109.5
N(7)-C(60)-H(60B)	108.8	C(61B)-C(63B)-H(63E)	109.5

Table A.34, Cont'd. Bond angles (deg.) for $[\text{Mo}_3\text{Se}_7(\text{S}_2\text{CN}^i\text{Bu}_2)_3]\text{I} \cdot \frac{1}{6}(\text{ClCH}_2\text{CH}_2\text{Cl}) \cdot \frac{1}{3}(\text{C}_5\text{H}_{10})$. Symmetry transformations used to generate equivalent atoms:

H(63D)-C(63B)-H(63E)	109.5	C(61B)-C(63B)-H(63F)	109.5
H(63D)-C(63B)-H(63F)	109.5	C(70)-C(71)-H(71A)	109.5
H(63E)-C(63B)-H(63F)	109.5	C(70)-C(71)-H(71B)	109.5
N(8)-C(64)-S(15)	123.6(5)	H(71A)-C(71)-H(71B)	109.5
N(8)-C(64)-S(16)	123.7(5)	C(70)-C(71)-H(71C)	109.5
S(15)-C(64)-S(16)	112.8(4)	H(71A)-C(71)-H(71C)	109.5
N(8)-C(65)-C(66)	113.9(7)	H(71B)-C(71)-H(71C)	109.5
N(8)-C(65)-H(65A)	108.8	C(70)-C(72)-H(72A)	109.5
C(66)-C(65)-H(65A)	108.8	C(70)-C(72)-H(72B)	109.5
N(8)-C(65)-H(65B)	108.8	H(72A)-C(72)-H(72B)	109.5
C(66)-C(65)-H(65B)	108.8	C(70)-C(72)-H(72C)	109.5
H(65A)-C(65)-H(65B)	107.7	H(72A)-C(72)-H(72C)	109.5
C(67)-C(66)-C(68)	111.6(10)	H(72B)-C(72)-H(72C)	109.5
C(67)-C(66)-C(65)	115.3(9)	N(9)-C(73)-S(17)	123.9(6)
C(68)-C(66)-C(65)	106.7(9)	N(9)-C(73)-S(18)	122.6(6)
C(67)-C(66)-H(66)	107.6	S(17)-C(73)-S(18)	113.6(4)
C(68)-C(66)-H(66)	107.6	N(9)-C(74)-C(75B)	119.8(11)
C(65)-C(66)-H(66)	107.6	N(9)-C(74)-C(75A)	106.9(10)
C(66)-C(67)-H(67A)	109.5	N(9)-C(74)-H(74A)	110.3
C(66)-C(67)-H(67B)	109.5	C(75A)-C(74)-H(74A)	110.3
H(67A)-C(67)-H(67B)	109.5	N(9)-C(74)-H(74B)	110.3
C(66)-C(67)-H(67C)	109.5	C(75A)-C(74)-H(74B)	110.3
H(67A)-C(67)-H(67C)	109.5	H(74A)-C(74)-H(74B)	108.6
H(67B)-C(67)-H(67C)	109.5	C(77A)-C(75A)-C(76A)	114.1(19)
C(66)-C(68)-H(68A)	109.5	C(77A)-C(75A)-C(74)	116.1(17)
C(66)-C(68)-H(68B)	109.5	C(76A)-C(75A)-C(74)	102.2(16)
H(68A)-C(68)-H(68B)	109.5	C(77A)-C(75A)-H(75A)	108.0
C(66)-C(68)-H(68C)	109.5	C(76A)-C(75A)-H(75A)	108.0
H(68A)-C(68)-H(68C)	109.5	C(74)-C(75A)-H(75A)	108.0
H(68B)-C(68)-H(68C)	109.5	C(75A)-C(76A)-H(76A)	109.5
N(8)-C(69)-C(70)	113.3(6)	C(75A)-C(76A)-H(76B)	109.5
N(8)-C(69)-H(69A)	108.9	H(76A)-C(76A)-H(76B)	109.5
C(70)-C(69)-H(69A)	108.9	C(75A)-C(76A)-H(76C)	109.5
N(8)-C(69)-H(69B)	108.9	H(76A)-C(76A)-H(76C)	109.5
C(70)-C(69)-H(69B)	108.9	H(76B)-C(76A)-H(76C)	109.5
H(69A)-C(69)-H(69B)	107.7	C(75A)-C(77A)-H(77A)	109.5
C(72)-C(70)-C(71)	110.4(9)	C(75A)-C(77A)-H(77B)	109.5
C(72)-C(70)-C(69)	111.4(8)	H(77A)-C(77A)-H(77B)	109.5
C(71)-C(70)-C(69)	109.1(7)	C(75A)-C(77A)-H(77C)	109.5
C(72)-C(70)-H(70)	108.6	H(77A)-C(77A)-H(77C)	109.5
C(71)-C(70)-H(70)	108.6	H(77B)-C(77A)-H(77C)	109.5
C(69)-C(70)-H(70)	108.6	C(74)-C(75B)-C(77B)	112.1(15)

Table A.34, Cont'd. Bond angles (deg.) for $[\text{Mo}_3\text{Se}_7(\text{S}_2\text{CN}^i\text{Bu}_2)_3]\text{I} \cdot \frac{1}{6}(\text{ClCH}_2\text{CH}_2\text{Cl}) \cdot \frac{1}{3}(\text{C}_5\text{H}_{10})$. Symmetry transformations used to generate equivalent atoms:

C(74)-C(75B)-C(76B)	112.5(16)	C(77B)-C(75B)-C(76B)	109.6(17)
C(74)-C(75B)-H(75B)	107.5	C(84)-C(82)-C(85)	21(3)
C(77B)-C(75B)-H(75B)	107.5	C(82)-C(83)-C(84)	58(4)
C(76B)-C(75B)-H(75B)	107.5	C(82)-C(83)-C(85)	47(4)
C(75B)-C(76B)-H(76D)	109.5	C(84)-C(83)-C(85)	12(3)
C(75B)-C(76B)-H(76E)	109.5	C(85)-C(84)-C(82)	110(9)
H(76D)-C(76B)-H(76E)	109.5	C(85)-C(84)-C(83)	137(9)
C(75B)-C(76B)-H(76F)	109.5	C(82)-C(84)-C(83)	28.7(18)
H(76D)-C(76B)-H(76F)	109.5	C(85)-C(84)-C(86)	20(8)
H(76E)-C(76B)-H(76F)	109.5	C(82)-C(84)-C(86)	94(3)
C(75B)-C(77B)-H(77D)	109.5	C(83)-C(84)-C(86)	119(2)
C(75B)-C(77B)-H(77E)	109.5	C(84)-C(85)-C(86)	150(10)
H(77D)-C(77B)-H(77E)	109.5	C(84)-C(85)-C(82)	49(7)
C(75B)-C(77B)-H(77F)	109.5	C(86)-C(85)-C(82)	106(5)
H(77D)-C(77B)-H(77F)	109.5	C(84)-C(85)-C(83)	31(7)
H(77E)-C(77B)-H(77F)	109.5	C(86)-C(85)-C(83)	121(5)
N(9)-C(78)-C(79)	113.1(8)	C(82)-C(85)-C(83)	19.3(16)
N(9)-C(78)-H(78A)	109.0	C(85)-C(86)-C(87)	108(4)
C(79)-C(78)-H(78A)	109.0	C(85)-C(86)-C(84)	10(4)
N(9)-C(78)-H(78B)	109.0	C(87)-C(86)-C(84)	117(2)
C(79)-C(78)-H(78B)	109.0	C(88)-C(87)-C(90)	90(3)
H(78A)-C(78)-H(78B)	107.8	C(88)-C(87)-C(86)	137(4)
C(81)-C(79)-C(80)	111.4(10)	C(90)-C(87)-C(86)	115(3)
C(81)-C(79)-C(78)	113.8(9)	C(88)-C(87)-C(89)	23(2)
C(80)-C(79)-C(78)	109.1(13)	C(90)-C(87)-C(89)	101(3)
C(81)-C(79)-H(79)	107.4	C(86)-C(87)-C(89)	115(2)
C(80)-C(79)-H(79)	107.4	C(89)-C(88)-C(87)	132(5)
C(78)-C(79)-H(79)	107.4	C(89)-C(88)-C(90)	136(4)
C(79)-C(80)-H(80A)	109.5	C(87)-C(88)-C(90)	51(3)
C(79)-C(80)-H(80B)	109.5	C(88)-C(89)-C(87)	26(3)
H(80A)-C(80)-H(80B)	109.5	C(87)-C(90)-C(91)	122(3)
C(79)-C(80)-H(80C)	109.5	C(87)-C(90)-C(88)	39(2)
H(80A)-C(80)-H(80C)	109.5	C(91)-C(90)-C(88)	161(3)
H(80B)-C(80)-H(80C)	109.5	C(93)-C(92)-Cl(1)	123(3)
C(79)-C(81)-H(81A)	109.5	C(93)-C(92)-H(92A)	106.6
C(79)-C(81)-H(81B)	109.5	Cl(1)-C(92)-H(92A)	106.6
H(81A)-C(81)-H(81B)	109.5	C(93)-C(92)-H(92B)	106.6
C(79)-C(81)-H(81C)	109.5	Cl(1)-C(92)-H(92B)	106.6
H(81A)-C(81)-H(81C)	109.5	H(92A)-C(92)-H(92B)	106.6
H(81B)-C(81)-H(81C)	109.5	C(92)-C(93)-Cl(2)	124(3)
C(83)-C(82)-C(84)	93(5)	C(92)-C(93)-H(93A)	106.4
C(83)-C(82)-C(85)	114(5)	Cl(2)-C(93)-H(93A)	106.4

Table A.34, Cont'd. Bond angles (deg.) for $[\text{Mo}_3\text{Se}_7(\text{S}_2\text{CN}^i\text{Bu}_2)_3]\text{I} \cdot \frac{1}{6}(\text{ClCH}_2\text{CH}_2\text{Cl}) \cdot \frac{1}{3}(\text{C}_5\text{H}_{10})$. Symmetry transformations used to generate equivalent atoms:

H(93A)-C(93)-H(93B)	106.4
C(92)-C(93)-H(93B)	106.4
Cl(2)-C(93)-H(93B)	106.4

Table A.35. Anisotropic displacement parameters ($\text{\AA}^2 \times 10^3$) for $[\text{Mo}_3\text{Se}_7(\text{S}_2\text{CN}^i\text{Bu}_2)_3]\text{I} \cdot \frac{1}{6}(\text{ClCH}_2\text{CH}_2\text{Cl}) \cdot \frac{1}{3}(\text{C}_5\text{H}_{10})$. The anisotropic displacement factor exponent takes the form: $-2\pi^2[h^2a^{*2}U^{11} + \dots + 2hka^*b^*U^{12}]$.

Atom	U^{11}	U^{22}	U^{33}	U^{23}	U^{13}	U^{12}
I(1)	48(1)	37(1)	51(1)	-6(1)	-2(1)	-14(1)
I(2)	36(1)	50(1)	23(1)	1(1)	-9(1)	-16(1)
I(3)	25(1)	25(1)	38(1)	-8(1)	1(1)	3(1)
Mo(1)	17(1)	20(1)	21(1)	-1(1)	-1(1)	2(1)
Mo(2)	27(1)	27(1)	21(1)	-2(1)	-1(1)	1(1)
Mo(3)	19(1)	24(1)	26(1)	-1(1)	-4(1)	3(1)
Mo(4)	14(1)	15(1)	17(1)	1(1)	0(1)	-4(1)
Mo(5)	13(1)	12(1)	20(1)	1(1)	-2(1)	-1(1)
Mo(6)	15(1)	12(1)	18(1)	1(1)	1(1)	0(1)
Mo(7)	15(1)	21(1)	22(1)	-5(1)	1(1)	0(1)
Mo(8)	17(1)	20(1)	20(1)	-6(1)	0(1)	1(1)
Mo(9)	15(1)	22(1)	22(1)	-7(1)	-1(1)	0(1)
Se(1)	31(1)	24(1)	31(1)	-4(1)	0(1)	3(1)
Se(2)	32(1)	40(1)	39(1)	-4(1)	5(1)	6(1)
Se(3)	31(1)	36(1)	32(1)	-5(1)	-9(1)	0(1)
Se(4)	48(1)	45(1)	35(1)	3(1)	-10(1)	3(1)
Se(5)	21(1)	28(1)	32(1)	-2(1)	1(1)	0(1)
Se(6)	25(1)	29(1)	29(1)	-6(1)	1(1)	2(1)
Se(7)	48(1)	53(1)	47(1)	0(1)	-1(1)	6(1)
Se(8)	15(1)	26(1)	26(1)	3(1)	-2(1)	-2(1)
Se(9)	24(1)	28(1)	27(1)	-3(1)	2(1)	4(1)
Se(10)	21(1)	22(1)	21(1)	3(1)	0(1)	-2(1)
Se(11)	18(1)	24(1)	32(1)	6(1)	2(1)	-4(1)
Se(12)	26(1)	19(1)	24(1)	-2(1)	0(1)	-8(1)
Se(13)	36(1)	19(1)	33(1)	3(1)	2(1)	-2(1)
Se(14)	36(1)	33(1)	43(1)	1(1)	2(1)	0(1)
Se(15)	18(1)	25(1)	28(1)	-5(1)	-1(1)	1(1)
Se(16)	25(1)	30(1)	34(1)	-8(1)	-4(1)	-3(1)
Se(17)	23(1)	28(1)	26(1)	-10(1)	2(1)	0(1)
Se(18)	34(1)	41(1)	27(1)	-6(1)	-2(1)	1(1)
Se(19)	23(1)	23(1)	28(1)	-6(1)	2(1)	0(1)
Se(20)	23(1)	27(1)	34(1)	-7(1)	6(1)	-1(1)
Se(21)	36(1)	47(1)	42(1)	-7(1)	1(1)	-2(1)
S(1)	22(1)	24(1)	29(1)	5(1)	-5(1)	-3(1)
S(2)	22(1)	21(1)	27(1)	2(1)	-5(1)	-1(1)
S(3)	45(1)	40(1)	26(1)	-8(1)	4(1)	-6(1)
S(4)	46(1)	36(1)	25(1)	-4(1)	6(1)	-5(1)
S(5)	22(1)	27(1)	56(1)	0(1)	-6(1)	5(1)
S(6)	25(1)	25(1)	46(1)	1(1)	-5(1)	3(1)

Table A.35, Cont'd. Anisotropic displacement parameters ($\text{\AA}^2 \times 10^3$) for $[\text{Mo}_3\text{Se}_7(\text{S}_2\text{CN}^i\text{Bu}_2)_3]\text{I} \cdot \frac{1}{6}(\text{ClCH}_2\text{CH}_2\text{Cl}) \cdot \frac{1}{3}(\text{C}_5\text{H}_{10})$. The anisotropic displacement factor exponent takes the form: $-2\pi^2[h^2a^{*2}U^{11} + \dots + 2hka^*b^*U^{12}]$.

Atom	U^{11}	U^{22}	U^{33}	U^{23}	U^{13}	U^{12}
S(7)	20(1)	37(1)	22(1)	5(1)	-2(1)	-12(1)
S(8)	20(1)	26(1)	19(1)	2(1)	0(1)	-7(1)
S(9)	25(1)	15(1)	32(1)	4(1)	-10(1)	0(1)
S(10)	28(1)	13(1)	34(1)	0(1)	-13(1)	-2(1)
S(11)	27(1)	24(1)	23(1)	-3(1)	2(1)	7(1)
S(12)	20(1)	22(1)	28(1)	-2(1)	-1(1)	6(1)
S(13)	21(1)	22(1)	36(1)	0(1)	9(1)	3(1)
S(14)	24(1)	23(1)	37(1)	-2(1)	7(1)	5(1)
S(15)	30(1)	24(1)	23(1)	-5(1)	0(1)	7(1)
S(16)	26(1)	24(1)	22(1)	-7(1)	-3(1)	6(1)
S(17)	20(1)	27(1)	36(1)	-12(1)	-6(1)	1(1)
S(18)	20(1)	26(1)	42(1)	-10(1)	-6(1)	2(1)
N(1)	20(2)	21(3)	21(3)	0(2)	-2(2)	1(2)
N(2)	48(4)	40(4)	17(3)	-1(3)	2(3)	1(3)
N(3)	30(3)	28(3)	36(3)	-3(3)	-4(3)	9(3)
N(4)	21(3)	30(3)	25(3)	6(2)	2(2)	-5(2)
N(5)	29(3)	14(2)	34(3)	2(2)	-7(2)	-1(2)
N(6)	26(3)	21(3)	29(3)	6(2)	5(2)	6(2)
N(7)	21(3)	21(3)	35(3)	2(2)	5(2)	1(2)
N(8)	23(3)	28(3)	21(3)	-7(2)	0(2)	2(2)
N(9)	19(3)	33(3)	29(3)	-6(2)	-3(2)	3(2)
C(1)	16(3)	26(3)	20(3)	0(2)	2(2)	5(2)
C(2)	21(3)	29(3)	23(3)	-6(3)	-4(2)	-1(3)
C(3)	19(3)	27(3)	38(4)	-1(3)	4(3)	2(3)
C(4)	22(3)	41(5)	62(6)	-7(4)	-2(3)	-5(3)
C(5)	34(4)	41(4)	36(4)	-2(3)	9(3)	2(3)
C(6)	28(3)	28(3)	19(3)	3(2)	-1(2)	3(3)
C(7)	25(3)	28(3)	38(4)	4(3)	2(3)	0(3)
C(8)	53(5)	29(4)	44(5)	-7(3)	6(4)	7(4)
C(9)	36(4)	37(4)	51(5)	19(4)	-2(4)	5(3)
C(10)	51(5)	38(4)	20(3)	-5(3)	-4(3)	0(4)
C(11)	60(5)	40(4)	19(3)	-1(3)	2(3)	-1(4)
C(12)	59(6)	47(5)	28(4)	-7(4)	7(4)	-1(4)
C(13)	65(7)	58(7)	51(6)	-6(5)	-2(5)	2(5)
C(14)	76(8)	74(8)	42(6)	7(5)	17(5)	-15(6)
C(15)	52(5)	49(5)	22(3)	-2(3)	-4(3)	0(4)
C(16)	50(5)	46(5)	31(4)	-7(4)	6(4)	1(4)
C(17)	76(8)	52(7)	80(9)	-16(6)	1(7)	-14(6)
C(18)	57(6)	52(6)	39(5)	-4(4)	8(4)	5(5)

Table A.35, Cont'd. Anisotropic displacement parameters ($\text{\AA}^2 \times 10^3$) for $[\text{Mo}_3\text{Se}_7(\text{S}_2\text{CN}^i\text{Bu}_2)_3]\text{I} \cdot \frac{1}{6}(\text{ClCH}_2\text{CH}_2\text{Cl}) \cdot \frac{1}{3}(\text{C}_5\text{H}_{10})$. The anisotropic displacement factor exponent takes the form: $-2\pi^2[h^2a^{*2}U^{11} + \dots + 2hka^*b^*U^{12}]$.

Atom	U^{11}	U^{22}	U^{33}	U^{23}	U^{13}	U^{12}
C(19)	24(3)	25(3)	37(4)	4(3)	-2(3)	9(3)
C(20)	39(4)	24(3)	40(4)	1(3)	-2(3)	5(3)
C(21)	44(5)	32(4)	46(5)	-4(4)	0(4)	-6(3)
C(22)	75(8)	47(6)	62(7)	-16(5)	11(6)	2(5)
C(23)	60(6)	55(6)	33(4)	-6(4)	-9(4)	-10(5)
C(24)	21(3)	35(4)	36(4)	-3(3)	-1(3)	10(3)
C(25)	29(4)	48(5)	37(4)	-6(4)	1(3)	9(3)
C(26)	50(5)	64(6)	31(4)	-8(4)	0(4)	-2(5)
C(27)	28(4)	52(5)	37(4)	-5(4)	-2(3)	6(4)
C(28)	21(3)	26(3)	18(3)	4(2)	4(2)	-6(2)
C(29)	23(3)	42(4)	38(4)	11(3)	5(3)	-13(3)
C(33)	37(4)	40(4)	18(3)	1(3)	-2(3)	-5(3)
C(37)	25(3)	14(3)	32(3)	0(2)	-3(3)	2(2)
C(38)	31(3)	15(3)	38(4)	5(3)	1(3)	3(3)
C(39)	45(4)	20(3)	42(4)	3(3)	7(4)	5(3)
C(40)	45(5)	31(4)	72(7)	3(4)	28(5)	0(4)
C(41)	85(8)	51(6)	41(5)	20(4)	12(5)	19(6)
C(42)	44(4)	17(3)	37(4)	0(3)	-12(3)	-8(3)
C(43)	64(6)	21(3)	38(4)	-3(3)	-7(4)	-7(4)
C(44)	92(9)	44(6)	51(6)	-12(5)	-30(6)	8(6)
C(45)	60(6)	29(4)	47(5)	0(4)	9(4)	-8(4)
C(46)	21(3)	20(3)	32(3)	1(3)	3(3)	2(2)
C(47)	32(4)	30(4)	30(4)	1(3)	9(3)	9(3)
C(48)	46(5)	33(4)	36(4)	9(3)	9(3)	14(3)
C(49)	53(6)	70(7)	54(6)	22(5)	15(5)	-14(5)
C(50)	74(7)	57(6)	35(5)	9(4)	10(5)	20(5)
C(51)	20(3)	27(3)	46(4)	3(3)	2(3)	5(3)
C(53)	80(8)	42(6)	68(7)	8(5)	-17(6)	-5(5)
C(54)	82(9)	78(9)	65(8)	20(7)	-32(7)	-8(7)
C(55)	19(3)	26(3)	33(4)	-2(3)	3(3)	2(2)
C(56)	23(3)	27(3)	43(4)	1(3)	7(3)	2(3)
C(57)	57(6)	50(5)	47(5)	12(4)	24(5)	17(5)
C(58)	76(8)	84(9)	42(6)	-15(6)	-3(5)	16(7)
C(59)	81(9)	93(10)	75(9)	23(8)	52(8)	32(8)
C(60)	34(4)	23(3)	38(4)	2(3)	7(3)	1(3)
C(64)	19(3)	24(3)	22(3)	-9(2)	-1(2)	1(2)
C(65)	28(3)	32(4)	23(3)	-2(3)	-2(3)	4(3)
C(66)	52(5)	41(5)	48(5)	6(4)	1(4)	-4(4)
C(67)	38(5)	82(9)	92(10)	33(8)	3(6)	-6(5)

Table A.35, Cont'd. Anisotropic displacement parameters ($\text{\AA}^2 \times 10^3$) for $[\text{Mo}_3\text{Se}_7(\text{S}_2\text{CN}^i\text{Bu}_2)_3]\text{I} \cdot \frac{1}{6}(\text{ClCH}_2\text{CH}_2\text{Cl}) \cdot \frac{1}{3}(\text{C}_5\text{H}_{10})$. The anisotropic displacement factor exponent takes the form: $-2\pi^2[h^2a^*U^{11} + \dots + 2hka^*b^*U^{12}]$.

Atom	U^{11}	U^{22}	U^{33}	U^{23}	U^{13}	U^{12}
C(68)	78(9)	45(6)	109(11)	38(7)	0(8)	-3(6)
C(69)	26(3)	36(4)	25(3)	-12(3)	0(3)	6(3)
C(70)	34(4)	40(4)	39(4)	-21(4)	-10(3)	5(3)
C(71)	63(6)	54(6)	49(6)	-33(5)	-12(5)	13(5)
C(72)	61(7)	50(6)	74(8)	-17(5)	10(6)	-21(5)
C(73)	20(3)	31(3)	27(3)	-5(3)	-3(2)	-2(3)
C(74)	22(3)	38(4)	35(4)	-13(3)	-5(3)	-8(3)
C(78)	23(3)	38(4)	53(5)	-1(4)	-14(3)	7(3)
C(79)	30(4)	62(6)	75(7)	-28(6)	1(4)	11(4)
C(80)	59(8)	57(8)	240(30)	-37(12)	25(12)	24(7)
C(81)	54(6)	76(8)	66(7)	-11(6)	17(6)	3(6)

Table A.36. Hydrogen coordinates ($\times 10^4$) and isotropic displacement parameters ($\text{\AA}^2 \times 10^3$) for $[\text{Mo}_3\text{Se}_7(\text{S}_2\text{CN}^i\text{Bu}_2)_3]\text{I} \cdot \frac{1}{6}(\text{ClCH}_2\text{CH}_2\text{Cl}) \cdot \frac{1}{3}(\text{C}_5\text{H}_{10})$.

H atom	x	y	z	U(eq)
H(2A)	192	7894	3031	29
H(2B)	5	8514	2721	29
H(3)	-530	9393	3069	34
H(4A)	-847	8092	2767	62
H(4B)	-1074	8008	3125	62
H(4C)	-640	7299	3024	62
H(5A)	-260	8000	3568	56
H(5B)	-683	8794	3600	56
H(5C)	-133	9148	3583	56
H(6A)	328	10012	2601	30
H(6B)	772	10442	2809	30
H(7)	-228	10782	2956	37
H(8A)	290	10794	3440	63
H(8B)	-6	11791	3381	63
H(8C)	553	11736	3290	63
H(9A)	-94	12375	2761	62
H(9B)	77	11616	2486	62
H(9C)	468	12153	2716	62
H(11A)	834	8396	5772	47
H(11B)	708	7897	5427	47
H(12)	93	9280	5746	54
H(13A)	-46	9294	5173	87
H(13B)	-499	8815	5352	87
H(13C)	-116	8124	5174	87
H(14A)	-69	7203	5683	96
H(14B)	-361	7947	5910	96
H(14C)	184	7663	6003	96
H(15A)	1403	10247	5594	49
H(15B)	947	10063	5820	49
H(16)	866	11231	5236	51
H(17A)	1013	12638	5555	104
H(17B)	1467	11914	5589	104
H(17C)	1084	11979	5878	104
H(18A)	116	10789	5432	74
H(18B)	191	11940	5500	74
H(18C)	257	11163	5793	74
H(20A)	2884	4395	4013	41
H(20B)	3411	4076	4139	41
H(21)	3680	4547	3581	49
H(22A)	3691	2924	3753	92

Table A.36, Cont'd. Hydrogen coordinates ($\times 10^4$) and isotropic displacement parameters ($\text{\AA}^2 \times 10^3$) for $[\text{Mo}_3\text{Se}_7(\text{S}_2\text{CN}^t\text{Bu}_2)_3]\text{I} \cdot \frac{1}{6}(\text{ClCH}_2\text{CH}_2\text{Cl}) \cdot \frac{1}{3}(\text{C}_5\text{H}_{10})$.

H atom	x	y	z	U(eq)
H(22B)	3518	2973	3376	92
H(22C)	3132	2802	3659	92
H(23A)	2671	4310	3429	74
H(23B)	3080	4419	3159	74
H(23C)	2962	5322	3397	74
H(24A)	3955	6367	4047	37
H(24B)	4062	5212	4080	37
H(25)	3723	6476	4591	46
H(26A)	3843	4409	4656	72
H(26B)	3338	4977	4664	72
H(26C)	3728	5139	4952	72
H(27A)	4463	6231	4847	59
H(27B)	4570	6518	4475	59
H(27C)	4608	5395	4591	59
H(29A)	365	3836	3442	41
H(29B)	434	3959	3055	41
H(30A)	75	5576	3077	48
H(31A)	237	6021	3638	77
H(31B)	-323	6165	3549	77
H(31C)	-149	5225	3756	77
H(32A)	-416	4181	2951	79
H(32B)	-553	4084	3330	79
H(32C)	-727	5024	3123	79
H(30B)	41	4574	3660	48
H(31D)	-329	5958	3453	77
H(31E)	245	6055	3434	77
H(31F)	-66	5801	3110	77
H(32D)	-734	4372	3396	79
H(32E)	-480	4216	3049	79
H(32F)	-414	3411	3333	79
H(33A)	865	5079	3812	38
H(33B)	1398	5155	3671	38
H(34A)	903	3358	3774	47
H(35A)	1653	2629	3663	79
H(35B)	1468	3249	3352	79
H(35C)	1879	3689	3590	79
H(36A)	1451	3164	4234	79
H(36B)	1672	4232	4166	79
H(36C)	1127	4126	4284	79
H(34B)	1757	4035	3583	47

Table A.36, Cont'd. Hydrogen coordinates ($\times 10^4$) and isotropic displacement parameters ($\text{\AA}^2 \times 10^3$) for $[\text{Mo}_3\text{Se}_7(\text{S}_2\text{CN}^t\text{Bu}_2)_3]\text{I} \cdot \frac{1}{6}(\text{ClCH}_2\text{CH}_2\text{Cl}) \cdot \frac{1}{3}(\text{C}_5\text{H}_{10})$.

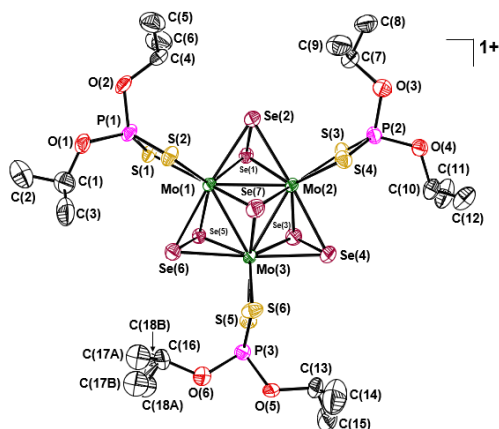
H atom	x	y	z	U(eq)
(35D)	1538	2434	3661	79
H(35E)	1001	2767	3748	79
H(35F)	1201	2934	3386	79
H(36D)	1751	4521	4155	79
H(36E)	1355	3694	4226	79
H(36F)	1887	3381	4121	79
H(38A)	1882	12191	2072	34
H(38B)	1630	11232	1919	34
H(39)	2260	11025	1549	43
H(40A)	2700	12787	1795	73
H(40B)	2913	12075	1520	73
H(40C)	2894	11716	1893	73
H(41A)	1904	13015	1540	88
H(41B)	1613	12091	1394	88
H(41C)	2101	12445	1225	88
H(42A)	2523	12092	2427	39
H(42B)	2749	11064	2542	39
H(43)	2114	10772	2893	49
H(44A)	2773	11819	3067	94
H(44B)	2298	11911	3283	94
H(44C)	2417	12736	3016	94
H(45A)	1679	12560	2666	68
H(45B)	1476	11901	2959	68
H(45C)	1474	11480	2592	68
H(47A)	3505	3604	1467	37
H(47B)	4033	3240	1578	37
H(48)	3833	5174	1328	46
H(49A)	4514	5240	1656	88
H(49B)	4683	5323	1283	88
H(49C)	4743	4305	1477	88
H(50A)	4266	3584	979	83
H(50B)	4168	4659	832	83
H(50C)	3724	3957	918	83
H(51A)	4181	4689	2258	37
H(51B)	4408	3821	2046	37
H(52A)	3624	3511	2479	55
H(53A)	3815	1858	2438	96
H(53B)	3680	2306	2085	96
H(53C)	4233	2112	2185	96
H(54A)	4318	4055	2780	113

Table A.36, Cont'd. Hydrogen coordinates ($\times 10^4$) and isotropic displacement parameters ($\text{\AA}^2 \times 10^3$) for $[\text{Mo}_3\text{Se}_7(\text{S}_2\text{CN}^i\text{Bu}_2)_3]\text{I} \cdot \frac{1}{6}(\text{ClCH}_2\text{CH}_2\text{Cl}) \cdot \frac{1}{3}(\text{C}_5\text{H}_{10})$.

H atom	x	y	z	U(eq)
H(54B)	4197	2937	2873	113
H(54C)	4629	3178	2629	113
H(56A)	6025	7380	5429	37
H(56B)	6227	8484	5417	37
H(57)	5863	8712	4887	61
H(58A)	5592	6692	4912	101
H(58B)	5519	7396	4600	101
H(58C)	5221	7594	4927	101
H(59A)	6678	8177	4935	124
H(59B)	6441	7712	4610	124
H(59C)	6510	7050	4932	124
H(60A)	5075	9595	5538	38
H(60B)	5355	9577	5198	38
H(61A)	6082	10074	5461	46
H(62A)	5531	11320	5267	88
H(62B)	5304	11399	5625	88
H(62C)	5850	11733	5567	88
H(63A)	6126	10519	5998	93
H(63B)	5588	10129	6052	93
H(63C)	6008	9371	5961	93
H(61B)	5360	9860	5931	46
H(62D)	5487	11612	5812	88
H(62E)	5570	11348	5435	88
H(62F)	5050	11190	5593	88
H(63D)	6168	10430	6007	93
H(63E)	6188	9338	5860	93
H(63F)	6276	10264	5626	93
H(65A)	4364	6053	8147	33
H(65B)	4594	5462	7848	33
H(66)	3858	4580	7776	56
H(67A)	3560	5443	8369	106
H(67B)	3292	4550	8186	106
H(67C)	3308	5613	8018	106
H(68A)	4316	4379	8405	116
H(68B)	4514	3921	8071	116
H(68C)	4021	3523	8221	116
H(69A)	3609	7100	7993	35
H(69B)	3697	7690	7659	35
H(70)	4381	7641	8194	45
H(71A)	4131	9257	8304	83

Table A.36, Cont'd. Hydrogen coordinates ($\times 10^4$) and isotropic displacement parameters ($\text{\AA}^2 \times 10^3$) for $[\text{Mo}_3\text{Se}_7(\text{S}_2\text{CN}^t\text{Bu}_2)_3]\text{I} \cdot \frac{1}{6}(\text{ClCH}_2\text{CH}_2\text{Cl}) \cdot \frac{1}{3}(\text{C}_5\text{H}_{10})$.

H atom	x	y	z	U(eq)
H(71B)	3687	8514	8336	83
H(71C)	3733	9189	8016	83
H(72A)	4754	7943	7696	92
H(72B)	4771	8918	7916	92
H(72C)	4389	8828	7619	92
H(74A)	1857	3826	5465	38
H(74B)	2368	3419	5599	38
H(75A)	2782	4025	5120	39
H(76A)	2393	2489	5107	81
H(76B)	1923	2979	4942	81
H(76C)	2417	2932	4744	81
H(77A)	2374	5448	5010	77
H(77B)	2408	4786	4686	77
H(77C)	1914	4833	4884	77
H(75B)	2772	3743	5178	39
H(76D)	2418	2587	4816	81
H(76E)	2391	2209	5187	81
H(76F)	1921	2658	5009	81
H(77D)	2418	4304	4687	77
H(77E)	1923	4504	4872	77
H(77F)	2394	5131	4965	77
H(78A)	1700	5514	5439	46
H(78B)	2072	6305	5586	46
H(79)	1879	5799	6128	67
H(80A)	1044	6423	5771	178
H(80B)	1478	7142	5873	178
H(80C)	1159	6638	6151	178
H(81A)	1231	4803	6233	97
H(81B)	1613	4202	6021	97
H(81C)	1135	4631	5849	97
H(92A)	584	6332	4447	121
H(92B)	258	6181	4760	121
H(93A)	958	5971	4932	134
H(93B)	1122	5390	4615	134



The thermal ellipsoid plot is drawn at the 50% level. All H atoms are omitted for clarity.

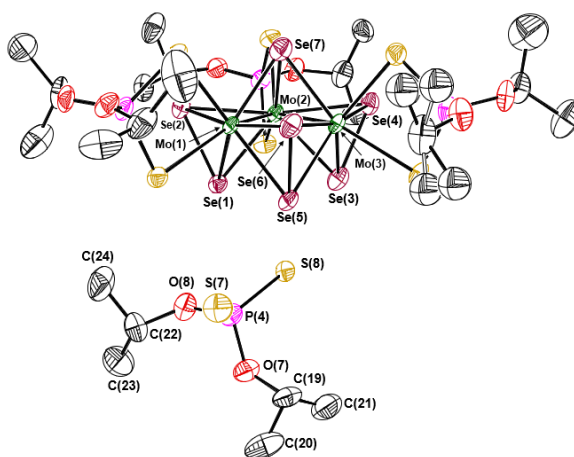


Table A.37. Crystal Data and Structure Refinement for $[\text{Mo}_3\text{Se}_7(\text{S}_2\text{PO}^i\text{Pr}_2)_3][\text{S}_2\text{PO}^i\text{Pr}_2] \cdot \frac{1}{4}\text{Et}_2\text{O}$.

Identification code	JPD1296_0m_a	
Empirical formula	$\text{C}_{25}\text{H}_{56}\text{Mo}_3\text{O}_{8.25}\text{P}_4\text{S}_8\text{Se}_7$	
Formula weight	1709.59	
Temperature	150(2) K	
Wavelength	0.71073 Å	
Crystal system	Triclinic	
Space group	$P\bar{1}$	
Unit cell dimensions	$a = 13.7582(4)$ Å	$\alpha = 72.260(2)^\circ$
	$b = 14.3562(4)$ Å	$\beta = 72.906(2)^\circ$
	$c = 16.1940(5)$ Å	$\gamma = 68.909(2)^\circ$
Volume	$2780.59(15)$ Å ³	
Z	2	
Density (calculated)	2.042 g/cm ³	
Absorption coefficient	5.701 mm ⁻¹	
F(000)	1648	

Table A.37, Cont'd. Crystal Data and Structure Refinement for $[\text{Mo}_3\text{Se}_7(\text{S}_2\text{PO}^i\text{Pr}_2)_3][\text{S}_2\text{PO}^i\text{Pr}_2] \cdot \frac{1}{4}\text{Et}_2\text{O}$.

Crystal size	0.326 x 0.173 x 0.139 mm ³
θ range for data collection	1.887 to 26.517°
Index ranges	$-17 \leq h \leq 17$, $-17 \leq k \leq 18$, $-20 \leq l \leq 20$
Reflections collected	105773
Independent reflections	11505 [R(int) = 0.0801]
Completeness to $\theta = 25.242^\circ$	99.9 %
Absorption correction	Semi-empirical from equivalents
Max. and min. transmission	0.7465 and 0.6798
Refinement method	Full-matrix least-squares on F^2
Data / restraints / parameters	11505 / 0 / 514
Goodness-of-fit on F^2	1.028
Final R indices [$I > 2\sigma(I)$]	R1 = 0.0656, wR2 = 0.1572
R indices (all data)	R1 = 0.1038, wR2 = 0.1916
Extinction coefficient	n/a
Largest diff. peak and hole	2.095 and -2.175 e·Å ⁻³

Table A.38. Atomic coordinates ($\times 10^4$) and equivalent isotropic displacement parameters ($\text{\AA}^2 \times 10^3$) for $[\text{Mo}_3\text{Se}_7(\text{S}_2\text{P}^i\text{Bu}_2)_3][\text{S}_2\text{P}^i\text{Bu}_2] \cdot \frac{1}{4}\text{Et}_2\text{O}$. $U(\text{eq})$ is defined as one third of the trace of the orthogonalized U^{ij} tensor.

Atom	x	y	z	U(eq)
Mo(1)	3120(1)	2507(1)	7940(1)	21(1)
Mo(2)	2762(1)	4609(1)	7352(1)	22(1)
Mo(3)	4836(1)	3291(1)	7174(1)	23(1)
Se(1)	2037(1)	3586(1)	6768(1)	27(1)
Se(2)	1217(1)	3819(1)	8198(1)	32(1)
Se(3)	4056(1)	4571(1)	5895(1)	37(1)
Se(4)	4436(1)	5292(1)	6785(1)	33(1)
Se(5)	4484(1)	2041(1)	6561(1)	27(1)
Se(6)	5061(1)	1354(1)	7899(1)	34(1)
Se(7)	3631(1)	3553(1)	8616(1)	38(1)
S(1)	2496(2)	1036(2)	7904(2)	30(1)
S(2)	2698(2)	1638(2)	9560(2)	32(1)
S(3)	1528(2)	6151(2)	6481(2)	32(1)
S(4)	2010(2)	5869(2)	8349(2)	31(1)
S(5)	6582(2)	3040(2)	5995(2)	34(1)
S(6)	6212(2)	3139(2)	7988(2)	36(1)
S(7)	3693(3)	746(2)	5623(2)	48(1)
S(8)	3567(2)	3249(2)	5033(2)	28(1)
P(1)	2191(2)	679(2)	9224(2)	30(1)
P(2)	1116(2)	6850(2)	7475(2)	31(1)
P(3)	7362(2)	2783(2)	6939(2)	33(1)
P(4)	3066(2)	2113(2)	4975(2)	35(1)
O(1)	2695(6)	-487(6)	9628(5)	37(2)
O(2)	996(6)	711(6)	9686(5)	38(2)
O(3)	-120(6)	7200(6)	7886(5)	38(2)
O(4)	1248(6)	7951(5)	7184(5)	37(2)
O(5)	8216(6)	3361(6)	6691(5)	38(2)
O(6)	8162(7)	1672(6)	7113(6)	46(2)
O(7)	3238(7)	2193(7)	3929(5)	44(2)
O(8)	1813(7)	2514(6)	5207(6)	45(2)
C(1)	3765(11)	-1085(11)	9319(8)	52(3)
C(2)	3718(14)	-2154(11)	9480(10)	66(4)
C(3)	4523(15)	-1048(12)	9792(15)	90(6)
C(4)	133(9)	1682(9)	9624(9)	46(3)
C(5)	-539(11)	1666(12)	10537(10)	60(4)
C(6)	-473(13)	1702(14)	8980(10)	73(5)
C(7)	-744(10)	6477(9)	8252(8)	42(3)
C(8)	-1834(10)	7074(11)	8033(10)	56(4)
C(9)	-818(11)	6122(12)	9223(9)	62(4)

Table A.38, Cont'd. Atomic coordinates ($\times 10^4$) and equivalent isotropic displacement parameters ($\text{\AA}^2 \times 10^3$) for $[\text{Mo}_3\text{Se}_7(\text{S}_2\text{P}^i\text{Bu}_2)_3][\text{S}_2\text{P}^i\text{Bu}_2] \cdot \frac{1}{4}\text{Et}_2\text{O}$. $U(\text{eq})$ is defined as one third of the trace of the orthogonalized U^{ij} tensor.

Atom	x	y	z	U(eq)
C(10)	2266(11)	8133(9)	6743(8)	46(3)
C(11)	2216(16)	8659(12)	5790(9)	71(5)
C(12)	2460(12)	8748(11)	7255(9)	54(3)
C(13)	7963(11)	4485(9)	6421(9)	48(3)
C(14)	8021(19)	4851(15)	7171(14)	97(7)
C(15)	8764(13)	4721(11)	5601(11)	71(5)
C(16)	7909(11)	720(9)	7274(11)	57(4)
C(17A)	7880(20)	190(20)	8163(18)	66(6)
C(18A)	8750(20)	130(20)	6583(18)	63(6)
C(17B)	8560(40)	60(40)	8100(30)	66(6)
C(18B)	8180(40)	240(30)	6600(30)	63(6)
C(19)	4301(11)	1806(10)	3436(8)	48(3)
C(20)	4289(14)	933(12)	3091(10)	70(5)
C(21)	4570(13)	2689(13)	2717(10)	67(4)
C(22)	1205(11)	1789(11)	5373(10)	53(3)
C(23)	456(14)	2195(16)	4744(12)	83(5)
C(24)	671(11)	1609(16)	6332(10)	76(5)
O(9)	-5000	5000	10000	170(20)
C(25B)	-4280(70)	4720(70)	10570(60)	101(19)
C(25A)	-3930(80)	5010(70)	9560(60)	101(19)
C(26)	-3000(30)	4720(30)	9570(30)	80(10)

Table A.39. Bond lengths (Å) for $[\text{Mo}_3\text{Se}_7(\text{S}_2\text{P}^i\text{Bu}_2)_3][\text{S}_2\text{P}^i\text{Bu}_2] \cdot \frac{1}{4}\text{Et}_2\text{O}$. Symmetry transformations used to generate equivalent atoms: #1 $-x - 1, -y + 1, -z + 2$.

Mo(1)-Se(7)	2.4831(14)	O(1)-C(1)	1.440(15)
Mo(1)-S(2)	2.532(2)	O(2)-C(4)	1.468(15)
Mo(1)-Se(1)	2.5357(13)	O(3)-C(7)	1.461(14)
Mo(1)-Se(5)	2.5498(12)	O(4)-C(10)	1.449(14)
Mo(1)-S(1)	2.571(3)	O(5)-C(13)	1.475(13)
Mo(1)-Se(6)	2.5798(14)	O(6)-C(16)	1.460(15)
Mo(1)-Se(2)	2.6197(13)	O(7)-C(19)	1.444(15)
Mo(1)-Mo(2)	2.7775(11)	O(8)-C(22)	1.477(15)
Mo(1)-Mo(3)	2.7782(11)	C(1)-C(3)	1.49(2)
Mo(2)-Se(7)	2.4817(14)	C(1)-C(2)	1.50(2)
Mo(2)-Se(3)	2.5059(13)	C(1)-H(1)	1.0000
Mo(2)-S(4)	2.529(3)	C(2)-H(2A)	0.9800
Mo(2)-Se(1)	2.5499(13)	C(2)-H(2B)	0.9800
Mo(2)-S(3)	2.564(3)	C(2)-H(2C)	0.9800
Mo(2)-Se(2)	2.5998(13)	C(3)-H(3A)	0.9800
Mo(2)-Se(4)	2.6338(13)	C(3)-H(3B)	0.9800
Mo(2)-Mo(3)	2.7865(12)	C(3)-H(3C)	0.9800
Mo(3)-Se(7)	2.4799(14)	C(4)-C(5)	1.494(18)
Mo(3)-S(6)	2.522(3)	C(4)-C(6)	1.50(2)
Mo(3)-Se(3)	2.5278(14)	C(4)-H(4)	1.0000
Mo(3)-Se(5)	2.5378(13)	C(5)-H(5A)	0.9800
Mo(3)-S(5)	2.579(3)	C(5)-H(5B)	0.9800
Mo(3)-Se(6)	2.6105(13)	C(5)-H(5C)	0.9800
Mo(3)-Se(4)	2.6290(13)	C(6)-H(6A)	0.9800
Se(1)-Se(2)	2.3263(14)	C(6)-H(6B)	0.9800
Se(3)-Se(4)	2.2719(17)	C(6)-H(6C)	0.9800
Se(5)-Se(6)	2.3335(15)	C(7)-C(9)	1.482(18)
S(1)-P(1)	1.993(4)	C(7)-C(8)	1.521(18)
S(2)-P(1)	2.011(4)	C(7)-H(7)	1.0000
S(3)-P(2)	1.989(4)	C(8)-H(8A)	0.9800
S(4)-P(2)	2.014(4)	C(8)-H(8B)	0.9800
S(5)-P(3)	1.990(4)	C(8)-H(8C)	0.9800
S(6)-P(3)	2.004(4)	C(9)-H(9A)	0.9800
S(7)-P(4)	1.938(4)	C(9)-H(9B)	0.9800
S(8)-P(4)	2.020(4)	C(9)-H(9C)	0.9800
P(1)-O(1)	1.574(8)	C(10)-C(11)	1.507(19)
P(1)-O(2)	1.583(8)	C(10)-C(12)	1.513(19)
P(2)-O(4)	1.567(8)	C(10)-H(10)	1.0000
P(2)-O(3)	1.585(8)	C(11)-H(11A)	0.9800
P(3)-O(5)	1.565(8)	C(11)-H(11B)	0.9800
P(3)-O(6)	1.574(8)	C(11)-H(11C)	0.9800
P(4)-O(8)	1.575(9)	C(12)-H(12A)	0.9800
P(4)-O(7)	1.613(8)	C(12)-H(12B)	0.9800

Table A.39, Cont'd. Bond lengths (Å) for $[\text{Mo}_3\text{Se}_7(\text{S}_2\text{P}^i\text{Bu}_2)_3][\text{S}_2\text{P}^i\text{Bu}_2]\cdot\frac{1}{4}\text{Et}_2\text{O}$. Symmetry transformations used to generate equivalent atoms: #1 $-x - 1, -y + 1, -z + 2$.

C(12)-H(12C)	0.9800	C(24)-H(24B)	0.9800
C(13)-C(15)	1.492(18)	C(24)-H(24C)	0.9800
C(13)-C(14)	1.49(2)	O(9)-C(25B)#1	1.41(9)
C(13)-H(13)	1.0000	O(9)-C(25B)	1.41(9)
C(14)-H(14A)	0.9800	O(9)-C(25A)#1	1.44(10)
C(14)-H(14B)	0.9800	O(9)-C(25A)	1.44(10)
C(14)-H(14C)	0.9800	C(25A)-C(26)	1.19(9)
C(15)-H(15A)	0.9800		
C(15)-H(15B)	0.9800		
C(15)-H(15C)	0.9800		
C(16)-C(18B)	1.36(4)		
C(16)-C(17A)	1.40(3)		
C(16)-C(18A)	1.55(3)		
C(16)-C(17B)	1.68(5)		
C(16)-H(16)	1.0000		
C(17A)-H(17A)	0.9800		
C(17A)-H(17B)	0.9800		
C(17A)-H(17C)	0.9800		
C(18A)-H(18A)	0.9800		
C(18A)-H(18B)	0.9800		
C(18A)-H(18C)	0.9800		
C(17B)-H(17D)	0.9800		
C(17B)-H(17E)	0.9800		
C(17B)-H(17F)	0.9800		
C(18B)-H(18D)	0.9800		
C(18B)-H(18E)	0.9800		
C(18B)-H(18F)	0.9800		
C(19)-C(21)	1.51(2)		
C(19)-C(20)	1.53(2)		
C(19)-H(19)	1.0000		
C(20)-H(20A)	0.9800		
C(20)-H(20B)	0.9800		
C(20)-H(20C)	0.9800		
C(21)-H(21A)	0.9800		
C(21)-H(21B)	0.9800		
C(21)-H(21C)	0.9800		
C(22)-C(24)	1.50(2)		
C(22)-C(23)	1.50(2)		
C(22)-H(22)	1.0000		
C(23)-H(23A)	0.9800		
C(23)-H(23B)	0.9800		
C(23)-H(23C)	0.9800		
C(24)-H(24A)	0.9800		

Table A.40. Bond angles (deg.) for $[\text{Mo}_3\text{Se}_7(\text{S}_2\text{P}^i\text{Bu}_2)_3][\text{S}_2\text{P}^i\text{Bu}_2]\cdot\frac{1}{4}\text{Et}_2\text{O}$. Symmetry transformations used to generate equivalent atoms: #1 $-x - 1, -y + 1, -z + 2$.

Se(7)-Mo(1)-S(2)	79.92(7)	Se(3)-Mo(2)-S(3)	85.46(7)
Se(7)-Mo(1)-Se(1)	112.73(5)	S(4)-Mo(2)-S(3)	76.72(9)
S(2)-Mo(1)-Se(1)	135.35(8)	Se(1)-Mo(2)-S(3)	83.32(7)
Se(7)-Mo(1)-Se(5)	112.17(5)	Se(7)-Mo(2)-Se(2)	85.40(4)
S(2)-Mo(1)-Se(5)	136.41(7)	Se(3)-Mo(2)-Se(2)	135.60(5)
Se(1)-Mo(1)-Se(5)	80.44(4)	S(4)-Mo(2)-Se(2)	88.52(7)
Se(7)-Mo(1)-S(1)	156.59(7)	Se(1)-Mo(2)-Se(2)	53.70(4)
S(2)-Mo(1)-S(1)	76.78(8)	S(3)-Mo(2)-Se(2)	91.93(7)
Se(1)-Mo(1)-S(1)	85.89(7)	Se(7)-Mo(2)-Se(4)	84.30(4)
Se(5)-Mo(1)-S(1)	83.92(7)	Se(3)-Mo(2)-Se(4)	52.39(4)
Se(7)-Mo(1)-Se(6)	84.57(5)	S(4)-Mo(2)-Se(4)	86.67(7)
S(2)-Mo(1)-Se(6)	87.71(7)	Se(1)-Mo(2)-Se(4)	134.14(5)
Se(1)-Mo(1)-Se(6)	134.38(5)	S(3)-Mo(2)-Se(4)	96.36(7)
Se(5)-Mo(1)-Se(6)	54.11(4)	Se(2)-Mo(2)-Se(4)	169.20(5)
S(1)-Mo(1)-Se(6)	92.31(7)	Se(7)-Mo(2)-Mo(1)	56.01(4)
Se(7)-Mo(1)-Se(2)	84.95(4)	Se(3)-Mo(2)-Mo(1)	96.91(4)
S(2)-Mo(1)-Se(2)	87.35(7)	S(4)-Mo(2)-Mo(1)	124.75(7)
Se(1)-Mo(1)-Se(2)	53.62(4)	Se(1)-Mo(2)-Mo(1)	56.65(3)
Se(5)-Mo(1)-Se(2)	133.80(5)	S(3)-Mo(2)-Mo(1)	138.85(7)
S(1)-Mo(1)-Se(2)	96.07(7)	Se(2)-Mo(2)-Mo(1)	58.20(3)
Se(6)-Mo(1)-Se(2)	169.05(5)	Se(4)-Mo(2)-Mo(1)	117.57(4)
Se(7)-Mo(1)-Mo(2)	55.96(4)	Se(7)-Mo(2)-Mo(3)	55.80(4)
S(2)-Mo(1)-Mo(2)	122.99(7)	Se(3)-Mo(2)-Mo(3)	56.76(3)
Se(1)-Mo(1)-Mo(2)	57.14(3)	S(4)-Mo(2)-Mo(3)	123.86(7)
Se(5)-Mo(1)-Mo(2)	95.86(4)	Se(1)-Mo(2)-Mo(3)	95.30(4)
S(1)-Mo(1)-Mo(2)	142.27(7)	S(3)-Mo(2)-Mo(3)	141.85(7)
Se(6)-Mo(1)-Mo(2)	118.08(4)	Se(2)-Mo(2)-Mo(3)	117.90(4)
Se(2)-Mo(1)-Mo(2)	57.50(3)	Se(4)-Mo(2)-Mo(3)	57.95(3)
Se(7)-Mo(1)-Mo(3)	55.91(3)	Mo(1)-Mo(2)-Mo(3)	59.91(3)
S(2)-Mo(1)-Mo(3)	123.87(7)	Se(7)-Mo(3)-S(6)	81.79(7)
Se(1)-Mo(1)-Mo(3)	95.83(4)	Se(7)-Mo(3)-Se(3)	111.20(5)
Se(5)-Mo(1)-Mo(3)	56.69(3)	S(6)-Mo(3)-Se(3)	135.13(8)
S(1)-Mo(1)-Mo(3)	139.41(7)	Se(7)-Mo(3)-Se(5)	112.69(5)
Se(6)-Mo(1)-Mo(3)	58.17(3)	S(6)-Mo(3)-Se(5)	133.59(8)
Se(2)-Mo(1)-Mo(3)	117.50(4)	Se(3)-Mo(3)-Se(5)	82.50(4)
Mo(2)-Mo(1)-Mo(3)	60.21(3)	Se(7)-Mo(3)-S(5)	158.07(8)
Se(7)-Mo(2)-Se(3)	111.88(5)	S(6)-Mo(3)-S(5)	76.40(9)
Se(7)-Mo(2)-S(4)	80.90(7)	Se(3)-Mo(3)-S(5)	83.47(7)
Se(3)-Mo(2)-S(4)	133.17(7)	Se(5)-Mo(3)-S(5)	84.59(7)
Se(7)-Mo(2)-Se(1)	112.29(5)	Se(7)-Mo(3)-Se(6)	83.99(4)
Se(3)-Mo(2)-Se(1)	82.03(4)	S(6)-Mo(3)-Se(6)	86.54(8)
S(4)-Mo(2)-Se(1)	136.54(7)	Se(3)-Mo(3)-Se(6)	135.95(5)
Se(7)-Mo(2)-S(3)	157.52(7)	Se(5)-Mo(3)-Se(6)	53.88(4)

Table A.40, Cont'd. Bond angles (deg.) for $[\text{Mo}_3\text{Se}_7(\text{S}_2\text{P}^i\text{Bu}_2)_3][\text{S}_2\text{P}^i\text{Bu}_2] \cdot \frac{1}{4}\text{Et}_2\text{O}$. Symmetry transformations used to generate equivalent atoms: #1 $-x - 1, -y + 1, -z + 2$.

S(5)-Mo(3)-Se(6)	96.78(7)	P(1)-S(1)-Mo(1)	88.82(12)
Se(7)-Mo(3)-Se(4)	84.44(4)	P(1)-S(2)-Mo(1)	89.51(12)
S(6)-Mo(3)-Se(4)	88.86(8)	P(2)-S(3)-Mo(2)	89.25(12)
Se(3)-Mo(3)-Se(4)	52.24(4)	P(2)-S(4)-Mo(2)	89.69(12)
Se(5)-Mo(3)-Se(4)	134.57(5)	P(3)-S(5)-Mo(3)	88.43(12)
S(5)-Mo(3)-Se(4)	92.84(7)	P(3)-S(6)-Mo(3)	89.70(13)
Se(6)-Mo(3)-Se(4)	168.04(5)	O(1)-P(1)-O(2)	96.0(4)
Se(7)-Mo(3)-Mo(1)	56.01(4)	O(1)-P(1)-S(1)	113.5(3)
S(6)-Mo(3)-Mo(1)	124.14(7)	O(2)-P(1)-S(1)	115.3(3)
Se(3)-Mo(3)-Mo(1)	96.38(4)	O(1)-P(1)-S(2)	114.2(3)
Se(5)-Mo(3)-Mo(1)	57.11(3)	O(2)-P(1)-S(2)	113.5(3)
S(5)-Mo(3)-Mo(1)	141.17(8)	S(1)-P(1)-S(2)	104.64(15)
Se(6)-Mo(3)-Mo(1)	57.11(3)	O(4)-P(2)-O(3)	95.6(4)
Se(4)-Mo(3)-Mo(1)	117.71(4)	O(4)-P(2)-S(3)	113.8(3)
Se(7)-Mo(3)-Mo(2)	55.86(4)	O(3)-P(2)-S(3)	115.5(3)
S(6)-Mo(3)-Mo(2)	125.95(8)	O(4)-P(2)-S(4)	113.8(3)
Se(3)-Mo(3)-Mo(2)	56.01(3)	O(3)-P(2)-S(4)	114.2(3)
Se(5)-Mo(3)-Mo(2)	95.91(4)	S(3)-P(2)-S(4)	104.24(16)
S(5)-Mo(3)-Mo(2)	138.82(7)	O(5)-P(3)-O(6)	95.9(4)
Se(6)-Mo(3)-Mo(2)	116.70(4)	O(5)-P(3)-S(5)	115.4(3)
Se(4)-Mo(3)-Mo(2)	58.12(3)	O(6)-P(3)-S(5)	113.5(4)
Mo(1)-Mo(3)-Mo(2)	59.88(3)	O(5)-P(3)-S(6)	113.1(4)
Se(2)-Se(1)-Mo(1)	65.04(4)	O(6)-P(3)-S(6)	114.9(4)
Se(2)-Se(1)-Mo(2)	64.25(4)	S(5)-P(3)-S(6)	104.35(16)
Mo(1)-Se(1)-Mo(2)	66.21(4)	O(8)-P(4)-O(7)	99.1(5)
Se(1)-Se(2)-Mo(2)	62.05(4)	O(8)-P(4)-S(7)	115.3(4)
Se(1)-Se(2)-Mo(1)	61.34(4)	O(7)-P(4)-S(7)	113.3(4)
Mo(2)-Se(2)-Mo(1)	64.30(3)	O(8)-P(4)-S(8)	105.5(3)
Se(4)-Se(3)-Mo(2)	66.70(4)	O(7)-P(4)-S(8)	104.5(4)
Se(4)-Se(3)-Mo(3)	66.17(5)	S(7)-P(4)-S(8)	117.1(2)
Mo(2)-Se(3)-Mo(3)	67.22(4)	C(1)-O(1)-P(1)	124.8(7)
Se(3)-Se(4)-Mo(3)	61.59(4)	C(4)-O(2)-P(1)	121.1(6)
Se(3)-Se(4)-Mo(2)	60.91(4)	C(7)-O(3)-P(2)	122.0(7)
Mo(3)-Se(4)-Mo(2)	63.94(3)	C(10)-O(4)-P(2)	122.0(7)
Se(6)-Se(5)-Mo(3)	64.65(4)	C(13)-O(5)-P(3)	123.3(7)
Se(6)-Se(5)-Mo(1)	63.60(4)	C(16)-O(6)-P(3)	125.7(8)
Mo(3)-Se(5)-Mo(1)	66.20(3)	C(19)-O(7)-P(4)	118.8(8)
Se(5)-Se(6)-Mo(1)	62.29(4)	C(22)-O(8)-P(4)	118.6(8)
Se(5)-Se(6)-Mo(3)	61.47(4)	O(1)-C(1)-C(3)	111.4(13)
Mo(1)-Se(6)-Mo(3)	64.72(4)	O(1)-C(1)-C(2)	105.7(11)
Mo(3)-Se(7)-Mo(2)	68.33(4)	C(3)-C(1)-C(2)	111.5(12)
Mo(3)-Se(7)-Mo(1)	68.08(4)	O(1)-C(1)-H(1)	109.4
Mo(2)-Se(7)-Mo(1)	68.03(4)	C(3)-C(1)-H(1)	109.4

Table A.40, Cont'd. Bond angles (deg.) for $[\text{Mo}_3\text{Se}_7(\text{S}_2\text{P}^i\text{Bu}_2)_3][\text{S}_2\text{P}^i\text{Bu}_2]\cdot\frac{1}{4}\text{Et}_2\text{O}$. Symmetry transformations used to generate equivalent atoms: #1 $-x - 1, -y + 1, -z + 2$.

C(2)-C(1)-H(1)	109.4	C(7)-C(9)-H(9A)	109.5
C(1)-C(2)-H(2A)	109.5	C(7)-C(9)-H(9B)	109.5
C(1)-C(2)-H(2B)	109.5	H(9A)-C(9)-H(9B)	109.5
H(2A)-C(2)-H(2B)	109.5	C(7)-C(9)-H(9C)	109.5
C(1)-C(2)-H(2C)	109.5	H(9A)-C(9)-H(9C)	109.5
H(2A)-C(2)-H(2C)	109.5	H(9B)-C(9)-H(9C)	109.5
H(2B)-C(2)-H(2C)	109.5	O(4)-C(10)-C(11)	107.8(12)
C(1)-C(3)-H(3A)	109.5	O(4)-C(10)-C(12)	107.0(11)
C(1)-C(3)-H(3B)	109.5	C(11)-C(10)-C(12)	114.4(10)
H(3A)-C(3)-H(3B)	109.5	O(4)-C(10)-H(10)	109.2
C(1)-C(3)-H(3C)	109.5	C(11)-C(10)-H(10)	109.2
H(3A)-C(3)-H(3C)	109.5	C(12)-C(10)-H(10)	109.2
H(3B)-C(3)-H(3C)	109.5	C(10)-C(11)-H(11A)	109.5
O(2)-C(4)-C(5)	106.0(10)	C(10)-C(11)-H(11B)	109.5
O(2)-C(4)-C(6)	107.1(11)	H(11A)-C(11)-H(11B)	109.5
C(5)-C(4)-C(6)	111.8(11)	C(10)-C(11)-H(11C)	109.5
O(2)-C(4)-H(4)	110.6	H(11A)-C(11)-H(11C)	109.5
C(5)-C(4)-H(4)	110.6	H(11B)-C(11)-H(11C)	109.5
C(6)-C(4)-H(4)	110.6	C(10)-C(12)-H(12A)	109.5
C(4)-C(5)-H(5A)	109.5	C(10)-C(12)-H(12B)	109.5
C(4)-C(5)-H(5B)	109.5	H(12A)-C(12)-H(12B)	109.5
H(5A)-C(5)-H(5B)	109.5	C(10)-C(12)-H(12C)	109.5
C(4)-C(5)-H(5C)	109.5	H(12A)-C(12)-H(12C)	109.5
H(5A)-C(5)-H(5C)	109.5	H(12B)-C(12)-H(12C)	109.5
H(5B)-C(5)-H(5C)	109.5	O(5)-C(13)-C(15)	106.8(11)
C(4)-C(6)-H(6A)	109.5	O(5)-C(13)-C(14)	107.5(12)
C(4)-C(6)-H(6B)	109.5	C(15)-C(13)-C(14)	112.5(14)
H(6A)-C(6)-H(6B)	109.5	O(5)-C(13)-H(13)	109.9
C(4)-C(6)-H(6C)	109.5	C(15)-C(13)-H(13)	109.9
H(6A)-C(6)-H(6C)	109.5	C(14)-C(13)-H(13)	109.9
H(6B)-C(6)-H(6C)	109.5	C(13)-C(14)-H(14A)	109.5
O(3)-C(7)-C(9)	110.0(11)	C(13)-C(14)-H(14B)	109.5
O(3)-C(7)-C(8)	105.0(10)	H(14A)-C(14)-H(14B)	109.5
C(9)-C(7)-C(8)	111.2(11)	C(13)-C(14)-H(14C)	109.5
O(3)-C(7)-H(7)	110.2	H(14A)-C(14)-H(14C)	109.5
C(9)-C(7)-H(7)	110.2	H(14B)-C(14)-H(14C)	109.5
C(8)-C(7)-H(7)	110.2	C(13)-C(15)-H(15A)	109.5
C(7)-C(8)-H(8A)	109.5	C(13)-C(15)-H(15B)	109.5
C(7)-C(8)-H(8B)	109.5	H(15A)-C(15)-H(15B)	109.5
H(8A)-C(8)-H(8B)	109.5	C(13)-C(15)-H(15C)	109.5
C(7)-C(8)-H(8C)	109.5	H(15A)-C(15)-H(15C)	109.5
H(8A)-C(8)-H(8C)	109.5	H(15B)-C(15)-H(15C)	109.5
H(8B)-C(8)-H(8C)	109.5	C(18B)-C(16)-O(6)	119(2)

Table A.40, Cont'd. Bond angles (deg.) for $[\text{Mo}_3\text{Se}_7(\text{S}_2\text{P}^i\text{Bu}_2)_3][\text{S}_2\text{P}^i\text{Bu}_2]\cdot\frac{1}{4}\text{Et}_2\text{O}$. Symmetry transformations used to generate equivalent atoms: #1 $-x - 1, -y + 1, -z + 2$.

C(17A)-C(16)-O(6)	110.7(17)	H(20B)-C(20)-H(20C)	109.5
C(17A)-C(16)-C(18A)	115.3(18)	C(19)-C(21)-H(21A)	109.5
O(6)-C(16)-C(18A)	105.1(14)	C(19)-C(21)-H(21B)	109.5
C(18B)-C(16)-C(17B)	114(3)	H(21A)-C(21)-H(21B)	109.5
O(6)-C(16)-C(17B)	97.3(19)	C(19)-C(21)-H(21C)	109.5
C(17A)-C(16)-H(16)	108.5	H(21A)-C(21)-H(21C)	109.5
O(6)-C(16)-H(16)	108.5	H(21B)-C(21)-H(21C)	109.5
C(18A)-C(16)-H(16)	108.5	O(8)-C(22)-C(24)	108.4(12)
C(16)-C(17A)-H(17A)	109.5	O(8)-C(22)-C(23)	109.2(12)
C(16)-C(17A)-H(17B)	109.5	C(24)-C(22)-C(23)	114.4(13)
H(17A)-C(17A)-H(17B)	109.5	O(8)-C(22)-H(22)	108.2
C(16)-C(17A)-H(17C)	109.5	C(24)-C(22)-H(22)	108.2
H(17A)-C(17A)-H(17C)	109.5	C(23)-C(22)-H(22)	108.2
H(17B)-C(17A)-H(17C)	109.5	C(22)-C(23)-H(23A)	109.5
C(16)-C(18A)-H(18A)	109.5	C(22)-C(23)-H(23B)	109.5
C(16)-C(18A)-H(18B)	109.5	H(23A)-C(23)-H(23B)	109.5
H(18A)-C(18A)-H(18B)	109.5	C(22)-C(23)-H(23C)	109.5
C(16)-C(18A)-H(18C)	109.5	H(23A)-C(23)-H(23C)	109.5
H(18A)-C(18A)-H(18C)	109.5	H(23B)-C(23)-H(23C)	109.5
H(18B)-C(18A)-H(18C)	109.5	C(22)-C(24)-H(24A)	109.5
C(16)-C(17B)-H(17D)	109.5	C(22)-C(24)-H(24B)	109.5
C(16)-C(17B)-H(17E)	109.5	H(24A)-C(24)-H(24B)	109.5
H(17D)-C(17B)-H(17E)	109.5	C(22)-C(24)-H(24C)	109.5
C(16)-C(17B)-H(17F)	109.5	H(24A)-C(24)-H(24C)	109.5
H(17D)-C(17B)-H(17F)	109.5	H(24B)-C(24)-H(24C)	109.5
H(17E)-C(17B)-H(17F)	109.5	C(25B)#1-O(9)-C(25B)	180.00(2)
C(16)-C(18B)-H(18D)	109.5	C(25B)#1-O(9)-C(25A)#1	65(5)
C(16)-C(18B)-H(18E)	109.5	C(25B)-O(9)-C(25A)#1	115(5)
H(18D)-C(18B)-H(18E)	109.5	C(25A)#1-O(9)-C(25A)	179.998(11)
C(16)-C(18B)-H(18F)	109.5	C(26)-C(25A)-O(9)	150(8)
H(18D)-C(18B)-H(18F)	109.5		
H(18E)-C(18B)-H(18F)	109.5		
O(7)-C(19)-C(21)	107.6(11)		
O(7)-C(19)-C(20)	106.5(12)		
C(21)-C(19)-C(20)	114.2(12)		
O(7)-C(19)-H(19)	109.5		
C(21)-C(19)-H(19)	109.5		
C(20)-C(19)-H(19)	109.5		
C(19)-C(20)-H(20A)	109.5		
C(19)-C(20)-H(20B)	109.5		
H(20A)-C(20)-H(20B)	109.5		
C(19)-C(20)-H(20C)	109.5		
H(20A)-C(20)-H(20C)	109.5		

Table A.41. Anisotropic displacement parameters ($\text{\AA}^2 \times 10^3$) for $[\text{Mo}_3\text{Se}_7(\text{S}_2\text{P}^i\text{Bu}_2)_3][\text{S}_2\text{P}^i\text{Bu}_2] \cdot \frac{1}{4}\text{Et}_2\text{O}$. The anisotropic displacement factor exponent takes the form: $-2\pi^2[h^2a^{*2}U^{11} + \dots + 2hka^*b^*U^{12}]$.

Atom	U^{11}	U^{22}	U^{33}	U^{23}	U^{13}	U^{12}
Mo(1)	23(1)	20(1)	17(1)	0(1)	0(1)	-9(1)
Mo(2)	24(1)	20(1)	18(1)	-2(1)	0(1)	-9(1)
Mo(3)	23(1)	23(1)	18(1)	0(1)	1(1)	-9(1)
Se(1)	32(1)	24(1)	24(1)	-2(1)	-4(1)	-10(1)
Se(2)	30(1)	30(1)	30(1)	-4(1)	1(1)	-11(1)
Se(3)	38(1)	35(1)	30(1)	-1(1)	0(1)	-12(1)
Se(4)	33(1)	30(1)	34(1)	-3(1)	-1(1)	-15(1)
Se(5)	30(1)	25(1)	21(1)	-3(1)	1(1)	-9(1)
Se(6)	36(1)	31(1)	29(1)	1(1)	-4(1)	-10(1)
Se(7)	40(1)	38(1)	32(1)	-4(1)	-2(1)	-16(1)
S(1)	41(2)	27(1)	24(1)	-3(1)	-2(1)	-18(1)
S(2)	43(2)	33(1)	19(1)	-1(1)	1(1)	-20(1)
S(3)	38(1)	26(1)	28(1)	-3(1)	-11(1)	-4(1)
S(4)	35(1)	29(1)	27(1)	-8(1)	-4(1)	-7(1)
S(5)	27(1)	36(1)	25(1)	0(1)	4(1)	-8(1)
S(6)	32(1)	48(2)	28(1)	0(1)	-7(1)	-19(1)
S(7)	59(2)	32(2)	48(2)	-2(1)	-15(2)	-10(1)
S(8)	36(1)	20(1)	27(1)	2(1)	-6(1)	-12(1)
P(1)	34(1)	29(1)	24(1)	0(1)	2(1)	-17(1)
P(2)	34(1)	24(1)	30(1)	-6(1)	-2(1)	-6(1)
P(3)	26(1)	28(1)	37(2)	3(1)	-4(1)	-9(1)
P(4)	39(2)	31(1)	30(1)	-4(1)	-4(1)	-9(1)
O(1)	47(5)	30(4)	26(4)	3(3)	-1(3)	-15(3)
O(2)	42(4)	35(4)	35(4)	0(3)	3(3)	-25(4)
O(3)	38(4)	40(4)	34(4)	-9(3)	-6(3)	-11(4)
O(4)	35(4)	27(4)	38(4)	1(3)	-3(3)	-7(3)
O(5)	22(4)	31(4)	51(5)	0(3)	0(3)	-10(3)
O(6)	40(5)	35(4)	59(5)	2(4)	-14(4)	-13(4)
O(7)	44(5)	51(5)	33(4)	-12(4)	-6(4)	-8(4)
O(8)	41(5)	36(4)	50(5)	-7(4)	-1(4)	-10(4)
C(1)	49(8)	55(8)	35(7)	8(6)	-9(6)	-9(6)
C(2)	82(11)	54(9)	53(9)	-16(7)	-24(8)	3(8)
C(3)	82(12)	39(8)	137(18)	24(10)	-48(12)	-19(8)
C(4)	35(6)	39(6)	53(7)	0(6)	7(5)	-21(5)
C(5)	47(8)	67(9)	63(9)	-31(8)	3(7)	-12(7)
C(6)	55(9)	82(11)	51(9)	3(8)	-3(7)	-5(8)
C(7)	39(6)	36(6)	47(7)	-6(5)	0(5)	-16(5)
C(8)	38(7)	64(9)	64(9)	-10(7)	-6(6)	-20(6)
C(9)	47(8)	64(9)	52(8)	12(7)	-7(6)	-13(7)

Table A.41, Cont'd. Anisotropic displacement parameters ($\text{\AA}^2 \times 10^3$) for $[\text{Mo}_3\text{Se}_7(\text{S}_2\text{P}^i\text{Bu}_2)_3][\text{S}_2\text{P}^i\text{Bu}_2] \cdot \frac{1}{4}\text{Et}_2\text{O}$. The anisotropic displacement factor exponent takes the form: $-2\pi^2[h^2a^*2U^{11} + \dots + 2hka^*b^*U^{12}]$.

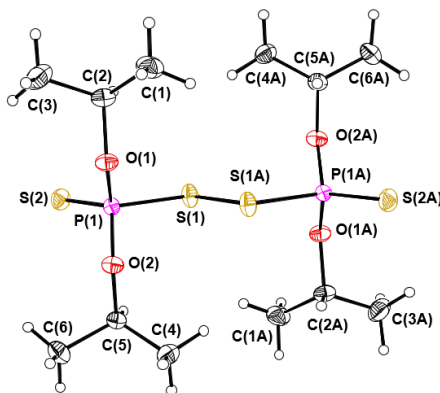
Atom	U^{11}	U^{22}	U^{33}	U^{23}	U^{13}	U^{12}
C(10)	52(7)	31(6)	45(7)	8(5)	-4(6)	-19(6)
C(11)	120(15)	60(9)	44(8)	-14(7)	4(8)	-54(10)
C(12)	64(9)	60(8)	49(8)	0(6)	-15(7)	-37(7)
C(13)	47(7)	28(6)	60(8)	1(5)	-2(6)	-17(5)
C(14)	130(18)	69(12)	96(15)	-27(11)	-4(13)	-41(12)
C(15)	77(11)	45(8)	66(10)	12(7)	11(8)	-29(8)
C(16)	45(7)	30(6)	80(10)	5(6)	-10(7)	-8(6)
C(19)	49(7)	57(8)	35(6)	-21(6)	-5(5)	-3(6)
C(20)	78(11)	60(9)	49(8)	-23(7)	-7(8)	10(8)
C(21)	60(9)	86(12)	50(8)	-26(8)	1(7)	-17(8)
C(22)	52(8)	50(8)	64(9)	-8(7)	-12(7)	-27(6)
C(23)	67(11)	120(16)	77(12)	-21(11)	-31(9)	-34(11)
C(24)	31(7)	128(16)	59(9)	-3(10)	-12(7)	-26(9)

Table A.42. Hydrogen coordinates ($\times 10^4$) and isotropic displacement parameters ($\text{\AA}^2 \times 10^3$) for $[\text{Mo}_3\text{Se}_7(\text{S}_2\text{P}^i\text{Bu}_2)_3][\text{S}_2\text{P}^i\text{Bu}_2] \cdot \frac{1}{4}\text{Et}_2\text{O}$.

H atom	x	y	z	U(eq)
H(1)	3991	-817	8668	63
H(2A)	3525	-2427	10119	99
H(2B)	4416	-2587	9237	99
H(2C)	3182	-2146	9189	99
H(3A)	4494	-334	9712	135
H(3B)	5246	-1438	9552	135
H(3C)	4326	-1346	10425	135
H(4)	428	2276	9416	55
H(5A)	-809	1072	10735	89
H(5B)	-1139	2295	10532	89
H(5C)	-109	1621	10943	89
H(6A)	-4	1696	8394	110
H(6B)	-1081	2324	8946	110
H(6C)	-729	1099	9182	110
H(7)	-410	5879	7963	50
H(8A)	-2136	7679	8291	84
H(8B)	-2306	6638	8277	84
H(8C)	-1763	7291	7388	84
H(9A)	-100	5816	9348	93
H(9B)	-1206	5611	9459	93
H(9C)	-1198	6706	9504	93
H(10)	2838	7461	6764	55
H(11A)	2164	8187	5488	106
H(11B)	2861	8868	5495	106
H(11C)	1590	9266	5767	106
H(12A)	1900	9406	7239	82
H(12B)	3154	8870	6986	82
H(12C)	2453	8368	7871	82
H(13)	7230	4793	6294	57
H(14A)	7353	4897	7614	146
H(14B)	8133	5528	6947	146
H(14C)	8615	4369	7444	146
H(15A)	9479	4294	5690	107
H(15B)	8724	5445	5471	107
H(15C)	8615	4579	5104	107
H(16)	7190	891	7144	69
H(17A)	7529	685	8547	100
H(17B)	8608	-168	8253	100
H(17C)	7482	-300	8311	100
H(18A)	9438	-154	6768	94

Table A.42, Cont'd. Hydrogen coordinates ($\times 10^4$) and isotropic displacement parameters ($\text{\AA}^2 \times 10^3$) for $[\text{Mo}_3\text{Se}_7(\text{S}_2\text{P}^i\text{Bu}_2)_3][\text{S}_2\text{P}^i\text{Bu}_2] \cdot \frac{1}{4}\text{Et}_2\text{O}$.

H atom	x	y	z	U(eq)
H(18B)	8827	607	6003	94
H(18C)	8523	-420	6544	94
H(17D)	8608	-666	8223	100
H(17E)	8165	323	8638	100
H(17F)	9272	136	7936	100
H(18D)	7882	721	6094	94
H(18E)	7892	-344	6795	94
H(18F)	8956	-3	6421	94
H(19)	4816	1534	3841	58
H(20A)	4040	424	3589	105
H(20B)	5010	610	2789	105
H(20C)	3810	1205	2674	105
H(21A)	4127	2898	2278	101
H(21B)	5323	2475	2427	101
H(21C)	4435	3267	2979	101
H(22)	1719	1124	5249	64
H(23A)	-78	2830	4876	124
H(23B)	100	1687	4814	124
H(23C)	858	2334	4134	124
H(24A)	1209	1351	6697	114
H(24B)	289	1106	6459	114
H(24C)	166	2255	6467	114



Thermal ellipsoid plot is drawn at the 50% level.

Table A.43. Crystal Data and Structure Refinement for $[(i\text{PrO})_2\text{P}(\text{S})\text{S}-\text{SP}(\text{S})(\text{O}^i\text{Pr})_2]$.

Identification code	JPD1268_xprep_a	
Empirical formula	$\text{C}_{12}\text{H}_{28}\text{O}_4\text{P}_2\text{S}_4$	
Formula weight	426.52	
Temperature	150(2) K	
Wavelength	0.71073 Å	
Crystal system	Triclinic	
Space group	$P-1$	
Unit cell dimensions	$a = 8.1001(8)$ Å	$\alpha = 97.731(4)^\circ$
	$b = 8.3522(8)$ Å	$\beta = 111.085(3)^\circ$
	$c = 8.4745(8)$ Å	$\gamma = 94.678(4)^\circ$
Volume	$524.82(9)$ Å ³	
Z	1	
Density (calculated)	1.350 g/cm ³	
Absorption coefficient	0.616 mm ⁻¹	
$F(000)$	226	
Crystal size	0.563 x 0.273 x 0.248 mm ³	
θ range for data collection	2.985 to 42.412°	
Index ranges	$-15 \leq h \leq 15, -15 \leq k \leq 15, -16 \leq l \leq 16$	
Reflections collected	40335	
Independent reflections	7197 [R(int) = 0.0362]	
Completeness to $\theta = 25.242^\circ$	88.3 %	
Absorption correction	Semi-empirical from equivalents	
Max. and min. transmission	0.7483 and 0.6825	
Refinement method	Full-matrix least-squares on F^2	
Data / restraints / parameters	7197 / 0 / 104	
Goodness-of-fit on F^2	1.063	
Final R indices [$I > 2\sigma(I)$]	R1 = 0.0253, wR2 = 0.0673	
R indices (all data)	R1 = 0.0318, wR2 = 0.0710	
Extinction coefficient	n/a	
Largest diff. peak and hole	0.395 and -0.216 e·Å ⁻³	

Table A.44. Atomic coordinates ($\times 10^4$) and equivalent isotropic displacement parameters ($\text{\AA}^2 \times 10^3$) for $[(^i\text{PrO})_2\text{P}(\text{S})\text{S}-\text{SP}(\text{S})(\text{O}^i\text{Pr})_2]$. $U(\text{eq})$ is defined as one third of the trace of the orthogonalized U^{ij} tensor.

Atom	x	y	z	U(eq)
S(1)	5586(1)	4324(1)	5975(1)	22(1)
S(2)	4167(1)	1792(1)	7831(1)	24(1)
P(1)	3297(1)	3108(1)	6093(1)	15(1)
O(1)	2062(1)	2255(1)	4222(1)	20(1)
O(2)	2072(1)	4406(1)	6317(1)	20(1)
C(1)	2329(1)	1246(1)	1568(1)	32(1)
C(2)	2557(1)	857(1)	3316(1)	23(1)
C(3)	1367(1)	-655(1)	3255(1)	36(1)
C(4)	2524(1)	7266(1)	7448(1)	27(1)
C(5)	2605(1)	5591(1)	7931(1)	20(1)
C(6)	1334(1)	5169(1)	8795(1)	36(1)

Table A.45. Bond lengths (Å) and angles (deg.) for [(ⁱPrO)₂P(S)S–SP(S)(OⁱPr)₂]. Symmetry transformations used to generate equivalent atoms: #1 –x + 1, –y + 1, –z + 1.

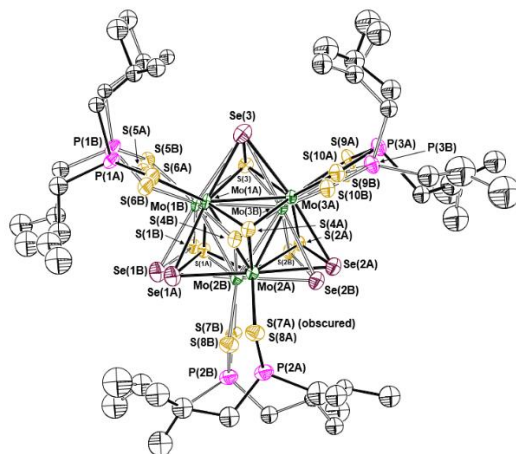
S(1)-P(1)	2.0822(3)	C(2)-C(1)-H(1B)	109.5
S(1)-S(1)#1	2.1106(3)	H(1A)-C(1)-H(1B)	109.5
S(2)-P(1)	1.9205(2)	C(2)-C(1)-H(1C)	109.5
P(1)-O(2)	1.5660(4)	H(1A)-C(1)-H(1C)	109.5
P(1)-O(1)	1.5689(4)	H(1B)-C(1)-H(1C)	109.5
O(1)-C(2)	1.4734(7)	O(1)-C(2)-C(1)	106.17(5)
O(2)-C(5)	1.4756(6)	O(1)-C(2)-C(3)	107.80(5)
C(1)-C(2)	1.5081(9)	C(1)-C(2)-C(3)	113.75(6)
C(1)-H(1A)	0.9800	O(1)-C(2)-H(2)	109.7
C(1)-H(1B)	0.9800	C(1)-C(2)-H(2)	109.7
C(1)-H(1C)	0.9800	C(3)-C(2)-H(2)	109.7
C(2)-C(3)	1.5089(10)	C(2)-C(3)-H(3A)	109.5
C(2)-H(2)	1.0000	C(2)-C(3)-H(3B)	109.5
C(3)-H(3A)	0.9800	H(3A)-C(3)-H(3B)	109.5
C(3)-H(3B)	0.9800	C(2)-C(3)-H(3C)	109.5
C(3)-H(3C)	0.9800	H(3A)-C(3)-H(3C)	109.5
C(4)-C(5)	1.5095(8)	H(3B)-C(3)-H(3C)	109.5
C(4)-H(4A)	0.9800	C(5)-C(4)-H(4A)	109.5
C(4)-H(4B)	0.9800	C(5)-C(4)-H(4B)	109.5
C(4)-H(4C)	0.9800	H(4A)-C(4)-H(4B)	109.5
C(5)-C(6)	1.5079(9)	C(5)-C(4)-H(4C)	109.5
C(5)-H(5)	1.0000	H(4A)-C(4)-H(4C)	109.5
C(6)-H(6A)	0.9800	H(4B)-C(4)-H(4C)	109.5
C(6)-H(6B)	0.9800	O(2)-C(5)-C(6)	107.33(5)
C(6)-H(6C)	0.9800	O(2)-C(5)-C(4)	106.86(4)
		C(6)-C(5)-C(4)	113.33(5)
P(1)-S(1)-S(1)#1	100.063(11)	O(2)-C(5)-H(5)	109.7
O(2)-P(1)-O(1)	96.97(2)	C(6)-C(5)-H(5)	109.7
O(2)-P(1)-S(2)	119.302(18)	C(4)-C(5)-H(5)	109.7
O(1)-P(1)-S(2)	119.164(19)	C(5)-C(6)-H(6A)	109.5
O(2)-P(1)-S(1)	108.086(19)	C(5)-C(6)-H(6B)	109.5
O(1)-P(1)-S(1)	107.835(19)	H(6A)-C(6)-H(6B)	109.5
S(2)-P(1)-S(1)	104.816(10)	C(5)-C(6)-H(6C)	109.5
C(2)-O(1)-P(1)	121.43(3)	H(6A)-C(6)-H(6C)	109.5
C(5)-O(2)-P(1)	120.73(3)	H(6B)-C(6)-H(6C)	109.5
C(2)-C(1)-H(1A)	109.5		

Table A.46. Anisotropic displacement parameters ($\text{\AA}^2 \times 10^3$) for (3,5-Cl₂-H₃C₆)C(O)C(O)(C₆H₃-3,5-Cl₂). The anisotropic displacement factor exponent takes the form: $-2\pi^2[h^2a^{*2}U^{11} + \dots + 2hka^*b^*U^{12}]$.

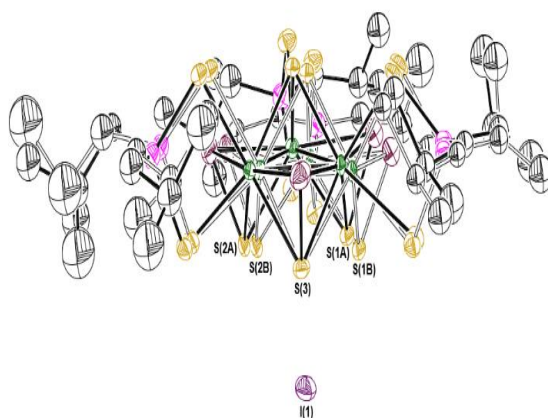
Atom	U^{11}	U^{22}	U^{33}	U^{23}	U^{13}	U^{12}
S(1)	14(1)	28(1)	24(1)	12(1)	6(1)	3(1)
S(2)	28(1)	23(1)	22(1)	10(1)	8(1)	4(1)
P(1)	15(1)	16(1)	15(1)	3(1)	5(1)	2(1)
O(1)	19(1)	21(1)	18(1)	-1(1)	3(1)	5(1)
O(2)	18(1)	22(1)	19(1)	0(1)	6(1)	5(1)
C(1)	39(1)	34(1)	21(1)	0(1)	12(1)	6(1)
C(2)	24(1)	22(1)	20(1)	-1(1)	5(1)	7(1)
C(3)	48(1)	21(1)	35(1)	3(1)	12(1)	1(1)
C(4)	30(1)	21(1)	30(1)	4(1)	11(1)	5(1)
C(5)	22(1)	20(1)	18(1)	1(1)	8(1)	4(1)
C(6)	46(1)	35(1)	35(1)	3(1)	28(1)	1(1)

Table A.47. Hydrogen coordinates ($\times 10^4$) and isotropic displacement parameters ($\text{\AA}^2 \times 10^3$) for (3,5-Cl₂-H₃C₆)C(O)C(O)(C₆H₃-3,5-Cl₂).

H atom	x	y	z	U(eq)
H(1A)	2631	343	904	48
H(1B)	3121	2249	1702	48
H(1C)	1085	1399	964	48
H(2)	3835	743	3954	28
H(3A)	1682	-1609	2674	55
H(3B)	116	-542	2625	55
H(3C)	1529	-798	4429	55
H(4A)	2867	8093	8488	40
H(4B)	1304	7339	6681	40
H(4C)	3347	7454	6860	40
H(5)	3854	5504	8693	24
H(6A)	1670	5918	9890	54
H(6B)	1391	4046	9006	54
H(6C)	114	5268	8050	54



Thermal ellipsoid plot is drawn at the 50% level. All H atoms are omitted for clarity. The cation is afflicted by a "whole-molecule" disorder by a pivot along the Se(3)–S(3) axis.



Thermal ellipsoid plot is drawn at the 30% level. All H atoms are omitted for clarity.

Table A.48. Crystal Data and Structure Refinement for $[\text{Mo}_3\text{S}_4\text{Se}_3(\text{S}_2\text{P}^i\text{Bu}_2)_3]\text{I} \cdot \frac{1}{2}\text{C}_5\text{H}_{12}$.

Identification code	JPD1097_0m_a	
Empirical formula	$\text{C}_{26.50}\text{H}_{60}\text{IMo}_3\text{P}_3\text{S}_{10}\text{Se}_3$	
Formula weight	1443.85	
Temperature	150(2) K	
Wavelength	0.71073 Å	
Crystal system	Monoclinic	
Space group	$C2/c$	
Unit cell dimensions	$a = 32.047(3)$ Å	$\alpha = 90^\circ$
	$b = 17.7330(14)$ Å	$\beta = 106.950(2)^\circ$
	$c = 20.1100(15)$ Å	$\gamma = 90^\circ$
Volume	$10931.9(15)$ Å ³	
Z	8	
Density (calculated)	1.755 g/cm ³	
Absorption coefficient	3.729 mm ⁻¹	
F(000)	5640	

Table A.48, Cont'd. Crystal Data and Structure Refinement for $[\text{Mo}_3\text{S}_4\text{Se}_3(\text{S}_2\text{P}^i\text{Bu}_2)_3]\text{I} \cdot \frac{1}{2}\text{C}_5\text{H}_{12}$.

Crystal size	0.217 x 0.206 x 0.060 mm ³
θ range for data collection	2.117 to 27.249°
Index ranges	$-41 \leq h \leq 41, -22 \leq k \leq 22, -25 \leq l \leq 25$
Reflections collected	144302
Independent reflections	12155 [R(int) = 0.0336]
Completeness to $\theta = 25.242^\circ$	99.9 %
Refinement method	Full-matrix least-squares on F^2
Data / restraints / parameters	12155 / 101 / 465
Goodness-of-fit on F^2	1.072
Final R indices [$I > 2\sigma(I)$]	R1 = 0.0638, wR2 = 0.1794
R indices (all data)	R1 = 0.0877, wR2 = 0.2066
Extinction coefficient	n/a
Largest diff. peak and hole	1.791 and -2.021 e·Å ⁻³

Table A.49. Atomic coordinates ($\times 10^4$) and equivalent isotropic displacement parameters ($\text{\AA}^2 \times 10^3$) for $[\text{Mo}_3\text{S}_4\text{Se}_3(\text{S}_2\text{P}^i\text{Bu}_2)_3]\text{I} \cdot \frac{1}{2}\text{C}_5\text{H}_{12}$. $U(\text{eq})$ is defined as one third of the trace of the orthogonalized U^{ij} tensor.

Atom	x	y	z	U(eq)
I(1)	1843(1)	8631(1)	3652(1)	66(1)
Se(3)	2344(1)	8383(1)	1332(1)	55(1)
S(3)	2163(1)	8506(1)	2285(1)	36(1)
Mo(1A)	1710(2)	7678(2)	1474(3)	28(1)
Mo(2A)	951(1)	8444(1)	1333(1)	32(1)
Mo(3A)	1689(1)	9200(2)	1298(2)	27(1)
Se(1A)	973(1)	6994(1)	1391(1)	59(1)
Se(2A)	951(1)	9889(1)	1128(1)	50(1)
S(1A)	1304(3)	7644(4)	2314(4)	34(1)
S(2A)	1297(3)	9446(4)	2142(5)	32(1)
S(4A)	1303(2)	8312(3)	452(3)	32(1)
S(5A)	2159(4)	6594(10)	2280(10)	38(2)
S(6A)	1877(7)	6712(14)	678(14)	43(2)
P(1A)	2157(3)	6027(9)	1405(8)	40(2)
C(1A)	2697(5)	5827(9)	1352(8)	39(3)
C(2A)	2992(6)	6514(11)	1395(9)	47(4)
C(3A)	2905(6)	6890(11)	677(9)	51(5)
C(4A)	3474(8)	6267(16)	1661(14)	76(8)
C(5A)	1945(7)	5070(11)	1484(11)	58(5)
C(6A)	1485(9)	5023(16)	1566(14)	83(7)
C(7A)	1442(12)	4400(20)	1993(17)	115(11)
C(8A)	1145(12)	5020(20)	853(16)	116(12)
S(7A)	344(1)	8517(2)	1899(2)	45(1)
S(8A)	284(1)	8334(3)	305(2)	51(1)
P(2A)	-89(1)	8532(3)	940(2)	53(1)
C(9A)	-345(10)	9459(15)	660(15)	89(8)
C(10A)	-301(6)	10035(10)	1228(9)	56(4)
C(11A)	-427(8)	10784(12)	838(12)	80(6)
C(12A)	-525(11)	9980(20)	1744(17)	115(11)
C(13A)	-515(6)	7863(11)	867(11)	67(5)
C(14A)	-389(7)	7042(12)	1047(13)	74(5)
C(15A)	-741(9)	6609(16)	1234(16)	105(9)
C(16A)	-251(9)	6599(15)	501(14)	95(7)
S(9A)	2108(3)	10376(6)	1808(5)	44(1)
S(10A)	1765(2)	9852(3)	226(3)	38(1)
P(3A)	2075(2)	10719(4)	836(3)	42(1)
C(17A)	1553(6)	11395(9)	550(9)	49(4)
C(18A)	1695(9)	12074(12)	1042(13)	79(6)
C(19A)	1845(8)	12744(13)	633(13)	83(6)

Table A.49, Cont'd. Atomic coordinates ($\times 10^4$) and equivalent isotropic displacement parameters ($\text{\AA}^2 \times 10^3$) for $[\text{Mo}_3\text{S}_4\text{Se}_3(\text{S}_2\text{P}^i\text{Bu}_2)_3]\text{I} \cdot \frac{1}{2}\text{C}_5\text{H}_{12}$. $U(\text{eq})$ is defined as one third of the trace of the orthogonalized U^{ij} tensor.

Atom	x	y	z	U(eq)
C(20A)	1726(16)	12180(20)	1674(16)	163(16)
C(21A)	2612(7)	10963(12)	784(12)	66(5)
C(22A)	2962(7)	10389(13)	1078(13)	71(6)
C(23A)	2979(11)	9795(17)	533(17)	99(11)
C(24A)	3383(9)	10718(19)	1368(18)	112(11)
Mo(1B)	1708(2)	7498(2)	1559(3)	28(1)
Mo(2B)	925(1)	8170(1)	1504(1)	32(1)
Mo(3B)	1596(1)	9030(1)	1337(2)	27(1)
Se(1B)	1042(1)	6731(1)	1618(1)	59(1)
Se(2B)	822(1)	9588(1)	1190(1)	50(1)
S(1B)	1366(3)	7463(4)	2482(3)	34(1)
S(2B)	1229(3)	9242(3)	2206(5)	32(1)
S(4B)	1226(2)	8079(2)	557(3)	32(1)
S(5B)	2275(4)	6685(9)	2305(9)	38(2)
S(6B)	1785(6)	6596(13)	625(13)	43(2)
P(1B)	2291(2)	6060(9)	1478(8)	40(2)
C(1B)	2836(5)	5984(8)	1394(7)	34(3)
C(2B)	3112(5)	6689(9)	1454(8)	42(4)
C(3B)	3015(5)	7089(9)	755(7)	36(3)
C(4B)	3575(7)	6461(13)	1714(12)	64(5)
C(5B)	2109(6)	5118(9)	1530(9)	47(4)
C(6B)	1662(7)	4978(12)	1612(10)	63(5)
C(7B)	1642(9)	4306(15)	2096(13)	90(7)
C(8B)	1308(10)	4875(18)	912(13)	97(9)
S(7B)	392(1)	8128(2)	2218(2)	45(1)
S(8B)	202(1)	7898(2)	600(2)	51(1)
P(2B)	-99(1)	7922(3)	1354(2)	53(1)
C(9B)	-522(5)	8627(8)	1225(8)	50(3)
C(10B)	-384(5)	9444(8)	1245(8)	47(3)
C(11B)	-387(8)	9752(15)	537(11)	76(6)
C(12B)	-686(7)	9873(11)	1530(10)	60(4)
C(13B)	-382(7)	7052(11)	1445(12)	72(5)
C(14B)	-106(8)	6330(13)	1619(13)	88(6)
C(15B)	-295(10)	5807(18)	2071(15)	124(10)
C(16B)	-84(13)	5910(20)	985(17)	152(14)
S(9B)	1968(3)	10264(5)	1797(5)	44(1)
S(10B)	1622(2)	9680(3)	236(3)	38(1)
P(3B)	1905(2)	10587(3)	804(3)	42(1)
C(17B)	1728(8)	11526(11)	544(12)	75(6)

Table A.49, Cont'd. Atomic coordinates ($\times 10^4$) and equivalent isotropic displacement parameters ($\text{\AA}^2 \times 10^3$) for $[\text{Mo}_3\text{S}_4\text{Se}_3(\text{S}_2\text{P}^i\text{Bu}_2)_3]\text{I} \cdot \frac{1}{2}\text{C}_5\text{H}_{12}$. $U(\text{eq})$ is defined as one third of the trace of the orthogonalized U^{ij} tensor.

Atom	x	y	z	U(eq)
C(18B)	1816(14)	12230(18)	990(20)	161(17)
C(19B)	1501(14)	12800(20)	300(20)	169(16)
C(20B)	1391(11)	12242(18)	1397(16)	119(10)
C(21B)	2422(5)	10896(9)	710(9)	48(3)
C(22B)	2812(6)	10361(10)	978(10)	55(4)
C(23B)	2837(8)	9712(12)	493(12)	65(5)
C(24B)	3229(8)	10853(15)	1144(16)	96(8)
C(25A)	-873(18)	3550(30)	1120(30)	98(15)
C(26A)	-480(20)	3550(50)	830(50)	170(40)
C(27A)	-150(20)	2950(30)	1240(40)	120(20)
C(28A)	297(17)	2570(30)	1530(60)	190(40)
C(29A)	220(20)	1720(30)	1620(30)	113(18)
C(25B)	-1025(16)	3530(30)	1530(30)	90(13)
C(26B)	-780(17)	3960(30)	1090(30)	88(13)
C(27B)	-600(20)	3480(40)	590(40)	130(30)
C(28B)	-120(20)	3730(40)	950(60)	220(50)
C(29B)	160(20)	3020(50)	1190(40)	160(30)

Table A.50. Bond lengths (Å) for $[\text{Mo}_3\text{S}_4\text{Se}_3(\text{S}_2\text{P}^i\text{Bu}_2)_3]\text{I}\cdot\frac{1}{2}\text{C}_5\text{H}_{12}$. Symmetry transformations used to generate equivalent atoms:

Se(3)-S(3)	2.1689(17)	C(3A)-H(3A3)	0.9800
Se(3)-Mo(1A)	2.472(5)	C(4A)-H(4A1)	0.9800
Se(3)-Mo(3A)	2.535(4)	C(4A)-H(4A2)	0.9800
Se(3)-Mo(3B)	2.660(3)	C(4A)-H(4A3)	0.9800
Se(3)-Mo(1B)	2.713(5)	C(5A)-C(6A)	1.53(3)
S(3)-Mo(1A)	2.354(6)	C(5A)-H(5A1)	0.9900
S(3)-Mo(3B)	2.405(4)	C(5A)-H(5A2)	0.9900
S(3)-Mo(3A)	2.451(4)	C(6A)-C(7A)	1.43(3)
S(3)-Mo(1B)	2.492(5)	C(6A)-C(8A)	1.53(3)
Mo(1A)-S(4A)	2.371(7)	C(6A)-H(6A)	1.0000
Mo(1A)-S(1A)	2.415(10)	C(7A)-H(7A1)	0.9800
Mo(1A)-S(6A)	2.51(3)	C(7A)-H(7A2)	0.9800
Mo(1A)-Se(1A)	2.617(6)	C(7A)-H(7A3)	0.9800
Mo(1A)-S(5A)	2.652(19)	C(8A)-H(8A1)	0.9800
Mo(1A)-Mo(3A)	2.720(4)	C(8A)-H(8A2)	0.9800
Mo(1A)-Mo(2A)	2.726(6)	C(8A)-H(8A3)	0.9800
Mo(2A)-S(4A)	2.372(5)	S(7A)-P(2A)	2.020(6)
Mo(2A)-S(1A)	2.425(5)	S(8A)-P(2A)	2.021(6)
Mo(2A)-S(2A)	2.446(8)	P(2A)-C(13A)	1.781(19)
Mo(2A)-S(8A)	2.512(4)	P(2A)-C(9A)	1.85(3)
Mo(2A)-S(7A)	2.529(4)	C(9A)-C(10A)	1.51(3)
Mo(2A)-Se(1A)	2.575(3)	C(9A)-H(9A1)	0.9900
Mo(2A)-Se(2A)	2.595(2)	C(9A)-H(9A2)	0.9900
Mo(2A)-Mo(3A)	2.736(2)	C(10A)-C(12A)	1.43(3)
Mo(3A)-S(4A)	2.382(6)	C(10A)-C(11A)	1.53(2)
Mo(3A)-S(2A)	2.428(9)	C(10A)-H(10A)	1.0000
Mo(3A)-S(10A)	2.520(6)	C(11A)-H(11A)	0.9800
Mo(3A)-S(9A)	2.531(8)	C(11A)-H(11B)	0.9800
Mo(3A)-Se(2A)	2.594(4)	C(11A)-H(11C)	0.9800
Se(1A)-S(1A)	2.180(9)	C(12A)-H(12A)	0.9800
Se(2A)-S(2A)	2.163(10)	C(12A)-H(12B)	0.9800
S(5A)-P(1A)	2.02(2)	C(12A)-H(12C)	0.9800
S(6A)-P(1A)	1.91(3)	C(13A)-C(14A)	1.52(3)
P(1A)-C(1A)	1.802(19)	C(13A)-H(13A)	0.9900
P(1A)-C(5A)	1.85(2)	C(13A)-H(13B)	0.9900
C(1A)-C(2A)	1.53(2)	C(14A)-C(15A)	1.50(3)
C(1A)-H(1A1)	0.9900	C(14A)-C(16A)	1.52(3)
C(1A)-H(1A2)	0.9900	C(14A)-H(14A)	1.0000
C(2A)-C(3A)	1.54(2)	C(15A)-H(15A)	0.9800
C(2A)-C(4A)	1.54(3)	C(15A)-H(15B)	0.9800
C(2A)-H(2A)	1.0000	C(15A)-H(15C)	0.9800
C(3A)-H(3A1)	0.9800	C(16A)-H(16A)	0.9800
C(3A)-H(3A2)	0.9800	C(16A)-H(16B)	0.9800

Table A.50, Cont'd. Bond lengths (Å) for $[\text{Mo}_3\text{S}_4\text{Se}_3(\text{S}_2\text{P}^i\text{Bu}_2)_3]\text{I}\cdot\frac{1}{2}\text{C}_5\text{H}_{12}$. Symmetry transformations used to generate equivalent atoms:

C(16A)-H(16C)	0.9800	Mo(2B)-Mo(3B)	2.737(2)
S(9A)-P(3A)	2.021(12)	Mo(3B)-S(4B)	2.372(6)
S(10A)-P(3A)	2.037(9)	Mo(3B)-S(2B)	2.404(8)
P(3A)-C(21A)	1.81(2)	Mo(3B)-S(10B)	2.518(6)
P(3A)-C(17A)	2.002(18)	Mo(3B)-S(9B)	2.535(8)
C(17A)-C(18A)	1.54(2)	Mo(3B)-Se(2B)	2.606(4)
C(17A)-H(17A)	0.9900	Se(1B)-S(1B)	2.176(9)
C(17A)-H(17B)	0.9900	Se(2B)-S(2B)	2.167(9)
C(18A)-C(20A)	1.26(3)	S(5B)-P(1B)	2.01(2)
C(18A)-C(19A)	1.60(3)	S(6B)-P(1B)	2.20(3)
C(18A)-H(18A)	1.0000	P(1B)-C(5B)	1.78(2)
C(19A)-H(19A)	0.9800	P(1B)-C(1B)	1.809(17)
C(19A)-H(19B)	0.9800	C(1B)-C(2B)	1.52(2)
C(19A)-H(19C)	0.9800	C(1B)-H(1B1)	0.9900
C(20A)-H(20A)	0.9800	C(1B)-H(1B2)	0.9900
C(20A)-H(20B)	0.9800	C(2B)-C(4B)	1.48(2)
C(20A)-H(20C)	0.9800	C(2B)-C(3B)	1.524(19)
C(21A)-C(22A)	1.50(3)	C(2B)-H(2B)	1.0000
C(21A)-H(21A)	0.9900	C(3B)-H(3B1)	0.9800
C(21A)-H(21B)	0.9900	C(3B)-H(3B2)	0.9800
C(22A)-C(24A)	1.43(3)	C(3B)-H(3B3)	0.9800
C(22A)-C(23A)	1.53(3)	C(4B)-H(4B1)	0.9800
C(22A)-H(22A)	1.0000	C(4B)-H(4B2)	0.9800
C(23A)-H(23A)	0.9800	C(4B)-H(4B3)	0.9800
C(23A)-H(23B)	0.9800	C(5B)-C(6B)	1.51(2)
C(23A)-H(23C)	0.9800	C(5B)-H(5B1)	0.9900
C(24A)-H(24A)	0.9800	C(5B)-H(5B2)	0.9900
C(24A)-H(24B)	0.9800	C(6B)-C(8B)	1.54(3)
C(24A)-H(24C)	0.9800	C(6B)-C(7B)	1.55(3)
Mo(1B)-S(4B)	2.386(7)	C(6B)-H(6B)	1.0000
Mo(1B)-S(1B)	2.417(9)	C(7B)-H(7B1)	0.9800
Mo(1B)-S(5B)	2.457(18)	C(7B)-H(7B2)	0.9800
Mo(1B)-S(6B)	2.53(2)	C(7B)-H(7B3)	0.9800
Mo(1B)-Se(1B)	2.564(6)	C(8B)-H(8B1)	0.9800
Mo(1B)-Mo(2B)	2.753(6)	C(8B)-H(8B2)	0.9800
Mo(1B)-Mo(3B)	2.760(4)	C(8B)-H(8B3)	0.9800
Mo(2B)-S(4B)	2.377(5)	S(7B)-P(2B)	2.009(6)
Mo(2B)-S(2B)	2.399(7)	S(8B)-P(2B)	2.023(6)
Mo(2B)-S(1B)	2.413(4)	P(2B)-C(9B)	1.807(15)
Mo(2B)-S(7B)	2.530(4)	P(2B)-C(13B)	1.824(19)
Mo(2B)-S(8B)	2.539(4)	C(9B)-C(10B)	1.512(19)
Mo(2B)-Se(1B)	2.579(3)	C(9B)-H(9B1)	0.9900
Mo(2B)-Se(2B)	2.591(2)	C(9B)-H(9B2)	0.9900

Table A.50, Cont'd. Bond lengths (Å) for $[\text{Mo}_3\text{S}_4\text{Se}_3(\text{S}_2\text{P}^i\text{Bu}_2)_3]\text{I}\cdot\frac{1}{2}\text{C}_5\text{H}_{12}$. Symmetry transformations used to generate equivalent atoms:

C(10B)-C(12B)	1.47(2)	C(23B)-H(23D)	0.9800
C(10B)-C(11B)	1.52(2)	C(23B)-H(23E)	0.9800
C(10B)-H(10B)	1.0000	C(23B)-H(23F)	0.9800
C(11B)-H(11D)	0.9800	C(24B)-H(24D)	0.9800
C(11B)-H(11E)	0.9800	C(24B)-H(24E)	0.9800
C(11B)-H(11F)	0.9800	C(24B)-H(24F)	0.9800
C(12B)-H(12D)	0.9800	C(25A)-C(26A)	1.547(10)
C(12B)-H(12E)	0.9800	C(25A)-H(25A)	0.9800
C(12B)-H(12F)	0.9800	C(25A)-H(25B)	0.9800
C(13B)-C(14B)	1.54(3)	C(25A)-H(25C)	0.9800
C(13B)-H(13C)	0.9900	C(26A)-C(27A)	1.550(10)
C(13B)-H(13D)	0.9900	C(26A)-H(26A)	0.9900
C(14B)-C(16B)	1.50(3)	C(26A)-H(26B)	0.9900
C(14B)-C(15B)	1.54(3)	C(27A)-C(28A)	1.551(10)
C(14B)-H(14B)	1.0000	C(27A)-H(27A)	0.9900
C(15B)-H(15D)	0.9800	C(27A)-H(27B)	0.9900
C(15B)-H(15E)	0.9800	C(28A)-C(29A)	1.546(10)
C(15B)-H(15F)	0.9800	C(28A)-H(28A)	0.9900
C(16B)-H(16D)	0.9800	C(28A)-H(28B)	0.9900
C(16B)-H(16E)	0.9800	C(29A)-H(29A)	0.9800
C(16B)-H(16F)	0.9800	C(29A)-H(29B)	0.9800
S(9B)-P(3B)	2.031(11)	C(29A)-H(29C)	0.9800
S(10B)-P(3B)	2.027(8)	C(25B)-C(26B)	1.550(10)
P(3B)-C(17B)	1.79(2)	C(25B)-H(25D)	0.9800
P(3B)-C(21B)	1.805(16)	C(25B)-H(25E)	0.9800
C(17B)-C(18B)	1.51(3)	C(25B)-H(25F)	0.9800
C(17B)-H(17C)	0.9900	C(26B)-C(27B)	1.548(10)
C(17B)-H(17D)	0.9900	C(26B)-H(26C)	0.9900
C(18B)-C(19B)	1.77(4)	C(26B)-H(26D)	0.9900
C(18B)-C(20B)	1.79(4)	C(27B)-C(28B)	1.548(10)
C(18B)-H(18B)	1.0000	C(27B)-H(27C)	0.9900
C(19B)-H(19D)	0.9800	C(27B)-H(27D)	0.9900
C(19B)-H(19E)	0.9800	C(28B)-C(29B)	1.551(10)
C(19B)-H(19F)	0.9800	C(28B)-H(28C)	0.9900
C(20B)-H(20D)	0.9800	C(28B)-H(28D)	0.9900
C(20B)-H(20E)	0.9800	C(29B)-H(29D)	0.9800
C(20B)-H(20F)	0.9800	C(29B)-H(29E)	0.9800
C(21B)-C(22B)	1.54(2)	C(29B)-H(29F)	0.9800
C(21B)-H(21C)	0.9900		
C(21B)-H(21D)	0.9900		
C(22B)-C(23B)	1.52(2)		
C(22B)-C(24B)	1.55(3)		
C(22B)-H(22B)	1.0000		

Table A.51. Bond angles (deg.) for $[\text{Mo}_3\text{S}_4\text{Se}_3(\text{S}_2\text{P}^i\text{Bu}_2)_3]\text{I}\cdot\frac{1}{2}\text{C}_5\text{H}_{12}$. Symmetry transformations used to generate equivalent atoms:

S(3)-Se(3)-Mo(1A)	60.55(14)	Se(3)-Mo(1A)-Mo(2A)	118.32(12)
S(3)-Se(3)-Mo(3A)	62.23(9)	S(6A)-Mo(1A)-Mo(2A)	128.6(6)
Mo(1A)-Se(3)-Mo(3A)	65.79(11)	Se(1A)-Mo(1A)-Mo(2A)	57.59(14)
S(3)-Se(3)-Mo(3B)	58.67(8)	S(5A)-Mo(1A)-Mo(2A)	137.2(3)
S(3)-Se(3)-Mo(1B)	60.17(12)	Mo(3A)-Mo(1A)-Mo(2A)	60.33(11)
Mo(3B)-Se(3)-Mo(1B)	61.80(10)	S(4A)-Mo(2A)-S(1A)	109.9(3)
Se(3)-S(3)-Mo(1A)	66.11(14)	S(4A)-Mo(2A)-S(2A)	110.3(2)
Se(3)-S(3)-Mo(3B)	70.92(8)	S(1A)-Mo(2A)-S(2A)	82.6(3)
Se(3)-S(3)-Mo(3A)	66.23(9)	S(4A)-Mo(2A)-S(8A)	81.56(18)
Mo(1A)-S(3)-Mo(3A)	68.92(11)	S(1A)-Mo(2A)-S(8A)	135.0(2)
Se(3)-S(3)-Mo(1B)	70.80(12)	S(2A)-Mo(2A)-S(8A)	135.7(3)
Mo(3B)-S(3)-Mo(1B)	68.58(11)	S(4A)-Mo(2A)-S(7A)	159.51(18)
S(3)-Mo(1A)-S(4A)	112.16(18)	S(1A)-Mo(2A)-S(7A)	84.3(2)
S(3)-Mo(1A)-S(1A)	83.1(3)	S(2A)-Mo(2A)-S(7A)	85.5(2)
S(4A)-Mo(1A)-S(1A)	110.2(3)	S(8A)-Mo(2A)-S(7A)	77.98(14)
S(3)-Mo(1A)-Se(3)	53.34(12)	S(4A)-Mo(2A)-Se(1A)	85.58(14)
S(4A)-Mo(1A)-Se(3)	85.60(16)	S(1A)-Mo(2A)-Se(1A)	51.6(2)
S(1A)-Mo(1A)-Se(3)	136.2(3)	S(2A)-Mo(2A)-Se(1A)	134.0(2)
S(3)-Mo(1A)-S(6A)	131.7(5)	S(8A)-Mo(2A)-Se(1A)	87.99(13)
S(4A)-Mo(1A)-S(6A)	86.3(7)	S(7A)-Mo(2A)-Se(1A)	92.59(13)
S(1A)-Mo(1A)-S(6A)	133.5(6)	S(4A)-Mo(2A)-Se(2A)	87.55(13)
Se(3)-Mo(1A)-S(6A)	86.3(5)	S(1A)-Mo(2A)-Se(2A)	133.2(2)
S(3)-Mo(1A)-Se(1A)	134.1(2)	S(2A)-Mo(2A)-Se(2A)	50.7(2)
S(4A)-Mo(1A)-Se(1A)	84.7(2)	S(8A)-Mo(2A)-Se(2A)	89.18(12)
S(1A)-Mo(1A)-Se(1A)	51.2(3)	S(7A)-Mo(2A)-Se(2A)	93.21(12)
Se(3)-Mo(1A)-Se(1A)	169.8(2)	Se(1A)-Mo(2A)-Se(2A)	172.88(10)
S(6A)-Mo(1A)-Se(1A)	89.9(4)	S(4A)-Mo(2A)-Mo(1A)	54.92(17)
S(3)-Mo(1A)-S(5A)	85.0(4)	S(1A)-Mo(2A)-Mo(1A)	55.5(2)
S(4A)-Mo(1A)-S(5A)	159.4(5)	S(2A)-Mo(2A)-Mo(1A)	94.3(3)
S(1A)-Mo(1A)-S(5A)	82.0(4)	S(8A)-Mo(2A)-Mo(1A)	124.48(17)
Se(3)-Mo(1A)-S(5A)	96.8(3)	S(7A)-Mo(2A)-Mo(1A)	139.39(14)
S(6A)-Mo(1A)-S(5A)	73.5(8)	Se(1A)-Mo(2A)-Mo(1A)	59.08(11)
Se(1A)-Mo(1A)-S(5A)	91.2(2)	Se(2A)-Mo(2A)-Mo(1A)	117.86(11)
S(3)-Mo(1A)-Mo(3A)	57.22(12)	S(4A)-Mo(2A)-Mo(3A)	55.04(15)
S(4A)-Mo(1A)-Mo(3A)	55.28(15)	S(1A)-Mo(2A)-Mo(3A)	96.1(2)
S(1A)-Mo(1A)-Mo(3A)	96.8(2)	S(2A)-Mo(2A)-Mo(3A)	55.5(2)
Se(3)-Mo(1A)-Mo(3A)	58.22(10)	S(8A)-Mo(2A)-Mo(3A)	123.46(13)
S(6A)-Mo(1A)-Mo(3A)	126.6(7)	S(7A)-Mo(2A)-Mo(3A)	140.43(13)
Se(1A)-Mo(1A)-Mo(3A)	117.7(2)	Se(1A)-Mo(2A)-Mo(3A)	118.59(11)
S(5A)-Mo(1A)-Mo(3A)	141.9(4)	Se(2A)-Mo(2A)-Mo(3A)	58.15(9)
S(3)-Mo(1A)-Mo(2A)	96.48(17)	Mo(1A)-Mo(2A)-Mo(3A)	59.73(12)
S(4A)-Mo(1A)-Mo(2A)	54.94(17)	S(4A)-Mo(3A)-S(2A)	110.6(2)
S(1A)-Mo(1A)-Mo(2A)	55.91(18)	S(4A)-Mo(3A)-S(3)	108.46(17)

Table A.51, Cont'd. Bond angles (deg.) for $[\text{Mo}_3\text{S}_4\text{Se}_3(\text{S}_2\text{P}^i\text{Bu}_2)_3]\text{I}\cdot\frac{1}{2}\text{C}_5\text{H}_{12}$. Symmetry transformations used to generate equivalent atoms:

S(2A)-Mo(3A)-S(3)	81.3(2)	Se(2A)-S(2A)-Mo(3A)	68.5(3)
S(4A)-Mo(3A)-S(10A)	81.49(19)	Se(2A)-S(2A)-Mo(2A)	68.2(3)
S(2A)-Mo(3A)-S(10A)	135.6(3)	Mo(3A)-S(2A)-Mo(2A)	68.3(3)
S(3)-Mo(3A)-S(10A)	137.05(19)	Mo(2A)-S(4A)-Mo(1A)	70.1(2)
S(4A)-Mo(3A)-S(9A)	159.7(3)	Mo(2A)-S(4A)-Mo(3A)	70.28(17)
S(2A)-Mo(3A)-S(9A)	83.7(3)	Mo(1A)-S(4A)-Mo(3A)	69.8(2)
S(3)-Mo(3A)-S(9A)	87.4(3)	P(1A)-S(5A)-Mo(1A)	88.0(8)
S(10A)-Mo(3A)-S(9A)	78.3(3)	P(1A)-S(6A)-Mo(1A)	94.9(12)
S(4A)-Mo(3A)-Se(3)	83.98(18)	C(1A)-P(1A)-C(5A)	102.0(11)
S(2A)-Mo(3A)-Se(3)	132.6(3)	C(1A)-P(1A)-S(6A)	108.9(12)
S(3)-Mo(3A)-Se(3)	51.54(8)	C(5A)-P(1A)-S(6A)	123.0(10)
S(10A)-Mo(3A)-Se(3)	89.99(18)	C(1A)-P(1A)-S(5A)	112.9(8)
S(9A)-Mo(3A)-Se(3)	97.0(3)	C(5A)-P(1A)-S(5A)	106.8(11)
S(4A)-Mo(3A)-Se(2A)	87.36(18)	S(6A)-P(1A)-S(5A)	103.4(12)
S(2A)-Mo(3A)-Se(2A)	50.9(2)	C(2A)-C(1A)-P(1A)	115.4(12)
S(3)-Mo(3A)-Se(2A)	131.97(13)	C(2A)-C(1A)-H(1A1)	108.4
S(10A)-Mo(3A)-Se(2A)	89.05(19)	P(1A)-C(1A)-H(1A1)	108.4
S(9A)-Mo(3A)-Se(2A)	91.2(3)	C(2A)-C(1A)-H(1A2)	108.4
Se(3)-Mo(3A)-Se(2A)	171.33(14)	P(1A)-C(1A)-H(1A2)	108.4
S(4A)-Mo(3A)-Mo(1A)	54.91(17)	H(1A1)-C(1A)-H(1A2)	107.5
S(2A)-Mo(3A)-Mo(1A)	94.90(19)	C(1A)-C(2A)-C(3A)	110.5(15)
S(3)-Mo(3A)-Mo(1A)	53.86(14)	C(1A)-C(2A)-C(4A)	109.5(16)
S(10A)-Mo(3A)-Mo(1A)	124.2(2)	C(3A)-C(2A)-C(4A)	109.7(16)
S(9A)-Mo(3A)-Mo(1A)	140.8(3)	C(1A)-C(2A)-H(2A)	109.0
Se(3)-Mo(3A)-Mo(1A)	55.99(15)	C(3A)-C(2A)-H(2A)	109.0
Se(2A)-Mo(3A)-Mo(1A)	118.10(15)	C(4A)-C(2A)-H(2A)	109.0
S(4A)-Mo(3A)-Mo(2A)	54.69(13)	C(2A)-C(3A)-H(3A1)	109.5
S(2A)-Mo(3A)-Mo(2A)	56.16(18)	C(2A)-C(3A)-H(3A2)	109.5
S(3)-Mo(3A)-Mo(2A)	93.96(8)	H(3A1)-C(3A)-H(3A2)	109.5
S(10A)-Mo(3A)-Mo(2A)	123.13(18)	C(2A)-C(3A)-H(3A3)	109.5
S(9A)-Mo(3A)-Mo(2A)	138.9(3)	H(3A1)-C(3A)-H(3A3)	109.5
Se(3)-Mo(3A)-Mo(2A)	115.71(10)	H(3A2)-C(3A)-H(3A3)	109.5
Se(2A)-Mo(3A)-Mo(2A)	58.19(8)	C(2A)-C(4A)-H(4A1)	109.5
Mo(1A)-Mo(3A)-Mo(2A)	59.94(14)	C(2A)-C(4A)-H(4A2)	109.5
S(1A)-Se(1A)-Mo(2A)	60.66(14)	H(4A1)-C(4A)-H(4A2)	109.5
S(1A)-Se(1A)-Mo(1A)	59.6(3)	C(2A)-C(4A)-H(4A3)	109.5
Mo(2A)-Se(1A)-Mo(1A)	63.34(12)	H(4A1)-C(4A)-H(4A3)	109.5
S(2A)-Se(2A)-Mo(3A)	60.6(3)	H(4A2)-C(4A)-H(4A3)	109.5
S(2A)-Se(2A)-Mo(2A)	61.07(19)	C(6A)-C(5A)-P(1A)	116.6(16)
Mo(3A)-Se(2A)-Mo(2A)	63.66(7)	C(6A)-C(5A)-H(5A1)	108.2
Se(1A)-S(1A)-Mo(1A)	69.2(3)	P(1A)-C(5A)-H(5A1)	108.2
Se(1A)-S(1A)-Mo(2A)	67.75(19)	C(6A)-C(5A)-H(5A2)	108.2
Mo(1A)-S(1A)-Mo(2A)	68.6(2)	P(1A)-C(5A)-H(5A2)	108.2

Table A.51, Cont'd. Bond angles (deg.) for $[\text{Mo}_3\text{S}_4\text{Se}_3(\text{S}_2\text{P}^i\text{Bu}_2)_3]\text{I}\cdot\frac{1}{2}\text{C}_5\text{H}_{12}$. Symmetry transformations used to generate equivalent atoms:

H(5A1)-C(5A)-H(5A2)	107.3	H(11A)-C(11A)-H(11C)	109.5
C(7A)-C(6A)-C(8A)	113(3)	H(11B)-C(11A)-H(11C)	109.5
C(7A)-C(6A)-C(5A)	112(2)	C(10A)-C(12A)-H(12A)	109.5
C(8A)-C(6A)-C(5A)	110(2)	C(10A)-C(12A)-H(12B)	109.5
C(7A)-C(6A)-H(6A)	107.2	H(12A)-C(12A)-H(12B)	109.5
C(8A)-C(6A)-H(6A)	107.2	C(10A)-C(12A)-H(12C)	109.5
C(5A)-C(6A)-H(6A)	107.2	H(12A)-C(12A)-H(12C)	109.5
C(6A)-C(7A)-H(7A1)	109.5	H(12B)-C(12A)-H(12C)	109.5
C(6A)-C(7A)-H(7A2)	109.5	C(14A)-C(13A)-P(2A)	118.3(15)
H(7A1)-C(7A)-H(7A2)	109.5	C(14A)-C(13A)-H(13A)	107.7
C(6A)-C(7A)-H(7A3)	109.5	P(2A)-C(13A)-H(13A)	107.7
H(7A1)-C(7A)-H(7A3)	109.5	C(14A)-C(13A)-H(13B)	107.7
H(7A2)-C(7A)-H(7A3)	109.5	P(2A)-C(13A)-H(13B)	107.7
C(6A)-C(8A)-H(8A1)	109.5	H(13A)-C(13A)-H(13B)	107.1
C(6A)-C(8A)-H(8A2)	109.5	C(15A)-C(14A)-C(13A)	112.5(19)
H(8A1)-C(8A)-H(8A2)	109.5	C(15A)-C(14A)-C(16A)	108.4(19)
C(6A)-C(8A)-H(8A3)	109.5	C(13A)-C(14A)-C(16A)	116(2)
H(8A1)-C(8A)-H(8A3)	109.5	C(15A)-C(14A)-H(14A)	106.5
H(8A2)-C(8A)-H(8A3)	109.5	C(13A)-C(14A)-H(14A)	106.5
P(2A)-S(7A)-Mo(2A)	88.65(19)	C(16A)-C(14A)-H(14A)	106.5
P(2A)-S(8A)-Mo(2A)	89.13(19)	C(14A)-C(15A)-H(15A)	109.5
C(13A)-P(2A)-C(9A)	107.9(12)	C(14A)-C(15A)-H(15B)	109.5
C(13A)-P(2A)-S(7A)	111.5(7)	H(15A)-C(15A)-H(15B)	109.5
C(9A)-P(2A)-S(7A)	115.0(9)	C(14A)-C(15A)-H(15C)	109.5
C(13A)-P(2A)-S(8A)	114.3(7)	H(15A)-C(15A)-H(15C)	109.5
C(9A)-P(2A)-S(8A)	104.7(9)	H(15B)-C(15A)-H(15C)	109.5
S(7A)-P(2A)-S(8A)	103.4(2)	C(14A)-C(16A)-H(16A)	109.5
C(10A)-C(9A)-P(2A)	115.8(18)	C(14A)-C(16A)-H(16B)	109.5
C(10A)-C(9A)-H(9A1)	108.3	H(16A)-C(16A)-H(16B)	109.5
P(2A)-C(9A)-H(9A1)	108.3	C(14A)-C(16A)-H(16C)	109.5
C(10A)-C(9A)-H(9A2)	108.3	H(16A)-C(16A)-H(16C)	109.5
P(2A)-C(9A)-H(9A2)	108.3	H(16B)-C(16A)-H(16C)	109.5
H(9A1)-C(9A)-H(9A2)	107.4	P(3A)-S(9A)-Mo(3A)	89.1(4)
C(12A)-C(10A)-C(9A)	123(2)	P(3A)-S(10A)-Mo(3A)	89.0(3)
C(12A)-C(10A)-C(11A)	108.5(19)	C(21A)-P(3A)-C(17A)	124.8(9)
C(9A)-C(10A)-C(11A)	104.3(17)	C(21A)-P(3A)-S(9A)	110.2(8)
C(12A)-C(10A)-H(10A)	106.6	C(17A)-P(3A)-S(9A)	105.2(7)
C(9A)-C(10A)-H(10A)	106.6	C(21A)-P(3A)-S(10A)	116.8(8)
C(11A)-C(10A)-H(10A)	106.6	C(17A)-P(3A)-S(10A)	93.4(6)
C(10A)-C(11A)-H(11A)	109.5	S(9A)-P(3A)-S(10A)	103.5(4)
C(10A)-C(11A)-H(11B)	109.5	C(18A)-C(17A)-P(3A)	102.6(13)
H(11A)-C(11A)-H(11B)	109.5	C(18A)-C(17A)-H(17A)	111.3
C(10A)-C(11A)-H(11C)	109.5	P(3A)-C(17A)-H(17A)	111.3

Table A.51, Cont'd. Bond angles (deg.) for $[\text{Mo}_3\text{S}_4\text{Se}_3(\text{S}_2\text{P}^i\text{Bu}_2)_3]\text{I}\cdot\frac{1}{2}\text{C}_5\text{H}_{12}$. Symmetry transformations used to generate equivalent atoms:

C(18A)-C(17A)-H(17B)	111.3	H(24A)-C(24A)-H(24C)	109.5
P(3A)-C(17A)-H(17B)	111.3	H(24B)-C(24A)-H(24C)	109.5
H(17A)-C(17A)-H(17B)	109.2	S(4B)-Mo(1B)-S(1B)	109.4(3)
C(20A)-C(18A)-C(17A)	134(3)	S(4B)-Mo(1B)-S(5B)	161.9(5)
C(20A)-C(18A)-C(19A)	117(3)	S(1B)-Mo(1B)-S(5B)	86.3(4)
C(17A)-C(18A)-C(19A)	109.2(17)	S(4B)-Mo(1B)-S(3)	108.04(15)
C(20A)-C(18A)-H(18A)	90.7	S(1B)-Mo(1B)-S(3)	83.5(3)
C(17A)-C(18A)-H(18A)	90.7	S(5B)-Mo(1B)-S(3)	82.0(4)
C(19A)-C(18A)-H(18A)	90.7	S(4B)-Mo(1B)-S(6B)	79.9(6)
C(18A)-C(19A)-H(19A)	109.5	S(1B)-Mo(1B)-S(6B)	135.8(6)
C(18A)-C(19A)-H(19B)	109.5	S(5B)-Mo(1B)-S(6B)	82.5(7)
H(19A)-C(19A)-H(19B)	109.5	S(3)-Mo(1B)-S(6B)	136.2(5)
C(18A)-C(19A)-H(19C)	109.5	S(4B)-Mo(1B)-Se(1B)	85.6(2)
H(19A)-C(19A)-H(19C)	109.5	S(1B)-Mo(1B)-Se(1B)	51.7(2)
H(19B)-C(19A)-H(19C)	109.5	S(5B)-Mo(1B)-Se(1B)	97.9(2)
C(18A)-C(20A)-H(20A)	109.5	S(3)-Mo(1B)-Se(1B)	134.9(2)
C(18A)-C(20A)-H(20B)	109.5	S(6B)-Mo(1B)-Se(1B)	87.8(4)
H(20A)-C(20A)-H(20B)	109.5	S(4B)-Mo(1B)-Se(3)	86.70(14)
C(18A)-C(20A)-H(20C)	109.5	S(1B)-Mo(1B)-Se(3)	132.5(3)
H(20A)-C(20A)-H(20C)	109.5	S(5B)-Mo(1B)-Se(3)	89.1(3)
H(20B)-C(20A)-H(20C)	109.5	S(3)-Mo(1B)-Se(3)	49.03(10)
C(22A)-C(21A)-P(3A)	115.5(16)	S(6B)-Mo(1B)-Se(3)	90.1(5)
C(22A)-C(21A)-H(21A)	108.4	Se(1B)-Mo(1B)-Se(3)	172.3(2)
P(3A)-C(21A)-H(21A)	108.4	S(4B)-Mo(1B)-Mo(2B)	54.54(16)
C(22A)-C(21A)-H(21B)	108.4	S(1B)-Mo(1B)-Mo(2B)	55.18(17)
P(3A)-C(21A)-H(21B)	108.4	S(5B)-Mo(1B)-Mo(2B)	141.4(4)
H(21A)-C(21A)-H(21B)	107.5	S(3)-Mo(1B)-Mo(2B)	94.82(15)
C(24A)-C(22A)-C(21A)	113(2)	S(6B)-Mo(1B)-Mo(2B)	121.8(5)
C(24A)-C(22A)-C(23A)	110(2)	Se(1B)-Mo(1B)-Mo(2B)	57.89(13)
C(21A)-C(22A)-C(23A)	111(2)	Se(3)-Mo(1B)-Mo(2B)	117.65(11)
C(24A)-C(22A)-H(22A)	107.3	S(4B)-Mo(1B)-Mo(3B)	54.32(14)
C(21A)-C(22A)-H(22A)	107.3	S(1B)-Mo(1B)-Mo(3B)	94.7(2)
C(23A)-C(22A)-H(22A)	107.3	S(5B)-Mo(1B)-Mo(3B)	135.6(4)
C(22A)-C(23A)-H(23A)	109.5	S(3)-Mo(1B)-Mo(3B)	54.21(10)
C(22A)-C(23A)-H(23B)	109.5	S(6B)-Mo(1B)-Mo(3B)	122.5(6)
H(23A)-C(23A)-H(23B)	109.5	Se(1B)-Mo(1B)-Mo(3B)	117.3(2)
C(22A)-C(23A)-H(23C)	109.5	Se(3)-Mo(1B)-Mo(3B)	58.17(8)
H(23A)-C(23A)-H(23C)	109.5	Mo(2B)-Mo(1B)-Mo(3B)	59.53(10)
H(23B)-C(23A)-H(23C)	109.5	S(4B)-Mo(2B)-S(2B)	109.6(2)
C(22A)-C(24A)-H(24A)	109.5	S(4B)-Mo(2B)-S(1B)	109.8(2)
C(22A)-C(24A)-H(24B)	109.5	S(2B)-Mo(2B)-S(1B)	83.7(3)
H(24A)-C(24A)-H(24B)	109.5	S(4B)-Mo(2B)-S(7B)	161.86(17)
C(22A)-C(24A)-H(24C)	109.5	S(2B)-Mo(2B)-S(7B)	85.1(2)

Table A.51, Cont'd. Bond angles (deg.) for $[\text{Mo}_3\text{S}_4\text{Se}_3(\text{S}_2\text{P}^i\text{Bu}_2)_3]\text{I}\cdot\frac{1}{2}\text{C}_5\text{H}_{12}$. Symmetry transformations used to generate equivalent atoms:

S(1B)-Mo(2B)-S(7B)	81.6(2)	S(2B)-Mo(3B)-Se(2B)	51.1(2)
S(4B)-Mo(2B)-S(8B)	84.94(17)	S(10B)-Mo(3B)-Se(2B)	90.01(18)
S(2B)-Mo(2B)-S(8B)	134.5(3)	S(9B)-Mo(3B)-Se(2B)	92.5(3)
S(1B)-Mo(2B)-S(8B)	133.0(2)	S(4B)-Mo(3B)-Se(3)	88.19(17)
S(7B)-Mo(2B)-S(8B)	77.06(13)	S(3)-Mo(3B)-Se(3)	50.40(7)
S(4B)-Mo(2B)-Se(1B)	85.48(13)	S(2B)-Mo(3B)-Se(3)	134.6(3)
S(2B)-Mo(2B)-Se(1B)	135.1(2)	S(10B)-Mo(3B)-Se(3)	86.21(16)
S(1B)-Mo(2B)-Se(1B)	51.6(2)	S(9B)-Mo(3B)-Se(3)	92.6(2)
S(7B)-Mo(2B)-Se(1B)	91.44(12)	Se(2B)-Mo(3B)-Se(3)	172.87(14)
S(8B)-Mo(2B)-Se(1B)	87.41(12)	S(4B)-Mo(3B)-Mo(2B)	54.90(11)
S(4B)-Mo(2B)-Se(2B)	85.59(12)	S(3)-Mo(3B)-Mo(2B)	97.28(9)
S(2B)-Mo(2B)-Se(2B)	51.3(2)	S(2B)-Mo(3B)-Mo(2B)	55.18(16)
S(1B)-Mo(2B)-Se(2B)	134.9(2)	S(10B)-Mo(3B)-Mo(2B)	126.26(17)
S(7B)-Mo(2B)-Se(2B)	96.22(11)	S(9B)-Mo(3B)-Mo(2B)	137.7(2)
S(8B)-Mo(2B)-Se(2B)	89.15(12)	Se(2B)-Mo(3B)-Mo(2B)	57.96(7)
Se(1B)-Mo(2B)-Se(2B)	170.69(9)	Se(3)-Mo(3B)-Mo(2B)	120.09(10)
S(4B)-Mo(2B)-Mo(3B)	54.73(13)	S(4B)-Mo(3B)-Mo(1B)	54.79(17)
S(2B)-Mo(2B)-Mo(3B)	55.34(18)	S(3)-Mo(3B)-Mo(1B)	57.21(13)
S(1B)-Mo(2B)-Mo(3B)	95.4(2)	S(2B)-Mo(3B)-Mo(1B)	96.02(18)
S(7B)-Mo(2B)-Mo(3B)	140.36(12)	S(10B)-Mo(3B)-Mo(1B)	123.8(2)
S(8B)-Mo(2B)-Mo(3B)	127.11(13)	S(9B)-Mo(3B)-Mo(1B)	140.0(3)
Se(1B)-Mo(2B)-Mo(3B)	117.58(11)	Se(2B)-Mo(3B)-Mo(1B)	117.88(14)
Se(2B)-Mo(2B)-Mo(3B)	58.49(8)	Se(3)-Mo(3B)-Mo(1B)	60.03(14)
S(4B)-Mo(2B)-Mo(1B)	54.84(16)	Mo(2B)-Mo(3B)-Mo(1B)	60.12(13)
S(2B)-Mo(2B)-Mo(1B)	96.3(2)	S(1B)-Se(1B)-Mo(1B)	60.7(2)
S(1B)-Mo(2B)-Mo(1B)	55.3(2)	S(1B)-Se(1B)-Mo(2B)	60.29(13)
S(7B)-Mo(2B)-Mo(1B)	136.26(12)	Mo(1B)-Se(1B)-Mo(2B)	64.73(11)
S(8B)-Mo(2B)-Mo(1B)	125.29(15)	S(2B)-Se(2B)-Mo(2B)	59.76(17)
Se(1B)-Mo(2B)-Mo(1B)	57.38(10)	S(2B)-Se(2B)-Mo(3B)	59.6(2)
Se(2B)-Mo(2B)-Mo(1B)	118.63(9)	Mo(2B)-Se(2B)-Mo(3B)	63.55(7)
Mo(3B)-Mo(2B)-Mo(1B)	60.35(10)	Se(1B)-S(1B)-Mo(2B)	68.16(19)
S(4B)-Mo(3B)-S(3)	111.47(17)	Se(1B)-S(1B)-Mo(1B)	67.6(3)
S(4B)-Mo(3B)-S(2B)	109.6(2)	Mo(2B)-S(1B)-Mo(1B)	69.50(19)
S(3)-Mo(3B)-S(2B)	84.3(2)	Se(2B)-S(2B)-Mo(2B)	68.9(3)
S(4B)-Mo(3B)-S(10B)	83.29(18)	Se(2B)-S(2B)-Mo(3B)	69.3(2)
S(3)-Mo(3B)-S(10B)	131.53(17)	Mo(2B)-S(2B)-Mo(3B)	69.5(2)
S(2B)-Mo(3B)-S(10B)	135.7(3)	Mo(3B)-S(4B)-Mo(2B)	70.37(16)
S(4B)-Mo(3B)-S(9B)	161.2(3)	Mo(3B)-S(4B)-Mo(1B)	70.9(2)
S(3)-Mo(3B)-S(9B)	83.0(3)	Mo(2B)-S(4B)-Mo(1B)	70.61(18)
S(2B)-Mo(3B)-S(9B)	82.9(3)	P(1B)-S(5B)-Mo(1B)	90.6(7)
S(10B)-Mo(3B)-S(9B)	78.1(2)	P(1B)-S(6B)-Mo(1B)	84.5(8)
S(4B)-Mo(3B)-Se(2B)	85.36(16)	C(5B)-P(1B)-C(1B)	106.0(10)
S(3)-Mo(3B)-Se(2B)	135.33(13)	C(5B)-P(1B)-S(5B)	112.4(10)

Table A.51, Cont'd. Bond angles (deg.) for $[\text{Mo}_3\text{S}_4\text{Se}_3(\text{S}_2\text{P}^i\text{Bu}_2)_3]\text{I}\cdot\frac{1}{2}\text{C}_5\text{H}_{12}$. Symmetry transformations used to generate equivalent atoms:

C(1B)-P(1B)-S(5B)	112.1(7)	C(6B)-C(7B)-H(7B3)	109.5
C(5B)-P(1B)-S(6B)	105.8(8)	H(7B1)-C(7B)-H(7B3)	109.5
C(1B)-P(1B)-S(6B)	118.1(11)	H(7B2)-C(7B)-H(7B3)	109.5
S(5B)-P(1B)-S(6B)	102.5(10)	C(6B)-C(8B)-H(8B1)	109.5
C(2B)-C(1B)-P(1B)	119.2(11)	C(6B)-C(8B)-H(8B2)	109.5
C(2B)-C(1B)-H(1B1)	107.5	H(8B1)-C(8B)-H(8B2)	109.5
P(1B)-C(1B)-H(1B1)	107.5	C(6B)-C(8B)-H(8B3)	109.5
C(2B)-C(1B)-H(1B2)	107.5	H(8B1)-C(8B)-H(8B3)	109.5
P(1B)-C(1B)-H(1B2)	107.5	H(8B2)-C(8B)-H(8B3)	109.5
H(1B1)-C(1B)-H(1B2)	107.0	P(2B)-S(7B)-Mo(2B)	90.19(18)
C(4B)-C(2B)-C(1B)	107.7(14)	P(2B)-S(8B)-Mo(2B)	89.65(18)
C(4B)-C(2B)-C(3B)	111.6(14)	C(9B)-P(2B)-C(13B)	103.1(8)
C(1B)-C(2B)-C(3B)	110.7(13)	C(9B)-P(2B)-S(7B)	111.4(6)
C(4B)-C(2B)-H(2B)	108.9	C(13B)-P(2B)-S(7B)	110.7(7)
C(1B)-C(2B)-H(2B)	108.9	C(9B)-P(2B)-S(8B)	114.1(6)
C(3B)-C(2B)-H(2B)	108.9	C(13B)-P(2B)-S(8B)	114.7(7)
C(2B)-C(3B)-H(3B1)	109.5	S(7B)-P(2B)-S(8B)	103.1(2)
C(2B)-C(3B)-H(3B2)	109.5	C(10B)-C(9B)-P(2B)	117.2(11)
H(3B1)-C(3B)-H(3B2)	109.5	C(10B)-C(9B)-H(9B1)	108.0
C(2B)-C(3B)-H(3B3)	109.5	P(2B)-C(9B)-H(9B1)	108.0
H(3B1)-C(3B)-H(3B3)	109.5	C(10B)-C(9B)-H(9B2)	108.0
H(3B2)-C(3B)-H(3B3)	109.5	P(2B)-C(9B)-H(9B2)	108.0
C(2B)-C(4B)-H(4B1)	109.5	H(9B1)-C(9B)-H(9B2)	107.2
C(2B)-C(4B)-H(4B2)	109.5	C(12B)-C(10B)-C(9B)	106.4(13)
H(4B1)-C(4B)-H(4B2)	109.5	C(12B)-C(10B)-C(11B)	110.7(15)
C(2B)-C(4B)-H(4B3)	109.5	C(9B)-C(10B)-C(11B)	113.4(15)
H(4B1)-C(4B)-H(4B3)	109.5	C(12B)-C(10B)-H(10B)	108.7
H(4B2)-C(4B)-H(4B3)	109.5	C(9B)-C(10B)-H(10B)	108.7
C(6B)-C(5B)-P(1B)	119.7(13)	C(11B)-C(10B)-H(10B)	108.7
C(6B)-C(5B)-H(5B1)	107.4	C(10B)-C(11B)-H(11D)	109.5
P(1B)-C(5B)-H(5B1)	107.4	C(10B)-C(11B)-H(11E)	109.5
C(6B)-C(5B)-H(5B2)	107.4	H(11D)-C(11B)-H(11E)	109.5
P(1B)-C(5B)-H(5B2)	107.4	C(10B)-C(11B)-H(11F)	109.5
H(5B1)-C(5B)-H(5B2)	106.9	H(11D)-C(11B)-H(11F)	109.5
C(5B)-C(6B)-C(8B)	112.8(19)	H(11E)-C(11B)-H(11F)	109.5
C(5B)-C(6B)-C(7B)	114.0(18)	C(10B)-C(12B)-H(12D)	109.5
C(8B)-C(6B)-C(7B)	109.2(19)	C(10B)-C(12B)-H(12E)	109.5
C(5B)-C(6B)-H(6B)	106.8	H(12D)-C(12B)-H(12E)	109.5
C(8B)-C(6B)-H(6B)	106.8	C(10B)-C(12B)-H(12F)	109.5
C(7B)-C(6B)-H(6B)	106.8	H(12D)-C(12B)-H(12F)	109.5
C(6B)-C(7B)-H(7B1)	109.5	H(12E)-C(12B)-H(12F)	109.5
C(6B)-C(7B)-H(7B2)	109.5	C(14B)-C(13B)-P(2B)	117.2(15)
H(7B1)-C(7B)-H(7B2)	109.5	C(14B)-C(13B)-H(13C)	108.0

Table A.51, Cont'd. Bond angles (deg.) for $[\text{Mo}_3\text{S}_4\text{Se}_3(\text{S}_2\text{P}^i\text{Bu}_2)_3]\text{I}\cdot\frac{1}{2}\text{C}_5\text{H}_{12}$. Symmetry transformations used to generate equivalent atoms:

P(2B)-C(13B)-H(13C)	108.0	C(18B)-C(19B)-H(19E)	109.5
C(14B)-C(13B)-H(13D)	108.0	H(19D)-C(19B)-H(19E)	109.5
P(2B)-C(13B)-H(13D)	108.0	C(18B)-C(19B)-H(19F)	109.5
H(13C)-C(13B)-H(13D)	107.2	H(19D)-C(19B)-H(19F)	109.5
C(16B)-C(14B)-C(13B)	113(2)	H(19E)-C(19B)-H(19F)	109.5
C(16B)-C(14B)-C(15B)	109(2)	C(18B)-C(20B)-H(20D)	109.5
C(13B)-C(14B)-C(15B)	110(2)	C(18B)-C(20B)-H(20E)	109.5
C(16B)-C(14B)-H(14B)	108.4	H(20D)-C(20B)-H(20E)	109.5
C(13B)-C(14B)-H(14B)	108.4	C(18B)-C(20B)-H(20F)	109.5
C(15B)-C(14B)-H(14B)	108.4	H(20D)-C(20B)-H(20F)	109.5
C(14B)-C(15B)-H(15D)	109.5	H(20E)-C(20B)-H(20F)	109.5
C(14B)-C(15B)-H(15E)	109.5	C(22B)-C(21B)-P(3B)	117.0(12)
H(15D)-C(15B)-H(15E)	109.5	C(22B)-C(21B)-H(21C)	108.0
C(14B)-C(15B)-H(15F)	109.5	P(3B)-C(21B)-H(21C)	108.0
H(15D)-C(15B)-H(15F)	109.5	C(22B)-C(21B)-H(21D)	108.0
H(15E)-C(15B)-H(15F)	109.5	P(3B)-C(21B)-H(21D)	108.0
C(14B)-C(16B)-H(16D)	109.5	H(21C)-C(21B)-H(21D)	107.3
C(14B)-C(16B)-H(16E)	109.5	C(23B)-C(22B)-C(21B)	115.6(16)
H(16D)-C(16B)-H(16E)	109.5	C(23B)-C(22B)-C(24B)	111.1(18)
C(14B)-C(16B)-H(16F)	109.5	C(21B)-C(22B)-C(24B)	106.9(16)
H(16D)-C(16B)-H(16F)	109.5	C(23B)-C(22B)-H(22B)	107.7
H(16E)-C(16B)-H(16F)	109.5	C(21B)-C(22B)-H(22B)	107.7
P(3B)-S(9B)-Mo(3B)	89.0(4)	C(24B)-C(22B)-H(22B)	107.7
P(3B)-S(10B)-Mo(3B)	89.6(3)	C(22B)-C(23B)-H(23D)	109.5
C(17B)-P(3B)-C(21B)	84.8(10)	C(22B)-C(23B)-H(23E)	109.5
C(17B)-P(3B)-S(10B)	121.5(8)	H(23D)-C(23B)-H(23E)	109.5
C(21B)-P(3B)-S(10B)	117.1(6)	C(22B)-C(23B)-H(23F)	109.5
C(17B)-P(3B)-S(9B)	118.8(8)	H(23D)-C(23B)-H(23F)	109.5
C(21B)-P(3B)-S(9B)	110.9(6)	H(23E)-C(23B)-H(23F)	109.5
S(10B)-P(3B)-S(9B)	103.3(3)	C(22B)-C(24B)-H(24D)	109.5
C(18B)-C(17B)-P(3B)	128(2)	C(22B)-C(24B)-H(24E)	109.5
C(18B)-C(17B)-H(17C)	105.4	H(24D)-C(24B)-H(24E)	109.5
P(3B)-C(17B)-H(17C)	105.4	C(22B)-C(24B)-H(24F)	109.5
C(18B)-C(17B)-H(17D)	105.4	H(24D)-C(24B)-H(24F)	109.5
P(3B)-C(17B)-H(17D)	105.4	H(24E)-C(24B)-H(24F)	109.5
H(17C)-C(17B)-H(17D)	106.0	C(26A)-C(25A)-H(25A)	109.5
C(17B)-C(18B)-C(19B)	93(2)	C(26A)-C(25A)-H(25B)	109.5
C(17B)-C(18B)-C(20B)	104(3)	H(25A)-C(25A)-H(25B)	109.5
C(19B)-C(18B)-C(20B)	91(2)	C(26A)-C(25A)-H(25C)	109.5
C(17B)-C(18B)-H(18B)	120.8	H(25A)-C(25A)-H(25C)	109.5
C(19B)-C(18B)-H(18B)	120.8	H(25B)-C(25A)-H(25C)	109.5
C(20B)-C(18B)-H(18B)	120.8	C(25A)-C(26A)-C(27A)	106(5)
C(18B)-C(19B)-H(19D)	109.5	C(25A)-C(26A)-H(26A)	110.5

Table A.51, Cont'd. Bond angles (deg.) for $[\text{Mo}_3\text{S}_4\text{Se}_3(\text{S}_2\text{P}^i\text{Bu}_2)_3]\text{I}\cdot\frac{1}{2}\text{C}_5\text{H}_{12}$. Symmetry transformations used to generate equivalent atoms:

C(27A)-C(26A)-H(26A)	110.5	C(27B)-C(28B)-H(28D)	110.0
C(25A)-C(26A)-H(26B)	110.5	C(29B)-C(28B)-H(28D)	110.0
C(27A)-C(26A)-H(26B)	110.5	H(28C)-C(28B)-H(28D)	108.3
H(26A)-C(26A)-H(26B)	108.7	C(28B)-C(29B)-H(29D)	109.5
C(26A)-C(27A)-C(28A)	155(6)	C(28B)-C(29B)-H(29E)	109.5
C(26A)-C(27A)-H(27A)	97.6	H(29D)-C(29B)-H(29E)	109.5
C(28A)-C(27A)-H(27A)	97.6	C(28B)-C(29B)-H(29F)	109.5
C(26A)-C(27A)-H(27B)	97.6	H(29D)-C(29B)-H(29F)	109.5
C(28A)-C(27A)-H(27B)	97.6	H(29E)-C(29B)-H(29F)	109.5
H(27A)-C(27A)-H(27B)	103.6		
C(29A)-C(28A)-C(27A)	107(3)		
C(29A)-C(28A)-H(28A)	110.2		
C(27A)-C(28A)-H(28A)	110.2		
C(29A)-C(28A)-H(28B)	110.2		
C(27A)-C(28A)-H(28B)	110.2		
H(28A)-C(28A)-H(28B)	108.5		
C(28A)-C(29A)-H(29A)	109.5		
C(28A)-C(29A)-H(29B)	109.5		
H(29A)-C(29A)-H(29B)	109.5		
C(28A)-C(29A)-H(29C)	109.5		
H(29A)-C(29A)-H(29C)	109.5		
H(29B)-C(29A)-H(29C)	109.5		
C(26B)-C(25B)-H(25D)	109.5		
C(26B)-C(25B)-H(25E)	109.5		
H(25D)-C(25B)-H(25E)	109.5		
C(26B)-C(25B)-H(25F)	109.5		
H(25D)-C(25B)-H(25F)	109.5		
H(25E)-C(25B)-H(25F)	109.5		
C(27B)-C(26B)-C(25B)	117(5)		
C(27B)-C(26B)-H(26C)	107.9		
C(25B)-C(26B)-H(26C)	107.9		
C(27B)-C(26B)-H(26D)	107.9		
C(25B)-C(26B)-H(26D)	107.9		
H(26C)-C(26B)-H(26D)	107.2		
C(26B)-C(27B)-C(28B)	93(6)		
C(26B)-C(27B)-H(27C)	113.2		
C(28B)-C(27B)-H(27C)	113.2		
C(26B)-C(27B)-H(27D)	113.2		
C(28B)-C(27B)-H(27D)	113.2		
H(27C)-C(27B)-H(27D)	110.5		
C(27B)-C(28B)-C(29B)	109(3)		
C(27B)-C(28B)-H(28C)	110.0		
C(29B)-C(28B)-H(28C)	110.0		

Table A.52. Anisotropic displacement parameters ($\text{\AA}^2 \times 10^3$) for $[\text{Mo}_3\text{S}_4\text{Se}_3(\text{S}_2\text{P}^i\text{Bu}_2)_3]\text{I} \cdot \frac{1}{2}\text{C}_5\text{H}_{12}$. The anisotropic displacement factor exponent takes the form: $-2\pi^2[h^2a^{*2}U^{11} + \dots + 2hka^*b^*U^{12}]$.

Atom	U^{11}	U^{22}	U^{33}	U^{23}	U^{13}	U^{12}
I(1)	89(1)	72(1)	38(1)	-8(1)	19(1)	-11(1)
Se(3)	64(1)	61(1)	42(1)	5(1)	19(1)	16(1)
S(3)	41(1)	42(1)	24(1)	-1(1)	8(1)	5(1)
Mo(1A)	43(1)	16(1)	25(1)	2(1)	11(1)	7(1)
Mo(2A)	36(1)	31(1)	28(1)	0(1)	10(1)	4(1)
Mo(3A)	35(1)	24(1)	22(1)	-1(1)	10(1)	1(1)
Se(1A)	71(1)	50(1)	56(1)	-4(1)	17(1)	-3(1)
Se(2A)	54(1)	44(1)	53(1)	0(1)	18(1)	8(1)
S(1A)	44(2)	32(3)	28(3)	3(2)	13(2)	3(2)
S(2A)	45(3)	23(3)	32(2)	-4(2)	16(1)	2(2)
S(4A)	42(2)	32(2)	23(2)	-1(2)	9(1)	3(2)
S(5A)	47(5)	37(3)	35(1)	-3(2)	20(4)	-2(3)
S(6A)	49(7)	41(6)	33(3)	-19(3)	5(5)	2(4)
P(1A)	39(5)	44(2)	33(3)	-8(2)	4(4)	13(4)
S(7A)	38(1)	55(2)	44(2)	2(1)	16(1)	5(1)
S(8A)	44(1)	62(2)	40(1)	1(1)	2(1)	-3(1)
P(2A)	41(1)	60(2)	54(2)	-3(1)	8(1)	4(1)
S(9A)	69(5)	37(3)	28(1)	-4(1)	18(3)	-18(3)
S(10A)	53(3)	38(2)	25(1)	3(1)	15(2)	-1(2)
P(3A)	56(3)	39(2)	34(1)	3(1)	18(2)	-7(2)
Mo(1B)	43(1)	16(1)	25(1)	2(1)	11(1)	7(1)
Mo(2B)	36(1)	31(1)	28(1)	0(1)	10(1)	4(1)
Mo(3B)	35(1)	24(1)	22(1)	-1(1)	10(1)	1(1)
Se(1B)	71(1)	50(1)	56(1)	-4(1)	17(1)	-3(1)
Se(2B)	54(1)	44(1)	53(1)	0(1)	18(1)	8(1)
S(1B)	44(2)	32(3)	28(3)	3(2)	13(2)	3(2)
S(2B)	45(3)	23(3)	32(2)	-4(2)	16(1)	2(2)
S(4B)	42(2)	32(2)	23(2)	-1(2)	9(1)	3(2)
S(5B)	47(5)	37(3)	35(1)	-3(2)	20(4)	-2(3)
S(6B)	49(7)	41(6)	33(3)	-19(3)	5(5)	2(4)
P(1B)	39(5)	44(2)	33(3)	-8(2)	4(4)	13(4)
S(7B)	38(1)	55(2)	44(2)	2(1)	16(1)	5(1)
S(8B)	44(1)	62(2)	40(1)	1(1)	2(1)	-3(1)
P(2B)	41(1)	60(2)	54(2)	-3(1)	8(1)	4(1)
S(9B)	69(5)	37(3)	28(1)	-4(1)	18(3)	-18(3)
S(10B)	53(3)	38(2)	25(1)	3(1)	15(2)	-1(2)
P(3B)	56(3)	39(2)	34(1)	3(1)	18(2)	-7(2)

Table A.53. Hydrogen coordinates ($\times 10^4$) and isotropic displacement parameters ($\text{\AA}^2 \times 10^3$) for $[\text{Mo}_3\text{S}_4\text{Se}_3(\text{S}_2\text{P}^i\text{Bu}_2)_3]\text{I} \cdot \frac{1}{2}\text{C}_5\text{H}_{12}$.

H atom	x	y	z	U(eq)
H(1A1)	2841	5476	1732	47
H(1A2)	2671	5564	907	47
H(2A)	2931	6886	1729	56
H(3A1)	3096	7329	714	77
H(3A2)	2963	6528	347	77
H(3A3)	2600	7052	513	77
H(4A1)	3663	6708	1689	114
H(4A2)	3530	6040	2124	114
H(4A3)	3535	5897	1340	114
H(5A1)	1948	4778	1065	69
H(5A2)	2149	4819	1889	69
H(6A)	1438	5493	1810	99
H(7A1)	1667	4430	2442	173
H(7A2)	1153	4413	2068	173
H(7A3)	1475	3926	1762	173
H(8A1)	1190	5457	585	174
H(8A2)	1174	4556	605	174
H(8A3)	852	5043	912	174
H(9A1)	-215	9672	310	107
H(9A2)	-659	9378	427	107
H(10A)	17	10070	1482	67
H(11A)	-275	10830	481	121
H(11B)	-743	10796	618	121
H(11C)	-343	11204	1167	121
H(12A)	-448	10413	2059	172
H(12B)	-840	9976	1519	172
H(12C)	-439	9513	2009	172
H(13A)	-691	8034	1169	81
H(13B)	-707	7878	382	81
H(14A)	-132	7050	1472	89
H(15A)	-645	6087	1345	158
H(15B)	-800	6843	1639	158
H(15C)	-1007	6614	840	158
H(16A)	-20	6875	372	142
H(16B)	-140	6105	689	142
H(16C)	-502	6532	89	142
H(17A)	1490	11549	57	58
H(17B)	1292	11146	619	58
H(18A)	1389	12272	902	94
H(19A)	1805	12592	150	124

Table A.53, Cont'd. Hydrogen coordinates ($\times 10^4$) and isotropic displacement parameters ($\text{\AA}^2 \times 10^3$) for $[\text{Mo}_3\text{S}_4\text{Se}_3(\text{S}_2\text{P}^i\text{Bu}_2)_3]\text{I} \cdot \frac{1}{2}\text{C}_5\text{H}_{12}$.

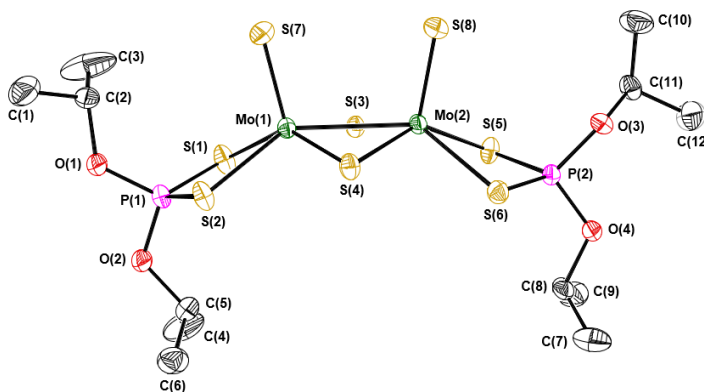
H atom	x	y	z	U(eq)
H(19B)	1668	13193	642	124
H(19C)	2153	12859	856	124
H(20A)	1830	12699	1803	245
H(20B)	1440	12118	1749	245
H(20C)	1933	11824	1961	245
H(21A)	2593	11047	289	80
H(21B)	2700	11445	1032	80
H(22A)	2884	10122	1462	85
H(23A)	2688	9575	338	148
H(23B)	3072	10033	160	148
H(23C)	3186	9398	751	148
H(24A)	3597	10319	1551	169
H(24B)	3466	11000	1007	169
H(24C)	3374	11061	1746	169
H(1B1)	2999	5625	1752	41
H(1B2)	2812	5753	936	41
H(2B)	3043	7038	1798	50
H(3B1)	2706	7232	597	53
H(3B2)	3196	7542	803	53
H(3B3)	3080	6750	413	53
H(4B1)	3762	6908	1758	96
H(4B2)	3629	6220	2170	96
H(4B3)	3643	6105	1387	96
H(5B1)	2123	4852	1103	56
H(5B2)	2324	4872	1926	56
H(6B)	1582	5440	1833	75
H(7B1)	1344	4249	2125	134
H(7B2)	1731	3842	1908	134
H(7B3)	1841	4401	2561	134
H(8B1)	1026	4786	995	145
H(8B2)	1291	5330	630	145
H(8B3)	1383	4441	666	145
H(9B1)	-739	8532	769	60
H(9B2)	-673	8554	1586	60
H(10B)	-82	9493	1570	56
H(11D)	-184	9460	357	114
H(11E)	-681	9712	215	114
H(11F)	-297	10282	584	114
H(12D)	-609	10409	1553	89
H(12E)	-985	9806	1229	89

Table A.53, Cont'd. Hydrogen coordinates ($\times 10^4$) and isotropic displacement parameters ($\text{\AA}^2 \times 10^3$) for $[\text{Mo}_3\text{S}_4\text{Se}_3(\text{S}_2\text{P}^i\text{Bu}_2)_3]\text{I} \cdot \frac{1}{2}\text{C}_5\text{H}_{12}$.

H atom	x	y	z	U(eq)
H(13C)	-525	7131	1814	86
H(13D)	-615	6966	1005	86
H(14B)	197	6474	1891	105
H(15D)	-310	6079	2487	187
H(15E)	-588	5644	1805	187
H(15F)	-106	5365	2209	187
H(16D)	95	5454	1126	228
H(16E)	-379	5761	712	228
H(16F)	46	6230	703	228
H(17C)	1838	11637	143	90
H(17D)	1407	11495	355	90
H(18B)	2121	12377	1248	193
H(19D)	1504	13320	458	254
H(19E)	1625	12776	-94	254
H(19F)	1200	12611	149	254
H(20D)	1424	12687	1697	178
H(20E)	1107	12261	1041	178
H(20F)	1408	11785	1678	178
H(21C)	2383	10991	211	58
H(21D)	2497	11383	956	58
H(22B)	2793	10137	1424	66
H(23D)	3095	9405	708	97
H(23E)	2574	9400	410	97
H(23F)	2857	9916	51	97
H(24D)	3205	11265	1456	144
H(24E)	3484	10542	1370	144
H(24F)	3263	11063	712	144
H(25A)	-1089	3917	871	147
H(25B)	-1006	3042	1057	147
H(25C)	-776	3671	1615	147
H(26A)	-340	4059	886	205
H(26B)	-570	3427	325	205
H(27A)	-321	2501	1033	146
H(27B)	-223	3011	1690	146
H(28A)	473	2638	1207	232
H(28B)	458	2795	1987	232
H(29A)	496	1462	1807	170
H(29B)	42	1661	1948	170
H(29C)	57	1505	1172	170
H(25D)	-1125	3896	1821	135

Table A.53, Cont'd. Hydrogen coordinates ($\times 10^4$) and isotropic displacement parameters ($\text{\AA}^2 \times 10^3$) for $[\text{Mo}_3\text{S}_4\text{Se}_3(\text{S}_2\text{P}^i\text{Bu}_2)_3]\text{I} \cdot \frac{1}{2}\text{C}_5\text{H}_{12}$.

H atom	x	y	z	U(eq)
H(25E)	-1278	3271	1226	135
H(25F)	-829	3167	1830	135
H(26C)	-980	4339	803	106
H(26D)	-533	4235	1405	106
H(27C)	-705	3646	99	157
H(27D)	-641	2933	629	157
H(28C)	-112	4057	1354	263
H(28D)	-8	4028	620	263
H(29D)	465	3173	1419	236
H(29E)	51	2735	1518	236
H(29F)	154	2706	786	236



Thermal ellipsoid plot is drawn at the 50% level. All H atoms are omitted for clarity.

Table A.54. Crystal Data and Structure Refinement for $[(i\text{PrO})_2\text{PS}_2]\text{Mo}(\text{S})(\mu_2\text{-S})_2\text{Mo}(\text{S})(\text{S}_2\text{P}(\text{O}^i\text{Pr})_2)]$

Identification code	JPD1309_0m_a	
Empirical formula	$\text{C}_{12}\text{H}_{28}\text{Mo}_2\text{O}_4\text{P}_2\text{S}_8$	
Formula weight	1493.28	
Temperature	150(2) K	
Wavelength	0.71073 Å	
Crystal system	Monoclinic	
Space group	$P2_1/c$	
Unit cell dimensions	$a = 12.6795(5)$ Å	$\alpha = 90^\circ$
	$b = 13.8455(6)$ Å	$\beta = 101.4810(10)^\circ$
	$c = 16.1584(6)$ Å	$\gamma = 90^\circ$
Volume	$2779.91(19)$ Å ³	
Z	4	
Density (calculated)	1.784 g/cm ³	
Absorption coefficient	1.635 mm ⁻¹	
F(000)	1496	
Crystal size	0.357 x 0.189 x 0.009 mm ³	
θ range for data collection	2.380 to 26.428°	
Index ranges	$-15 \leq h \leq 15, -17 \leq k \leq 17, -20 \leq l \leq 20$	
Reflections collected	88748	
Independent reflections	5684 [R(int) = 0.0497]	
Completeness to $\theta = 25.242^\circ$	99.6 %	
Absorption correction	Semi-empirical from equivalents	
Max. and min. transmission	0.99 and 0.87	
Refinement method	Full-matrix least-squares on F^2	
Data / restraints / parameters	5684 / 0 / 261	
Goodness-of-fit on F^2	1.018	
Final R indices [$I > 2\sigma(I)$]	R1 = 0.0230, wR2 = 0.0574	
R indices (all data)	R1 = 0.0345, wR2 = 0.0642	
Extinction coefficient	n/a	
Largest diff. peak and hole	0.439 and -0.343 e·Å ⁻³	

Table A.55. Atomic coordinates ($\times 10^4$) and equivalent isotropic displacement parameters ($\text{\AA}^2 \times 10^3$) for $[(\text{iPrO})_2\text{PS}_2)\text{Mo}(\text{S})(\mu_2\text{-S})_2\text{Mo}(\text{S})(\text{S}_2\text{P}(\text{O}^i\text{Pr})_2)]$. $U(\text{eq})$ is defined as one third of the trace of the orthogonalized U^{ij} tensor.

Atom	x	y	z	$U(\text{eq})$
Mo(1)	6942(1)	2201(1)	7749(1)	19(1)
Mo(2)	5196(1)	2058(1)	6368(1)	18(1)
S(1)	8814(1)	2747(1)	7784(1)	31(1)
S(2)	7270(1)	3272(1)	9014(1)	27(1)
S(3)	7001(1)	2119(1)	6334(1)	21(1)
S(4)	5203(1)	2733(1)	7678(1)	23(1)
S(5)	5086(1)	2424(1)	4847(1)	25(1)
S(6)	3503(1)	3026(1)	6030(1)	23(1)
S(7)	7050(1)	776(1)	8210(1)	32(1)
S(8)	4770(1)	596(1)	6412(1)	29(1)
P(1)	8820(1)	3352(1)	8915(1)	22(1)
P(2)	3538(1)	2758(1)	4816(1)	20(1)
O(1)	9635(1)	2890(1)	9663(1)	26(1)
O(2)	9293(1)	4397(1)	8985(1)	27(1)
O(3)	2723(1)	1937(1)	4484(1)	22(1)
O(4)	3122(1)	3613(1)	4196(1)	26(1)
C(1)	9784(3)	1810(2)	10822(2)	58(1)
C(2)	9578(2)	1858(2)	9891(2)	29(1)
C(3)	10396(4)	1326(3)	9521(3)	86(2)
C(4)	9657(3)	5565(3)	7977(2)	61(1)
C(5)	8791(2)	5160(2)	8391(2)	33(1)
C(6)	8295(2)	5880(2)	8883(2)	41(1)
C(7)	2789(3)	5283(2)	4418(2)	47(1)
C(8)	3645(2)	4573(2)	4305(2)	31(1)
C(9)	4131(2)	4748(2)	3544(2)	42(1)
C(10)	2510(3)	336(2)	3967(2)	46(1)
C(11)	2789(2)	1336(2)	3736(2)	27(1)
C(12)	2039(3)	1738(2)	2981(2)	49(1)

Table A.56. Bond lengths (Å) for $[(i\text{PrO})_2\text{PS}_2]\text{Mo}(\text{S})(\mu_2\text{-S})_2\text{Mo}(\text{S})(\text{S}_2\text{P}(\text{O}^i\text{Pr})_2)$. Symmetry transformations used to generate equivalent atoms:

Mo(1)-S(7)	2.1044(7)	C(7)-H(7B)	0.9800
Mo(1)-S(3)	2.3044(6)	C(7)-H(7C)	0.9800
Mo(1)-S(4)	2.3059(7)	C(8)-C(9)	1.501(4)
Mo(1)-S(1)	2.4804(7)	C(8)-H(8)	1.0000
Mo(1)-S(2)	2.4921(6)	C(9)-H(9A)	0.9800
Mo(1)-Mo(2)	2.8199(3)	C(9)-H(9B)	0.9800
Mo(2)-S(8)	2.0994(7)	C(9)-H(9C)	0.9800
Mo(2)-S(3)	2.3016(7)	C(10)-C(11)	1.494(4)
Mo(2)-S(4)	2.3122(6)	C(10)-H(10A)	0.9800
Mo(2)-S(5)	2.4859(6)	C(10)-H(10B)	0.9800
Mo(2)-S(6)	2.4972(7)	C(10)-H(10C)	0.9800
S(1)-P(1)	2.0088(9)	C(11)-C(12)	1.497(4)
S(2)-P(1)	2.0060(9)	C(11)-H(11)	1.0000
S(5)-P(2)	2.0064(9)	C(12)-H(12A)	0.9800
S(6)-P(2)	2.0048(8)	C(12)-H(12B)	0.9800
P(1)-O(2)	1.5615(18)	C(12)-H(12C)	0.9800
P(1)-O(1)	1.5629(17)		
P(2)-O(3)	1.5580(17)		
P(2)-O(4)	1.5721(17)		
O(1)-C(2)	1.481(3)		
O(2)-C(5)	1.483(3)		
O(3)-C(11)	1.483(3)		
O(4)-C(8)	1.481(3)		
C(1)-C(2)	1.475(4)		
C(1)-H(1A)	0.9800		
C(1)-H(1B)	0.9800		
C(1)-H(1C)	0.9800		
C(2)-C(3)	1.492(4)		
C(2)-H(2)	1.0000		
C(3)-H(3A)	0.9800		
C(3)-H(3B)	0.9800		
C(3)-H(3C)	0.9800		
C(4)-C(5)	1.503(4)		
C(4)-H(4A)	0.9800		
C(4)-H(4B)	0.9800		
C(4)-H(4C)	0.9800		
C(5)-C(6)	1.490(4)		
C(5)-H(5)	1.0000		
C(6)-H(6A)	0.9800		
C(6)-H(6B)	0.9800		
C(6)-H(6C)	0.9800		
C(7)-C(8)	1.502(4)		
C(7)-H(7A)	0.9800		

Table A.57. Bond angles (deg.) for $[(i\text{PrO})_2\text{PS}_2]\text{Mo}(\text{S})(\mu_2\text{-S})_2\text{Mo}(\text{S})(\text{S}_2\text{P}(\text{O}^i\text{Pr})_2)]$. Symmetry transformations used to generate equivalent atoms:

S(7)-Mo(1)-S(3)	107.02(2)	O(3)-P(2)-S(6)	109.27(7)
S(7)-Mo(1)-S(4)	108.11(3)	O(4)-P(2)-S(6)	114.46(7)
S(3)-Mo(1)-S(4)	100.72(2)	O(3)-P(2)-S(5)	114.75(7)
S(7)-Mo(1)-S(1)	106.46(3)	O(4)-P(2)-S(5)	113.06(7)
S(3)-Mo(1)-S(1)	79.51(2)	S(6)-P(2)-S(5)	103.32(3)
S(4)-Mo(1)-S(1)	143.61(3)	C(2)-O(1)-P(1)	122.02(15)
S(7)-Mo(1)-S(2)	106.19(3)	C(5)-O(2)-P(1)	120.18(15)
S(3)-Mo(1)-S(2)	144.06(2)	C(11)-O(3)-P(2)	123.34(15)
S(4)-Mo(1)-S(2)	81.53(2)	C(8)-O(4)-P(2)	120.99(14)
S(1)-Mo(1)-S(2)	78.30(2)	C(2)-C(1)-H(1A)	109.5
S(7)-Mo(1)-Mo(2)	101.53(2)	C(2)-C(1)-H(1B)	109.5
S(3)-Mo(1)-Mo(2)	52.204(16)	H(1A)-C(1)-H(1B)	109.5
S(4)-Mo(1)-Mo(2)	52.468(15)	C(2)-C(1)-H(1C)	109.5
S(1)-Mo(1)-Mo(2)	129.522(18)	H(1A)-C(1)-H(1C)	109.5
S(2)-Mo(1)-Mo(2)	131.868(17)	H(1B)-C(1)-H(1C)	109.5
S(8)-Mo(2)-S(3)	107.48(2)	C(1)-C(2)-O(1)	106.9(2)
S(8)-Mo(2)-S(4)	108.22(2)	C(1)-C(2)-C(3)	113.0(3)
S(3)-Mo(2)-S(4)	100.61(2)	O(1)-C(2)-C(3)	107.7(2)
S(8)-Mo(2)-S(5)	105.43(2)	C(1)-C(2)-H(2)	109.7
S(3)-Mo(2)-S(5)	80.18(2)	O(1)-C(2)-H(2)	109.7
S(4)-Mo(2)-S(5)	144.27(2)	C(3)-C(2)-H(2)	109.7
S(8)-Mo(2)-S(6)	108.00(2)	C(2)-C(3)-H(3A)	109.5
S(3)-Mo(2)-S(6)	142.21(2)	C(2)-C(3)-H(3B)	109.5
S(4)-Mo(2)-S(6)	80.21(2)	H(3A)-C(3)-H(3B)	109.5
S(5)-Mo(2)-S(6)	78.30(2)	C(2)-C(3)-H(3C)	109.5
S(8)-Mo(2)-Mo(1)	102.001(19)	H(3A)-C(3)-H(3C)	109.5
S(3)-Mo(2)-Mo(1)	52.295(15)	H(3B)-C(3)-H(3C)	109.5
S(4)-Mo(2)-Mo(1)	52.264(16)	C(5)-C(4)-H(4A)	109.5
S(5)-Mo(2)-Mo(1)	130.429(17)	C(5)-C(4)-H(4B)	109.5
S(6)-Mo(2)-Mo(1)	129.846(16)	H(4A)-C(4)-H(4B)	109.5
P(1)-S(1)-Mo(1)	88.77(3)	C(5)-C(4)-H(4C)	109.5
P(1)-S(2)-Mo(1)	88.51(3)	H(4A)-C(4)-H(4C)	109.5
Mo(2)-S(3)-Mo(1)	75.50(2)	H(4B)-C(4)-H(4C)	109.5
Mo(1)-S(4)-Mo(2)	75.27(2)	O(2)-C(5)-C(6)	107.6(2)
P(2)-S(5)-Mo(2)	86.21(3)	O(2)-C(5)-C(4)	107.3(2)
P(2)-S(6)-Mo(2)	85.94(3)	C(6)-C(5)-C(4)	114.2(3)
O(2)-P(1)-O(1)	97.89(9)	O(2)-C(5)-H(5)	109.2
O(2)-P(1)-S(2)	114.45(7)	C(6)-C(5)-H(5)	109.2
O(1)-P(1)-S(2)	115.00(8)	C(4)-C(5)-H(5)	109.2
O(2)-P(1)-S(1)	112.66(7)	C(5)-C(6)-H(6A)	109.5
O(1)-P(1)-S(1)	114.55(8)	C(5)-C(6)-H(6B)	109.5
S(2)-P(1)-S(1)	102.87(4)	H(6A)-C(6)-H(6B)	109.5
O(3)-P(2)-O(4)	102.33(9)	C(5)-C(6)-H(6C)	109.5

Table A.57, Cont'd. Bond angles (deg.) for $[(i\text{PrO})_2\text{PS}_2]\text{Mo}(\text{S})(\mu_2\text{-S})_2\text{Mo}(\text{S})(\text{S}_2\text{P}(\text{O}^i\text{Pr})_2)]$. Symmetry transformations used to generate equivalent atoms:

H(6A)-C(6)-H(6C)	109.5
H(6B)-C(6)-H(6C)	109.5
C(8)-C(7)-H(7A)	109.5
C(8)-C(7)-H(7B)	109.5
H(7A)-C(7)-H(7B)	109.5
C(8)-C(7)-H(7C)	109.5
H(7A)-C(7)-H(7C)	109.5
H(7B)-C(7)-H(7C)	109.5
O(4)-C(8)-C(7)	106.5(2)
O(4)-C(8)-C(9)	107.2(2)
C(7)-C(8)-C(9)	114.7(2)
O(4)-C(8)-H(8)	109.4
C(7)-C(8)-H(8)	109.4
C(9)-C(8)-H(8)	109.4
C(8)-C(9)-H(9A)	109.5
C(8)-C(9)-H(9B)	109.5
H(9A)-C(9)-H(9B)	109.5
C(8)-C(9)-H(9C)	109.5
H(9A)-C(9)-H(9C)	109.5
H(9B)-C(9)-H(9C)	109.5
C(11)-C(10)-H(10A)	109.5
C(11)-C(10)-H(10B)	109.5
H(10A)-C(10)-H(10B)	109.5
C(11)-C(10)-H(10C)	109.5
H(10A)-C(10)-H(10C)	109.5
H(10B)-C(10)-H(10C)	109.5
O(3)-C(11)-C(10)	105.2(2)
O(3)-C(11)-C(12)	109.0(2)
C(10)-C(11)-C(12)	113.8(2)
O(3)-C(11)-H(11)	109.5
C(10)-C(11)-H(11)	109.5
C(12)-C(11)-H(11)	109.5
C(11)-C(12)-H(12A)	109.5
C(11)-C(12)-H(12B)	109.5
H(12A)-C(12)-H(12B)	109.5
C(11)-C(12)-H(12C)	109.5
H(12A)-C(12)-H(12C)	109.5
H(12B)-C(12)-H(12C)	109.5

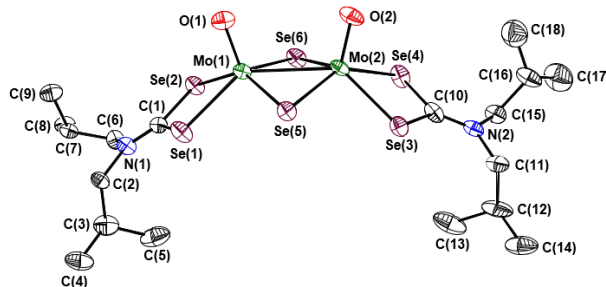
Table A.58. Anisotropic displacement parameters ($\text{\AA}^2 \times 10^3$) for $[(i\text{PrO})_2\text{PS}_2]\text{Mo}(\text{S})(\mu_2\text{-S})_2\text{Mo}(\text{S})(\text{S}_2\text{P}(\text{O}^i\text{Pr})_2)]$. The anisotropic displacement factor exponent takes the form: $-2\pi^2[h^2a^{*2}U^{11} + \dots + 2hka^*b^*U^{12}]$.

Atom	U^{11}	U^{22}	U^{33}	U^{23}	U^{13}	U^{12}
Mo(1)	19(1)	21(1)	16(1)	-1(1)	1(1)	-1(1)
Mo(2)	19(1)	19(1)	16(1)	0(1)	1(1)	-2(1)
S(1)	22(1)	48(1)	25(1)	-12(1)	7(1)	-7(1)
S(2)	21(1)	37(1)	23(1)	-10(1)	4(1)	-4(1)
S(3)	21(1)	25(1)	17(1)	-2(1)	2(1)	1(1)
S(4)	21(1)	31(1)	18(1)	-3(1)	3(1)	-1(1)
S(5)	20(1)	38(1)	18(1)	4(1)	2(1)	1(1)
S(6)	24(1)	25(1)	21(1)	-2(1)	3(1)	1(1)
S(7)	40(1)	27(1)	27(1)	5(1)	1(1)	1(1)
S(8)	32(1)	22(1)	31(1)	0(1)	2(1)	-6(1)
P(1)	19(1)	27(1)	20(1)	-3(1)	1(1)	-3(1)
P(2)	20(1)	19(1)	19(1)	1(1)	0(1)	-1(1)
O(1)	24(1)	24(1)	27(1)	1(1)	-2(1)	-4(1)
O(2)	23(1)	25(1)	28(1)	2(1)	-2(1)	-4(1)
O(3)	24(1)	20(1)	24(1)	-4(1)	6(1)	-3(1)
O(4)	27(1)	21(1)	25(1)	3(1)	-4(1)	-4(1)
C(1)	97(3)	40(2)	33(2)	8(1)	6(2)	9(2)
C(2)	30(2)	24(1)	31(1)	4(1)	4(1)	-6(1)
C(3)	133(4)	42(2)	110(3)	27(2)	85(3)	38(2)
C(4)	70(2)	51(2)	71(2)	28(2)	39(2)	19(2)
C(5)	34(2)	30(1)	32(1)	4(1)	-2(1)	4(1)
C(6)	37(2)	37(2)	51(2)	-4(1)	10(1)	6(1)
C(7)	68(2)	26(2)	51(2)	-2(1)	23(2)	-5(2)
C(8)	36(2)	22(1)	30(1)	5(1)	-4(1)	-10(1)
C(9)	44(2)	34(2)	50(2)	10(1)	14(2)	-5(1)
C(10)	72(2)	25(2)	40(2)	-9(1)	8(2)	-2(2)
C(11)	27(1)	30(1)	23(1)	-10(1)	5(1)	-1(1)
C(12)	68(2)	43(2)	28(2)	-3(1)	-6(2)	6(2)

Table A.59. Hydrogen coordinates ($\times 10^4$) and isotropic displacement parameters ($\text{\AA}^2 \times 10^3$) for $[(i\text{PrO})_2\text{PS}_2]\text{Mo}(\text{S})(\mu_2\text{-S})_2\text{Mo}(\text{S})(\text{S}_2\text{P}(\text{O}^i\text{Pr})_2)$.

H atom	x	y	z	U(eq)
H(1A)	9758	1135	11000	87
H(1B)	9234	2183	11031	87
H(1C)	10497	2080	11052	87
H(2)	8844	1600	9654	34
H(3A)	10379	640	9665	130
H(3B)	11113	1589	9748	130
H(3C)	10234	1400	8905	130
H(4A)	9350	6066	7572	91
H(4B)	9959	5048	7682	91
H(4C)	10228	5847	8409	91
H(5)	8216	4864	7950	40
H(6A)	7961	6397	8506	62
H(6B)	8852	6154	9329	62
H(6C)	7747	5562	9137	62
H(7A)	3102	5931	4499	70
H(7B)	2496	5102	4913	70
H(7C)	2212	5277	3915	70
H(8)	4227	4569	4823	37
H(9A)	4479	5383	3591	64
H(9B)	3565	4729	3034	64
H(9C)	4667	4247	3510	64
H(10A)	2539	-102	3496	69
H(10B)	1783	333	4088	69
H(10C)	3026	123	4468	69
H(11)	3542	1346	3636	32
H(12A)	2059	1330	2488	73
H(12B)	2263	2395	2871	73
H(12C)	1306	1752	3088	73

Structure Determination Summary



Thermal ellipsoid plot is drawn at the 50% probability level. Hydrogen atoms are omitted for clarity.

Table A.60. Crystal Data and Structure Refinement for $[(t\text{-Bu}_2\text{NCSe}_2)\text{MoO}(\mu\text{-Se})_2\text{MoO}(\text{Se}_2\text{CN}^i\text{Bu}_2)]$.

Identification code	JPD1293_0m	
Empirical formula	$\text{C}_{18}\text{H}_{36}\text{Mo}_2\text{N}_2\text{O}_2\text{Se}_6$	
Formula weight	978.13	
Temperature	273(2) K	
Wavelength	0.71073 Å	
Crystal system	Monoclinic	
Space group	Cc	
Unit cell dimensions	$a = 11.3342(6)$ Å	$\alpha = 90^\circ$
	$b = 17.9266(10)$ Å	$\beta = 95.7698(19)^\circ$
	$c = 14.5595(8)$ Å	$\gamma = 90^\circ$
Volume	$2943.3(3)$ Å ³	
Z	4	
Density (calculated)	2.207 g/cm ³	
Absorption coefficient	8.289 mm ⁻¹	
F(000)	1848	
Crystal size	$0.286 \times 0.221 \times 0.090$ mm ³	
θ range for data collection	2.272 to 30.553°	
Index ranges	$-16 \leq h \leq 16, -25 \leq k \leq 25, -20 \leq l \leq 20$	
Reflections collected	29564	
Independent reflections	8643 [R(int) = 0.0370]	
Completeness to $\theta = 25.242^\circ$	99.7 %	
Absorption correction	Semi-empirical from equivalents	
Max. and min. transmission	0.52 and 0.33	
Refinement method	Full-matrix least-squares on F^2	
Data / restraints / parameters	8643 / 2 / 280	
Goodness-of-fit on F^2	1.054	
Final R indices [$I > 2\sigma(I)$]	R1 = 0.0356, wR2 = 0.0818	
R indices (all data)	R1 = 0.0435, wR2 = 0.0876	
Absolute structure parameter	0.049(10)	
Extinction coefficient	n/a	
Largest diff. peak and hole	1.568 and -1.037 e·Å ⁻³	

Table A.61. Atomic coordinates ($\times 10^4$) and equivalent isotropic displacement parameters ($\text{\AA}^2 \times 10^3$) for $[(i\text{Bu}_2\text{NCSe}_2)\text{MoO}(\mu\text{-Se})_2\text{MoO}(\text{Se}_2\text{CN}^i\text{Bu}_2)]$. $U(\text{eq})$ is defined as one third of the trace of the orthogonalized U^{ij} tensor.

Atom	x	y	z	$U(\text{eq})$
Mo(1)	-7584(1)	-1864(1)	-368(1)	23(1)
Mo(2)	-7545(1)	-3317(1)	-1243(1)	25(1)
Se(1)	-6786(1)	-1420(1)	1261(1)	33(1)
Se(2)	-9240(1)	-1096(1)	263(1)	29(1)
Se(3)	-6770(1)	-4587(1)	-620(1)	28(1)
Se(4)	-9170(1)	-4283(1)	-1722(1)	36(1)
Se(5)	-6155(1)	-2862(1)	38(1)	26(1)
Se(6)	-9289(1)	-2513(1)	-1182(1)	32(1)
O(1)	-7016(5)	-1283(3)	-1110(4)	36(1)
O(2)	-6931(6)	-3164(4)	-2225(4)	42(1)
N(1)	-8472(5)	-502(4)	2033(4)	27(1)
N(2)	-8351(5)	-5752(4)	-1297(4)	27(1)
C(1)	-8209(6)	-891(4)	1340(5)	23(1)
C(2)	-7660(7)	-419(4)	2887(5)	28(2)
C(3)	-8114(8)	-764(6)	3726(6)	41(2)
C(4)	-7172(9)	-688(6)	4550(6)	48(2)
C(5)	-8467(10)	-1585(7)	3546(8)	58(3)
C(6)	-9659(6)	-147(4)	2048(6)	30(2)
C(7)	-9600(6)	671(4)	2301(5)	26(1)
C(8)	-10885(7)	964(5)	2267(6)	35(2)
C(9)	-8885(7)	1124(5)	1683(6)	36(2)
C(10)	-8137(6)	-5041(5)	-1240(5)	30(2)
C(11)	-7578(7)	-6310(5)	-793(5)	32(2)
C(12)	-8129(9)	-6657(6)	20(6)	49(3)
C(13)	-8496(12)	-6063(9)	691(7)	71(4)
C(14)	-7229(11)	-7191(7)	502(7)	60(3)
C(15)	-9431(7)	-6053(5)	-1840(6)	33(2)
C(16)	-9201(7)	-6289(6)	-2805(6)	40(2)
C(17)	-10262(13)	-6828(9)	-3178(10)	76(4)
C(18)	-8963(12)	-5745(8)	-3482(9)	70(3)

Table A.62. Bond lengths (Å) for [*i*Bu₂NCSe₂)MoO(μ-Se)₂MoO(Se₂CN^{*i*}Bu₂)]. Symmetry transformations used to generate equivalent atoms:

Mo(1)-O(1)	1.674(6)	C(9)-H(9B)	0.9600
Mo(1)-Se(5)	2.4461(9)	C(9)-H(9C)	0.9600
Mo(1)-Se(6)	2.4570(10)	C(11)-C(12)	1.526(11)
Mo(1)-Se(2)	2.5708(9)	C(11)-H(11A)	0.9700
Mo(1)-Se(1)	2.5770(10)	C(11)-H(11B)	0.9700
Mo(1)-Mo(2)	2.9017(9)	C(12)-C(14)	1.518(16)
Mo(2)-O(2)	1.675(6)	C(12)-C(13)	1.530(17)
Mo(2)-Se(6)	2.4545(10)	C(12)-H(12)	0.9800
Mo(2)-Se(5)	2.4565(9)	C(13)-H(13A)	0.9600
Mo(2)-Se(3)	2.5724(10)	C(13)-H(13B)	0.9600
Mo(2)-Se(4)	2.5734(10)	C(13)-H(13C)	0.9600
Se(1)-C(1)	1.885(7)	C(14)-H(14A)	0.9600
Se(2)-C(1)	1.895(7)	C(14)-H(14B)	0.9600
Se(3)-C(10)	1.897(7)	C(14)-H(14C)	0.9600
Se(4)-C(10)	1.883(8)	C(15)-C(16)	1.516(12)
N(1)-C(1)	1.285(9)	C(15)-H(15A)	0.9700
N(1)-C(2)	1.478(9)	C(15)-H(15B)	0.9700
N(1)-C(6)	1.491(9)	C(16)-C(18)	1.431(17)
N(2)-C(10)	1.297(11)	C(16)-C(17)	1.594(15)
N(2)-C(11)	1.477(11)	C(16)-H(16)	0.9800
N(2)-C(15)	1.490(9)	C(17)-H(17A)	0.9600
C(2)-C(3)	1.506(11)	C(17)-H(17B)	0.9600
C(2)-H(2A)	0.9700	C(17)-H(17C)	0.9600
C(2)-H(2B)	0.9700	C(18)-H(18A)	0.9600
C(3)-C(4)	1.530(13)	C(18)-H(18B)	0.9600
C(3)-C(5)	1.540(16)	C(18)-H(18C)	0.9600
C(3)-H(3)	0.9800		
C(4)-H(4A)	0.9600		
C(4)-H(4B)	0.9600		
C(4)-H(4C)	0.9600		
C(5)-H(5A)	0.9600		
C(5)-H(5B)	0.9600		
C(5)-H(5C)	0.9600		
C(6)-C(7)	1.512(11)		
C(6)-H(6A)	0.9700		
C(6)-H(6B)	0.9700		
C(7)-C(9)	1.508(11)		
C(7)-C(8)	1.543(10)		
C(7)-H(7)	0.9800		
C(8)-H(8A)	0.9600		
C(8)-H(8B)	0.9600		
C(8)-H(8C)	0.9600		
C(9)-H(9A)	0.9600		

Table A.63. Bond angles (deg.) for $[(i\text{Bu}_2\text{NCSe}_2)\text{MoO}(\mu\text{-Se})_2\text{MoO}(\text{Se}_2\text{CN}^i\text{Bu}_2)]$. Symmetry transformations used to generate equivalent atoms:

O(1)-Mo(1)-Se(5)	108.8(2)	N(1)-C(1)-Se(2)	125.6(5)
O(1)-Mo(1)-Se(6)	108.6(2)	Se(1)-C(1)-Se(2)	108.2(3)
Se(5)-Mo(1)-Se(6)	103.85(3)	N(1)-C(2)-C(3)	114.0(7)
O(1)-Mo(1)-Se(2)	103.9(2)	N(1)-C(2)-H(2A)	108.7
Se(5)-Mo(1)-Se(2)	142.64(4)	C(3)-C(2)-H(2A)	108.7
Se(6)-Mo(1)-Se(2)	81.89(3)	N(1)-C(2)-H(2B)	108.7
O(1)-Mo(1)-Se(1)	106.3(2)	C(3)-C(2)-H(2B)	108.7
Se(5)-Mo(1)-Se(1)	80.81(3)	H(2A)-C(2)-H(2B)	107.6
Se(6)-Mo(1)-Se(1)	140.89(4)	C(2)-C(3)-C(4)	109.3(7)
Se(2)-Mo(1)-Se(1)	72.98(3)	C(2)-C(3)-C(5)	111.0(8)
O(1)-Mo(1)-Mo(2)	104.5(2)	C(4)-C(3)-C(5)	111.6(8)
Se(5)-Mo(1)-Mo(2)	53.87(2)	C(2)-C(3)-H(3)	108.3
Se(6)-Mo(1)-Mo(2)	53.75(3)	C(4)-C(3)-H(3)	108.3
Se(2)-Mo(1)-Mo(2)	132.95(3)	C(5)-C(3)-H(3)	108.3
Se(1)-Mo(1)-Mo(2)	131.38(3)	C(3)-C(4)-H(4A)	109.5
O(2)-Mo(2)-Se(6)	109.9(2)	C(3)-C(4)-H(4B)	109.5
O(2)-Mo(2)-Se(5)	107.7(2)	H(4A)-C(4)-H(4B)	109.5
Se(6)-Mo(2)-Se(5)	103.61(3)	C(3)-C(4)-H(4C)	109.5
O(2)-Mo(2)-Se(3)	106.8(2)	H(4A)-C(4)-H(4C)	109.5
Se(6)-Mo(2)-Se(3)	138.94(4)	H(4B)-C(4)-H(4C)	109.5
Se(5)-Mo(2)-Se(3)	81.71(3)	C(3)-C(5)-H(5A)	109.5
O(2)-Mo(2)-Se(4)	103.1(2)	C(3)-C(5)-H(5B)	109.5
Se(6)-Mo(2)-Se(4)	81.23(3)	H(5A)-C(5)-H(5B)	109.5
Se(5)-Mo(2)-Se(4)	144.72(4)	C(3)-C(5)-H(5C)	109.5
Se(3)-Mo(2)-Se(4)	73.11(3)	H(5A)-C(5)-H(5C)	109.5
O(2)-Mo(2)-Mo(1)	104.7(2)	H(5B)-C(5)-H(5C)	109.5
Se(6)-Mo(2)-Mo(1)	53.83(3)	N(1)-C(6)-C(7)	113.6(6)
Se(5)-Mo(2)-Mo(1)	53.55(2)	N(1)-C(6)-H(6A)	108.8
Se(3)-Mo(2)-Mo(1)	131.26(3)	C(7)-C(6)-H(6A)	108.8
Se(4)-Mo(2)-Mo(1)	132.95(3)	N(1)-C(6)-H(6B)	108.8
C(1)-Se(1)-Mo(1)	89.3(2)	C(7)-C(6)-H(6B)	108.8
C(1)-Se(2)-Mo(1)	89.3(2)	H(6A)-C(6)-H(6B)	107.7
C(10)-Se(3)-Mo(2)	88.8(3)	C(9)-C(7)-C(6)	113.0(6)
C(10)-Se(4)-Mo(2)	89.1(2)	C(9)-C(7)-C(8)	111.1(6)
Mo(1)-Se(5)-Mo(2)	72.58(3)	C(6)-C(7)-C(8)	107.7(6)
Mo(2)-Se(6)-Mo(1)	72.43(3)	C(9)-C(7)-H(7)	108.3
C(1)-N(1)-C(2)	122.8(6)	C(6)-C(7)-H(7)	108.3
C(1)-N(1)-C(6)	121.6(6)	C(8)-C(7)-H(7)	108.3
C(2)-N(1)-C(6)	115.5(6)	C(7)-C(8)-H(8A)	109.5
C(10)-N(2)-C(11)	122.4(6)	C(7)-C(8)-H(8B)	109.5
C(10)-N(2)-C(15)	121.8(7)	H(8A)-C(8)-H(8B)	109.5
C(11)-N(2)-C(15)	115.7(6)	C(7)-C(8)-H(8C)	109.5
N(1)-C(1)-Se(1)	126.1(5)	H(8A)-C(8)-H(8C)	109.5

Table A.63, Cont'd. Bond angles (deg.) for [*i*Bu₂NCSe₂)MoO(μ-Se)₂MoO(Se₂CN^{*i*}Bu₂)]. Symmetry transformations used to generate equivalent atoms:

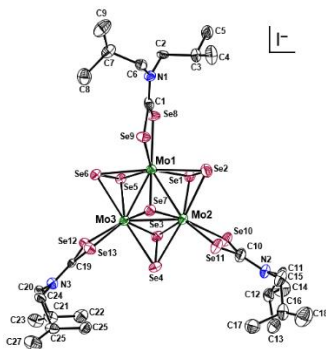
H(8B)-C(8)-H(8C)	109.5	C(18)-C(16)-H(16)	105.6
C(7)-C(9)-H(9A)	109.5	C(15)-C(16)-H(16)	105.6
C(7)-C(9)-H(9B)	109.5	C(17)-C(16)-H(16)	105.6
H(9A)-C(9)-H(9B)	109.5	C(16)-C(17)-H(17A)	109.5
C(7)-C(9)-H(9C)	109.5	C(16)-C(17)-H(17B)	109.5
H(9A)-C(9)-H(9C)	109.5	H(17A)-C(17)-H(17B)	109.5
H(9B)-C(9)-H(9C)	109.5	C(16)-C(17)-H(17C)	109.5
N(2)-C(10)-Se(4)	125.4(5)	H(17A)-C(17)-H(17C)	109.5
N(2)-C(10)-Se(3)	126.2(6)	H(17B)-C(17)-H(17C)	109.5
Se(4)-C(10)-Se(3)	108.3(4)	C(16)-C(18)-H(18A)	109.5
N(2)-C(11)-C(12)	113.1(7)	C(16)-C(18)-H(18B)	109.5
N(2)-C(11)-H(11A)	109.0	H(18A)-C(18)-H(18B)	109.5
C(12)-C(11)-H(11A)	109.0	C(16)-C(18)-H(18C)	109.5
N(2)-C(11)-H(11B)	109.0	H(18A)-C(18)-H(18C)	109.5
C(12)-C(11)-H(11B)	109.0	H(18B)-C(18)-H(18C)	109.5
H(11A)-C(11)-H(11B)	107.8		
C(14)-C(12)-C(11)	107.9(8)		
C(14)-C(12)-C(13)	111.0(9)		
C(11)-C(12)-C(13)	111.8(9)		
C(14)-C(12)-H(12)	108.7		
C(11)-C(12)-H(12)	108.7		
C(13)-C(12)-H(12)	108.7		
C(12)-C(13)-H(13A)	109.5		
C(12)-C(13)-H(13B)	109.5		
H(13A)-C(13)-H(13B)	109.5		
C(12)-C(13)-H(13C)	109.5		
H(13A)-C(13)-H(13C)	109.5		
H(13B)-C(13)-H(13C)	109.5		
C(12)-C(14)-H(14A)	109.5		
C(12)-C(14)-H(14B)	109.5		
H(14A)-C(14)-H(14B)	109.5		
C(12)-C(14)-H(14C)	109.5		
H(14A)-C(14)-H(14C)	109.5		
H(14B)-C(14)-H(14C)	109.5		
N(2)-C(15)-C(16)	112.6(6)		
N(2)-C(15)-H(15A)	109.1		
C(16)-C(15)-H(15A)	109.1		
N(2)-C(15)-H(15B)	109.1		
C(16)-C(15)-H(15B)	109.1		
H(15A)-C(15)-H(15B)	107.8		
C(18)-C(16)-C(15)	120.6(10)		
C(18)-C(16)-C(17)	111.5(9)		
C(15)-C(16)-C(17)	106.9(8)		

Table A.64. Anisotropic displacement parameters ($\text{\AA}^2 \times 10^3$) for $[(i\text{Bu}_2\text{NCSe}_2)\text{MoO}(\mu\text{-Se})_2\text{MoO}(\text{Se}_2\text{CN}^i\text{Bu}_2)]$. The anisotropic displacement factor exponent takes the form: $-2\pi^2[h^2 a^{*2}U^{11} + \dots + 2hka^*b^*U^{12}]$.

Atom	U^{11}	U^{22}	U^{33}	U^{23}	U^{13}	U^{12}
Mo(1)	19(1)	31(1)	21(1)	2(1)	2(1)	3(1)
Mo(2)	20(1)	38(1)	18(1)	-3(1)	4(1)	2(1)
Se(1)	20(1)	49(1)	28(1)	-8(1)	-3(1)	12(1)
Se(2)	18(1)	41(1)	29(1)	-5(1)	-2(1)	7(1)
Se(3)	21(1)	33(1)	29(1)	-6(1)	-3(1)	-3(1)
Se(4)	20(1)	46(1)	40(1)	-11(1)	-4(1)	2(1)
Se(5)	18(1)	32(1)	29(1)	-1(1)	-1(1)	2(1)
Se(6)	22(1)	43(1)	29(1)	-3(1)	-5(1)	6(1)
O(1)	32(3)	42(3)	35(3)	10(2)	7(2)	4(2)
O(2)	44(4)	60(4)	24(3)	-1(3)	14(3)	-3(3)
N(1)	18(3)	36(3)	28(3)	-2(2)	3(2)	3(2)
N(2)	20(3)	42(3)	20(3)	-2(2)	1(2)	-10(3)
C(1)	15(3)	30(3)	24(3)	2(3)	3(2)	0(2)
C(2)	25(4)	37(4)	24(3)	-3(3)	4(3)	4(3)
C(3)	28(4)	57(6)	40(5)	8(4)	13(3)	7(4)
C(4)	46(5)	73(7)	29(4)	9(4)	15(4)	10(5)
C(5)	44(6)	68(7)	61(7)	31(6)	1(5)	-9(5)
C(6)	18(3)	36(4)	35(4)	-4(3)	7(3)	2(3)
C(7)	19(3)	38(4)	23(3)	2(3)	4(3)	3(3)
C(8)	27(4)	44(4)	35(4)	5(3)	11(3)	9(3)
C(9)	28(4)	44(5)	38(4)	10(4)	10(3)	4(3)
C(10)	19(3)	43(4)	28(4)	-12(3)	5(3)	-4(3)
C(11)	29(4)	42(4)	24(4)	5(3)	-1(3)	-18(3)
C(12)	43(5)	80(7)	25(4)	12(4)	2(4)	-36(5)
C(13)	67(8)	118(11)	32(5)	2(6)	22(5)	-5(7)
C(14)	65(7)	73(7)	38(5)	22(5)	-9(5)	-37(6)
C(15)	22(3)	45(4)	31(4)	-3(3)	1(3)	-14(3)
C(16)	23(4)	71(6)	26(4)	-6(4)	-3(3)	-12(4)
C(17)	67(8)	89(10)	68(9)	-12(7)	-11(7)	-23(7)
C(18)	70(8)	72(8)	64(8)	-5(6)	-3(6)	3(6)

Table A.65. Hydrogen coordinates ($\times 10^4$) and isotropic displacement parameters ($\text{\AA}^2 \times 10^3$) for $[(i\text{Bu}_2\text{NCSe}_2)\text{MoO}(\mu\text{-Se})_2\text{MoO}(\text{Se}_2\text{CN}^i\text{Bu}_2)]$.

H atom	x	y	z	U(eq)
H(2A)	-7522	108	3003	34
H(2B)	-6905	-646	2792	34
H(3)	-8821	-488	3866	49
H(4A)	-6451	-923	4407	72
H(4B)	-7447	-925	5080	72
H(4C)	-7026	-169	4679	72
H(5A)	-9093	-1610	3051	87
H(5B)	-8736	-1796	4094	87
H(5C)	-7793	-1860	3380	87
H(6A)	-10096	-410	2488	36
H(6B)	-10096	-200	1443	36
H(7)	-9231	716	2937	32
H(8A)	-11293	864	1670	52
H(8B)	-10873	1492	2379	52
H(8C)	-11286	717	2732	52
H(9A)	-8076	957	1754	54
H(9B)	-8917	1641	1850	54
H(9C)	-9206	1062	1052	54
H(11A)	-6834	-6074	-568	39
H(11B)	-7403	-6703	-1217	39
H(12)	-8834	-6940	-217	59
H(13A)	-8782	-6301	1216	107
H(13B)	-9113	-5758	386	107
H(13C)	-7824	-5757	891	107
H(14A)	-6991	-7547	63	90
H(14B)	-7579	-7448	985	90
H(14C)	-6548	-6916	760	90
H(15A)	-10046	-5674	-1881	39
H(15B)	-9720	-6478	-1517	39
H(16)	-8494	-6606	-2726	48
H(17A)	-10947	-6535	-3382	114
H(17B)	-10447	-7156	-2692	114
H(17C)	-10030	-7117	-3685	114
H(18A)	-9670	-5463	-3659	104
H(18B)	-8711	-5991	-4014	104
H(18C)	-8349	-5415	-3226	104



Thermal ellipsoid plot is drawn at the 50% probability level. Hydrogen atoms are omitted for clarity.

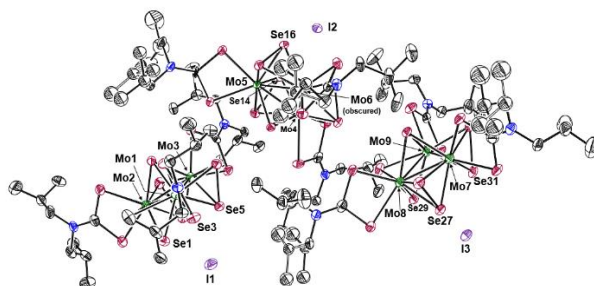


Table A.66. Crystal Data and Structure Refinement for $[\text{Mo}_3\text{Se}_7(\text{Se}_2\text{CN}^i\text{Bu}_2)_3]\text{I}$.

Identification code	jpd1375_0m_a_sq	
Empirical formula	$\text{C}_{27}\text{H}_{54}\text{IMo}_3\text{N}_3\text{Se}_{13}$	
Formula weight	1861.93	
Temperature	150(2) K	
Wavelength	0.71073 Å	
Crystal system	monoclinic	
Space group	$P2_1/c$	
Unit cell dimensions	$a = 28.1698(14)$ Å	$\alpha = 90^\circ$
	$b = 13.6823(7)$ Å	$\beta = 90.8760(10)^\circ$
	$c = 41.079(2)$ Å	$\gamma = 90^\circ$
Volume	$15831.3(14)$ Å ³	
Z	12	
Density (calculated)	2.344 g/cm ³	
Absorption coefficient	10.276 mm ⁻¹	
F(000)	10296	
Crystal size	0.364 x 0.145 x 0.022 mm ³	
θ range for data collection	1.788 to 26.444°	
Index ranges	$-35 \leq h \leq 35, -17 \leq k \leq 17, -51 \leq l \leq 51$	
Reflections collected	285209	
Independent reflections	32504 [R(int) = 0.1040]	
Completeness to $\theta = 25.242^\circ$	99.9 %	
Absorption correction	Semi-empirical from equivalents	
Max. and min. transmission	0.78 and 0.63	

Table A.66, Cont'd. Crystal Data and Structure Refinement for $[\text{Mo}_3\text{Se}_7(\text{Se}_2\text{CN}^i\text{Bu}_2)_3]\text{I}$.

Refinement method	Full-matrix least-squares on F^2
Data / restraints / parameters	32504 / 0 / 1290
Goodness-of-fit on F^2	1.019
Final R indices [$I > 2\sigma(I)$]	R1 = 0.0519, wR2 = 0.0935
R indices (all data)	R1 = 0.1003, wR2 = 0.1116
Extinction coefficient	n/a
Largest diff. peak and hole	1.344 and -1.641 $\text{e} \cdot \text{\AA}^{-3}$

Table A.67. Atomic coordinates ($\times 10^4$) and equivalent isotropic displacement parameters ($\text{\AA}^2 \times 10^3$) for $[\text{Mo}_3\text{Se}_7(\text{Se}_2\text{CN}^i\text{Bu}_2)_3]\text{I}$. $U(\text{eq})$ is defined as one third of the trace of the orthogonalized U^{ij} tensor.

Atom	x	y	z	U(eq)
I(1)	7344(1)	3757(1)	5887(1)	45(1)
I(2)	8868(1)	8955(1)	8519(1)	37(1)
I(3)	5114(1)	3217(1)	8775(1)	33(1)
Mo(1)	7715(1)	7100(1)	5921(1)	23(1)
Mo(2)	8373(1)	6140(1)	5538(1)	26(1)
Mo(3)	8470(1)	6134(1)	6210(1)	21(1)
Mo(4)	7937(1)	7274(1)	7761(1)	17(1)
Mo(5)	8286(1)	8941(1)	7459(1)	17(1)
Mo(6)	7506(1)	9058(1)	7862(1)	18(1)
Mo(7)	5458(1)	6497(1)	8939(1)	23(1)
Mo(8)	5781(1)	5998(1)	8325(1)	23(1)
Mo(9)	6321(1)	5542(1)	8874(1)	23(1)
Se(1)	7490(1)	5775(1)	5509(1)	31(1)
Se(2)	7716(1)	7272(1)	5288(1)	35(1)
Se(3)	8406(1)	4573(1)	5872(1)	29(1)
Se(4)	9120(1)	5422(1)	5835(1)	31(1)
Se(5)	7608(1)	5713(1)	6329(1)	26(1)
Se(6)	7881(1)	7174(1)	6549(1)	26(1)
Se(7)	8560(1)	7637(1)	5869(1)	24(1)
Se(8)	6795(1)	7434(1)	5950(1)	32(1)
Se(9)	7590(1)	8979(1)	5966(1)	30(1)
Se(10)	8450(1)	4929(1)	5043(1)	38(1)
Se(11)	8959(1)	6906(1)	5122(1)	35(1)
Se(12)	8721(1)	5005(1)	6700(1)	29(1)
Se(13)	9166(1)	6977(1)	6521(1)	26(1)
Se(14)	8789(1)	7854(1)	7829(1)	22(1)
Se(15)	8600(1)	7191(1)	7322(1)	24(1)
Se(16)	8265(1)	10033(1)	7963(1)	24(1)
Se(17)	7794(1)	10545(1)	7523(1)	25(1)
Se(18)	7842(1)	8011(1)	8325(1)	22(1)
Se(19)	7146(1)	7435(1)	8083(1)	23(1)
Se(20)	7495(1)	8193(1)	7326(1)	18(1)
Se(21)	8201(1)	5677(1)	8076(1)	26(1)
Se(22)	7551(1)	5779(1)	7467(1)	27(1)
Se(23)	9084(1)	9861(1)	7311(1)	29(1)
Se(24)	8273(1)	9316(1)	6835(1)	23(1)
Se(25)	7091(1)	10076(1)	8323(1)	28(1)
Se(26)	6670(1)	9566(1)	7648(1)	26(1)
Se(27)	4984(1)	5441(1)	8540(1)	26(1)

Table A.67, Cont'd. Atomic coordinates ($\times 10^4$) and equivalent isotropic displacement parameters ($\text{\AA}^2 \times 10^3$) for $[\text{Mo}_3\text{Se}_7(\text{Se}_2\text{CN}^i\text{Bu}_2)_3]\text{I}$. $U(\text{eq})$ is defined as one third of the trace of the orthogonalized U^{ij} tensor.

Atom	x	y	z	U(eq)
Se(28)	5032(1)	7093(1)	8409(1)	29(1)
Se(29)	6038(1)	4261(1)	8467(1)	26(1)
Se(30)	6637(1)	5283(1)	8284(1)	29(1)
Se(31)	5642(1)	4868(1)	9211(1)	27(1)
Se(32)	6036(1)	6214(1)	9430(1)	30(1)
Se(33)	6170(1)	7258(1)	8683(1)	24(1)
Se(34)	4671(1)	6524(1)	9281(1)	31(1)
Se(35)	5342(1)	8249(1)	9179(1)	31(1)
Se(36)	5522(1)	5240(1)	7755(1)	32(1)
Se(37)	6021(1)	7212(1)	7868(1)	29(1)
Se(38)	6837(1)	4136(1)	9148(1)	30(1)
Se(39)	7157(1)	6251(1)	9018(1)	32(1)
N(1)	6609(3)	9465(5)	5942(2)	24(2)
N(2)	9099(3)	5639(6)	4580(2)	31(2)
N(3)	9587(3)	5676(6)	6980(2)	25(2)
N(4)	7832(3)	3999(6)	7765(2)	26(2)
N(5)	9111(3)	10283(6)	6637(2)	27(2)
N(6)	6211(3)	10823(6)	8090(2)	26(2)
N(7)	4481(3)	8417(6)	9529(2)	28(2)
N(8)	5898(3)	6373(6)	7243(2)	28(2)
N(9)	7727(3)	4876(6)	9360(2)	26(2)
C(1)	6932(3)	8767(7)	5955(2)	26(2)
C(2)	6123(3)	9232(7)	5835(2)	26(2)
C(3)	6072(4)	9122(8)	5465(2)	37(3)
C(4)	6299(5)	9920(10)	5278(3)	58(4)
C(5)	5566(4)	8940(9)	5365(3)	41(3)
C(6)	6721(4)	10500(7)	6007(2)	28(2)
C(7)	6599(4)	10804(7)	6354(3)	34(3)
C(8)	6964(4)	10426(8)	6601(3)	42(3)
C(9)	6542(4)	11904(8)	6378(3)	54(3)
C(10)	8877(4)	5795(8)	4863(3)	37(3)
C(11)	8980(4)	4745(8)	4384(3)	40(3)
C(12)	9202(4)	3783(8)	4514(3)	40(3)
C(13)	9731(4)	3698(8)	4438(3)	43(3)
C(14)	8927(5)	2946(9)	4356(3)	64(4)
C(15)	9346(4)	6442(8)	4412(3)	40(3)
C(16)	9870(4)	6296(8)	4371(3)	39(3)
C(17)	10135(4)	6247(9)	4694(3)	46(3)
C(18)	10055(5)	7148(10)	4166(3)	65(4)

Table A.67, Cont'd. Atomic coordinates ($\times 10^4$) and equivalent isotropic displacement parameters ($\text{\AA}^2 \times 10^3$) for $[\text{Mo}_3\text{Se}_7(\text{Se}_2\text{CN}^i\text{Bu}_2)_3]\text{I}$. $U(\text{eq})$ is defined as one third of the trace of the orthogonalized U^{ij} tensor.

Atom	x	y	z	U(eq)
C(19)	9229(3)	5843(7)	6774(2)	21(2)
C(20)	9595(3)	4786(7)	7186(2)	27(2)
C(21)	9918(4)	3971(7)	7069(3)	33(3)
C(22)	9805(4)	3618(8)	6730(3)	42(3)
C(23)	9886(4)	3127(8)	7309(3)	44(3)
C(24)	9959(3)	6408(7)	7041(2)	26(2)
C(25)	10427(3)	6262(8)	6871(3)	33(3)
C(26)	10382(4)	6301(8)	6503(2)	35(3)
C(27)	10789(4)	7032(8)	6998(3)	49(3)
C(28)	7852(3)	4970(6)	7770(2)	27(2)
C(29)	8066(4)	3395(7)	8014(2)	28(2)
C(30)	7783(4)	3290(7)	8329(3)	41(3)
C(31)	8070(5)	2619(9)	8563(3)	59(4)
C(32)	7289(4)	2899(8)	8273(3)	50(3)
C(33)	7583(3)	3484(7)	7493(2)	28(2)
C(34)	7876(4)	3433(7)	7184(3)	40(3)
C(35)	8372(4)	3005(7)	7243(3)	38(3)
C(36)	7602(5)	2885(9)	6924(3)	58(4)
C(37)	8872(3)	9884(6)	6881(2)	22(2)
C(38)	9581(3)	10724(8)	6695(3)	38(3)
C(39)	9983(4)	9966(13)	6691(4)	73(5)
C(40)	10438(4)	10545(15)	6794(4)	105(7)
C(41)	10036(5)	9396(12)	6404(5)	111(7)
C(42)	8908(4)	10315(8)	6301(2)	37(3)
C(43A)	8546(7)	11195(13)	6244(4)	35(4)
C(44A)	8721(6)	12142(13)	6356(4)	44(4)
C(45A)	8409(7)	11201(17)	5887(5)	52(5)
C(43B)	8818(12)	11290(20)	6172(7)	35(4)
C(44B)	8380(11)	11680(20)	6385(8)	44(4)
C(45B)	8673(13)	11200(30)	5819(9)	52(5)
C(46)	6585(3)	10268(6)	8035(2)	24(2)
C(47)	6147(4)	11244(7)	8417(2)	31(2)
C(48)	5934(4)	10513(8)	8653(3)	38(3)
C(49)	5955(4)	10924(9)	8998(3)	52(3)
C(50)	5438(4)	10225(9)	8552(3)	53(4)
C(51)	5859(3)	11044(7)	7837(3)	30(2)
C(52A)	5883(7)	12129(15)	7711(5)	33(4)
C(53A)	5557(8)	12222(17)	7407(5)	48(5)
C(54A)	6396(8)	12348(18)	7595(6)	57(5)

Table A.67, Cont'd. Atomic coordinates ($\times 10^4$) and equivalent isotropic displacement parameters ($\text{\AA}^2 \times 10^3$) for $[\text{Mo}_3\text{Se}_7(\text{Se}_2\text{CN}^i\text{Bu}_2)_3]\text{I}$. $U(\text{eq})$ is defined as one third of the trace of the orthogonalized U^{ij} tensor.

Atom	x	y	z	U(eq)
C(52B)	6033(9)	11731(18)	7596(6)	33(4)
C(53B)	5724(10)	11710(20)	7294(7)	48(5)
C(54B)	6127(11)	12720(20)	7729(7)	57(5)
C(55)	4771(4)	7838(7)	9362(2)	32(2)
C(56)	4041(3)	8047(8)	9672(3)	35(3)
C(57)	4069(4)	8000(9)	10047(3)	51(3)
C(58)	4449(5)	7340(11)	10166(3)	74(4)
C(59)	3578(5)	7671(12)	10161(4)	91(5)
C(60)	4595(4)	9470(7)	9580(3)	38(3)
C(61A)	4449(7)	10094(13)	9292(5)	44(4)
C(62A)	4580(9)	11150(18)	9372(6)	79(7)
C(63A)	3930(8)	10075(17)	9211(6)	63(6)
C(61B)	4206(13)	10220(20)	9469(9)	44(4)
C(62B)	4409(17)	11220(30)	9573(13)	79(7)
C(63B)	4133(16)	10050(30)	9106(11)	63(6)
C(64)	5827(3)	6281(7)	7560(3)	31(2)
C(65)	5715(3)	5640(8)	7009(2)	33(2)
C(66A)	6045(7)	4819(15)	6971(6)	32(4)
C(67A)	5792(8)	4057(18)	6776(6)	47(5)
C(68A)	6510(8)	4786(19)	6935(7)	53(5)
C(66B)	6094(7)	5098(17)	6781(6)	32(4)
C(67B)	5822(9)	4329(19)	6581(7)	47(5)
C(68B)	6522(9)	5120(20)	6773(8)	53(5)
C(69)	6149(3)	7209(7)	7099(3)	32(3)
C(70)	5817(4)	7907(8)	6922(3)	39(3)
C(71)	6109(4)	8699(9)	6761(3)	53(3)
C(72)	5439(4)	8332(10)	7139(3)	59(4)
C(73)	7317(3)	5051(7)	9206(2)	24(2)
C(74)	7817(3)	3942(7)	9522(2)	31(2)
C(75)	7609(4)	3881(10)	9864(3)	52(3)
C(76)	7746(5)	2876(11)	10004(3)	78(5)
C(77)	7745(5)	4709(12)	10083(3)	77(5)
C(78)	8101(3)	5631(8)	9369(3)	34(3)
C(79)	8392(4)	5667(9)	9059(3)	46(3)
C(80)	8727(5)	6530(10)	9084(4)	82(5)
C(81)	8660(4)	4728(10)	8994(3)	65(4)

Table A.68. Bond lengths (Å) for [Mo₃Se₇(Se₂CNⁱBu₂)₃]**I**. Symmetry transformations used to generate equivalent atoms:

Mo(1)-Se(7)	2.5041(12)	Mo(6)-Se(18)	2.5499(12)
Mo(1)-Se(5)	2.5533(13)	Mo(6)-Se(26)	2.5958(12)
Mo(1)-Se(1)	2.5541(13)	Mo(6)-Se(17)	2.6015(12)
Mo(1)-Se(9)	2.6020(13)	Mo(6)-Se(19)	2.6091(12)
Mo(1)-Se(2)	2.6108(14)	Mo(6)-Se(25)	2.6377(12)
Mo(1)-Se(6)	2.6185(13)	Mo(7)-Se(33)	2.5046(12)
Mo(1)-Se(8)	2.6367(12)	Mo(7)-Se(31)	2.5429(12)
Mo(1)-Mo(3)	2.7574(11)	Mo(7)-Se(27)	2.5482(13)
Mo(1)-Mo(2)	2.7786(11)	Mo(7)-Se(28)	2.5999(13)
Mo(2)-Se(7)	2.5091(13)	Mo(7)-Se(32)	2.6024(13)
Mo(2)-Se(1)	2.5391(13)	Mo(7)-Se(35)	2.6153(13)
Mo(2)-Se(3)	2.5465(13)	Mo(7)-Se(34)	2.6442(13)
Mo(2)-Se(4)	2.6088(13)	Mo(7)-Mo(9)	2.7757(11)
Mo(2)-Se(11)	2.6121(13)	Mo(7)-Mo(8)	2.7779(12)
Mo(2)-Se(2)	2.6126(14)	Mo(8)-Se(33)	2.5068(13)
Mo(2)-Se(10)	2.6353(13)	Mo(8)-Se(27)	2.5435(12)
Mo(2)-Mo(3)	2.7687(12)	Mo(8)-Se(29)	2.5490(12)
Mo(3)-Se(7)	2.5034(12)	Mo(8)-Se(37)	2.6030(12)
Mo(3)-Se(3)	2.5517(13)	Mo(8)-Se(30)	2.6100(12)
Mo(3)-Se(5)	2.5518(12)	Mo(8)-Se(28)	2.6148(13)
Mo(3)-Se(13)	2.5957(13)	Mo(8)-Se(36)	2.6546(14)
Mo(3)-Se(4)	2.6004(12)	Mo(8)-Mo(9)	2.7697(12)
Mo(3)-Se(6)	2.6072(12)	Mo(9)-Se(33)	2.5088(12)
Mo(3)-Se(12)	2.6258(13)	Mo(9)-Se(29)	2.5412(13)
Mo(4)-Se(20)	2.5028(12)	Mo(9)-Se(31)	2.5522(12)
Mo(4)-Se(14)	2.5385(11)	Mo(9)-Se(32)	2.6033(14)
Mo(4)-Se(18)	2.5441(12)	Mo(9)-Se(39)	2.6050(13)
Mo(4)-Se(22)	2.6048(12)	Mo(9)-Se(30)	2.6167(13)
Mo(4)-Se(15)	2.6174(12)	Mo(9)-Se(38)	2.6524(13)
Mo(4)-Se(19)	2.6180(12)	Se(1)-Se(2)	2.3327(15)
Mo(4)-Se(21)	2.6413(12)	Se(3)-Se(4)	2.3315(14)
Mo(4)-Mo(6)	2.7606(10)	Se(5)-Se(6)	2.3211(14)
Mo(4)-Mo(5)	2.7821(11)	Se(8)-C(1)	1.864(9)
Mo(5)-Se(20)	2.5058(11)	Se(9)-C(1)	1.875(10)
Mo(5)-Se(14)	2.5418(12)	Se(10)-C(10)	1.851(11)
Mo(5)-Se(16)	2.5549(12)	Se(11)-C(10)	1.868(11)
Mo(5)-Se(17)	2.6115(12)	Se(12)-C(19)	1.854(9)
Mo(5)-Se(24)	2.6139(12)	Se(13)-C(19)	1.875(9)
Mo(5)-Se(15)	2.6166(12)	Se(14)-Se(15)	2.3265(14)
Mo(5)-Se(23)	2.6544(12)	Se(16)-Se(17)	2.3320(14)
Mo(5)-Mo(6)	2.7756(11)	Se(18)-Se(19)	2.3225(13)
Mo(6)-Se(20)	2.5011(12)	Se(21)-C(28)	1.856(10)
Mo(6)-Se(16)	2.5476(12)	Se(22)-C(28)	1.859(9)

Table A.68, Cont'd. Bond lengths (Å) for [Mo₃Se₇(Se₂CN^{*i*}Bu₂)₃]. Symmetry transformations used to generate equivalent atoms:

Se(23)-C(37)	1.856(9)	C(6)-C(7)	1.530(13)
Se(24)-C(37)	1.864(9)	C(7)-C(9)	1.517(14)
Se(25)-C(46)	1.857(10)	C(7)-C(8)	1.524(14)
Se(26)-C(46)	1.875(9)	C(11)-C(12)	1.549(15)
Se(27)-Se(28)	2.3272(14)	C(12)-C(14)	1.522(15)
Se(29)-Se(30)	2.3265(13)	C(12)-C(13)	1.530(14)
Se(31)-Se(32)	2.3235(15)	C(15)-C(16)	1.502(15)
Se(34)-C(55)	1.848(10)	C(16)-C(17)	1.516(14)
Se(35)-C(55)	1.872(10)	C(16)-C(18)	1.534(15)
Se(36)-C(64)	1.850(10)	C(20)-C(21)	1.522(13)
Se(37)-C(64)	1.872(11)	C(21)-C(22)	1.503(14)
Se(38)-C(73)	1.855(9)	C(21)-C(23)	1.523(14)
Se(39)-C(73)	1.867(10)	C(24)-C(25)	1.512(13)
N(1)-C(1)	1.321(11)	C(25)-C(26)	1.517(14)
N(1)-C(2)	1.467(11)	C(25)-C(27)	1.550(14)
N(1)-C(6)	1.474(11)	C(29)-C(30)	1.534(14)
N(2)-C(10)	1.345(12)	C(30)-C(32)	1.507(15)
N(2)-C(15)	1.476(13)	C(30)-C(31)	1.548(15)
N(2)-C(11)	1.501(12)	C(33)-C(34)	1.528(14)
N(3)-C(19)	1.326(11)	C(34)-C(36)	1.508(15)
N(3)-C(24)	1.468(11)	C(34)-C(35)	1.530(14)
N(3)-C(20)	1.484(11)	C(38)-C(39)	1.536(17)
N(4)-C(28)	1.330(11)	C(39)-C(41)	1.43(2)
N(4)-C(29)	1.465(11)	C(39)-C(40)	1.559(18)
N(4)-C(33)	1.487(12)	C(42)-C(43B)	1.46(3)
N(5)-C(37)	1.333(11)	C(42)-C(43A)	1.59(2)
N(5)-C(38)	1.471(11)	C(43A)-C(44A)	1.46(2)
N(5)-C(42)	1.488(12)	C(43A)-C(45A)	1.51(3)
N(6)-C(46)	1.321(11)	C(43B)-C(45B)	1.51(4)
N(6)-C(51)	1.456(12)	C(43B)-C(44B)	1.61(4)
N(6)-C(47)	1.476(12)	C(47)-C(48)	1.524(13)
N(7)-C(55)	1.335(12)	C(48)-C(50)	1.504(15)
N(7)-C(56)	1.471(12)	C(48)-C(49)	1.524(15)
N(7)-C(60)	1.491(12)	C(51)-C(52B)	1.46(3)
N(8)-C(64)	1.328(12)	C(51)-C(52A)	1.57(2)
N(8)-C(69)	1.473(12)	C(52A)-C(53A)	1.54(3)
N(8)-C(65)	1.478(12)	C(52A)-C(54A)	1.56(3)
N(9)-C(73)	1.329(11)	C(52B)-C(54B)	1.49(4)
N(9)-C(74)	1.463(12)	C(52B)-C(53B)	1.51(3)
N(9)-C(78)	1.476(12)	C(56)-C(57)	1.545(15)
C(2)-C(3)	1.528(13)	C(57)-C(58)	1.478(17)
C(3)-C(4)	1.485(15)	C(57)-C(59)	1.536(17)
C(3)-C(5)	1.499(13)	C(60)-C(61A)	1.51(2)

Table A.68, Cont'd. Bond lengths (Å) for $[\text{Mo}_3\text{Se}_7(\text{Se}_2\text{CN}^i\text{Bu}_2)_3]\text{I}$. Symmetry transformations used to generate equivalent atoms:

C(60)-C(61B)	1.56(3)
C(61A)-C(63A)	1.50(3)
C(61A)-C(62A)	1.53(3)
C(61B)-C(63B)	1.52(6)
C(61B)-C(62B)	1.55(5)
C(65)-C(66A)	1.47(2)
C(65)-C(66B)	1.61(2)
C(66A)-C(68A)	1.32(3)
C(66A)-C(67A)	1.49(3)
C(66B)-C(68B)	1.21(3)
C(66B)-C(67B)	1.53(3)
C(69)-C(70)	1.514(13)
C(70)-C(72)	1.515(15)
C(70)-C(71)	1.519(14)
C(74)-C(75)	1.530(15)
C(75)-C(77)	1.494(18)
C(75)-C(76)	1.537(17)
C(78)-C(79)	1.525(15)
C(79)-C(80)	1.513(16)
C(79)-C(81)	1.516(16)

Table A.69. Bond angles (deg.) for $[\text{Mo}_3\text{Se}_7(\text{Se}_2\text{CN}^i\text{Bu}_2)_3]\text{I}$. Symmetry transformations used to generate equivalent atoms:

Se(7)-Mo(1)-Se(5)	113.36(4)	Se(1)-Mo(2)-Se(11)	132.55(5)
Se(7)-Mo(1)-Se(1)	112.25(4)	Se(3)-Mo(2)-Se(11)	132.21(5)
Se(5)-Mo(1)-Se(1)	82.93(4)	Se(4)-Mo(2)-Se(11)	86.75(4)
Se(7)-Mo(1)-Se(9)	81.16(4)	Se(7)-Mo(2)-Se(2)	82.60(4)
Se(5)-Mo(1)-Se(9)	132.09(5)	Se(1)-Mo(2)-Se(2)	53.82(4)
Se(1)-Mo(1)-Se(9)	135.71(5)	Se(3)-Mo(2)-Se(2)	136.93(5)
Se(7)-Mo(1)-Se(2)	82.73(4)	Se(4)-Mo(2)-Se(2)	165.75(5)
Se(5)-Mo(1)-Se(2)	136.29(5)	Se(11)-Mo(2)-Se(2)	87.49(4)
Se(1)-Mo(1)-Se(2)	53.69(4)	Se(7)-Mo(2)-Se(10)	155.80(5)
Se(9)-Mo(1)-Se(2)	89.06(4)	Se(1)-Mo(2)-Se(10)	86.06(4)
Se(7)-Mo(1)-Se(6)	85.25(4)	Se(3)-Mo(2)-Se(10)	83.33(4)
Se(5)-Mo(1)-Se(6)	53.31(3)	Se(4)-Mo(2)-Se(10)	92.81(4)
Se(1)-Mo(1)-Se(6)	136.04(5)	Se(11)-Mo(2)-Se(10)	71.77(4)
Se(9)-Mo(1)-Se(6)	85.07(4)	Se(2)-Mo(2)-Se(10)	97.75(5)
Se(2)-Mo(1)-Se(6)	167.31(5)	Se(7)-Mo(2)-Mo(3)	56.37(3)
Se(7)-Mo(1)-Se(8)	152.84(5)	Se(1)-Mo(2)-Mo(3)	97.39(4)
Se(5)-Mo(1)-Se(8)	88.44(4)	Se(3)-Mo(2)-Mo(3)	57.20(3)
Se(1)-Mo(1)-Se(8)	85.32(4)	Se(4)-Mo(2)-Mo(3)	57.75(3)
Se(9)-Mo(1)-Se(8)	72.00(4)	Se(11)-Mo(2)-Mo(3)	126.81(4)
Se(2)-Mo(1)-Se(8)	92.56(4)	Se(2)-Mo(2)-Mo(3)	116.91(4)
Se(6)-Mo(1)-Se(8)	96.29(4)	Se(10)-Mo(2)-Mo(3)	139.42(5)
Se(7)-Mo(1)-Mo(3)	56.57(3)	Se(7)-Mo(2)-Mo(1)	56.25(3)
Se(5)-Mo(1)-Mo(3)	57.28(3)	Se(1)-Mo(2)-Mo(1)	57.20(3)
Se(1)-Mo(1)-Mo(3)	97.32(4)	Se(3)-Mo(2)-Mo(1)	96.43(4)
Se(9)-Mo(1)-Mo(3)	123.21(4)	Se(4)-Mo(2)-Mo(1)	117.01(4)
Se(2)-Mo(1)-Mo(3)	117.37(4)	Se(11)-Mo(2)-Mo(1)	127.88(4)
Se(6)-Mo(1)-Mo(3)	57.95(3)	Se(2)-Mo(2)-Mo(1)	57.83(3)
Se(8)-Mo(1)-Mo(3)	144.71(5)	Se(10)-Mo(2)-Mo(1)	142.86(5)
Se(7)-Mo(1)-Mo(2)	56.42(3)	Mo(3)-Mo(2)-Mo(1)	59.61(3)
Se(5)-Mo(1)-Mo(2)	96.15(4)	Se(7)-Mo(3)-Se(3)	112.97(4)
Se(1)-Mo(1)-Mo(2)	56.68(3)	Se(7)-Mo(3)-Se(5)	113.44(4)
Se(9)-Mo(1)-Mo(2)	126.82(4)	Se(3)-Mo(3)-Se(5)	81.69(4)
Se(2)-Mo(1)-Mo(2)	57.89(3)	Se(7)-Mo(3)-Se(13)	80.10(4)
Se(6)-Mo(1)-Mo(2)	117.76(4)	Se(3)-Mo(3)-Se(13)	133.39(4)
Se(8)-Mo(1)-Mo(2)	140.55(4)	Se(5)-Mo(3)-Se(13)	136.08(5)
Mo(3)-Mo(1)-Mo(2)	60.01(3)	Se(7)-Mo(3)-Se(4)	84.14(4)
Se(7)-Mo(2)-Se(1)	112.60(4)	Se(3)-Mo(3)-Se(4)	53.80(4)
Se(7)-Mo(2)-Se(3)	112.96(5)	Se(5)-Mo(3)-Se(4)	135.28(5)
Se(1)-Mo(2)-Se(3)	83.52(4)	Se(13)-Mo(3)-Se(4)	85.68(4)
Se(7)-Mo(2)-Se(4)	83.85(4)	Se(7)-Mo(3)-Se(6)	85.51(4)
Se(1)-Mo(2)-Se(4)	137.00(5)	Se(3)-Mo(3)-Se(6)	135.01(4)
Se(3)-Mo(2)-Se(4)	53.76(4)	Se(5)-Mo(3)-Se(6)	53.46(3)
Se(7)-Mo(2)-Se(11)	84.09(4)	Se(13)-Mo(3)-Se(6)	88.63(4)

Table A.69, Cont'd. Bond angles (deg.) for $[\text{Mo}_3\text{Se}_7(\text{Se}_2\text{CN}^i\text{Bu}_2)_3]\text{I}$. Symmetry transformations used to generate equivalent atoms:

Se(4)-Mo(3)-Se(6)	168.90(5)	Se(20)-Mo(4)-Mo(6)	56.49(3)
Se(7)-Mo(3)-Se(12)	152.10(5)	Se(14)-Mo(4)-Mo(6)	97.15(4)
Se(3)-Mo(3)-Se(12)	86.59(4)	Se(18)-Mo(4)-Mo(6)	57.29(3)
Se(5)-Mo(3)-Se(12)	88.07(4)	Se(22)-Mo(4)-Mo(6)	125.64(4)
Se(13)-Mo(3)-Se(12)	72.01(4)	Se(15)-Mo(4)-Mo(6)	117.52(4)
Se(4)-Mo(3)-Se(12)	92.85(4)	Se(19)-Mo(4)-Mo(6)	57.97(3)
Se(6)-Mo(3)-Se(12)	94.44(4)	Se(21)-Mo(4)-Mo(6)	141.16(4)
Se(7)-Mo(3)-Mo(1)	56.60(3)	Se(20)-Mo(4)-Mo(5)	56.31(3)
Se(3)-Mo(3)-Mo(1)	96.84(4)	Se(14)-Mo(4)-Mo(5)	56.85(3)
Se(5)-Mo(3)-Mo(1)	57.33(3)	Se(18)-Mo(4)-Mo(5)	97.09(4)
Se(13)-Mo(3)-Mo(1)	124.82(4)	Se(22)-Mo(4)-Mo(5)	125.82(4)
Se(4)-Mo(3)-Mo(1)	118.05(4)	Se(15)-Mo(4)-Mo(5)	57.88(3)
Se(6)-Mo(3)-Mo(1)	58.35(3)	Se(19)-Mo(4)-Mo(5)	117.72(4)
Se(12)-Mo(3)-Mo(1)	144.00(4)	Se(21)-Mo(4)-Mo(5)	142.95(4)
Se(7)-Mo(3)-Mo(2)	56.57(3)	Mo(6)-Mo(4)-Mo(5)	60.10(3)
Se(3)-Mo(3)-Mo(2)	57.02(3)	Se(20)-Mo(5)-Se(14)	112.20(4)
Se(5)-Mo(3)-Mo(2)	96.43(4)	Se(20)-Mo(5)-Se(16)	112.60(4)
Se(13)-Mo(3)-Mo(2)	123.51(4)	Se(14)-Mo(5)-Se(16)	82.96(4)
Se(4)-Mo(3)-Mo(2)	58.04(3)	Se(20)-Mo(5)-Se(17)	83.91(4)
Se(6)-Mo(3)-Mo(2)	118.51(4)	Se(14)-Mo(5)-Se(17)	136.31(4)
Se(12)-Mo(3)-Mo(2)	141.93(4)	Se(16)-Mo(5)-Se(17)	53.65(3)
Mo(1)-Mo(3)-Mo(2)	60.37(3)	Se(20)-Mo(5)-Se(24)	82.33(4)
Se(20)-Mo(4)-Se(14)	112.41(4)	Se(14)-Mo(5)-Se(24)	134.45(4)
Se(20)-Mo(4)-Se(18)	113.13(4)	Se(16)-Mo(5)-Se(24)	132.83(4)
Se(14)-Mo(4)-Se(18)	83.61(4)	Se(17)-Mo(5)-Se(24)	86.26(4)
Se(20)-Mo(4)-Se(22)	82.17(4)	Se(20)-Mo(5)-Se(15)	83.18(4)
Se(14)-Mo(4)-Se(22)	133.12(4)	Se(14)-Mo(5)-Se(15)	53.59(3)
Se(18)-Mo(4)-Se(22)	133.17(4)	Se(16)-Mo(5)-Se(15)	136.22(4)
Se(20)-Mo(4)-Se(15)	83.23(4)	Se(17)-Mo(5)-Se(15)	166.51(4)
Se(14)-Mo(4)-Se(15)	53.62(3)	Se(24)-Mo(5)-Se(15)	88.17(4)
Se(18)-Mo(4)-Se(15)	136.96(4)	Se(20)-Mo(5)-Se(23)	153.80(5)
Se(22)-Mo(4)-Se(15)	86.76(4)	Se(14)-Mo(5)-Se(23)	86.99(4)
Se(20)-Mo(4)-Se(19)	84.24(4)	Se(16)-Mo(5)-Se(23)	86.47(4)
Se(14)-Mo(4)-Se(19)	136.78(4)	Se(17)-Mo(5)-Se(23)	94.42(4)
Se(18)-Mo(4)-Se(19)	53.45(3)	Se(24)-Mo(5)-Se(23)	71.46(3)
Se(22)-Mo(4)-Se(19)	86.99(4)	Se(15)-Mo(5)-Se(23)	95.44(4)
Se(15)-Mo(4)-Se(19)	166.65(4)	Se(20)-Mo(5)-Mo(6)	56.25(3)
Se(20)-Mo(4)-Se(21)	154.06(4)	Se(14)-Mo(5)-Mo(6)	96.69(4)
Se(14)-Mo(4)-Se(21)	86.92(4)	Se(16)-Mo(5)-Mo(6)	56.92(3)
Se(18)-Mo(4)-Se(21)	85.10(4)	Se(17)-Mo(5)-Mo(6)	57.65(3)
Se(22)-Mo(4)-Se(21)	71.91(4)	Se(24)-Mo(5)-Mo(6)	125.04(4)
Se(15)-Mo(4)-Se(21)	95.96(4)	Se(15)-Mo(5)-Mo(6)	117.02(4)
Se(19)-Mo(4)-Se(21)	93.29(4)	Se(23)-Mo(5)-Mo(6)	142.15(4)

Table A.69, Cont'd. Bond angles (deg.) for $[\text{Mo}_3\text{Se}_7(\text{Se}_2\text{CN}^i\text{Bu}_2)_3]\text{I}$. Symmetry transformations used to generate equivalent atoms:

Se(20)-Mo(5)-Mo(4)	56.21(3)	Mo(4)-Mo(6)-Mo(5)	60.33(3)
Se(14)-Mo(5)-Mo(4)	56.74(3)	Se(33)-Mo(7)-Se(31)	112.95(4)
Se(16)-Mo(5)-Mo(4)	96.04(4)	Se(33)-Mo(7)-Se(27)	112.44(4)
Se(17)-Mo(5)-Mo(4)	116.90(4)	Se(31)-Mo(7)-Se(27)	83.54(4)
Se(24)-Mo(5)-Mo(4)	126.75(4)	Se(33)-Mo(7)-Se(28)	83.17(4)
Se(15)-Mo(5)-Mo(4)	57.90(3)	Se(31)-Mo(7)-Se(28)	136.99(5)
Se(23)-Mo(5)-Mo(4)	142.79(4)	Se(27)-Mo(7)-Se(28)	53.74(4)
Mo(6)-Mo(5)-Mo(4)	59.57(3)	Se(33)-Mo(7)-Se(32)	83.81(4)
Se(20)-Mo(6)-Se(16)	113.01(4)	Se(31)-Mo(7)-Se(32)	53.67(4)
Se(20)-Mo(6)-Se(18)	112.99(4)	Se(27)-Mo(7)-Se(32)	136.91(5)
Se(16)-Mo(6)-Se(18)	82.62(4)	Se(28)-Mo(7)-Se(32)	166.19(5)
Se(20)-Mo(6)-Se(26)	80.17(4)	Se(33)-Mo(7)-Se(35)	83.27(4)
Se(16)-Mo(6)-Se(26)	132.03(4)	Se(31)-Mo(7)-Se(35)	131.49(5)
Se(18)-Mo(6)-Se(26)	136.63(4)	Se(27)-Mo(7)-Se(35)	134.05(5)
Se(20)-Mo(6)-Se(17)	84.21(4)	Se(28)-Mo(7)-Se(35)	88.29(4)
Se(16)-Mo(6)-Se(17)	53.85(3)	Se(32)-Mo(7)-Se(35)	85.60(4)
Se(18)-Mo(6)-Se(17)	136.25(4)	Se(33)-Mo(7)-Se(34)	154.21(5)
Se(26)-Mo(6)-Se(17)	84.17(4)	Se(31)-Mo(7)-Se(34)	86.86(4)
Se(20)-Mo(6)-Se(19)	84.46(4)	Se(27)-Mo(7)-Se(34)	85.05(4)
Se(16)-Mo(6)-Se(19)	135.91(4)	Se(28)-Mo(7)-Se(34)	93.45(4)
Se(18)-Mo(6)-Se(19)	53.49(3)	Se(32)-Mo(7)-Se(34)	96.26(4)
Se(26)-Mo(6)-Se(19)	89.42(4)	Se(35)-Mo(7)-Se(34)	71.06(4)
Se(17)-Mo(6)-Se(19)	167.79(5)	Se(33)-Mo(7)-Mo(9)	56.45(3)
Se(20)-Mo(6)-Se(25)	151.92(4)	Se(31)-Mo(7)-Mo(9)	57.15(3)
Se(16)-Mo(6)-Se(25)	89.21(4)	Se(27)-Mo(7)-Mo(9)	97.06(4)
Se(18)-Mo(6)-Se(25)	85.71(4)	Se(28)-Mo(7)-Mo(9)	117.42(4)
Se(26)-Mo(6)-Se(25)	72.04(4)	Se(32)-Mo(7)-Mo(9)	57.79(3)
Se(17)-Mo(6)-Se(25)	96.64(4)	Se(35)-Mo(7)-Mo(9)	125.62(4)
Se(19)-Mo(6)-Se(25)	91.22(4)	Se(34)-Mo(7)-Mo(9)	143.20(4)
Se(20)-Mo(6)-Mo(4)	56.55(3)	Se(33)-Mo(7)-Mo(8)	56.37(3)
Se(16)-Mo(6)-Mo(4)	96.74(4)	Se(31)-Mo(7)-Mo(8)	96.71(4)
Se(18)-Mo(6)-Mo(4)	57.08(3)	Se(27)-Mo(7)-Mo(8)	56.86(3)
Se(26)-Mo(6)-Mo(4)	125.79(4)	Se(28)-Mo(7)-Mo(8)	58.07(3)
Se(17)-Mo(6)-Mo(4)	118.01(4)	Se(32)-Mo(7)-Mo(8)	117.25(4)
Se(19)-Mo(6)-Mo(4)	58.28(3)	Se(35)-Mo(7)-Mo(8)	127.78(4)
Se(25)-Mo(6)-Mo(4)	140.88(4)	Se(34)-Mo(7)-Mo(8)	140.80(4)
Se(20)-Mo(6)-Mo(5)	56.42(3)	Mo(9)-Mo(7)-Mo(8)	59.83(3)
Se(16)-Mo(6)-Mo(5)	57.17(3)	Se(33)-Mo(8)-Se(27)	112.53(4)
Se(18)-Mo(6)-Mo(5)	97.12(4)	Se(33)-Mo(8)-Se(29)	112.79(4)
Se(26)-Mo(6)-Mo(5)	122.42(4)	Se(27)-Mo(8)-Se(29)	83.68(4)
Se(17)-Mo(6)-Mo(5)	58.01(3)	Se(33)-Mo(8)-Se(37)	82.41(4)
Se(19)-Mo(6)-Mo(5)	118.26(4)	Se(27)-Mo(8)-Se(37)	132.97(5)
Se(25)-Mo(6)-Mo(5)	145.28(4)	Se(29)-Mo(8)-Se(37)	133.18(5)

Table A.69, Cont'd. Bond angles (deg.) for $[\text{Mo}_3\text{Se}_7(\text{Se}_2\text{CN}^i\text{Bu}_2)_3]\text{I}$. Symmetry transformations used to generate equivalent atoms:

Se(33)-Mo(8)-Se(30)	84.25(4)	Se(32)-Mo(9)-Se(30)	167.09(5)
Se(27)-Mo(8)-Se(30)	137.06(5)	Se(39)-Mo(9)-Se(30)	86.65(4)
Se(29)-Mo(8)-Se(30)	53.59(3)	Se(33)-Mo(9)-Se(38)	154.23(5)
Se(37)-Mo(8)-Se(30)	86.70(4)	Se(29)-Mo(9)-Se(38)	86.80(4)
Se(33)-Mo(8)-Se(28)	82.83(4)	Se(31)-Mo(9)-Se(38)	85.21(4)
Se(27)-Mo(8)-Se(28)	53.61(3)	Se(32)-Mo(9)-Se(38)	93.22(4)
Se(29)-Mo(8)-Se(28)	136.90(4)	Se(39)-Mo(9)-Se(38)	71.73(4)
Se(37)-Mo(8)-Se(28)	87.05(4)	Se(30)-Mo(9)-Se(38)	95.97(4)
Se(30)-Mo(8)-Se(28)	166.28(5)	Se(33)-Mo(9)-Mo(8)	56.45(3)
Se(33)-Mo(8)-Se(36)	153.92(5)	Se(29)-Mo(9)-Mo(8)	57.17(3)
Se(27)-Mo(8)-Se(36)	87.51(4)	Se(31)-Mo(9)-Mo(8)	96.70(4)
Se(29)-Mo(8)-Se(36)	84.87(4)	Se(32)-Mo(9)-Mo(8)	117.51(4)
Se(37)-Mo(8)-Se(36)	71.58(4)	Se(39)-Mo(9)-Mo(8)	125.72(4)
Se(30)-Mo(8)-Se(36)	92.19(4)	Se(30)-Mo(9)-Mo(8)	57.89(3)
Se(28)-Mo(8)-Se(36)	97.39(4)	Se(38)-Mo(9)-Mo(8)	143.13(5)
Se(33)-Mo(8)-Mo(9)	56.52(3)	Se(33)-Mo(9)-Mo(7)	56.31(3)
Se(27)-Mo(8)-Mo(9)	97.32(4)	Se(29)-Mo(9)-Mo(7)	96.96(4)
Se(29)-Mo(8)-Mo(9)	56.90(3)	Se(31)-Mo(9)-Mo(7)	56.83(3)
Se(37)-Mo(8)-Mo(9)	125.78(4)	Se(32)-Mo(9)-Mo(7)	57.76(3)
Se(30)-Mo(8)-Mo(9)	58.12(3)	Se(39)-Mo(9)-Mo(7)	126.31(4)
Se(28)-Mo(8)-Mo(9)	117.12(4)	Se(30)-Mo(9)-Mo(7)	117.65(4)
Se(36)-Mo(8)-Mo(9)	140.35(4)	Se(38)-Mo(9)-Mo(7)	140.77(4)
Se(33)-Mo(8)-Mo(7)	56.30(3)	Mo(8)-Mo(9)-Mo(7)	60.12(3)
Se(27)-Mo(8)-Mo(7)	57.02(3)	Se(2)-Se(1)-Mo(2)	64.70(4)
Se(29)-Mo(8)-Mo(7)	96.72(4)	Se(2)-Se(1)-Mo(1)	64.40(4)
Se(37)-Mo(8)-Mo(7)	126.12(4)	Mo(2)-Se(1)-Mo(1)	66.12(4)
Se(30)-Mo(8)-Mo(7)	117.80(4)	Se(1)-Se(2)-Mo(1)	61.91(4)
Se(28)-Mo(8)-Mo(7)	57.55(3)	Se(1)-Se(2)-Mo(2)	61.48(4)
Se(36)-Mo(8)-Mo(7)	143.85(4)	Mo(1)-Se(2)-Mo(2)	64.28(4)
Mo(9)-Mo(8)-Mo(7)	60.05(3)	Se(4)-Se(3)-Mo(2)	64.49(4)
Se(33)-Mo(9)-Se(29)	112.99(4)	Se(4)-Se(3)-Mo(3)	64.17(4)
Se(33)-Mo(9)-Se(31)	112.50(4)	Mo(2)-Se(3)-Mo(3)	65.78(4)
Se(29)-Mo(9)-Se(31)	82.95(4)	Se(3)-Se(4)-Mo(3)	62.03(4)
Se(33)-Mo(9)-Se(32)	83.71(4)	Se(3)-Se(4)-Mo(2)	61.76(4)
Se(29)-Mo(9)-Se(32)	136.27(4)	Mo(3)-Se(4)-Mo(2)	64.21(3)
Se(31)-Mo(9)-Se(32)	53.56(4)	Se(6)-Se(5)-Mo(3)	64.49(4)
Se(33)-Mo(9)-Se(39)	82.57(4)	Se(6)-Se(5)-Mo(1)	64.78(4)
Se(29)-Mo(9)-Se(39)	132.83(5)	Mo(3)-Se(5)-Mo(1)	65.39(3)
Se(31)-Mo(9)-Se(39)	133.86(5)	Se(5)-Se(6)-Mo(3)	62.05(4)
Se(32)-Mo(9)-Se(39)	87.64(4)	Se(5)-Se(6)-Mo(1)	61.90(4)
Se(33)-Mo(9)-Se(30)	84.07(4)	Mo(3)-Se(6)-Mo(1)	63.70(3)
Se(29)-Mo(9)-Se(30)	53.60(4)	Mo(3)-Se(7)-Mo(1)	66.83(3)
Se(31)-Mo(9)-Se(30)	136.26(5)	Mo(3)-Se(7)-Mo(2)	67.06(4)

Table A.69, Cont'd. Bond angles (deg.) for [Mo₃Se₇(Se₂CNⁱBu₂)₃]. Symmetry transformations used to generate equivalent atoms:

Mo(1)-Se(7)-Mo(2)	67.32(4)	Se(29)-Se(30)-Mo(8)	61.86(4)
C(1)-Se(8)-Mo(1)	88.0(3)	Se(29)-Se(30)-Mo(9)	61.54(4)
C(1)-Se(9)-Mo(1)	88.9(3)	Mo(8)-Se(30)-Mo(9)	64.00(3)
C(10)-Se(10)-Mo(2)	88.1(3)	Se(32)-Se(31)-Mo(7)	64.47(4)
C(10)-Se(11)-Mo(2)	88.5(3)	Se(32)-Se(31)-Mo(9)	64.34(4)
C(19)-Se(12)-Mo(3)	87.7(3)	Mo(7)-Se(31)-Mo(9)	66.02(3)
C(19)-Se(13)-Mo(3)	88.2(3)	Se(31)-Se(32)-Mo(7)	61.85(4)
Se(15)-Se(14)-Mo(4)	64.93(4)	Se(31)-Se(32)-Mo(9)	62.09(4)
Se(15)-Se(14)-Mo(5)	64.85(4)	Mo(7)-Se(32)-Mo(9)	64.45(4)
Mo(4)-Se(14)-Mo(5)	66.41(3)	Mo(7)-Se(33)-Mo(8)	67.33(4)
Se(14)-Se(15)-Mo(5)	61.56(4)	Mo(7)-Se(33)-Mo(9)	67.24(3)
Se(14)-Se(15)-Mo(4)	61.46(4)	Mo(8)-Se(33)-Mo(9)	67.04(4)
Mo(5)-Se(15)-Mo(4)	64.22(3)	C(55)-Se(34)-Mo(7)	89.0(3)
Se(17)-Se(16)-Mo(6)	64.26(4)	C(55)-Se(35)-Mo(7)	89.4(3)
Se(17)-Se(16)-Mo(5)	64.42(4)	C(64)-Se(36)-Mo(8)	87.5(3)
Mo(6)-Se(16)-Mo(5)	65.91(3)	C(64)-Se(37)-Mo(8)	88.6(3)
Se(16)-Se(17)-Mo(6)	61.90(4)	C(73)-Se(38)-Mo(9)	87.6(3)
Se(16)-Se(17)-Mo(5)	61.93(4)	C(73)-Se(39)-Mo(9)	88.8(3)
Mo(6)-Se(17)-Mo(5)	64.34(3)	C(1)-N(1)-C(2)	119.6(8)
Se(19)-Se(18)-Mo(4)	64.90(4)	C(1)-N(1)-C(6)	122.8(8)
Se(19)-Se(18)-Mo(6)	64.56(4)	C(2)-N(1)-C(6)	117.4(7)
Mo(4)-Se(18)-Mo(6)	65.63(3)	C(10)-N(2)-C(15)	120.9(9)
Se(18)-Se(19)-Mo(6)	61.95(4)	C(10)-N(2)-C(11)	119.3(9)
Se(18)-Se(19)-Mo(4)	61.65(4)	C(15)-N(2)-C(11)	117.3(8)
Mo(6)-Se(19)-Mo(4)	63.76(3)	C(19)-N(3)-C(24)	121.8(8)
Mo(6)-Se(20)-Mo(4)	66.97(3)	C(19)-N(3)-C(20)	120.7(8)
Mo(6)-Se(20)-Mo(5)	67.33(3)	C(24)-N(3)-C(20)	117.2(7)
Mo(4)-Se(20)-Mo(5)	67.48(3)	C(28)-N(4)-C(29)	122.2(8)
C(28)-Se(21)-Mo(4)	87.5(3)	C(28)-N(4)-C(33)	120.3(8)
C(28)-Se(22)-Mo(4)	88.5(3)	C(29)-N(4)-C(33)	117.4(8)
C(37)-Se(23)-Mo(5)	87.9(3)	C(37)-N(5)-C(38)	120.8(8)
C(37)-Se(24)-Mo(5)	89.0(3)	C(37)-N(5)-C(42)	121.4(8)
C(46)-Se(25)-Mo(6)	87.9(3)	C(38)-N(5)-C(42)	117.9(8)
C(46)-Se(26)-Mo(6)	88.7(3)	C(46)-N(6)-C(51)	122.3(8)
Se(28)-Se(27)-Mo(8)	64.76(4)	C(46)-N(6)-C(47)	119.1(8)
Se(28)-Se(27)-Mo(7)	64.27(4)	C(51)-N(6)-C(47)	118.5(8)
Mo(8)-Se(27)-Mo(7)	66.13(3)	C(55)-N(7)-C(56)	121.8(8)
Se(27)-Se(28)-Mo(7)	61.99(4)	C(55)-N(7)-C(60)	121.0(8)
Se(27)-Se(28)-Mo(8)	61.63(4)	C(56)-N(7)-C(60)	117.2(8)
Mo(7)-Se(28)-Mo(8)	64.38(3)	C(64)-N(8)-C(69)	123.1(9)
Se(30)-Se(29)-Mo(9)	64.86(4)	C(64)-N(8)-C(65)	121.3(8)
Se(30)-Se(29)-Mo(8)	64.54(4)	C(69)-N(8)-C(65)	115.6(8)
Mo(9)-Se(29)-Mo(8)	65.93(4)	C(73)-N(9)-C(74)	121.2(8)

Table A.69, Cont'd. Bond angles (deg.) for [Mo₃Se₇(Se₂CNⁱBu₂)₃]. Symmetry transformations used to generate equivalent atoms:

C(73)-N(9)-C(78)	120.1(8)	C(36)-C(34)-C(35)	112.2(9)
C(74)-N(9)-C(78)	118.6(8)	C(36)-C(34)-C(33)	109.4(9)
N(1)-C(1)-Se(8)	124.4(7)	C(35)-C(34)-C(33)	112.9(9)
N(1)-C(1)-Se(9)	124.7(7)	N(5)-C(37)-Se(23)	124.3(7)
Se(8)-C(1)-Se(9)	110.9(5)	N(5)-C(37)-Se(24)	124.1(7)
N(1)-C(2)-C(3)	113.1(8)	Se(23)-C(37)-Se(24)	111.6(4)
C(4)-C(3)-C(5)	113.2(10)	N(5)-C(38)-C(39)	112.6(10)
C(4)-C(3)-C(2)	114.1(9)	C(41)-C(39)-C(38)	117.7(13)
C(5)-C(3)-C(2)	111.2(9)	C(41)-C(39)-C(40)	113.9(12)
N(1)-C(6)-C(7)	112.3(8)	C(38)-C(39)-C(40)	105.0(13)
C(9)-C(7)-C(8)	111.4(9)	C(43B)-C(42)-N(5)	115.3(14)
C(9)-C(7)-C(6)	110.9(9)	N(5)-C(42)-C(43A)	113.2(10)
C(8)-C(7)-C(6)	111.7(8)	C(44A)-C(43A)-C(45A)	112.5(16)
N(2)-C(10)-Se(10)	123.9(8)	C(44A)-C(43A)-C(42)	114.3(14)
N(2)-C(10)-Se(11)	124.5(8)	C(45A)-C(43A)-C(42)	107.5(15)
Se(10)-C(10)-Se(11)	111.6(5)	C(42)-C(43B)-C(45B)	109(2)
N(2)-C(11)-C(12)	114.9(9)	C(42)-C(43B)-C(44B)	104(2)
C(14)-C(12)-C(13)	110.3(9)	C(45B)-C(43B)-C(44B)	111(3)
C(14)-C(12)-C(11)	106.9(9)	N(6)-C(46)-Se(25)	125.5(7)
C(13)-C(12)-C(11)	112.6(9)	N(6)-C(46)-Se(26)	123.4(7)
N(2)-C(15)-C(16)	115.1(9)	Se(25)-C(46)-Se(26)	111.1(5)
C(15)-C(16)-C(17)	112.3(9)	N(6)-C(47)-C(48)	112.3(8)
C(15)-C(16)-C(18)	107.7(10)	C(50)-C(48)-C(47)	111.6(9)
C(17)-C(16)-C(18)	110.3(10)	C(50)-C(48)-C(49)	112.1(9)
N(3)-C(19)-Se(12)	125.2(7)	C(47)-C(48)-C(49)	109.9(9)
N(3)-C(19)-Se(13)	124.0(7)	N(6)-C(51)-C(52B)	112.7(12)
Se(12)-C(19)-Se(13)	110.8(5)	N(6)-C(51)-C(52A)	113.4(10)
N(3)-C(20)-C(21)	115.1(8)	C(53A)-C(52A)-C(54A)	106.1(17)
C(22)-C(21)-C(20)	114.3(8)	C(53A)-C(52A)-C(51)	108.4(15)
C(22)-C(21)-C(23)	110.2(9)	C(54A)-C(52A)-C(51)	109.1(16)
C(20)-C(21)-C(23)	108.0(9)	C(51)-C(52B)-C(54B)	114(2)
N(3)-C(24)-C(25)	117.1(8)	C(51)-C(52B)-C(53B)	110(2)
C(26)-C(25)-C(24)	113.3(8)	C(54B)-C(52B)-C(53B)	115(2)
C(26)-C(25)-C(27)	110.7(9)	N(7)-C(55)-Se(34)	125.2(7)
C(24)-C(25)-C(27)	109.2(9)	N(7)-C(55)-Se(35)	124.3(7)
N(4)-C(28)-Se(21)	123.6(7)	Se(34)-C(55)-Se(35)	110.5(5)
N(4)-C(28)-Se(22)	124.4(8)	N(7)-C(56)-C(57)	112.4(9)
Se(21)-C(28)-Se(22)	112.0(5)	C(58)-C(57)-C(59)	111.8(12)
N(4)-C(29)-C(30)	114.0(8)	C(58)-C(57)-C(56)	112.4(10)
C(32)-C(30)-C(29)	113.3(9)	C(59)-C(57)-C(56)	106.5(11)
C(32)-C(30)-C(31)	110.8(9)	N(7)-C(60)-C(61A)	112.2(10)
C(29)-C(30)-C(31)	107.9(9)	N(7)-C(60)-C(61B)	116.1(15)
N(4)-C(33)-C(34)	113.0(8)	C(63A)-C(61A)-C(60)	114.8(16)

Table A.69, Cont'd. Bond angles (deg.) for $[\text{Mo}_3\text{Se}_7(\text{Se}_2\text{CN}^i\text{Bu}_2)_3]\text{I}$. Symmetry transformations used to generate equivalent atoms:

C(63A)-C(61A)-C(62A)	107.3(17)
C(60)-C(61A)-C(62A)	107.6(16)
C(63B)-C(61B)-C(60)	106(3)
C(63B)-C(61B)-C(62B)	117(3)
C(60)-C(61B)-C(62B)	104(3)
N(8)-C(64)-Se(36)	125.1(8)
N(8)-C(64)-Se(37)	123.5(7)
Se(36)-C(64)-Se(37)	111.4(5)
C(66A)-C(65)-N(8)	111.8(10)
N(8)-C(65)-C(66B)	117.6(10)
C(68A)-C(66A)-C(65)	132.0(19)
C(68A)-C(66A)-C(67A)	112(2)
C(65)-C(66A)-C(67A)	107.1(16)
C(68B)-C(66B)-C(67B)	120(2)
C(68B)-C(66B)-C(65)	132(2)
C(67B)-C(66B)-C(65)	107.3(16)
N(8)-C(69)-C(70)	112.6(8)
C(72)-C(70)-C(71)	111.9(10)
C(72)-C(70)-C(69)	113.3(9)
C(71)-C(70)-C(69)	109.0(9)
N(9)-C(73)-Se(38)	124.4(7)
N(9)-C(73)-Se(39)	123.9(7)
Se(38)-C(73)-Se(39)	111.7(4)
N(9)-C(74)-C(75)	113.6(9)
C(77)-C(75)-C(74)	114.4(10)
C(77)-C(75)-C(76)	113.1(11)
C(74)-C(75)-C(76)	107.1(10)
N(9)-C(78)-C(79)	113.2(9)
C(80)-C(79)-C(81)	111.3(10)
C(80)-C(79)-C(78)	108.1(11)
C(81)-C(79)-C(78)	113.4(10)

Table A.70. Anisotropic displacement parameters ($\text{\AA}^2 \times 10^3$) for $[\text{Mo}_3\text{Se}_7(\text{Se}_2\text{CN}^i\text{Bu}_2)_3]\text{I}$. The anisotropic displacement factor exponent takes the form: $-2\pi^2[h^2a^{*2}U^{11} + \dots + 2hka^*b^*U^{12}]$.

Atom	U^{11}	U^{22}	U^{33}	U^{23}	U^{13}	U^{12}
I(1)	49(1)	34(1)	53(1)	-5(1)	4(1)	-13(1)
I(2)	40(1)	45(1)	25(1)	0(1)	-5(1)	-14(1)
I(3)	31(1)	24(1)	42(1)	8(1)	3(1)	-3(1)
Mo(1)	23(1)	20(1)	24(1)	-1(1)	1(1)	3(1)
Mo(2)	30(1)	25(1)	23(1)	-3(1)	5(1)	1(1)
Mo(3)	22(1)	19(1)	23(1)	-1(1)	3(1)	2(1)
Mo(4)	19(1)	11(1)	21(1)	0(1)	1(1)	-1(1)
Mo(5)	21(1)	13(1)	18(1)	0(1)	2(1)	-3(1)
Mo(6)	21(1)	12(1)	20(1)	-1(1)	4(1)	-1(1)
Mo(7)	22(1)	21(1)	25(1)	6(1)	2(1)	-2(1)
Mo(8)	23(1)	23(1)	23(1)	7(1)	1(1)	-2(1)
Mo(9)	22(1)	22(1)	26(1)	9(1)	1(1)	-1(1)
Se(1)	32(1)	31(1)	30(1)	-6(1)	-1(1)	-1(1)
Se(2)	41(1)	36(1)	28(1)	3(1)	-4(1)	2(1)
Se(3)	34(1)	21(1)	33(1)	-4(1)	5(1)	4(1)
Se(4)	28(1)	29(1)	37(1)	-4(1)	8(1)	6(1)
Se(5)	25(1)	23(1)	29(1)	-1(1)	4(1)	0(1)
Se(6)	28(1)	24(1)	25(1)	-3(1)	4(1)	2(1)
Se(7)	27(1)	23(1)	24(1)	1(1)	3(1)	0(1)
Se(8)	24(1)	22(1)	51(1)	-3(1)	-1(1)	2(1)
Se(9)	26(1)	22(1)	40(1)	1(1)	-1(1)	1(1)
Se(10)	46(1)	37(1)	30(1)	-10(1)	11(1)	-7(1)
Se(11)	46(1)	33(1)	28(1)	-5(1)	12(1)	-5(1)
Se(12)	28(1)	25(1)	33(1)	7(1)	-2(1)	-3(1)
Se(13)	27(1)	21(1)	31(1)	3(1)	-2(1)	0(1)
Se(14)	20(1)	22(1)	24(1)	3(1)	1(1)	-2(1)
Se(15)	26(1)	22(1)	23(1)	-4(1)	5(1)	4(1)
Se(16)	30(1)	17(1)	24(1)	-3(1)	2(1)	-7(1)
Se(17)	34(1)	13(1)	27(1)	2(1)	3(1)	-1(1)
Se(18)	25(1)	20(1)	19(1)	1(1)	3(1)	-3(1)
Se(19)	21(1)	20(1)	28(1)	5(1)	4(1)	-4(1)
Se(20)	20(1)	14(1)	20(1)	-1(1)	0(1)	-1(1)
Se(21)	33(1)	15(1)	31(1)	4(1)	-6(1)	-1(1)
Se(22)	33(1)	13(1)	34(1)	-1(1)	-9(1)	-2(1)
Se(23)	25(1)	36(1)	25(1)	5(1)	0(1)	-12(1)
Se(24)	26(1)	24(1)	20(1)	3(1)	1(1)	-6(1)
Se(25)	33(1)	25(1)	26(1)	-4(1)	6(1)	6(1)
Se(26)	26(1)	23(1)	30(1)	-5(1)	1(1)	5(1)
Se(27)	23(1)	25(1)	31(1)	5(1)	0(1)	-3(1)

Table A.70, Cont'd. Anisotropic displacement parameters ($\text{\AA}^2 \times 10^3$) for $[\text{Mo}_3\text{Se}_7(\text{Se}_2\text{CN}^i\text{Bu}_2)_3]\text{I}$. The anisotropic displacement factor exponent takes the form: $-2\pi^2[h^2a^{*2}U^{11} + \dots + 2hka^*b^*U^{12}]$.

Atom	U^{11}	U^{22}	U^{33}	U^{23}	U^{13}	U^{12}
Se(28)	27(1)	25(1)	34(1)	9(1)	-4(1)	2(1)
Se(29)	26(1)	23(1)	28(1)	6(1)	2(1)	-2(1)
Se(30)	27(1)	27(1)	33(1)	8(1)	6(1)	0(1)
Se(31)	27(1)	26(1)	29(1)	12(1)	2(1)	-2(1)
Se(32)	33(1)	34(1)	24(1)	7(1)	-1(1)	-3(1)
Se(33)	24(1)	23(1)	26(1)	7(1)	2(1)	-3(1)
Se(34)	29(1)	23(1)	42(1)	2(1)	10(1)	-6(1)
Se(35)	28(1)	23(1)	41(1)	4(1)	7(1)	-6(1)
Se(36)	37(1)	31(1)	27(1)	6(1)	0(1)	-10(1)
Se(37)	33(1)	29(1)	26(1)	10(1)	-2(1)	-8(1)
Se(38)	28(1)	26(1)	38(1)	12(1)	-4(1)	-3(1)
Se(39)	25(1)	26(1)	44(1)	12(1)	-5(1)	-4(1)
N(1)	25(4)	19(4)	29(5)	-4(4)	-1(4)	3(3)
N(2)	39(5)	34(5)	19(5)	-3(4)	5(4)	0(4)
N(3)	27(4)	23(4)	26(5)	3(4)	-1(4)	1(3)
N(4)	33(5)	22(4)	22(5)	3(4)	3(4)	0(4)
N(5)	23(4)	27(5)	32(5)	5(4)	5(4)	-8(3)
N(6)	29(4)	24(4)	26(5)	2(4)	6(4)	7(4)
N(7)	25(4)	28(5)	31(5)	6(4)	1(4)	0(4)
N(8)	23(4)	36(5)	25(5)	6(4)	-4(4)	-2(4)
N(9)	25(4)	24(4)	28(5)	1(4)	-1(4)	3(3)
C(1)	41(6)	17(5)	19(5)	1(4)	-6(4)	0(4)
C(2)	16(5)	26(5)	36(6)	-6(5)	-5(4)	5(4)
C(3)	39(6)	48(7)	25(6)	-5(5)	-5(5)	5(5)
C(4)	70(9)	72(10)	30(7)	1(7)	-6(6)	-6(8)
C(5)	34(6)	60(8)	30(6)	-8(6)	-3(5)	-5(6)
C(6)	36(6)	22(5)	27(6)	4(5)	-1(5)	8(4)
C(7)	38(6)	27(6)	38(7)	-6(5)	11(5)	-2(5)
C(8)	44(7)	43(7)	40(7)	-7(6)	-4(6)	-9(6)
C(9)	63(8)	40(7)	59(9)	-22(6)	13(7)	-2(6)
C(10)	42(6)	42(7)	26(6)	-3(5)	5(5)	2(5)
C(11)	54(7)	43(7)	23(6)	-12(5)	10(5)	-2(6)
C(12)	47(7)	44(7)	27(6)	-10(5)	-1(5)	1(6)
C(13)	50(7)	37(7)	42(7)	-9(6)	8(6)	0(5)
C(14)	68(9)	45(8)	78(11)	-15(7)	-2(8)	-9(7)
C(15)	57(7)	36(7)	28(6)	-1(5)	16(5)	-2(6)
C(16)	55(7)	36(6)	26(6)	-2(5)	1(5)	-4(5)
C(17)	42(7)	50(8)	46(8)	-17(6)	-5(6)	6(6)
C(18)	66(9)	68(10)	60(9)	-1(8)	15(7)	-18(8)

Table A.70, Cont'd. Anisotropic displacement parameters ($\text{\AA}^2 \times 10^3$) for $[\text{Mo}_3\text{Se}_7(\text{Se}_2\text{CN}^i\text{Bu}_2)_3]\text{I}$. The anisotropic displacement factor exponent takes the form: $-2\pi^2[h^2a^{*2}U^{11} + \dots + 2hka^*b^*U^{12}]$.

Atom	U^{11}	U^{22}	U^{33}	U^{23}	U^{13}	U^{12}
C(19)	21(5)	24(5)	18(5)	-8(4)	3(4)	6(4)
C(20)	29(5)	32(6)	20(5)	3(4)	-2(4)	0(4)
C(21)	29(5)	27(6)	43(7)	12(5)	0(5)	-4(4)
C(22)	51(7)	27(6)	48(8)	1(5)	6(6)	8(5)
C(23)	39(6)	35(7)	58(8)	9(6)	-1(6)	-7(5)
C(24)	20(5)	25(5)	32(6)	-3(4)	-7(4)	1(4)
C(25)	23(5)	31(6)	44(7)	-1(5)	-2(5)	4(4)
C(26)	38(6)	39(6)	28(6)	3(5)	7(5)	8(5)
C(27)	35(6)	40(7)	70(9)	-2(6)	-7(6)	-10(5)
C(28)	36(6)	10(5)	34(6)	8(4)	7(5)	4(4)
C(29)	43(6)	11(5)	31(6)	9(4)	6(5)	8(4)
C(30)	77(9)	15(5)	31(7)	-1(5)	2(6)	-3(5)
C(31)	87(10)	42(8)	48(8)	3(6)	12(7)	18(7)
C(32)	58(8)	34(7)	61(9)	-1(6)	28(7)	-9(6)
C(34)	54(7)	13(5)	52(8)	0(5)	-5(6)	-6(5)
C(35)	54(7)	21(6)	38(7)	5(5)	6(6)	-2(5)
C(36)	73(9)	44(8)	55(9)	-15(7)	-10(7)	3(7)
C(37)	31(5)	19(5)	17(5)	4(4)	20(4)	-2(4)
C(38)	26(5)	52(7)	37(7)	15(6)	4(5)	-17(5)
C(39)	25(6)	125(14)	70(11)	-19(10)	4(7)	-5(8)
C(40)	25(7)	190(20)	97(13)	-10(13)	-7(8)	-21(10)
C(41)	51(10)	81(13)	200(20)	-24(14)	31(12)	2(9)
C(42)	39(6)	46(7)	26(6)	7(5)	0(5)	-16(5)
C(46)	32(5)	13(5)	27(6)	-5(4)	13(4)	-2(4)
C(47)	40(6)	28(6)	24(6)	6(5)	15(5)	14(5)
C(48)	41(6)	38(6)	34(7)	10(5)	18(5)	16(5)
C(49)	66(8)	51(8)	38(7)	5(6)	18(6)	15(7)
C(50)	50(7)	49(8)	63(9)	32(7)	21(7)	5(6)
C(51)	22(5)	29(6)	39(7)	5(5)	0(5)	2(4)
C(55)	35(6)	30(6)	30(6)	0(5)	-2(5)	-3(5)
C(56)	29(6)	40(6)	37(7)	-1(5)	11(5)	-6(5)
C(57)	56(8)	45(8)	52(8)	-14(6)	26(7)	-9(6)
C(58)	92(11)	75(11)	54(10)	25(8)	3(8)	-13(9)
C(59)	83(11)	102(13)	91(13)	1(11)	43(10)	-19(10)
C(60)	34(6)	22(6)	57(8)	-13(5)	7(5)	-9(5)
C(64)	24(5)	35(6)	33(6)	16(5)	-4(4)	1(4)
C(65)	35(6)	42(7)	20(6)	5(5)	5(5)	-6(5)
C(69)	25(5)	40(6)	33(6)	17(5)	1(5)	-5(5)
C(70)	38(6)	47(7)	32(7)	12(5)	2(5)	0(5)

Table A.70, Cont'd. Anisotropic displacement parameters ($\text{\AA}^2 \times 10^3$) for $[\text{Mo}_3\text{Se}_7(\text{Se}_2\text{CN}^i\text{Bu}_2)_3]\text{I}$. The anisotropic displacement factor exponent takes the form: $-2\pi^2[h^2a^{*2}U^{11} + \dots + 2hka^*b^*U^{12}]$.

Atom	U^{11}	U^{22}	U^{33}	U^{23}	U^{13}	U^{12}
C(71)	73(9)	54(8)	32(7)	17(6)	-1(6)	-11(7)
C(72)	59(8)	71(9)	48(8)	25(7)	-2(7)	26(7)
C(73)	10(4)	38(6)	23(5)	2(5)	1(4)	5(4)
C(74)	21(5)	34(6)	38(6)	14(5)	-2(4)	6(4)
C(75)	48(7)	70(9)	39(8)	23(7)	0(6)	-1(7)
C(76)	95(11)	97(12)	42(9)	40(8)	6(8)	11(10)
C(77)	100(12)	109(13)	21(7)	-10(8)	5(7)	3(10)
C(78)	25(5)	36(6)	40(7)	-2(5)	-9(5)	-3(5)
C(79)	34(6)	55(8)	50(8)	9(6)	4(6)	-6(6)
C(80)	56(9)	60(10)	131(15)	25(10)	19(9)	-18(7)
C(81)	54(8)	67(10)	74(10)	-5(8)	37(7)	-6(7)

Table A.71. Hydrogen coordinates ($\times 10^4$) and isotropic displacement parameters ($\text{\AA}^2 \times 10^3$) for $[\text{Mo}_3\text{Se}_7(\text{Se}_2\text{CN}^i\text{Bu}_2)_3]\text{I}$.

H atom	x	y	z	U(eq)
H(2A)	5907	9756	5908	31
H(2B)	6023	8615	5939	31
H(3)	6249	8513	5409	45
H(4A)	6275	9775	5045	86
H(4B)	6634	9974	5343	86
H(4C)	6137	10539	5323	86
H(5A)	5375	9518	5415	62
H(5B)	5444	8375	5485	62
H(5C)	5548	8809	5131	62
H(6A)	6542	10915	5850	34
H(6B)	7064	10611	5971	34
H(7)	6287	10502	6407	41
H(8A)	7275	10711	6556	64
H(8B)	6983	9712	6586	64
H(8C)	6867	10612	6821	64
H(9A)	6458	12081	6601	81
H(9B)	6289	12119	6227	81
H(9C)	6840	12223	6321	81
H(11A)	9086	4849	4158	48
H(11B)	8630	4668	4377	48
H(12)	9161	3751	4755	48
H(13A)	9859	3100	4537	64
H(13B)	9900	4267	4527	64
H(13C)	9772	3673	4202	64
H(14A)	8936	3014	4118	96
H(14B)	8597	2963	4427	96
H(14C)	9072	2322	4420	96
H(15A)	9296	7053	4536	48
H(15B)	9197	6529	4195	48
H(16)	9922	5672	4250	47
H(17A)	10100	6869	4810	69
H(17B)	10473	6123	4656	69
H(17C)	10005	5717	4826	69
H(18A)	9856	7220	3970	97
H(18B)	10383	7016	4104	97
H(18C)	10044	7752	4294	97
H(20A)	9268	4529	7199	32
H(20B)	9698	4975	7409	32
H(21)	10252	4220	7073	40
H(22A)	9480	3364	6720	63

Table A.71, Cont'd. Hydrogen coordinates ($\times 10^4$) and isotropic displacement parameters ($\text{\AA}^2 \times 10^3$) for $[\text{Mo}_3\text{Se}_7(\text{Se}_2\text{CN}^i\text{Bu}_2)_3]\text{I}$.

H atom	x	y	z	U(eq)
H(22B)	10028	3099	6671	63
H(22C)	9835	4163	6576	63
H(23A)	9556	2908	7323	66
H(23B)	9998	3345	7524	66
H(23C)	10085	2585	7235	66
H(24A)	10024	6430	7278	31
H(24B)	9832	7055	6976	31
H(25)	10550	5601	6932	39
H(26A)	10169	5780	6427	52
H(26B)	10696	6211	6408	52
H(26C)	10253	6937	6437	52
H(27A)	10650	7686	6977	73
H(27B)	11078	6995	6869	73
H(27C)	10866	6901	7227	73
H(29A)	8380	3685	8068	34
H(29B)	8122	2736	7923	34
H(30)	7758	3950	8432	49
H(31A)	7911	2588	8773	88
H(31B)	8391	2882	8594	88
H(31C)	8089	1961	8470	88
H(32A)	7126	3292	8106	76
H(32B)	7112	2934	8476	76
H(32C)	7306	2218	8200	76
H(33A)	7280	3825	7444	34
H(33B)	7505	2811	7563	34
H(34)	7919	4118	7104	47
H(35A)	8344	2322	7312	57
H(35B)	8537	3381	7413	57
H(35C)	8553	3037	7041	57
H(36A)	7605	2185	6974	86
H(36B)	7749	2994	6712	86
H(36C)	7273	3120	6916	86
H(38A)	9583	11060	6908	46
H(38B)	9639	11220	6525	46
H(39)	9918	9496	6872	88
H(40A)	10706	10092	6816	157
H(40B)	10385	10870	7003	157
H(40C)	10508	11036	6628	157
H(41A)	9742	9036	6358	167
H(41B)	10298	8932	6435	167

Table A.71, Cont'd. Hydrogen coordinates ($\times 10^4$) and isotropic displacement parameters ($\text{\AA}^2 \times 10^3$) for $[\text{Mo}_3\text{Se}_7(\text{Se}_2\text{CN}^i\text{Bu}_2)_3]\text{I}$.

H atom	x	y	z	U(eq)
H(41C)	10106	9827	6220	167
H(42A)	8743	9691	6255	44
H(42B)	9171	10376	6145	44
H(43A)	8254	11044	6369	43
H(44A)	9022	12289	6250	66
H(44B)	8772	12123	6593	66
H(44C)	8488	12649	6301	66
H(45A)	8099	11520	5859	79
H(45B)	8389	10527	5807	79
H(45C)	8648	11559	5765	79
H(43B)	9102	11720	6199	43
H(44D)	8091	11319	6325	66
H(44E)	8330	12380	6341	66
H(44F)	8452	11589	6617	66
H(45D)	8818	10614	5726	79
H(45E)	8781	11778	5700	79
H(45F)	8327	11152	5800	79
H(47A)	5936	11821	8400	37
H(47B)	6458	11467	8503	37
H(48)	6135	9910	8650	45
H(49A)	6282	11114	9052	77
H(49B)	5849	10425	9152	77
H(49C)	5748	11497	9011	77
H(50A)	5243	10814	8526	80
H(50B)	5302	9804	8719	80
H(50C)	5447	9872	8345	80
H(51A)	5538	10919	7923	36
H(51B)	5906	10596	7651	36
H(52A)	5786	12598	7885	40
H(53A)	5571	12892	7323	72
H(53B)	5229	12067	7466	72
H(53C)	5663	11766	7239	72
H(54A)	6479	11891	7421	85
H(54B)	6620	12273	7778	85
H(54C)	6411	13019	7512	85
H(52B)	6349	11473	7529	40
H(53D)	5674	11030	7226	72
H(53E)	5880	12070	7119	72
H(53F)	5417	12013	7340	72
H(54D)	6141	13195	7550	85

Table A.71, Cont'd. Hydrogen coordinates ($\times 10^4$) and isotropic displacement parameters ($\text{\AA}^2 \times 10^3$) for $[\text{Mo}_3\text{Se}_7(\text{Se}_2\text{CN}^i\text{Bu}_2)_3]\text{I}$.

H atom	x	y	z	U(eq)
H(54E)	6431	12723	7849	85
H(54F)	5872	12907	7877	85
H(56A)	3974	7384	9585	42
H(56B)	3774	8477	9605	42
H(57)	4133	8672	10133	61
H(58A)	4476	7385	10404	111
H(58B)	4752	7530	10069	111
H(58C)	4373	6666	10104	111
H(59A)	3522	6993	10094	137
H(59B)	3334	8094	10064	137
H(59C)	3565	7715	10399	137
H(60A)	4941	9541	9620	46
H(60B)	4431	9705	9776	46
H(61A)	4630	9880	9097	53
H(62A)	4553	11549	9175	118
H(62B)	4907	11175	9457	118
H(62C)	4364	11403	9537	118
H(63A)	3840	9421	9135	94
H(63B)	3861	10553	9039	94
H(63C)	3749	10240	9405	94
H(61B)	3903	10084	9586	53
H(62D)	4730	11299	9488	118
H(62E)	4422	11265	9812	118
H(62F)	4205	11745	9487	118
H(63D)	4397	9659	9023	94
H(63E)	4123	10681	8993	94
H(63F)	3834	9701	9067	94
H(65A)	5406	5389	7084	39
H(65B)	5661	5956	6794	39
H(66A)	6022	4521	7192	38
H(67A)	6020	3563	6705	71
H(67B)	5641	4361	6584	71
H(67C)	5549	3747	6909	71
H(68A)	6638	5452	6936	80
H(68B)	6582	4469	6727	80
H(68C)	6654	4412	7114	80
H(66B)	6060	5602	6605	38
H(67D)	6045	3960	6447	71
H(67E)	5587	4653	6439	71
H(67F)	5659	3881	6728	71

Table A.71, Cont'd. Hydrogen coordinates ($\times 10^4$) and isotropic displacement parameters ($\text{\AA}^2 \times 10^3$) for $[\text{Mo}_3\text{Se}_7(\text{Se}_2\text{CN}^i\text{Bu}_2)_3]\text{I}$.

H atom	x	y	z	U(eq)
H(68D)	6645	4456	6748	80
H(68E)	6646	5404	6977	80
H(68F)	6622	5523	6589	80
H(69A)	6387	6963	6945	39
H(69B)	6321	7568	7274	39
H(70)	5652	7530	6746	47
H(71A)	6270	9094	6928	79
H(71B)	5900	9117	6629	79
H(71C)	6347	8396	6621	79
H(72A)	5274	7802	7251	89
H(72B)	5210	8701	7005	89
H(72C)	5587	8769	7300	89
H(74A)	8165	3837	9538	37
H(74B)	7681	3410	9387	37
H(75)	7256	3892	9838	63
H(76A)	8092	2833	10028	117
H(76B)	7633	2361	9856	117
H(76C)	7600	2792	10217	117
H(77A)	8091	4734	10108	115
H(77B)	7603	4612	10297	115
H(77C)	7630	5324	9989	115
H(78A)	8316	5501	9557	40
H(78B)	7952	6277	9403	40
H(79)	8169	5786	8872	55
H(80A)	8545	7125	9128	123
H(80B)	8896	6604	8879	123
H(80C)	8956	6420	9262	123
H(81A)	8789	4748	8774	97
H(81B)	8443	4171	9012	97
H(81C)	8920	4657	9153	97